Modelling of Salt Solubilities for Smart Water flooding in Carbonate Reservoirs using Extended UNIQUAC Model

PHD THESIS
MARCH 2016

Krishna Hara Chakravarty

Supervisor

Kaj Thomsen

Philip Loldrup Fosbøl

DTU-KT

Department of Chemical and Biochemical Engineering

KT-DTU
Department of Chemical and Biochemical Engineering
Technical University of Denmark

Søltofts Plads, Building 229
2800 Kongens Lyngby, Denmark
Phone +45 4225 2800
http://www.kt.dtu.dk

Preface

This thesis is submitted as partial fulfilment of the requirement for the PhD degree at the Technical University of Denmark (DTU). The work has been carried out at the Department of Chemical and Biochemical Engineering from 2012 to 2016 under the supervision of Associate Professor Kaj Thomsen and Associate Professor Philip Loldrup Fosbøl. This PhD project was funded by DTU, Maersk Oil, DONG Energy and the Danish Energy Agency as a part of the Smart Water project. The experimental work for this thesis was carried out at DTU and Geological Survey of Denmark and Greenland (GEUS).

This thesis contains three introduction chapters (I-III). Chapter I describes the state of art literature review of smart water enhanced oil recovery water flooding for both sandstones and carbonates. Chapter II describes the theory behind conducted density functional theory calculations in the PhD work. Chapter III describes the theory behind conducted Extended UNIQUAC speciation calculations in the PhD work. Chapter IV is the discussion section. Herein results from the different papers produced from the thesis work (which are put as Paper I-XV to the thesis) are discussed and compared with reported experimental data and proposed mechanisms for smart water enhanced oil recovery for carbonates. This is a paper-based thesis and Chapter IV refers to the Papers in the Appendix which has to be read conjointly. The results in the PhD work have been put in as 15 individual Papers to the PhD thesis. Paper I-VIII and X include 9 SPE publications which have been presented at different SPE conferences. Four of these 9 papers have been submitted for peer review publications as well (with two of the papers being in initial review while the other two being in the revision stage). Paper IX and XI-XV are prospective papers which shall be sent for peer review publication after contributions from other researchers in the smart water group have been obtained.

All experiments and simulations in Paper I-IX and XIV-XV were conducted by Krishna Hara Chakravarty. Core flooding equipment used in paper X-XIII was designed and produced by Ida Fabricius and Mohamed Monzurul Alam from DTU-Civil Engineering, and Philip L. Fosbøl, Ioannis Xiarchos from DTU-Chemical Engineering. Plots in Paper X were jointly produced by Krishna and Mehrdad Ahkami of DTU-Chemical Engineering. Core flooding experiments in paper XI-XIII was conducted primarily by Ioannis Xiarchos. Dan Olsen and Hans Jørgen of Geological Survey of Greenland and Denmark (GEUS) Sinh Nguyen and Hector Diaz of DTU-Environment and Tran Thuong Dang, Zacarias Tecle and Duc Thuong Vu, Philip L. Fosbøl, Mehrdad Ahkami and Krishna Hara

Chakravarty of DTU-Chemical Engineering and assisted in the core flooding experiments. The coreplug preparation and measurement of petrophysical properties was conducted by Mohamed Monzurul Alam, Konstantina Katika and Ida Fabricius from Civil Engineering with collaboration from Dan Olsen and Hans Jørgen of Geological Survey of Greenland and Denmark (GEUS). These petrophysical properties have been previously published in Konstantina's PhD thesis. Duc Thuong Vu has also produced the CT-scan images used in paper 11-13. Processing of the pressure profiles, Oil recovery and effluent brine composition and preparation of final plots are presented in Paper 11-13 was done by Krishna.

Acknowledgements

I would like to express my most sincere gratitude to my supervisors for their full support throughout the project. First of all I would like to express my deep appreciation to my supervisor, Associate Professor Kaj Thomsen. He provided support and advice during this project and allowed me the freedom to address the challenge from different ways. He also supported and guided me in all steps of modelling, writing of the articles, its revision and presentation. I have benefited a lot from the data bank and programs. This guidance enhanced my knowledge in Thermodynamics, Chemical Engineering, Chemistry, Geology and many other aspects of science and life.

I would like to thank my Co-supervisor, Associate Professor Philip Loldrup Fosbøl for his guidance and support on the core flooding research presented in this thesis. Your deep involvement and enthusiasm in the experimental work has been very helpful in this project. I also say thank for the constant encouragement, support and many valuable inputs.

I acknowledge the Danish Energy Agency, Mærsk Oil and DONG Energy for funding the research and providing the core data. I am thankful to Alexander Shapiro, Ida Fabricius Ioannis Xiarchos; Mehrdad Ahkami and all members of the Center for Energy Resource Engineering for valuable discussions, suggestions and technical assistance. A huge thank to Sinh Nguyen and Hector Diaz of DTU-Environment and Tran Thuong Dang, Zacarias Tecle and Duc Thuong Vu of DTU-Chemical Engineering for assisting in laboratory work.

I would like to thank representatives from Maersk and Dong Energy who provided valuable input to various discussions. Particularly I would like to thank Vural Sander Suicmez and Niels Lindeloff from Maersk Oil and Christian Schack Pedersen from DONG Energy for their valuable question and BSTFA samples for GC analysis. I would like to thank all reviewers to my SPE Papers and other Journal Papers; their comments have helped me improve the work significantly. I would like to thank various research groups for their published smart water and low salinity EOR studies. The core flooding experiments conducted by various groups in Denmark, Norway, Middle East and US have been the central part of my analysis. Without these available online data I could not have been able to submit my thesis in the present format.

I would like to also thank my family for being so.

Krishna Hara Chakravarty
March 2016
Kgs Lyngby Denmark

,

from the steadfast efforts of Tripti Banerjee (Meenakshi)

Summary

For most oil reservoirs which were drilled with conventional methods, the expected initial recovery of available hydrocarbons maybe as low as 15% – thus leaving 85+% of hydrocarbons in the reservoir. Implementation of mechanical methods including pump jacks and initial gas injection or thermal recovery can increase that capture up to 25-30% of original oil in place (OOIP). But cost effective Enhanced Oil Recovery (EOR) techniques if implemented correctly can be used to produce another 10-15% of the initially available hydrocarbons.

Advanced water flooding (i.e. altering injection brine compositions by varying concentration of selected ions) is an enhanced oil recovery method which in a low cost, non-toxic manner increases oil recovery from various carbonate reservoirs. Dan and Halfdan are chalk reservoirs from the Danish North Sea, which are matured oil fields that have been flooded with water for more than a decade and are potential candidates for brine composition based EOR. Advanced water flooding through alteration in brine composition has been termed as Smart Water(SmW) Flooding, Designed Water flooding, Low salinity brine injection, LowSal$^{(™)}$ EOR, and Advanced Water flooding in different research studies.

Several spontaneous imbibition and water flooding experiments have been conducted in order to understand the fundamental mechanism behind the observed increase in oil recovery for variation in injection of brine composition. When reported in literature, this observed increase in oil recovery has been explained using the wettability alteration mechanism. The wettability alteration mechanism reported in literature can be divided into two parts:

1. Substitution of calcium by magnesium: When Mg containing brine is injected into a core plug, the existing Ca^{2+} from the mineral surface/lattice is gradually replaced by the injected Mg^{2+}. Decrease in magnesium concentration in the effluent and the corresponding increase in calcium concentration further support this phenomenon.

2. Adsorption of SO_4^{2-} ions:- When SO_4^{2-} ions are injected into the core plugs along with Ca^{2+} and/or Mg^{2+} ions, then SO_4^{2-} ions gets adsorbed on the mineral surface. This leads to desorption of carboxyl ions from the mineral surface and makes the oil more mobile. Thus, eventually leading to an increase in oil recovery.

According to the wettability alteration mechanism, an increase in oil recovery therefore takes place when brines with high concentrations of Ca^{2+}, Mg^{2+}, and

SO_4^{2-} ions are injected. It has been further recommended that precipitation of ions must be avoided as precipitation can choke the pore throats and thus have an adverse effect on the sweep efficiency of the flooded water.

Several questions have been raised to the wettability alteration mechanism due to fundamental contradictions with experiments. It has been observed that Stevns Klint chalk from Denmark shows consistent increase in oil recovery for an increase in injection brine SO_4^{2-} concentration. But similar increases in oil recovery are not observed for Niobrara or Rørdal outcrop chalk core plugs. Observed increases in oil recovery for completely water wet core plugs are also contradictory to the proposed wettability alteration mechanism. No increase in oil recovery observed when injecting brines with high concentrations of SO_4^{2-} ions is also contradictory to the proposed wettability alteration mechanism. Therefore, understanding the fundamental mechanism behind SmW-EOR is quite important. In this study it is attempted to conduct geochemical modeling of salt solubility at reservoir conditions to explore the possible correlation between different brine properties and the corresponding increase in oil recovery (as reported in literature).

The possibility of ion substitution on mineral surfaces has been studied using density functional theory based molecular dynamic simulation. It has been observed that adsorption of magnesium releases energy which can thereafter lead to the release of calcium ions from the mineral surface. Based on DFT calculations it was observed that ion substitution on mineral surfaces can take place if enough time is provided.

This ion substitution causes an increase in Ca^{2+} concentration in the pore space (which is also observed the effluent brine analysis). Thus, additional Ca^{2+} in the pore space can cause change in brine speciation and cause insoluble salt precipitation. The interaction of insoluble salt with crude oil has thereafter been studied. It has been observed that crude oil interacts with insoluble salt to form water soluble emulsion. Both acids and base fractions have shown consistent tendency to oil emulsion formation. The pattern and composition of these emulsions was further studied using Gas Chromatographic analysis. The availability of different soluble salts was shown to influence the amount of emulsification taking place. Ca^{2+}, Mg^{2+}, SO_4^{2-} and PO_4^{3-} ions were observed to enhance oil emulsion formation considerably. Formation of this emulsion takes place only when insoluble fines and polar fraction are present in water and oil respectively. This emulsification therefore indicates an increased adhesion at the oil water interface with release of residue oil from the mineral surface.

Subsequently, the amount of fines formed in the coreplug due to change in brine speciation following ion substitution has been correlated to the oil recovery. Using Extended UNIQUAC model, speciation calculations were conducted for different brine compositions and it was observed that the amount of fines formation taking place after ion substitution consistently was correlated to the reported oil recovery for more than 128 core plugs. This

correlation remains consistent over variations in temperature, pressure, acid number, acid type, base number, aging temperature, aging time, formation water, composition and coreplug wettability. The fraction of soluble SO_4^{2-} (at reservoir condition speciation after ion substitution) showed only partial correlation to the reported oil recovery.

The brines produced from the coreplug (stored into the effluent tubes at room temperature) are analyzed to determine the effluent brine composition. This brine composition (at room temperature) is subsequently correlated to the injection brine composition and to the increased oil production. But the speciation properties of the brine when produced from the coreplug at reservoir conditions can get considerably altered as it changes to ambient conditions. So, the speciation analysis of effluent brines at reservoir conditions was also performed. Calculations showed that most brines are supersaturated at reservoir conditions when produced, and the amount of insoluble salt existing (mobile fines) was determined using extended UNIQUAC model. The amount of mobile fines produced from the core plug shows a one-to-one correlation to the reported EOR. Furthermore it has been observed that speciation variation can take place if soluble CO_2 (aq) is present in the injected water during WAG or carbonated water injection.

Extended UNIQUAC speciation calculations to establish a distinction between fines formation (after ion substitution) and precipitation (on injection) was conducted and it was observed that precipitation on injection take place for most of the recommended brines. Injection brines which have shown significant increase in oil recovery were also found to be supersaturated at the reservoir/experimental conditions. Contrary to the proposed wettability alteration mechanism, speciation calculation at reservoir condition showed no inverse correlation between amount of precipitation and oil recovery. And for highly precipitating brines, also the amount of fines formation taking place (after ion substitution) showed good correlation to the observed increase in oil recovery. This showed a clear distinction between injection brine (at room temperature) and actually injected brine (at reservoir condition).

Subsequently, core flooding experiments were conducted using reservoir core plugs from the Danish North Sea. Core flooding experiments were conducted at high and low temperature conditions (130°C and 60°C) for carbonate core plugs and at low temperature for greensand core plugs (60°C). It was observed that pauses in water flooding can cause additional ion substitution and release of calcite fines from the mineral surface. The amount of released Ca^{2+} and CO_3^{2-} /SO_4^{2-} was observed to be beyond the solubility limit (at flooding conditions). Thus, it indicates that insoluble $CaCO_3$ was produced because of attrition on the mineral surface. This attrition based fines production showed consistent correlation to the observed increase in oil recovery. A similar ion substitution did not/cannot take place in greensands so, correspondingly no major increase in oil recovery was observed for greensand core plugs.

Based on this correlation between fines formation and oil recovery, possible implementation strategies has been developed for different sections of the most oil producing field of the Danish north sea including the Dan field and the Halfdan field. Finally the amount of insoluble salt and soluble ions for various commonly used compositions has been reported. The fines migration based oil recovery mechanism has been proposed to explain variation in oil production during injection/imbibition of smart water floods. Further experimentation to scrutinize this mechanism has also been recommended. Finally, for implementation of SmW-EOR, the iron fertilization based ion alteration method has been proposed. It can be considered for implementation in several oil fields including the Dan field of North Sea.

Resume på dansk

For de fleste oliereservoirer der blev boret med konventionelle metoder, forventede indledende bedring af tilgængelige kulbrinter måske så lave som 15% - hvilket giver 85 +% af kulbrinter i reservoiret. Implementering af mekaniske metoder, herunder pumpe stik og indledende injektion gas eller varmegenvinding kan øge at fange op til 25-30% af den oprindelige olie på plads (OOIP). Men omkostningseffektive Enhanced Oil Recovery (EOR) teknikker, hvis implementeret korrekt, kan bruges til at producere en anden 10-15% af de oprindeligt tilgængelige kulbrinter.

Avanceret vand fyldning (dvs. ændring injektion saltlage kompositioner af varierende koncentration af udvalgte ioner) er en øget olieudvinding metode, som i en lav pris, ikke-toksisk måde øger olieudvinding fra forskellige carbonatreservoirer. Dan og Halfdan er kalkreservoirer fra den danske del af Nordsøen, som er modnet oliefelter, der er blevet oversvømmet med vand i mere end et årti og er potentielle kandidater til saltlage sammensætning baseret EOR. Avanceret vand oversvømmelser gennem ændring i saltlage sammensætning er blevet betegnet som Smart Water (SMW) Oversvømmelser, Designet vand oversvømmelser, lav saltholdighed saltlage injektion, LowSal (™) EOR, og Advanced Water oversvømmelser i forskellige forskningsundersøgelser.

Der er blevet udført flere spontane opsugning og vand oversvømmelsesforsøg for at forstå den grundlæggende mekanisme bag den observerede stigning i olieudvinding for variation i injektion af saltvand sammensætning. Når rapporteret i litteraturen, bemærkede denne stigning i olieindvinding er blevet forklaret ved hjælp af befugtningsevne ændring mekanisme. Fugtningsmuligheden ændring mekanisme rapporteret i litteraturen kan opdeles i to dele:

1. Udskiftning af calcium ved magnesium: Når Mg indeholdende saltlage indsprøjtes i en kerne stik, er den eksisterende Ca^{2+} fra den mineralske overflade / gitter gradvist erstattet af den injicerede Mg^{2+}. Fald i koncentrationen magnesium i spildevandet og den tilsvarende stigning i calciumkoncentration yderligere støtte dette fænomen.

2. Adsorption af SO_4^{2-} ioner: - Når SO_4^{2-} ioner injiceres i de centrale propper sammen med Ca^{2+} og / eller Mg^{2+} -ioner, derefter SO42- ioner bliver adsorberet på mineralske underlag. Dette fører til desorption af carboxylgrupper ioner fra det mineralske overflade og gør olien mere mobile. Således i sidste ende fører til en stigning i olieudvinding.

Ifølge befugteligheden ændring mekanisme, en stigning i olieindvinding foregår derfor når saltopløsninger med høje koncentrationer af Ca^{2+}, Mg^{2+}, og SO_4^{2-} ioner injiceres. Det er yderligere blevet anbefalet, at udfældning af ioner skal undgås, da nedbøren kan kvæle de porehalsene og dermed har en negativ indvirkning på sweep effektiviteten af den oversvømmede vand.

Flere spørgsmål er blevet rejst til befugtningsevne ændring mekanisme skyldes grundlæggende modsætninger med eksperimenter. Det er blevet observeret, at Stevns Klint kridt fra Danmark viser konsekvent stigning i olieudvinding for en stigning i injektion saltlage SO_4^{2-} koncentration. Men lignende stigninger i olieudvinding er ikke observeret for Niobrara eller Rørdal outcrop kridt kerne stik. Observerede stigninger i olieudvinding for helt vand våde core stik er også i modstrid med den foreslåede befugtningsevne ændring mekanisme. Ingen stigning i olieudvinding observeret, når injektion saltlager med høje koncentrationer af SO_4^{2-} ioner er også i modstrid med den foreslåede befugtningsevne ændring mekanisme. Derfor forstå den grundlæggende mekanisme bag SMW-EOR er ret vigtigt. I denne undersøgelse er det forsøgt at foretage geokemiske modellering af salt opløselighed ved reservoir betingelser for at undersøge mulig sammenhæng mellem forskellige saltlage egenskaber og den tilsvarende stigning i olieindvinding (som rapporteret i litteraturen).

Muligheden for ion substitution på mineralske overflader er blevet undersøgt ved hjælp af tæthedsfunktionalteori baseret molekylær dynamisk simulering. Det er blevet observeret, at adsorption af magnesium frigiver energi, som derefter kan føre til frigivelsen af calciumioner fra mineralet overflade. Adsorption af magnesiumioner i sites på mineralske overflade kan også finde sted. Baseret på DFT beregninger blev det observeret, at ion substitution på mineralske overflader kan finde sted, hvis der er tilvejebragt tilstrækkelig tid.

Dette ion substitution forårsager en stigning i Ca^{2+} -koncentration i porerummet (som også observeret effluenten saltlage analyse). Således kan yderligere Ca^{2+} i porerummet forårsage ændring i saltlage artsdannelse og forårsage uopløseligt salt udfældning. Interaktionen af uopløseligt salt med råolie er derefter undersøgt. Det er blevet observeret, at råolie interagerer med uopløseligt salt til dannelse vandopløseligt emulsion. Både syrer og baser fraktioner har vist konstant tendens til olie-emulsion formation. Mønstret og sammensætningen af disse emulsioner blev yderligere undersøgt ved hjælp gaskromatografisk analyse. Tilgængeligheden af forskellige opløselige salte viste sig at påvirke den mængde emulgering finder sted. Ca^{2+}, Mg^{2+}, iagttoges SO_4^{2-} og PO_4^{3-} ioner kan forbedre olie-emulsion dannelse betydeligt. Dannelse af denne emulsion finder sted, når uopløselige bøder og polære fraktion er til stede i vand og olie hhv. Denne emulgering indikerer derfor en øget vedhæftning på olie vand grænsefladen med frigivelse af olivenpresserester fra mineralet overflade.

Efterfølgende har størrelsen af de bøder, der er dannet i coreplug følge af ændring i saltlage artsdannelse efter ion substitution blevet korreleret til

olieudvinding. Brug Udvidet UNIQUAC model blev speciering beregninger foretaget for forskellige saltlage kompositioner, og det blev observeret, at størrelsen af de bøder dannelse finder sted efter ion substitution konsekvent var korreleret til den rapporterede olieudvinding i mere end 128 centrale stik. Denne korrelation er fortsat konsekvent over variationer i temperatur, tryk, syretal, syretype, basetal, ældningstemperatur, ældningstid, formationsvand, sammensætning og coreplug befugtelighed. Fraktionen af opløselige SO_4^{2-} (ved reservoir tilstand artsdannelse efter ion substitution) viste kun delvis korrelation til den rapporterede olieudvinding.

Saltopløsningerne fremstillet fra coreplug (gemt i spildevand rør ved stuetemperatur) analyseres for at bestemme den udstrømmende saltlage sammensætning. Dette saltvand sammensætning (ved stuetemperatur) efterfølgende korreleret til injektion saltlage sammensætning og den øgede olieproduktion. Men specieringen egenskaber af saltlage, når der produceres fra coreplug ved reservoirforhold kan få ændret betydeligt, da den skifter til omgivelserne. Så blev artsbestemmelse analyse af spildevand saltlager på reservoirforhold også udført. Beregninger viste, at de fleste saltopløsninger er overmættet ved reservoirforhold når de produceres, og mængden af uopløseligt salt eksisterende (mobile bøder) blev bestemt ved hjælp af udvidet UNIQUAC model. Mængden af mobile bøder produceret fra kernen stik viser en en-til-en korrelation til den rapporterede EOR. Endvidere er det blevet observeret, at artsdannelse variation kan finde sted, hvis opløseligt CO_2 (aq) er til stede i det injicerede vand under WAG eller kulsyreholdigt injektion.

Extended UNIQUAC speciering beregninger for at etablere en sondring mellem bøder dannelse (efter ion substitution) og nedbør (på injektion) blev udført, og det blev observeret, at nedbør på injektion ske for de fleste af de anbefalede saltopløsninger. Injektion saltopløsninger, som har vist betydelig stigning i olieindvinding fandtes også at være overmættet ved reservoiret / forsøgsbetingelser. I modsætning til den foreslåede befugtningsevne ændring mekanisme, artsdannelse beregning på reservoir tilstand viste ingen invers korrelation mellem mængden af nedbør og olieudvinding. Og til meget fældning af saltopløsninger, også størrelsen af de bøder dannelse finder sted (efter ion substitution) viste god korrelation til den observerede stigning i olieudvinding. Dette viste en klar sondring mellem injektion saltlage (ved stuetemperatur) og faktisk indsprøjtet saltvand (ved reservoir tilstand).

Efterfølgende blev gennemført centrale oversvømmelsesforsøg hjælp reservoir kerne stik fra den danske del af Nordsøen. Core oversvømmelsesforsøg blev udført ved høje og lave temperaturer (130 °C og 60 °C) i carbonat core stikpropper og ved lav temperatur i greensand core plugs (60 °C). Det blev observeret, pauser i vand oversvømmelser kan forårsage yderligere ion substitution og frigivelse af calcit bøder fra mineralet overflade. Mængden af frigivet Ca^{2+} og CO_3^{2-} / SO_4^{2-} blev observeret at være uden opløselighedsgrænsen (ved oversvømmelser forhold). Det indikerer således, at uopløselig $CaCO_3$ blev

produceret på grund af nedslidning på mineralsk overflade. Denne nedslidning baseret bøder produktion viste konsekvent korrelation til den observerede stigning i olieudvinding. En lignende ion substitution ikke / kan ikke finde sted i Greensands så blev tilsvarende ingen større stigning i olieindvinding observeret for greensand kerne stik.

Baseret på denne sammenhæng mellem bøder dannelse og olieudvinding, har mulige implementeringsstrategier blevet udviklet til forskellige dele af det mest olieproducerende felt af den danske nordsøen herunder Dan feltet og feltet Halfdan. Endelig mængde uopløseligt salt og opløselige ioner til forskellige almindeligt anvendte præparater er blevet rapporteret. Den bøder migration baseret olieindvinding mekanisme er blevet foreslået til at forklare variation i olieproduktionen under injektion / opsugning af oversvømmelser smarte vand. Yderligere forsøg at undersøge denne mekanisme er også blevet anbefalet. Endelig for gennemførelsen af SmW-EOR, er blevet foreslået jern befrugtning baseret ion ændring metode. Det kan betragtes til implementering i flere oliefelter, herunder Dan feltet i Nordsøen.

List of publication

The work of the PhD thesis has resulted in the following research papers.

- Paper I: Chakravarty, K. H., Fosbøl, P. L., & Thomsen, K. (2015, November). Behavior of Ca^{2+} and Mg^{2+} ions During Smart Water Flooding On Chalk Reservoirs. In *SPE Oil & Gas India Conference and Exhibition*. Society of Petroleum Engineers.
- Paper II: Chakravarty, K. H., Fosbøl, P. L., & Thomsen, K. (2015, April). Interactions of Fines with Oil and its Implication in Smart Water Flooding. In *SPE Bergen One Day Seminar*. Society of Petroleum Engineers.
- Paper III: Chakravarty, K. H., Fosbøl, P. L., & Thomsen, K. (2015, June). Interactions of Fines with Base Fractions of Oil and its Implication in Smart Water Flooding. In *EUROPEC 2015*. Society of Petroleum Engineers.
- Paper IV: Chakravarty, K. H., Fosbøl, P. L., & Thomsen, K. (2015, August). Brine Crude Oil Interactions at the Oil-Water Interface. In *SPE Asia Pacific Enhanced Oil Recovery Conference*. Society of Petroleum Engineers.
- Paper V: Chakravarty, K. H., Fosbøl, P. L., & Thomsen, K. (2015, June). Importance of Fines in Smart Water Enhanced Oil Recovery (SmW-EOR) for Chalk Outcrops. In *EUROPEC 2015*. Society of Petroleum Engineers.
- Paper VI: Chakravarty, K. H., Fosbøl, P. L., & Thomsen, K. (2015, November). Fine Formation during brine-crude oil-calcite interaction in Smart Water flooding and its correlation to Enhanced Oil Recovery. In *SPE Annual Caspian Technical Conference & Exhibition*. Society of Petroleum Engineers.
- Paper VII: Chakravarty, K. H., Fosbøl, P. L., & Thomsen, K. (2015, November). Significance of Fines and their Correlation to Reported Oil Recovery. In *Abu Dhabi International Petroleum Exhibition and Conference*. Society of Petroleum Engineers.
- Paper VIII: Chakravarty, K. H., & Thomsen, K. (2015, November). Formation of Anhydrite Due to Interaction between Water Soluble CO_2 (aq) and Calcite Mineral during Enhanced Oil Recovery. In *SPE Oil & Gas India Conference and Exhibition*. Society of Petroleum Engineers.
- Paper IX: Chakravarty, K. H., Fosbøl, P. L., & Thomsen, K. (2016) Modeling of salt solubility and dissolution during smart water flooding for carbonate reservoir. *Journal of Petroleum Science and Engineering* (Draft Manuscript: To be submitted)

- Paper X: Ahkami, M., Chakravarty, K. H., Xiarchos, I., Thomsen, K., & Fosbøl, P. L., (2016), April Determining Optimum Aging Time Using Novel Core Flooding Equipment. In *SPE Bergen One Day Seminar*. Society of Petroleum Engineers.

- Paper XI: Chakravarty, K. H., Ahkami, M., Xiarchos, I., Fosbøl, P. L., & Thomsen, K. (2016) Effect of pause in brine injection during Smart Water-Enhanced Oil Recovery (SmW-EOR) for low temperature chalks: A case study from North Sea. *Journal of Petroleum Science and Engineering* (Draft Manuscript: To be submitted)

- Paper XII: Chakravarty, K. H., Ahkami, M., Xiarchos, I., Fosbøl, P. L., & Thomsen, K. (2016) Effect of pause in brine injection during Smart Water-Enhanced Oil Recovery (SmW-EOR) for low temperature chalks: A case study from North Sea. *Journal of Petroleum Science and Engineering* (Draft Manuscript: To be submitted)

- Paper XIII: Chakravarty, K. H., Ahkami, M., Xiarchos, I., Fosbøl, P. L., & Thomsen, K. (2016) Smart Water-Enhanced Oil Recovery (SmW-EOR) in low temperature Sandstone reservoirs: A case study from North Sea. *Journal of Petroleum Science and Engineering* (Draft Manuscript: To be submitted)

- Paper XIV: Chakravarty, K. H., Fosbøl, P. L., & Thomsen, K. (2016) Parallel injection of multiple brines through various injection wells for optimum fines formation during smart water flooding. *Journal of Petroleum Science and Engineering* (Draft Manuscript: To be submitted)

- Paper XV: Chakravarty, K. H., Fosbøl P. L., Thomsen K. Extended UNIQUAC Calculation of Solubilities of various smart water floods at reservoir conditions.

This study is based on documentation done in form of 15 research papers as listed above. The Paper I-VIII and X are SPE papers presented in conference and are published online in onepetro. Papers II and V have also been submitted for journal publication in *SPE reservoir evaluation & engineering;* while Papers III and IV have been submitted for journal publication in *Journal of Petroleum Science and Engineering*. Response from reviewers on Paper IV and V have been received and in revision while for Paper II and III the response is awaited. The intention is to submit and publish all of the sated papers in peer review scientific journal. Paper X-XIII are incomplete manuscripts which is in preparation as post flooding petrophysical measurements and flow modelling are yet to conducted. Konstantina Katika, Ida Fabricius, Alexander Shapiro and Artem Alexeev are likely to further contribute and be co-authors to these papers (Paper XI-XIII) when submitted for peer review publications.

Contents

Chapter 1 - A brief literature Review of Smart Water Enhanced Oil Recovery and its influencing factors 1
1.1 Introduction 1
1.2 Smart Water: Introduction 2
1.3 Wettability 3
1.4 Smart Water: Low salinity water flooding and sandstone reservoirs 5
1.5 Smart Water: High Salinity and Carbonates reservoirs 12
1.6 Modeling low salinity water flood 17
1.7 Conclusion 18
Chapter 2 - Theory of Density Functional Theory for adsorption/desorption from mineral surface 21
2.1 Introduction 21
2.2 A b-initio, first principle methods 23
2.3 Mineral Properties and Behavior 29
2.4 Thermodynamic Properties 33
Chapter 3 - Modeling electrolyte solutions with the extended universal quasichemical (UNIQUAC) model 37
3.1 Introduction 37
3.2 Extended UNIQUAC model 38
3.3 Model parameters 41
3.4 Standard-state properties 43
3.5 Results 45
3.6 Application in Smart Water Enhanced Oil Recovery (EOR) 49
3.7 Conclusion 50
Chapter 4 - Discussion 53
4.1 Ion Substitution 54
4.2 Emulsification 61
4.3 Extended UNIQUAC calculation and fines-SmW EOR correlation 70
4.4 What is the mechanism for SW-EOR? 80

4.5 Precipitation on injection and after substitution 86
Chapter 5 - Conclusion and Future Scope of work 91
5.1 Scrutinizing fines based SW-EOR mechanism 91
5.2 Implementation of fines based SW-EOR 93
5.3 Conclusion 97
References 101
Appendix 114
Paper I - Behavior of Ca2+ and Mg2+ ions During Smart Water Flooding On Chalk Reservoirs *115*
Paper II - Interactions of Fines with Oil and its Implication in Smart Water Flooding *128*
Paper III - Interactions of Fines with Base Fractions of Oil and its Implication in Smart Water Flooding *144*
Paper IV - Brine Crude Oil Interactions at the Oil-Water Interface *163*
Paper V - Importance of Fines in Smart Water Enhanced Oil Recovery (SmW-EOR) for Chalk Outcrops *180*
Paper VI - Fine Formation during brine-crude oil-calcite interaction in Smart Water flooding and its correlation to Enhanced Oil Recovery *201*
Paper VII - Significance of Fines and their Correlation to Reported Oil Recovery *221*
Paper VIII - Formation of Anhydrite Due to Interaction Between Water Soluble CO2 (aq) and Calcite Mineral During Enhanced Oil Recovery *239*
Paper IX - Modeling of salt solubility and dissolution during smart water flooding for carbonate reservoir *256*
Paper X Determining Optimum Aging Time Using Novel Core Flooding Equipment *274*
Paper XI Effect of pause in brine injection during Smart Water-Enhanced Oil Recovery (SmW-EOR) for low temperature chalks: A case study from North Sea *290*
Paper XII Effect of pause in low temperature chalks during Smart Waterflooding: A case study from North Sea *308*
Paper XIII Smart Water-Enhanced Oil Recovery (SmW-EOR) in low temperature Sandstone reservoirs: A case study from North Sea *333*
Paper XIV Parallel injection of multiple brines through various injection wells for optimum fines formation during smart water flooding *352*
Paper XV Extended UNIQUAC Calculation of Solubilities of various smart water floods at reservoir conditions *370*

CHAPTER 1

A brief literature Review of Smart Water Enhanced Oil Recovery and its influencing factors

1.1 Introduction

Recovery stages: A reservoir begins to produce when petroleum travels from the reservoir pores to the production well. The production processes of oil recovery are traditionally divided in three stages:

a. Primary recovery: Primarily, crude reservoir oil and gas moves naturally from the reservoir pores to the well and thereafter to the surface by natural energy present in the reservoir. Natural energy source in the reservoir condition are solution-gas drive, gas-cap drive, natural water drive, fluid and rock expansion, and gravity drainage (Green 1998). The existence of the high natural differential pressure between the reservoir and the inside of the well supports the natural movement of captured reservoir oil towards the well. With the progress in the recovery process a pressure depletion will occur. Then it becomes compulsory to implement artificial lift processes to increase the differential pressure and keep up the production (Ahmed 2006). Primary recovery is a comparatively inefficient process were only 10-30 % of the Original oil in place (OOIP) are produced (Green 1998).

b. Secondary recovery: In this stage, supplemental energy is provided to continue the oil recovery when primary recovery has reached its limit of production. External techniques like water injection or gas injection are used to maintain the reservoir pressure and/or to improve sweep competence so that the remaining oil is displaced towards producing wells (Green 1998). Over the past few decades, water flooding is perhaps the most common method (Green 1998; Ahmed 2006). Secondary recovery is now the major stage of oil recovery producing 30-50 % of the original oil in place (OOIP).

c. Tertiary recovery/EOR: The third phase of oil recovery, also known as (Enhanced Oil Recovery) EOR is applied after both primary and secondary oil recovery becomes uneconomical, as oil left in the reservoir

can be displaced by injection of gases or water, or by use of thermal energy. These EOR techniques supplement the natural energy present in the reservoir to interact with the reservoir rock /oil system to displace the oil and enhance the movement of oil towards the production well (Green 1998; Ahmed 2006; Fanchi 2010). Several studies over the past decade have proven that through wettability modification towards a more water-wet condition, oil recovery can be increased by smart use of different ions in the injected water. This smartly modified water with a particular brine composition decided through rock-oil system studies is called 'Smart Water'. The fact that the composition of the injected smart water is different from the formation water (FW), may characterize water flooding as an EOR process (Green 1998).

1.2 Smart Water: Introduction

Water flooding was first practiced for pressure maintenance after primary pressure diminution and has since then become the most extensively applied improved oil recovery technique. Various technologies and practices have been previously used to improve the percentage of oil recovery by water flooding, such as multilateral wells, infill drilling, improved reservoir characterization and modern monitoring and surveillance, and other. Conventionally, a slender consideration has been specified in reservoir engineering practice to the role of chemistry of injection water on displacement efficiency or its impact on oil recovery.

Some earlier scholars had pointed out the effect that the salinity of brine can have on recovery in sandstones rocks. But it was in the 90's that studies by Morrow and co-workers (Tang and Morrow 1997; Tang and Morrow 1999; Yildiz and Morrow 1996) reawakened the understanding that the composition of the brine is crucial; "water is not just water!". Since then, extensive research has been presented showing that the configuration of the injected water can affect oil/brine/rock systematically in a favorable way to increase oil recovery. Morrow and Buckley 2011 have a long list of published works on smart water floods.

Optimal seawater flooding in high temperature carbonate reservoirs and low salinity water flooding in sandstone reservoirs are two major broad examples of smart water flooding. The interest generated by smart water flooding is largely related to the benefits that can be derived from its injection in petroleum reservoirs. Some of the most feasible benefits include:

a. Cost benefit related with the extra oil that can be produced.
b. Cost benefit associated with the savings that can be made from carrying out other Enhanced Oil Recovery (EOR) chemical processes.

c. The adversarial environmental impact of injecting smart water is minimal compared with injection of EOR chemicals.
d. The possibility of altering the composition of produced water and re-injecting it.
e. Combined with other EOR methods (e.g. surfactant and polymer flooding) to further improve recovery.
f. It may be readily accessible or producible in some fields.
g. Potentially reduce the scaling and corrosion of field equipment

1.3 Wettability

Wettability is a phenomenon that can be defined as the tendency of one fluid to spread on or adhere to a solid surface in the presence of other immiscible fluids (Ahmed 2006). Reservoir wettability controls the flow rate of oil and water in the reservoir. The wetting circumstance in a rock-fluid system depends on the interfacial tension (IFT), which refers to the tension amongst liquids at a liquid-liquid interface. IFT depends on the configuration of the two fluids at the interface between phases (Fanchi 2010). Wettability is calculated by the contact angle where two immiscible fluids interface meets the solid surface, as illustrated in Figure 1.1. Five various wetting conditions and their corresponding angle of contact are listed in Table 1.1. The angle is calculated via the denser phase (Dandekar 2013).

$$\sigma_{so} - \sigma_{sw} = \sigma_{ow} cos\theta \qquad (1.1)$$

Where:

σ_{so} = IFT between oil and solid [dynes/cm or N/m]

σ_{sw} = IFT between water and solid [dynes/cm or N/m]

σ_{ow} = IFT between oil and water [dynes/cm or N/m]

θ = tangential angle made by the water phase at oil-water-solid interface [degrees]

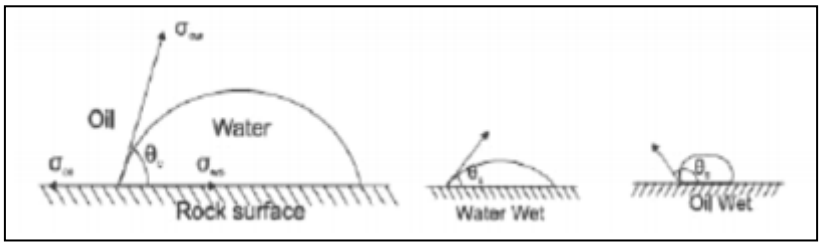


Figure 1.1: Illustration of the contact angle θ, through the water phase (Strand 2005).

Wetting Condition	Contact Angle [degrees]
Strongly water-wet	0-30
Moderately water-wet	30-75
Neutrally wet	75-105
Moderately oil-wet	105-150
Strongly oil-wet	150-180

Table 1.1: Wetting conditions for a water-oil system (Fanchi 2010).

The angle of contact indicates the wettability situation in a reservoir. There are five major wetting environments concomitant with this phenomenon.

a. Water-wet: In a water-wet rock, the surface favors the water phase rather than the oil. For an entirely water-wet rock, the oil is concentrated in the pore center and droplets surrounded by water, not touching any of the rock surfaces, as illustrated in Figure 1.2. The potential for enhanced oil recovery by continuous water flooding is low for these systems, as the water would preferentially flow along the narrow path along the grain walls and leave the oil behind. An entirely water-wet system has an angle of contact of 0° (Dandekar 2013).

b. Oil-wet: An oil-wet rock is exactly the reverse of a water-wet rock. The oil exists like a film on the surface of the grain, and the water is concentrated in the pore center as droplets, as illustrated in Figure 1.2. An entirely oil-wet system has a contact angle of 180° (Dandekar 2013). An oil-wet system is neither ideal as a significant part of the oil will remain attached along the walls of the grains.

c. Fractional wet: Fractional wettability denotes a situation where some of the pores are water-wet, while others are oil-wet. This is mostly associated with rock consisting of different minerals having different chemical properties leading to the formation of particular zones of preferential wetting of water and oil throughout the rock surface (Dandekar 2013).

d. Mixed wet: Fractional wettability associated with pore structural dynamics creates a mixed wet system. In some situations, water occupies the smaller pores and are water-wet containing no oil, while oil fill up larger pores forming continuous paths, resulting in an oil-wet surface (Dandekar 2013).

e. Intermediate wet: Intermediate wet denotes a state where the rock surface favors both the oil and water phases. This is a situation which includes the sub-classes of both fractional and mixed wettability. The state where the rock surface has an equal preference of oil and water is

called neutral wettability. The contact angle in this case is 90° (Dandekar 2013).

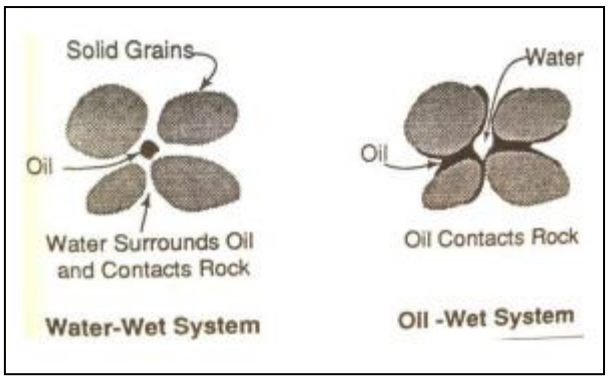


Figure 1.2: Illustration of a water-wet and an oil-wet system (Green 1998).

The reservoir wettability can be modified by changing the parameters that influence the wettability. Some of the parameters which influence the wettability during a water flooding include:

a. Rock
b. Brine
c. Oil
d. Initial water of saturation
e. Aging time
f. Aging temperature
g. Temperature of measurement

Numerous reports of experimental work on wettability situations have been published. Jadhunandan and Morrow 1995 found the optimum wetting condition for oil recovery by water flooding to be weakly water-wet. The potential for enhanced oil recovery by continuous water flooding is low in a wet system. By decreasing the water-wetness during the recovery process by smart variation of the effecting parameters increases the oil recovery, and an increasing oil-wetness decreases the oil recovery.

1.4 Smart Water: Low salinity water flooding and sandstone reservoirs

The idea of Low Salinity Effect (LSE) has been addressed since the 1960s. Work by Bernard 1967 revealed that the injection of fresh water can increase oil recovery from clay containing sandstone cores. Permeability reduction and the development of a relatively high pressure drop were also observed. This work did not get the attention of the oil industry. The pioneering work by Morrow and co-workers conveyed improved recovery of crude oil by low salinity EOR

(Tang and Morrow 1997; Tang and Morrow 1999). Numerous recent examples of increased oil recovery by LSE also confirmed this emerging trend (Morrow and Buckley 2011; Nasralla et al. 2011; Hadia et al. 2011). In most of these studies, 15-20 % extra oil recovery from low salinity water flooding is reported. Lager and co-workers (Lager et al. 2008) stated that by injecting low salinity water with the right composition to the right reservoir, it is possible to reach an increased recovery of up to 40%.

The recovery method is grossly affected by the interactions between the crude oil, brine and rock. These interactions are fairly complex and several mechanisms, both physical and chemical, have been proposed in the last decade. None of them has so far been generally accepted as the main one responsible for the observed low salinity effect. It is therefore important to review the requirements and conditions for successful EOR using LSE (Lager et al. 2008; RezaeiDoust et al. 2009; Austad et al. 2010).

1.4.1 Requirements:

a. **Rock:** It is vital that to have a porous medium such as sandstone. The presence of clay was initially believed to be a prime necessity. When Tang and Morrow, 1999 used cores fired at 800 °C and acidized (to remove the clay) they did not observe LSE . Using 3D imaging technique, (Lebedeva et al. 2009), it was shown that low salinity brine mobilized the dolomite and anhydrite crystals found in the rocks. In another study, Pu et al. (2010) correlated the LSE perceived in three different sandstone cores to formation of a more water-wet from weakly water-wet situation by the dissolution of anhydrite and dolomite cements available in the rocks. They also reported that the cores that were already strongly water wet did not respond to low salinity water injection. Thereafter, in a study of tertiary low salinity imbibition in dolostone (composed primarily by dolomite) containing anhydrite substrate, Suijkerbuijk et al. 2012 clinched that anhydrite dissolution could be a contributory mechanism but not the main mechanism of the improved oil recovery. Low salinity effects have been documented only with carbonates containing dolomite and anhydrite, the mechanisms differ from those in sandstone as surface charges, bonds and cation exchange will all affect the recovery percentage when injecting low salinity water.

b. **Oil:** The oil should contain polar components like acids and bases to make the oil surface-active agents, which can change the wettability away from water-wet (Jerauld et al 2008). No effect has been observed for oil free from polar components (Tang and Morrow 1999; Sharma and Filoco 2000).

   When water is present, the oil and rock surfaces become charged. Their polar components behave as acids and bases (Buckley and Liu 1998). These surface charges affect the adsorption behavior and thus wettability

throughout the injection of low salinity water. To explore the role played by the different polar components, RezaeiDoust et al. (2011) conducted two core floods, one with an oil with a high acid number-low basic number while the other oil had a low acid number-high basic number. They stated that both oils had similar LSE and recommended that the phenomenon works with both acidic and basic oils.

In a recent study, Suijkerbuijk et al. (2012) carried out imbibition tests with many different crude oils and identical core types and brine types (high and low salinity). They varied only the oil in their imbibition tests. The oil types were characterized by interfacial tension (IFT) with formation water, density, viscosity, total acid number (TAN), total basic number (TBN), sulphur content, saturates, aromatic content, resin content, asphaltene contents and asphaltene stability. The oil types gave diverse responses to tertiary low salinity water imbibition. Yet they were unable to find a good correlation between any of these oil properties and the tertiary imbibition low salinity effects recorded. They concluded that conventional classification of the oil with the properties (TAN, TBN, SARA etc.) was not enough, and recommended that fractionation of the oil into functional groups is essential.

c. **Brine:** Tang (1998) concluded that the salinity and pH of the brine affect the surface charge of the mineral and oil/brine interfaces which affect the adsorption of polar components and therefore the wettability.

   Initially FW must be present and the efficiency of oil recovery is related to the initial water saturation (S_{wi}). Tang and Morrow (1999) suggested that when a core is originally 100% saturated with crude oil, $S_{wi} = 0$, then the oil recovery will not be affected by variations in salinity of the injected brine by water flooding. Lager et al., (2008) reported that the FW must comprise divalent cations, like Ca^{2+} and Mg^{2+}, which can interact with the oil and the mineral surface and create bonds.

d. **Low salinity injection fluid:** RezaeiDoust and his group (RazeiDoust 2011) presented that the general belief is that the low salinity injection fluid must have a salinity ranging from 1000-2000 ppm, but LSE have been observed up to 40 000 ppm. They stated that the fluid also seems to be sensitive to ionic composition (Ca^{2+} vs. Na^{+}), affecting the interactions between the injected and the initial water, the rock mineral composition and the crude oil, resulting in possible wettability alteration.

e. **Produced water:** The produced water has been examined by pH measurements and for a non-buffered system, the pH of the run-off water increases about 1-3 pH units when injecting the low salinity fluid. It has not been verified that an increase in pH is needed to observe low salinity effects. In some cases, production of fines has been detected, but low salinity effects have also been observed without visible production of fines (Lager et al. 2009).

f. **Temperature:** When considering temperature, there seems to be no limitations to where low salinity effects can be observed. However, most of the reported studies have been performed at temperatures below 100 °C. Recent low salinity work indicates that an effect may be difficult at high temperatures. Tang (1998) proposed that increasing the aging time and temperature, changes the wetting from strongly water-wet towards oil-wet.

1.4.2 Mechanisms

With the present research trend it seems that probably the low salinity effect is a result of different mechanisms acting together, each with its own contribution. The different mechanisms, which have been proposed up to now, include:

a. **Migration of fines:** The migration of fines concept was first suggested by Tang and Morrow (1999). They reported that Low salinity water will release fines, which are small clay particles. Polar part of the crude oil will stick to the fine particles as droplets and when injecting low salinity water some of the oil will be produced together with these fines as shown in Figure 1.3. A wettability alteration occurs, by making the clay more water-wet. Skauge et al. (2008) proposed that the released fines will also improve the sweep efficiency as the released extra fines will slowly block the pore throats. This leads to a pressure buildup forcing the water to flow into the non-swept pores and wash the residual oil and consequently improve the sweep efficiency. However, low salinity effects without production of fines have been observed in later work.

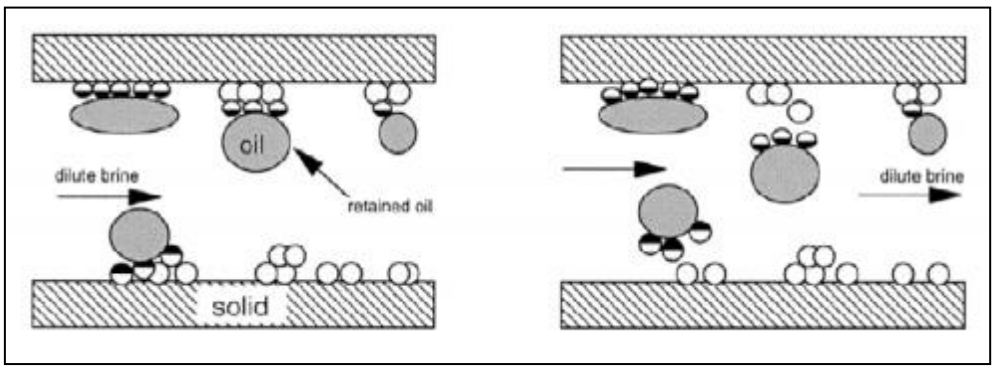


Figure 1.3: Illustration to the left shows the oil before low salinity water flooding and the illustration to the right shows the oil detached from the rock during low salinity water flooding (Tang & Morrow, 1999).

b. **Increase in pH:** McGuire et al. (2005) proposed in their paper that the observed increase in oil recovery by injection of Low salinity water was analogous to alkaline flooding. Moreover, they stated that the increase in pH, normally 1-3 pH units, after low salinity water flooding is caused by the generation of surfactants from the residual oil. This generation

requires that the crude oil should have a TAN more than 0.2 mg KOH/g (RezaeiDoust et al., 2009). Low salinity effects have however been observed with lower AN (Suijkerbuijk et al. 2012), which also makes this mechanism doubtful. Reduction in reservoir oil/water IFT and changes in wettability may also occur with elevated pH, increasing oil recovery.

Lager et al. (2006) proposed that carbonate dissolution and cation exchange can lead to increased pH. As seen from the dissolution reactions, Equation 1.2 and 1.3, when carbonate dissolves there will be an additional OH^-. Cation exchange occurs between the clay and the injected water. At the clay surface adsorbed cations will be replaced by H^+ in the fluid, leading to increased pH due to a decrease in H^+-concentration (Lager et al. 2008), but in reservoirs, the presence of CO_2 may act as a buffer that may prevent the attainment of such high pH as noticed in the lab.

$$CaCO_3 \rightleftharpoons Ca^{2+} + CO_3^{2-} \qquad (1.2)$$

$$CO_3^{2-} + H_2O \rightleftharpoons HCO_3^- + OH^- \qquad (1.3)$$

c. **Multicomponent Ionic Exchange (MIE):** Lager et al. (2006) suggested that multicomponent ionic exchange (MIE) among clay mineral surfaces and the injected brine could be responsible for the increase in oil recovery by LSE. As presented in the Table 1.2, eight different mechanisms for adsorption of organic matter onto clays were suggested by Sposito (1999). The mechanisms are likely to be dependent on the condition of the clay surface and the organic function of the organic matter.

Mechanism	*Organic functional group involved*
Cation exchange	Amino, ring NH, heterocyclic N (aromatic ring)
Protonation	Amino, heterocyclic N, carbonyl, carboxylate
Anion exchange	Carboxylate
Water bridging	Amino, Carboxylate, carbonyl, alcoholic OH
Cation bridging	Carboxylate, amines, carbonyl, alcoholic OH
Ligand exchange	Carboxylate
Hydrogen bonding	Amino, carbonyl, carboxyl, phenolic OH
Van der Waals interaction	Uncharged organic units

Table 1.2: Possible adsorption mechanisms between organic compounds onto clay and calcite minerals (Sposito, 1999).

When polar compounds like resins, asphaltene or hydrocarbons with acetic or amino functional group in the oil bonds with multivalent cations at the clay surface, and when organic polar compounds adsorb directly onto clay mineral surfaces by displacement of the most unstable cations present at the clay surface, the reservoir rock becomes oil-wet.

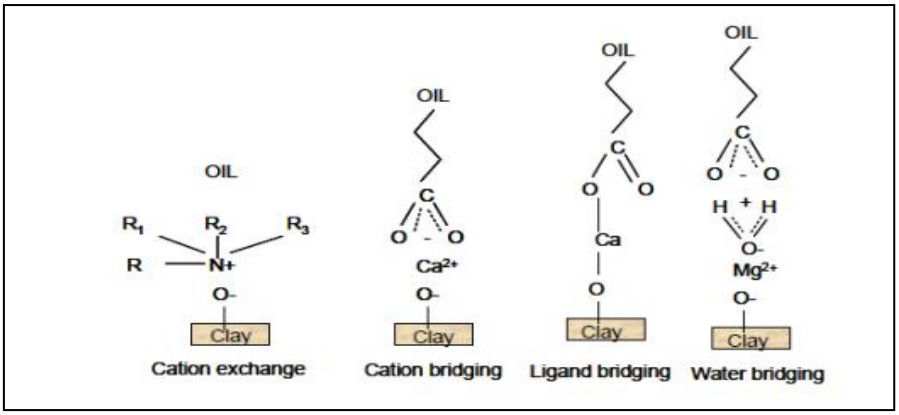


Figure 1.4: Clay/oil attraction by divalent cations (Lager et al. 2008).

The polar compounds in the oil are bonded to the negatively charged surface, and divalent cations like calcium and magnesium act as bridges between the negatively charged compounds in the oil and the negatively charged clay surface, illustrated in Figure 1.4. When low salinity brine is injected, the divalent ions exchange with either cationic organic compounds or with bases due to the change in ion exchange equilibrium. The consequence of this will be that the bonded oil will become mobile, wettability alters towards more water-wet and the oil recovery will increase (Lager et al. 2008; Sposito et al. 1999). Furthermore, Lager et al. (2006) suggest that injecting Low salinity water will change the charge density of the clay resulting in expansion of the electric double layer by the MIE mechanism and enabling desorption of the oil from the surface.

d. **Double layer effect:** Ligthelm et al. (2009) reported that the electrical double layer between the clay and the oil interfaces expands when the salinity decreases. The oil will detach from the surface and the wettability of the reservoir rock surface becomes more water-wet causing LSE. Similar to Figure 1.4, proposed by Lager et al. (2008), Ligthelm et al. (2009) suggests there is a Ca^{2+} bridge between the negatively charged clay and oil. The expansion of the electrical double layer due to low salinity associated with MIE enables desorption of polar compounds from the clay surface. This results in an increased oil recovery because the bonds holding oil in contact with the grain surface are broken (Lager et al. 2008).

e. **Salting-in Effect:** RezaeiDoust et al. (2011) suggested that the main mechanism for LSE was related to changes in the solubility of polar organic hydrocarbons and their salts with the brine ions in the aqueous phase, called a salting-in effect.

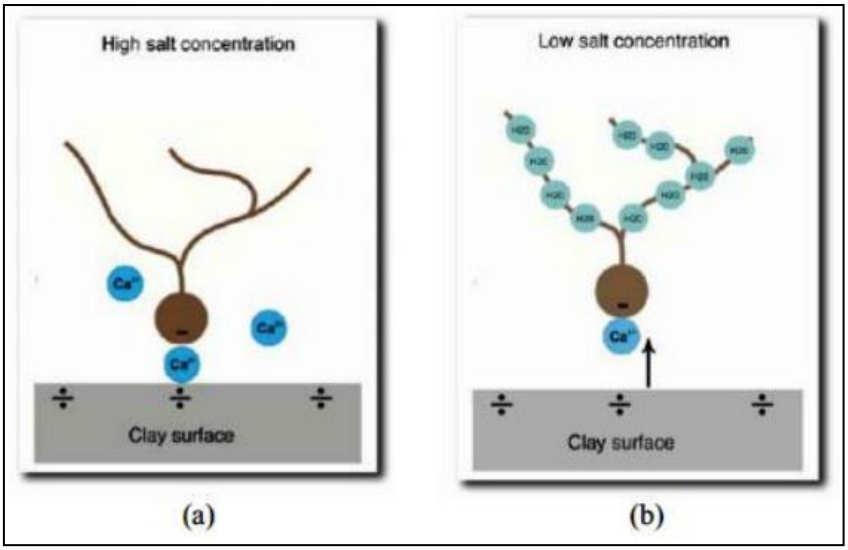


Figure 1.5: Illustration of (a) salting-out effect and (b) salting-in effect (Melberg, 2010).

Organic material in water is solvated because the hydrogen bonds between water molecules form water structures around the hydrophobic part of the material. In high saline water, inorganic ions like Ca^{2+}, Mg^{2+} and Na^{+} will break up these water structures and consequently decrease the solubility. Moreover, the organic material will move to and adsorb at the rock surface. Between the negatively charged clay surface and the organic material the cations create a bond, illustrated in Figure 1.5(a). This phenomena is called a salting-out effect, where the solubility of organic material in water drops by adding salt to the solution. Low salinity water will have the opposite effect. By eliminating salt from the water, the solubility of organic material in water increases, and salting-in effect is obtained. When the salinity is under the critical ionic strength, the bond between the ions and the mineral surface will weaken as a result of the decreased ionic strength in the water phase. Then, organic material will move from the surface and desorb, contributing to the LSE . This is illustrated in Figure 1.5(b).

f. **Local pH increase:** One of the newest proposed mechanisms of LSE is desorption of acids and bases by pH increase made by Austad et al. (2010). The mechanism is illustrated in Figure 1.6. A structural discrepancy in the silica or in the aluminum layer or at the edge surfaces, cause a negative charge on the clay surface. The clay minerals are consequently able to exchange cations between their layers and cations at the external surfaces. At basin conditions, acidic and basic organic material is adsorbed onto the clay together with inorganic ions, especially Ca^{2+}, and a chemical equilibrium is established. By injecting low salinity water this equilibrium is disturbed because of the difference in ion concentration between the injected water and the initial FW, leading to desorption of cations, especially Ca^{2+}. Protons, H^{+}, from the water close to the clay surface, adsorb onto the clay and replace the Ca^{2+}. A local

increase in pH close to the clay surface occurs, as illustrated by Equation 1.4 (Austad et al., 2010).

$$\text{Clay-}Ca^{2+} + H_2O \rightarrow \text{Clay-}\ H^+ + Ca^{2+} + OH^- \qquad (1.4)$$

Because of the local increase in pH adjacent to the clay surface, the adsorbed acidic and basic material reacts as in an ordinary acid-base proton transfer reaction, supporting desorption of organic material, and the rock becomes more water wet and increased oil recovery is observed. The acid base reaction takes place between the OH^- and the adsorbed acid and protonated base shown by Equation 1.5 and 1.6 (Austad et al., 2010).

$$\text{Clay-}NHR_3^+ + OH^- \rightarrow \text{Clay} + R_3N + H_2O \qquad (1.5)$$

$$\text{Clay-RCOOH} + OH^- \rightarrow \text{Clay} + RCOO^- + H_2O \qquad (1.6)$$

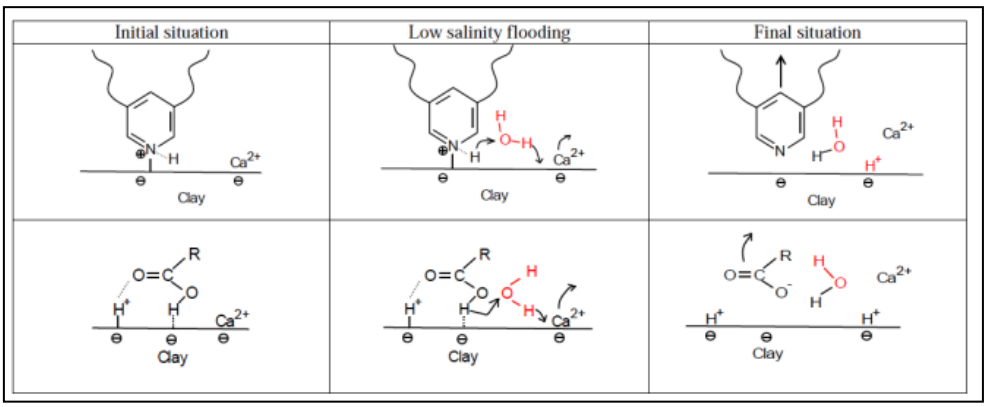


Figure 1.6: Illustration of the proposed mechanism for low salinity EOR effects (Austad et al., 2010). Upper: Desorption of basic material. Lower: Desorption of acidic material. Initial pH at reservoir conditions may be in the range of 5.

1.5 Smart Water: High Salinity and Carbonates reservoirs

The remarkable success of seawater injection in different chalk reservoirs (Austad et al. 2008) has been the motivation for a number of experimental studies to understand complex crude oil/water/rock chemical interactions for carbonate reservoirs. Improved oil recovery by smart variation of the sea water in chalk reservoirs was first reported by Austad et al. 2005. Since then, several laboratory experimental studies of varied water injection were carried out using different core plugs, crude oils, concentrations and aqueous phase compositions at various wettability and temperature conditions (Austad et al. 2008; Faithi et al. 2010; Faithi et al. 2011; RezaeiDoust et al. 2011 Shariatpanahi et al. 2010). Cationic surfactants of the type alkyl trimethyl ammonium, R-$N(CH_3)_3^+$, dissolved in seawater (SW) are able to increase water wetness in chalk, limestone, and dolomite (Strand et al. 2008; Standnes and Austad 2000). The mechanism for the wettability variation was suggested to be an interaction between the cationic surfactant monomers and adsorbed negatively charged carboxylic material, forming a cat-anionic complex, which is released from the

mineral surface (Standnes 2000). Through systematic experimental studies, it was verified that Ca^{2+}, Mg^{2+}, and SO_4^{2-} were the active ions in the wettability alteration process. The wettability alteration became more efficient as the temperature increased above 100°C. Each of the concentrations of Ca^{2+}, Mg^{2+}, SO_4^{2} and the temperature were varied separately to study the impact on oil recovery in a spontaneous imbibition process (Fernø et al. 2011; Hadia et al. 2011). In some spontaneous imbibition experiments no increment in oil recovery for enhanced SO_4^{2-} concentration was observed (Fernø et al. 2011).

1.5.1 Requirements

a. **Reactive Potential:** SW contains reactive ions, Ca^{2+}, Mg^{2+}, and SO_4^{2-} which have been shown to act as potential determining ions since they can change the surface charge of $CaCO_3$ (Pierre et al. 1990; Zhang et al. 2006). The impact on oil recovery for each of these ions in SW has been explored by Zhang and his group with Stevns Klint outcrop chalk (Zhang et al. 2006; Zhang et al. 2007). The concentration of SO_4^{2-} in the imbibing SW varied from 0 to 4 times the concentration in ordinary sea water (SW), the oil recovery improved from less than 10% to about 50% of OOIP. And they concluded that, there was a remarkable effect on oil recovery by just changing the concentration of one single ion. For increased calcium, the oil recovery increased from 28 to 60 % after 30 days of imbibition. Strand et al 2006 performed chromatographic studies which showed the adsorption of SO_4^{2-} onto the rock increased as the temperature increased and the co-adsorption of Ca^{2+} increased as the concentration of Ca^{2+} in the runoff decreased. They concluded that the increased adsorption of SO_4^{2-} onto the chalk surface reduces the positive charge, and causes increased affinity for Ca^{2+} due to less electrostatic interaction. Brines with equal proportions of $Ca^{2+}$and Mg^{2+} were tested by Zhang et. al (2007). It was concluded that the reactivity of Mg^{2+} ion towards carbonate surfaces increases dramatically as the temperature increases.

b. **Rock types:** Austad and co-workers performed numerous displacement experiments of oil by seawater from chalk rock samples (Austad et al. 2010; Zhang et al. 2006; Faithi et al. 2011). A large number of them were carried out with Stevns Klint outcrop chalk core plugs. A significant increase in oil recovery was observed with sulfate enriched Smart Water flooded core plugs as compared to cores flooded with brine without sulfate ions.

   Fjelde et al. 2011 conducted spontaneous imbibition experiments using SW and formation brine with core plugs from two fractured chalk fields at reservoir temperature. Only a small increase in oil recovery was observed with the seawater as compared to the formation brine (containing no SO_4^{2}) for reservoir core plugs as compared to Stevns Klint outcrop chalk core plugs.

Fernø et al. 2011 examined core plugs from three different quarries (Niobrara, Rørdal and Stevns Klint) and concluded that the effect of sulfate could be grossly dependent on the chalk type (i.e., rock mineral composition). Niobrara and Rørdal outcrop chalk core plugs, unlike Stevns Klint, showed no added improvement from sulfate on oil recovery during spontaneous imbibition.

Strand et al. 2003 experimentally explored the oil recovery possibility by SW flooding for limestone core plugs. Previous spontaneous imbibition studies on chalk have revealed that the oil recovery improved when the concentration of SO_4^{2-} increased (Austad et al. 2005; Zhang and Austad 2005). But no additional increase in oil recovery from the limestone core was detected, when the concentration of SO_4^{2-} was increased 3 times the concentration in seawater.

c. **Optimization of injected water** Standnes and Austad 2000 reported improved spontaneous imbibition of water into neutral to preferential oil-wet chalk with application of cationic surfactants. Later Strand et al. 2003 conducted a spontaneous imbibition study using cationic surfactants for chalk and dolomite cores, concentrating on the effect of brine salinity and composition. It was observed that spontaneous imbibition can be improved for some chalk core plugs by sulfate addition to the imbibed fluid. The sulfate concentration had a much lesser effect on dolomite as on chalk, suggesting that sulfate somewhat reacted with chalk. Among the divalent ions present in seawater, Mg^{2+} has a concentration twice that of SO_4^{2-} and four times higher than the Ca^{2+} concentration. Hence, Zhang et al. 2007 carried out spontaneous imbibition experiments to investigate the impact of Mg^{2+} ions on oil recovery. It was observed that Mg^{2+} without SO_4^{2-} resulted only in marginal extra oil recovery, but Mg^{2+}along with SO_4^{2-} resulted in a significant increase in oil recovery. Neither SO_4^{2-}nor Ca^{2+} alone was able to increase recovery under spontaneous imbibition. Lager et al. 2008 presented a comparative study of the oil recovery from a North Sea (Valhall) carbonate core sample with synthetic SO_4^{2-} free brine (formation water) and with seawater containing SO_4^{2-} under reservoir conditions. The imbibition tests were executed with a core saturated by olive oil. A clear enhancement in oil recovery was observed with SW in comparison to the formation water.

Fathi et al. 2011 carried out spontaneous imbibition study using Stevns Klint core plugs to optimize the concentration of the active ions, especially SO_4^{2-} and Ca^{2+} in seawater depleted of NaCl. The ultimate oil recovery increased by 5-18 % of OOIP when the concentration of SO_4^{2-} was increased to four times that in seawater. The concentration of Ca^{2+}did not have a significant effect on oil recovery at 100 °C, but showed some improvements at 120 °C.

d. **Temperature:** Temperature has been a constant point of consideration and analysis in most of the water based EOR studies in chalk reservoirs. Austad et. al 2010 conducted spontaneous imbibition experiments with Stevns Klint outcrop chalk core plugs at different temperatures (70, 90, 110 and 130 °C). The oil recovery increased with both the concentration of sulfate and the temperature. The typical oil recovery increased from 22 to 45%, when increasing the temperature from 90 to 130 °C.

   Strand and Austad 2000 studied enhanced oil recovery from Stevns Klint chalk core plugs using seawater, by both spontaneous imbibition and viscous flooding at 90, 110 and 120 °C. At the first temperature, no variation in oil recovery was observed in the spontaneous imbibition process with application of seawater and formation water (without any sulfate). However, in the forced flooding process, seawater increased oil recovery by 14% compared to formation water. At 110 and 120 °C, the impact of seawater became even more significant.

   Puntervold et al. 2009 performed both spontaneous imbibition and forced flooding experiments with chalk core plugs inserting various mixtures of seawater and produced water. At 50 and 70 °C, no discrimination in oil recovery was observed for different mixtures of seawater and produced water. At 90 °C, a small difference in the oil displacement potential for the different mixtures could be detected. The fluids containing sulfate ions seemed to give 5-10 % higher oil recovery compared to the produced water having no sulfate. Seawater appeared to be much more effective than produced water above 100 °C. Fathi et al. 2011 also observed great difference in oil recovery between different imbibing fluids (seawater, seawater depleted in NaCl, seawater depleted in NaCl spiked by sulfate) above 100°C.

1.5.2 Mechanisms

Although a huge body of experimental data exists on the effect of potential determining ions on oil recovery, there is still no overall consensus regarding the mechanisms behind the observed effect.Several experimental studies have been carried out on seawater flooding in chalk reservoirs by Austad and co-workers (Strand et al. 2008; Standnes and Austad 2000; Zhang et al. 2006; Zhang et al. 2006; Faithi et al. 2009; Strand et al. 2003; Puntervold et al 2009). Based on these experimental results, wettability alteration was proposed to be a key reason for the improvement of the oil recovery. A schematic model of the chemical mechanism for wettability alteration was suggested. Figure 1.7 shows this schematic model.

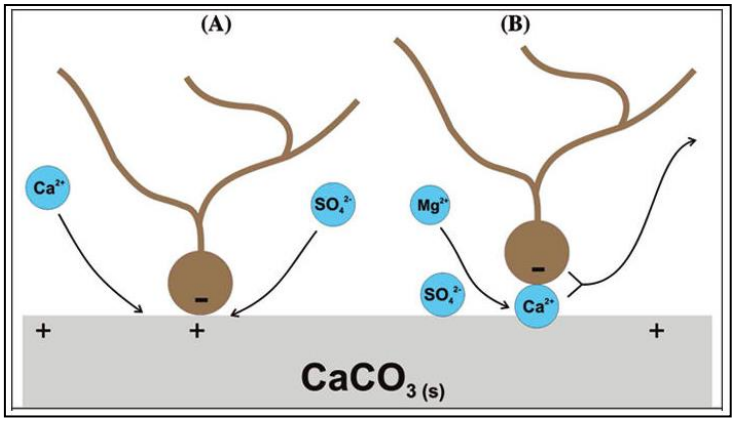


Figure 1.7: Schematic model of the wettability alteration induced by sea water. (A) Proposed mechanism when Ca^{2+} and SO_4^{2-} are active. (B) Proposed mechanism when Mg^{2+} and SO_4^{2-} are active (Zhang et al. 2007).

According to this idea, negatively charged carboxylic acidic components of crude oil are adsorbed on positively charged parts of the chalk surface. When seawater is injected into the reservoir, sulfate ions adsorb to the rock surface, which changes the surface charge, so that some of the adsorbed crude oil may be removed from the rock. Due to less electrostatic repulsion, calcium ions also approach the chalk surface and displace more crude oil by ion-binding. At high temperature (> 90-100 °C), magnesium is also involved vigorously in the wettability variation process. Experimental results have shown that magnesium substitutes calcium on the chalk surface when seawater is slowly flooded through an outcrop chalk core. Thus, magnesium may displace the calcium-carboxylate complex (Figure 1.7b).

Hiroth et al. 2010 examined how water chemistry affects surface charge and rock dissolution in a pure calcium carbonate rock. A chemical model is constructed that couples bulk aqueous and surface chemistry to predict the surface potential of calcite and adsorption of sulfate ions from the pore water. It was shown that temperature dependence of the surface charge does not follow the temperature dependence of oil recovery. They concluded that surface potential changes (caused by injection water chemistry) are not able to explain the observed changes in the oil recovery. Chalk dissolution appeared to be the controlling factor which can explain compaction and increase in oil recovery.

Fernø et al. 2011 fundamentally questioned the wettability alteration through a series of imbibition experiment with different core plugs. Spontaneous imbibition tests at 130°C with Niobrara outcrop chalk did not give added oil recovery with the presence of sulfate in the imbibing brine. The wettability of four Niobrara chalk cores aged to less water-wet conditions actually changed toward strongly water-wet conditions after spontaneous imbibition at 130°C, but no additional oil was produced. This wettability alteration happened regardless of sulfate presence in the imbibing brine. Aged Rørdal outcrop chalk also showed no added effect from sulfate on oil recovery during spontaneous imbibition at 130°C. But in this case, wettability alteration towards water

wetness was neither observed for sulphate containing brine nor for sulphate deficient brine during imbibition. Thus, the claimed wettability alteration effect from sulfate ions was not observed. Mineral depositions and compositional differences were claimed to be the deciding features responsible for the reported differences in the benefit of sulfate interacting with the calcite surfaces.

According to the above described schematic model of wettability modification, no potential determining ions (Ca^{2+}, Mg^{2+} and SO_4^{2-}) alone could increase the oil recovery. Karoussi et al. 2007 documented that water saturated with Mg^{2+}ions (without SO_4^{2-} and Ca^{2+} ions) could also enhance the oil recovery in spontaneous imbibition experiments with chalk core plugs. Madland et al. 2009 studied the effect of aqueous chemistry on the mechanical strength of chalk. Hydrostatic creep tests were carried out with continuous flooding of seawater, distilled water, NaCl and $MgCl_2$. It was concluded that only the presence of Mg^{2+} in the injected brine can deform the rock. Both these studies indicated that oil recovery increase could be caused by some other recovery mechanisms than wettability alteration.

1.5.3 Environment:

It has been reported that produced water contains some low molecular weight aromatic hydrocarbons. And so, it is suggested that the easiest way to avoid polluting the seawater is to re-inject the produced water into the reservoir. Puntervold et al. 2009 investigated the oil recovery potential using different mixtures of produced water and seawater by spontaneous imbibition. The oil recovery with different mixtures of produced water and seawater was significantly higher than under injection of the pure produced water. Fathi et al. 2011 observed that not only the concentrations of active ions (SO_4^{2-}, Ca^{2+} and Mg^{2+}) are important for improving the oil recovery, but the amount of NaCl could also have some impact on this process. Spontaneous imbibition experiments were carried out on Stevns Klint chalk core plugs with seawater and seawater depleted of NaCl. Both the imbibition rate and the oil recovery increased with seawater depleted of NaCl in comparison to seawater. A decrease in oil recovery was observed with the increase of the amount of NaCl in seawater.

1.6 Modeling low salinity water flood

Relatively few low salinity modeling works have been reported in the literature. The mechanisms put forward in the literature are still being debated and none of the mechanisms have been universally accepted until now. Nevertheless, it can be useful to present the modeling mechanisms put forward so far, at least for verification purposes. In this section a brief review of some modeling works is presented.

Jerauld et al. (2008), Tripathi & Mohanty (2008) and Yu-shu & Baojun (2009) modeled beneficial low salinity effects by directly linking the brine salinity to the flow conditions (relative permeability and/or capillary pressure). In the model presented by Jerauld et al. (2008), salt is modeled as a single component in the water phase. The salinity can then be tracked and made to determine the residual saturation by simple linear interpolation. Also Yu-shu & Baojun (2009) included the possible adsorption-desorption of salt but did not link the adsorbed salt to improved flow functions. Two major disadvantages of this model is that, the work did not include the adsorption of hydrocarbons and organic salts and it modeled salt as a single component in water phase, while there is various example of composition variation and its effect in the efficiency of oil recovery.

Eclipse 100 is commercial software that has a brine tracking function. Herein interpolation of the saturation and relative permeability end points for water and oil phases on the basis of salinity/salt concentration can be simulated. Also there is an option to adjust the water-oil capillary pressure as a function of salt concentration according to the description given by Jerauld et al. (2008). A major shortcoming of this type of modeling is that it only takes into account the total salt concentration and not the composition of the brine and as such cannot capture the role played by divalent ions (Kunnas,2012).

Fjelde et. al (2012) has made an attempt to take up extensive modeling incorporating adsorption/desorption of divalent cations and organic salts to explain LSE in EOR by MIE reaction. They conducted semi-empirical modeling and considered various experimental data, including ionic concentration, pH, relative permeability, capillary pressure etc. They concluded that inclusion of aqueous chemistry, mineral solubility, and crude oil divided into a functional group based analysis of oil/rock/brine system as a prior requirement for modeling the smart water flow, and suggested case by case study of each hydrocarbon group with the different brine/rock systems.

Zaretskiy et al (2012) developed a two phase single phase flow model in which he tried to incorporate fluid-solid interaction by externally linking to the chemical software package GEM-selector (Kulik et al 2003). According to the simulation, they claimed that brine ions are easily adsorbed unto the rock surface and the pore geometry had a more significant role in the flow role. These results did not take into account the variation of concentration of the different ions in the brine, which is proposed to be an important factor, Suijkerbuijk et al. (2012).

1.7 Conclusion

As seen from the previous reports in literature there are a number of different views on the mechanism(s) responsible for Smart Water EOR. Moreover, the influencing parameters on Smart Water EOR are numerous and quite

complicated. Despite these, most of the models presented in the literature are qualitative and the few simulators are quite simple and do not attempt to capture the complexities involved.

Cluster formation of brine-water (Kerisit and Parker 2004), water-hydrocarbon (Rigo et al. 2012) in fluid and their compact adsorption on calcite surface has been previously studied by software like Quantum Expresso (Giannozzi et al. 2009). Therefore, using DFT calculation in Quantum Expresso, the feasibility of ion substitution and adsorption can be studied.

Thomsen & Rasmussen developed a chemical software package, the Extended UNIQUAC model (Thomsen and Rasmussen 1999) which is being used in studying the thermodynamics of different EOR mechanisms and carbon capture and storage techniques (Darde et al. 2012; Riazi et al. 2009). It has been used to calculate solubilities of different salts with great accuracy. It can be used to calculate the brine properties at reservoir condition and thus identify suitable parameter which consistently correlates to oil recovery over various reports in literature.

Theory of Density Functional
Theory for adsorption/desorption from mineral surface

2.1 Introduction

Computational Materials Science (CMS) is a young discipline and is growingly finding its way and acceptance in various different fields, and is being considered as a bridge connecting theory and experiment. The computer experiments in material science allow theory to examine and to predict experiments (Hafner et al. 2000) and sometimes even to substitute them, when experiment is not practicable. CMS is an interdisciplinary subject, implying the synergy of quantum, classical and statistical mechanical physics, of chemistry and even biochemistry.

CMS investigates for several properties of materials, both existing and new, and their applications, with the use and analysis of numerical models on high performance computers. It provides qualitative and quantitative information for phenomena that may be too complex to be dealt with analytical methods, like:

a. The atomic structure of the material (Adam and Krasheninnikov 1996), like bond lengths and angles, crystal lattice parameters, surface reconstructions, structural phase transitions,
b. Its electronic and transport properties,
c. Elasticity and other mechanical properties (bulk modulus, elastic constants),
d. Reactivity of surfaces,
e. Chemical reactions (on a microscopic scale),
f. Catalytic behavior,
g. Magnetic properties and
h. Novel materials with predetermined properties.

One should acknowledge the computer performance that has been increased dramatically over the last few decades (Thijssen et al. 2007), making possible the investigation of bigger systems. However, the cases for which analytical solutions are possible are limited. Therefore, most calculations done in

computational physics involve some degree of approximation (Thijssen et al. 2007). The challenge of CMS is to find the method with the most appropriate approximations to solve the investigated system.

A computational model is an approximate, but well-defined mathematical procedure of simulation. Generally, there are five different stages in the development and use of such a model: a required accuracy must be selected, qualitatively; a model should be able to provide clear distinction between possible differences of the behavior of the system under investigation. The quantitative aim is the reproduction of the data and the prediction of the calculated quantities within experimental accuracy. For energies, an accuracy of at least 10meV/particle (1kJ/mol) would be appropriate. Formulation: the mathematical procedure must be precisely formulated and should be general and continuous as far as possible. Implementation: the method has to be implemented in a form which permits its application in reasonable time and cost. This stage involves the development of efficient and easy-to-be used computer programs. Verification: then one should compare the results of the model with experimental data, to determine whether the expected quantitative accuracy is reached. Prediction is the final step: an application of the model to problems to which the answer is unknown or in dispute (Pople 1999), should be possible for a reliable package.

Models which utilize only the fundamental constants of physics are generally termed "a b initio"; if some parameters have to be introduced, which are determined by fitting to some experimental data, the methods are "semi-empirical" (Pople 1999), like classical Monte Carlo, Brownian motion, Lattice Dynamics, and classical Molecular Dynamics. There is also a third category the hybrid methods, which use both empirical and a b-initio approaches, like a b-initio molecular dynamics (AIMD) simulations (Balbuena and Seminario 1999).

Apart from the a b-initio and semi-empirical methods, one can divide the methods, according to the time and length scale of the systems to be calculated, in: Atomistic Simulations, Meso-scale Methods and Continuum Methods.

2.2 A b-initio, first principle methods

2.2.1 Schrodinger equation

First principle calculation originate from the basic equation of quantum mechanics, the Schrodinger equation (Schrödinger 1926), which in the time independent form of any given system is

$$\widehat{H}\Psi(R_1, R_2..R_M; r_1, r_2, r_3, ..r_n) = E\Psi(R_1, R_2..R_M; r_1, r_2, r_3, ..r_n) \quad (2.1)$$

where $\hat{H}$ is the Hamiltonian of concerned the system, Ψ is the many-body Schrodinger wave function, which is a dependent on the position of the M nuclei $\{R_i\}$ and the N electrons $\{r_i\}$: $\Psi = \Psi(R_1, R_2, \ldots, R_M; r_1, r_2, \ldots, r_N)$, and E is the total energy of this system. If the system is isolated, in the non-relativistic approximation, the Hamiltonian is given by

$$\hat{H} = -\sum_{i=1}^{M} \frac{\hbar^2}{2M_i} \nabla^2 R_i - \sum_{i=1}^{N} \frac{\hbar^2}{2m} \nabla^2 r_i + \sum_{i=1}^{M} \sum_{j>i}^{M} \frac{Z_i Z_j e^2}{4\pi\epsilon_o |R_i - R_j|} - \sum_{i=1}^{N} \sum_{j=i}^{M} \frac{Z_j e^2}{4\pi\epsilon_o |r_i - R_j|} + \sum_{i=1}^{N} \sum_{j>i}^{N} \frac{e^2}{4\pi\epsilon_o |r_i - r_j|} \quad (2.2)$$

where the first and the second term are the kinetic energy operators of nuclei and electrons, each with mass M_i and m respectively. While the third to the fifth term in the equation deals with the potential developed by the Coulomb forces for charge Z_i and e of the nuclei and the electron respectively and ϵ_o is the dielectric constant of the vacuum, which can be changed according to the medium of concern. Fundamentally speaking only experimental contribution in the Schrodinger equation in a non-relativistic environment are four primary constants: the Plank's constant h, the charge of the electron e, the mass of the electron m, and the dielectric constant of the vacuum ϵ_o, which are the equal for every system, plus the mass of the nuclei.

2.2.2 Born-Oppenheimer approximation:

Solving the Schrodinger equation is practically impossible for any real system which contains two or more electrons or nuclei, and consequently smart and adequate approximation becomes a fundamental requirement. The first successful formulation that can be applied is the Born- Oppenheimer approximation (Born and Oppenheimer 1927). This formulation brings in light the significant difference between the mass of electron and the mass of any nuclei (the light possible nuclei is also 2000 times more heavily than the electron). Hence the electrons movement is on a much faster timescale. This in turn means that, without any noticeable loss of accuracy for most systems, one can isolate the electronic problem from that of the nuclei. So, we can solve the Schrodinger equation for the electrons only, with the nuclei positions are kept fixed. Therefore, we can rewrite equation 2.1 thus:

$$\hat{H}(r_1, r_2, r_3, \ldots r_n; \{R_i\}) \Psi(r_1, r_2, r_3, \ldots r_n; \{R_i\}) = E\{R_i\} \Psi(r_1, r_2, r_3, \ldots r_n; \{R_i\}) \quad (2.3)$$

Where, the Hamiltonian depends only parametrically from the positions of the nuclei $\{R_i\}$, and so do the wave function Ψ and the energy E.

The first simplification of this problem is done by Born and Oppenheimer (BO) (Born and Oppenheimer 1927), as mentioned at the introduction, in which the nuclear and electronic degrees of freedom are decoupled, since the nuclei are ~ 2000 times heavier than the electrons and can be considered to be stationary

compared to them, while electrons are moving within a fixed external potential due to the nuclei. With the BO approximation the full many-body Hamiltonian equation 2.2 becomes simpler to that of an electronic Hamiltonian:

$$\hat{H} = -\frac{1}{2}\sum_{i=1}^{N}\nabla^2 r_i - \sum_{i=1}^{N}\sum_{j=i}^{M}\frac{Z_j}{|r_i - R_j|} + \sum_{i=1}^{N}\sum_{j>i}^{N}\frac{1}{|r_i - r_j|} \qquad (2.4)$$

But, solving the Schrodinger equation with the above Hamiltonian equation 2.3 is still too complex for most cases, since the many-electron wave function contains 3N variables. Therefore, for solids calculations are performed for a small part of a crystal, the computational cell. To take periodicity into account periodic boundary conditions are imposed on super-cell, molecules and adsorption complexes. This is the way to transform the task of calculation of a system of large number of electrons into a task of calculation of much smaller super-cell.

But, once equation 2.3 is solved, the energy $E\{R_i\}$ can be interpreted as a potential energy for the motion of nuclei. When the quantum nature of the nuclei becomes negligible, and with essentially no loss of accuracy one can treat their motion as they were classical particles. As shown in the flow diagram bellow , this allows to perform MD simulations, in which the Newton equations of motion for the nuclei are solved using the quantum mechanical forces evaluated from the derivative of $E\{R_i\}$ with respect to the positions $\{R_i\}$.

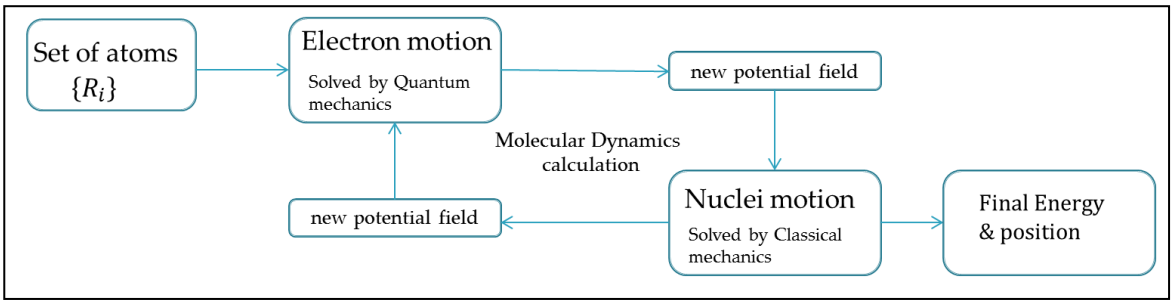


Figure 2.1: Explaining the flow dynamics of Molecular dynamics calculation by treating Nuclei in classical motion and Electron in quantum motion.

2.2.3 Density Functional Theory (DFT)

In 1964 Hohenberg and Kohn undertook the many-body problem using a completely new approach. Here the main ideas of DFT are briefly developed. Hohenberg and Kohn showed that the external potential V_{ex}, on the electrons can be uniquely obtained (to a trivial additive constant) by the electron ground-state density $n(r) = \langle\Psi|\hat{n}(r)|\Psi\rangle = \int dr_1, dr_2, \ldots dr_1, |\Psi(r, r_2, \ldots r_N)|^2$, where Ψ is the ground-state wave-function of the system and $\hat{n}$ *(r)* is the density operator. Here we have omitted the dependence of Ψ from the positions of the nuclei for simplicity. Since *n(r)* determines the number of electrons N, and since V_{ex} and N fix the Hamiltonian of the system, it turns out that the electron density completely determines all the electronic ground-state properties of the

system, and in fact, as shown later (Kohn and Sham 1965) also the finite temperature properties.

In the work by Hohenberg and Kohn 1964, one important property of the system is the energy, which can be written as:

$$E[n] = F_{HK}[n] + \int V_{ext}(r)n(r)dr \quad (2.5)$$

With

$$F_{HK}[n] = \langle \Psi[n] | \hat{T} + \hat{V}_{ee} | \Psi[n] \rangle \quad (2.6)$$

and $\hat{T}$ are $\hat{V}_{ee}$ respectively the kinetic energy and the electron-electron interaction operators, and $\Psi[n]$ is the ground-state wave function of the system. It is important to note that $F_{HK}[n]$ is independent of the external potential and therefore it is a universal functional. This is the crucial result of DFT. By the use of vibrational principle, it was also demonstrated that the ground state density of the system is the one that minimizes $E[n]$, and the minimum of $E[n]$ is equal to the ground-state energy E_o. The significance of these two results is clear; the only quantity that is needed is the electron density, no matter how many electrons are present in the system.

A year after the paper, (Ceperley and Alder 1985) invented an indirect method to solve the problem. The idea is to write the energy functional as an easy part plus a difficult part:

$$F[n] = T_o[n] + E_H[n] + E_{XC}[n] \quad (2.7)$$

where $T_o[n]$ is the ground-state kinetic energy of an auxiliary non-interacting system with density is the same as the one of the real system, $E_H[n]$ is the repulsive electrostatic energy of the classical charge distribution $n(r)$, and $E_{XC}[n]$ is the XC energy defined through Equation 2.7.

Minimizing the total energy $E[n]$ under the constraints of orthonormality for the one-particle orbitals of the auxiliary system $\int \Psi_i^*(r)\Psi_j(r)dr = \delta_{ij}$, one finds a set of one-particle Schrodinger-like equations:

$$\left[-\frac{\hbar^2}{2m}\nabla^2 + V_{KS}(r)\right]\psi_i(r) = \epsilon_i\psi_i(r) \quad (2.8)$$

where the KS potential is given by

$$V_{KS}(r) = V_{ext}(r) + \int \frac{n(r)}{|r-r'|}dr' + V_{XC}(r) \quad (2.9)$$
$$V_{XC}(r) = \frac{\delta E_{XC}[n]}{\delta n(r)} \;\&\; n(r) = \sum_i f(\epsilon_i - \epsilon_F)|\psi_i(r)|^2$$

With $f(x)$ the Fermi-Dirac distribution and the ϵ_F Fermi energy fixed by the condition:

$$\int n(r)dr = N \quad (2.10)$$

These are the famous KS equations; they must be solved self-consistently because V_{KS} is a functional of the orbitals itself. The generalization to finite temperature is obtained by replacing E with the electronic free energy $U = E - TS$, where S is the electronic entropy, given by the independent-electron formula $S = -k_B T \sum_i [f_i ln f_i + (1 - f_i)\ln(1 - f_i)]$, with f_i; the thermal (Fermi-Dirac) occupation number of orbital i.

It is important to note that calculating the single-particle eigen-values ϵ_i with the energy of quasi-particles, and therefore their distribution with the electronic density of states of the system would be conceptually incorrect, as the KS eigenvalues are only an artificial mathematical tool to arrive at the ground-state density of the system. Nevertheless, it has been shown that the DFT density of states mostly resembles very accurately the real density of states of systems, and they are therefore can be used to analyze their electronic structure and thereby calculating the material properties. But, the exact XC functional $E_{XC}[n]$ are not known, so one should not expect the DFT density of states to be an exact representation of the real density of states of the system.

Once the self-consistency is attained, the electronic free energy of the system is

$$U = \sum_{i=1}^{N} f(\epsilon_i - \epsilon_F)\epsilon_i - \frac{1}{2}\int \frac{n(r)n(r')}{|r-r'|} dr + E_{XC}[n] - \int V_{XC}(r)n(r)dr + E^{ion} - TS \qquad (2.11)$$

where E^{ion} is the ionic electrostatic repulsion term. This would be the exact electronic free energy of the system if we knew $E_{XC}[n]$ (which also depends on temperature, though very little is known about this dependence). Unfortunately, the exact form of the XC (free) energy is not (yet) known.

2.4.4 XC functionals

An approximate expression for the XC functional, called the LDA was provided. In the LDA, the dependence of functional on the density has the form

$$E_{XC}^{LDA}[n] = \int n(r)\epsilon_{XC}\big(n(r)\big)dr \qquad (2.12)$$

and $E_{xc}(n)$ is taken to be the XC energy per particle of a uniform electron gas whose density is $n(r)$. This has been very accurately calculated using Monte Carlo simulations (Perdew and Zunger 1981) and parameterized in order to be given in an analytic form (Wang and Perdew 1991).

By construction, this approximation yields exact results if the density of the system is uniform, and should not be very accurate for those systems whose density is highly inhomogeneous, as for example atoms and molecules. However, it turns out to work better than expected for a wide range of materials. In molecules, for example, the LDA usually overestimates the binding energies, but it yields in general good results for equilibrium distances

and vibrational frequencies. It was the evidence of the very high quality of the LDA that has been the main factor responsible for the tremendous success of DFT.

Nowadays, a number of sophisticated functionals have become available, like the so-called generalized gradient approximation (GGA) (Tao et al. 2003), or the thereafter developed meta GGA (Staroverov et al. 2004; Hamann et al. 1979), but it is not obvious which one to prefer in general, with the good old LDA itself being competitive in accuracy in a variety of cases. It is also worth mentioning that, when used in combination with plane-waves methods, XC hybrid functionals usually require a computational effort that is several orders of magnitudes higher than what is required by local XC functionals like the LDA or the GGAs.

Whatever functional is used, these type of calculations all go under the classification of a b initio, in the sense that no experimental input is allowed, apart from the four fundamental constants mentioned above. Of course, it would be desirable to have a unique functional with the highest possible accuracy for any system, but this stage has not been reached yet (at the time of writing).

2.2.5 PPs and basis sets

In practical cases, it is often necessary to introduce one additional approximation in order to speed up the calculations, known as the PP approximation. In essence, this is a way to freeze the electrons of the core of the atoms, and remove them from the calculations. The justification for doing this is that the core electrons are so tightly bound to the nuclei that they are essentially undisturbed by the chemical bonding, or, conversely, the chemistry of materials is unaffected by the behavior of the core electrons. This implies a saving in complexity and computer time which is proportional to the number of electrons that have been frozen, but, as discussed shortly, the saving becomes enormous in the most widely diffused computer codes which are based on plane-wave expansions of the single-particle KS orbitals.

In order to solve the KS equations, it is necessary to expand the auxiliary KS orbitals in terms of some known basis functions. A variety of possible choices are available. Traditional quantum chemistry codes often use Gaussians, which are quite well-suited for much localized orbitals, and in the course of the years a large amount of expertise has accumulated to create high-quality basis sets for a wide range of materials. The drawback of Gaussians is that the quality of the basis set depends on the choice of the user, and transferability can be an issue when different systems are compared. An alternative set of functions which are totally unbiased and systematically improvable is plane waves. They also have the additional advantage of adapting naturally to calculations in which periodically boundary conditions are employed, which is a very useful

setup even in systems that have no periodicity, in order to reduce finite size effects. Plane-wave calculations are relatively simple, and the evaluation of forces and the stress tensor are not much more difficult than the evaluation of the total energy. A drawback of plane waves is that a large number of them may be needed for describing rapidly varying functions, like the very localized core orbitals, or the valence wave functions in the core region, which need to oscillate widely in order to be orthogonal to the core orbitals. For this reason, plane-wave calculations are almost always associated with the use of PPs.

The first aim of PPs is to eliminate the core electrons from the explicit calculations because they do not participate in the chemical properties of matter, at least until their binding energy is much higher than the energy involved in the chemical properties one wants to study. So one freezes them around the nuclei and redefines the system as it was formed by ions plus valence electrons. We are left now with the problem of dealing with the oscillations in the core region of the valence wave functions, due to the orthogonalization to the core wave functions. The solution to this is the introduction of a PP, which substitutes the ionic Coulomb potential in such a way that the valence pseudo-eigenvalues are the same as the all-electron (AE) ones on some reference configuration in the atom. The pseudo-wave functions coincide with the AE ones from a fixed core radius one, and are as smooth as possible below the core radius, with the only constraint to be normalized (norm-conserving (NC) PPs). To satisfy these requirements the PP usually must be angular momentum dependent, that is, pseudo-wave functions corresponding to different angular momenta are eigen functions of different potentials. However, the long-range behavior of these different potentials must resemble the true one, because above the core radius the pseudo-wave functions are identical to the AE ones. This means that the difference must be confined in the core region and then the PP can be written in the following form (Kerker1980; Bachelet et al. 1982; Voigt 1892).

$$V_a(r,r') = V_a^{loc}(r)\delta(r-r') + \sum V_{a,l}(r)P_l(\hat{r},\hat{r}')\delta(r-r') \qquad (2.13)$$

$$P_l(\hat{r},\hat{r}') = \sum_{m=-l}^{l} Y_{l,m}(\theta,\phi)Y_{l,m}^{*}(\theta,\phi)$$

where $V_a^{loc}(r)$is the local long-range (spherical) part and approaches the AE potential above a cutoff radius r', and $V_{a,l}(t^{+})$ is the short-range angular-momentum-dependent part, the index a indentifies the atom, and Pl is the projector onto the angular momentum I, with $Y_{l,m}$ being the spherical harmonics. The quality of the PP depends on its transferability properties, that is, the capability to reproduce the AE results over a wide range of electronic configurations, and of course for the atom in different environments.

To simulate materials under pressure is not much more difficult than to perform calculations at zero pressure; all that needs to be done is to change the volume of the simulation cell appropriately. In doing so, one possible problem can be the shortening of the nearest-neighbors distance among the atoms, which if drops below the sum of the core radii of the PPs employed (or PAW potentials), may affect the quality of the results. Therefore, some care is necessary in designing the potentials appropriate for the conditions where they need to be used. However, apart from this possible shortcoming, it is often the case that simulations at high pressure are even more accurate than those at low pressure. The reason is that as the pressure increases the charge density becomes more homogeneous, which helps the XC functionals in their work.

By contrast, high-temperature simulations are much more demanding than zero-temperature ones. The reason is that at high temperature it is the free energy that plays the essential role, and an accurate calculation of this requires expensive sampling of the phase space. For solids at not too high temperature, it is often accurate enough to use the quasi-harmonic approximation, in which the potential energy of the crystal is expanded to second order in the displacement of the atoms from their equilibrium positions. This quasi-harmonic potential usually provides a very accurate description of the dynamical properties of the system at low temperature, and gives easy access to the free energy of the system, which can be calculated analytically as a function of temperature. The prefix quasi- is there to indicate that this quasi-harmonic potential depends on the volume of the system. In practice, the quality of the thermodynamics obtained within the quasi-harmonic approximation is often preserved also to temperatures not far from the melting temperature, although at such high temperatures a full account of an harmonic effects becomes necessary, at least to assess the validity of the quasi-harmonic approximation. For highly an harmonic solid and for liquids, one has to resort to MD or Monte Carlo techniques to sample the phase space. MD simulations are particularly attractive because they also provide dynamical information like diffusion, or autocorrelation properties which can be used together with the fluctuation-dissipation theorem to evaluate a number of physical properties of the system, as seen below. The next section presents the zero-temperature properties of materials, and the following section discusses finite temperature.

2.3.1 Elastic constants

Most of what we know about the interior of our planet comes from seismology, and therefore from the elastic behavior of the minerals inside the Earth. The theory of elasticity of crystals has been established in 1660 by R. Hooke and the fundamentals have remained the same. Briefly, if a crystal is subjected to an

infinitesimal stress $d\sigma_{ij}$, with i and j running through the three Cartesian directions in space, then it will deform according to the strain matrix $d\epsilon_{ij}$

$$d\sigma_{ij} = \sum_{k.l} c_{ijkl}\, d\epsilon_{ij} \qquad (2.14)$$

The constant of proportionality between stress and strain, c_{ijkl}, is a fourth-rank tensor of elastic constants. With no loss of generality we can assume $d\sigma_{ij}$ and $d\epsilon_{ij}$, to be symmetric ($d\sigma_{ij} \neq d\sigma_{ji}$ would imply a nonzero torque on the crystal, which would simply impose an angular acceleration and not a deformation), and therefore the elastic constant tensor is also sym- metric. It is therefore possible to rewrite the second-rank tensors $d\sigma_{ij}$, and $d\epsilon_{ij}$ as six components (vectors), in the Voigt notation (Stixrude and Cohen 1995), with the index pairs 11, 22, 33, 23, 31, and 12 represented by the six symbols 1, 2, 3, 4, 5, and 6, respectively. In this notation, the stress-strain relation appears as

$$d\sigma_i = \sum_j c_{ij}\, d\epsilon_j \qquad (2.15)$$

with *i* and going from 1 to 6. Elastic constants are given as the coefficients C, in this notation. The matrix c_{ij} is symmetric, so that the maximum number of independent elastic constants of a crystal is 21. Because of crystal symmetries, the number of independent constants is usually much smaller. For example, in cubic crystals, there are only three elastic constants, in h.c.p Fe there are five, and in orthorhombic $MgSiO_3$ perovskite there are nine, while for calcite it would be six.

Equation provides the route to the calculation of the elastic properties of materials, and it can be applied both at zero and high temperatures. At zero temperature, the components of stress tensor can be calculated as (minus) the partial derivative of the internal energy with respect to the components of the strain:

$$\sigma_{ij} = -\partial E/\partial \epsilon_{ij}\big|_{\epsilon} \qquad (2.16)$$

Examples of zero-temperature calculations of elastic constants include the DFT calculations of (Oganov and Ono 2004) on the h.c.p crystal structure of iron at Earth's inner core conditions, which suggested a possible mechanism based on the partial alignment of h.c.p crystallites to explain the seismic anisotropy of the Earth's inner core. Several recent studies in the GGA and LDA calculations of the elastic constant of the recently discovered calcite, post-perovskite & kaolinite phase by three groups (Oganov et al. 2003; Tsuchiya et al. 2004; Prenkel and Smit 1996), which showed that this phase is elastically very anisotropic, and that with a proper alignment it is possible to explain the observed seismic anisotropy of the D'' region.

2.3.2 Finite Temperature

The extension to finite temperature properties of materials could simply be obtained by substituting the internal energy E with the Helmholtz free energy F. The ij component of the stress tensor σ_{ij} is (minus) the partial derivative of F with respect to strain ϵ_{ij}taken at constant T, and holding constant all the other components of the strain tensor:

$$\sigma_{ij} = -\partial A/\partial \epsilon_{ij}\big|_{\epsilon,T} \tag{2.17}$$

Similarly, the pressure p is obtained as (minus) the partial derivative of F with respect to volume, taken at constant temperature:

$$p = -\partial A/\partial V|_T \tag{2.18}$$

If the system of interest is at sufficiently high temperature the nuclei can be treated as classical particles, and the expression of the Helmholtz free energy A for a system of N identical particles enclosed in a volume V, and in thermal equilibrium at temperature T is (Alder and Wainwright 1959):

$$A = -k_B T ln\left\{\frac{1}{N!\Lambda^{3N}}\int dR\, e^{-\beta U(R,T)}\right\} \tag{2.19}$$

where $\Delta = h/(2pMk_BT)^{½}$ is the thermal wave length, with M the mass of the particles, h the Planck's constant, β= l/k_BT, k_B is the Boltzmann constant, and $U(R_l,\ldots R_N; T)$ the potential energy function, which depends on the positions of the N particles in the system, and possibly on temperature, in which case U is the electronic free energy. The multidimensional integral extends over the total volume of the system V.

2.3.3 Molecular dynamics

If the system is isolated, thermal averages (represented in the equations above as (19)) can be calculated as time averages along an MD simulation (Gibson et l. 1960; Verlet 1960). The main idea here is to move the ions according to the Newton's equations of motion. This is achieved in practice by discretizing the equation of motion $m\partial v_i/\partial t = F_i$ (m_i is the mass of atom i, v_i is its velocity, and F_i is the force acting on it). This is done by dividing into steps Δt, and approximate the solution of the equation of motion, for example, as proposed by (Allen and O'shea 1987; Andersen 1980; Bose et al. 1984; Alder and Wainwright 1959)

$$r_i(t+\Delta t) = r_i(t) + v_i(t)\Delta t + \frac{1}{2m_i}F_i(t)\Delta t^2 \tag{2.20}$$

$$v_i(t+\Delta t) = v_i(t) + \frac{1}{2m_i}(F_i(t) + F_i(t+\Delta t))\Delta t \tag{2.21}$$

If the time step is small enough (usually less than 1/ 20 of a typical vibrational period), the Verlet algorithm conserves well the total energy of the system,

both on short and long timescales. If the volume of the simulation cell V and the number of atoms N are kept constant, this so-called (N, V, E) simulation generates configurations in phase space that are distributed according to the microcanonical ensemble.

It is a standard result of statistical mechanics that thermal averages evaluated either in the micro- or in the canonical ensemble are equivalent if the system is sufficiently large, but it is useful to be able to perform simulations in ensembles other than the microcanonical one. For example, in order to obtain thermal averages in the canonical ensemble (i.e. , constant N, V, and T), like the pressure in Equation 2.19, one can couple the system with an external heat (Bose et al. 1984; Hoover 1985; Parrinello and Rahman 1980). When combined with the Parrinello- Rahman constant-stress technique (Wentzcovitch et al. 1993), this also allows simulations to be performed at constant T and σ_{ab} (de Wijs et al. 1998).

2.3.4 Diffusion and Viscosity

Using MD simulations, it is also possible to study the properties of liquids, For example, in a liquid, the atoms are free to diffuse throughout the whole volume, and this behavior can be characterized by diffusion coefficients D_α, where a runs over different species in the system. These D_α,, are straightforwardly related to the mean square displacement of the atoms through the Einstein relation (Andersen 1980):

$$\frac{1}{N_\alpha}\langle\sum_{i=1}^{N_\alpha}|r_{\alpha i}(t_o+t)-r_{\alpha i}(t_o)|^2\rangle \rightarrow 6D_\alpha, as\ t\rightarrow\infty \qquad (2.22)$$

where $r_{\alpha i}$ (t) is the vector position at time t of the ith atom of species α, N_α, is the number of atoms of species a in the cell, and <> means time average over t_o. The diffusion coefficient can also be used to obtain a rough estimate of the viscosity η of the liquid, by using the relation between the two stated by the Stokes-Einstein relation:

$$D_\eta = \frac{k_B T}{2\pi a} \qquad (2.23)$$

This technique was used (Alfe and Gillan 1998a) to estimate the viscosity of liquid iron at Earth's core conditions. The Stokes-Einstein relation Equation 2.23 is exact for the Brownian motion of a macroscopic particle of diameter a in a liquid of viscosity η. The relation is only approximate when applied to atoms; however, if α is chosen to be the nearest-neighbors distance of the atoms in the solid, Equation 2.23 provide results that agree within 40% for a wide range of liquid metals. To calculate the viscosity rigorously, it is possible to use the Green-Kubo relation.

$$\eta = \frac{V}{k_B T}\int_0^\infty dt\langle\sigma_{xy}(t)\sigma_{xy}(0)\rangle \qquad (2.24)$$

where σ_{xy} is the off-diagonal component of the stress tensor $\sigma_{\alpha\beta}$ (α and β are Cartesian components). This relation was used in the context of first-principles calculations for the first time by Alfe and Gillan 1998b, who first calculated the viscosity of liquid aluminum at ambient pressure and a temperature of 1000 K, showing that the method provided results in good agreement with the experiments, and then applied the method to the calculation of the viscosity of a liquid mixture of iron and sulfur under Earth core conditions (Alfe and Gillan 1998b).

2.4 Thermodynamic Properties

The phase stability of a system is determined by the minimum of its Gibbs free energy $G = A + pV$ .Since $p = -\partial F/\partial V|_T$, also knowledge of F as function of V and Tallows the computation of G. More generally, equilibrium in a multispecies system is determined by the chemical potentials μ_i, with i running over the different species, which represents the constant of proportionality between the energy of the system and the amount of the specie i (Adamson and Gast 1967)

$$\mu_i = \left(\frac{\partial E}{\partial N_i}\right)_{S,V} \tag{2.25}$$

where S is the entropy, and Ni is the number of particles of the species i. Alternative equivalent definitions of the chemical potential are (Adamson and Gast 1967):

$$\mu_i = \left(\frac{\partial F}{\partial N_i}\right)_{T,V} = \left(\frac{\partial G}{\partial N_i}\right)_{T,p} = -T\left(\frac{\partial S}{\partial N_i}\right)_{E,V} \tag{2.26}$$

Equilibrium between two phases is determined by the condition of equality of the chemical potential of each individual species in the two phases.

2.4.1 Solutions

As mentioned in the above, the behavior of solutions can be understood in terms of the chemical potential μ_i, defined in Equations 2.25 and 2.26. Consider now a solutions with N_A particles of solvent A and N_x particles of solute X, with $N = N_A + N_X$. In the high-temperature limit, the Helmholtz free energy of this system is (Alder and Wainwright 1959)

$$A = -k_B T ln \frac{1}{\Lambda_A^{3N_A}\Lambda_B^{3N_B} N_A! N_X!} \int dR_1 \dots dR_N e^{-U(R_1 \dots R_N;T)/k_B T} \tag{2.27}$$

And thereafter we can calculate the chemical potential as

$$\mu_X = \left(\frac{\partial F}{\partial N_X}\right)_{T,V} = F(N_A, N_X + 1) - F(N_A, N_X) \tag{2.28}$$

2.4.2 First-principle calculations of chemical potentials

To calculateμ_X, it is useful to consider the difference in chemical potential between the solute and the solvent $\mu_{XA} = \mu_X - \mu_A$, which is equal to the change of Helmholtz free energy of the system as one atom of solvent is transmuted into an atom of solute at constant volume V and constant temperature p. This transmutation does not obviously correspond to real physical process, but provides a perfectly rigorous way of calculating the difference of chemical potentials:

$$\mu_{XA} = k_B T ln \frac{c_X}{1-c_X} + 3k_B T ln\left(\frac{\Lambda_X}{\Lambda_A}\right) + m(C_X) \qquad (2.29)$$

Where Λ_X and Λ_A are thermal wavelength of solute and solvent, and

$$m(C_X) = -k_B T ln \frac{\int dR e^{-\beta U(N_A-1,N_X+1;R)}}{\int dR e^{-\beta U(N_A,N_X;R)}} \qquad (2.30)$$

With $U(N_A,N_X;R)$ the potential energy of the system with N_A atom of solvent and N_x atom of solute, atom $U(N_A-1,N_X+1;R)$the one for the system in which one of the atoms of solvent has been transmuted into solute.

The thermodynamic integration can now be used to compute $m(c_X)$ in the liquid state. This is done by defining an intermediate potential $U_\lambda = \lambda U(N_A-1,N_X+1;R) + (1-\lambda)U(N_A,N_X;R)$, so that $m(c_X)$ can be expressed as :

$$m(c_X) = \int_0^1 d\lambda \langle U(N_A - 1, N_X + 1) - U(N_A, N_X)\rangle_\lambda \qquad (2.31)$$

In practice, the calculation of $m(c_X)$ is done by performing two separate simulation, one with N_A atom of solvent and N_x of solute and the other with N_A-1 atoms of solvent and N_x+1 atoms of solute . At the end of each step, forces are computed in both system and their linear combination $f_\lambda = \lambda f(N_A - 1, N_X + 1) f(N_A, N_X)$ is used to evolve the system in time in order to compute the thermal average$\langle U(N_A - 1, N_X + 1) - U(N_A, N_X)\rangle_\lambda$. This is repeated at a number of different values of λ and the integral is performed numerically.

To improve statistics, it is useful to transmute many atoms of solvent into solute. In this case one does not obtain directly μ_{XA} at a chosen concentration but an integral of this range of concentration. However, by repeating the calculation transmuting a different number of atoms at a time, it is possible to extract information about value of μ_{XA} in the whole range of concentration, as described in Alfe et. al (2002).

2.4.3 Solid-liquid equilibrium:

Thermodynamic equilibrium is reached when the Gibbs free energy of the system is minimum and therefore $0=dG=d\ (G^l+G^s+G^{ad})$ where l, s and ad indicate liquid, solid and adsorb particles respectively. In a multi component

system, the Gibbs free energy can be expressed in terms of the chemical potential of the species in the system (McGlynn 1996 , Adamson and Gast 1967)

$$G = \sum_i \mu_i N_i \qquad (2.32)$$

Using equation 2.32 and the Gibbs-Duhem equation we obtain:

$$dG = \sum_i \mu_i dN_i \qquad (2.33)$$

If the system is isolated, particles can only flow between the solid and the liquid and we have $dN^s_i = \sum_i dN_i(\mu_i^l - \mu_i^s)$ which implies:

$$dG = \sum_i dN_i(\mu_i^l - \mu_i^s) \qquad (2.34)$$

If $\mu_i^l < \mu_i^s$ there will be a flow of particles from the solid to the liquid region ($dN_i > 0$)and the visa vasa, so that the Gibbs Energy of the system in lowered. In case of formation of adsorbed cluster we form a 3 volume case and the system is in equilibrium when the minimum Gibbs energy is attained. These obtained chemical potential can be thereafter optimized to obtain the least energy state. The obtained theoretical results for chemical potential can also be correlated with available experimental results and model. In case of successful correlation these results can further be incorporated in the data bank.

2.5 Application in smart water EOR:

From the DFT calculation feasibility of individual ion adsorption on calcite and its associated adsorption energy can be studied for varied pressure temperature conditions (Kerisit and Parker 2004). Furthermore possible complex formation on the calcite surface due to its interaction with the polar fraction of oil can be thereafter explored (Bennetzen et al. 2014). Proposed multiple ion exchange based wettability alteration mechanism (Austad et al. 2009) can be therefore examined from these first principle calculation and the feasibility of Ca^{2+}/Mg^{2+} substitution on the calcite surface can be thereby explored (Bennetzen et al. 2014). Effect of polar acids in this ion substitution is an integral part of the proposed wettability alteration mechanism (Austad et al. 2009); therefore the adsorption energy of the possible complexes that can form on the mineral surface can be further studied.

CHAPTER 3

Modeling electrolyte solutions with the extended universal quasichemical (UNIQUAC) model

The Extended UNIQUAC mode (or the extended universal quasichemical) model is a thermodynamic model for solutions containing both electrolytes and non-electrolytes. The model is a Gibbs excess function which constitutes of a Debye–Hückel term and a standard UNIQUAC term. The model just requires parallel particle particular association parameters. The model can accurately predict and reproduce experimental data for solid–liquid, vapor–liquid, and vapour–liquid equilibria in addition to solutions properties like Osmotic coefficient, Enthalpy, Specific heat etc. for any brine combination by utilizing one arrangement of parameters. These calculations can be accurately made both at room temperatures and at high pressure (100bars) and high temperature (300 °C) using the Extended UNIQUAC model.

3.1 Introduction

Most thermodynamic models for electrolyte solutions consist of two interaction term; long-range, electrostatic interactions derived from the Debye–Hückel theory (Debye and Hückel 1923) and a short-range interactions term. The interaction of charged particles in an ideal solution is explained by the Debye and Hückel theory. For non-ideal systems therefore this Debye–Hückel needs to be combined with a term for short-range interactions. For such short range interactions virial expansion of terms in molality is used by the Pitzer model (Pitzer 1991). In electrolyte nonrandom two-liquid (NRTL) model (Chen et al. 1982; Chen and Evans 1986; Chen and Song 2004) the NRTL local composition model is used to include the short range interactions. In the Extended UNIQUAC model (Thomsen et al. 1996; Thomsen and Rasmussen 1999) along with the Debye–Hückel term; UNIQUAC local composition model is included for studying short-range interactions. The model parameters are ion-specific, and both ion and nonionic species have the same parameters. Instead of Debye–Hückel theory; using the mean spherical approximation (MSA) theory an substitute term for long-range electrostatic interactions has been also derived (Waisman and Lebowitz 1970; Harvey et al. 1988). This term has mostly been applied in combination with short-range interactions that are

derived from cubic equations of state (Wu and Prausnitz 1998; Myers et al. 2002).

3.2 Extended UNIQUAC model

Initially UNIQUAC model was presented and developed by Sander et al. 1986. Thereafter the Nocolaisen et al. altered the model by supplanting the altered UNIQUAC term utilized by Sander et al. with a standard UNIQUAC term. These model parameters presented by Nicolaisen et al. 1993, has been thereafter used in the Extended UNIQUAC model as reported in previous studies (Thomsen et al. 1996; Thomsen and Rasmussen 1999). But in Extended UNIQUAC Model an improved method for determining the model parameters has been developed (Thomsen et al. 1996). Thus there is no longer any upper limit to the number of ions or other solutes that can be simultaneously accommodated by the model.

3.2.1 Concentration units and standard states

Mole fraction scale is used as the concentration unit in Extended UNIQUAC model. Mole fractions are here defined on the basis of the speciation in the solution. It is assumed that water is the only solvent where ions can be dissolved. Other species including Ions, non-electrolytes including alcohols, and dissolved gasses are taken solutes. The chemical potential of water is calculated from:

$$\mu_w = \mu_w^0 + RTln(x_w\gamma_w) \tag{3.1}$$

In equation 3.1 μ_w^0 is the standard-state chemical potential of water. It is equal to the chemical potential of pure water at the system temperature and pressure. The system temperature T is in Kelvin. R is the gas constant, γ_w is the activity coefficient of water, and x_w is the mole fraction of water, following the symmetric convention, the activity coefficient for water activity coefficient is equal to one for the pure component. The synthetic capability of solute *i* is given by equation 3.2:

$$\mu_i = \mu_i^0 + RTln(x_i\gamma_i^*) \tag{3.2}$$

In equation 3.2, $\mu_i^0$is the standard-state chemical potential corresponding to the unsymmetric convention, with activity coefficient being equal to one at infinite dilution in water. γ_i^* is the unsymmetric activity coefficient for solute *i*. Symmetric action coefficient at given concentration when divided by that at infinite dilution gives the unsymmetric activity coefficient for the solute *i*, as shown in equation 3.3:

$$\gamma_i^* = \gamma_i / \gamma_i^\infty \tag{3.3}$$

Mostly experimental measurements of activity coefficients are normally reported in literature in molality scale. Therefore conversion between molal activity coefficient and unsymmetric mole fraction activity coefficient is important, to be able to compare calculated and experimental activity coefficients. The molal activity coefficient is derived from the unsymmetric mole fraction activity coefficient by multiplication with the water mole fraction:

$$\gamma_i^m = \gamma_i^* x_w \tag{3.4}$$

3.2.2 Model equations:

For the long range interactions the Debye–Hückel contribution term is required to Extended UNIQUAC model. The superscript D–H is used to mark the Debye–Hückel contribution to the excess Gibbs energy term , which is given by the following expression:

$$\frac{G^{E,D-H}}{RT} = -x_w M_w 4A\left[ln\left(1 + bI^{½}\right) - bI^{½} + 0.5b^2 I\right]/b^3 \tag{3.5}$$

Equation 3.5 has been derived by simplifying the original expression by Debye and Hückel (Equation 3.1). Herein, Mw is the molar mass of water (kg mol^{-1}), b = 1.5 (kg $mol^{-1})^{1/2}$ is a constant. G^E is the molar excess Gibbs energy. A is the temperature and pressure-dependent Debye–Hückel parameter. The following equation gives the temperature dependence of A, at saturation pressure of water. Equation 3.6 can be applied up to temperatures of 500 K and T_o equation 3.6 is equal to 273.15 K.

$$A = [1.131 + 1.335 * 10^{-3} * (T - T_0) + 1.164 * 10^{-5} * (T - T_o)^2]\ (kg\ mol^{-1})^{½} \tag{3.6}$$

Temperature dependence of the relative permittivity of water is accounted in the Debye–Hückel equation by the parameter A. Solutes, such as ions or alcohols; also have a strong influence on the relative permittivity of solutions. But, the relative permittivity in the Extended UNIQUAC model considered independent of composition. The ionic strength of the solution I is calculated as a function of concentrations and ionic charges z_i given by equation 3.7:

$$I = 0.5 \sum_i \frac{x_i z_i^2}{x_w M_w}\ (mol\ kg^{-1}) \tag{3.7}$$

By proper differentiation of equation 3.5, the electrostatic contributions to the activity coefficients are obtained. For ions and water the, contribution terms are:

$$ln\gamma_i^{D-H} = -z_i^2 AI^{½}/\left(1 + bI^{½}\right) \tag{3.8}$$

$$ln\gamma_i^{D-H} = M_w 2A\left[1 + bI^{½} - \left(1 + bI^{½}\right)^{-1} - 2ln\left(1 + bI^{½}\right)\right]/b^3 \tag{3.9}$$

respectively. Combinatorial part and a residual part the two UNIQUAC contributions to the excess Gibbs energy function. Superscript C is used for the combinatorial part and is given as:

$$\frac{G^{E,C}}{(RT)} = \sum_i x_i ln\left(\frac{\phi_i}{x_i}\right) - 5.0 \sum_i q_i x_i ln\left(\frac{\phi_i}{\theta_i}\right) \quad (3.10)$$

In equation 3.10, ϕ_i is the volume fraction, θ_i is the surface area fraction and x_i is the mole fraction component *i*. Fir species *i* the volume and surface area fractions are calculated as:

$$\phi_i = {x_i r_i}/{\sum_j x_j r_j} \quad \theta_i = {x_i q_i}/{\sum_j x_j q_j} \quad (3.11)$$

In the Extended UNIQUAC model there are two adjustable parameters for each species including the volume parameter r_i and the surface area parameter q_i(Thomsen et al. 1996). No direct correlation between the two model parameters and density of the solution has been reported in literature. The combinatorial contribution to the activity coefficient of species *i* is obtained from:

$$ln\gamma_i^C = ln\left({\phi_i}/{x_i}\right) + 1 - {\phi_i}/{x_i} - 5.0 q_j \left[ln\left(\frac{\phi_i}{\theta_i}\right) + 1 - \frac{\phi_i}{\theta_i}\right] \quad (3.12)$$

Superscript R is used for the residual part of the excess Gibbs capacity. This term is calculated using equation 3.13:

$$\frac{G^{E,R}}{(RT)} = \sum_i x_i q_i ln\left(\sum_j \theta_i \Psi_{ij}\right) \quad (3.13)$$

Where $\Psi_{ij}$is defined as:

$$\Psi_{ij} = exp\left[-u_{ij} - u_{ii}\right]/T \quad (3.14)$$

Herein the two interaction energy terms, u_{ij} and u_{ii} are independent of composition, but are temperature- dependent given as:

$$u_{ij} = u_{ij}^0 + u_{ij}^t (T - 298.15) \quad (3.15)$$

The two parameters u_{ij}^0 & u_{ij}^t in equation 3.15 are Extended UNIQUAC model adjustable parameters that is specific to each pair. It can be determined by optimizing experimental data. By separation of equation 3.13, the residual contribution to the activity coefficients is obtained:

$$ln\gamma_i^R = q_i \left[1 - ln\left(\sum_l \theta_l \Psi_{ij}\right) - \sum_j \left(\frac{\theta_j \Psi_{ij}}{\sum_l \theta_l \Psi_{lj}}\right)\right] \quad (3.16)$$

The combinatorial and the residue parts of the activity coefficients obtained from equations 3.12 and 3.16 are symmetric activity coefficients. While, the electrostatic part of the solute activity coefficient, equation 3.8, is an unsymmetric mole fraction activity coefficient. Therefore both the combinatorial and the residual parts of the activity coefficients should be converted to unsymmetric activity coefficients, to calculate the unsymmetric

mole fraction activity coefficient for a solute. This is obtained by dividing with the corresponding infinite dilution activity coefficients. An expression for the latter can be derived by setting the water mole fraction equal to 1 in equations 3.12 and 3.16. Thus the solute activity coefficient is given as:

$$ln\gamma_i^* = ln\left(\frac{\gamma_i^C}{\gamma_i^{C,\infty}}\right) + ln\left(\frac{\gamma_i^R}{\gamma_i^{R,\infty}}\right) + ln\left(\gamma_i^{D-H}\right) \quad (3.17)$$

The expression for the dissolvable (water) activity coefficient is basically:

$$ln\gamma_w = ln\gamma_i^C + ln\gamma_i^R + ln\gamma_i^{D-H} \quad (3.18)$$

Excess enthalpy and excess heat capacity and other thermal properties can be obtained by the model by calculating the temperature derivatives of equations 3.17 and 3.18. The combinatorial part of the activity coefficient is independent of temperature (as observable in equation 3.12). Moreover the residual part of the activity coefficient is proportional to the surface area parameter q_i (as shown in equation 3.16). Therefore, the residual part of the excess enthalpy is, also proportional to the surface area parameter. Thus experimental data of excess enthalpy can be used for determining the value of the surface area parameters.

Aqueous solutions of gases like CO_2, NH_3, and SO_2 in the temperature range up to 110 °C can have vapor pressures that exceed ideal gas behavior. In the extended UNIQUAC model, gas-phase fugacities are calculated with the Soave–Redlich–Kwong cubic equation of state to take such non-ideality into account. Gas-stage fugacities are computed for water and volatile solutes such as alcohols and gases, not for ions.

3.3 Model parameters

The parameters needed in order to perform calculations with the extended UNIQUAC model are the Debye–Hückel A parameter (equation 3.9); the Debye–Hückel b parameter (which is a constant value 1.5 $(kg\ mol^{-1})^{1/2}$). The necessary parameters are derived from the critical properties of the volatile solutes, for calculation of gas-phase fugacities with the Soave–Redlich–Kwong cubic equation of state.

Therefore the main parameters in the model that needs to be adjusted are:

- UNIQUAC volume and surface area parameters r_i and q_i for each species, and
- UNIQUAC interaction energy parameters u_{ij}^0 and u_{ij}^t for each pair of interacting species.

The UNIQUAC volume and surface area parameters assigned to water by the authors of the UNIQUAC model (Abrams and Prausnitz 1975) are retained in the Extended UNIQUAC model. Every single other parameter has been optimized

from the basis of experimental CERE data bank for electrolyte solutions (Thomsen 2004). Hence the total unknown parameters that needs to be optimized for performing Extended UNIQUAC calculations is comparable to the number of parameters used in the electrolyte NRTL model, but is much lower than the number of parameters required for the Pitzer model. Electrolyte solutions fundamentally contain more than one kind of ion, thus only relative properties of ions can be determined. It is applicable both for experimental data (Wilson et al. 2002) as well as for thermodynamic models. In Extended UNIQUAC model (Thomsen et al. 1996; Thomsen and Rasmussen 1999; Thomsen 2005) the parameter values were moored by arbitrarily settling the values to that of hydrogen ion.

3.3.1 Electrolyte databank

An extensive databank for aqueous electrolyte solutions has been compiled in the CERE research group at the Department of Chemical Engineering, Technical University of Denmark. The databank presently contains more than 100000 experimental data points concerning liquid–liquid equilibrium, vapor–liquid equilibrium, activity coefficients, degree of dissociation, gas solubility, enthalpy of mixing, heat capacity, salt solubility, density, and gas hydrate formation, all in binary, ternary, and quaternary solutions. The databank can be accessed on-line.

Data from this databank has been previously used optimize the Extended UNIQUAC model parameters. In order to minimize the difference between calculated and experimental data, herein nonlinear, least-squares minimization is performed. The difference between calculated and experimental data has been calculated in several different ways, depending on the type of data and the system in question (Iliuta et al. 2000; Iliuta et al. 2002; Christensen, and Thomsen 2003; Thomsen and Rasmussen 1999; Thomsen et al. 2004). All data of the same type (e.g., osmotic coefficients, salt solubility, and density) are weighted identically. These optimized parameters and thermodynamic properties needed for performing calculations with the extended UNIQUAC model have been published, and various experimental data has been reproduced by the model (Thomsen et al. 1996; Thomsen and Rasmussen 1999; Thomsen 2005; Pereda et al. 2000; Iliuta et al. 2000; Iliuta et al. 2002; Christensen, and Thomsen 2003; Thomsen et al. 2004).

3.3.2 Equilibrium Calculations

Moreover along with Phase equilibrium calculations, speciation equilibrium calculations have also been performed using Extended UNIQUAC model. In simple speciation study only auto protolysis of water had to be considered. While in more complex cases, a number of speciation equilibria have been considered. The speciation equilibria can be formulated as a mathematical

equation in terms of activity coefficients, concentrations, and standard chemical potentials (similar the solid–liquid equilibria and vapor–liquid equilibria formulation). The condition for equilibrium between two phases is that the chemical potential is identical in the two phases. The chemical potentials of water and solutes are given by equations 3.1 and 3.2.

3.4 Standard-state properties

For evaluating the chemical potentials of water and solutes (as given in equations 3.1 and 3.2), the standard state chemical potentials is required. "The NBS Tables of Chemical Thermodynamic Properties" (Wagman et al. 1982) provides the standard-state chemical potentials of solutes at 298.15 K. These standard-state properties are reported with reference to the. And in the Extended UNIQUAC model the calculations are conducted with unsymmetric mole fraction scale, so molality standard state needs to be converted according to the following equation:

$$\mu_i^m = \mu_i^* + RTln(M_w\gamma_w) \tag{3.19}$$

Superscript m is used for molality standard state. Using the Gibbs–Helmholtz equation the standard-state chemical potentials at temperatures different from 298.15 K are evaluated:

$$d(\mu_i^*/RT)/_{dT} = -\Delta_f H_i/(RT^2) \tag{3.20}$$

The standard-state heat capacity of ionic solutes was found to be described well by the three-para- meter correlation (Thomsen et al. 1996):

$$C_{p,i}^* = a_i + b_iT + c_i/(T - 200) \tag{3.21}$$

This standard-state heat capacity is used for evaluating the temperature dependence of the standard-state enthalpy of formation $\Delta f\ Hi$ in equation 3.20, and for calculating the heat capacity of electrolyte solutions. It is necessary to know the standard thermodynamic properties of the various solid phases, in solid–liquid equilibrium calculations,. Such properties for many salts are listed in the NBS tables (Wagman et al. 1982). Such properties have been fitted to experimental solid–liquid equilibrium data for salts not found in these tables.

3.4.1 Solid-liquid equilibrium

For solid–liquid equilibrium between crystalline glauber salt [$Na_2SO_4.10H_2O$ (c)] and an aqueous solution containing sodium sulfate the flowing equation must be satisfied: The equilibrium condition for this can be expressed as:

$$\mu^0_{Na_2SO_4\bullet 10H_2O} = 2\mu_{Na^+} + \mu_{SO_4^{2-}} + 10\mu_{H_2O} \tag{3.22}$$

Herein it is required that the chemical potential of 2 mol sodium ions plus the chemical potential of 1 mol sulfate ions and 10 mol water is identical to the chemical potential of 1 mol crystalline glauber salt. Chemical potential of a pure, crystalline phase is represented with Superscript 0 on the chemical potential of glauber. By using equations 3.1 and 3.2, equation 3.22 can be further written as:

$$ln\left[\left(x_{Na^+}\gamma^*_{Na^+}\right)^2 x_{SO_4^{2-}}\gamma^*_{SO_4^{2-}}(x_w\gamma_w)^{10}\right] = \left(\mu^0_{Na_2SO_4\bullet 10H_2O} - 2\mu^*_{Na^+} - \mu^*_{SO_4^{2-}} - 10\mu^0_w\right) \quad (3.23)$$

Using the tabulated values (Wagman et al. 1982) of the standard- state chemical potentials, the right-hand side of equation 3.23 can be calculated. By iteration, the concentration on the left-hand side of equation 3.23 can then be adjusted until the activity product yields the desired value.

3.4.2 Vapor-liquid equilibrium

Vapor–liquid equilibrium calculations can also be conducted in a similar way. The chemical potentials of these volatile components must be equal in the in the gas phase and in the liquid phase for the solution to attain equilibrium. Example: For equilibrium to exist between sulfur dioxide in the gas phase and in an aqueous phase, it is required that the chemical potential of sulfur dioxide in the two phases is equal:

$$\mu_{SO_2}(g) = \mu_{SO_2}(aq) \quad (3.24)$$

The chemical potential of SO_2 in the gas phase includes; an ideal gas chemical potential (superscript ig) and a term that varies with fugacity. Similarly, the chemical potential of SO_2 in the aqueous phase can be expressed in terms of the standard-state chemical potential of solutes and the activity coefficient (as explained in equation 3. 2). Overall equation 3.24 can be re written as:

$$\mu^{ig}_{SO_2} + RTln\left(\gamma_{SO_2}\hat{\varphi}_{SO_2}P\right) = \mu^*_{SO_2} + RTln\left(x_{SO_2}\gamma^*_{SO_2}\right) \quad (3.25)$$

This is the so-called gamma-phi approach to vapor–liquid equilibrium calculation. y_{SO_2} is the corresponding mole fraction and $\hat{\varphi}_{SO_2}$ is the fugacity coefficient of SO_2 in the vapor phase.

3.4.2 Liquid-liquid equilibrium

For liquid–liquid equilibrium to occur, the chemical potential of each independent component must equal in the two liquid phases. In this connection, an independent component is a neutral species. Example: NaCl has to be considered an independent component, for liquid–liquid equilibrium in a system consisting of NaCl, water, and iso-propanol. One equation can be written for the equilibrium of each of the three independent components

between liquid phase I and liquid phase II. By using equation 3.2, the equation for NaCl can be expressed as:

$$\mu^*_{Na^+} + \mu^*_{Cl^-} + RTln\left(x^I_{Na^+}\gamma^{*,I}_{Na^+}x^I_{Cl^-}\gamma^{*,I}_{Cl^-}\right) = \mu^*_{Na^+} + \mu^*_{Cl^-} + RTln\left(x^{II}_{Na^+}\gamma^{*,II}_{Na^+}x^{II}_{Cl^-}\gamma^{*,II}_{Cl^-}\right) \quad (3.26)$$

Herein, the standard chemical potentials cancel each other, and the condition for equilibrium between the two phases for NaCl gets simplified to:

$$x^I_{Na^+}\gamma^{*,I}_{Na^+}x^I_{Cl^-}\gamma^{*,I}_{Cl^-} = x^{II}_{Na^+}\gamma^{*,II}_{Na^+}x^{II}_{Cl^-}\gamma^{*,II}_{Cl^-} \quad (3.27)$$

For the other two components also a similar equilibrium equation can be written.

3.5 Results

Based on this Extended UNIQUAC model several parameters have been optimized. And experimental data for various different conditions have been reproduced. As shown in Figure 3.1; the solubility of $Mn(NO_3)_2$ as a function of temperature from −16 to 90°C is shown. Experimental data from varied sources are plotted along with the calculated curve. The solubility line consists of five parts, one for ice, and one for each of the four salt hydrates including manganous nitrate: the hexahydrate, the tetrahydrate, the dihydrate, and the monohydrate.

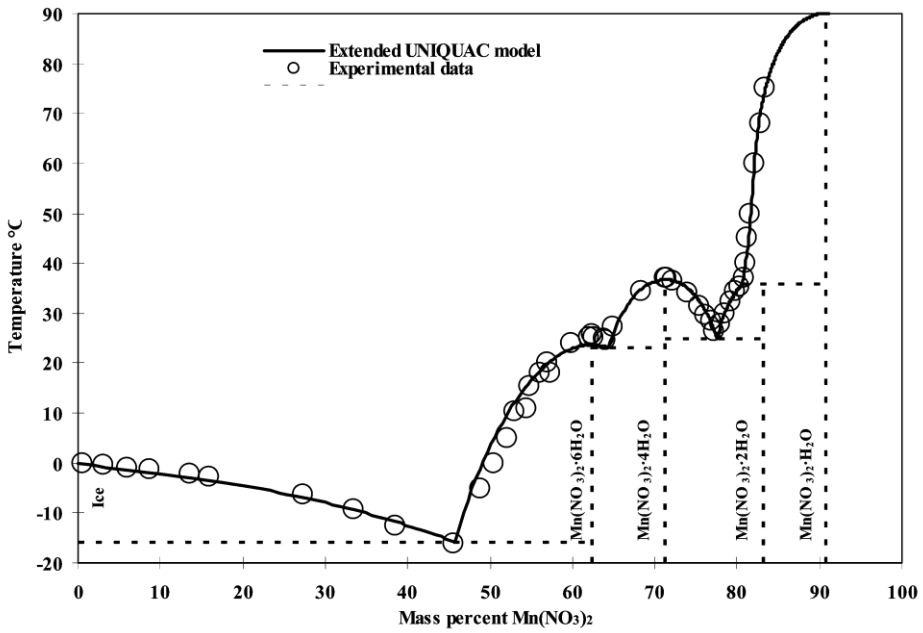


Figure 3.1: The solubility of manganese nitrate as a function of temperature calculated with the Extended UNIQUAC model and plotted along with experimental data (Thomsen 2005).

The very particular shape of this solubility diagram is reproduced quite accurately by the model and consistent correlation between the calculated

values and experimental data is observed. Above 75°C, Decomposition of manganous nitrate starts at 75 °C (Ewing and Rasmussen 1942), therefore there are no experimental data.

In another study as shown in Figure 3.2, eight different solid phases can precipitate from this ternary system has been reproduced consistently using Extended UNIQUAC model. The various salt formations have been modelled over a temperature range from -40 to 110°C. One of these, $NaKCO_3.6H_2O$, has been considered to be a solid solution rather than a pure, crystalline salt (Hill and Miller 1927).

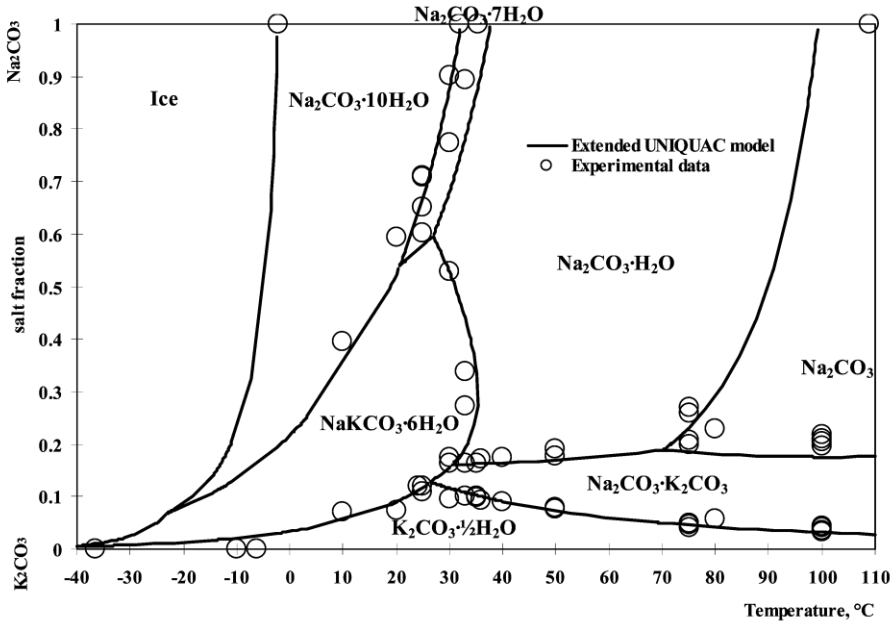


Figure 3.2: Temperature-composition diagram for saturated solutions in the Na2CO3–K2CO3–H2O system at temperatures from −40 to 110 °C. Consistent correlation is observed between Extended UNIQUAC model and experimental data for multi species system (Thomsen 2005).

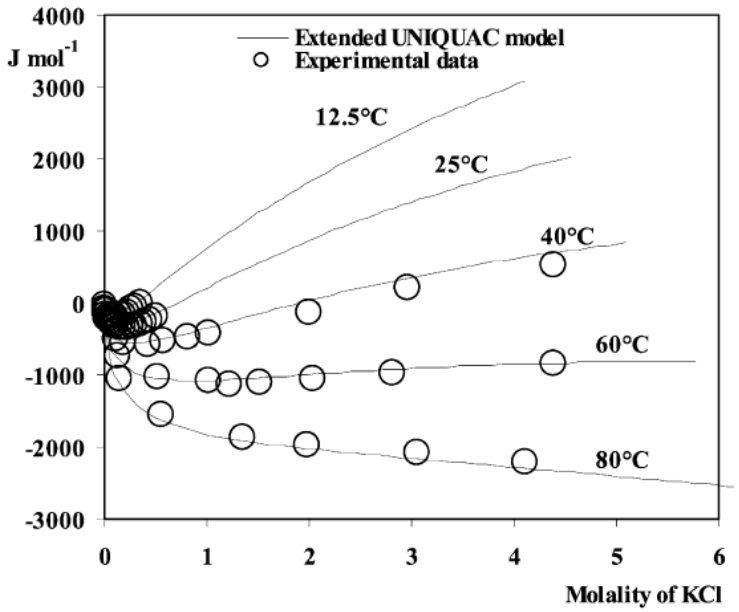


Figure 3.3: The heat of dilution to infinite dilution for KCl calculated at 5 different temperatures and plotted along with experimental data (Thomsen 2005).

Thermal property data, such as heat of dilution data, are also included in the data used to determine the parameters in the model (Thomsen 2005). An improved temperature dependence of the activity coefficients is obtained by including such thermal properties in the parameter estimation. Moreover the model itself is upgraded as it obtains the capability to calculate and reproduce the thermal properties. Example: as shown in Figure 3.3, heat of dilution where calculated to infinite dilution data are compared with experimental data of the same type at five different temperatures. It is observable that for varied temperatures head of dilution can be accurately predicted by the model.

Furthermore because of modeling of gas solubility (as shown in Figure 3.4); modeling system like of the aqueous NH_3–CO_2 which requires formation of carbamate has also been taken into consideration:

$$NH_3(aq) + HCO_3^- \rightarrow NH_2COO^- + H_2O(l)$$

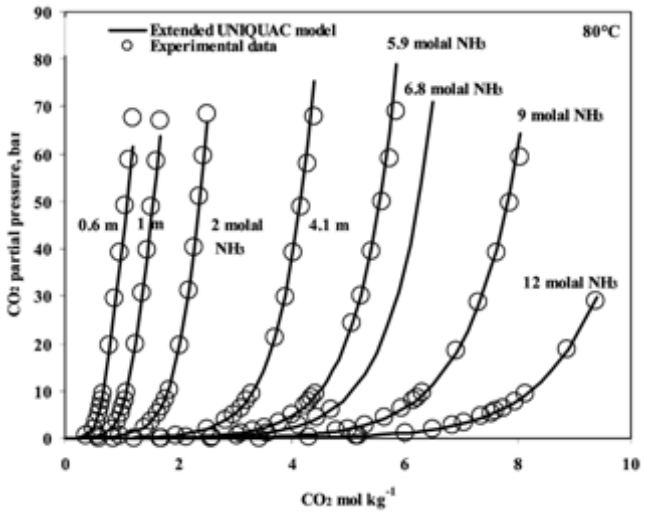


Figure 3.4: The incomplete weight of carbon dioxide over watery arrangements of carbon dioxide and smelling salts. Model estimations are demonstrated together with test information.

A significant amount of ammonia and carbon dioxide will be converted to carbamate, especially in a small pH range around pH = 9–11. The amounts of gases that are converted to carbamate do not contribute to the vapor pressure of the solution.

Salt solubilizes between multiple brines in a two liquid system (containing both water-alcohol) can be successfully calculated using Extended UNIQUAC model. Solubility for sodium sulphate/potassium sulphate in methanol-water solutions has been accurately calculated by the model for varied temperatures (Iliuta et al. 2000).

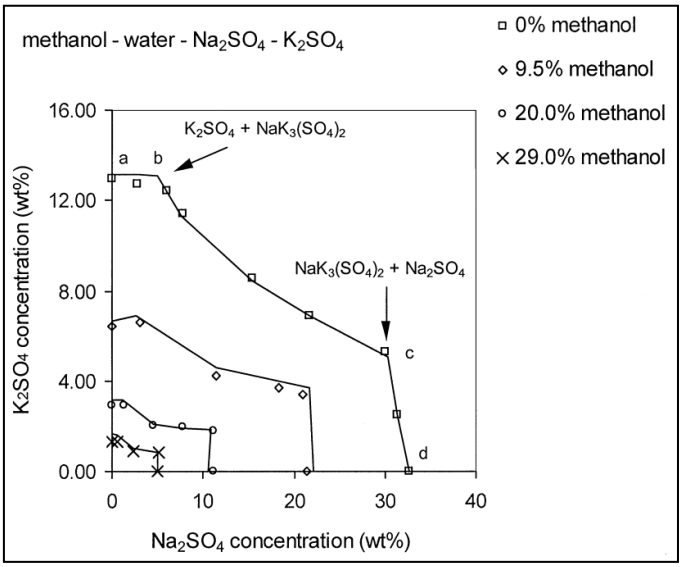


Figure 3.5: Solubility diagram for sodium sulphate/potassium sulphate in methanol-water solutions at 313.15 K. Herein calculated equilibrium using Extended UNIQUAC model show consistent correlation to experimental data (Iliuta et al. 2000)

3.6 Application in Smart Water Enhanced Oil Recovery (EOR)

Smart water based EOR involves variation in concentration of the various ions including: Na^+, Ba^{2+}, K^+, Cl^-, SO_4^{2-}, Ca^{2+}, Mg^{2+}, CO_3^{2-}, HCO_3^-, $CO_2(aq)$, H^+ and OH^-. Availability of soluble ions of SO_4^{2-}, Ca^{2+} and Mg^{2+} salts in reservoir condition has been recommended in literature (Austad et al. 2009). Furthermore precipitation of any salts must also be avoided according to wettability alteration mechanism (Austad et al. 2009). Smart Water EOR has also been considered along with WAG-CO_2 injection. Therefore modelling of solubility/dissolution for both modified sea water electrolyte solution with and without dissolved CO_2 is important. Both parameters (volume and surface area parameters r_i and q_i for each species, and interaction energy parameters u_{ij}^0 and u_{ij}^t for each pair of interacting species) have been optimized for the these ions (Garcia et al. 2005; Garcia et al. 2006). As shown in Figure 3.6, experimental data has been consistently reproduced by the Extended UNIQUAC model for various salts. Solubility experimental data up to 1000 bars and 300°C have been previously reproduced by the optimized model parameters (Garcia et al. 2006). Reservoir conditions being considered for smart water flooding are up to 150°C and 400 bars (Zahid et al. 2010; Austad et al 2009). Therefore the model is suitable to calculate salt solubilizes for given variation in brine composition is reservoir conditions.

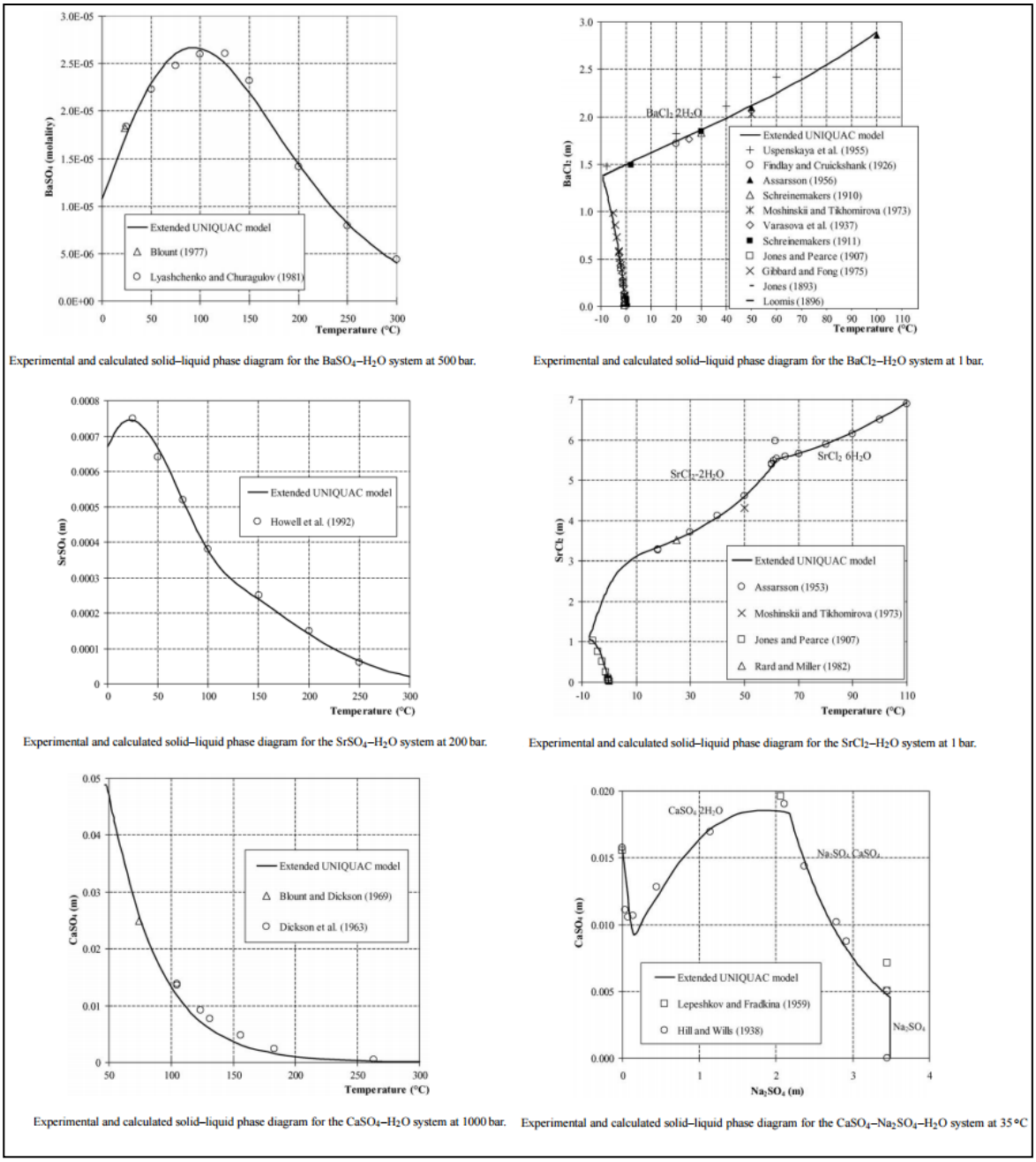


Figure 3.6: Salt solubility calculated from extended UNIQUAC model at high pressure high temperature conditions for various cations (Gracia et al. 2006).

3.7 Conclusion

The Extended UNIQUAC model is a very simple thermodynamic model for electrolytes. Yet it is able to describe solid–liquid, liquid–liquid, and vapor–liquid equilibria using one set of parameters. In addition, thermal properties such as the heat of dilution and the heat capacities of electrolyte solutions are calculated quite accurately by the model. The model can be used at elevated pressure up to 1000 bars and 300°C. Necessary parameters for major ions present in smart water brines including Na^+, K^+, Cl^-, SO_4^{2-}, Ca^{2+}, Mg^{2+}, CO_3^{2-},

HCO_3^-, CO_2(aq), H^+ and OH^- have already been optimized, and several experimental data at elevated reservoir conditions have been reproduced. Thus the model perfectly is suitable for modelling Salt solubility's and dissolution during Smart water Enhanced Oil Recovery.

Discussion

In various cited references it has been observed that smart water EOR water flooding/imbibition experiments with higher sulfate concentration in the injected brine has led to a higher oil recovery. In these studies during interpretation, the composition of the injected brines is correlated to the reported oil recovery. But, the proposed wettability alteration mechanism suggest the injected/imbibing Mg^{2+} ions replaces Ca^{2+} ions from the mineral surfaces. So, the feasibility of this ion substitution has been studied using DFT calculation in Paper I. This ion substitution leads to decrease is Mg^{2+} concentration with associated increase in Ca^{2+} concentration in the pore space. Thus, the probability of insoluble precipitation/fine salt formation can be considerably enhanced. Thus correspondingly interaction of insoluble salts has been studied with Polar acids (Paper II) and basic (Paper III) fractions of oil. Consistent emulsification due to interaction between insoluble salts and polar fraction of oil is observed. Effect of soluble ions in this emulsification was further studied in Paper IV. This ion substitution and associated change in electrolyte speciation eventually leads to the formation of a new brine composition in the pore space. To calculate the properties of the brine present in pore space at reservoir condition, Extended UNIQUAC modeling was conducted in Paper V and Paper VI. Consistent correlation between fine formation and oil recovery was observed in reservoir conditions. The brine and fines in the pore space interacts with the crude oil and alters its displacement efficiency. Therefore, the properties of produced brine at reservoir condition were calculated from reported effluent brine composition in ambient condition (Paper VII). It was also observed available soluble salts in reservoir brines can also alter brine speciation particularly during carbonated water floods. Its correlation to oil recovery has been studied in Paper VIII. The injection brine composition at ambient condition can have different speciation from that in reservoir conditions. And calculations show that injection brine and injected brine have significantly different speciation and most recommend brines actually starts precipitating at reservoir conditions (Paper IX). Paper IX also distinguishes between fine formation within reservoir and precipitation on injection. Pause in brine injection has shown to increase oil recovery in few low salinity EOR studies and subsequently core flooding experiments was conducted to explore the effect of fine in the same. A continuous resistivity

monitoring smart water coreflooding equipment was developed (Paper X). In which coreflooding experiments with only soluble salts and pause injections was studied for High temperature (130°C) chalk water floods (Paper XI), Low temperature (60°C) chalk water floods (Paper XI); Low temperature (60°C) greensand water floods (Paper XIII). An attrition based fine production with directed correlation to oil recovery was observed over various pauses in brine injection. Based on these studies optimum brine composition for maximum fine formation was reported in Paper XIV. And all solubility properties of commonly used brines in reservoir conditions as calculated from Extended UNIQUAC model was reported in Paper XV. In this section, the correlation between the experimental results and Extended UNIQUAC calculations (as stated above) is discussed. A possible correlation between fines formation, emulsification and oil recovery has also included. The obtained results are compared to studies reported in the literature (Austad et al. 2009; Gupta et al. 2011; Pu et al. 2012; Zahid et al. 2012), to explore the possible mechanism behind SmW-EOR.

4.1 Ion Substitution

4.1.1 Types of Cation Substitution

The DFT calculations in this study (Paper I) and another similar previous study (Sánchez et al. 2014) shows that substitution of Ca^{2+} by Mg^{2+} on the calcite surface is possible in two different ways:

a. The adsorbed Ca^{2+} ion on the mineral surface can be replaced by the injected Mg^{2+} ions. Herein there is no associated formation of magnesite or dolomite (Karimi et al. 2015). This substitution only requires the ions to have enough entropy to pass the energy barrier for adsorption or desorption on the mineral surface. Herein total amount of additional Ca^{2+} released must not increase above a monolayer of Ca^{2+} of the mineral surface. For North Sea chalks such substitution can readily take place at a flooding rate of 0.2 ml/min (Strand et al. 2008). The total amount of additional Mg^{2+} adsorbed by this process remains limited by the total amount adsorbed Ca^{2+} available on the mineral surface.

   Example (Strand et al. 2008): In Figure 4.1a it is observable that injecting Mg^{2+} into the coreplug increases the release of Ca^{2+} ions from the coreplug. Initially, there is no production of Mg^{2+} in the effluent brine. After 2 PV of effluent brine production, the concentration of Ca^{2+} decreases and no additional Ca^{2+} is observed in the effluent. The effluent Mg^{2+} concentration also becomes equal to the injected brine concentration. This indicates that after the initial substitution on the mineral surface further substitution gets constrained. Lack of further availability of adsorbed surface Ca^{2+} is likely to be the associated reason.

b. The other process of possible mineral substitution is the substitution on the calcite surface. As explained by Austad (Austad et al. 2009) and DFT calculations (Sánchez et al. 2014) herein the Ca^{2+} from the grain is removed from its crystal lattice permanently and is released in the pore space. And in place of the Ca^{2+} ion in the lattice, the Mg^{2+} ion from the brine gets introduced. During continuous flooding the mineral changes from calcite to dolomite and eventually to magnesite (Austad et al. 2009). In comparison to the amount of Mg^{2+} present in sea water, the amount of Ca^{2+} available in the chalk minerals is significantly greater. Thus, this mineral surface substitution is not limited by Ca^{2+} and can be observed for several PVI (Strand et al. 2008).

   Example (Strand et al. 2008): Figure 4.1b shows effluent resulting from sea water injection to a reservoir coreplug at 1 PV/day. Slow injection into a high specific surface coreplug was conducted. The effluent brine concentration observed in this experiment is shown in Figure 4.1b. Herein it is observable that the injection of Mg^{2+} was continued for 5.5 PV and throughout this injection the produced brine contained significantly less Mg^{2+} and an elevated amount of Ca^{2+}. Unlike the previous example, the substitution did not stop after 2 PV of brine injection in this case and thus replacement of ions from the mineral lattice must have taken place. The total Ca^{2+} released from the mineral surface is equivalent to 5 Ca^{2+} ion monolayers on the mineral surface. This also indicates that along with adsorbed Ca^{2+} ions, ions in the mineral crystal must have participated in the substitution.

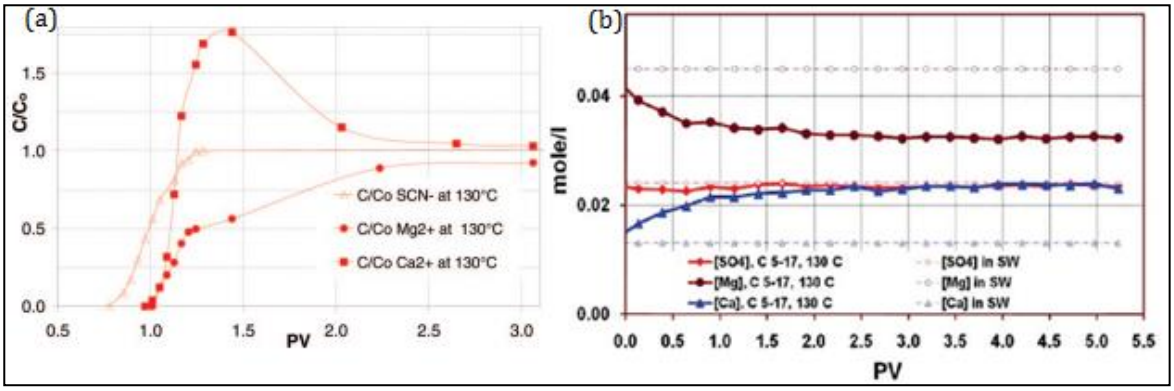


Figure 4.1: Enriched Ca^{2+} and depleted Mg^{2+} in effluent indicate ion substitution on mineral surface. (a) ions substitution only observed for 1 PV (b) ion substitution consistently observable for 5 PV (Strand et al. 2008).

It must be noted that surface Mg^{2+} adsorption does not necessarily always lead to release or desorption of Ca^{2+} ions. Mg^{2+} adsorption can take place on a free calcite surface. But this phenomenon can only be observed for 1-2 PV since it is limited by the amount of available free surface. Substitution from the mineral lattice is always associated with a decrease in Mg^{2+} and corresponding increase

in Ca^{2+} concentration. Observed decrease in concentration of Mg^{2+} for 1 PV at 70°C during water flooding, with no associated increase in Ca^{2+} indicate free site adsorption of Mg^{2+} on calcite (Zahid et al. 2012). These two types of ion substitution in the coreplug are schematically represented in Figure 4.2.

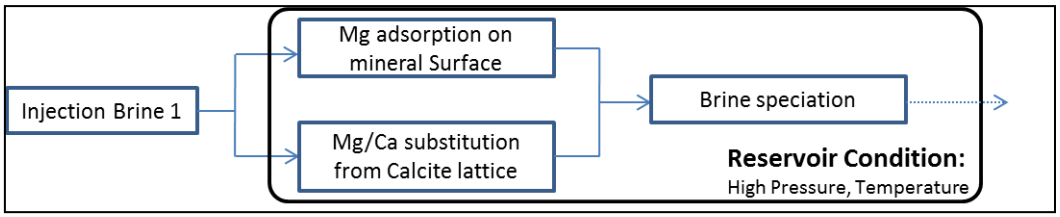


Figure 4.2: Schematic representation of the two types of ion substitution at reservoir condition

These are the two types of substitution which can take place on the mineral surface. Thus, release of Ca^{2+} ion from the coreplug, with associated absence of Mg^{2+} ions must not be associated directly to the formation of dolomite in the coreplug. The amount of substitution that takes place is not just dependent on the brine injection rate but is also dependent significantly on coreplug (Zahid et al. 2012). For example, ion substitution readily takes place in experiments conducted with outcrop chalks from Stevns Klint Denmark. Similar ion substitution has not been observed in experiments conducted with reservoir coreplugs (Zahid et al. 2012).

4.1.2 Extent of Ion Substitution

The ion substitutions of Ca^{2+} by Mg^{2+} are well established in literature (Elstnerova et al. 2010; Austad et al. 2009; Veizer 1983; Boggs 2009; Gupta et al. 2011; Vo et al. 2012). Because the common cations in the carbonate mineral have the same charges and similar ionic radii, substitution of cations is common. Substitution of Mg^{2+} (ionic radius 0.072 nm) for Ca^{2+} (ionic radius 0.100 nm) is readily obtained. On the other hand, the larger Ca^{2+} ion does not substitute for Mg^{2+} in the mineral surface (Boggs 2009). In the calcite structure, disordered cation substitution of Mg^{2+} for Ca^{2+} can occur, up to several mole percentages. Calcite containing more than 4–5 mol % magnesite can be easily obtained with various calcite minerals (Boggs 2009). Some calcite has shown to produce up to 30% mol $MgCO_3$ (Veizer, 1983; Boggs 2009). The extents of ion substitution that takes place with reservoir and outcrops have also been proved to be significantly different; as explained in the following experiments from literature.

a. In Stevns Klint Chalk up to 100% of the lattice surface Ca^{2+} has been shown to be substituted consistently by Mg^{2+} injection (Austad et al. 2009). Herein both surface absorbed ions and mineral lattice ions have shown to be substituted easily. Through XRD analysis, it has also been

shown that dolomite can be formed on the mineral surface (Megawati et al. 2015).

b. Similar studies with reservoirs rocks from the North Sea have not shown similar ion substitution for the same rate of brine injection (Zahid et al. 2012). Herein both Dan field coreplugs and Stevns Klint chalk where flooded with a similar scheme at 2 PV/day. In the case of Dan field chalks, both the injected brine composition and the effluent Mg^{2+} was 1093.73 ppm, while similar injection of brine with 1093.73 ppm of Mg^{2+} into Stevns klint chalk showed production of only 900-920 ppm of Mg^{2+} in the effluent brine (at 70°C). This indicates that Mg^{2+} must have been adsorbed during the waterflood. This ion substitution for Stevns Klint chalk was associated with increase in oil production by 10.2% of OOIP, while Dan field outcrop neither showed a decrease in effluent concentration during the flooding nor was an increase in oil production observed. It was concluded that coreplug behavior of outcrops are different from that of reservoir coreplugs (Zahid et al. 2012).

c. Advanced ion management of limestone coreplugs from the Middle East was studied using various brine compositions (Gupta et al. 2011; Vo et al. 2012). The rate of brine injection was 5-10 PV/day (1-2 ft/day displacement). The amount of additional Ca^{2+} ion produced in the effluent was plotted against the amount of missing Magnesium ion in the effluent. In Figure 4.3, a one-to-one correlation between increase in Ca^{2+} ion concentration and decrease in Mg^{2+} ion concentration can be observed. It can be attributed to ion substitution. The amount of ion substitution that took place was typically around 0.003-0.005 mol/liter with a maximum of 0.009 mol. The injected Mg^{2+} concentration was 0.053 mol. Therefore, with an injection rate of 5-10 PV/day into Middle East coreplugs typically 7.54% (with a maximum of 16.98%) of Mg^{2+} gets substituted on the mineral surface. Other studies with Middle East coreplugs have consistently shown 50% Mg^{2+} for 12 PV when the brine injection rate was controlled at 1 PV/day (Shariatpanahi et al. 2010; Vo et al. 2012).

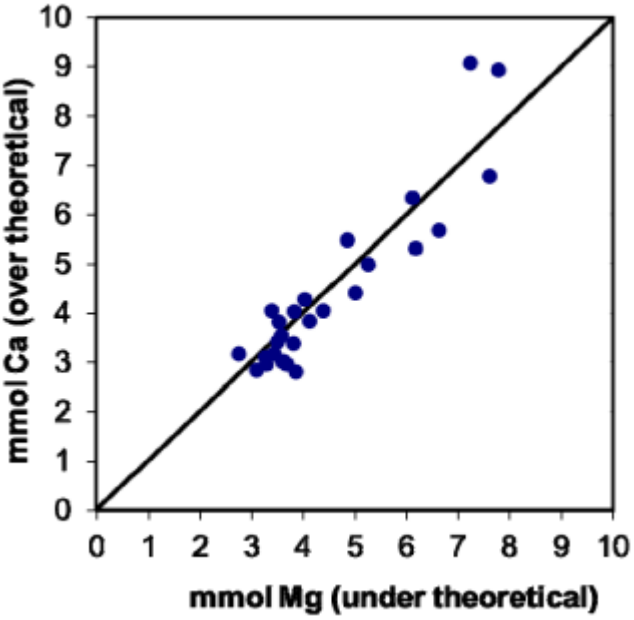


Figure 4.3: Increase in Ca^{2+} concentration in effluent vs decrease in Mg^{2+} concentration in effluent brine (Vo et al. 2012)

d. Furthermore, a spontaneous imbibition experiment was conducted with highly porous (30 to 45 %) and moderately permeable (3-8 mD) outcrops originating from various sites including Stevns Klint chalk (Denmark), Rørdal chalk (Denmark) and Niobara chalk (United States) respectively (Fernø et al. 2011). Same flooding and aging conditions were maintained for all the coreplugs. No additional increase in oil recovery was observed for increased SO_4^{2-} concentration at 130°C for Niobara and Rørdal chalks. A consistent increase in oil recovery was observed for aged Stevns Klint chalk. Ion substitution is an essential step for increased oil production according to wettability alteration (Austad et al. 2009), calcite dissolution (Pu et al. 2010) and fines formation (Chakravarty et al. 2015) mechanism. No additional oil production was observed for Niobara and Rørdal coreplugs (when flooded at identical condition) (Fernø et al. 2011) also imply that the extent of ion substitution for Stevns Klint chalk must have been significantly different from that of Niobara and Rørdal chalks.

It is well accepted and proven that ion substitution on calcite surfaces can take place when Mg^{2+} brines are injected in Chalk and limestone coreplugs. The effect of pressure and temperature on Mg^{2+}/Ca^{2+} ion substitution has been extensively studied in literature. It has been studied meticulously for both chalks and limestone coreplugs over a temperature range from 70°C to 130°C (Puntervold et al. 2008). This certainly provides information about the effect of individual ions in smart water flooding, and thus helps in understanding the underlying fundamental mechanism (Austad et al. 2009). But the reservoir temperature does not undergo any major change during injection of different

smart water floods. Therefore, these properties are constant for the reservoir and cannot be altered to attain more favorable flooding conditions. If the reservoir temperature is intentionally altered (alike to laboratory variations (RezaeiDoust et al. 2009)) by additional processes during smart water flooding then considering its effect on ion substitution is very important. Other than the temperature and pressure condition of the water flood, the extent of substitution depends on two major parameters:

a. Origin of the coreplug: Outcrops like Stevns Klint chalk readily substitute on mineral surface (Strand et al. 2008), while North Sea reservoir chalk does not show the same extent of ion substitution (Zahid et al. 2011). Also, not all outcrops show similar ion exchange, as Rørdal chalk (from Denmark) and Niobara chalk (from United States) show no major ion substitution (Fernø et al. 2011); while even reservoir coreplugs from Middle East show consistent ion substitution (Shariatpanahi et al. 2010).

b. Rate of brine injection: Quick injection at 5 PV/day or more shows release of only adsorbed ions from the mineral surface from Stevns Klint chalk (Strand et al. 2008). A pause of 10 hours or more can cause ion substitution from tight North Sea reservoirs coreplugs as well (Paper XII; Figure 8-9). Furthermore, when brine was injected at 2 PV/day, no ion substitution was observed for the same reservoir coreplugs from North Sea (Zahid et al. 2011). The measured composition of injected and effluent brines was identical. Therefore, it was suggested that substitution does not take place for coreplugs from North Sea reservoirs. But experiments in this study show that ion substitution on the mineral lattice can be observed (Paper XII; Figure 8) on reinjection of brine after following a pause (in water injection) of 8 hours or more. Pause time and degree of ion substitution showed a linear correlation. This correlation was studied up to 78 hours of pause time. This indicates that ion substitution does take place for North Sea reservoir chalks, but its substitution kinetics is much slower than Stevns Klint outcrop chalk.

In the literature recommendations for reservoirs chalks have been made (Puntervold et al. 2014) based on ion substitution experiments on Stevns Klint outcrop chalks. But ion substitution experiments with Stevns Klint chalk have shown to be different from North Sea reservoir coreplugs (Zahid et al. 2011). In the above discussion and in previous studies (Zahid et al. 2011; Fernø et al. 2011) it has been shown that the origin of core plugs has a major effect on the extent of ion substitution that takes place during water floods. Before recommending a suitable Smart Water for any oil fields, a detailed ion substitution variation at reservoir condition for variation in injection rate must be studied. It must be noted that the release of additional Ca^{2+} during effluent analysis is fundamental to all proposed mechanisms including wettability alteration (Austad et al. 2009), mineral dissolution (Pu et al. 2010) and fines formation (Chakravarty et al. 2015). Therefore, experiments on degree of ion

substitution as a function of injection rate at reservoir conditions must be conducted for every oil field to understand the behavior of the proposed brine when injected in the reservoir.

Smart water flooding is mostly being considered for oil fields that are presently being flooded with sea water. Therefore, the effluent brine composition data during initial water flooding and after a pause in production/reinjection can be used to study the extent of ion substitution that takes place for the given reservoir (Yousef et al. 2012). Also, the oil industry can use the data from previously conducted water flooding experiments to study the degree on Mg^{2+}/Ca^{2+}ion substitution for each reservoir.

This study emphasizes that the degree of Mg^{2+}/Ca^{2+} ion substitution against rate of brine injection must be studied individually for each reservoir. Unlike temperature, the rate of injection can be easily altered in oil fields to attain optimum ion substitution and EOR irrespective of the associated mechanism. Based on FTIR and TGA analysis it has been shown that the ion substitution on mineral surfaces cannot be the sole cause of an increase in oil production (Karimi et al. 2015). Therefore, change in brine composition, speciation and possibility of insoluble fines formation because of ion substitution should be considered.

4.1.3 Implication of Ion substitution:

Irrespective of the type of substitution that take place, an additional amount of Ca^{2+} is produced in the coreplug (Shariatpanahi et al. 2010). This release of Ca^{2+} from the coreplug and associated absence of Mg^{2+} changes the brine speciation significantly. Since $CaSO_4$(s) has very low solubility (Marshall et al. 1964), particularly at high temperatures, the additional Ca^{2+} cause a significant increase in the amount of anhydrite precipitation in the coreplug (Paper V, Figure 4.1). This anhydrite formation thus can cause a decrease in sulphate concentration in the effluent as previously observed (Strand et al. 2008). Normally, in most calcite water flooding experiments, a decrease in sulphate concentration in the effluent is associated with adsorption of SO_4^{2-} ions on the mineral surface (Strand et al. 2006). But due to the release of additional Ca^{2+} ions from the mineral surface, precipitation of $CaSO_4$(s) could also be the reason. Therefore, during water flooding (where ion substitution is observable), all SO_4^{2-} that remains inside the coreplug cannot be associated to adsorption on the core plug. A fraction of the SO_4^{2-} has likely precipitated as $CaSO_4$.

In a smart water study (Fathi et al. 2011), a flow through experiment was conducted and it was observed that a fraction of Ca^{2+}, Mg^{2+} and SO_4^{2-} ions remained inside the coreplug. It was interpreted as adsorption of ions due to their adhesion to the calcite surface. But, as a parallel interpretation, the decrease in Mg^{2+} concentration in the effluent can be explained by ion

substitution on the mineral surface (as proposed Austad et al. 2009); while anhydrite precipitation in the coreplug (following the ion substitution) may have led to an associated decrease in $Ca^{2+}$and SO_4^{2-} concentration in the effluent. Thus, all SO_4^{2-} ions that remain inside the coreplug may not necessarily be associated to SO_4^{2-} adsorption on the calcite surface.

This understanding can therefore be summarized in two points:

a. Coreplug dependent ion substitution can alter the brine speciation and lead to salt precipitation.

b. Decrease in effluent SO_4^{2-} concentration can be caused by SO_4^{2-} adsorption and by anhydrite precipitation.

4.2 Emulsification

4.2.1 Fines interaction with Crude oil:

The possible change in brine speciation following ion substitution has not been considered when interpreting water flooding experiments. A decrease in SO_4^{2-} concentration in the effluent has been assumed directly associated to its adsorption on the mineral surface (Fathi et al. 2011). All of the injected brine has generally been considered to remain soluble. Correspondingly, properties such as interfacial tension (IFT) and contact angle analysis are used to analyze the interaction of different brines with oil and water. But, the formation of insoluble salts in the coreplug has not been previously realized so the interaction of insoluble salts with crude oil had not attained much attention. Therefore, an analysis of fines-crude oil interaction in the presence of different brines was conducted. As discussed in the SPE-173855-MS (Paper II) and SPE-174335-MS (Paper III) and SPE-179765 (Paper IV) it was observed that the fines grains of insoluble salts can produce water soluble oil emulsions. The availability of polar compounds in the oil and insoluble salts in the brine solution were observed to be prerequisites for the formation of these emulsions. But the amount of emulsion formation did not show any direct correlation to the amount of acid/base present in the oil. This was consistently observed for more than 70 different samples (including both crude and designed oil). It was observed that stearic acid doped crude oil readily emulsified in the presence of fines, but heptanoic acid only showed partial emulsification. This indicates that two different crude oils with the same acid number but with different acid composition can lead to significantly different amounts of emulsification.

Furthermore, crude oils from different sources (oil fields) have different acid compositions. Therefore, for oil originating from different sources, a linear relation between acid number and amount of oil emulsification can't be

expected. This phenomenon shows a direct correlation to observed oil production from different waterfloods (Zahid et al. 2010; Standnes and Austad 2000; Zhang and Austad 2005) as discussed below.

a. Zahid et al. 2010 observed that dissimilarity of oil type had significant effect on oil recovery, but no correlation was established between Total Acid Number and EOR. Herein water flooding experiments were conducted where oil originating from 3 different sources was used including Latin America, North Sea and Middle East. The experimental setup and flooding scheme was completely identical for the three crude oils. The three oil samples had the following acid number trend: *Latin America>Middle East>North Sea*. It is expected that reservoirs with oil with higher acid number shall produce less oil because of the strong adhesion between oil and mineral surface (Standnes and Austad 2000) so the expected oil recovery trend was: *Latin America < Middle East <North Sea*. But when smart water was injected the observed oil recovery trend was: *North Sea<Latin America<Middle East*. Least oil production for North Sea Oil, and highest oil production for Middle East oil was consistently observed over nine different core flooding experiments. Latin American oil had significantly higher acid number and should have produced significantly less amounts of oil (as proposed by Standnes and Austad 2000), but that wasn't observed. This showed that for oil originating from different sources, the acid number shows no direct correlation to oil production (Zahid et al. 2010). And oils with similar acid number may not necessarily have similar recovery fractions.

   This observed pattern in oil recovery, (wherein availability of acid affects the oil production, but shows no correlation precisely) is very similar to the pattern of emulsification observed in the conducted experiments (wherein availability of acid affects the oil emulsification, but shows no correlation precisely). This shows a correlation between fines based emulsification and oil production.

b. Standnes and Austad 2000 observed a very consistent decrease in oil production for an increase in acid number. Both rate of oil production and ultimate oil recovery decreased with increasing acid number (from AN=0 to 1.73 (mg KOH/g)). A spontaneous imbibition experiment achieving 10% production of OOIP took more than 1000 hours for AN=0.52; while the same was attained in less than 10 hours with lower acids numbers. In a similar study (Zhang and Austad 2005) the wettability index was shown to have an inverse correlation to acid number in the temperature range from 40°C to 120°C. At 40°C, the wettability index dropped from 0.88 to 0.57 with a gradual increase in acid number. These studies show that the acid number has a direct correlation to oil production and mineral wettability. But unlike the previous example (Zahid et al. 2010), oil originating from different

sources was not used for obtaining variation in acid number. In both the experiments (Standnes and Austad 2000; Zhang and Austad 2005) a specific oil originating from the North Sea was used. It was diluted with hexane to decrease the acid number. Therefore, the various oil samples used in this experiment did not have any variation in type of acid, only its amount varied with samples. So, for the increase in composition of a specific acid, a consistent correlation between acid number and oil production was observed.

Paper II: Figure 3; increase in concentration of heptanoic acid shows a linear increase in amount of acid participation in emulsification. This indicates increased adhesion between the grains and crude oil. For a given acid type, an increase in Acid Number shows direct correlation to both fines based oil emulsification and oil production. Correlation between acid number and oil recovery (Zahid et al. 2010) or acid number and fines based emulsification (Paper II) is lost if the samples have dissimilar acid types.

To summarize; oil originating from the same source when diluted with alkane show direct correlation between acid number, fines based emulsification and oil production. Oils originating from different sources show no direct correlation between acid number, fines based emulsification and oil production. Therefore, an detailed compositional analysis is required. Nevertheless, the pattern of fines based emulsification and oil production remains consistent over variation in oil types and composition. Thus, fines based emulsification of oil as observed in this study could be a possible reason for the observed EOR for entirely water wet systems.

Furthermore, contact angle measurements with both aged and unaged chalks have shown similar results (Jabbar et al. 2013). Contact angle measurements have shown that oil soluble heavy fatty acids (like stearic acid) play a significant role in wettability alteration on calcite and carbonate surfaces. Moreover, the chain length (or heavier acids) showed higher contact angles indicating more oil wetness. It further shows that oil with similar acid numbers, when containing heptanoic acid have significantly less contact angle as compared to stearic acids (Jabbar et al. 2013). In Paper II, the same phenomenon was observed during fines based emulsification, stearic acid showed more active participation in emulsification than heptanoic acid. Contact angle studies further reestablishes the point that if oil samples contain different acidic compounds, then direct correlation between acid number and oil production cannot be obtained, and further analysis of the oil is required.

The behavior of Kaolinite (clay mineral) during fines based emulsification was also reported in Paper II and Paper III. No consistency between acid number and emulsification is observed here; while and the acid type present in the oil is shown to play a prominent role. Spontaneous imbibition experiments with kaolinite containing Berea sandstone have also shown that for crude oil

originating from different sources, no correlation is observed between variation in acid number and oil production (Suijkerbuijk et al. 2012).

In the proposed wettability alteration mechanism (Austad et al. 2009), the increase in oil recovery is primarily caused by desorption of carboxyl acids from the mineral surface. Therefore, the acid number should show a direct correlation to oil production (Standnes and Austad 2000). But we observe that it is only observed for a specific type of variation in acid number. As discussed above, there is suitable evidence (Zahid et al. 2010; Jabbar et al. 2013; Moradi et al. 2013) that the acid number shows no direct correlation to oil production. Therefore, a more detailed analysis of oil composition is required, when oils originating from different sources are compared.

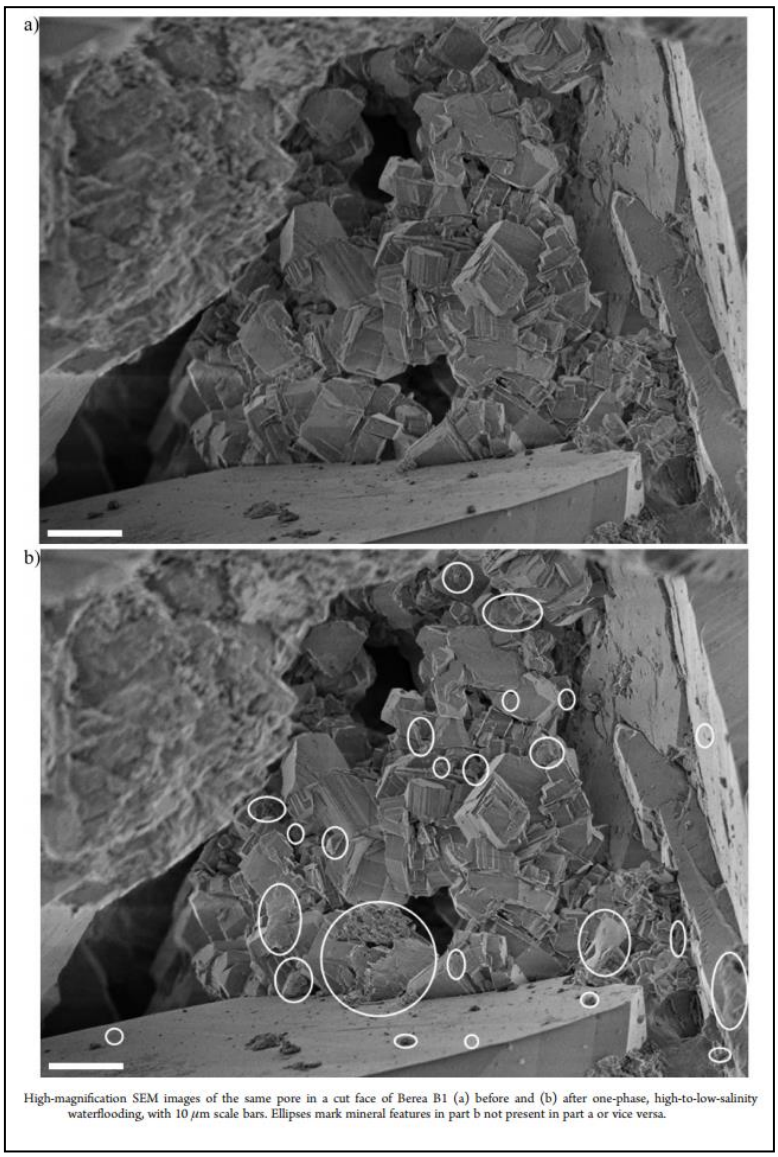


Figure 4.4: High magnification SEM images of the pore space before (a) and after (b) waterflood. Ellipses mark minerals in part (b) that was not present in part (a) or vice versa. This proves that small fine particles from the mineral became mobile during the water flood and migrated ahead in the coreplug (Fogden et al. 2011).

Through Scanning electron Microscope, micro-CT scans and X-ray analysis, emulsification of oil has been observed due to interactions with clay fines particles in sandstone coreplugs (Fogden et al. 2011). The images show that loosely bound, partially oil-fines lining sandstone grains are stripped by the adhering oil during its recovery and redeposited on grains further downstream (Figure 4.4). Low salinity brine injection increases the fraction of fines thus mobilized by weakening their bonds to grains and strengthening their bonds to oil. It was thereafter suggested that these more oil-wet fines stabilize the water-in-oil curved menisci. Therefore, the fines aid in maintaining the connectivity of the oil phase and thus increase its production. Overall it was concluded that mobilization of fine particles is a major candidate in the mechanism for low salinity enhanced oil recovery. More importantly, the images from this study (as shown below in Figure 4.5) clearly show that oil-in-water emulsions do form in coreplugs at elevated temperature and availability of fine particles in water increases the stability of the oil droplets significantly (Fogden et al. 2011). Experiments without fine particles yielded no oil droplets in water for any variation in brine composition. The reported results within coreplugs (Fogden et al. 2011) are consistent with the observed pattern of emulsification using Gas Chromatographic analysis. It further supports the importance of mobile fines interaction with residual oil in its displacement and increased production.

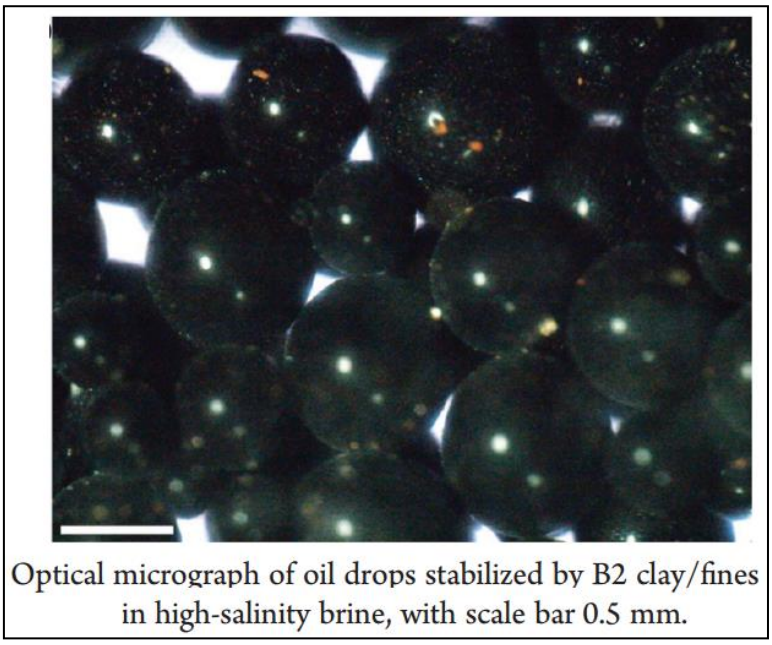


Figure 4.5: In high salinity brine, formation of oil droplets in water takes place due to interaction between clay fines and crude oil (Fogden et al. 2011).

4.2.2 Fines based emulsification at reservoir condition:

The conducted experiments reported in Paper II, III and IV were not conducted at reservoir temperature. So, the possible formation of water soluble emulsions

due to the interaction between polar fractions of oil and insoluble salt fines in reservoir condition has remained unexplored.

Fine particle based oil droplets formations in water have been previously observed through CT-scan studies (Fogden et al. 2011). These observations were made for clay particles which were completely insoluble fine grains already available in the core plugs. Changing high salinity to low salinity brine allows the mobilization of these clay particles, which in turn increase the displacement of oil (as shown in Figure 4.4 and 4.5).

But unlike sandstones, in case of chalk reservoirs there are no insoluble, potentially mobile fine particles (like clay) already present in the coreplug. The presented work (Paper V) shows that brines with a high fraction of potential ions (Ca^{2+}, Mg^{2+} and SO_4^{2-}), when undergoing ion substitution in the coreplug, leads to the formation of insoluble anhydrite salt. The produced insoluble anhydrite fine particles can emulsify the residue oil. Therefore, experimental evidence of emulsification of crude oil on interaction with insoluble salts formed from Smart Waters (like SW-4SO_4: sea water with four times sulphate) should be observable at reservoir condition as well.

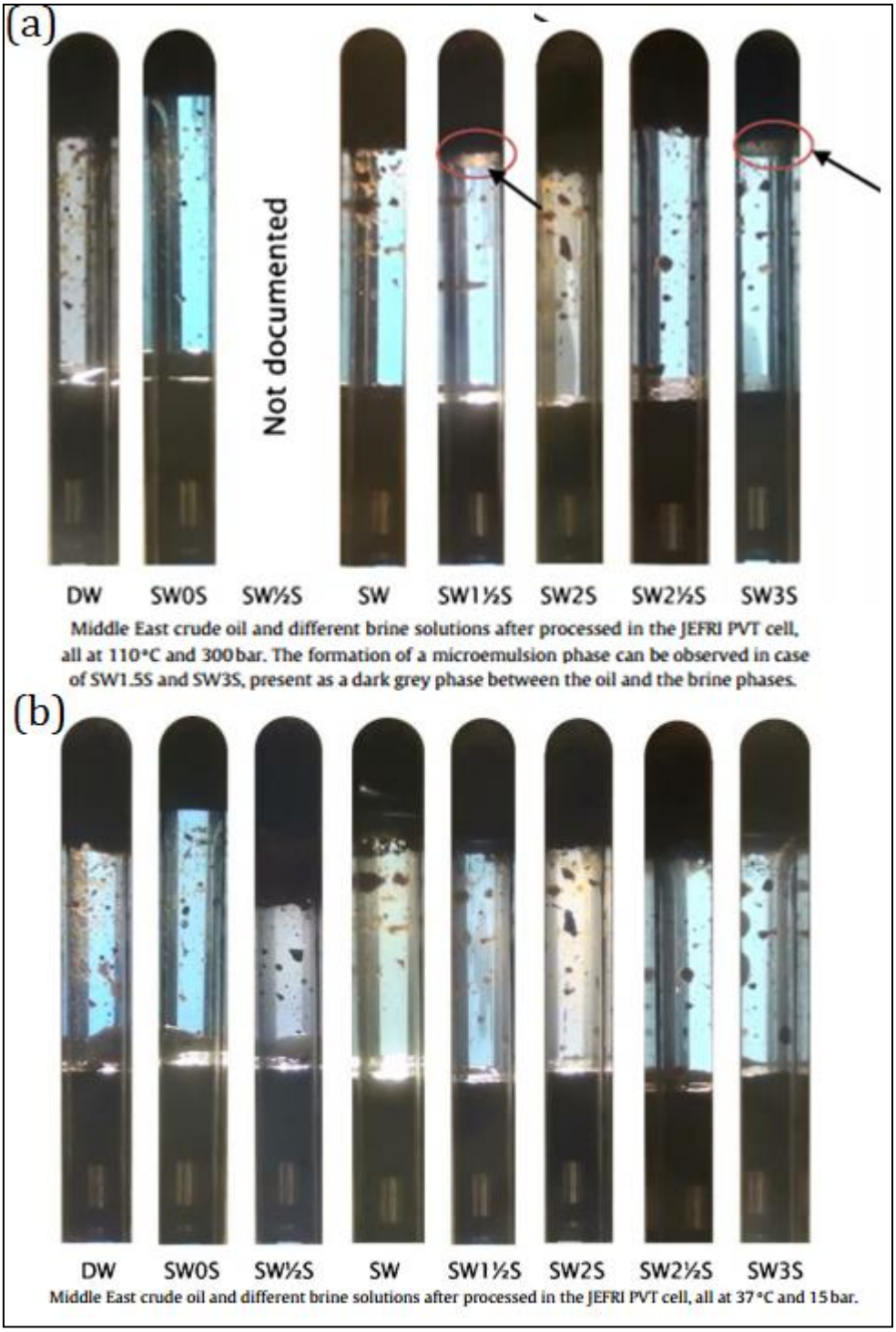


Figure 4.6: Micro-emulsion formation for high sulphate brines (sea water with 1½ times sulphate concentration or more) at 110°C; while no such micro-emulsions were observed at 37°C.(Zahid et al. 2011)

Previously, emulsification of oil at reservoir conditions has been observed with different high salinity smart waters. In crude oil from the middle east, different brine solutions were added, including DW (deionized water), SW0S (sea water without sulphate), SW½S (sea water with ½ sulphate concentration), SW (normal sea water with no alteration to sulphate

concentration), SW1½S (sea water with 1½ times sulphate concentration), SW2S (sea water with twice sulphate concentration), SW2½S (sea water with 2½ times sulphate concentration) and SW3S (sea water with 3 times sulphate concentration).

Emulsification experiments had been conducted at 37°C and 110°C (as shown in Figure 4.6, Zahid et al. 2011). It was observed that at 110°C the brine containing enriched sulphate concentration resulted in a new micro emulsion phase. It was reported that emulsification of crude oil takes place with increase in sulphate concentration at high pressure/temperature condition in the DBR JEFRI PVT cell (Zahid et al. 2011).

Speciation calculation for the reported brine compositions were conducted at various pressure/temperature conditions using Extended UNIQUAC model. The amount of fines formation taking place because of changes in brine composition and pressure, temperature variation is plotted in Figure 4.7. It was observed that with increase in pressure and temperature the stated brines gradually became super saturated which resulted in the formation of insoluble fine particles. As shown in Figure 4.7, brines enriched with SO_4^{2-} (sea water with 1½ times sulphate concentration or more) gradually started fines formation from 70°C and beyond. At 110°C the amount of fines formation that took place was directly proportional to the available SO_4^{2-} concentration. Micro-emulsion formation was observed for SW1½S to SW3S at 110°C (Zahid et al. 2011) and at the same conditions, it is observed that the brines become supersaturated and leads to formation of fines. As shown in Figure 4.6a, low sulphate brines including SW, SW½S and SW0S showed no micro-emulsion formation (Zahid et al. 2011) even at 110°C.

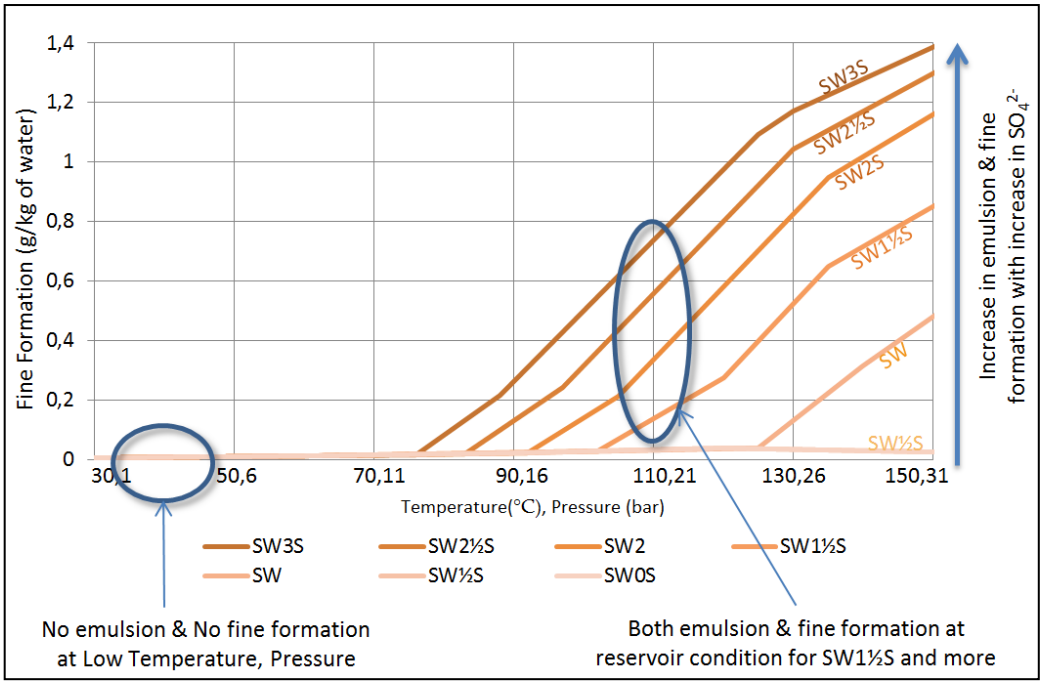


Figure 4.7: Extended UNIQUAC calculation of amount of fines formation for various brine compositions as previously reported (Zahid et al. 2011). It shows fines formation for high sulphate brines (SW1½S, SW2S, SW2½S and SW3S) at 110°C.

The Extended UNIQUAC brine speciation calculation also shows that all low sulphate brines including SW, SW½S and SW0S remained soluble at 110°C. Moreover, at 37°C no micro-emulsion formation was observed in the reported experiment for all brine variations including low sulphate and high sulphate brines. As shown in Figure 4.7 at 37°C none of the brines were supersaturated. This shows a one-to-one correlation between fines formation and oil emulsification at reservoir conditions for high salinity smart water floods as well. This further reestablishes the idea that formation of insoluble mobile salts can increase the adhesion between the residue oil and flooded water through formation of emulsions. Thus, it can increase the displacement of oil and lead to an increased oil production.

The established one-to-one correlation between fines formation and oil emulsification is valid for the experiment conducted at reservoir temperature for oil brine combination. But a similar correlation between oil emulsification and fines formation during core flooding has not been established. Nevertheless in a subsequent study, exactly the same oil (Middle East oil) and same brine composition (SW0S and SW3S) was used in water flooding experiments of completely water wet core plugs, and a significant increase in oil recovery was observed (Zahid et al. 2010). In Paper V (Figure 4.8, 9 and 10) a direct correlation between fines formation and oil recovery for this particular set of experiments (Zahid et al. 2010) has been established for 15 core plug waterfloods. Figure 4.7 establishes a direct correlation between the amount of fines formation and emulsification, while Paper V establishes a one-to one correlation between fines formation and oil production. Therefore, collectively

it establishes a step by step correlation between fines formation, oil emulsification and oil recovery even for a completely water wet coreplug; thus proving a more detailed correlation between fines formation and SW–EOR.

4.3 Extended UNIQUAC calculation and fines-SmW EOR correlation

Emulsification indicates an increased adhesion between the oil water interfaces due to the presence of insoluble mobile salts. These emulsifications can be caused by the interaction of insoluble fines with crude oil. Previous studies for Berea sandstone indicated that mobile fines available in flooded water can release trapped oil from the mineral surface and increase its mobility by making the surface more water wet (Tang and Morrow 1999). It is possible that the insoluble fines may have a similar behavior in chalk as well, but strong correlation between the amount of fines and the observed oil recovery needs to be established to prove this. This called for a reanalysis of all smart water core flooding experiments reported in the literature, by taking the above two points in consideration.

4.3.1 Traditional waterflooding interpretation:

In spite of the observed correlation between fines based oil emulsification and oil recovery, the wettability alteration mechanism has been proposed in the literature (Austad et al. 2009). In this proposed mechanism it has been consistently suggested that SO_4^{2-} must remain soluble in the coreplug (Austad et al. 2009). After ion substitution on the calcite surface, the soluble sulphate gets adsorbed and leads to a release of adsorbed carboxyl compounds. This changes the mineral wettability to a more water wet state and enhances oil displacement. It is represented as a flow chart in Figure 4.8. In the supporting data to this mechanism it has been shown that when the injection brine contained high concentrations of SO_4^{2-} ions a corresponding increase in oil production was observed (Fathi et al. 2011). Increasing Mg^{2+} and Ca^{2+} concentration in the injection brine has also shown an increase in oil recovery (Fathi et al. 2010). Decreasing NaCl concentration also leads to higher oil recovery (Zhang et al. 2006). It has been re-established over several studies that a high concentration of soluble sulphate (in presence of calcium or magnesium ions) has the most prominent influence on increasing oil recovery. It is the soluble SO_4^{2-} ion that replaces the adsorbed carboxyl ions from the calcite surface (Zhang et al. 2006; Austad et al. 2005; Austad et al. 2009; Fathi et al. 2011; Fathi et al. 2010).

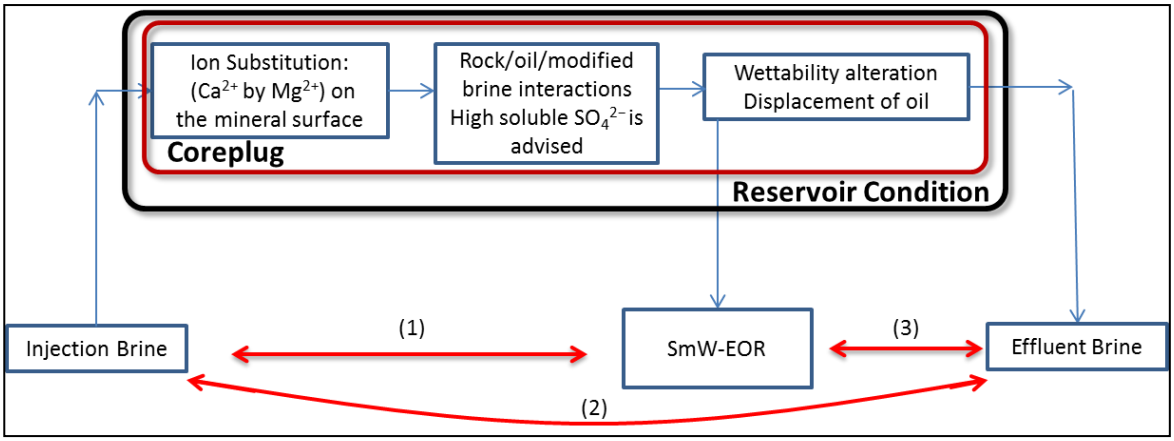


Figure 4.8: Flow diagram of proposed wettability alteration mechanism. (1), (2), and (3) indicate the three correlational analysis used for smart water –EOR interpretation.

According to the mechanism, the ionic composition of the interacting brine (at reservoir condition, after ion substitution) should correlate to oil recovery, as following adsorption of soluble SO_4^{2-} ions on the mineral surface release of adsorbed carboxyl compound takes place. As shown in Figure 4.8, three major correlation analyses are conducted for the interpretation:

a. The variation in composition of injection brine is correlated to the observed oil recovery. Herein the composition and speciation of the injection brine at room temperature is used during correlation to the oil recovery. Based on this correlation, the efficiency of different ions in oil production is measured.

b. Secondly, the composition of the injection brine (at room temperature) is correlated to the composition of effluent brine obtained in effluent tubes at room temperature. Based on this correlation ion substitution, surface adsorption and salt precipitation are quantified.

c. The obtained adsorption, substitution or precipitation from the correlation study between the two brine compositions in injection and effluent tubes at room temperature is correlated to oil production from the high temperature core plug.

4.3.2 Brine speciation in coreplug:

Based on the above stated three analysis steps, interpretations are made on the individual effects of each ion during smart water flooding in chalk and limestone reservoirs. But it has been neglected previously that ion substitution modifies the brine composition leading to dissolution and precipitation of various salts. Various salts including $CaSO_4$, $CaCO_3$, $BaSO_4$ and $MgCO_3$ (Marshall et al. 1964) have very low solubilities. Thus, their precipitation cannot be ignored. As shown in the flow chart (Figure 4.9), in this thesis work it is attempted to correlate the reported oil recovery with the amount of soluble

SO_4^{2-} present in the modified brine and the corresponding fines formation taking place using Extended UNIQUAC model (Thomsen and Rasmussen 1999).

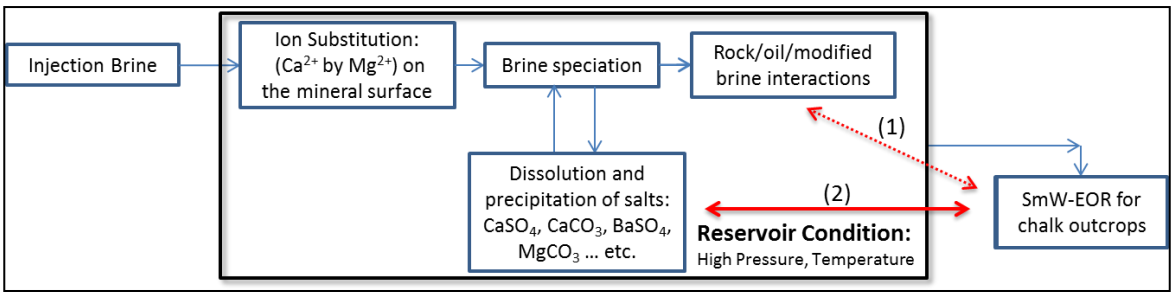


Figure 4.9: Flow chart of correlation of oil recovery with soluble and insoluble fraction of injection brine at reservoir pressure and temperature conditions. Dotted arrow (1) indicates only partial correlation between soluble salts and oil recovery; while arrow (2) indicates consistent correlation between oil recovery and fines/precipitation formation after substitution from injection brine.

The Extended UNIQUAC model is a thermodynamic model for aqueous solutions of electrolytes and non-electrolytes (Thomsen and Rasmussen 1999).The optimized parameters of this model are based on a large amount of experimental data (Garcia et al. 2005; Thomsen and Rasmussen 1999; Christensen and Thomsen 2003; Garcia et al. 2006). The experimental basis of this model enables it to describe the phase behavior and the thermal properties of solutions containing electrolytes with great accuracy.

As explained in Paper V, 62 coreflooding experiments were analyzed. A direct correlation between the amount of fines formation and the reported oil recovery was observed. These calculations clearly show that the properties of the brine present in the pore space – after substitution - should be correlated with the reported oil recovery. Substitution of Ca^{2+} by Mg^{2+} can change the brine properties significantly and fines formation through possible precipitation of $CaSO_4$ is significantly enhanced. The amount of fines formed consistently correlates with the observed oil recovery for several core flooding experiments. This correlation between fines formation and oil recovery has been observed during variation of all major coreplug properties, including Acid Number (Paper V: Figure 4.2 and 3); temperature (Paper V: Figure 4.2-5,7-11); rock type (Paper V: Figure 4.5 and 6); wettability (Paper V: Figure 4.9-11); aging temperature (Paper V: Figure 4.4); formation brine (Paper V: Figure 4.8), origin of oil (Paper V: Figure 4.10) and brine composition (Paper V and VI). And the amount of soluble SO_4^{2-} ions present in the brine solutions is only partially correlated with the observed oil recovery. This proves that Extended UNIQUAC model can be used as a very useful tool to exactly calculate the amount of fines formation for different brine combinations for a diverse range of pressure and temperature conditions. The calculated amount of fines formed can then be used for determining the expected amount of oil recovery.

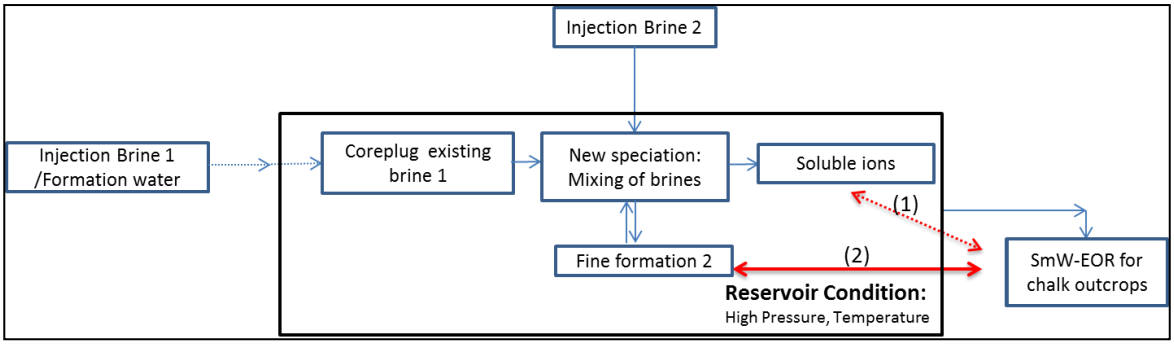


Figure 4.10: Flow chart showing oil recovery correlation with soluble salts and insoluble fines present in the coreplug, after interaction of injection brine with the existing brine in the coreplug at reservoir condition. Fines formation 2 indicates additional fines formation because of Brine 2 injection leading to additional oil recovery.

Further, Extended UNIQUAC brine speciation calculation of various water floods of chalk and limestone coreplugs from reports in literature show that brine speciation gets altered due to the interaction between two brines. When formation water is replaced by injection of new smart waters, or when one smart water flood is replaced by another (with different brine compositions) then the interaction between the two brines leads to a new brine speciation and new fines formation in certain cases. Herein the combined effect of ion substitution and brine mixing can also be observed (Paper VI, Figure 2-5). Therefore, correlation was studied between fines formation and oil recovery for multiple brine injection water floods. As shown in Paper VI, further correlation between oil production and fines formation has been observed for 76 additional coreflooding experiments, involving multiple temperature variations and multiple brine injections. As indicated in Figure 4.10, the observed correlation in Paper VI clearly shows that the efficiency of the injected brine clearly depends on the composition of the brine previously injected in the coreplug. The amount of fines formed due to the interaction of the existing brine with the new injection brine show a one-to-one correlation to the oil recovery. The soluble salts thereafter available in the coreplug only show partial correlation to the oil recovery. This correlation between fines formation (due to mixing of brines) and oil recovery has been observed for, completely water-wet, mixed wet and oil wet coreplugs. Therefore, even when wettability alteration (to greater water wetness) is not possible, a correlation between fines formation and oil recovery is observed.

Thus, brine properties/speciation in coreplugs at reservoir conditions is significantly different from brine properties/speciation at ambient conditions. And the amount of fines formation taking place in the coreplug show good correlation to oil recovery.

4.3.3 Produced brine vs Effluent brine:

When brine is produced from the coreplug, it is stored into effluent tubes at room temperature. Samples of these effluent brines are thereafter taken for accurate brine compositional analysis using ICP-MS (or similar other tools) (Gupta et al. 2012). The obtained brine composition (at room temperature) is thereafter correlated to injection brine composition and increased oil production.

Speciation properties of the brine when produced from the coreplug at reservoir condition can be significantly different from that at room temperature. As shown in Paper V, Figure 1, at elevated pressures, the solubility of $CaSO_4(s)$ significantly increases when moving from reservoir condition (110°C-130°C) to lower temperature (50°C or less). The speciation of the produced brine after cooling no longer reflects the speciation of the brine which was produced along with the increased oil productions, at elevated pressure and temperature conditions. The brine speciation at the flooding conditions was calculated by Extended UNIQUAC model using the composition of the reported effluent brines at room temperature. This gives the exact composition of the soluble ions and insoluble salts produced from the coreplug at the flooding conditions (Elevated pressure and temperature). In Paper VII (and represented in the flow chart Figure 4.11) this distinction between effluent brine and produced brine was established. The amount of mobile, insoluble fines particles that actually passed through the small pore throats of the porous coreplugs showed a direct correlation to the observed oil recovery.

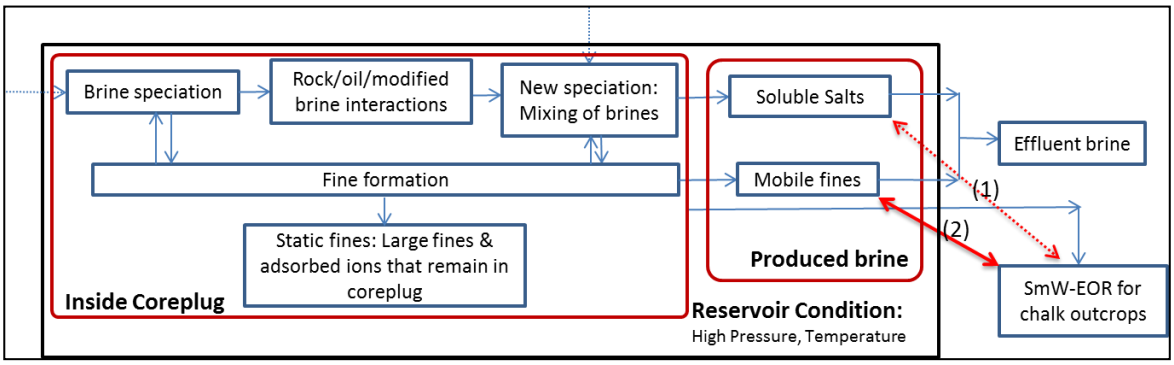


Figure 4.11: Flow chart of distinction between the Produced brine from reservoir/experimental condition and the effluent brine at room temperature. Produced soluble salts (1) and insoluble mobile fines (2) are correlated to oil recovery in Paper VII

In this study it is observed that, following ion substitution, the amount of mobile fines produced from the coreplug is comparable to the soluble salt fraction in the produced brine. Therefore this prominent existence of mobile fines cannot be ignored during water flood interpretations. Moreover oil recovery has also been shown to increase with increase in temperature, with a direct correlation to the corresponding increase in fines formation (Paper VII, Figure 4.2-4). On the other hand, the decrease in soluble sulphate

concentration of the produced brine (Shariatpanahi et al. 2010) show an inverse correlation to oil production for high temperature water flooding (Paper VII, Figure 4.2-4). Decreased solubility of anhydrite fines is the primary associated reason. Furthermore, mobile fines are also produced exactly when brine alteration takes place (Paper VII, Figure 4.5-7). This indicates that fines formation takes place because of mixing of existing and injected brine as previously predicted in the coreplug brine calculations (in Paper V and VI). This fines production is exactly observed for the specific PVI (Paper VII, Figure 4.5-6) when an associated increase in oil production was observed (Gupta et al. 2012). Emulsification experiments also showed strong adhesion between fines and crude oil. This further reestablishes the point that trapped oil from the mineral surface can be released and made transportable along the water flood by adhesive interaction with small mobile fine particles as previously recommended (Tang and Morrow 1999).

The amount of static fines observed in a water flood experiment can be directly calculated from the mass difference between the injection and the effluent brine. These static fines account for adsorbed ions and insoluble salts particles that may have been initially mobile, but with increase in grain size became stuck in the pore throat, and thus was not produced in the effluent. These static fines, when stuck in the pore throats, can alter the flow of the flooded water, and therefore its optimal utilization is essential as it can also block the inject neck and choke the core plug. The observed variation in oil recovery between permeable outcrop chalks and low permeable reservoir chalks (Zahid et al. 2012; Strand et al. 2005, Faith et al. 2011) could be associated to variations in fines mobility, and static fines formation in different porous networks. Flow through simulation of porous media need to be conducted to further quantify this phenomenon. It must be also noticed that the ratio of static fines to mobile fines observed in small coreplugs will not remain the same when implemented at reservoir scale. As with further mobilization of fines the grain size of the mobile fines may continuously increase because of their interaction with the supersaturated brine and thus they can eventually get stuck in the pore throats (Muecke 1979). This gradual conversion of mobile fines into static fines with increase in grain size is an important kinetics phenomenon which needs to be well studied before consideration of implementation of these supersaturated brines in typically low permeability chalk reservoirs like Dan field in North Sea (Røgen et al. 2005).

Scaling challenges is another important issue that may arise during implementation of smart water EOR in high temperature reservoirs (Moghadasi et al. 2003a; Moghadasi et al. 2003b; Haarberg et al. 1992). As shown previously, the produced brine contains significant amounts of mobile fines in coreplug water flooding experiments. But in these experiments the produced brines quickly move to the effluent tubes at room temperature, (where solids like anhydrite are completely soluble Paper VII: Figure 4.2-5). Therefore there is no risk of precipitation of brine in the experimental

production pipes. But unlike coreplug waterflooding experiments conducted in laboratory (Zahid et al. 2011;Strand et al. 2005; Gupta et al. 2012), at reservoir scale these supersaturated brines have ample time in the production pipe, where it remains at elevated pressure/temperature condition (Moghadasi et al. 2003b). Thus there is a significant possibility of precipitation of salts in the production pipes (Moghadasi et al. 2003a). It must be noted that in core flooding equipment the production brine undergoes an almost instant change from reservoir temperatures of 110°C-130°C to ambient conditions of 24°C. But in reservoir productions pipes, as the brine moves towards the surface, no such instant change in surrounding temperature take place (Moghadasi et al. 2003b). These supersaturated brines are therefore susceptible to precipitation and thus can cause hindrance in oil production. To mimic the reservoir scenario and study the possibility of scaling, the effluent pipe in the core flooding equipment can be elongated and kept in a high temperature/pressure bath, so as to ensure ample time is provided for studying the kinetics of anhydrite precipitation during oil recovery from production pipes.

In this study, the observed correlation between insoluble mobile fines and oil production is consistent over various studies. But through high resolution imaging (including use of micro-CT scan) the exact interaction between the two should be further studied. Herein the study provides no information on whether the supersaturated brine fraction is in the form of nucleated grains or remains non-nucleated throughout its flow through the porous network in the coreplug. Because of the continuous mobility of the supersaturated brine and significant availability of nucleation mineral surfaces it is not expected that the supersaturated brine may have remained completely non-nucleated (Bird et al. 1986). But nevertheless, the grain size still remains unknown. And interaction of these adhesive fines with the crude oil also requires further investigations of SEM/micro-CT scan (and Nano-CT scan if possible) of chalk coreplugs while smart water flooding. Study of SEM/micro-CT scan of chalk coreplugs during water flooding can be done similarly to previously conducted SEM/micro-CT scan studies for clay bearing sandstone coreplugs (Fogden et al. 2011).

4.3.4 Injection brine Vs Injected brine:

Just like the produced brine and the effluent brine do not have same speciation, it is possible that the injection brine (i.e. composition of brine at room temperature) and the injected brine (i.e. the same brine at reservoir condition) may have different speciation (Paper IX).

Injection of various brines including SW0NaCl (Sea Water with no NaCl); SW0NaCl-2SO4 (Sea Water with no NaCl, twice SO_4^{2-}); SW0NaCl-3SO4 (Sea Water with no NaCl, thrice SO_4^{2-}), SW0NaCl-4SO4 (Sea Water with no NaCl, four times SO_4^{2-}) have been recommended for North Sea Chalk reservoirs at 130°C (Puntervold et al. 2014). Extended UNIQUAC brine speciation calculations have been conducted for the brines that have been recommended in literature for injection in North Sea Chalk reservoirs at 130°C. Significant differences in

soluble ion composition between injection brine and injected brine are observed due to change in pressure/temperature conditions (Paper IX). Correspondingly, a considerable amount of anhydrite precipitation is observed for all recommended brines including SW0NaCl-nSO_4 ∀ n= 2,3,4. Most spontaneous imbibition experiments are conducted at 10 bars to 50 bars (Puntervold et al. 2014; Faithi et al. 2011; Strand et al. 2006), while reservoir pressure can easily go up to 400 bars (Yousef et al. 2012). Extended UNIQUAC calculations of brine speciation of injection brines were conducted over pressure variations from 10 bars to 600 bars. Precipitation of anhydrite fines in the reservoir is observed at both experimental and at reservoir conditions (as shown in Paper IX, Figure 4.2-5). According to this observation the flow chart of coreplug smart water studies was further modified as shown in Figure 4.11.

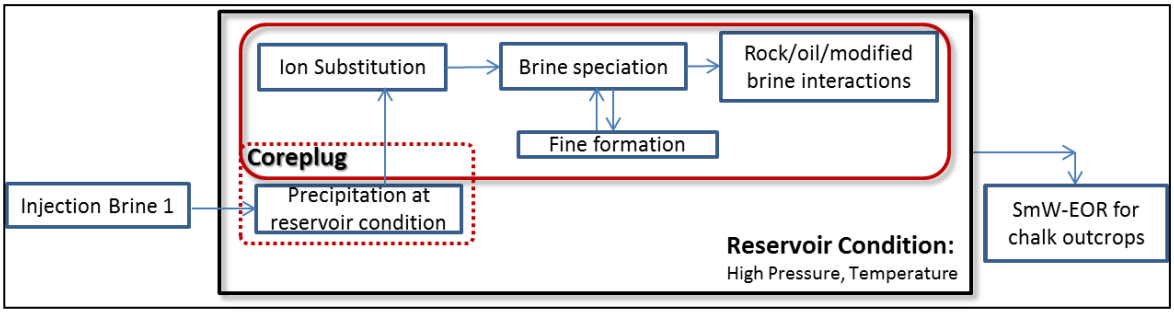


Figure 4.11: Flow chart shows that the injection brine becomes supersaturated and thus can cause precipitation when raised to reservoir conditions. Dotted Red lines indicate that this precipitation may take place inside the coreplug, or before in the injection pipeline depending upon the kinetics of nucleation.

This initial precipitation does not depend on the mechanism of smart water EOR. Neither does it depend on whether ion substitution takes place on the mineral surface or not. It is a phenomenon of the recommended brines at reservoir conditions, and is independent of the associated smart water EOR mechanism. But it certainly has three important implications for smart water floodings.

a. According to the wettability alteration mechanism, the use of high potential ion fraction (either by removing NaCl: SW0NaCl or by enhancing potential ions: SW-4SO_4) is recommended for North Sea chalk fields at 130°C (Austad et al. 2009; Puntervold et al. 2014). And it has been suggested that while using these brines, precipitation in the coreplug must be avoided (Austad et al. 2009). But as shown in Paper IX the recommended brine will cause precipitation at North Sea chalk fields at reservoir conditions 120-140°C irrespective of interaction with oil or mineral surface. Therefore, the use of recommended high potential ion fraction brines (SW0NaCl-nSO_4 ∀ n= 2,3,4) and avoiding precipitation are two contradictory requirements for all coreplugs at 130°C.

b. As shown in Paper IX, the previously observed high oil recovery for high potential ion fraction brines (SW0NaCl-nSO_4 ∀ n= 2,3,4) (Puntervold et

al. 2014), can be explained using fines formation mechanism. Herein subtracting the initial precipitation from the total precipitation taking place in the core plug after ion substitution shows a consistent correlation to oil recovery even for brines containing very high potential ion fraction (like SW0NaCL, SW4Ca). It must be noted that the amount of supersaturation caused in the core plug following the ion substitution must be dominant over the precipitation taking place during injection before ion substitution.

c. Most oil producing chalk reservoirs including chalks from North Sea reservoirs are known for their extremely low permeability (Røgen et al. 2005). Therefore irrespective of the associated mechanism, if these (SW0NaCl-nSO_4 ∀ n= 2,3,4) recommended brines (Puntervold et al. 2014) are considered for injection into reservoirs, it must be injected with full awareness that these brines are supersaturated at reservoir conditions and its implication in these low permeability chalks needs to be pre-considered. Furthermore particularly for low permeability coreplugs (like Dan field from North Sea, Røgen et al. 2005) it must be noted that additional precipitation after ion substitution will also take place. Unlike precipitation on injection (which is a brine property), this precipitation depends on the extent of ion substitution taking place in the pore space, thus in effected by coreplug properties and injection rate.

To summarize: Precipitation shall take place when these previously mentioned recommended brines (Puntervold et al. 2014) are injected into low permeability reservoirs. The amount of fines formation taking place after substitution shows good correlation to the observed oil recovery. Based on the above stated Extended UNIQUAC Speciation calculation, and water flood interpretation, a summarized flow chart has been developed as shown in Figure 4.12.

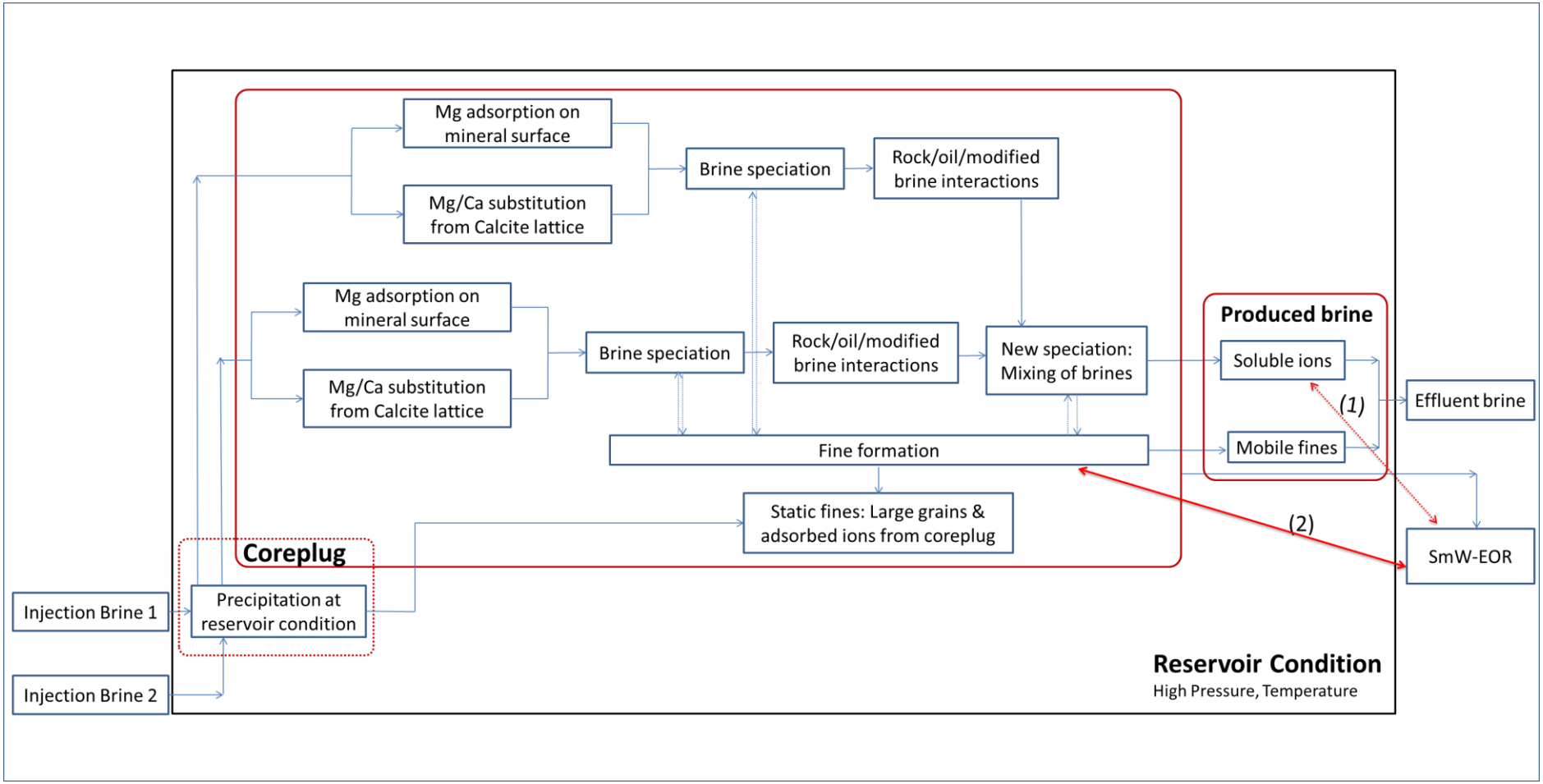


Figure 4.12: Flow chart of various steps taking place during SmW-EOR: (1) soluble salts at reservoir condition and (2) insoluble fines have been attempted to correlate to oil production for various SmW-EOR experiments. Amount of fines shows consistent correlation to oil production.

4.3.5 Fines formation with soluble CO_2

Water alternate Gas (WAG) injection, and carbonated water injection for increasing oil recovery has been implemented in various oil fields (Dang et al. 2014). The injection of soluble CO_2 coupled with smart water can alter the brine speciation significantly (Dang et al. 2014). Availability of CO_2 leads to dissolution of calcite in the pore space (Mackay et al. 2014). This not only changes the permeability of the core but the additional Ca^{2+} in the pore space can lead to anhydrite fines formation. Initial study in Paper VIII show good correlation between anhydrite fines formation and additional oil recovery due to brine alterations in the presence of soluble CO_2 with WAG- CO_2 and carbonated water injection. This further opens the possibility of smart water flooding implementation into oil fields in which CO_2 is already being injected.

4.4 What is the mechanism for SW-EOR?

In the founding work for enhanced oil recovery through salinity variation, by Tang and Morrow 1999; it was reported that fines were essential for observing any increase in oil recovery. Based on a series of studies the following conclusion was made:

''Repeated waterfloods on a single reservoir sandstone core indicated that potentially mobile fine particles play a key role in the sensitivity of oil recovery to salinity. This conclusion was tested using Berea sandstone after fines had been stabilized by firing at 800°C and metal oxides removed by acidizing. Recovery of crude oil from this fired and acidized sandstone was essentially independent of salinity.'' -(Tang and Morrow 1999)

In sandstone coreplugs the fine particles in form of kaolinite clay are already present in the coreplug. Decreasing the salinity leads to the removal of Na^+/Cl^- electric double layer (Nasralla et al. 2014) and allows the clay fines to mobilize in the pore space. In this study we observe a similar behavior for chalk core plugs. Although fines are not present in the chalk coreplug but from the various reported (high potential ion) (Faithi et al. 2010; Faithi et al. 2011; Zahid et al. 2010; Strand et al. 2005; Zhang et al. 2006) smart water floods and based on Extended UNIQUAC calculation it is observed that fines formation was consistently taking place (Paper V & VIII). Four major reasons have been identified why fines formation can take place in the core plug.

a. Ion Substitution: Mg^{2+}/Ca^{2+} substitution on the mineral surface can change the brine speciation by release of additional Ca^{2+} in the pore space, thus causing fines formation (Paper V)

b. Mixing of two different brines can also cause supersaturation in the pore space and cause fines formation. Herein it must be noted that fines formation can take place during (Paper VI):

   i. interaction of injected brine with formation water
   ii. during alteration of injection brine, thus interaction between two injected brines

c. Available soluble gas in the brine like CO_2 can cause significant change in the speciation. Insoluble, yet readily available salts like $CaCO_3$; $MgCO_3$ and $CaMg(CO_3)_2$ can easily get dissolved in presence of water dissolved CO_2. Thus altering both permeability of coreplug and brine speciation (Paper VIII).

d. In several experiments the pressure and temperature conditions of the coreplug have been consistently varied to study the effect of injection brine at different conditions. This variation in pressure and temperature condition can also alter the brine speciation and lead to fines formation (Paper V& VI).

Fines have been shown to have an affinity for oil, as it can emulsify the crude oil in water both at room temperature and at reservoir conditions (Paper II–IV). The fines formed in the coreplug (as a result of the variations in brine injection) also interacts with the trapped oil. And if the affinity between the residue oil and the fines is greater than the oils affinity to the mineral surface then it can release the trapped oil from the mineral surface (Fogden et al. 2011). These mixed wet fines which have consistent interaction to both the oil phase and the smart water, ensures flow of residue oil along with the flooded water. Herein adhesion of these mixed wet mobile fines with residue oil causes release of trapped oil from the mineral surface (Fogden et al. 2011; Tang and Morrow; Nasralla et al. 2014) which leads to increased water wetness on the mineral surface (Strand et al. 2006).

It must be noted that the fines must remain mobile in the coreplug and should interact with the flooded water and the residue oil for increasing the displacement efficient of the oil (Tang and Morrow; Nasralla et al. 2014; Paper VII). In previous experiments there was also no EOR effect for cores that were initially 100% saturated with crude oil when fines were initially immersed in the oil phase (Tang and Morrow 1999). These fines did not interact with any flooded water and could therefore not form any adhesive complex between the two fluid phases. Development of mixed-wet fine particles, and change in colloidal forces with brine composition does not occur when the fines remain completely associated with a single fluid phase i.e. crude oil or brine. It was therefore suggested that adsorption from crude oil, the presence of mobile fines, and initial water saturation are all necessary prerequisite conditions for increase in oil recovery for salinity variations. As shown in Figure 4.13, this

observed recovery behavior in sandstone was ascribed to partial stripping of mixed-wet fines from pore walls during the course of waterflooding (Tang and Morrow 1999).

Adsorption onto surfaces in sandstone includes the outer surfaces of fine particles that coat the pore walls as illustrated in Fig. 8a (Tang and Morrow 1999). Electron microscopy has shown the distribution of the predominant kaolinite on sandstone grains (Fogden et al. 2011). While chalk coreplugs also have adsorbed Ca^{2+} /Mg^{2+} ions adsorbed on the calcite surface (Kerisit et al. 2004). Supersaturation of brine following ion substitution takes place when Mg^{2+} rich brine substitutes on this mineral surface (Paper V & VI). Due to supersaturation, insoluble fine particles are likely to nucleate on the available mineral surface. Therefore, the core will contain crude oil which adheres to fine particles, which during water flooding has two possibilities:

a. Crude oil can remain as drops which adhere to fines at pore walls as part of the trapped oil fraction. From cryo-microscopic analysis (Robin et al. 1991), it has been reported that residual crude oil consistently associate with patches of fines in the coreplug. An observed decrease in oil production rate for high precipitation in coreplug (static fines) also supports this.

b. The mixed-wet fine particles are stripped away from the pore walls by the flowing oil and tend to locate at the oil–water interface (Fig. 8b). Previous studies have also shown stable formation of mixed-wet particles at the oil/water interface (Muecke 1979).

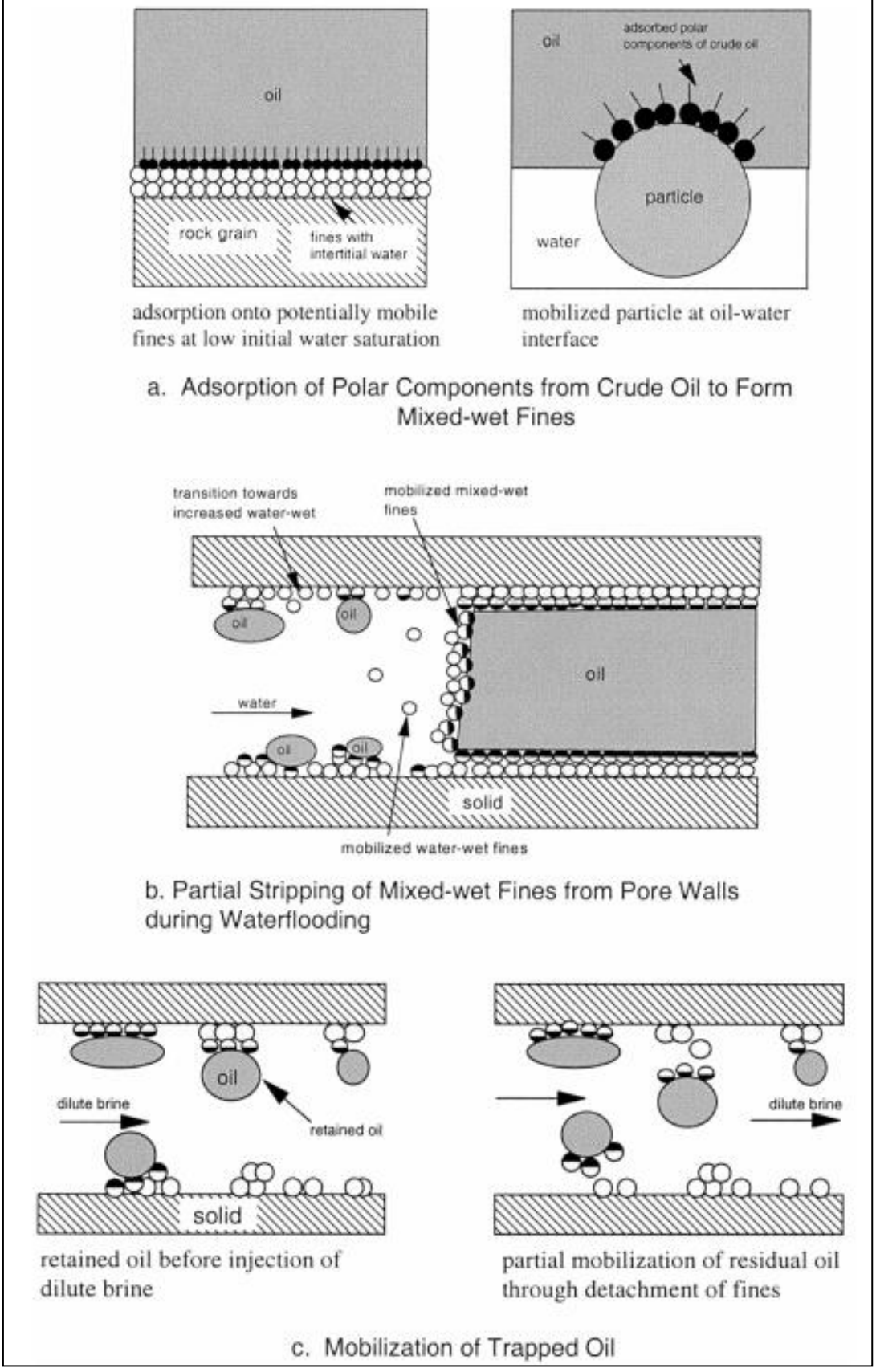


Figure 4.13: Role of mobile fines in crude oil/brine/rock interaction and increased oil recovery (Tang and Morrow 1999)

Israelachvili has shown that the forces which determine stripping of mixed-wet fines from pore walls depend on a balance between mechanical and colloidal (DLVO) forces (Israelachvili, 1991). Mechanical forces include capillary forces, resulting from adhesion of crude oil to the fines, and viscous forces from the flooding water, which tend to promote stripping. Any mechanical barrier to dislodgment will oppose stripping. Colloidal forces between fine particles will depend on the balance between van der Waals attractive forces and ion selective electrostatic repulsion. Consequently, the forces that govern the stability of colloids also come into play in the displacement of oil. The ion substitution and fines formation alters the forces on the mineral surface when brine 1 (mostly sea water) is injected. But, after continuous flooding a preferential flow path is developed in most fractured low permeability oil fields (Brown 1987). Thus Ca^{2+} ions on the pore walls of the preferential flow path gradually undergoes ion substitution by the Mg^{2+} ions of the injected brine as shown in Figure 4.14 (a).

A majority of the water flows through these preferential flow paths (Brown 1987). The injected (Mg^{2+} ions) brine therefore does not have the same extent of interaction with the remaining calcite pore walls.

When brines typically containing higher concentrations of potential ions (compared to sea water) are injected into the coreplug, formation of new insoluble salts take place on injection or after substitution (Paper V). These additional, newly formed fines are initially small grains which can flow through the porous network (Zhang et al. 2000). The mobile fines present in the flooded water form mixed-wet surfaces because of its natural adhesion of fines to oil (Muecke 1979). These fines therefore can enhance the adhesion on the oil water interface, thus leading to release of trapped oil from the mineral surface, and eventually making the surface water wet. The observed increase in wettability is caused by the increased adhesion between residue oil and mobile fines from imbibing fluid or flooded water (Tang and Morrow 1999). In case ion substitution doesn't take place (for the specific injection rate), then no fines formation take places and neither any increase in oil recovery is observed (Zahid et al. 2011) nor any variation in wettability is expected. For Rørdal outcrop chalks, spontaneous imbibition of $SW4SO_4$ neither led to any variation in mineral wettability nor was production of any additional oil observed (Fernø et al. 2011). These observations support the notion that the rate of ion substitution plays a major role in fines formation and displacement of oil.

Thus, the injection of additional fines forming smart water brines enhances the displacement efficiency of the residue oil. Furthermore, with continued flow and interaction of these mobile fines with the supersaturated brine solution, a gradual increase in grain size takes place (Wellman et al. 2003). After sufficient increase in size, fines eventually get stopped at the pore throats (As shown in Figure 4.14b). This leads to the formation of static fines in the pore space (Zhang et al. 2000). Formation of static fines blocks the pore throats and thus

forces the water to divert its flow from its initial preferential flow path (Nasralla et al. 2014). Therefore the sweep efficiency is altered and new surfaces for further ion substitution are made available (as shown in Figure 4.14c). When large amounts of water are flooded through these new surfaces, the interaction between Mg^{2+} ions and pore walls also increase (as recommended by Austad et al. 2009). Ca^{2+} in these new surfaces can undergo ion substitution because of the injected Mg^{2+} ions thus leading to new brine speciation and fines formation on the newly swept pore walls. These newly formed fines can also increase the adhesion between the flooded water and residue oil (Tang and Morrow 1999). When the forces at the oil-water interface (due to interaction with mobile fines) are greater than the corresponding adhesion on the mineral surface, the release of residue oil from these newly flooded regions, takes place. Thus, the mobility of oil is increased and eventually leads to enhanced oil recovery. After ion substitution in the pore walls is completed, further flooding of brine will produce no additional fines and thus this channel will also behave similar to the preferential flow paths. Static fines formation can still take place due to the gradual increase in grain size from the newly formed fines (Zhang et al. 2000). Formation of static fines can thereafter further alter the flow pattern of injected brine and produce new surfaces for ion substitutions and thus causing further water wetness and increased displacement efficiency of residue oil. Kinetics of fines formation and its rate of growth in the supersaturated brine solution in the pore space therefore play a major role in altering the sweep efficiency of the flooded water. Influence on reservoir permeability will be observed when static fines formation takes place in the reservoir. Expected precipitation because of existence of super saturated brines/mobile fines causes no alteration in the reservoir permeability.

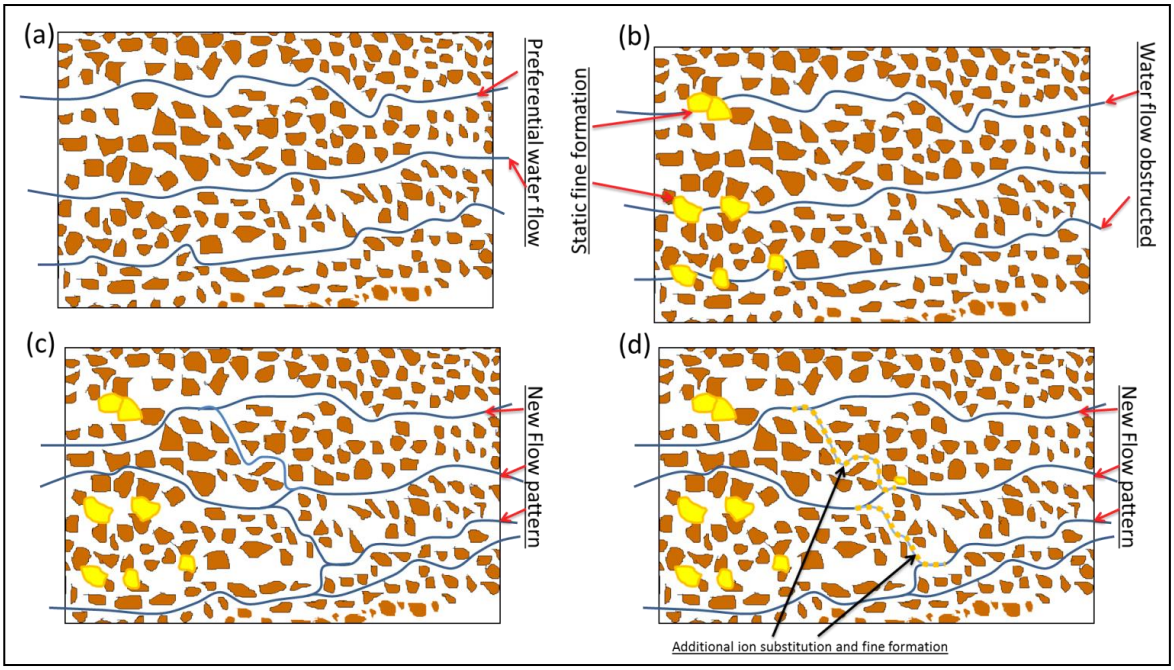


Figure 4.14: Schematic representation of water flow pattern alteration due to static fines: (a) initial preferential water flow established with flooded sea water (injection brine 1) (b) large static fines formations obstruct the flow of water along the traditional path (c) Water flow path altered leading to significant water foods through new regions (d) Fines formation following ion substitution further takes place along the pore walls.

For low salinity brine injection in sandstone, both (1) sweep alteration based on fines migration (Nasralla et al. 2014) and (2) mixed-wet fines based wettability alteration of mineral surface (Tang and Morrow 1999) have been recommended as possible mechanisms. Increasing oil recovery with a decrease in salinity gives possibility of supersaturation; only mobilization of already present fines (clay) particles can take place in either case (Nasralla et al. 2014; Tang and Morrow 1999). Injection of high salinity brines in chalks consistently results in supersaturated solutions in the coreplug. Depending on the kinetics of growth in grain size these will eventually lead to enhanced oil recovery. As previously stated these fines can form mixed-wet particles when they are small and mobile (Tang and Morrow 1999). This results in an increase of the adhesion at the oil/water interface. The increase in grain size results in static fines which can alter the flow pattern and the sweep efficiency of the injected brine as previously proposed for sandstones (Nasralla et al. 2014). The existence of supersaturated brine results in the continued growth of fines and allows fines to behave both as felicitator and obstructer of fluid flow depending upon their size in porous chalk reservoirs during smart water flooding.

4.5 Precipitation on injection and after substitution

Formation of small fines particles of insoluble salts can take place when the brine solution is supersaturated. The kinetics depends on the availability of a surface for nucleation and on the flow rate of the supersaturated brine (Zhang

et al. 2000). Recommended brines for injection into North sea chalk reservoirs (SW0NaCl-nSO_4 ∀ n= 2, 3 and 4) (Puntervold et al. 2014), are shown to supersaturate at reservoir condition (Paper IX). Therefore injection brines (like SW0NaCl-nSO_4 ∀ n= 2,3,4) will form insoluble salt grains near the point of injection. These insoluble salts can either form in the injection pipes or near the injection point in the reservoir. All injected water will pass through the particular injection well and the same pipe line and injection region. Grain formed due to supersaturation will be continuously interacting with major fractions of the injected supersaturated water. This allows a quick growth of the insoluble salt grains. All of the injection brine become supersaturated at the same temperature (thus same region) in the pipe line, and follows a similar kinetics when injected into the coreplug (Pruess and Müller 2009). Therefore, the growth of these insoluble salt nuclei and their precipitation will always take place near the injection point. The kinetics of this process therefore needs further attention. Unlike precipitation on injection, a supersaturated solution produced as a result of ion substitution has a very different kinetics as described below.

a. The brine injected in a reservoir gets diverted in different directions in the porous network. Therefore, the amount of brine flowing through a specific pore space in the reservoir is much less than the amount passing through the injection pipe or the injection region. Thus, the fines formed in the reservoir are in contact with smaller volumes of supersaturated brines. Therefore, the grains of insoluble salts likely have a relatively low growth rate.

b. Once ion substitution has completely taken place at a specific pore wall, the pore wall becomes inert to further flow of brines and thus promotes no growth of the insoluble salts. Precipitation of salts on injection is a property of the brine and is independent of ion substitution. Continued flow of brine through the injection point consistently creates supersaturated solution (because of increase in temperature) thus continuous formation of insoluble precipitated grains will take place specifically near the injection point.

c. After continued injection, the precipitation of additional insoluble salt (or fines formation) only takes place when a new surface is accessed (either through wettability alteration or by alteration of the sweep efficiency). Thus, fines formation following ion substitution takes place throughout the flooded pore space in the reservoir, and no specific region can be selected.

d. Fines formation can also take place because of mixing of injection brine with formation brine, or mixing of two injected brines. Dissolved sour gases like CO_2 in carbonated water also affect the solubility and cause fines formation. In coreplug experiments, the temperature and pressure of the

coreplug are often altered. Each of these phenomena can cause supersaturation of brine in the entire flooded region of the reservoir, and not at any specific location. Therefore small insoluble fine particles start forming throughout the reservoir with continued flooding. Thus forming mobile fines and enhancing oil displacement.

e. The mobile fines formed from smart water flooding are likely to gradually interact with each other and with the supersaturated brine. As a result, the fines will increase in size and eventually form static fines. Since these fines are formed throughout the reservoir, static fines will remain spread in the flooded regions of the reservoirs. North Sea reservoir chalks are known for their Medium-high porosity and yet low permeability porous network, constituting very small pore throats of 10 nm to 100nm (D'Heur 1984). Therefore fines are likely to get blocked at pore throats after their initial growth (10 nm to 100nm). Thus small grains of static fines are likely to be observable throughout the reservoir. This ensures that even the static fine grains forming in the reservoir are likely to remain separated and no specific region can be selected where static fines are likely to get accumulated.

Precipitation on injection is region specific and associated with quick growth. A large amount of precipitation on injection can also choke coreplugs and thereby have a negative influence on oil recovery. Consequently, if precipitation on injection is greater than that after ion substitution, then the expected increase in oil recovery for injection of high potential ions is no longer observed. Thus only the amount of fine formation taking place after ion substitution shows a one-to-one correlation to the oil recovery for high potential ion containing brine as well.

It must be noted that precipitation on injection takes place near the injection area; fines formation takes place throughout the reservoir. Both have an associated kinetics of growth of its grain size. In coreflooding studies, the injection point and the rest of the coreplug are not at distances corresponding to reservoir conditions. So a greater overlap of the two kinetic patterns is more likely to take place in a coreplug study. In reservoir flooding, the precipitation on injection would take place near the injection point and only the soluble salts will move into the reservoir. And following ion substitution (Austad et al. 2009), these soluble salts will get supersaturated; form fines (Paper V), and follow their own growth kinetics (Zhang et al. 2000).

At reservoir scale, precipitation on injection takes place near the injection point, while fine formation takes place throughout the reservoir whenever a new surface is available. In reservoirs, the injection point and reservoir pore space are separated over hundreds of meter. Also the fine forming brine may have been injected several months or years ago. Thus the injection precipitation shall have taken place considerably prior to the fine formation.

Therefore the influence of precipitation on injection over precipitation after ion substitution is limited as they are separated over large distances and time. In core plugs the injection point and a new pore space in the core plug are few millimeters away so the precipitation on injection can have a major influence on fine formation kinetics. Typically 1 PV/day to 5 PV/day is injected in a core plug. The fine forming brine is only supersaturated for a few hours. Because of close proximity in both time and distance in core flooding experiments, the kinetics of precipitation on injection can have a considerable effect on fine formation following ion substitution.

Therefore the influence of precipitation on injection will have relative much less influence on fines formation taking place in the entire flooded region (because of separation over distance) at reservoir scale than at coreplug scale as the injection point and the flooded region remain in close proximity of each other at coreplug scale.

Besides fines formation, there are other parameters influencing the final oil recovery. It has been shown through DFT calculation (Paper I) that adsorption of Mg^{2+} on calcite surfaces releases energy which can desorb corresponding carboxyl from the mineral surfaces. Ion substitution causes a change in mineral properties (from $CaCO_3$ to $CaMg(CO_3)_2$), which also decreases the adhesion between crude oil and mineral surface. Therefore, injection of Mg^{2+} (in absence of SO_4^{2-} or fines formation) can also cause a minor increase in oil recovery. Imbibition of brines with soluble salts like $SW0SO_4$+Mg^{2+} (i.e. sea water without SO_4^{2-} but with added Mg^{2+}), have shown to alter oil recovery (Zhang et al. 2006). But compared to fines forming brines like SW4S+Mg (which produced 62 % of OOIP at 130°C), brines with soluble salt $SW0SO_4$+Mg (produced 27% of OOIP at 130°C) had significantly smaller effect on the displacement efficiency of oil. Furthermore, instead of injecting pure NaCl brine (dominant in sea water), injection of a brine with dissolved $CaCl_2$ has been shown to alter the oil production (Ligthelm et al. 2014). Minor oil recovery variations have been observed for various soluble salts concentration in the water flooding experiments as well (Paper XI and XII). Soluble salts can also alter the forces at the oil water interface. In the presence of fines, the effect of soluble salts has therefore been studied in Paper III. Injection of large amounts of $MgCl_2$ dissolved in sea water after completely removing all NaCl will be significantly more expensive than injecting brines with high concentration of potential ions (Yousef and Ayirala 2014).

When water flooding is conducted at higher temperature, the increase in temperature causes adsorbed carboxyl groups to be more readily desorbed following adsorption of Mg^{2+} ions on calcite surfaces (Paper 1, Figure 9), This desorption of carboxyl groups also promotes the mobility of oil and effects final oil production as previously observed (for SW0S-Mg RezaeiDoust et al. 2009).

Instead of water flooding at higher temperature core plugs can be aged at a higher temperature in Ca^{2+} rich brine. Aging under these conditions also leads to higher adsorption of oil (Paper 1; Zhang et al. 2005). Thus aging coreplugs at high temperature creates strong mineral adhesion between surface polar fractions of oil. If imbibition experiments are subsequently performed at lower temperature it will show that oil production is adversely affected due to the high adhesion between mineral surface and polar oil fractions (Zhang et al. 2005). But these parameters, including aging temperature and aging time can only be altered in laboratory scale core plug experiments. In field scale implementations, these parameters remain specific to the reservoir and cannot be changed as the reservoir oil has already aged over millions of years at specific temperatures.

For mimicking specific oil fields, recovery parameters such as aging temperature and crude oil properties should be the same as the reservoir conditions so that realistic water flooding can be conducted (Zhang et a. 2006). Optimum aging through resistivity monitoring should also be conducted (Paper X), to ensure that reservoir wettability is attained. During field specific implementation properties such as injection rate and brine speciation can be easily altered. Before reservoir scale implementation such properties should be further studied in laboratory experiments. Parameters such as core plug lithology, pressure, temperature (both flooding and aging), formation brine, and aging time shall anyways remain constant for a given reservoir. The variation of some of these parameters in laboratory investigations before field specific implementation may not be equally important.

Conclusion and Future Scope of work

Fines formation and the correlation of fines formation to oil recovery is a new finding of this study. Based on the available experimental evidence (Austad et. al. 2005; Fernø et al. 2011; Zahid et. al. 2010; Gupta et al. 2011; Alvardo et al. 2014; Tang and Morrow 1999; Nasralla et al. 2014) Extended UNIQUAC calculations were performed. The results were compared to other previously proposed mechanisms and an impression of the possible behavior of soluble salts and fines was found. The results have been explained in the above mechanism. The observed correlation is based on previous literature reports (Zhang et al. 2006, Zahid et al. 2010; Faithi et al. 2010; Faithi et al. 2011; Strand et al. 2006) and geochemical modelling. This proposed mechanism should be scrutinized from, petrophysical, geological, and flow behavior angles. Particularly the grain size of the formed fines, their distribution in the coreplug (during and after flooding) and their exact pattern of interaction with the residue oil are phenomena which require further experimental investigations.

For further exploring fines behavior and understanding the mechanism, the following experimental and simulation studies are recommended.

5.1 Scrutinizing fines based SW-EOR mechanism

a. It must be noted that (unlike clay bearing sandstone) Micro CT-scan/SEM analysis of chalk coreplugs during smart water flooding at reservoir condition to study fines-oil interaction, during enhanced oil recovery remains unexplored. Attempts of CT-scan studies during the conducted water floods (Paper XI, Figure 6) were made. The image resolution obtained was not sufficient to identify and oil, brine and fine fractions. To obtain high resolution images Micro-CT/Nano-CT scans and SEM analysis of chalk coreplugs (like it was done with sandstone (Fogden et al. 2011) are recommended. For obtaining optimum information about the correlation between oil recovery and fine formation, these analyses should be conducted before, during and after flooding.

b. The emulsification experiments were conducted with micro size clay, anhydrite and carbonate fines. In low permeability chalk reservoirs, the pore throats can be much smaller (Teufel et al. 1991). Therefore, nano size fines particle analysis can also be conducted to further study the fines-oil interactions at more realistic reservoir conditions. No correlation has been established between oil production during smart water floods and observed alkane selectivity during micro fines based oil emulsification. In low permeable tight reservoirs of North Sea only nano scale fines can pass through the tiny core plugs (D'Heur 1984). Therefore the alkane selectivity during emulsification with nano size fines should be studied, for mimicking fines interactions in tight reservoirs of North Sea.

c. NMR studies are consistently used for wettability and petro physical measurements of rock properties (Johannesen et al. 2006). The T2 relaxation time during Low field NMR completely depends on the relative distance of protons from the mineral surface (Johannesen et al. 2006). During emulsification, fines (or small mineral grains) are in close distance to both proton sources oil and water (Tang and Morrow 1999). Therefore the T2 distribution due to the spin relaxation of proton from water and oil should be studied for fines based oil emulsions. And following the individual study of emulsions, their influence in coreplug Low NMR studies can be further considered. This method may also be beneficial in identifying emulsion formation in core plugs during smart water floods.

d. It must also be noted that all emulsification and fines formation due to the smart water flooding is largely dependent on the degree of ion substitution (Austad et al. 2009) that takes place in the pore space. It is depending on the injection rate and the coreplug properties. Therefore, detailed investigation of the extent of ion substitution vs injection rate must be studied individually for each oil field. In oil fields that are presently being flooded with sea water, the existing effluent brine data from produced water and data from previous flooding experiments with coreplug from the same oil field can be used to obtain information on the extent of ion substitution vs injection rate variation. Previously conducted regular core flooding experiments with sea water can also be used for determining the extent of ion substitution in the specific field, as ion substitution takes place even when normal sea water is injected in chalk coreplugs.

e. Studying the kinetics of growth of fines in the reservoir is also very important. If mobile fines grains grow very quickly compared to reservoir pore throats then they will quickly form static fines. As a result, oil particles will remain segregated from the preferential flow paths, thus oil recovery may not be observed even though ion substitution took place.

Observed increase in water wetness without associated increase in oil recovery for spontaneous imbibition experiment at 130°C for Niobara Chalks (US) also indicates the same (Fernø et al. 2011).

f. The porous network of chalk reservoirs is much different from Berea sandstone reservoirs, with much smaller pore throats and lower permeability (Alvardo et al. 2014; Ligthelm et al. 2009, Strand et al. 2006). Therefore the flow behaviors of the fines in chalk reservoirs are likely to be much different. Darcy equation based flow behavior modelling (Blunt et al. 2002) of fines and its interaction with oil also needs to be conducted to predict the flow properties during smart water floods. Micro-CT scan images obtained during water flooding, and with experimental/simulation information on kinetics of fines formation and its growth will be important inputs which should be considered for developing a realistic model of smart water floods. Herein ions substitution based fines flow behavior in both imbibition and water flood studies needs further attention.

g. In Advanced Ion Management studies, the uses of phosphate and borate ions have been shown to increase oil production (Gupta et al. 2012). Extended UNIQUAC correlation of oil recovery to fines formation for these brines also remains undone and therefore its correlational analysis is recommended for examining the mechanism.

h. Both the soluble ions and the polar fractions of crude oil have a tendency to be adsorbed on the mineral surface (Jabbar et al. 2013). In static conditions, the relative adhesion between the two determines the wettability. Amott-Harvey-index and contact angle measurements are used to study this wettability analysis (Jabbar et al. 2013; Standnes and Austad 2000). In flooding condition, mobile fines adhesion at oil/water interface acts against the trapped oil's adhesion to the calcite surface, thus promotes increased wettability (Tang and Morrow 1999). But in static condition, during contact angle measurements fines can sit on both the mineral surface and at the oil water interface and thus can have opposite effects. Therefore experiments to study the effect of fines during static wettability should be conducted. Available data on contact angle measurements for different smart water brines should be thereafter correlated.

5.2 Implementation of fines based SW-EOR

Important points where further studies can be conducted for implementation of SmW-EOR have also been identified. During implementation of SmW-EOR there is a major challenge of obtaining cheap smart water in near offshore oil

rigs. Future research recommendation for cheap smart water is addressed in this section.

Low Salinity-EOR can increase oil production from most sandstone reservoirs and certain chalk reservoirs (RezaeiDoust et al. 2009). It can be implemented both individually and with other EOR methods (surfactant flooding and WAG-CO_2). The general process of obtaining low salinity water is by doing reverse osmosis of sea water, which is an expensive, energy consuming process. In smart water EOR the suggested alterations to seawater, like SW0NaCl (sea water without NaCl) and SW0NaCl-4SO_4 (sea water without NaCl and 4 times SO_4^{2-} concentration) are more difficult to produce from seawater (Zahid et al. 2011). Moreover, bringing tons of chemicals offshore is also not economically viable (RezaeiDoust et al. 2009; Zahid et al. 2011; Austad et al. 2009; Gupta et al. 2012).

An alternative way of achieving desalination of seawater is through iron fertilization. Iron fertilization is the intentional introduction of iron to the upper ocean and sea areas to stimulate a phytoplankton algal bloom (Moore et al. 2006). It is intended to enhance biological productivity, which can increase carbon dioxide removal from the atmosphere. Iron is a trace element necessary for photosynthesis in all plants. Iron is highly insoluble in seawater and it is often the limiting nutrient for phytoplankton growth. Large algal blooms can be created by supplying iron to iron-deficient waters (Moore et al. 2006). A number of ocean labs, scientists, and businesses are exploring fertilization as a means to sequester atmospheric carbon dioxide in the deep ocean, and to increase marine biological productivity. Since 1993, thirteen international research teams have completed ocean trials demonstrating that diatoms blooms can be stimulated by iron addition (Moore et al. 2006). However, several questions have been raised over its adverse impact in marine ecology (Stewart and Hessami 2005). It has been suggested to remove these phytoplankton algae, which becomes economically unfeasible for major implementations.

The two technologies individually have major application challenges but when combined together can produce a value chain where the waste product of one process can be used in another process as a primary input source. There has been no previous study that has explored the parallel implementations of these two technologies.

5.2.1 Hypothesis

Algae like spirulina contain significant amounts of NaCl, while it can only grow in Ca^{2+} and Mg^{2+} depleted sea water. Their NaCl consumption will cause a decrease in salinity of seawater. This low NaCl, high Ca^{2+}, Mg^{2+} when injected in carbonate petroleum reserves is known for increasing oil production from carbonate reservoirs (RezaeiDoust et al. 2009). Thus, instead of doing

expensive energy consuming reverse osmosis of seawater, low saline water (produced after filtration of salt rich algae) can be directly injected into reservoirs for EOR processes. If specific useful algae like spirulina are grown during iron fertilization the produced algae will (when brought on land for the designated purposes) automatically recycle the phosphorus present in seawater which otherwise would eventually be settled in the oceanic bed.

It must be noted that Phosphorus is a vital element for life with no available or prospective biological or technological substitutes (Childers et al. 2011). Phosphate rock (P-rock) fertilizers currently dominate the Phosphorus supply for agriculture. However, in a period ranging from 50 to 100 years, depending on the study (Cordell et al. 2009; Dawson and Hilton 2011) the reserves of this mineral are estimated to be depleted. Thus, insufficiency is likely to increase phosphate production costs by a factor 3 to 5 times in this century (Dawson and Hilton 2011) and geopolitical disputes might also influence both the cost and availability. In European Union presently, only about one-fourth of the phosphorus applied to agricultural fields is actually recycled (Childers et al. 2011). Moreover, phosphate-rock fertilizers have caused an increase in heavy metal concentrations like cadmium in soils over the last decades (McBride and Spiers 2001; Mar and Okazaki 2012). For all these reasons, innovative recycling and technologies need to be developed and implemented.

In sea water regions with high nutrient content, low chlorophyll zones adding small amounts of iron (measured by mass parts per trillion) can trigger large phytoplankton blooms. Recent marine trials suggest that one kilogram of fine iron particles may generate over 100,000 kilograms of plankton biomass (Moore et al. 2006; Stewart and Hessami 2005). These planktons are suggested to have affected the ecology in sea and oceanic environment. Removal of these algae from the sea becomes a costly process and thus addressing the ecological challenges remains an issue. Moreover, iron fertilization studies primarily aim at optimizing the amount of plankton growth. But several algae (like spirulina) are edible for humans and other animals on earth (Keskinkan et al. 2004). Thus, removal of them from the sea water becomes advantageous as it provides an additional feeding value for humans and animals. Spirulina, when grown on lakes on-shore, has a tendency of absorbing heavy metal with it, which makes the algae toxic for human consumption (Keskinkan et al. 2004) and maintaining high standard of monitoring becomes important. However, seawater is depleted of heavy metals since they are insoluble in water. The absence of heavy metals ensures that the produced spirulina during iron fertilization will be able to meet high food quality standards.

Thus, seawater desalination through iron fertilized algae productions could be a financially and ecologically sound alternative to existing methods.

5.2.2 Recommended Experiments and Modeling

The initial scope of the study may be limited to laboratory experiments and UNIQUAC modelling to test the stated hypothesis and possibly create awareness on its field implementation. It includes three major sections as stated below.

a. High-Nutrient, low-chlorophyll zones have been identified as possible locations for Iron fertilization (Minas and Minas 1992). Current and possible hydrocarbon reserves have also been identified and confirmed by using seismic and geophysical modelling. Using the Extended UNIQUAC model, brine speciation calculations at high pressure and temperature conditions can be conducted (Thomsen and Rasmussen 1999) to identify all synergies' location in the sea, wherein both iron fertilization and oil production can be simultaneously conducted. Some prospective regions where both nitrate concentration is high (thus suitable for engineering an algal boom) and oil is presently being produced. Some possible oil fields are listed below:

    i. Corvina oil and gas field in South Pacific ocean in the offshore of Peru (Freire 1989)
    ii. Cook inlet oil field in Gulf of Alaska in the offshore of United States (Fisher and Magoon 1978)
    iii. Chinguetti oil field in South Atlantic ocean in the offshore of Mauritania(Africa) (Colman et al. 2005)
    iv. Dan field in North Sea in the offshore of Denmark (Jorgensen 1992)
    v. Sea of Okhotsk (no oil production presently) near Sakhalin Island at the offshore of Russia
    vi. Further analysis shall provide target location in the offshore sea surface for which experimental studies can be performed.

b. To specific seawater, iron fertilization experiments can be conducted to produce algal boom (Moore et al. 2006) which also alter selective ion composition in sea water. In this modified seawater, various salt eating and/or edible algae can be produced. This phytoplankton can be thereafter filtered out and the changes in salinity of the brine will be recorded using ICP-MS analysis. Possible fines formation at reservoir conditions due to mixing of these brines with seawater can thereafter be modeled using the Extended UNIQUAC. This experimental and modeling study can be iterated multiple times to produce optimum conditions for phytoplankton growth and possible EOR.

c. Standard core flooding experiments with these modified brines can be thereafter conducted. Any observed increase in oil recovery following injection of modified seawater will verify the hypothesis that iron fertilization can be used as a tool to increase the oil production and

sequestrate CO_2 at the same time. This can not only produce cheap smart water for EOR implementation but growth of edible algae like spirulina during this process shall provide a sea cultivation and phosphorus recycling technique.

5.3 Conclusion

In this study, geochemical modeling of salt solubility at reservoir conditions and with correlation to the oil recovery has been studied. Based on which the following conclusions have been made:

a. Through DFT based molecular dynamic calculation; it has been observed that substitution of Ca^{2+} by Mg^{2+} on the mineral surface can take place. At reservoir conditions, the feasibility of ion substitution is further enhanced with increase in core plug temperature. It has been observed that ion substitution on mineral surfaces may not necessarily cause changes in the mineral lattice and only adsorbed Ca^{2+} ions may be replaced from the mineral surface. This ion substitution leads to an increase in Ca^{2+} concentration in the pore space, which can change the brine speciation.

b. Brine speciation variation can lead to formation of insoluble salts and therefore the behavior of insoluble salts with crude oil and different brine composition has been studied. It has been observed that water insoluble acid/amine (polar) fractions of crude oil interact with insoluble salt to from soluble emulsions. For various compositions of alkanes (carboxyl) acids and (amines) bases these emulsions have been observed. All possible fines including carbonates, sulfates, and clay promotes the formation of oil emulsions in water. Fines and polar hydrocarbons must be available in the crude oil and water for any such emulsion formation. The observed pattern of emulsification with model fines and design oil were also observed for reservoir fines and crude oil from the Dan field of the North Sea. The emulsification amount varies with the types of acids present in the oil, therefore no direct correlation between acid number and fines-oil emulsion is observed. Available soluble fractions of $Ca^{2+}$and Mg^{2+} ions are the most useful cations in enhancing the amount of fines based-oil emulsion formation. Among anions $SO_4^{2-}$and HPO_4^{2-} was found to considerably increase the oil emulsion formation. This emulsification therefore indicates an increase adhesion at the oil water interface with release of residue oil from the mineral surface.

c. Subsequently, extended UNIQUAC model based solubility calculations have been conducted to explore the correlation between fines formation and oil recovery for 128 core plugs. It has been observed that in previous core flooding/imbibition experiments, properties of the injection brine

have been used during interpretation of the observed oil recovery. But the composition and properties of the injected brine can get significantly altered on ion substitution on the mineral surface. Therefore the interacting brine present in the pore space – after substitution – has been correlated with the reported oil recovery. Calculations using Extended UNIQUAC model show that Mg^{2+}/Ca^{2+} substitution can alter the brine properties significantly and fines formation through supersaturation of $CaSO_4$ is significantly enhanced. Fines formation can take place because of multiple reasons including:

i. Change in brine speciation following ion substitution on the mineral surface
ii. Interaction between two individually soluble injected brine compositions
iii. Variation in pressure/temperature condition of the core plug during imbibition experiment
iv. Existence of soluble CO_2(aq) causes dissolution of $CaCO_3$ followed by anhydrite formation
v. Pause and reinjection of Na and Mg salts causes attrition based $CaCO_3$ fines formation
vi. For all of these 5 cases, solubility at reservoir condition has been studied and thereafter has been co-related to the total oil recovery reported in the literature including 128 core flooding experiments. Studies have shown consistently good correlation between oil production and amount of fines formation. But the soluble SO_4^{2-} fraction at reservoir condition, (speciation after ion substitution) only partially correlates with the observed oil recovery. This study also shows that the observed wettability alteration (to water wetness) could be an effect and not the primary cause of SmW-EOR.

d. Various studies from literature reports the effluent brine compositions measured at ambient conditions and attempts to directly correlate these to the oil recovery. Reanalyzing these brine compositions at experimental/reservoir conditions show that substantial quantities of fines were released from the core plugs. As temperature and pressure decreased to ambient conditions, the produced fines were dissolved in the effluent water. Cases with unaccounted fines at flooding conditions directly correlated (as dissolved ions) to oil recovery were reported for the following types of experiments:

i. Rock type: chalk, limestone and dolostone
ii. Core plug type: outcrop and reservoir core plug
iii. Flooding type: spontaneous imbibition and water flooding experiment
iv. EOR strategy: low salinity, smart waterfloods and advanced ion management
v. Rock origin: Middle East, North Sea and United States

vi. This observed co-relation between produced fines and oil recovery show that insoluble salts can pass through the pores network and be produced in the effluent. Thus, the real amount of soluble ions produced from the core plug at flooding/imbibition conditions is less than that at room temperature and is mistakenly overestimated. Furthermore, only a fraction of the supersaturated salts actually precipitates in the core plug, and correspondingly precipitation can also be overestimated.

e. In the literature, precipitation of salts during water flooding has been perceived to have a negative impact on the oil production. Therefore, the amounts of precipitation for different core plugs have been studied. It has been observed that a large amount of precipitate can produce significantly high oil recovery in many cases. But in some cases, high precipitation of salt has an adverse effect. This shows that precipitation has no clear inverse correlation to the observed increase in oil recovery; while the amount of fines formation taking place after ion substitution in the reservoir shows consistent co-relation to oil recovery for highly precipitating brines as well. Here, a significant distinction has been made between precipitation at injection and fines formation in the reservoirs.

f. Water flooding experiments have been conducted and thorough continuous core plug resistance measurements of variation in wettability during aging has been monitored. Observed oil recovery show that pausing the water floods can cause attrition of insoluble calcite based fines production from the coreplug. This release of fines formed from the core plug shows consistent correlation to the increase in oil recovery. Following pauses/reinjections, increases in oil recovery were consistently observed for both high temperature (130°C; EOR of 5.1% of OOIP) and low temperature (60 °C; EOR of 17.8% of OOIP) water floods. Similar pause based water flooding experiment conducted for sandstone does not show a major increase in oil recovery. This indicates that following ion substitution, insoluble fines formation through attrition of $CaCO_3$ is the primary parameter related to the observed EOR.

g. Based on these studies, the optimum amount of fines formation has been calculated for different conditions and prospective fines formation based mechanism has been proposed. For optimum use of both ion substitutions based fines formation and mixing based fines formation, the use of core slab flooding equipment has been proposed. In particular, it can be used for analysis of core flooding experiments for Dan field block A in the Danish North Sea. Speciation properties of all commonly used smart water floods have been calculated and various pressure/temperature conditions and amount of fines precipitate and soluble ions have been reported.

These studies collectively show that fines formation have a good co-relation to oil recovery and therefore further experiments have been proposed to scrutinize the proposed mechanism and develop further understanding of the same.

References

- Abrams, D. S., & Prausnitz, J. M. (1975). Statistical thermodynamics of liquid mixtures: a new expression for the excess Gibbs energy of partly or completely miscible systems. AIChE Journal, 21(1), 116-128.
- Adamson, A. W., & Gast, A. P. (1967). Physical chemistry of surfaces.
- Ahmed, T. (2006). Reservoir engineering handbook. Gulf Professional Publishing..
- Alder, B. J., & Wainwright, T. E. (1959). Studies in molecular dynamics. I. General method. The Journal of Chemical Physics, 31(2), 459-466.
- Alfe, D., & Gillan, M. J. (1998a). First-principles calculation of transport coefficients. Physical review letters, 81(23), 5161.
- Alfè, D., & Gillan, M. J. (1998b). First-principles simulations of liquid Fe-S under Earth's core conditions. Physical Review B, 58(13), 8248.
- Alfe, D., Gillan, M. J., & Price, G. D. (2002). Composition and temperature of the Earth's core constrained by combining ab initio calculations and seismic data. Earth and Planetary Science Letters, 195(1), 91-98.
- Allen, M. P., & O'shea, S. F. (1987). A Monte Carlo simulation study of orientational domain clusters in the planar quadrupole model. Molecular Simulation, 1(1-2), 47-66.
- Andersen, H. C. (1980). Molecular dynamics simulations at constant pressure and/or temperature. The Journal of chemical physics, 72(4), 2384-2393.
- Austad, T., RezaeiDoust, A., & Puntervold, T. (2010, January). Chemical mechanism of low salinity water flooding in sandstone reservoirs. In SPE improved oil recovery symposium. Society of Petroleum Engineers.
- Austad, T., Strand, S., & Puntervold, T. (2009, September). Is wettability alteration of carbonates by seawater caused by rock dissolution. In Paper SCA2009-43 presented at the International Symposium of the Society of Core Analysts held in Noordwijk, The Netherlands, September (pp. 27-30).
- Austad, T., Strand, S., Høgnesen, E. J., & Zhang, P. (2005, January). Seawater as IOR fluid in fractured chalk. In SPE International Symposium on Oilfield Chemistry. Society of Petroleum Engineers.
- Bachelet, G. B., Hamann, D. R., & Schlüter, M. (1982). Pseudopotentials that work: From H to Pu. Physical Review B, 26(8), 4199.

- Balbuena, P., & Seminario, J. M. (Eds.). (1999). Molecular dynamics: from classical to quantum methods (Vol. 7). Elsevier.
- Bennetzen, M. V., Mogensen, K., Ataman, E., & Andersson, M. (2014, November). A Predictive Model to Link Molecular Structures to Carbonate Rock Wettability: Adsorption of Various Organic Molecules on Flat and Rugged Calcite Surfaces. In Abu Dhabi International Petroleum Exhibition and Conference. Society of Petroleum Engineers.
- Bernard, G. G. (1967, January). Effect of floodwater salinity on recovery of oil from cores containing clays. In SPE California Regional Meeting. Society of Petroleum Engineers.
- Bird, G., Boon, J., & Stone, T. (1986). Silica transport during steam injection into oil sands: 1. Dissolution and precipitation kinetics of quartz: New results and review of existing data. Chemical geology, 54(1), 69-80.
- Boggs, Sam. Petrology of sedimentary rocks. Cambridge University Press, 2009.
- Born, M., & Oppenheimer, R. (1927). Zur quantentheorie der molekeln.Annalen der Physik, 389(20), 457-484.
- Bose, S., Mannan, R. M., & Arntzen, C. J. (1984). Increased synthesis of photosystem II in Triticum vulgare when grown in the presence of BAS 13-338. Zeitschrift für Naturforschung C, 39(5), 510-514.
- Brown, D. A. (1987). The flow of water and displacement of hydrocarbons in fractured chalk reservoirs. Geological Society, London, Special Publications,34(1), 201-218.
- Buckley, J. S., & Liu, Y. (1998). Some mechanisms of crude oil/brine/solid interactions. Journal of Petroleum Science and Engineering, 20(3), 155-160.
- Ceperley, D., & Alder, B. J. (1985). Muon–alpha-particle sticking probability in muon-catalyzed fusion. Physical Review A, 31(4), 1999.
- Chakravarty, K. H., Fosbøl, P. L., & Thomsen, K. (2015, June). Importance of Fines in Smart Water Enhanced Oil Recovery (SmW-EOR) for Chalk Outcrops. In EUROPEC 2015. Society of Petroleum Engineers.
- Chakravarty, K. H., Fosbøl, P. L., & Thomsen, K. (2015, November). Significance of Fines and their Correlation to Reported Oil Recovery. In Abu Dhabi International Petroleum Exhibition and Conference. Society of Petroleum Engineers.
- Chen, C. C., & Evans, L. B. (1986). A local composition model for the excess Gibbs energy of aqueous electrolyte systems. AIChE Journal, 32(3), 444-454.
- Chen, C. C., & Song, Y. (2004). Generalized electrolyte-NRTL model for mixed-solvent electrolyte systems. AIChE Journal, 50(8), 1928-1941.
- Chen, C. C., Britt, H. I., Boston, J. F., & Evans, L. B. (1982). Local composition model for excess Gibbs energy of electrolyte systems. Part I: Single solvent, single completely dissociated electrolyte systems. AIChE Journal, 28(4), 588-596.

- Childers, D. L., Corman, J., Edwards, M., & Elser, J. J. (2011). Sustainability challenges of phosphorus and food: solutions from closing the human phosphorus cycle. BioScience, 61(2), 117-124.
- Christensen, S. G., & Thomsen, K. (2003). Modeling of vapor-liquid-solid equilibria in acidic aqueous solutions. Industrial & engineering chemistry research, 42(18), 4260-4268.
- Colman, J. G., Gordon, D. M., Lane, A. P., Forde, M. J., & Fitzpatrick, J. J. (2005). Carbonate mounds off Mauritania, Northwest Africa: status of deep-water corals and implications for management of fishing and oil exploration activities. In Cold-water corals and ecosystems (pp. 417-441). Springer Berlin Heidelberg.
- Cordell, D., Drangert, J. O., & White, S. (2009). The story of phosphorus: global food security and food for thought. Global environmental change,19(2), 292-305.
- Dandekar, A. Y. (2013). Petroleum reservoir rock and fluid properties. CRC press.
- Dang, C. T., Nghiem, L. X., Chen, Z., Nguyen, N. T., & Nguyen, Q. P. (2014, April). CO2 Low Salinity Water Alternating Gas: A New Promising Approach for Enhanced Oil Recovery. In SPE Improved Oil Recovery Symposium. Society of Petroleum Engineers.
- Darde, V., Maribo-Mogensen, B., van Well, W. J., Stenby, E. H., & Thomsen, K. (2012). Process simulation of CO 2 capture with aqueous ammonia using the Extended UNIQUAC model. International Journal of Greenhouse Gas Control, 10, 74-87.
- Dawson, C. J., & Hilton, J. (2011). Fertiliser availability in a resource-limited world: Production and recycling of nitrogen and phosphorus. Food Policy, 36, S14-S22.
- de Wijs, G. A., Kresse, G., Vočadlo, L., Dobson, D., Alfe, D., Gillan, M. J., & Price, G. D. (1998). The viscosity of liquid iron at the physical conditions of the Earth's core. Nature, 392(6678), 805-807.
- Debye, P., & Hückel, E. (1923). De la théorie des électrolytes. i. abaissement du point de congélation et phénomènes associés.Physikalische Zeitschrift, 24(9), 185-206.
- Elstnerová, P., Friák, M., Fabritius, H. O., Lymperakis, L., Hickel, T., Petrov, M.,& Neugebauer, J. (2010). Ab initio study of thermodynamic, structural, and elastic properties of Mg-substituted crystalline calcite. Acta biomaterialia, 6(12), 4506-4512.
- Ewing, W. W., & Rasmussen, H. E. (1942). The Temperature—Composition Relations of the Binary System Manganous Nitrate—Water. Journal of the American Chemical Society, 64(6), 1443-1445.
- Fanchi, J. (2010). Integrated reservoir asset management: principles and best practices. Gulf Professional Publishing.
- Fathi, S. J., Austad, T., & Strand, S. (2010). "Smart Water" as a Wettability Modifier in Chalk: The Effect of Salinity and Ionic Composition. Energy & fuels, 24 (4), 2514-2519.

- Fathi, S. J., Austad, T., & Strand, S. (2011). Water-based enhanced oil recovery (EOR) by "smart water": Optimal ionic composition for EOR in carbonates. Energy & fuels, 25(11), 5173-5179.
- Fernø, M. A., Grønsdal, R., Åsheim, J., Nyheim, A., Berge, M., & Graue, A. (2011). Use of sulfate for water based enhanced oil recovery during spontaneous imbibition in chalk. Energy & fuels, 25(4), 1697-1706.
- Fisher, M. A., & Magoon, L. B. (1978). Geologic framework of lower Cook inlet, Alaska. AAPG Bulletin, 62(3), 373-402.
- Fjelde, I. F., & Aasen, S. M. A. (2009, April). Improved spontaneous imbibition of water in reservoir chalks. In IOR 2009-15th European Symposium on Improved Oil Recovery.
- Fjelde, I., Asen, S. M., & Omekeh, A. V. (2012, January). Low salinity water flooding experiments and interpretation by simulations. In SPE Improved Oil Recovery Symposium. Society of Petroleum Engineers.
- Fogden, A., Kumar, M., Morrow, N. R., & Buckley, J. S. (2011). Mobilization of fine particles during flooding of sandstones and possible relations to enhanced oil recovery. Energy & Fuels, 25(4), 1605-1616.
- Fredenslund, A., & Rasmussen, P. (1986). Separations from dilute solutions: group-contribution methods. Fluid phase equilibria, 27, 347-372.
- Freire, W. (1989, January). Campos basin deepwater giant fields. In Offshore Technology Conference. Offshore Technology Conference.
- García, A. V., Thomsen, K., & Stenby, E. H. (2005). Prediction of mineral scale formation in geothermal and oilfield operations using the extended UNIQUAC model: part I. Sulfate scaling minerals. Geothermics, 34(1), 61-97.
- García, A. V., Thomsen, K., & Stenby, E. H. (2006). Prediction of mineral scale formation in geothermal and oilfield operations using the Extended UNIQUAC model: Part II. Carbonate-scaling minerals. Geothermics, 35(3), 239-284.
- Giannozzi, P., Baroni, S., Bonini, N., Calandra, M., Car, R., Cavazzoni, C & Dal Corso, A. (2009). QUANTUM ESPRESSO: a modular and open-source software project for quantum simulations of materials. Journal of Physics: Condensed Matter, 21(39), 395502.
- Gibson, J. B., Goland, A. N., Milgram, M., & Vineyard, G. (1960). Dynamics of radiation damage. Physical Review, 120(4), 1229.
- Green, D. W., & Willhite, G. P. (1998). Enhanced oil recovery; Henry L. Doherty Memorial Fund of AIME. Society of Petroleum Engineers: Richardson, TX.
- Gupta, R., Smith, G. G., Hu, L., Willingham, T., Lo Cascio, M., Shyeh, J. J., & Harris, C. R. (2011, January). Enhanced Waterflood for Carbonate Reservoirs-Impact of Injection Water Composition. In SPE Middle East Oil and Gas Show and Conference. Society of Petroleum Engineers.
- Haarberg, T., Selm, I., Granbakken, D. B., Ostvold, T., Read, P., & Schmidt, T. (1992). Scale formation in reservoir and production equipment during oil recovery: An equilibrium model. SPE production Engineering,7(01), 75-84.

- Hadia, N., Lehne, H. H., Kumar, K. G., Selboe, K. A., Stensen, F. Å., & Torsater, O. (2011, January). Laboratory Investigation of Low Salinity Waterflooding on Reservoir Rock Samples from the Fr? y Field. In SPE Middle East Oil and Gas Show and Conference. Society of Petroleum Engineers.
- Hafner, J. (2000). Atomic-scale computational materials science. Acta Materialia, 48(1), 71-92.
- Hamann, D. R., Schlüter, M., & Chiang, C. (1979). Norm-conserving pseudopotentials. Physical Review Letters, 43(20), 1494.
- Harvey, A. H., Copeman, T. W., & Prausnitz, J. M. (1988). Explicit approximations to the mean spherical approximation for electrolyte systems with unequal ion sizes. The Journal of Physical Chemistry, 92(22), 6432-6436.
- Hermansen, H., Landa, G. H., Sylte, J. E., & Thomas, L. K. (2000). Experiences after 10 years of waterflooding the Ekofisk Field, Norway.Journal of Petroleum Science and Engineering, 26(1), 11-18.
- Hill, A. E., & Miller Jr, F. W. (1927). Ternary Systems. IV. Potassium Carbonate, Sodium Carbonate and Water. Journal of the American Chemical Society, 49(3), 669-686.
- Hiorth, A., Cathles, L. M., & Madland, M. V. (2010). The impact of pore water chemistry on carbonate surface charge and oil wettability. Transport in porous media, 85(1), 1-21.
- Hohenberg, P., & Kohn, W. (1964). Inhomogeneous electron gas. Physical review, 136(3B), B864.
- Hoover, W. G. (1985). Canonical dynamics: equilibrium phase-space distributions. Physical Review A, 31(3), 1695.
- Iliuta, M. C., Thomsen, K., & Rasmussen, P. (2000). Extended UNIQUAC model for correlation and prediction of vapour–liquid–solid equilibria in aqueous salt systems containing non-electrolytes. Part A. Methanol–water–salt systems. Chemical Engineering Science, 55(14), 2673-2686.
- Iliuta, M. C., Thomsen, K., & Rasmussen, P. (2002). Modeling of heavy metal salt solubility using the extended UNIQUAC model. AIChE journal,48(11), 2664-2689.
- IVC-SEP Databank for Electrolyte Solutions <http://www.ivc-sep.kt.dtu.dk/databank> (2004).
- Jabbar, M. Y., Al-Hashim, H. S., & Abdallah, W. (2013, May). Effect of brine composition on wettability alteration of carbonate rocks in the presence of polar compounds. In SPE Saudi Arabia Section Technical Symposium and Exhibition. Society of Petroleum Engineers.
- Jadhunandan, P. P., & Morrow, N. R. (1995). Effect of wettability on waterflood recovery for crude-oil/brine/rock systems. SPE reservoir engineering, 10(01), 40-46.
- Jerauld, G. R., Webb, K. J., Lin, C. Y., & Seccombe, J. C. (2008). Modeling low-salinity waterflooding. SPE Reservoir Evaluation & Engineering, 11(06), 1-000.

- Jorgensen, L. N. (1992). Dan Field--Denmark Central Graben, Danish North Sea
- Karimi, M., Al-Maamari, R. S., Ayatollahi, S., & Mehranbod, N. (2015). Mechanistic study of wettability alteration of oil-wet calcite: The effect of magnesium ions in the presence and absence of cationic surfactant. Colloids and Surfaces A: Physicochemical and Engineering Aspects, 482, 403-415.
- Karoussi, O., & Hamouda, A. A. (2007). Imbibition of sulfate and magnesium ions into carbonate rocks at elevated temperatures and their influence on wettability alteration and oil recovery. Energy & fuels, 21(4), 2138-2146.
- Kerisit, S., & Parker, S. C. (2004). Free energy of adsorption of water and metal ions on the {1014} calcite surface. Journal of the American Chemical Society, 126(32), 10152-10161.
- Kerker, G. P. (1980). Non-singular atomic pseudopotentials for solid state applications. Journal of Physics C: Solid State Physics, 13(9), L189.
- Keskinkan, O., Goksu, M. Z. L., Basibuyuk, M., & Forster, C. F. (2004). Heavy metal adsorption properties of a submerged aquatic plant (Ceratophyllum demersum). Bioresource Technology, 92(2), 197-200.
- Kohn, W., & Sham, L. J. (1965). Self-consistent equations including exchange and correlation effects. Physical Review, 140(4A), A1133.
- Kulik, D. A., Berner, U., & Curti, E. (2003). Modelling chemical equilibrium partitioning with the GEMS-PSI code. PSI Scientific Report, 4, 109-122.
- Kunnas, J. (2012). LWSF simulation at larger scale.
- Lager, A., Webb, K. J., Black, C. J. J., Singleton, M., & Sorbie, K. S. (2008). Low Salinity Oil Recovery-An Experimental Investigation1.Petrophysics, 49(01).
- Lebedeva, E., Senden, T. J., Knackstedt, M., & Morrow, N. (2009, April). Improved oil recovery from Tensleep sandstone–studies of brine-rock interactions by micro-CT and AFM. In IOR 2009-15th European Symposium on Improved Oil Recovery.
- Ligthelm, D. J., Gronsveld, J., Hofman, J., Brussee, N., Marcelis, F., & van der Linde, H. (2009, January). Novel Waterflooding Strategy By Manipulation Of Injection Brine Composition. In EUROPEC/EAGE Conference and Exhibition. Society of Petroleum Engineers.
- Lorimer, J. W. (1993). Thermodynamics of solubility in mixed solvent systems. Pure and applied chemistry, 65(2), 183-191.
- Mackay, E. J., & Martins de Souza, A. P. (2014, May). Modelling of CO2 and Seawater Injection in Carbonate Reservoirs to Evaluate Inorganic Scaling Risk. In SPE International Oilfield Scale Conference and Exhibition. Society of Petroleum Engineers.
- Madland, M. V., Zangiabadi, B., Korsnes, R. I., Evje, S., Cathles, L., Kristiansen, T. G., & Hiorth, A. (2009, April). Rock Fluid Interactions in Chalk with MgCl2 and Na2CI4 Brines with Equal Ionic Strength. In 15th European Symposium on Improved Oil Recovery.

- Mar, S. S., & Okazaki, M. (2012). Investigation of Cd contents in several phosphate rocks used for the production of fertilizer. Microchemical Journal,104, 17-21.
- Marshall, W. L., Slusher, R., & Jones, E. V. (1964). Aqueous Systems at High Temperatures XIV. Solubility and Thermodynamic Relationships for CaSO4 in NaCl-H2O Solutions from 40° to 200° C., 0 to 4 Molal NaCl.Journal of Chemical & Engineering Data, 9(2), 187-191.
- McBride, M. B., & Spiers, G. (2001). Trace element content of selected fertilizers and dairy manures as determined by ICP–MS. Communications in Soil Science and Plant Analysis, 32(1-2), 139-156.
- McGlynn, E. (1996). a photoluminescence study of cadmium and aluminium-related defects in silicon (Doctoral dissertation, Dublin City University).
- McGuire, P. L., Chatham, J. R., Paskvan, F. K., Sommer, D. M., & Carini, F. H. (2005, January). Low salinity oil recovery: An exciting new EOR opportunity for Alaska's North Slope. In SPE Western Regional Meeting. Society of Petroleum Engineers.
- Megawati, M., Madland, M. V., & Hiorth, A. (2015). Mechanical and physical behavior of high-porosity chalks exposed to chemical perturbation. Journal of Petroleum Science and Engineering, 133, 313-327.
- Melberg, E. (2010). Experimental study of low salinity EOR effects from the Varg field.
- Mermin, N. D. (1965). Thermal properties of the inhomogeneous electron gas. Physical Review, 137(5A), A1441.
- Minas, H. J., & Minas, M. (1992). Net community production in high nutrient-low chlorophyll waters of the tropical and Antarctic Oceans-grazing vs iron hypothesis. Oceanologica Acta, 15(2), 145-162.
- Moghadasi, J., Jamialahmadi, M., Müller-Steinhagen, H., & Sharif, A. (2003a, January). Scale formation in oil reservoir and production equipment during water injection (Kinetics of CaSO4 and CaCO3 crystal growth and effect on formation damage). In SPE European Formation Damage Conference. Society of Petroleum Engineers.
- Moghadasi, J., Jamialahmadi, M., Müller-Steinhagen, H., Sharif, A., Ghalambor, A., Izadpanah, M. R., & Motaie, E. (2003b, January). Scale formation in Iranian oil reservoir and production equipment during water injection. In International Symposium on Oilfield Scale. Society of Petroleum Engineers.
- Moore, C., Mills, M. M., Milne, A., Langlois, R., Achterberg, E. P., Lochte, K., & La Roche, J. (2006). Iron limits primary productivity during spring bloom development in the central North Atlantic. Global Change Biology, 12(4), 626-634.
- Morrow, N., & Buckley, J. (2011). Improved oil recovery by low-salinity waterflooding. Journal of Petroleum Technology, 63(05), 106-112.
- Myers, J. A., Sandler, S. I., & Wood, R. H. (2002). An equation of state for electrolyte solutions covering wide ranges of temperature, pressure, and

composition. Industrial & engineering chemistry research, 41(13), 3282-3297.
- Nasralla, R. A., & Nasr-El-Din, H. A. (2014). Double-layer expansion: is it a primary mechanism of improved oil recovery by low-salinity waterflooding?.SPE Reservoir Evaluation & Engineering, 17(01), 49-59.
- Nasralla, R. A., Alotaibi, M. B., & Nasr-El-Din, H. A. (2011, January). Efficiency of oil recovery by low salinity water flooding in sandstone reservoirs. In SPE Western North American Region Meeting. Society of Petroleum Engineers.
- Nicolaisen, H., Rasmussen, P., & Soerensen, J. M. (1993). Correlation and prediction of mineral solubilities in the reciprocal salt system (Na+, K+)(Cl-, SO 2- 4)- H 2 O at 0–100° C. Chemical Engineering Science, 48(18), 3149-3158.
- Oganov, A. R., & Ono, S. (2004). Theoretical and experimental evidence for a post-perovskite phase of MgSiO3 in Earth's D ″layer. Nature, 430(6998), 445-448.
- Oganov, A. R., Gillan, M. J., & Price, G. D. (2003). Ab initio lattice dynamics and structural stability of MgO. The Journal of chemical physics, 118(22), 10174-10182.
- Parrinello, M., & Rahman, A. (1980). Crystal structure and pair potentials: A molecular-dynamics study. Physical Review Letters, 45(14), 1196.
- Perdew, J. P., & Zunger, A. (1981). Self-interaction correction to density-functional approximations for many-electron systems. Physical Review B,23(10), 5048.
- Pereda, S., Thomsen, K., & Rasmussen, P. (2000). Vapor–liquid–solid equilibria of sulfur dioxide in aqueous electrolyte solutions. Chemical engineering science, 55(14), 2663-2671.
- Pierre, A., Lamarche, J. M., Mercier, R., Foissy, A., & Persello, J. (1990). Calcium as potential determining ion in aqueous calcite suspensions.JOURNAL OF DISPERSION SCIENCE ANDTECHNOLOGY, 11(6), 611-635.
- Pitzer, K. S. (1991). Activity Coefficients in Electrolyte Solutions CRC. Ann Arbor.
- Pople, J. A. (1999). Nobel lecture: Quantum chemical models. Reviews of Modern Physics, 71(5), 1267.
- Prenkel, D., & Smit, B. (1996). Understanding molecular simulation. Aca.
- Pruess, K., & Müller, N. (2009). Formation dry-out from CO2 injection into saline aquifers: 1. Effects of solids precipitation and their mitigation. Water Resources Research, 45(3).
- Pu, H., Xie, X., Yin, P., & Morrow, N. R. (2010, January). Low-salinity waterflooding and mineral dissolution. In SPE Annual Technical Conference and Exhibition. Society of Petroleum Engineers.
- Puntervold, T., & Austad, T. (2008). Injection of seawater and mixtures with produced water into North Sea chalk formation: impact of fluid–rock

interactions on wettability and scale formation. Journal of Petroleum Science and Engineering, 63(1), 23-33.
- Puntervold, T., Strand, S., & Austad, T. (2009). Coinjection of seawater and produced water to improve oil recovery from fractured North Sea chalk oil reservoirs. Energy & fuels, 23(5), 2527-2536.
- Puntervold, T., Strand, S., Ellouz, R., & Austad, T. (2014, December). Why is it Possible to Produce Oil from the Ekofisk Field for Another 40 Years?. InInternational Petroleum Technology Conference. International Petroleum Technology Conference.
- RazeiDoust, A., (2011) Low Salinity Water Flooding in Sandstone Reservoirs – A Chemical Wettability Alteration Mechanism. Ph.D Thesis, University of Stavanger,
- RezaeiDoust, A., Puntervold, T., Strand, S., & Austad, T. (2009). Smart water as wettability modifier in carbonate and sandstone: A discussion of similarities/differences in the chemical mechanisms. Energy & fuels, 23(9), 4479-4485.
- Riazi, M. R., & Moshfeghian, M. (2009). A thermodynamic model for LLE behavior of oil/brine/ionic-surfactant/alcohol co-surfactant systems for EOR processes. Journal of Petroleum Science and Engineering, 67(3), 75-83.
- Rigo, V. A., Metin, C. O., Nguyen, Q. P., & Miranda, C. R. (2012). Hydrocarbon Adsorption on Carbonate Mineral Surfaces: A First-Principles Study with van der Waals Interactions. The Journal of Physical Chemistry C,116(46), 24538-24548.
- Røgen, B., Fabricius, I. L., Japsen, P., Høier, C., Mavko, G., & Pedersen, J. M. (2005). Ultrasonic velocities of North Sea chalk samples: Influence of porosity, fluid content and texture. Geophysical Prospecting, 53(4), 481-496.
- Sánchez, V. M., & Miranda, C. R. (2014). Modeling acid oil component interactions with carbonate reservoirs: a first-principles view on low salinity recovery mechanisms. The Journal of Physical Chemistry C, 118(33), 19180-19187.
- Schrödinger, E. (1926). An undulatory theory of the mechanics of atoms and molecules. Physical Review, 28(6), 1049.
- Shariatpanahi, S. F., Strand, S., & Austad, T. (2010). Evaluation of Water-Based Enhanced Oil Recovery (EOR) by Wettability Alteration in a Low-Permeable Fractured Limestone Oil Reservoir. Energy & Fuels, 24(11), 5997-6008.
- Sharma, M. M., & Filoco, P. R. (2000). Effect of brine salinity and crude-oil properties on oil recovery and residual saturations. SPE Journal, 5(03), 293-300.
- Skauge, A., Fallah, S., & McKay, E. (2008). Modeling of LPS Linked Polymer Solutions. In The 29th IEA Workshop & Symposium (pp. 3-5).
- Sposito, G., Skipper, N. T., Sutton, R., Park, S. H., Soper, A. K., & Greathouse, J. A. (1999). Surface geochemistry of the clay

minerals.Proceedings of the National Academy of Sciences, 96(7), 3358-3364.
- Standnes, D. C., & Austad, T. (2000). Wettability alteration in chalk: 2. Mechanism for wettability alteration from oil-wet to water-wet using surfactants. Journal of Petroleum Science and Engineering, 28(3), 123-143.
- Standnes, D. C., & Austad, T. (2000). Wettability alteration in chalk: 2. Mechanism for wettability alteration from oil-wet to water-wet using surfactants. Journal of Petroleum Science and Engineering, 28(3), 123-143.
- Staroverov, V. N., Scuseria, G. E., Tao, J., & Perdew, J. P. (2004). Tests of a ladder of density functionals for bulk solids and surfaces. Physical Review B, 69(7), 075102.
- Stewart, C., & Hessami, M. A. (2005). A study of methods of carbon dioxide capture and sequestration––the sustainability of a photosynthetic bioreactor approach. Energy Conversion and Management, 46(3), 403-420.
- Stixrude, L., & Cohen, R. E. (1995). High-pressure elasticity of iron and anisotropy of Earth's inner core. SCIENCE-NEW YORK THEN WASHINGTON-, 1972-1972.
- Strand, S. (2005). Wettability Alteration in Chalk-A Study of Surface Chemistry. University of Stavanger: Dr. Ing. Thesis.
- Strand, S., Austad, T., Puntervold, T., Høgnesen, E. J., Olsen, M., & Barstad, S. M. F. (2008). "Smart water" for oil recovery from fractured limestone: a preliminary study. Energy & fuels, 22(5), 3126-3133.
- Strand, S., Høgnesen, E. J., & Austad, T. (2006). Wettability alteration of carbonates—Effects of potential determining ions (Ca 2+ and SO 4 2-) and temperature. Colloids and Surfaces A: Physicochemical and Engineering Aspects, 275(1), 1-10.
- Strand, S., Standnes, D. C., & Austad, T. (2003). Spontaneous imbibition of aqueous surfactant solutions into neutral to oil-wet carbonate cores: Effects of brine salinity and composition. Energy & fuels, 17(5), 1133-1144.
- Suijkerbuijk, B., Hofman, J., Ligthelm, D. J., Romanuka, J., Brussee, N., van der Linde, H., & Marcelis, F. (2012, January). Fundamental investigations into wettability and low salinity flooding by parameter isolation. In SPE Improved Oil Recovery Symposium. Society of Petroleum Engineers.
- Tang, G. Q. (1998). Brine composition and waterflood recovery for selected crude oil/brine/rock systems (Doctoral dissertation, University of Wyoming).
- Tang, G. Q., & Morrow, N. R. (1997). Salinity, temperature, oil composition, and oil recovery by waterflooding. SPE Reservoir Engineering, 12(04), 269-276.
- Tang, G. Q., & Morrow, N. R. (1999). Influence of brine composition and fines migration on crude oil/brine/rock interactions and oil recovery. Journal of Petroleum Science and Engineering, 24(2), 99-111..
- Tao, J., Perdew, J. P., Staroverov, V. N., & Scuseria, G. E. (2003). Climbing the density functional ladder: Nonempirical meta–generalized gradient

approximation designed for molecules and solids. Physical Review Letters,91(14), 146401.
- Teufel, L. W., Rhett, D. W., & Farrell, H. E. (1991, January). Effect of reservoir depletion and pore pressure drawdown on in situ stress and deformation in the Ekofisk field, North Sea. In The 32nd US Symposium on Rock Mechanics (USRMS). American Rock Mechanics Association.
- Thijssen, J. (2007). Computational physics. Cambridge University Press.
- Thomsen, K., & Rasmussen, P. (1999). Modeling of vapor–liquid–solid equilibrium in gas–aqueous electrolyte systems. Chemical Engineering Science, 54(12), 1787-1802.
- Thomsen, K., Iliuta, M. C., & Rasmussen, P. (2004). Extended UNIQUAC model for correlation and prediction of vapor–liquid–liquid–solid equilibria in aqueous salt systems containing non-electrolytes. Part B. Alcohol (ethanol, propanols, butanols)–water–salt systems. Chemical engineering science,59(17), 3631-3647.
- Thomsen, K., Rasmussen, P., & Gani, R. (1996). Correlation and prediction of thermal properties and phase behaviour for a class of aqueous electrolyte systems. Chemical Engineering Science, 51(14), 3675-3683.
- Tripathi, I., & Mohanty, K. K. (2008). Instability due to wettability alteration in displacements through porous media. Chemical Engineering Science, 63(21), 5366-5374.
- Tsuchiya, T., Tsuchiya, J., Umemoto, K., & Wentzcovitch, R. M. (2004). Phase transition in MgSiO 3 perovskite in the Earth's lower mantle. Earth and Planetary Science Letters, 224(3), 241-248.
- Van Vuuren, D. P., Bouwman, A. F., & Beusen, A. H. (2010). Phosphorus demand for the 1970–2100 period: a scenario analysis of resource depletion.Global environmental change, 20(3), 428-439.
- Veizer, Jan. "Chemical diagenesis of carbonates: theory and application of trace element technique." (1983).
- Verlet, L. (1967). Computer" experiments" on classical fluids. I. Thermodynamical properties of Lennard-Jones molecules. Physical review,159(1), 98.
- Vo, L. T., Gupta, R., & Hehmeyer, O. J. (2012, January). Ion chromatography analysis of advanced ion management carbonate coreflood experiments. In Abu Dhabi International Petroleum Conference and Exhibition. Society of Petroleum Engineers.
- Voigt, W. (1892). Ueber innere Reibung fester Körper, insbesondere der Metalle. Annalen der Physik, 283(12), 671-693.
- Wagman, D. D., Evans, W. H., Parker, V. B., & Schumm, R. H. (1982). F Halow, SM Bailey, KL Churney, RL Nuttall. NBS tables of chemical thermodynamic properties. J. Phys. Chem. Ref. Data, 11.
- Waisman, E., & Lebowitz, J. L. (1970). Exact solution of an integral equation for the structure of a primitive model of electrolytes. The Journal of Chemical Physics, 52(8), 4307-4309.

- Wang, Y., & Perdew, J. P. (1991). Correlation hole of the spin-polarized electron gas, with exact small-wave-vector and high-density scaling.Physical Review B, 44(24), 13298.
- Webb, K., Lager, A., & Black, C. (2008, October). Comparison of high/low salinity water/oil relative permeability. In International symposium of the society of core analysts, Abu Dhabi, UAE (Vol. 29).
- Wellman, T. P., Grigg, R. B., McPherson, B. J., Svec, R. K., & Lichtner, P. C. (2003, January). Evaluation of CO2-brine-reservoir rock interaction with laboratory flow tests and reactive transport modeling. In International symposium on oilfield chemistry. Society of Petroleum Engineers.
- Wentzcovitch, R. M., Martins, J. L., & Price, G. D. (1993). Ab initio molecular dynamics with variable cell shape: application to MgSiO 3.Physical Review Letters, 70(25), 3947.
- Wilson, G. S., Buck, R. P., Rondinini, S., Covington, A. K., Baucke, F. G. K., Brett, C. M. A & Pratt, K. W. (2002). Measurement of pH. Definition, Standards, and Procedures.
- Wu, J., & Prausnitz, J. M. (1998). Phase equilibria for systems containing hydrocarbons, water, and salt: An extended Peng-Robinson equation of state. Industrial & engineering chemistry research, 37(5), 1634-1643.
- Wu, Y. S., & Bai, B. (2009, January). Efficient simulation for low salinity waterflooding in porous and fractured reservoirs. In SPE Reservoir Simulation Symposium. Society of Petroleum Engineers.
- Yildiz, H. O., & Morrow, N. R. (1996). Effect of brine composition on recovery of Moutray crude oil by waterflooding. Journal of Petroleum science and Engineering, 14(3), 159-168.
- Yousef, A. A., Liu, J., Blanchard, G., Al-Saleh, S., Al-Zahrani, T., Al-Zahrani, R., & Al-Mulhim, N. (2012, October). Smartwater flooding: industry's first field test in carbonate reservoirs. In Proceedings of the SPE Annual Technical Conference and Exhibition (pp. 8-10)
- Zahid, A., Shapiro, A. A., & Skauge, A. (2012, January). Experimental Studies of Low Salinity Water Flooding Carbonate: A New Promising Approach. In SPE EOR Conference at Oil and Gas West Asia. Society of Petroleum Engineers.
- Zahid, A., Stenby, E. H., & Shapiro, A. A. (2010, January). Improved Oil Recovery in Chalk: Wettability Alteration or Something Else?. In SPE EUROPEC/EAGE Annual Conference and Exhibition. Society of Petroleum Engineers.
- Zaretskiy, Y., Geiger, S., & Sorbie, K. (2012). Direct numerical simulation of pore-scale reactive transport: applications to wettability alteration during two-phase flow. International Journal of Oil, Gas and Coal Technology, 5(2-3), 142-156.
- Zhang, P., & Austad, T. (2005, January). The relative effects of acid number and temperature on chalk wettability. In SPE International Symposium on Oilfield Chemistry. Society of Petroleum Engineers.

- Zhang, P., & Austad, T. (2005, June). Waterflooding in Chalk–Relationship between Oil Recovery, New Wettability Index, Brine Composition and Cationic Wettability Modifier (SPE94209). In 67th EAGE Conference & Exhibition.
- Zhang, P., Tweheyo, M. T., & Austad, T. (2006). Wettability alteration and improved oil recovery in chalk: The effect of calcium in the presence of sulfate. Energy & fuels, 20(5), 2056-2062.
- Zhang, P., Tweheyo, M. T., & Austad, T. (2007). Wettability alteration and improved oil recovery by spontaneous imbibition of seawater into chalk: Impact of the potential determining ions Ca2+, Mg2+, and SO42-.Colloids and Surfaces A: Physicochemical and Engineering Aspects, 301(1), 199-208.
- Zhang, Y., & Dawe, R. A. (2000). Influence of Mg 2+ on the kinetics of calcite precipitation and calcite crystal morphology. Chemical Geology,163(1), 129-138.

Appendix

Paper I

Chakravarty, K. H., Fosbøl, P. L., & Thomsen, K. (2015, November). Behavior of Ca^{2+} and Mg^{2+} ions During Smart Water Flooding On Chalk Reservoirs. In *SPE Oil & Gas India Conference and Exhibition*. Society of Petroleum Engineers.

SPE-178137-MS

Behavior of Ca^{2+} and Mg^{2+} ions During Smart Water Flooding on Chalk Reservoirs

Krishna Hara Chakravarty, Philip Loldrup Fosbøl and Kaj Thomsen, Center for Energy Resources Engineering (CERE), Department of Chemical and Biochemical Engineering, Technical University of Denmark

Copyright 2015, Society of Petroleum Engineers

This paper was prepared for presentation at the SPE Oil and Gas India Conference and Exhibition held in Mumbai, India, 24–26 November 2015.

This paper was selected for presentation by an SPE program committee following review of information contained in an abstract submitted by the author(s). Contents of the paper have not been reviewed by the Society of Petroleum Engineers and are subject to correction by the author(s). The material does not necessarily reflect any position of the Society of Petroleum Engineers, its officers, or members. Electronic reproduction, distribution, or storage of any part of this paper without the written consent of the Society of Petroleum Engineers is prohibited. Permission to reproduce in print is restricted to an abstract of not more than 300 words; illustrations may not be copied. The abstract must contain conspicuous acknowledgment of SPE copyright.

Abstract

In an oil reservoir, a thermodynamic equilibrium has been established between the minerals, formation water and oil through millions of years. Modifying the ionic composition during water flooding can lead to enhanced oil recovery (EOR) by altering the equilibrium. The observed alteration is because of changes in wettability by desorption of polar organic fractions from the mineral surface. Herein we simulate the fundamental microscopic mechanism associated to this phenomenon.

We used Density Functional Theory (DFT) for calculating the feasible mineral surface reactions; based on free energy profiles of the different combinations of water, metal ions (Ca^{2+}, Sr^{2+} and Mg^{2+}) and hydrocarbons over a temperature regime of 273K to 373K. The approach uses DFT based Local Density Approximation on molecular dynamic simulation.

We observe that a thin water film exist between chalk and brine/hydrocarbons. At a distance of 2.4Å from the calcite mineral surface a unique energy well containing only water is formed. While at height 4.2Å a major reaction platform containing many complexes is formed. The most stable adsorption complex for each ion was calculated for water-ion [M^{2+}—$(H_2O)_n$] and for water-ion-acetate complex complexes [CH_3COO—M^{2+}—$(H_2O)_n$] (where n =1-9, M^{2+}= Ca^{2+}, Sr^{2+} and Mg^{2+}) at different temperatures. Thereafter a free energy profile was developed for each of the adsorbing complexes. It was observed that Mg^{2+} behaves significantly different from Ca^{2+} on the calcite surface. Mg^{2+} preferred to be adsorbed alone, while Ca^{2+} preferred to be adsorbed with the carboxyl ion. Calculations show that Mg^{2+} adsorption releases energy. This energy supports desorption of organic acids with release of Ca^{2+} bound carboxyl ions. Existence of a thin film of saline water between the mineral surface and the bulk oil; helps in desorption of carboxyl group. In calcite/brine/alkane system Mg^{2+} absorption is favored on the calcite surface. While in the calcite/polar-oil/brine system the carboxyl-Ca^{2+} structure is likely to desorb more quickly by addition of Mg^{2+} ions. The obtained results were in agreement with diverse experimental data in the literature. A large part of the work also includes the categorical rejection of many other possible structures, complexes and clusters formations. The results supports that mineral substitution can take place during Smart Water EOR.

This study explains the detailed molecular bond mechanism behind smart water EOR which can help in better design of optimized oil recovery. The study also highlights the utility of DFT based molecular simulation in better understand EOR phenomena at mineral surfaces.

Introduction

Carbonate/chalk oil reservoirs, in both the North Sea and the Middle East, have been flooded with modified seawater to attain EOR sufficient recovery (Austad et al. 2008; Morrow et al. 2001; RezaeiDoust et al. 2009). Seawater is typically used to sweep reservoir oil to the producing wells. It is well-documented in the literature that laboratory studies have established that seawater can be used to change the wetting condition in an advantageous way to enhance the oil recovery from high temperature oil reservoirs, T > 100°C (Morrow, et al. 2001; Tang, et al. 1997; Jerauld, et al. 2008; Austad, et al. 2008). Some studies claim the sulfate in seawater acts as a reagent for desorbing carboxylic material from the carbonate surface (Austad et al.2008; RezaeiDoust et al. 2009). The group of Austad has conducted several experiments (Austad et al. 2008; Strand, et al. 2006; Zhang, et al. 2005; Zhang et al. 2006) by changing the brine composition of water flooding for Stevns Klint outcrop chalk (Denmark). They concluded that

Ca^{2+}, Mg^{2+}, and $SO_4^{2-}$are the most active ions in the wettability alteration process. Increased effect was seen at higher temperatures. On the basis of experimental results, a qualitative micro-scale model was proposed (Austad et al. 2008).

$$\text{Reaction 1: } RCOO^- - Ca - CaCO_3(s) + (Mg^{2+}, Ca^{2+}) + SO_4^{2-} \rightarrow (Mg, Ca) - CaCO_3(s) + RCOO - Ca^+ + SO_4^{2-}$$

As described in Reaction 1, the model states that SO_4^{2-} adsorbs onto the cations at the positively charged chalk. As a consequence Ca^{2+} can be attracted to the surface due to less electrostatic repulsion. Now Ca^{2+} can react with the carboxylic material and release it from the surface. In case of Mg^{2+} and SO_4^{2-}, it is proposed that Mg^{2+} is able to displace Ca^{2+} (Zhang et al. 2006), which is connected to the carboxylic group, thus making the hydrocarbons mobile. Other studies have concluded that the temperature does not have a consistent recovery effect over different cores (Zahid et al. 2012). The Stevns Klint outcrop chalk showed significant increase in recovery but reservoir cores did have varied effects (Zahid et al. 2010; Fernø et al. 2011). Furthermore contrary to the proposed mechanism in some experiment with Stevns Klint cores, substitution of Ca^{2+} ions by Mg^{2+} was not observed at high temperatures, and the effect of SO_4^{2-} decreased significantly in reservoir rocks compared to outcrops. (Zahid et al. 2012).

In order to address the phenomenon at microscopic scale and exploring the principles to this theory, a platform needs to be developed on a strong mathematical basis. In this work the calcite bulk properties are presented, followed by the calculated properties of energetics, structural characteristics, and kinetic reactions for cation and hydrocarbon complex formation on calcite surfaces.

First principle calculation represents an important and accurate tool to obtain information about the wettability process at atomistic level. Literature in this concern mainly employs classical force field models (Freeman et al. 2007; Freeman et al. 2009). In this work a model for exploring the calcite surface reactions has been developed using free energy contours. The interactions between water, calcium, strontium, and magnesium ions with hydrocarbon species are calculated from 0°C to 100°C. The goal is to understand the adsorption and desorption mechanism of a carboxyl group on the calcite surface over varied temperatures in the presence of brine.

In order to validate the model, different physical properties including an optimized calcite mineral structure and elastic constants of the calcite mineral was calculated and compared with experimental results (Dandekar et al. 1968; Peselnick and Robie 1962). Subsequently a basic framework was developed on which all adsorption simulation was conducted. Thereafter the adsorption pattern of water on calcite surface was simulated and the obtained results were compared with existing athermal calculations (Kerisit et al. 2004) to validate the developed framework.

As in most flooding experiments, the chalk samples are flooded with sea water, so it is important to obtain the possible adsorption complexes formed during interaction between sea water and ions on the calcite surface. The stability of various possible cation-water adsorption complexes on the calcite surface was explored over the entire temperature regime. Thereafter free energy profiles for the most stable structures were obtained using Molecular Dynamics (MD) simulations. These explain the possible arrangement of cations and water molecules on calcite surfaces during the water wet situations. Once the oil is introduced into the core plug, polar ends can interact with the cations and form hydrocarbon-cation complexes on the calcite surfaces. Stability and free energy profiles were developed for possible complex formations. These results were together used to examine the existing controversy on Mg^{2+} substitution by Ca^{2+} on calcite surfaces (Austad et al. 2008; Fernø et al. 2011; Zahid et al. 2010; Zhang et al. 2012). Finally, peculiar behaviors of Ca^{2+} and Mg^{2+} ions during smart water flooding have been established.

Model basis and validation

The basis of the calculations is a first principles quantum mechanical calculation using the total-energy pseudo potential method (Payne, et al. 1992). It is based on the plane wave implementation of DFT (Hohenberg et al. 1965; Kohn et al. 1965), using the Perdew and Wang (PW91) (Vanderbilt 1990) approximation to the exchange and correlation energy term. The Quantum Espresso package (Giannozzi et al. 2009) was used to run the simulations. Ultra-soft pseudo potentials (Vanderbilt 1990; Kresse et al. 1994) were used to describe the core valence electron interaction. The plane wave expansions energy cutoff was chosen to be 560 eV to reduce computational time. This approximation was tested by calculating also at 740 eV, which gave a negligible difference of approximately 20 meV in adsorption energy. The convergence criteria for structural optimization was 10^{-6} eV, ensuring that the total energies converged to less than 0.1 meV/atom. The gamma centered Monkhost–Pack method (Monkhost et al. 1976) was used for the Brillouin-zone sampling integration. For the minimal super-cell, a total of seven inequivalent k-points were used, while the isolated adsorption clusters were simulated at the gamma point only. The BFGS (Broyden 1970) algorithm was employed for the geometry relaxation, maintaining the total forces on atoms to less than, 0.01eV/Å. For bulk calculations the cell vectors were relaxed until the pressure on the cell reached 0.5 kbar. 0.5 kbar pressure was selected to mimic reservoir elevated pressure conditions.

Calcite mineral properties calculation

The initial conditions for the bulk calcite modeling uses fully relaxed crystal parameters of atomic positions and cell vectors. The hexagonal structure of calcite space group was obtained through the geometry optimization calculation. Cell vectors of the optimized crystal lattice obtained are a = b =4.997 Å and c= 17.051 Å, while the atomic distance C-O is 1.295 Å and the Ca-O bond length is 2.374 Å. The obtained results are compared with experimental values in Table 1. It shows that calculated crystals properties in this study are in good correlation to both, previously reported experiments (Graf 1961; Markgraf and Reeder 1985). Previ-

ously predicted optimized cell lattice using different simulations methods DCACP and PW91 (Rigo et al. 2012) are also congruent to the obtained crystal properties. It can be concluded that the results in this work are consistent with experimentally obtained values and other calculation studies.

Elastic constants of calcite were calculated using the finite strain technique (Ravindran et al. 1998). This method provides strain versus energy equations (Ravindran et al. 1998; Mehl et al. 1990). The elastic constants, C_{ij}, are related to strain, ε and stress, σ, by:

$$\text{Equation 1a: } \sigma_{ij} = \frac{\partial U}{\partial \varepsilon_{ij}}$$

$$\text{Equation 1b: } \delta\sigma_i = \sum_j C_{ij}\,\delta\varepsilon_i$$

The elastic tensor of the calcite mineral has seven different parameters; C_{11}, C_{33}, C_{44}, C_{66}, C_{12}, C_{13} and C_{14}. For small strains ($\delta\varepsilon_i$) imposed to the optimized unit cells, the resulting energy change (∂U) in the lattice structure was calculated from the "first principle method" and the corresponding change in energy gives the associated stress (σ_{ij}) using Equation 1a. As previously recommended (Ravindran et al.1998) a set of 24 different strains were provided and the corresponding stress was calculated. These calculated strains versus stress correlation were applied in Equation 1b for obtaining the constant of linear relation between the two. The elastic constant properties were thereby calculated using the linear correlation, Equation 1b.

The calculated elastic constants are listed in Table 2. Previously obtained elastic constants from ultrasonic phase comparison experiments are also shown in Table 2 (Peselnick and Robie 1962; Dandekar et al. 1968). The calculated values of this work were found consistent with the experimental values, as shown in Table 2. But for C_{16} all elastic constants match fairly well with the experimentally obtained values. In previous studies the obtained value of C_{14} was -20.8 GPa (Dandekar et al. 1968), C_{14} =-20.5 GPa (Peselnick and Robie 1962), C_{14} =10.8 GPa (Pavese et al. 1992) and C_{14} =7.3 GPa (Pavese et al. 1992). It should also be noted that the obtained and calculated values of C_{16} in previous studies are also not consistent with each other. In general the crystal structure and the elastic properties match with experimental values.

Basic model for adsorption simulation

First a consistent framework was developed to simulate the behavior of different ions, molecules and adsorption complexes on a calcite surface. The calcite surface was simulated by cleaving the calcite in the hexagonal structure along the (10 −14) surface. The surface contains an equal number of Ca^{2+} and CO_3^{2-} sections which keeps the surface neutral. The stability of this surface has previously been studied by different theoretical methods. This includes classical force fields (de Leeuw et al. 1998; Titiloye et al. 1998; Bruno et al. 2010) and DFT calculations (Kerisit et al. 2004; Lardge et al. 2010). In this work a model with two layers, one of them fixed, formed the crystal volume. Beyond the two layers a vacuum was maintained for the adsorption complexes. We tested the accuracy of this approximation by simulations of 2, 3, 4, and 6 layers. It was concluded that variation less than 2% was observed. Therefore a surface containing 2 layers was used. With this basis the interactions of brine-hydrocarbons clusters on calcite surfaces, plus the effect on adsorption volume was studied. It describes the simulation cell volume (V) consisting of the Crystal + Adsorption Volume System (CAVS). The simulation was performed with the time average of atomic movements using MD simulations considering Newton's equations of motion governed by Equation 2. At each step (for a given set of atomic positions) the force F_i on each atom (i) was calculated from first principles calculation as prescribed in literature (Ravindran et al. 1998). This calculated force was thereafter used in MD simulation.

$$\text{Equation 2a: } R_i(t+\Delta t) = R_i(t) + v_i(t)\Delta t + \frac{1}{2m_i}F_i(t)\Delta t^2$$

$$\text{Equation 2b: } V_i(t+\Delta t) = V_i(t) + \frac{1}{2m_i}\left(F_i(t) + F_i(t+\Delta t)\right)\Delta t$$

Using Equation 2a first, the new positions attained by the atoms were obtained after Δt time. The forces were also used to calculate the corresponding velocities of the atoms using Equation 2b. The updated velocity was used to obtain the next step position of the atoms.

The simulation was started assuming no initial velocity of the atoms. In the simulations the time step was less than 1/20 of a typical vibrational period. 20000 steps were chosen in one oscillation with a minimum of 10 ns. For each simulation set, the volume of the simulation cell V and the number of atoms N were kept constant applying a so called N-V-T simulation. To ensure 0.5 kbar at a specified temperature, the partial derivative were used of the Helmholtz free energy, A, with respect to volume (V) using the Clapeyron slope (Andersen 1980; Nosé 1984). Equation 3a was used to obtain the Helmholtz Free energy from the electron free potential energy which is obtained by the dynamic simulations (Frenkel et al. 1996). The Helmholtz free energy is applied for calculation of the Gibbs free energy profile for the system at a given temperature.

$$\text{Equation 3a: } A = -k_B T \ln\left\{\frac{1}{N!\Delta^{3N}}\int_V dr_i e^{-\beta E(r_i;T)}\right\}$$

$$\text{Equation 3b: } G = A + \left.\frac{\partial A}{\partial V}\right|_T V$$

For each adsorbing complex, an initial calculation was conducted at the adsorption volume boundary (which is also the furthest point from the crystal surface), and the obtained energy was treated as the Gibbs energy of the adsorbing complex at infinite distance from the crystal surface. Its difference to the cluster at any particular location (ΔG), gives the relative stability at the given location. Negative ΔG value indicates a more stable zone than that at infinite distance from the crystal surface. All calculations of adsorption were made in reference to its height (z), which is defined as the perpendicular distance of the central atom of the cluster to the 10-14 cleavage planes. Herein to keep the study simple, competitive adsorption was not considered and in each simulation a single adsorbing complex was placed at particular heights from the crystal surface and the dynamics simulation was conducted.

Water adsorption on Calcite

The adsorption dynamics of water on calcite surface has been studied previously (Kerisit et al. 2004). The oxygen in the water molecule was treated as the central atom. The MD system was composed of two phases (1) a 2X1X2 crystal slab with the 10-14 crystal lattices as the active mineral surface or crystal volume (2) on the crystal volume a cuboid of vacuum was maintained. The 2X1 mineral surface was the base area of the cuboid. And the height of the cuboid was altered according to the size of the adsorption complex. This vacuum cuboid provided enough space for analyzing the stability of adsorbing complex at different distance from the mineral surface. This vacuum cuboid has been referred as the adsorption volume). Similar to previous calculations (Kerisit et al. 2004), the crystal volume and adsorption volume system collectively formed the CAVS model. The calculation was conducted for 33 locations up to a height of 15 Å. On this setup, a water molecule was first introduced at a particular height in the adsorption volume and the dynamics was simulated for 20,000 steps. The average Helmholtz free energy was calculated using Equation 3 for the last 5000 steps. This ensured that energy for the most stable geometric orientation of the water molecule was obtained at the given height. Then simulations were conducted by introducing the water molecule at various heights from the calcite surface.

In this work the obtained Gibbs free energy (ΔG) are plotted in Figure 1 Noticeable water stability is obtained at an average height of 2.4 Å (layer I) and 4.2 Å (layer II) from the crystal surface the observed two layer adsorption patterns are in agreement with previous studies (Kerisit et al. 2004).Herein layer I correspond to bonding of surface calcium with the oxygen atom while layer II corresponds to hydrogen bonds to surface oxygen.

Results

Establishment of Sr, Ca and Mg hydration by MD

In most water flooding experiments, formation water is first introduced into the dried and cleaned cores (Austad et al. 2008; Fernø et al. 2011; Karoussi et al. 2007 ; Zhang et al. 2007; Tang et al. 1997). This provides a possibility of cation-water interaction on the calcite surface. Thus cation adsorption and water behavior on the calcite surface need to be explored. Possible adsorption complexes have been previously observed in for constant temperature conditions (Kerisit et al. 2004).But injection into coreplugs can take place at various temperatures. So, it is important to further explore the stability and adsorption dynamics of the water-cation complexes (metal ion hydrates) on calcite surfaces over the entire temperature regime from 273 K to 373 K. As the basic model of CAVS system was used in order to analyze the cation-water adsorption on calcite surfaces. It was studied at different temperatures.

Figure 2 shows how the cation was chosen to be the central atom in the calculations. The height of the adsorption volume was increased to 20 Å because of the increase in size of the cluster. The reported most stable orientation of absorption complex by Kerisit, et al. 2004 was used for the calculations at different temperatures.

Stability calculation was conducted for different cation hydrations for $[Ca(H_2O)_n]^{2+}$, $[Mg(H_2O)_n]^{2+}$, and $[Sr(H_2O)_n]^{2+}$, where n = 1-9. The individual energy of a single water molecule on the calcite surface was calculated (E_{H_2O}) at various temperatures as shown in Figure 3 The energy of the 'n' hydrated complex was calculated ($E_{[X(H_2O)_n]^{2+}}$) after complete geometric optimization. Thereby the binding energy E_{TOT} for each value of the n = 1-9 was calculated using Equation 4. The $[Ca(H_2O)_9]^{2+}$ and $[Sr(H_2O)_9]^{2+}$ clusters formed complexes with eight coordinating water molecules and one water molecule remained uncoordinated. The magnesium-water complexes with n > 5 relaxed to form clusters with six water molecules. The energetically preferred configuration of the $[Ca(H_2O)_8]^{2+}$ and $[Sr(H_2O)_8]^{2+}$ complexes is the square anti-prism, whereas the $[Mg(H_2O)_6]^{2+}$ complex is octahedral as shown in Figure 2 which is consistent with Kerisit, et al. (Kerisit, et al. 2004).

$$\text{Equation 4: } E_{TOT} = \left(E_{[X(H_2O)_n]^{2+}} - nE_{H_2O}\right)/n$$

The most stable hydration for each water-cation complex was obtained. As shown in figure 3 the binding energy optimized at 8 water molecules for water complexes with Ca^{2+} and Sr^{2+}. While binding energy optimized at 8 water molecules for water complexes with Mg^{2+}. The stability of these hydrated state ($[Ca(H_2O)_8]^{2+}$, $[Mg(H_2O)_6]^{2+}$ and $[Sr(H_2O)_8]^{2+}$) were not much affected by

temperature. The number of hydration molecule and its corresponding binding energy obtained for different cations at 0°C were consistent with previous results (Kerisit, et al. 2004). It has been shown in Table 3.

Surface bond length of hydrated species

For the three most stable metal ion hydrates: $[Ca(H_2O)_8]^{2+}$, $[Mg(H_2O)_6]^{2+}$ and $[Sr(H_2O)_8]^{2+}$ MD simulations were conducted and the free energy contours were obtained at different heights using Equation 3. 33 calculations were performed at z = 1.8 Å to 11.4 Å from the mineral surface. The obtained free energy (using Equation 3) for the adsorption of the three hydrate clusters at different temperatures was plotted in Figure 4. It shows that the relative free energy as a function of distance from the surface. For all three hydrated species a large energy barrier exist between the adsorption height and the bulk water. As observable in Figure 3 this energy barrier is observable at a distance of 5Å to 8Å from the mineral surface. Figure 2 shows that a similar energy barrier (at a distance of 5Å to 8Å) exists for water molecules as well. Thus a region of low ion and water density is formed at a height of 5-8Å from the mineral surface. The metal ion hydrates adsorb directly above the surface carbonate group at a height of 3.9, 4.1, and 4.2 Å for calcium, strontium and magnesium, respectively, at 0°C. It is interesting to note that even with increase in temperature the most stable height for all the hydrates is fairly consistent around 4.2 Å, as indicated by the red circles in Figure 4. This also clearly indicates that adsorption of magnesium ions remains more favorable even at higher temperatures. Moreover, energy is released during adsorption of Mg on the calcite surface. This release of energy consistently observed with increase in temperature.

Both Ca^{2+} and Sr^{2+} have an energy barrier at a distance of 5Å to 8Å from the mineral surface. This energy barrier keeps the ion adsorbed on the mineral surface. But the released energy due to Magnesium adsorption can enhance desorption of other adsorbed cations (including Ca^{2+} and Sr^{2+}). Thus adsorption of Mg ion on the mineral surface will promote desorption of Ca^{2+} and Sr^{2+} from the mineral surface.

The blue line in Figure 4; shows the energy well for water molecule at a height of 2.4 Å from the mineral surface. At this height none of the cation can form any adsorption complex, since 3.9Å was found to be the minimum distance at which cations can be adsorbed on the mineral surface. But during adsorption of cations (at the height of 3.9-4.2Å), the hydrating water molecules continue to occupy the energy well at 2.4Å. This implies that energy well at 2.4Å remains inaccessible to the cations, but is consistently occupied by water molecules. Thus the adsorption of cation ensures the existence of a water film between the calcite and the crude oil.

Hydrocarbon-cation complex formation on calcite surfaces

Some hydrocarbons in crude oil contain polar fractions (like compounds with carboxylic acid ends). These compounds are capable of interacting with cations; present in brine or adsorbed on mineral surfaces. These can together form complexes on mineral surface and affect the displacement efficiency of the oil. The stability of such possible complexes was simulated in this study. Thereafter free energy profiles were developed for analyzing the adsorption and desorption possibilities of carboxyl acid at various temperatures.

To obtain the most stable cation-carboxyl complex, energy calculation for different hydration was conducted. Herein binding energy calculation for $[CH_3COO^-—Ca^{2+}— (H_2O)n]^+$, $[CH_3COO^-—Mg^{2+}— (H_2O)_n]^+$, and $[CH_3COO^-—Sr^{2+}— (H_2O)_n]^+$ (for n= 1 to 9) was conducted. Carboxyl complex with Ca^{2+} and Sr^{2+} showed that most stable complex was formed with hydration of 4 water molecules. While carboxyl complex with Mg^{2+} showed that most stable complex was formed with hydration of 3 water molecules. The water molecules of the complex stayed at a height of 2.3 Å to 2.38 Å from the calcite surface, while the acetate kept pointing outwards as shown in Figure 2. The energetically preferred configuration for $[CH_3COO^{(-)}—Ca^{2+}—(H_2O)_4]^+$ and $[CH_3COO^{(-)}—Sr^{2+}— (H_2O)_4]^+$ complexes were square pyramid, whereas the $[CH_3COO^{(-)}—Mg^{2+}—(H_2O)_3]^+$ complex formed tetrahedron geometry between water molecules and Mg^{2+} ion.

MD simulations for oil-cation complexes were conducted, and the free energy was calculated using the CAVS model. Since the size of the adsorption complex increased so the corresponding height of the adsorbed volume was increased to 25 Å. 33 calculations were performed to obtain points between z=2.1 Å to 11.7 Å. Simulation for 20000 steps were run, while the Helmholtz free energy was calculated from the average of the last 1000 steps to obtain the energy values at steady state. As shown in Figure 2, the cation was taken to be the central atom for these clusters. The obtained free energy for the adsorption of the three oil-cation clusters at different temperatures is plotted in Figure 5. It is observed how all stabilize around an average height of 4.2 Å independent of temperature. The minimum Gibbs free energy is obtained in the carboxyl-Ca^{2+} complex at a height of 4.12 Å (indicated by the red circle in Figure 5). It shows how the free carboxylic acid ion would prefer to form a complex with the calcium ion on the calcite surface. Since the carboxyl-Ca^{2+} complex is more stable, a carboxyl-Mg^{2+} complex can leave the carboxyl group and be alone on the calcite surface when it interacts with a free Ca^{2+} ion. It is found that Mg^{2+} is more stable alone, while the calcium ion is more stable with the carboxyl group. The highly unstable zone around 6 Å form an energy barrier for desorption of the carboxyl ions. In Figure 6 there is a significant energy barrier between the complex adsorbed around 4.2 Å and the clusters at a height of around 9-11 Å. It is observed that the energy barrier significantly changes with change in temperature. This energy barrier decreases significantly with increase in temperature for the carboxyl-Ca^{2+} complexes. While it remains almost unaffected in the other case (Figure 7). This indicates that at higher temperature the release of carboxyl group becomes more preferable. Release of carboxyl groups at elevated temperature enhances that the displacement efficiency of trapped oil.

Several previous studies have shown a consistent increase in oil recovery with increase in temperature (Austad et al. 2008, Zahid et. al 2010, Gupta et al. 2012). Previously it has believed that adsorption of SO_4^{2-} should take place for the release of carboxyl acid from the mineral surface (Austad et al. 2008). But this calculation shows that with increase in temperature, the possible release of carboxyl groups significantly increase and carboxyl groups can be released without compulsory adsorption of SO_4^{2-} ions. Previously experiments have been conducted wherein consistent increase in oil recovery is observed for injecting formation water without SO_4^{2-} followed by sea water without SO_4^{2-} ion. In this case (Gupta et al. 2012) the Mg^{2+} concentration in the effluent brine was consistently less than that in the injected brine. Therefore adsorption of Mg^{2+} may lead to desorption of Ca^{2+}-carboxyl ions. Thus observed increase in oil recovery in absence of SO_4^{2-} (Gupta et al. 2012) can be explained according through calculation.

Discussion

Do calcium Mg^{2+}/Ca^{2+} substitution take place?

In some experimental results using outcrop chalks it has been suggested that substitution of Mg^{2+} by Ca^{2+} takes place in the core. Increase in Ca^{2+} has been consistently observed in the effluent brine (Austad et al. 2008; Korsnes et al. 2006) with Stevens Klint outcrop chalks. While experiments with both outcrops and reservoir coreplug have suggested that substitution of Mg^{2+} by Ca^{2+} do not take place (Zahid, et al. 2012). As an increase in Ca^{2+} concentration was not consistently observable in the effluent brine.

The simulations performed in this work were used to examine these varying experimental observations. From the simulations described in Figure 4, the Mg^{2+} ion is significantly more stable on the calcite surface than the Ca^{2+} or Sr^{2+} ions are. The behavior of Mg^{2+} is described by Reaction 2. Mg^{2+} ions get readily adsorbed on the calcite surface by forming hydration complexes with 6 water molecules. The formation of this hydrate releases energy. In absence of any polar molecules this energy favors desorption of Ca^{2+} ions. It becomes even more feasible at higher temperatures, explained by the lower energy barrier for adsorption of $Mg^{2+}(H_2O)_6$ in Figure 7. This is also shown by Figure 4, the $Mg^{2+}(H_2O)_6$ complex remains stable at higher temperatures.

$$\text{Reaction 2: } Mg^{2+} + \text{Calcite} + 6H_2O \rightarrow Mg^{2+}(H_2O)_6 - \text{Calcite} + eV$$

Korsnes et al. 2006 conducted water flooding experiments with Steavn Klint chalk and model oil. Decane was used as model oil. An increase in the effluent calcium concentration during seawater flooding at temperatures higher than 70℃ is reported (Korsnes et al. 2006). Here competitive adsorption was analyzed and it was observed that Mg^{2+} adsorption was favored at higher temperature. But in this experiment polar hydrocarbons were not introduced to the cores before water flooding. The release of Ca^{2+} after Mg^{2+} substitution is consistent with the simulation results. The Mg^{2+} ion has more affinity towards the calcite surface than Ca^{2+} as described in Reaction 2. Thus according to the conducted simulation the proposed Ca^{2+} substitution by Mg^{2+} (Austad et al. 2008; Korsnes et al. 2006) is completely feasible.

Zahid et al. conducted a similar set of experiments (Zahid et al. 2012). Herein both Stevns Klint chalks outcrops and North Sea reservoir chalks where used. Oil containing polar components was initially introduced to the cores. And sea water with times sulphate concentration was injected in the first case. Herein with increase in decrease in Ca^{2+} concentration was observed in the effluent brine. Thus it was suggested that the substitution did not take place.

The simulation in this study show that Ca^{2+} is more likely to bind with polar hydrocarbon, and with increase in temperature the energy barrier decreases. According to reaction 2 the injected Mg^{2+} are likely to get adsorbed on the mineral surface. The energy released during this adsorption can lead to desorption of Ca^{2+}-carboxyl complex from the mineral surface. As shown in reaction 3.

$$\text{Reaction 3: } \text{Calcite} - [H_2O]_4 - Ca^{2+} - CH_3COO^- + eV + SO_4^{2-} + M^{2+} \rightarrow \text{Calcite} - [H_2O]_n - M^{2+} - SO_4^{2-} + Ca^{2+} - CH_3COO^-$$

Now this desorption of Ca^{2+}-carboxyl complex will increase the amount of Ca^{2+} ion present in the pore space. Since the energy barrier of Ca^{2+}-carboxyl group decreases with increase in temperature so the amount of Ca^{2+} ion present in the pore space will further increase. Herein the injected brine is significantly sulphate rich. And solubility of $CaSO_4$ decreases significantly with increase in temperature. Thus possible fine formation (precipitation) of $CaSO_4$ may have taken place. Herein it is interesting to note that , in the effluent brine a decrease in Mg^{2+} and SO_4^{2-} concentration was also observed because for increase in temperature (Zahid et al. 2012). Thus the decrease in Mg^{2+} could be because of its absorption on the mineral surface, while decrease in Ca^{2+} and SO_4^{2-} could be because of $CaSO_4$(s) formation.

The mobility of this fine will depend on the porosity and permeability of the core sample. Stevens Klint chalk has a greater porosity and permeability than North Sea reservoir chalks. Thus in case of Stevns Klint chalk the formed fines remained mobile, while for North Sea chalk it became static. This formation of mobile fines may have led to the observed increase in oil recovery for increase in temperature. While no increase in oil recovery for increase in temperature could be because of formation of static fines with North Sea chalks.

In the second set of experiments conducted by Zahid et al. (Zahid et al. 2012) sea water with no sulphate ion was injected in the core plug. In this case with increase in temperature a gradual decrease in Mg^{2+} concentration was observed. After significant increase in temperature Ca^{2+} started increasing. This was reported as an unexpected increase of Ca^{2+} concentration at elevated temperature.

The consistent decrease in Mg^{2+} ion the effluent indicates that Mg^{2+} adsorption did take place. Since $MgCl_2$ is very soluble so no possible precipitation of Magnesium can take place. Furthermore in this case again Ca^{2+} is more likely to bind with polar hydrocarbon, and with increase in temperature the energy barrier decreases. And release of the Ca^{2+}-Carboxyl becomes feasible only at elevated temperature. Thus the Ca^{2+} increases in the pore space with desorption of Ca^{2+}-Carboxyl complex. In this case there is no possibility of precipitate formation the as the injected brine does not contain sulphate ions. Thus the reported unexpected increase of Ca^{2+} ion is because of desorption of Ca^{2+}-carboxyl ions. It is interesting to note that this case there is no possibility of fine formation and no increase in oil recovery was observed.

Therefore substitution of Ca^{2+} by Mg^{2+} can take place on the mineral surface. But release of Ca^{2+} may lead to $CaSO_4$(s) anhydrite fine formation. Thus increased Ca^{2+} concentration may not always be observable in the effluent brine.

Effect of Ca^{2+} and Mg^{2+}in EOR

Reaction 2 and Reaction 3 when combined describes a possible reaction mechanism towards carboxylic groups. It can be explained by:

a. The carboxylic group prefers to be adsorbed on the Ca^{2+} ion as shown in Figure 5
b. Energy is released during $[Mg(H_2O)_6]^{2+}$ adsorption on the calcite surface as shown in Figure 4
c. The carboxyl-Ca^{2+} complex are desorbed from the calcite surface by absorbing the energy released during Mg^{2+} adsorption.

Figure 2, arrow 1, 2 and 3 is a pictorial representation of these 3 steps. This is quite similar to the previously noted qualitative mechanism by (Austad et al. 2008; Zhang, et al. 2006) as explained in Reaction 1. The first point of difference is that in Austad's mechanism substitution of Ca^{2+} by Mg^{2+} is treated as a single phenomenon. But in this study adsorption of Mg^{2+} and desorption of Ca^{2+} are treated as two different phenomenon. It suggests that for model oil (containing only alkane and polar acids) adsorption of Mg^{2+} will be followed by desorption of Ca^{2+} ion from the mineral surface. Thus for decrease in Mg^{2+} concentration in the effluent brine a corresponding equivalent increase in Ca^{2+} concentration is observed in the effluent brine (Korsnes et al. 2006). But for crude oil (containing polar acids) Mg^{2+} adsorption on mineral surface does not directly lead to release of Ca^{2+} ions at low temperature. Thus at low temperature decrease of Mg^{2+} concentration in the effluent is not followed by corresponding increase in Ca^{2+} concentration in the effluent brine (Zahid et al. 2012). Only with sufficient increase in temperature the release of Ca^{2+}-Carboxyl complex take place, and correspondingly a sudden increase in Ca^{2+} concentration in the effluent brine is observed (Zahid et al. 2012). Secondly it clarifies that the release of Ca^{2+} may not be always observable in the effluent water because of precipitation of $CaSO_4$(s) (particularly insoluble at higher temperatures). Furthermore these calculations clearly show the role of Ca^{2+} and Mg^{2+} on EOR, that they are significantly different. While the Mg^{2+} ion prefers to stay alone on the calcite surface the Ca^{2+} ion prefers to be adsorbed with other polar hydrocarbon, even at high temperatures. Cations with and without the carboxyl complex are adsorbed at the same height from the crystal surface i.e. around 4.2 Å so interchanging of binding groups is possible. For example, an adsorbed Carboxyl-Mg^{2+} in contact with an adsorbed Ca^{2+} can rearrange itself to a carboxyl-Ca^{2+} and Mg^{2+} form, but in both cases it has an energy barrier which can only be crossed by help of external energy. So, any possible substitution reaction alone cannot affect desorption of the complexes. But adsorption of Mg^{2+} on to the mineral surface can provide the required external energy which can cause desorption of the complexes. The study supports the importance of $Ca^{2+}$and Mg^{2+} as an important factor in deciding the surface wettability. As shown in Figure 7, the energy barrier for the release of carboxyl-Ca^{2+} complex decreases with increase in temperature. It explains the experimental observations of how oil recovery increases as function of temperature. It supports the studies on the surface behavior to a great extent and provides a mathematical base to the study of Austad et al. (Austad et al. 2008).

It has previously been shown that imbibition of Mg^{2+} to a rock/brine/oil system, without the addition of SO_4^{2-} can result in enhanced oil recovery (Karoussi et al. 2007). In this study it was found that the addition of extra Mg^{2+} ions will result in the release of adsorption energy, which in turn will be used by the carboxyl-Ca^{2+} and will produce some free carboxyl ions and thus help in increasing the oil recovery. If SO_4^{2-} ions are lacking, the Ca^{2+} ions are likely to start adsorbing on polar hydrocarbons. Thus it is expected to result in a small increase in oil recovery, which is supported by the previous experiment (Karoussi et al. 2007; RezaeiDoust et al. 2009). Addition of Mg^{2+} ions without SO_4^{2-} ions increases the oil recovery slightly, but oil recovery is optimized only when released Ca^{2+} ions are not reabsorbed on the mineral surface. Formation of minute anhydrite fines could be a possible way to maintain the mobility of Ca.

It has also been observed that aging temperature play a key role in deciding the recovery fraction (Shariatpanahi et al. 2011). Significantly low oil recovery is obtained for coreplugs that are aged at high temperature (Shariatpanahi et al. 2011). In this reported experiment (Shariatpanahi et al. 2011) the formation water (unlike sea water) contained significantly high concentration of Ca^{2+} over Mg^{2+}. Thus significantly amount of carboxyl adsorption should have taken place. Since at higher temperature the energy barrier of Ca^{2+}-carboxyl complex decreases, so the possibility of carboxyl adsorption further increases. Thus aging at higher temperature led to higher adsorption of carboxyl ions. Thereafter the oil recovery was calculated for injection of the same Ca^{2+} enriched formation water. Using this Mg^{2+} depleted brine meant that the required energy for release of Carboxyl ions was not obtained. Thus a lower oil recovery was observed for cores aged at higher temperature (Shariatpanahi et al. 2011).

Conclusion

Molecular scale behavior of brine and hydrocarbon during water flooding on calcite surfaces has been simulated using first principle MD. A calcite crystal structure was optimized and the elastic constant was calculated. The obtained values were in agreement with the experimental data. Primary adsorption studies for different complexes of water, carboxyl group and Ca^{2+}, Mg^{2+} and Sr^{2+} ions on the calcite surface was studied from 0℃ to 100℃. Through the simulations it was observed that water molecules are more stable at two locations; at an average height of 2.4 Å and 4.2 Å from the calcite surface. $[Ca(H_2O)_8]^{2+}$,$[Sr(H_2O)_8]^{2+}$ and $[Mg(H_2O)_6]^{2+}$ were found to be most stable hydrate complexes. Furthermore, by free energy calculations maximum stability was found around a height of 4.2 to 4.4 Å from the calcite surface over the entire temperature regime, 0 to 100 °C. The carboxyl complexes $[CH_3COO^-—Ca^{2+}—(H_2O)_4]$, $[CH_3COO^-—Sr^{2+}—(H_2O)_4]$ and $[CH_3COO^-—Mg^{2+}—(H_2O)_3]$ were found to be the most stable. The most stable height of adsorption was found to be 4.2 Å (i.e. 3.9 Å to 4.4 Å) from the calcite surface.

Simulations showed that Mg adsorption on calcite surface released energy. This energy helped to release carboxyl complexes $[CH_3COO^-—Ca^{2+}—(H_2O)_4]$ from the calcite surface. The temperature barrier for the release of carboxyl group decreases with increase in temperature, thus at higher temperature EOR is favored. The released Ca^{2+} ion may further precipitate and form $CaSO_4$(s) because of its low solubility. Due to the precipitation of $CaSO_4$(s) it is possible that desorption of Ca^{2+} from the mineral surface may not always be reflected in the effluent water which may create a misunderstanding of the experimentalist. The observed EOR for injection of Sea water without SO_4^{2-} ion is also explained in this study. Collectively these results provide a fundamental distinction between the behaviors of Ca^{2+} and Mg^{2+} ions during smart water EOR.

Acknowledgement

This article is a part of research study in smart water project and center for energy resource engineering. The authors acknowledge Maersk Oil, Dong Energy, and The Danish Energy Agency (EUDP) for funding the Smart Water project.

References

- Andersen, H. C. (1980). Molecular dynamics simulations at constant pressure and/or temperature. *The Journal of chemical physics*, 72 (4), 2384-2393.
- Austad, T., Strand, S., Madland, M. V., Puntervold, T., & Korsnes, R. I. (2008). Seawater in chalk: An EOR and compaction fluid. *SPE Reservoir Evaluation & Engineering*, 11 (04), 648-654.
- Broyden, C. G. (1970). The convergence of a class of double-rank minimization algorithms 2. The new algorithm. *IMA Journal of Applied Mathematics*, 6 (3), 222-231.
- Bruno, M., Massaro, F. R., Rubbo, M., Prencipe, M., & Aquilano, D. (2010). (10.4),(01.8),(01.2), and (00.1) Twin Laws of Calcite (CaCO3): Equilibrium Geometry of the Twin Boundary Interfaces and Twinning Energy. *Crystal Growth & Design*, 10 (7), 3102-3109.
- Dandekar, D. P. (1968). Pressure dependence of the elastic constants of calcite. *Physical Review*, 172 (3), 873.
- de Leeuw, N. H., & Parker, S. C. (1998). Surface structure and morphology of calcium carbonate polymorphs calcite, aragonite, and vaterite: an atomistic approach. *The Journal of Physical Chemistry B*, 102 (16), 2914-2922.
- Fernø, M. A., Grønsdal, R., Åsheim, J., Nyheim, A., Berge, M., & Graue, A. (2011). Use of Sulfate for Water Based Enhanced Oil Recovery during Spontaneous Imbibition in Chalk. *Energy & fuels*, 25 (4), 1697-1706.
- Freeman, C. L., Asteriadis, I., Yang, M., & Harding, J. H. (2009). Interactions of organic molecules with calcite and magnesite surfaces. *The Journal of Physical Chemistry C*, 113 (9), 3666-3673.
- Freeman, C. L., Harding, J. H., Cooke, D. J., Elliott, J. A., Lardge, J. S., & Duffy, D. M. (2007). New forcefields for modeling biomineralization processes.*The Journal of Physical Chemistry C*, 111 (32), 11943-11951.
- Frenkel, D., & Smit, B. Understanding molecular simulation: from algorithms to applications, 1996. *Academic, San Diego*.
- Giannozzi, P., Baroni, S., Bonini, N., Calandra, M., Car, R., Cavazzoni, C., Ceresoli, D., Chiarotti, G. L., Cococcioni, M., Dabo, I., Corso, A. D., Gironcoli, S. D., Fabris, S., Fratesi, G., Gebauer, R., Gerstmann, U., Gougoussis, C.,Kokalj, A.,Lazzeri, M., Martin-Samos, L., Marzari, N., Mauri, C., Mazzarello, R., Paolini, S.,Pasquarello, A., Paulatto, L., Sbraccia, C., Scandolo, S., Sclauzero, G., Seitsonen, P. A.,Smogunov, A.,Umari, P. & Wentzcovitch, R. M. (2009). QUANTUM ESPRESSO: a modular and open-source software project for quantum simulations of materials. *Journal of Physics: Condensed Matter*, 21 (39), 395502.
- Graf, D. L. (1961). Crystallographic tables for the rhombohedral carbonates.*American Mineralogist*, 46 (11-2), 1283-1316.
- Vo, L. T., Gupta, R., & Hehmeyer, O. J. (2012, January). Ion Chromatography Analysis of Advanced Ion Management Carbonate Coreflood Experiments. In*Abu Dhabi International Petroleum Conference and Exhibition*. Society of Petroleum Engineers.
- Hohenberg, P. (1965). P hys. Rev. 1964, 136, B864–B871; b) W. Kohn, LJ Sham. *Phys. Rev*, 140, A1133-A1138.

- Jerauld, G. R., Webb, K. J., Lin, C. Y., & Seccombe, J. C. (2008). Modeling low-salinity waterflooding. *SPE Reservoir Evaluation & Engineering*, 11 (06), 1-000.
- Karoussi, O., & Hamouda, A. A. (2007). Imbibition of sulfate and magnesium ions into carbonate rocks at elevated temperatures and their influence on wettability alteration and oil recovery. *Energy & fuels*, 21 (4), 2138-2146.
- Kerisit, S., & Parker, S. C. (2004). Free energy of adsorption of water and metal ions on the {1014} calcite surface. *Journal of the American Chemical Society*, 126 (32), 10152-10161.
- Kohn, W., & Sham, L. J. (1965). Self-consistent equations including exchange and correlation effects. *Physical Review*, 140 (4A), A1133.
- Korsnes, R. I., Strand, S., Hoff, Ø., Pedersen, T., Madland, M. V., & Austad, T. (2006). Does the chemical interaction between seawater and chalk affect the mechanical properties of chalk? EUROCK 2006-Multiphysics Coupling and Long Term Behaviour in Rock Mechanics-ISBN 0 415 41001 0.
- Kresse, G., & Hafner, J. (1994). Norm-conserving and ultrasoft pseudopotentials for first-row and transition elements. *Journal of Physics: Condensed Matter*, 6 (40), 8245.
- Lardge, J. S., Duffy, D. M., Gillan, M. J., & Watkins, M. (2010). Ab initio simulations of the interaction between water and defects on the calcite (101 4) surface. *The Journal of Physical Chemistry C*, 114 (6), 2664-2668.
- Markgraf, S. A., & Reeder, R. J. (1985). High-temperature structure refinements of calcite and magnesite. *American Mineralogist*, 70 (5-6), 590-600.
- Mehl, M. J., Osburn, J. E., Papaconstantopoulos, D. A., & Klein, B. M. (1990). Structural properties of ordered high-melting-temperature intermetallic alloys from first-principles total-energy calculations. *Physical Review B*, 41 (15), 10311.
- Morrow, N. R., & Mason, G. (2001). Recovery of oil by spontaneous imbibition.*Current Opinion in Colloid & Interface Science*, 6 (4), 321-337.
- Nosé, S. (1984). A unified formulation of the constant temperature molecular dynamics methods. *The Journal of Chemical Physics*, 81 (1), 511-519.
- Omekeh A. V. PhD thesis Department of Petroleum Engineering University of Stavenger 2012 .
- Pavese, A., Catti, M., Price, G. D., & Jackson, R. A. (1992). Interatomic potentials for CaCO3 polymorphs (calcite and aragonite), fitted to elastic and vibrational data. *Physics and chemistry of minerals*, 19 (2), 80-87.
- Payne, M. C., Teter, M. P., Allan, D. C., Arias, T. A., & Joannopoulos, J. D. (1992). Iterative minimization techniques for ab initio total-energy calculations: molecular dynamics and conjugate gradients. *Reviews of Modern Physics*,64 (4), 1045.
- Peselnick, L., & Robie, R. A. (1962). Elastic constants of calcite. *Journal of Applied Physics*, 33 (9), 2889-2892.
- Ravindran, P., Fast, L., Korzhavyi, P. A., Johansson, B., Wills, J., & Eriksson, O. (1998). Density functional theory for calculation of elastic properties of orthorhombic crystals: Application to TiSi2. *Journal of Applied Physics*, 84 (9), 4891-4904.
- RezaeiDoust, A., Puntervold, T., Strand, S., & Austad, T. (2009). Smart water as wettability modifier in carbonate and sandstone: A discussion of similarities/differences in the chemical mechanisms. *Energy & fuels*, 23 (9), 4479-4485.
- Rigo, V. A., Metin, C. O., Nguyen, Q. P., & Miranda, C. R. (2012). Hydrocarbon Adsorption on Carbonate Mineral Surfaces: A First-Principles Study with van der Waals Interactions. *The Journal of Physical Chemistry C*, 116(46), 24538-24548.
- Shariatpanahi, S. F., Strand, S., & Austad, T. (2011). Initial wetting properties of carbonate oil reservoirs: effect of the temperature and presence of sulfate in formation water. *Energy & Fuels*, *25*(7), 3021-3028.
- Strand, S., Høgnesen, E. J., & Austad, T. (2006). Wettability alteration of carbonates—Effects of potential determining ions (Ca^{2+} and SO^{4}_{2-}) and temperature. *Colloids and Surfaces A: Physicochemical and Engineering Aspects*, 275 (1), 1-10.
- Suijkerbuijk, B., Hofman, J., Ligthelm, D. J., Romanuka, J., Brussee, N., van der Linde, H., & Marcelis, F. (2012, January). Fundamental investigations into wettability and low salinity flooding by parameter isolation. In *SPE Improved Oil Recovery Symposium*. Society of Petroleum Engineers.
- Tang, G. Q., & Morrow, N. R. (1997). *Salinity, Temperature, Oil Composition, and Oil Recovery by Waterflooding. SPE Res Eng* 12 *(4): 269–276*. SPE-36680-PA.
- Titiloye, J. O., De Leeuw, N. H., & Parker, S. C. (1998). Atomistic simulation of the differences between calcite and dolomite surfaces. *Geochimica et cosmochimica acta*, 62 (15), 2637-2641.
- Vanderbilt, D. (1990). Soft self-consistent pseudopotentials in a generalized eigenvalue formalism. *Physical Review B*, 41 (11), 7892.
- Zahid, A., Shapiro, A., Stenby, E. H., & Yan, W. (2012). Managing injected water composition to improve oil recovery: A case study of North Sea chalk reservoirs. *Energy & Fuels*, 26 (6), 3407-3415.
- Zahid, A., Stenby, E. H., & Shapiro, A. A. (2010, January). Improved Oil Recovery in Chalk: Wettability Alteration or Something Else?. In *SPE EUROPEC/EAGE Annual Conference and Exhibition*. Society of Petroleum Engineers.

- Zhang, P., & Austad, T. (2005, June). Waterflooding in Chalk–Relationship between Oil Recovery, New Wettability Index, Brine Composition and Cationic Wettability Modifier (SPE94209). In *67th EAGE Conference & Exhibition*.
- Zhang, P., Tweheyo, M. T., & Austad, T. (2006). Wettability alteration and improved oil recovery in chalk: The effect of calcium in the presence of sulfate.*Energy & fuels*, 20 (5), 2056-2062.

Table

Table 1: Correlation of calcite crystal lattice values and atomic bond length between previously calculated experimental and computational values, with this work and showing good correlation with experimental values.

	exp1 (Markgraf and Reeder 1985)	exp 2 (Graf 1961)	DCACP (Rigo et al. 2012)	PW91 (Rigo et al.2012)	This work
a(Å)	4.988	4.99	5.122	5.042	4.997
c(Å)	17.068	17.0615	17.512	17.220	17.051
c/a	3.422	3.419	3.419	3.415	3.412
C-O (Å)	1.29		1.305	1.298	1.295
Ca-O (Å)	2.36		2.430	2.381	2.374

Table 2: Correlation of elastic constant between previously calculated experimental and computational values, with this work and showing good correlation with experimental values.

C_{ij} (GPa)	Exp1 (Dandekar 1968)	Exp2 (Peselnick 1962)	Cal1-RIM (Pavese, et al. 1992)	Cal2-SM (Pavese, et al. 1992)	This Work
C_{11}	146.3	144.5	152.7	152.6	148
C_{33}	85.3	83.1	77.8	79.0	85
C_{44}	34.0	32.265	30.4	24.4	34
C_{66}	43.3	43.7	48.0	47.6	46
C_{12}	59.7	57.1	56.8	57.3	55
C_{13}	50.8	53.4	53.9	50.8	54
C_{14}	-20.8	-20.5	10.8	7.3	-21

Table 3: Binding energy at 0°C of the most stable complex and its corresponding hydration compared with athermal simulations by Kerisit et al. 2004.

Atoms	This Work (n, E_{tot}(eV))	(Kerisit et al. 2004) (n, E_{tot}(eV))
Ca	8,-1.41	8,-1.22
Sr	8,-1.30	8,-0.74
Mg	6, -3.54	6,-2.42

Figures

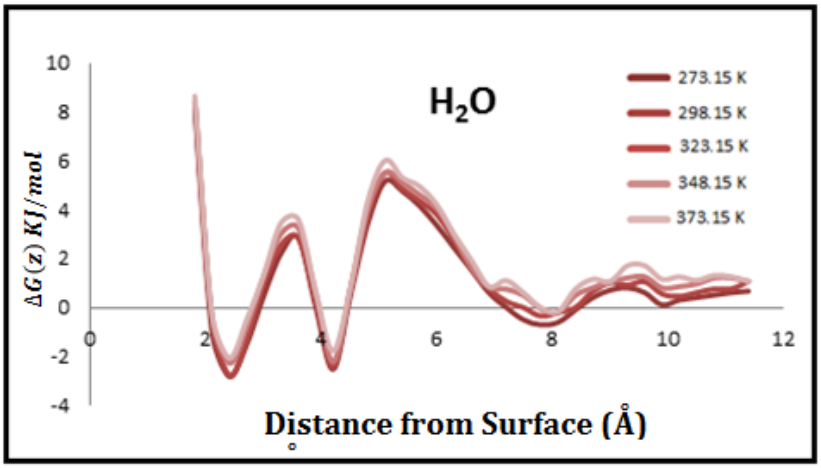


Figure1: Free energy profile of water at different temperatures, showing consistent high stability zones around 2.4 Å and 4.2Å.

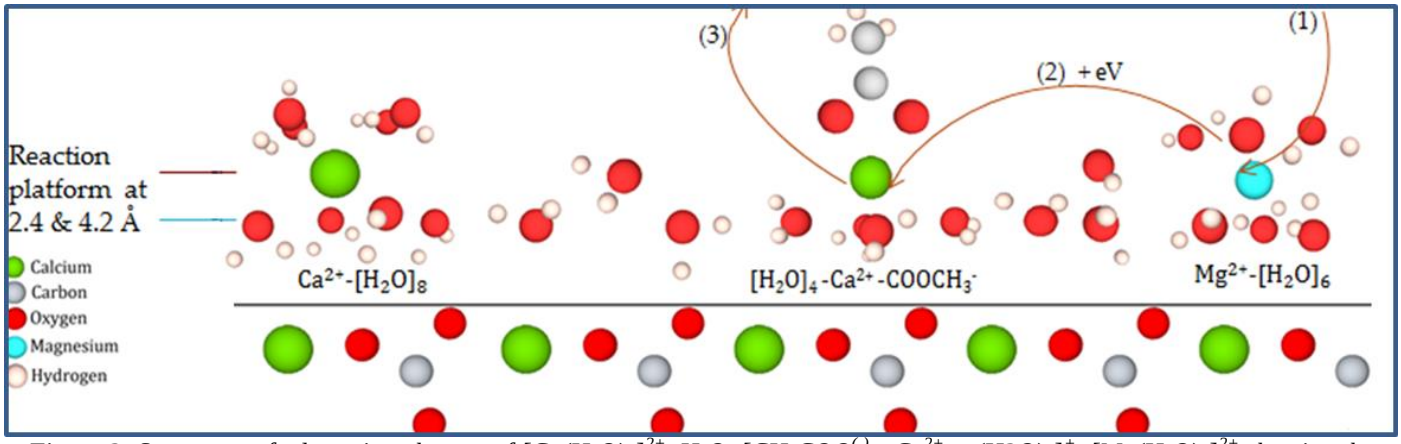


Figure 2: Structures of adsorption clusters of $[Ca(H_2O)_8]^{2+}$,H_2O, $[CH_3COO^{(-)}—Ca^{2+}— (H2O)_4]^{+}$, $[Mg(H_2O)_6]^{2+}$ showing the cation stability at a height of 4.2Å, and H_2O stability at 2.4 and 4.2Å. Arrows (1-3) indicate desorption of the carboxyl group by the energy released in adsorption of Mg^{2+}

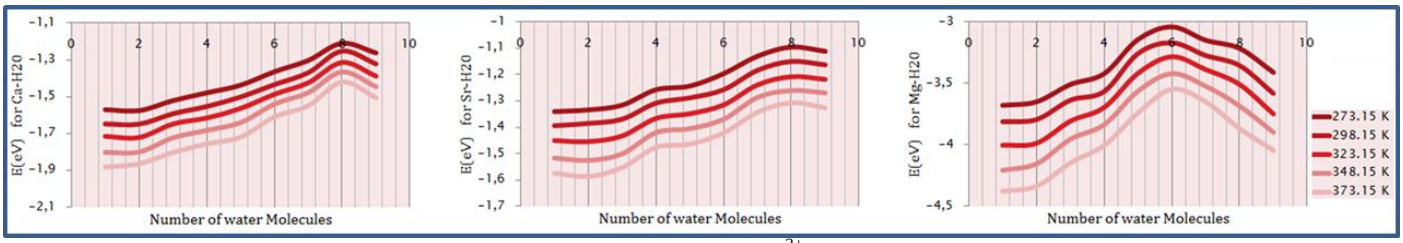


Figure 3: Binding energy for different complexes of the form $[C(H_2O)_n]^{2+}$ for C= Ca, Sr, and Mg and n=1-9. A consistent maximum stability at n=8 for Ca^{2+} and Sr^{2+} and n=6 for Mg^{2+}at all temperatures is indicated.

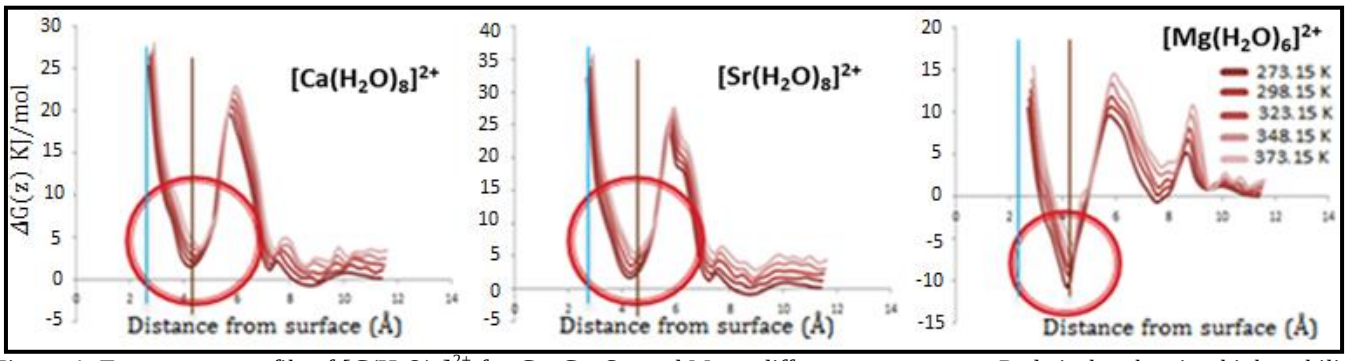


Figure 4: Free energy profile of $[C(H_2O)_n]^{2+}$ for C= Ca, Sr, and Mg at different temperature. Red circles showing high stability zone 4.2 Å, also showing negative free energy in Mg^{2+} adsorption.

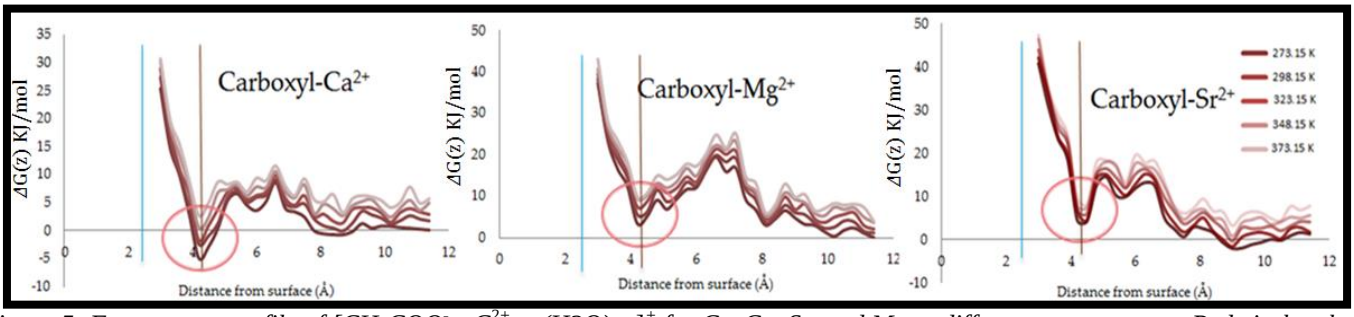


Figure 5: Free energy profile of $[CH_3COO^-—C^{2+}— (H2O)_{3-4}]^+$ for C= Ca, Sr, and Mg at different temperatures. Red circles show the high stability zone at 4.2 Å, also indicating the high stability of the carboxyl-Ca^{2+} complex.

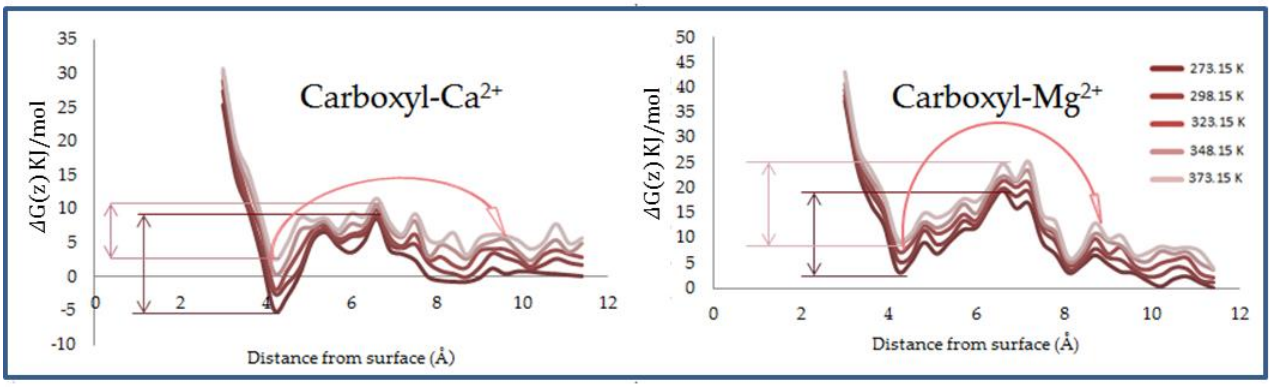


Figure 6: Temperature effect on the energy barrier to move the carboxyl from the surface to the bulk. At high temperature, a decrease in energy barrier for carboxyl-Ca^{2+} is observed, while no major effect is seen for the carboxyl-Mg^{2+} cluster.

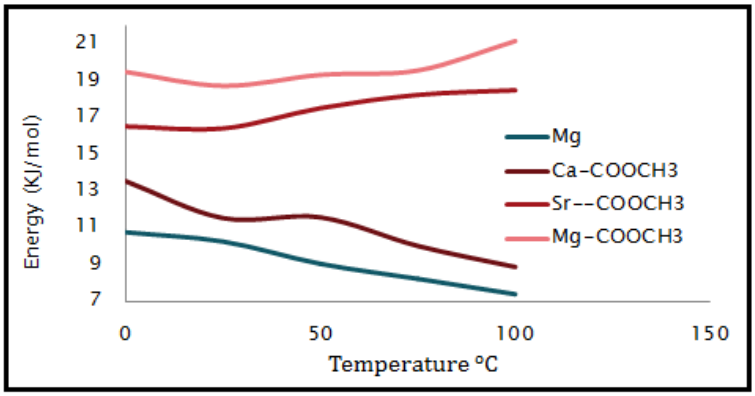


Figure 8: The energy barrier increases with temperature for carboxyl-Sr^{2+} and carboxyl-Mg^{2+}. The energy barrier to release carboxyl-Ca^{2+} is similar to the energy released by Mg^{2+} adsorption on the calcite surface. Both decreases with temperature rise.

Paper II

Chakravarty, K. H., Fosbøl, P. L., & Thomsen, K. (2015, April). Interactions of Fines with Oil and its Implication in Smart Water Flooding. In *SPE Bergen One Day Seminar*. Society of Petroleum Engineers.



SPE-173855-MS

Interactions of Fines with Oil and its Implication in Smart Water Flooding

Krishna Hara Chakravarty, Philip Loldrup Fosbøl and Kaj Thomsen, Center for Energy Resources Engineering (CERE), Department of Chemical and Biochemical Engineering, Technical University of Denmark

Copyright 2015, Society of Petroleum Engineers

This paper was prepared for presentation at the SPE Bergen One Day Seminar held in Bergen, Norway, 22 April 2015.

This paper was selected for presentation by an SPE program committee following review of information contained in an abstract submitted by the author(s). Contents of the paper have not been reviewed by the Society of Petroleum Engineers and are subject to correction by the author(s). The material does not necessarily reflect any position of the Society of Petroleum Engineers, its officers, or members. Electronic reproduction, distribution, or storage of any part of this paper without the written consent of the Society of Petroleum Engineers is prohibited. Permission to reproduce in print is restricted to an abstract of not more than 300 words; illustrations may not be copied. The abstract must contain conspicuous acknowledgment of SPE copyright.

Abstract

Migration of fines has been observed during water flooding in chalk reservoirs and has been suggested to play a key role in enhanced oil recovery (EOR). But, the exact role of fines is not well studied for carbonate reservoirs. This study shows that addition of water and crude oil on calcite fines leads to formation of soluble oil emulsions in the water phase. Formation of these emulsions and its implication in EOR has been experimentally analyzed.

To study this phenomenon, different water insoluble salts were used as fines including: Li_2CO_3, $MgCO_3$, $CaCO_3$, $CaSO_4$, $SrSO_4$ and $BaSO_4$ to which oil and water were added. To study conditions of oil emulsions formation, design oil was used consisting of hexane and hexadecane. Heptanoic acid and stearic acid were doped in various compositions to mimic the acid number of the oil. Experiments were conducted for pure crude oil and doped oil to understand its implications in EOR. Composition of initial and final (floating) oil was obtained through gas chromatographic (GC) analysis. The two were thereafter compared to obtain the composition of emulsions formed.

The experiments showed that oil emulsions are only formed when polar hydrocarbons are present in the oil. Different mixtures of alkanes did not produce any emulsion. In oil containing stearic acid it was observed that around 95% of the initial stearic acid was accumulated in the emulsions and only 5% was found in the floating oil. In oil samples containing heptanoic acid only 50-60% of its initial amount was accumulated in the emulsions. This indicates heavier acids can form more stable emulsions. Oil emulsions were produced with all the different fines used, but the composition of these emulsions where dependent on the salt anions. With all carbonates, lighter acids preferred emulsions formation with lighter alkane, (indicated by intensification of heavier alkane in the floating oil compared to the initial oil) and vice versa for heavier acids. While no such selectivity in emulsions formation was observed with any of the sulphates. Results obtained with crude oil and doped oil and designed oil were consistent. These results show that fines (of insoluble carbonate) released during core fracturing, or (sparingly soluble sulphates) formed during smart water flooding can form mixed wet water-soluble oil emulsions and help in mobilization of trapped oil along with increasing sweep efficiency. The results clearly show oil emulsion formation in the water phase from the interactions of oil with fines, and also provide a detailed understanding of its composition under different conditions. The study highlights the significance of fines during smart water flooding in carbonate reservoirs and shows how its role in EOR can be mistakenly underestimated.

Introduction

In the last decade, flooding of reservoirs with different salinity brines have emerged into a possible method of EOR technology that does not require toxic or expensive chemicals (Webb et al. 2005; Karoussi et al. 2007; Fjelde et al. 2009; Strand et al. 2006; Tweheyo et al. 2006; Zhang et al. 2007). In general it is universally accepted that altering the brine composition and its salinity can increase the recovery fractions for chalk reservoirs (Webb et al. 2005; Karoussi et al. 2007; Zhang et al. 2007), but fundamental mechanism of this EOR method is still not completely understood. To comprehend this innovative water flooding method, various research groups have applied a range of scientific engineering disciplines: It includes colloid and surface chemistry, thermodynamics of crude oil and brine, and flow behavior in porous media (Zhang et al. 2007a; Bagci et al. 2001; Austad et al. 2005; Fernø et al. 2011; Zahid et al. 2010).

Austad and co-workers have done a broad scale laboratory research, in order to understand the process of EOR from chalk using altered sea water (Strand et al. 2006; Zhang et al. 2007; Austad et al. 2005; Zhang et al. 2006; Puntervold et al. 2009). Herein, it

has been documented that SO_4^{2-} is a potential determining ion for increasing oil recovery in chalks. It is further proposed that the SO_4^{2-} ion must act along with Ca^{2+} and Mg^{2+} because sulphate alone cannot lead to enhanced oil recovery (Austad et al. 2005). Over a series of presented experiments, wettability alteration has been shown as the basis of enhanced oil recovery. Among these publications, majority of the reported experiments were conducted with Danish Stevns Klint outcrop chalk (Strand et al. 2006). The proposed mechanism constitutes two processes: (1) substitution of calcium by magnesium on calcite surfaces. (2) Adsorption of sulphate ions on the mineral surface associated with release of adsorbed carboxylic compounds which makes the surfaces more water wet. In the effluent water, decrease in sulphate concentration also shows that sulphate acts as a reagent in this process (Zhang et al. 2007a; Bagci et al. 2001). In most situations, the importance of soluble Ca^{2+}, Mg^{2+} and SO_4^{2-} ions in brine solution have been emphasized for obtaining enhanced oil recovery (Strand et al. 2006; Zhang et al. 2007;Austad et al. 2005;Zhang et al. 2006; Puntervold et al. 2009).

The wettability alteration mechanism has several unanswered questions (Fernø et al. 2011; Zahid et al. 2010; Zahid et al. 2012). It has been determined that the effect of sulphate concentration in EOR is highly dependent on the origin of the core sample. In chalk samples from Niobara in United States and Rørdal in Denmark the effect of sulphate in the enhancement of oil recovery was negligible while Stevns Klint outcrop chalk in Denmark showed a consistent increase in oil recovery with increase in sulphate concentration (Fernø et al. 2011). Moreover for totally water wet systems, 10% increase of oil recovery has been detected through smart water flooding experimentations (Zahid et al. 2010), which is contrary to the wettability alteration mechanism (Austad et al. 2005). Oil Emulsion formation and fine migration have also been suggested to be related to oil recovery, but no concrete evidence of this has been provided (Zahid et al. 2010; Zahid et al. 2011a; Zahid et al. 2012). Increased oil recovery has been found in connection to pressure drop, and fines migration was suggested as a possible reason (Zahid et al. 2010). It is also reported that experiments with variation of total acid number and the total base number of oil do not provide any direct co-relation to oil recovery (Suijkerbuijk et al. 2012). These experiments show vital points of differences (Fernø et al. 2011; Zahid et al. 2010; Zahid et al. 2012) from the wettability alteration model (Austad et al. 2005).

The pioneering study by Tang and Morrow (Tang and Morrow et al. 1999) has provided some primary condition for EOR through brine alternation, which includes (1) availability of potential mobile fines, (2) desorption of crude oil from mineral surface during water flooding and (3) initial water saturation. The study showed that variation of brine conditions had no effect in oil recovery for cores devoid of mobile fines. The study also proposed that mobile fines can bring trapped oil from the mineral surface to the flooded water phase and enhance its mobility during water flooding (Tang and Morrow et al. 1999).But formation of such micelles/emulsions due to interaction between oil and fines has been physically observed in previous studies. Some formation of emulsions has previously been shown (Zahid et al. 2011a), but the exact reason has not been explored in details. In reservoir oil production, considerable amounts of fines/sediments are often observed during water flooding (Stewart 1980). It has been known for decades that there are considerable amounts of basic sediment and water (BS&W) in the produced oil (Demny and Stewart 1985). Thus clearly during smart waterfloods, interaction between fines and the crude oil is possible. The pattern of these interactions affects the displacement efficiency of the oil; which would in turn affect the final oil recovery. This interaction between fines and oil has not been studied in details. Consequently its contribution in increasing the displacement efficiency of oil during smart waterfloods has not been calculated. It is important to analyze this adhesion phenomenon through a series of experiments on a more fundamental scale.

A series of experiments were conducted in this work, to study the interaction of the crude oil with fines. A simple experimental setup was used for emulsification of oil, as shown in Figure 1. Formation of emulsion due to interaction between $CaCO_3$ fines and crude oil originating from Dan field of Danish North Sea is shown in figure 1b.In this study, different kinds of fines (as listed in Table 1) have been used to study this phenomenon. Each type of fines has been individually analyzed together with several designed oils (listed in Table 1). These various combinations show the exact behavior of each hydrocarbon with different types of fines during these interactions. In this work we have considered calcium carbonate (C1), magnesium carbonate (C2), and lithium carbonate (C3), as three carbonate fines, calcium sulphate (S1), barium sulphate (S2), and strontium sulphate (S3) as three sulphate fines, and kaolinite (K1) as a clay mineral. The composition of the designed oil was varied significantly: one set of designed oil (O1) was prepared with heavy acid while the second designed oil (O2) includes light acid. Formation of emulsion was thereafter observed for different doped and designed oils as shown in figure2b. Patterns and conditions of emulsions formations of O1 and O2 with the various fines were studied through a series of experiments (shown in figure 3-7). Thereafter similar experiments were conducted with crude oil containing heavy acid (O3) and light acid (O4) to further correlate the observed results (as shown in figure 8). Formation of these micro emulsions was observed for the various different cases and consistent sets of patterns were established to characterize the properties of these emulsions.

Experimental details

Experimental setup

A simple experimental setup was developed (Figure 1) to study the conditions of the emulsion formation. First, 2 grams of the insoluble fines were added to 10ml of oil and 50ml of deionized water (Table 1). This system was stirred for 1 hour and the solution was kept in a closed container at room temperature for 18 hours to attain equilibrium. Subsequently it was observed that an emulsion was formed, as shown in Figure 1. Along with the fines (precipitates), water, and oil, the formation of water soluble oil emulsion takes place. Experiments with pure alkanes including hexane and decane did not show any emulsion formation on interactions with fines. As observable in figure 2a no emulsion formation takes place when the oil is devoid of polar components. Also

experiments with different oil combinations and water in absence of fines did not lead to any emulsion formation (as observable in figure 2a). It was thus concluded that presence of both fines and polar acid fraction are required for emulsion formation. Thus in all further experiments alkane combinations doped with polar acids were used. This generated a significant amount of emulsion formation, while a considerable amount of oil remained floating at the top of the emulsions. The emulsion formation caused by interactions between polar fractions of oil and fines is observable in figure 2b. To further study the properties of these oil emulsions, samples of oil were extracted from the floating fraction. This floating oil (final oil) and the oil added to the system originally (initial oil) was analyzed by gas chromatography and the compositions of the two oils were obtained. The compositions were plotted in triangular diagrams so that any change in composition could be analyzed.

Sample analysis

The ASTM D2887 method (Chorn et al. 1984), recommended for alkane analysis was used for the compositional analysis of crude oil mixtures (Blomberg et al. 2002; Adahchour et al. 2008; Dutriez et al. 2010). The acquisition instrument was Agilent 7890A, as previously used for alkane analysis (Dutriez et al. 2010; Saleh et al. 2009). The oven had an equilibrium time of 3mins, maximum temperature of 350°C and initial temperature of 40°C. It was heated 350°C in 4mins. The runtime of each sample was 19.5 mins. A 1μL front injector, with each injection volume 0.05 μL was used. After each analysis the injector was washed three times with toluene with each sample volume of 0.8 μL. In the front inlet He gas had a pressure of 0.226 bars and a total flow rate of 42.9 ml/min, with a septum purge flow of 3 ml/min. The inlet temperature was initially 50°C. It was then raised to 330°C for 5 min. The Agilent 125-10HB10 m x 530 μm x 2.65 μm column was used. It has void time of 0.173 min and maximum temperature of 350.0°C. The outlet had an initial temperature of 40°C, and a pressure of 0.226 bars. The flow rate of the outlet was 13.3 mL/min and it had an average velocity of 96.52 cm/sec. The front detector was heated to 375°C. HereintheH_2 flow rate was 40 mL/min and air flowrate was 450 mL/min. For each run the relative compositions of the oil components were calculated using Agilent simulated distillation. For all initial samples up to 5 repetitions was made, and consistency in obtained composition was more than 95%.

Experimental components

Three types of fines were studied: First, emulsion formations with carbonate fines (Table 1) were studied. These carbonates are sparingly soluble in water (solubility in water: $CaCO_3$0.0013 g/100 mL; $MgCO_3$0.0106 g/100ml; $Li_2CO_3$1.29 g/100 mL at STP (Garrels et al. 1961)) and thus most of the carbonate remains as fines in the solution (containing 2g of fines per 50 ml of water). While $CaCO_3$ makes up the major fraction of chalk and lime stone, $MgCO_3$is also found in reservoirs in small fractions. Li_2CO_3 was used to further develop a general understanding of the carbonates in emulsion formation. The fines were obtained from Sigma-Aldrich (Product Number $CaCO_3$: Z545643; $MgCO_3$: M7179; Li_2CO_3:62470).

The second sets of chemicals were sulphate fines (Table 1). Three different sulphates were used ($CaSO_4$, $BaSO_4$ and $SrSO_4$). All of these three sulphates are sparingly soluble in water ($CaSO_4$: 0.21g/100ml, $BaSO_4$:0.0002448 g/100 mL and $SrSO_4$:0.0135 g/100 mL at STP (Carlsberg et al. 1973). Thus, stable fines can exist in these solutions (containing 2g of fines per 50ml of water). In many previous SW-EOR studies it is mentioned that increasing concentrations of Ca^{2+}, $Mg^{2+}$and SO_4^{2-} can lead to higher oil recovery (Zhang et al. 2007; Austad et al. 2005). Increasing the concentrations of Ca^{2+} and SO_4^{2-} will cause precipitation of $CaSO_4$(s) as the brine is already saturated with this salt. Thus, it is equally important to understand the pattern of emulsion formations due to $CaSO_4$(s) precipitation. To explore the general behavior of sulphates in emulsion formation, $BaSO_4$, and$SrSO_4$ was used in addition to $CaSO_4$. The fines were obtained from Sigma-Aldrich (Product Number $CaSO_4$: 238988; $BaSO_4$: 202762; $SrSO_4$:433365). These chemicals have been previously used for similar geochemical analysis with sedimentary rocks (McLennan et al. 2014) thus was presumed suitable for this analysis.

In the third set of experiments, kaolinite was used as the only clay mineral. Small fines of kaolinite are often available in reservoirs and have been shown to influence the displacement efficiency of the crude oil (Tang and Morrow et al. 1999). Kaolinite is also sparingly soluble in water (Kittrick 1980) and forms stable fines that can actively contribute to emulsion formation by interacting with the oil and water. Kaolinite,$Al_2Si_2O_5(OH)_4$, was obtained from Sigma-Aldrich (Product Number: 03584).

Four types of oil were designed to study the interactions profoundly. The first set of designed oil (O1) consisted of hexane, hexadecane and stearic acid (Table 1). This ensured that the acid was of similar length to a fraction of the alkanes (hexadecane) and significantly heavier than the rest (hexane). The composition of hexane and hexadecane and stearic acid was varied in 12 different samples. These were used to conduct the experiment with each of the different fines. The second set of designed oil (O2) consisted of hexane, hexadecane and heptanoic acid. This ensured that the acid was of similar length to a fraction of the alkanes (hexane) and significantly lighter than the rest (hexadecane). The composition of these three chemicals was also varied. 12 different samples were made and these different oil samples were used to analyze their effect with the different fines (as stated above). Thereafter crude oil from the Dan field in the Danish North Sea was obtained from Maersk oil. This crude oil was used to further study the emulsion formations. The third set of oil (O3) was obtained by toting O1 with crude oil in various fractions. This ensures that the oil selectively contained stearic acid with varying fractions of different alkanes in the crude oil. By varying the concentration of the alkanes, 10 different oil samples were prepared. In the fourth oil set (O4) the crude oil was doped with O2 in various fractions. This ensures that the oil selectively contained heptanoic acid with varying fractions of different alkanes in the crude oil. By varying the concentration of the alkanes, 10 different oil samples were prepared. These oil samples were used for studying their behavior with the fines and understand the composition of the emulsion and the characteristics of the mechanism. In this experi-

ment it is observed that stirring water and crude oil with calcite fines leads to the formation of water soluble oil emulsions as shown in figure 2b. The composition of the initial and final oil was obtained through gas chromatographic analysis. Best grade chemicals were obtained for the fines and organic compounds to avoid any error in the conducted experiments.

Results & Discussion

In the first set of experiments, O1, water, and $CaCO_3$ fines were stirred and left for equilibration. After attaining equilibrium, significant amount of oil emulsion was observable in the water as shown in figure 2b. Samples from the floating oil and initial oil were taken for chromatographic analysis and the composition of the oil samples were calculated. Through gas chromatography it was observed that the composition of stearic acid was significantly reduced in the final oil (as shown in Figure 3). The hexadecane concentration was also reduced significantly in the final oil as compared to the initial oil, while the hexane concentration increased. In other words, the oil emulsion formed consisted mainly of stearic acid and hexadecane. This indicates that stearic acid plays an active role in the formation of this oil emulsion. The same set of experiments was repeated with magnesium carbonate fines (as also shown in Figure 3). Also in this case stearic acid together with hexadecane was depleted from the final oil and must have formed the emulsion together with the magnesium carbonate fines. The emulsion formation with lithium carbonate showed the same trend.

In all of the carbonate experiments it was observed that approximately 95wt% of the stearic acid was missing in the final oil and instead contributed to the water soluble emulsion formation (as shown in Figure 3). Approximately 50 wt% of the initial hexadecane was removed from the final oil and contributed to the formation of oil emulsions. These results remain consistent while changing the cation of the fines (Ca^{2+}, Mg^{2+}, Li^{+}) indicating that it is a property of the carbonates (Figure 3), not Ca^{2+}, Mg^{2+}or Li^{+}).

A similar set of experiments was conducted with the different sulphate fines. First calcium sulphate fines were used and their interaction with stearic acid containing oil (O1) was analyzed. The gas chromatographic results showed that the stearic acid content was significantly reduced; but neither hexane nor hexadecane concentrations changed selectively. This indicated that the oil emulsions formed had no selectivity of hexadecane over hexane in case of calcium sulphate fines (as shown in Figure 4). The same experiment was conducted for barium sulphate fines and the observed results were quite similar to that of calcium sulphate fines. The stearic acid concentration was significantly reduced in the final oil but there was no selectivity of hexane or hexadecane in the oil emulsion formations. To further scrutinize this trend, the experiment was also conducted with strontium sulphate fines. Exactly the same trend was again observed (Figure 4). With all these three sulphate fines the results are quite consistent over the variations in oil composition and variation in the alkane. With all the sulphate fines it was observed that approximately 95 wt% of the stearic acid was depleted from the oil and was contributing to the formation of the water soluble emulsions.

The experiments with carbonate fines and sulphate fines document that the alkane selectivity is dependent on the anion of the fines. Carbonate fines have selectivity for hexadecane, but no such selectivity was observed for sulphate fines. In both cases it was observed that around 95-96% of the stearic acid was contributing to the formation of the oil emulsion. Only 4-5% of the initial amount of stearic acid was available in the final oil, indicating that stearic acid played a significant role in the formation of emulsions irrespective of the type of fines.

The same set of experiments was conducted with O2 (oil composed of heptanoic acid instead of stearic acid). Considerable emulsion formation took place as shown in figure2b.When calcium carbonate fines were used, it was observed through gas chromatographic analysis that the behavior of the light heptanoic acid was significantly different from the behavior of stearic acid. The heptanoic acid concentration was reduced in the final oil as compared to initial oil but was not removed to the same extent as was seen with stearic acid. Around 50% of the initial heptanoic acid content was available in the final oil indicating that this acid participated in the oil emulsion formation, but with less affinity than stearic acid (Figure 5). Supplementary it was observed that the hexadecane concentration in the final oil increased significantly while the concentration of hexane was reduced, indicating selectivity of hexane over hexadecane in the emulsion formation with the light (heptanoic) acid (Figure 5). To further analyze this phenomenon, the experiment was conducted with the magnesium carbonate fines. Again it was observed that heptanoic acid was partially removed from the final oil indicating that it did contribute to oil emulsion formation but only partially (Figure 5). Also in this case, hexane concentration was diminished along with heptanoic acid. Thus the oil emulsion formation showed selectivity of hexane over hexadecane indicating that it was the light acid that caused the formation of the oil emulsion. Finally, lithium carbonate fines were used. The gas chromatographic analysis of the initial and the final oil showed the same pattern as with calcium and magnesium carbonate fines: The oil emulsion formation was selective of hexane over hexadecane. Heptanoic acid partially participated in the emulsion formation (as shown in figure 5). These results together suggest that light acids prefer to form oil emulsions with light alkanes and heavy acids prefer to form oil emulsions with heavy alkanes.

The same set of experiments was carried out with sulphate fines and oil O2 (oil composed of heptanoic acid instead of stearic acid). The results are shown in Figure 6. Heptanoic acid contributed partially to the oil emulsion formation. 45-50% of the initial heptanoic acid content was still available in the final oil; indicating less affinity than stearic acid (similar to the oil O2 interactions with carbonate fines). As previously observed with sulphate fines, no selectivity of alkane in the oil emulsions formation could be seen. The relative concentrations of hexane and hexadecane did not change in the final oil. The experiment was repeated with barium sulphate fines and with strontium sulphate fines. The same phenomena were again observed in these two cases: no selec-

tivity of one alkane over the other and the heptanoic acid was reduced to around 45-50% of the initial heptanoic acid content (Figure 6). These results further show that amount of fines participating in emulsion formation is dependent on the type of acid present in the oil.

Next, experiments were conducted with different clay fines. First, the interaction of kaolinite fines with a stearic acid containing oil (O1) was analyzed. The gas chromatographic results showed that the stearic acid content of the oil was significantly reduced but the ratio between hexane and hexadecane concentrations did not change much. The results are shown in figure 7. The same experiment was conducted with kaolinite fines and oil O2 (oil composed of heptanoic acid instead of stearic acid). As shown in figure 7 the heptanoic acid only partially contributed to the oil emulsion formation. The amount of heptanoic acid in the final oil was reduced to around 40-50% of the content in the initial oil. This result is similar to the results obtained with oil O2 and sulphate fines. No selectivity of alkanes in the emulsion formation was observed (figure 7). These results show that clay mineral behaves similar to sulphate fines and can readily form oil emulsions irrespective of the available alkanes.

These results together suggests that the light acids do not participate in oil emulsion formation as extensively as heavy acids do, furthermore, sulphate fines do not have any selectivity of any particular alkane in oil emulsions formation. To investigate these trends with crude oil, further experiments were conducted with oils O3 and O4 using calcium carbonate fines. The oils were composed of several compounds (Table 1).In both cases, considerable emulsion formation took place as shown in figure2b. The initial oil and the final oil compositions were plotted in a triangular diagram for analysis (Figure 8). In the three corners of the diagram are the acid, the hydrocarbons from C5 (Pentane) to C10 (Decane), and the hydrocarbons from C15 (Pentadecane) to C20 (Dodecane). The same type of experiment was conducted with this mixture. The gas chromatographic analysis of the final oil shows that the stearic acid content was significantly diminished, indicating that stearic acid was the main component in emulsion formation by interacting with the fines. The content of C5 to C10 slightly increased in the final oil, indicating that the heavier fractions were selectively chosen for oil emulsion formation (Figure 8). The content of the lighter alkanes increased in the floating oil and stearic acid was completely depleted from the final oil in these experiments. Similar experiments were conducted with heptanoic acid doped crude oil O4, for varying concentrations of the alkanes. Also here it was observed that the heptanoic acid content was partially removed in the final oil, implying that it contributed partially to the emulsion formation. The content of the heavy fraction of oil i.e. C15 to C20 increased slightly in the final oil and the fraction of lighter hydrocarbons, C5 to C10, decreased in the final oil. This indicated that the emulsions formed in this process selectively favored the light alkanes over the heavier alkanes (Figure 8).This is in agreement with the previously observed trend for carbonate fines.

The results from all these experiments suggest that oil emulsion formation can take place with various reservoir fines. The only primary criterion for emulsion formation from trapped oil is the availability of polar fractions in the crude oil and mobile fines in the pore space. It is further observed that light acids do not participate in oil emulsions formation as extensively as heavy acids do. Around 95% of the stearic acid content of oil participates in emulsion formation, whereas only 40-50% of the heptanoic acid content participates. Furthermore sulphate fines have no selectivity of any particular alkane in emulsion formation. Carbonate fines on the other hand cause light acids to prefer forming oil emulsions with light alkanes and heavy acids prefer forming oil emulsions with heavy alkanes. The amount of oil emulsion formation significantly depends on the kind of acids available in the crude oil. This shows that oil with same/similar total acid number (TAN) may result in different amount of emulsion formation. Thus, it is important to further analyze the crude oil and obtain the exact amount of each acid available in the oil in order to predict the amount of oil emulsion formation. Inconsistent variation in oil recovery with changes in TAN (Austad et al. 2008; Suijkerbuijk et al. 2012) could be related to the variation in the amount of emulsion formation.

Zahid et al. 2010 showed that SW-EOR can be observed for completely water wet systems. No wettability alteration can take place and emulsification of oil was suggested to be the primary reason. Furthermore Zahid et al. 2010 observed that variation of oil type had significant effect in oil recovery, but did not observe any correlation between TAN and EOR. The observed emulsification in this study shows a similar trend. The type of acid present in the oil plays a dominant role in deciding the amount of emulsion formation. TAN of the oil cannot be correlated to the amount of emulsion formation. Thus emulsification of oil as observed in this study could be a possible reason for the observed EOR for completely water wet system. Nevertheless, further studies are required to prove or disprove the same.

In pioneering study by Tang and Morrow 1999, it has also been observed that variation of salinity has no effect on EOR for cores devoid of fines. Herein it was suggested that mobile fines can bring trapped oil into the water phase. Although such emulsion/micelles formation due to interaction between insoluble fines and oil have not been previously recorded. Through this experimental study it is clearly observed that oil emulsion formation combines insoluble fines, water, and crude oil. It also shows that fines are capable of bringing small oil droplets into the water phase. This study supports the proposed mechanism by Tang and Morrow 1999, and provides supporting evidence to the same.

The formation of water soluble oil emulsions can significantly enhance the mobility of the oil. Oil emulsions formed in the pores can thus be a possible reason behind the observed EOR. Although there is not enough experimental evidence to prove that these water soluble oil emulsions contribute to SW-EOR the phenomenon needs to be considered for further experimental analysis. Besides wettability alteration, formation of fines due to changes in brine composition may have additional effects in SW-EOR. It

also needs to be considered that there are several cases of fine formations in previously conducted experiments (Tang and Morrow et al. 1999; Zahid et al. 2010; Zahid et al. 2011a).

Conclusion

In the pioneering work Tang and Morrow et al. 1999 it was suggested that fines can bring trapped oil into the water phase, which can in turn increase the mobility of trapped oil significantly. This study provides ample evidence to support this claim. As we observe that different kinds of insoluble fines can interact with in soluble oil and produce water soluble emulsions. This study further provides the following characterization for emulsions formation.

1. The crude oil must contain polar fractions for any such emulsions to form.
2. The amount of emulsion formation does not depend on the cation of the available fines.
3. All different kinds of carbonate, sulphate and clay fines used in these experiments showed formation of oil emulsions in the water.
4. The oil emulsion formation actively takes place when heavier acids are present. This is irrespective of the kinds of fines available in the system.
5. Carbonate fines show selectivity of alkanes in emulsion formation: light alkanes prefer to form emulsions with light acids while heavier alkanes prefer to form emulsions with heavy acids.
6. No such selectivity was observed for sulphate fines or clay fines.

These results together shows that fines in the system can act as a major catalyst in bringing trapped oil into water phase. And thus it supports the idea that formation of fines can enhance the displacement efficiency of oil during smart water floods.

Acknowledgment

This article is a part of research study in smart water project and center for energy resource engineering. The authors acknowledge Maersk Oil, Dong Energy, and The Danish Energy Agency (EUDP) for funding the Smart Water project.

References

- Adahchour, M., Beens, J., & Brinkman, U. A. (2008). Recent developments in the application of comprehensive two-dimensional gas chromatography. *Journal of Chromatography A*, **1186**(1), 67-108.
- Akbar, M., Vissapragada, B., Alghamdi, A. H., Allen, D., Herron, M., Carnegie, A., &Saxena, K. (2000). A snapshot of carbonate reservoir evaluation.*Oilfield Review*, **12**(4), 20-21.
- Austad, T., Strand, S., Madland, M. V., Puntervold, T., & Korsnes, R. I. (2008). Seawater in chalk: An EOR and compaction fluid. *SPE Reservoir Evaluation & Engineering*, **11**(04), 648-654.
- Austad, T., Strand, S., Høgnesen, E. J., & Zhang, P. (2005, January). Seawater as IOR fluid in fractured chalk. In *SPE International Symposium on Oilfield Chemistry*. Society of Petroleum Engineers.
- ASTM D2887-06, Standard Test Method for Boiling Range Distribution of Petroleum Fractions by Gas Chromatography, http://www.astm.org/DATABASE.CART/HISTORICAL/D2887-06.htm.
- Bagci, S., Kok, M. V., &Turksoy, U. (2001). Effect of brine composition on oil recovery by waterflooding. *Petroleum science and technology*, **19**(3-4), 359-372.
- Blomberg, J., Schoenmakers, P. J., & Brinkman, U. A. (2002). Gas chromatographic methods for oil analysis. *Journal of Chromatography A*,**972**(2), 137-173.
- Carlberg, B. L. (1973, January). Solubility of calcium sulphate in brine. In *SPE Oilfield Chemistry Symposium*. Society of Petroleum Engineers.
- Chorn, L. G. (1984). Simulated Distillation of Petroleum Crude Oil by Gas Chromatography. Characterizing the Heptanes-Plus Fraction. *Journal of Chromatographic Science*, **22**(1), 17-21.
- Demny, F. C., & Stewart, T. L. (1985). *U.S. Patent No. 4,543,191*. Washington, DC: U.S. Patent and Trademark Office.
- Dutriez, T., Courtiade, M., Thiébaut, D., Dulot, H., &Hennion, M. C. (2010). Improved hydrocarbons analysis of heavy petroleum fractions by high temperature comprehensive two-dimensional gas chromatography. *Fuel*, **89**(9), 2338-2345.
- Fernø, M. A., Grønsdal, R., Åsheim, J., Nyheim, A., Berge, M., &Graue, A. (2011). Use of Sulphate for Water Based Enhanced Oil Recovery during Spontaneous Imbibition in Chalk. *Energy &fuels*, **25**(4), 1697-1706.
- Fjelde, I. F., &Aasen, S. M. A. (2009, April). Improved spontaneous imbibition of water in reservoir chalks. In *15th European Symposium on Improved Oil Recovery*.
- Garrels, R. M., Thompson, M. E., &Siever, R. (1961). Control of carbonate solubility by carbonate complexes. *American Journal of Science*, **259**(1), 24-45.

- Karoussi, O., &Hamouda, A. A. (2007). Imbibition of sulphate and magnesium ions into carbonate rocks at elevated temperatures and their influence on wettability alteration and oil recovery. *Energy & fuels*, **21**(4), 2138-2146.
- Kittrick, J. A. (1980). Gibbsite and kaolinite solubilities by immiscible displacement of equilibrium solutions. *Soil Science Society of America Journal*,**44**(1), 139-142.
- McLennan, S. M., Anderson, R. B., Bell, J. F., Bridges, J. C., Calef, F., Campbell, J. L.,&Yingst, R. A. (2014). Elemental geochemistry of sedimentary rocks at Yellowknife Bay, Gale crater, Mars. *Science*, **343** (6169), 1244734.
- Puntervold, T., Strand, S., &Austad, T. (2009). Coinjection of seawater and produced water to improve oil recovery from fractured North Sea chalk oil reservoirs. *Energy & fuels*, **23**(5), 2527-2536.
- Saleh, A., Yamini, Y., Faraji, M., Rezaee, M., &Ghambarian, M. (2009). Ultrasound-assisted emulsification microextraction method based on applying low density organic solvents followed by gas chromatography analysis for the determination of polycyclic aromatic hydrocarbons in water samples. *Journal of Chromatography A*, **1216**(39), 6673-6679.
- Stewart, T. L. (1980). *U.S. Patent No. 4,184,952*. Washington, DC: U.S. Patent and Trademark Office.
- Strand, S., Høgnesen, E. J., &Austad, T. (2006). Wettability alteration of carbonates—Effects of potential determining ions (Ca^{2+} and SO_4^{2-}) and temperature. *Colloids and Surfaces A: Physicochemical and Engineering Aspects*, **275**(1), 1-10.
- Suijkerbuijk, B., Hofman, J., Ligthelm, D. J., Romanuka, J., Brussee, N., van der Linde, H., &Marcelis, F. (2012, January). Fundamental investigations into wettability and low salinity flooding by parameter isolation. In *SPE Improved Oil Recovery Symposium*. Society of Petroleum Engineers.
- Tang, G. Q., & Morrow, N. R. (1999). Influence of brine composition and fines migration on crude oil/brine/rock interactions and oil recovery. *Journal of Petroleum Science and Engineering*, **24**(2), 99-111.
- Tweheyo, M. T., Zhang, P., &Austad, T. (2006, January). The effects of temperature and potential determining ions present in seawater on oil recovery from fractured carbonates. In *SPE/DOE Symposium on Improved Oil Recovery*. Society of Petroleum Engineers.
- Webb, K. J., Black, C. J. J., &Tjetland, G. (2005, November). A laboratory study investigating methods for improving oil recovery in carbonates. In*International Petroleum Technology Conference*. Doha, Qatar: International Petroleum Technology Conference.
- Zahid, A., Stenby, E. H., & Shapiro, A. A. (2010, January). Improved Oil Recovery in Chalk: Wettability Alteration or Something Else?. In *SPE EUROPEC/EAGE Annual Conference and Exhibition*. Society of Petroleum Engineers.
- Zahid, A., Sandersen, S. B., Stenby, E. H., von Solms, N., & Shapiro, A. (2011). Advanced waterflooding in chalk reservoirs: Understanding of underlying mechanisms. *Colloids and Surfaces A: Physicochemical and Engineering Aspects*, **389**(1), 281-290.
- Zahid, A., Shapiro, A. A., &Skauge, A. (2012, January). Experimental Studies of Low Salinity Water Flooding Carbonate: A New Promising Approach. In *SPE EOR Conference at Oil and Gas West Asia*. Society of Petroleum Engineers.
- Zahid, A., Stenby, E. H., & Shapiro, A. A. (2012, January). Smart Waterflooding (High Sal/Low Sal) in Carbonate Reservoirs. In *SPE Europec/EAGE Annual Conference*. Society of Petroleum Engineers.
- Zhang, P., Tweheyo, M. T., &Austad, T. (2007). Wettability alteration and improved oil recovery by spontaneous imbibition of seawater into chalk: Impact of the potential determining ions Ca^{2+}, Mg^{2+}, and SO_4^{2-}. *Colloids and Surfaces A: Physicochemical and Engineering Aspects*, **301**(1), 199-208.
- Zhang, P., &Austad, T. (2006). Wettability and oil recovery from carbonates: Effects of temperature and potential determining ions. *Colloids and Surfaces A: Physicochemical and Engineering Aspects*, **279**(1), 179-187.

Tables:

Table 1: Different Carbonate, sulphate and clay fines used to study emulsion formations with different designed oils O1, O2, O3, O4

Fines:				
Carbonates:	C1: $CaCO_3$	C2: $MgCO_3$	C3:Li_2CO_3	
Sulphates:	S1: $CaSO_4$	S2: $BaSO_4$	S3: $SrSO_4$	
Clay:	K1: Kaolinite			
Designed Oil:				
Oil O1	Hexane	Hexadecane	Stearic Acid	
Oil O2	Hexane	Hexadecane	Heptanoic Acid	
Oil O3	Crude oil	Stearic Acid	Hexane	Hexadecane
Oil O4	Crude oil	Heptanoic Acid	Hexane	Hexadecane

Figures

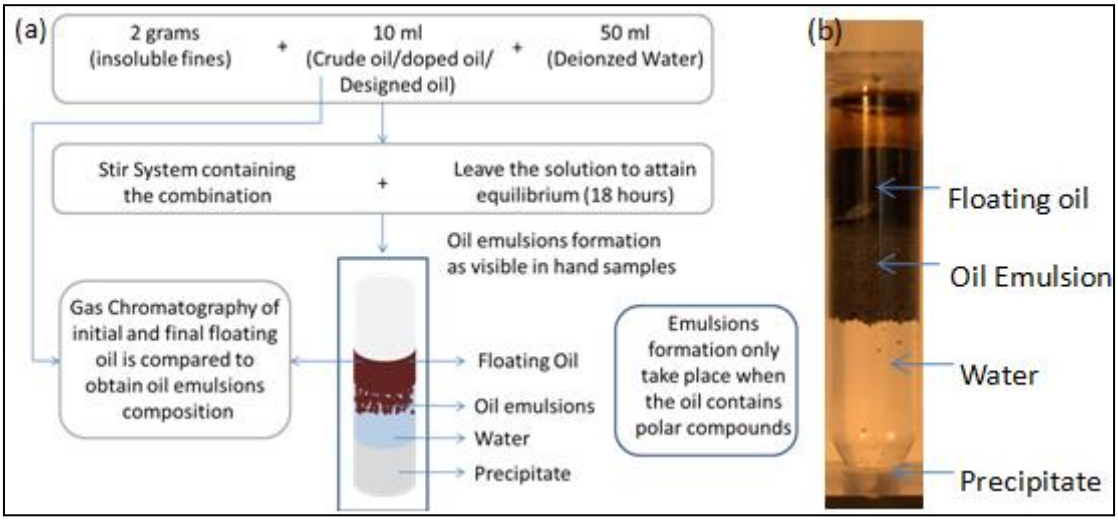
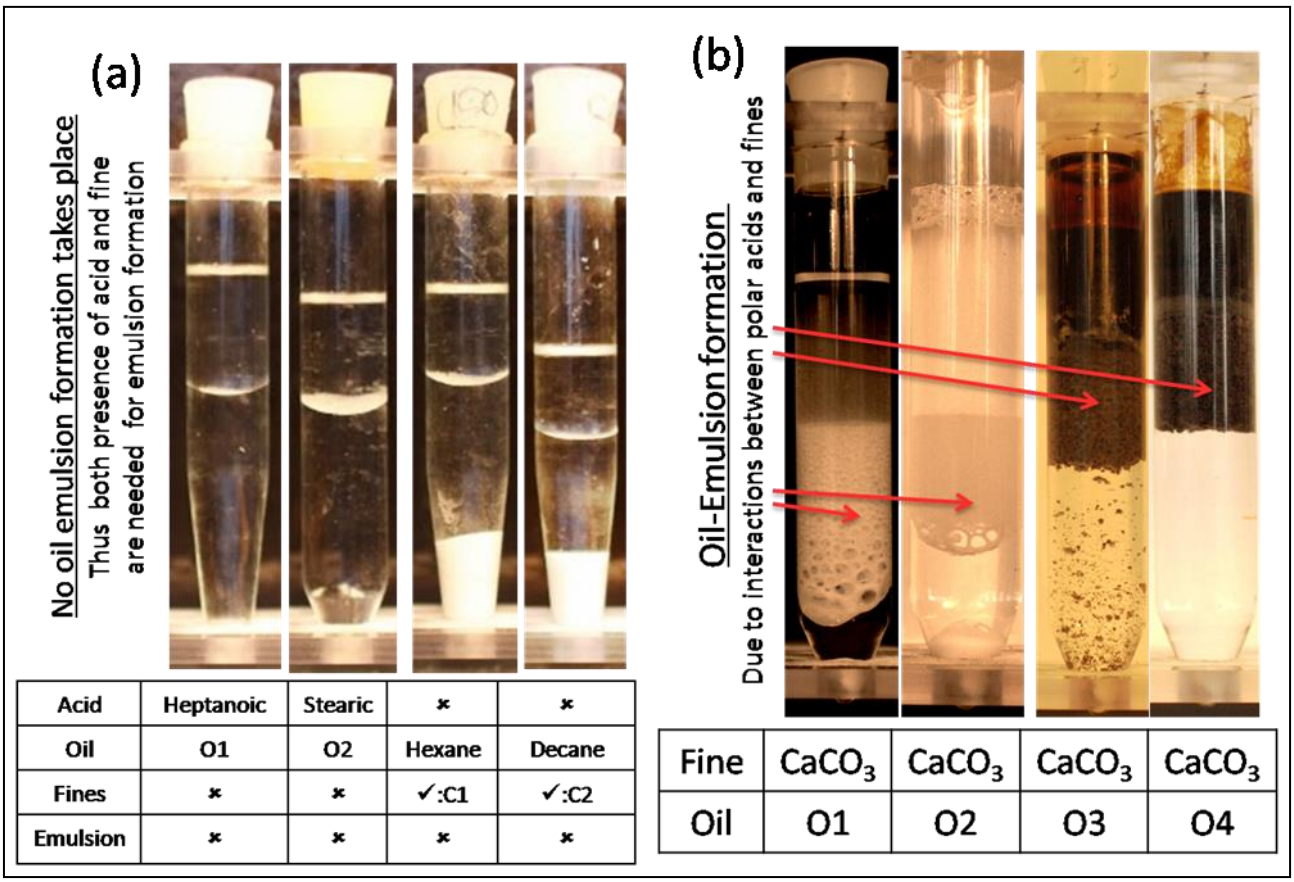


Figure 1: Schematic diagram of the experimental setup and procedure for emulsion formation.



Acid	Heptanoic	Stearic	×	×
Oil	O1	O2	Hexane	Decane
Fines	×	×	✓:C1	✓:C2
Emulsion	×	×	×	×

Fine	$CaCO_3$	$CaCO_3$	$CaCO_3$	$CaCO_3$
Oil	O1	O2	O3	O4

Figure 2(a): No emulsion formation in absence of either polar acid or fines (b): Emulsion formation with different designed oils and doped oils in the presence of acids and $CaCO_3$ fines.

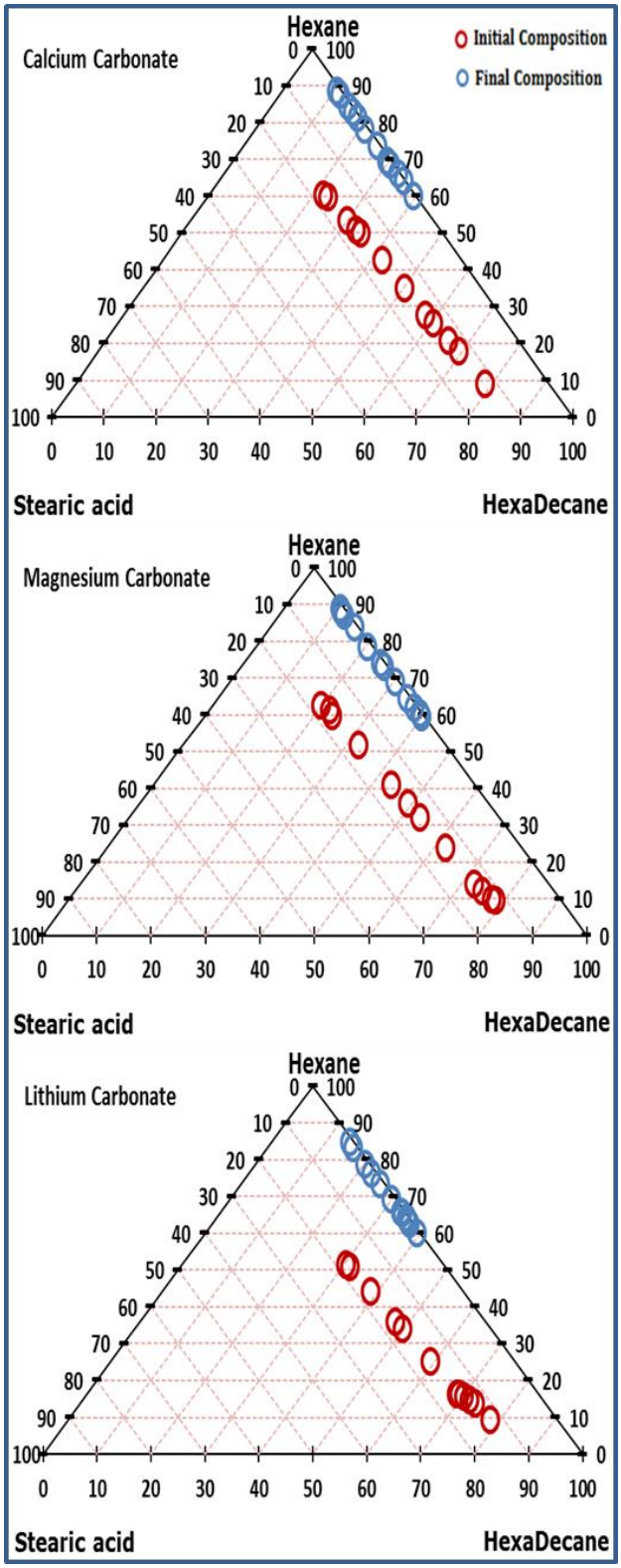


Figure 3: Representation of initial and final oil composition in (triangular diagram for hexane, hexadecane and stearic acid) for calcium, magnesium and lithium carbonate fines with oil O1.

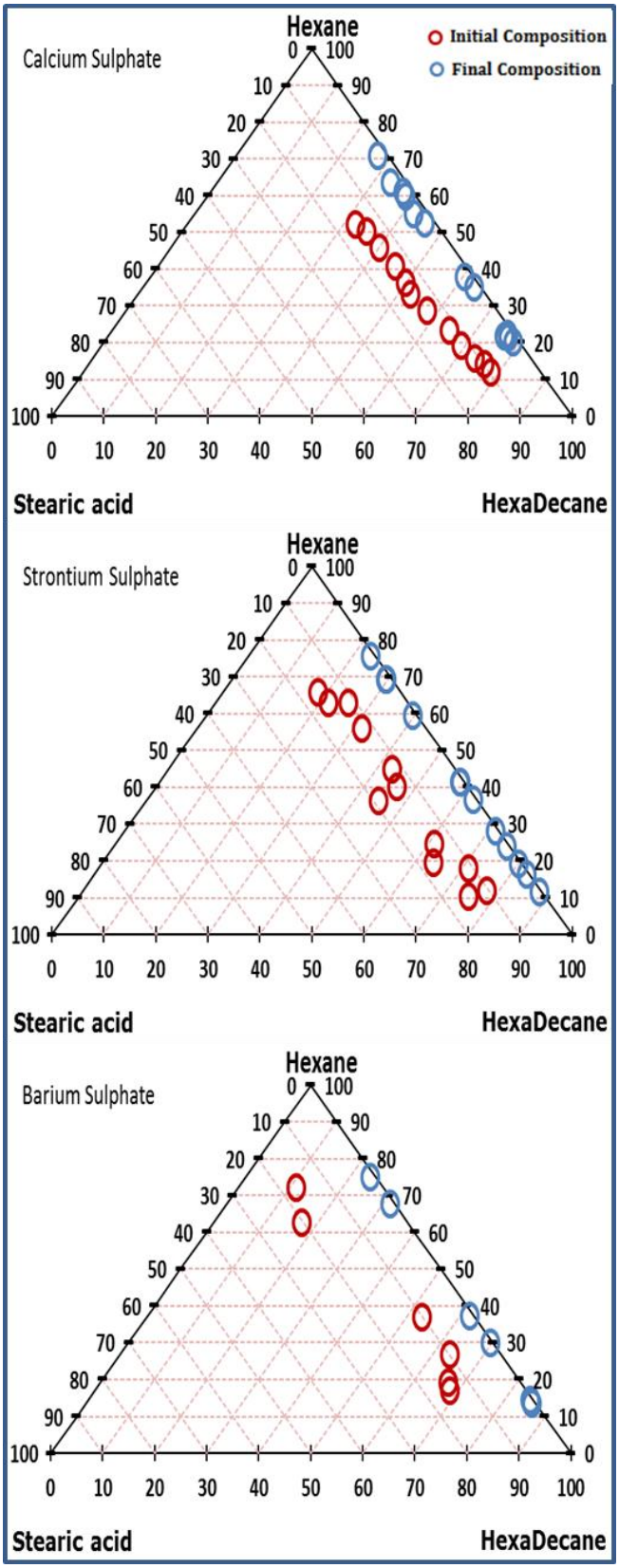


Figure 4: Representation of initial and final oil composition (triangular diagram with hexane, hexadecane and stearic acid) for calcium, barium and strontium sulphate fines with oil O2.

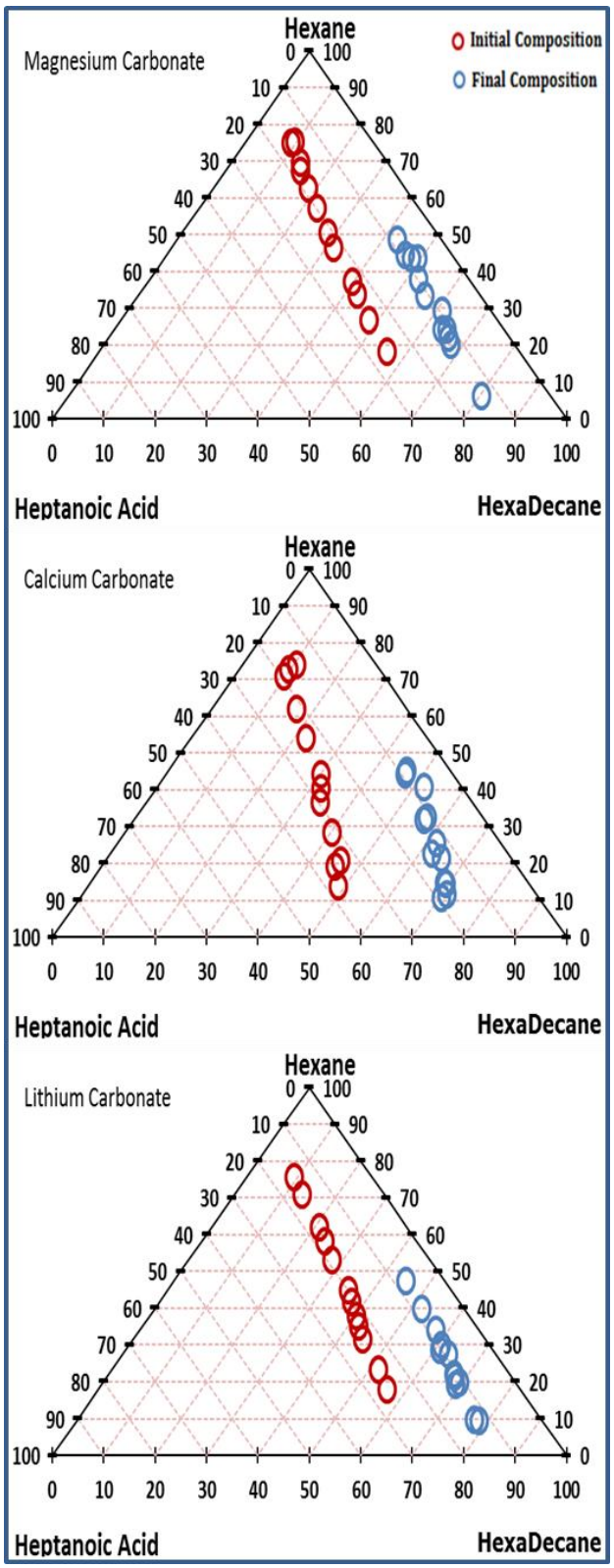


Figure 5: Heptanoic acid, hexane and hexadecane composition in the initial and final oil after emulsion formation with calcium, magnesium, and lithium carbonate fines with oil O2.

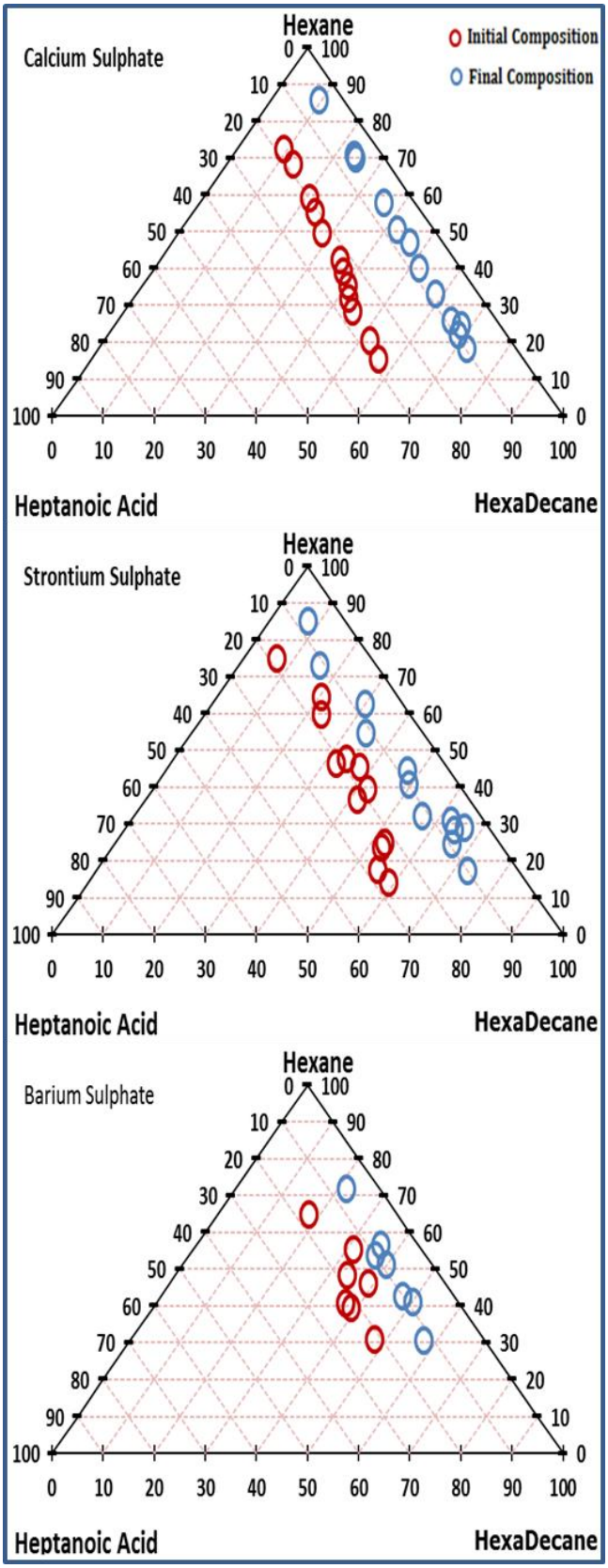


Figure 6: Heptanoic acid, hexane and hexadecane composition in the initial and floating oil after emulsion formation with calcium, strontium, and barium sulphate fines with Oil O2.

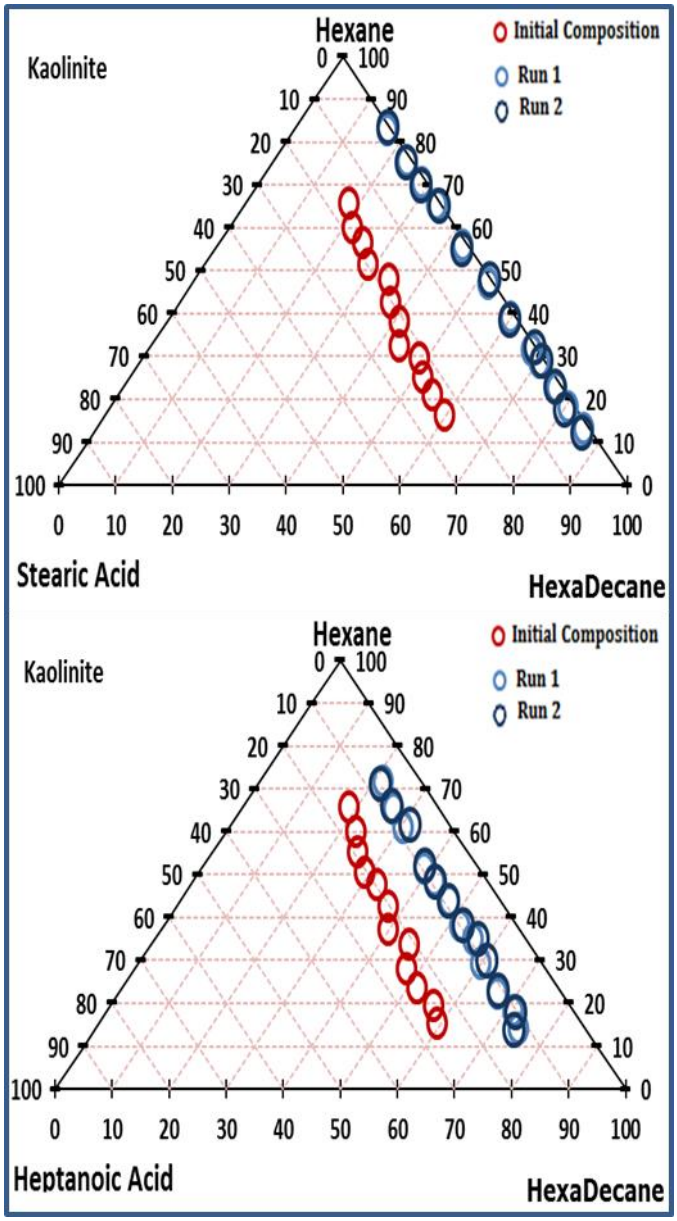


Figure 7: Representation of initial and floating oil composition in two runs (triangular diagram for hexane, hexadecane and acid) for kaolinite fines with oils O1(with stearic acid) and O2(with heptanoic acid).The two series of experiments were performed twice to ensure consistency(data represented : Run1 light blue, Run2 dark blue circles).

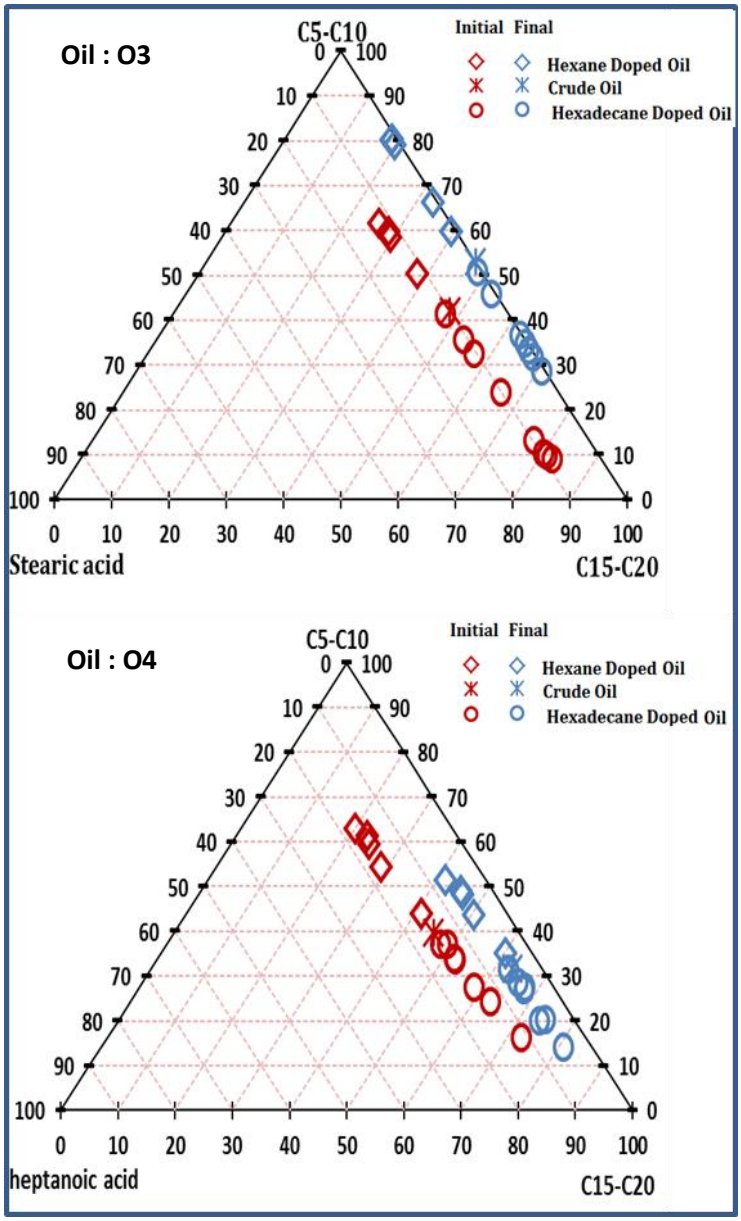


Figure 8: Representation of initial and floating oil composition in two runs (triangular diagram for C5-C10, C15-C20, and stearic/heptanoic acid acid) for calcium carbonate fines with oils O3 and O4.

Paper III

Chakravarty, K. H., Fosbøl, P. L., & Thomsen, K. (2015, June). Interactions of Fines with Base Fractions of Oil and its Implication in Smart Water Flooding. In *EUROPEC 2015*. Society of Petroleum Engineers.

SPE-174335-MS

Interaction of Fines with Base Fractions of Oil and its Implication in Smart Water Flooding

Krishna Hara Chakravarty, Philip Loldrup Fosbøl and Kaj Thomsen, Center for Energy Resources Engineering (CERE), Department of Chemical and Biochemical Engineering, Technical University of Denmark

Copyright 2015, Society of Petroleum Engineers

This paper was prepared for presentation at the EUROPEC 2015 held in Madrid, Spain, 1–4 June 2015.

This paper was selected for presentation by an SPE program committee following review of information contained in an abstract submitted by the author(s). Contents of the paper have not been reviewed by the Society of Petroleum Engineers and are subject to correction by the author(s). The material does not necessarily reflect any position of the Society of Petroleum Engineers, its officers, or members. Electronic reproduction, distribution, or storage of any part of this paper without the written consent of the Society of Petroleum Engineers is prohibited. Permission to reproduce in print is restricted to an abstract of not more than 300 words; illustrations may not be copied. The abstract must contain conspicuous acknowledgment of SPE copyright.

Abstract

Migration of fines and formation of oil emulsion have been independently observed during smart water flooding. Both have been suggested to play a vital role in enhanced oil recovery (EOR). The exact role of fines and the reason for emulsion formation are not well understood for carbonate reservoirs. This study shows that the addition of water and crude oil to calcite fines leads to the formation of soluble oil emulsions in the water phase. The formation of emulsions and their implication in EOR has been experimentally analyzed in this work.

A study was conducted to characterize the formation of these emulsions. It entailed aqueous mixtures with solids of Li_2CO_3, $MgCO_3$, $CaCO_3$, $CaSO_4$, $SrSO_4$, $BaSO_4$, and reservoir calcite fines. Different types of oils and water were also used. Three types of oil systems were applied. (1) A designed oil consisting of hexane and hexadecane; (2) Design oil, doped with different amounts of heptylamine and hexadecylamine to mimic the base number of the oil; (3) Experiments were conducted for pure North Sea crude oil and doped oil to understand its implications in EOR.

The composition of initial and final floating oil was determined through gas chromatographic (GC) analysis. Interaction between polar fraction of oil and the different fines led to production of oil emulsions. Designed oil containing only alkanes (without polar fractions) did not produce any emulsions during its interaction with fines. In oils containing hexadecylamine, 95% of the initial amount was accumulated in the emulsions and only 5% was found in the final oil. In oil samples containing heptylamine, up to 45-50% of the initial amount was accumulated in the emulsions. This indicates that heavier amines form more stable emulsions.

The emulsions formed depend on the fines present. Carbonates seem to promote emulsion formation consisting of, light amines and light alkanes. No such selectivity was observed for any of the sulfates. The conclusion is obtained for design oil, doped design oil, crude oil and doped crude oil. The conclusion is the same for pure $CaCO_3$ fines and reservoir $CaCO_3$ fines. These results show that fines of carbonate released during fracturing, or sulfates formed during smart water flooding can form water soluble oil emulsions which help to mobilize trapped oil and increase the sweep efficiency.

The results clearly show that oils having the same base number can form significantly different amounts of emulsion with fines, and provide detailed trends of emulsion formations with varied oil compositions. The study shows that interaction between fines and polar fractions of oil can enhance the oil-water interaction and it can lead to oil-emulsification during Smart Water flooding.

Introduction

In the founding work by Tang and Morrow (Tang and Morrow et al. 1999) it was shown that alteration of brine salinity and composition affects the oil recovery from sandstone reservoirs. Subsequently, through a series of research studies, smart water flooding has emerged as a possible EOR technology that does not require injection of toxic or expensive chemicals (Webb et al. 2005; Karoussi et al. 2007; Fjelde et al. 2009; Strand et al. 2006; Tweheyo et al. 2006; Zhang et al. 2007). It is universally accepted that altering the brine composition and its salinity can increase the recovery fractions both in sandstone and carbonate reservoirs (Yildiz et al. 1999; Fogden 2011; Lebedeva and Fogden 2011; Gupta et al. 2011; Delshad et al. 2013; Parracello et al. 2013; Robertson, 2007; McGuire et al. 2005; Alagic et al. 2011; Webb et al. 2005; Karoussi et al. 2007; Zhang et al. 2007). Different methods have been suggested for potential EOR, but no clear mechanism for this technology has been universally accepted. There are several

extensive investigation programs established to understand the scientific basis (Austad et al. 2005; Zahid et al. 2010; Gupta et al. 2011; Alvardo et al. 2014).

Austad and his co-workers have performed laboratory research for various brine solutions, in order to understand the process of enhanced oil recovery for chalk reservoirs (Strand et al. 2006; Zhang et al. 2007; Austad et al. 2005; Zhang et al. 2006; Puntervold et al. 2009). In these studies, it has been shown that SO_4^{2-} is a potential determining ion for increasing oil recovery from chalks. It is further proposed that the SO_4^{2-} ion must act in combination with Ca^{2+} and Mg^{2+} because SO_4^{2-} alone cannot increase the oil recovery. Over a series of presented experiments, wettability alteration (towards water wetness) has been shown to be the basis of enhanced oil recovery. Amongst these publications, Stevns Klint outcrop chalk from Denmark has been used in the majority of the reported experiments (Strand et al. 2006). The proposed mechanism consists of two processes: (1) substitution of calcium by magnesium on the calcite surface (2) Sulfate ions are adsorbed on the mineral surface, giving rise to the release of adsorbed carboxylic compounds (making the surface more water wet). In the effluent water, a decrease in sulfate concentration shows that sulfate acts as a reagent in this process (Zhang et al. 2007a; Bagci et al. 2001). In most studies, the importance of soluble Ca^{2+}, Mg^{2+} and SO_4^{2-} ions in brine solutions has been recognized as the reason for obtaining enhanced oil recovery.

In parallel, another series of experimental analysis with reservoir rock samples have shown contradicting results (Zahid et al. 2010; Zahid et al. 2011; Zahid et al. 2012a; Zahid et al. 2012b). For totally water wet systems, a 10% increase of oil recovery has been observed through smart water flooding experiments (Zahid et al. 2010). According to the wettability alteration mechanism, an increase in oil recovery should be a result of increased water wetness in the core plug (Austad et al. 2005). But an increase in oil recovery because of high concentration of the SO_4^{2-} ion in the injected brine has shown no corresponding increase in water wetness (Zahid et al. 2010). Emulsification of oil and dissolution of rock were suggested to be the possible reasons for the observed EOR in completely water wet systems, but no detailed mechanism was provided. A series of published studies in recent years also show that oil emulsions can be formed by a buildup of a viscoelastic interface with low salinity flooded water (Moradi et al. 2011; Moradi et al. 2013; Wang and Alvardo, 2012; Alvardo et al. 2014). Previously, it has been shown that polar organic acids can play a significant role in the buildup of viscoelastic brine-crude oil interfaces (Moradi et al. 2013). The formation of oil emulsion was also observed for brine solutions containing high concentrations of sulfate ions (more evidently at higher temperature) (Zahid et al. 2011). In the following work we recognize that at high temperature, the solubility of $CaSO_4(s)$ is low. Fines formation may therefore have been associated with the observed emulsions. In another study, increased oil recovery was found to be accompanied by a pressure drop (Zahid et al. 2012b). A possible correlation between fines formation and smart water EOR has been suggested, but no detailed mechanism has been proposed (Zahid et al. 2012b).

Fines formation has been proved useful in several other studies (Tang and Morrow, 1999; Pu et al. 2010; Hadia et al. 2012; Ligthelm et al. 2009) as well. Proposed correlation between mobile fine formation and EOR is as follows.

1. Certain reservoirs are covered with fines (clay particles) that have a high specific surface area and a high degree of reactivity towards the crude oil (Clementz, 1976).
2. The fines in contact with the brine solution form an electric double layer, and which causes fines to coagulate and remain attached to the mineral surface. Flooding with low salinity brine can remove the ion layer from the fines and can lead to the detachment of fines from the mineral surface (Alvarado 2014; Ligthelm et al. 2009).
3. Detachment of mobile fine particles from the pore wall can bring attached oil droplets (emulsions) into the water phase during injection of dilute brine solution (Tang and Morrow et al. 1999). It is further shown that that a variation of brine properties had no effect on fine absent cores. Thus presence of mobile fines was suggested to be a necessary condition for observing successful EOR (Tang and Morrow et al. 1999). However release of oil droplets (through emulsion formation) due to its interaction with mobile fines has not been suggested and not observed in previous studies.
4. Moreover it has been suggested that fines migration can block the pore throats and thus divert the flooded water towards upswept pores and increase the sweep efficiency of the flooding water (Pu et al. 2010; Hadia et al. 2012).

It is also reported that experiments with a variation of total base number show that the total base number of oil do not provide any direct correlation to oil recovery (Suijkerbuijk et al. 2012). These experiments do not support the wettability alteration mechanism (Austad et al. 2005), as additional amounts of polar components should lead to quicker and easier change in wettability and increase the importance of the brines. In produced oil, considerable amounts of fines/sediments are often observed during water flooding (Stewart 1980). It has been known for decades that there are considerable amounts of sediments and water (BS&W) in the produced oil (Demny and Stewart 1985). There is clear evidence that the availability of fines is important for the EOR technology, but there is no clear mechanism that can explain all the experimental observations.

The aim of this study is therefore to profoundly analyze the interaction between different fines and polar fractions of oil. Figure 1 outlines such kind of experiments conducted in this work. Oil emulsion formation takes place on interaction of fines with oils. A series of experiments were conducted to study the interaction of a simple designed oils and crude oil interacting with fines. In this study, different kinds of fines (Table 1) have been used to study their impact on oil-emulsion formation. Each type of fines has been individually analyzed together with two designed oils and their mixtures with crude oil (Table 1). These various combina-

tions show the exact behavior of each hydrocarbon with different types of fines during these interactions. In this work we have tested three types of carbonate fines: calcium carbonate (C1), magnesium carbonate (C2), and lithium carbonate (C3). Three sulfate fines were also tested: calcium sulfate (S1), barium sulfate (S2), and strontium sulfate (S3). In addition, we tested kaolinite (K1) as a clay mineral and fines made from carbonate reservoir rock from the Dan field in the Danish North Sea (D1). Previously it has been observed that reservoir rock behave differently from outcrops or model fines in water flooding experiments (Zahid et al. 2012a). Therefore, the same experiments were carried out both with synthetic fines and with fines of carbonate reservoir.

The composition of the designed oils was varied: one set of designed oil (O1) was prepared with the lighter hexylamine (as the single basic component) while the second designed oil (O2) includes the heavier hexadecylamine (as the single basic component). Patterns and conditions of emulsions formations of O1 and O2 with the various fines were generated through a series of experiments (Figure 7). It was shown by Puntervold et al. that design oil and crude oil may show different properties (Puntervold et al. 2007). Therefore, experiments were conducted with North Sea crude oil containing light bases (O3) and heavy base (O4) in addition to the experiments with designed oil.

Experiments

A simple experimental arrangement was established to study the circumstances of the emulsion formation. A schematic diagram is shown in Figure 1. First, 2 grams of the insoluble fines were added to 10 ml of oil and 50 ml of deionized water (Table 1). This mixture was stirred for 1 hour and the solution was kept in a closed container in ambient condition for 18 hours to attain equilibrium. As shown in Figure 1, a layer of water soluble oil emulsion was formed between the oil phase and the water phase. These were not observed using pure alkanes instead of the design oils, probably due to the unavailability of a polar component. Compositions of the floating oil (final oil) and the original oil added to the system (initial oil) were determined by GC. Triangular plots were used in the compositional comparison. ASTM method D2887 was applied for the analysis (Chorn et al. 1984) as recommended previously (Blomberg et al. 2002; Adahchour et al. 2008; Dutriez et al. 2010). An Agilent 7890A was used, as previously used for alkane analysis (Dutriez et al. 2010; Saleh et al.). 1 µL samples were introduced and 0.05 µL was used through the front GC injector. After each analysis the injector was thrice washed with toluene with each sample volume of 0.8 µL. In the front inlet He gas had a pressure of 0.226 bar gauge, a total flow rate of 42.9 ml/min and a septum purge flow rate of 3 ml/min. The temperature inlet was initially 50 °C, then rose from 200°C to 330°C for 5 min. The Agilent 125-10HB 10m x 530 µm x 2.65 µm column according to ASTM D2887-06 was used. The oven had an equilibrium time of 3 mins, with maximum temperature of 350 °C with an initial temperature of 40°C and thereafter heated up to 350°C in 4 mins. The runtime of each sample was 19.5 mins. The outlet stream had an initial temperature of 40 °C, and a pressure 0.226 bar gauge with flow rate of 13.3 mL/min and average velocity 96.52 cm/sec. The Front Detector (FID) was heated to 375 °C, the H_2 flow was 40 mL/min, and air flow was 450 mL/min. A column manufactured by Agilent (Model: 125-10HB) was used. It had the following specifications; Diameter: 530.00 µm, Length: 10.0 m, Film thickness: 2.65 µm, Void time: 0.173 min and maximum temperature: 350.0 °C. For each run the relative compositions of the oil components were calculated using Agilent's simulated distillation method. For all initial samples, up to 3 repetitions were made, and consistency in obtained composition was more than 95%.

Four types of fines were studied:

1. First, emulsion formations with carbonate fines were investigated (Table 1). These carbonates are sparingly soluble in water (solubility in water: $CaCO_3$ 0.0013 g/100 mL; $MgCO_3$ 0.0106 g/100ml; Li_2CO_3 1.29 g/100 mL at STP (Garrels et al. 1961) and thus most of the carbonate remain as fines in the solution (containing 2g of fines per 50 ml of water). While $CaCO_3$ makes up the major fraction of chalk and lime stone, $MgCO_3$ is found as a chemical component in reservoirs in small fractions. Testing the two carbonates also gives an idea of the behavior of oil emulsion formation with dolomite (which is present as a mineral in carbonate reservoir, as it is more stable than magnesite at reservoir conditions). Li_2CO_3 was used to further develop a general understanding of the carbonates in emulsion formation. The fines were obtained from Sigma-Aldrich (Product Number $CaCO_3$: Z545643; $MgCO_3$: M7179; Li_2CO_3: 62470).
2. The second sets of chemicals were sulfate fines (Table 1). Three different sulfate fines were used (including $CaSO_4$, $BaSO_4$ and $SrSO_4$). These are sparingly soluble in water ($CaSO_4$: 0.21g/100ml, $BaSO_4$: 0.0002448 g/100 mL and $SrSO_4$: 0.0135 g/100 mL at Standard Temperature and Pressure) (Carlsberg et al. 1973). Thus stable fines can exist in these solutions (containing 2g of fines per 50ml of water). Injecting $CaSO_4$ along with Sea water has been in suggested in different SmW-EOR experiments (Zhang et al. 2007; Austad et al. 2005), so its effect in emulsion formations has been analyzed. To explore the general behavior of sulfates in emulsion formation $BaSO_4$ and $SrSO_4$ were used in addition to $CaSO_4$. The fines were obtained from Sigma-Aldrich (Product Number $CaSO_4$: 238988; $BaSO_4$: 202762; $SrSO_4$: 433365).
3. In the third set of experiments, kaolinite was used as the only clay mineral. Small fines of kaolinite are often available in reservoirs and have been shown to influence the displacement efficiency of the crude oil (Tang and Morrow et al. 1999). Kaolinite is also sparingly soluble in water (Kittrick 1980) and forms stable fines that can actively contribute to emulsion formation by interacting with the oil and water. Kaolinite was obtained from Sigma-Aldrich (Product Number $Al_2Si_2O_5(OH)_4$: 03584).

4. In the fourth set of experiments, core samples from the Dan field in the Danish part of the North Sea were used. The Dan field reservoir Chalk is mainly of Maastrichtian age, characterized by a porosity range of 20-35% and permeability of 1.75 mD (Jørgensen 1992) and has more than 98% carbonate content (Fabricius et al. 2007). Recovery from the field is based on the simultaneous production of oil and injection of water to maintain reservoir pressure. Water injection was initiated in 1989 and has gradually been extended to the whole field. The recovery of oil is optimized by flooding the reservoir with sea water (Bæk 2013). Thus any possible release of carbonate fines during the water flooding can interact with the residue oil. And these interactions between the residue oil and produced fine will have a significant practical importance. Cleaned North Sea core samples were provided by Maersk Oil. The core samples were grinded so that they could be used for emulsion analysis. The fines were thereafter dried for 3 days. Constant weight of the fines ensured no condensation or evaporation of water droplets.

Four different types of oil were designed:

1. The first set of designed oil (O1) contained different fractions of hexane, hexadecane and hexadecylamine (Table 1). This ensured that the base (polar component) was of comparable dimension to a fraction hydrocarbon, as a fraction of the alkanes (hexadecane) and significantly heavier than the rest (hexane). The content of hexane and hexadecane and hexadecylamine was varied in 12 different samples. Oil emulsion formation with different fines was studied with each of these 12 samples. Pure alkane and amine hydrocarbons were obtained from Sigma-Aldrich (Product No: Hexane: 296090, Hexadecane: 296317 and Hexadecylamine: 445312).
2. The second set of designed oil (O2) consisted of hexane, hexadecane and heptylamine. In this case the basic amine was also of comparable dimension to a fraction of the alkanes (hexane) but was significantly lighter than the rest (hexadecane). The content of these three chemicals was also varied. Again 12 different samples were made and these different oil samples were used to analyze their effect with the different fines (as listed above). Pure alkane and amine hydrocarbons were obtained from Sigma-Aldrich (Product No: Hexane: 296090, Hexadecane: 296317 and Heptylamine: 126802)
   Subsequently, crude oil originating from the Dan field in the Danish North Sea was obtained from Maersk oil. This crude oil was used to further study the emulsion formation in the same manner.
3. The third set of oil (O3) was obtained by mixing O1 with crude oil in various fractions. This ensures that the oil selectively contained hexadecylamine (in significantly higher concentration than any other polar fraction) with varying fractions of different alkanes in the crude oil. By varying the concentration of the alkanes, 12 different oil samples were prepared.
4. The fourth oil set (O4) was developed by mixing O2 with crude oil in different proportions. Thus in this case the oil selectively contained heptylamine (in significantly higher concentration than any other polar fraction), with varying fractions of different alkanes in the crude oil. By varying the concentration of the alkanes, 12 different oil samples were prepared.

The above oils were used to study the behavior with the fines and understand the composition of the emulsion and the characteristics of the EOR mechanism. Best grade chemicals were obtained for the fines and organic compounds to avoid any error in the conducted experiments. These experiments were conducted in coherence with the previous study for oil emulsion formation with acidic fractions of crude oil (Chakravarty et al. 2015).

Results & Discussion
Emulsion formation between heavy basic hydrocarbons and carbonate fines (O1 & C)

In the first set of experiments, O1, water, and $CaCO_3$ fines were stirred and left for equilibration. The same set of experiments was performed twice to ensure consistency in the obtained compositions. Through GC it was observed that the composition of hexadecylamine was significantly reduced in the final oil (as shown in Figure 2). The hexadecane concentration was also reduced significantly in the final oil as compared to the initial oil, while the hexane concentration increased. In other words, the oil emulsion formed consisted mainly of hexadecylamine and hexadecane. This indicates that hexadecylamine plays an active role in the formation of this oil emulsion. The same set of experiment was repeated with magnesium carbonate fines (as also shown in Figure 2). Also in this case, hexadecylamine together with hexadecane was depleted from the oil and must have formed the emulsion together with the magnesium carbonate fines. The emulsion formation with lithium carbonate showed the same trend.

In all of the carbonate experiments (irrespective of the corresponding cation) it was witnessed that approximately 94 wt% of the hexadecylamine was missing from the final oil and it instead contributed to the water soluble emulsions formation (as shown in Figure 2). Along with the polar fractions, approximately 45 wt% of the initial hexadecane was removed from the final oil and contributed to the formation of oil emulsions. These results remain consistent irrespective of the cation of the fines (Ca^{2+}, Mg^{2+}, Li^{+}) indicating that it is a property of the carbonate ion (Figure 2).

Emulsion formation between heavy basic hydrocarbons and sulfate fines (O1 & S)

A similar set of experiments was conducted with various sulfate fines. First calcium sulfate was used and the interaction with hexadecylamine containing oil (O1) was analyzed. The GC results showed that the hexadecylamine content was significantly reduced; but neither hexane nor hexadecane concentrations was altered. As shown in Figure 3, there are clear indications that the oil emulsions formed with sulfate fines had no selectivity of hexadecane over hexane (unlike the selectivity previously observed with carbonates). The same set of experiments was conducted for barium sulfate fines and the obtained results were quite similar to that of calcium sulfate fines. The hexadecylamine concentration was significantly reduced in the final oil but there was no selectivity of hexane or hexadecane in the oil emulsion formations. To further examine this trend, the experiment was also conducted with strontium sulfate fines. A comparison between the final oil and the initial oil showed exactly the same trend (Figure 3). With all these three sulfate fines, the results are quite consistent during variations in oil composition and variation in the alkane fractions (Figure 3). Approximately 94-95 wt% of the hexadecylamine was depleted from the oil and was contributing to the formation of the water soluble oil emulsions.

The experiments with carbonate fines and sulfate fines document that the alkane selectivity is dependent on the anion of the fines. Carbonate fines have selectivity for hexadecane, but no such selectivity was observed for sulfate fines. In both cases it was observed that around 95-96% of the hexadecylamine was contributing to the formation of the oil emulsion. Only 4-5% of the initial amount of hexadecylamine was available in the final oil, indicating that hexadecylamine played a role in the formation of emulsions irrespective of the type of fines (Figure 3).

Emulsion formation between light basic hydrocarbons and carbonate fines (O2 & C)

The same set of experiments was conducted with O2 (oil composed of heptylamine instead of hexadecylamine). Two samples of the remaining oil were analyzed to ensure complete reliability of the acquired results. When calcium carbonate fines were used, it was observed through GC analysis that the behavior of the light heptylamine was significantly different from the behavior of hexadecylamine. The heptylamine concentration was reduced in the final oil as compared to initial oil but was not removed to the same extent as was seen with hexadecylamine. Around 55% of the initial heptylamine content was available in the final oil indicating that this base participated in the oil emulsion formation, but with less affinity than hexadecylamine (Figure 4). Supplementary it was observed that the hexadecane concentration in the final oil increased significantly while the concentration of hexane was reduced, indicating selectivity of hexane over hexadecane in the emulsion formation with the light base, heptylamine (Figure 4). To further analyze this phenomenon, the experiment was conducted with magnesium carbonate fines. Again, it was observed that heptylamine was partially removed from the final oil indicating that it did contribute to oil emulsion formation but only partially (Figure 4). Also in this case, the oil emulsion formation showed selectivity of hexane over hexadecane indicating that it was the light base that caused the formation of the oil emulsion. Finally, lithium carbonate fines were used. The GC analysis of the initial and the final oil showed the same pattern as with calcium and magnesium carbonate fines: The oil emulsion formation was selective of hexane over hexadecane and the heptylamine content of the initial oil participated in the emulsion formation.

These results together suggest that light bases prefer to form oil emulsions with light alkanes and heavy bases prefer to form oil emulsions with heavy alkanes. Since the presence of carbonate is the deciding factor, and the cation variation does not have any major effect so, it is quite possible that similar oil emulsion formation patterns can also be observed with dolomite fines. And it is expected that this phenomena of oil emulsion formation with alkane selectivity will be continuously observed for any mineralogical combination of carbonates. Although a detailed experiment with dolomite will be required to confirm the same.

Emulsion formation between light basic hydrocarbons and sulfate fines (O2 & S)

The same set of experiments was carried out with sulfate fines and oil O2 (oil composed of heptylamine instead of hexadecylamine). The results are shown in Figure 5. Heptylamine contributed partially to the oil emulsion formation. 50-55% of the initial heptylamine content was still available in the final oil; indicating less affinity for emulsion formation than hexadecylamine (similar to the oil O2 interactions with carbonate fines). As previously observed with sulfate fines, no selectivity of alkane in the oil emulsions formation could be seen. The relative concentrations of hexane and hexadecane did not change in the final oil. The experiment was repeated with barium sulfate fines and with strontium sulfate fines. The same phenomena were again observed in these two cases: no selectivity of one alkane over the other and the heptylamine was reduced to around 50-55% of the initial heptylamine content (Figure 5).

Emulsion formation between basic hydrocarbons and clay fines (O & K1)

Subsequently, experiments were conducted with different clay fines. GC analysis of the floating oil was conducted for two samples (indicated as Run 1 & Run 2 in Figure 6). First, the interaction of kaolinite fines with a hexadecylamine containing oil (O1) was analyzed. The composition obtained from the GC of the final and the initial oils showed that the hexadecylamine content of the oil was significantly reduced but the ratio between hexane and hexadecane concentrations did not change much. The results are shown in Figure 6. The same experiment was conducted with kaolinite fines and oil O2 (oil containing heptylamine instead of hexadecylamine). As shown in figure 6, heptylamine only partially contributed to the oil emulsion formation. The amount of heptylamine in the final oil was reduced to around 50-60% of the content in the initial oil. This result is similar to the results obtained

with oil O2 and carbonate fines. No selectivity of alkanes in the emulsion formation was observed (Figure 6). These results show that clay mineral behaves similar to sulfate fines and can readily form oil emulsions irrespective of the available alkanes.

Emulsion formation between crude oil and carbonate fines (O3-4& C1)

The obtained patterns from oils O1 and O2 collectively show that the light amines do not contribute to oil emulsion formation as extensively as heavier amines do. Furthermore, sulfate fines do not shown any selectivity of any particular alkane in oil emulsions formation irrespective of the associated cation. It has been previously observed that behavior of design oil and crude oil can be dissimilar in some cases of SW-EOR (Puntervold et al. 2007), so it is important to further check these observed trends with crude oil. To examine these trends with crude oil additional experiments were conducted with oils O3 and O4 using calcium carbonate fines. The oils were composed of several compounds (Table 1) in varying fractions. The same set of experiments was conducted and formation of oil emulsions was observed in the water. The initial oil and the final oil compositions were plotted in a triangular diagram for analysis (Figure 7). In the three corners of the diagram are the base, the hydrocarbons from C5 (Pentane) to C10 (Decane), and the hydrocarbons from C15 (Pentadecane) to C20 (Dodecane). The GC analysis of the final oil shows that the hexadecylamine content was significantly diminished, indicating that hexadecylamine was the main component in emulsion formation by interacting with the fines. The content of C5 to C10 slightly increased in the final oil, indicating that the heavier fractions were selectively chosen for oil emulsion formation (Figure 7). The content of the lighter alkanes increased in the floating oil and hexadecylamine was completely depleted from the final oil in these experiments. Similar experiments were conducted with heptylamine doped crude oil O4, for varying concentrations of the alkanes. Herein it was observed that the heptylamine content was partially removed in the final oil, implying that it contributed partially to the emulsion formation. The content of the heavy fraction of oil i.e. C15 to C20 increased slightly in the final oil and the fraction of lighter hydrocarbons, C5 to C10, decreased in the final oil. This indicated that the emulsions formed in this process selectively favored the light alkanes over the heavier alkanes (Figure 7). This result is in agreement with the previously observed trend for carbonate fines. The results obtained with the basic hydrocarbons were in coherence with the acidic analogs (Chakravarty et al. 2015).

In some experiments it has been proved that behavior of model oil may different from that of crude oil (Tina et al. 2009). So, experiments with both model oil and crude oil were compared. It is consistently observed that experiments with crude oil produced similar emulsions as observed for designed oil. For both set of oil (designed and crude) it is observed that heptylamine preferred emulsion formation with light alkanes while hexadecylamine preferred emulsion formation with heavier alkanes. Furthermore partial participation of heptylamine and complete participation of hexadecylamine in emulsion formation is observed for both designed oil and crude oil samples. This proves that the trends observed for oil emulsion formation with designed oil samples are relevant and reproducible with crude oil samples.

With crude oil samples it is observed the hexadecylamine shows higher participation in emulsion formation than heptylamine. This observed effect of in emulsion formation also proves that crude oils with similar base number can have significantly different interaction with fines. And total base number alone cannot estimate the amount of emulsion formation, nor can it explain the adhesion between fines and amines at oil-water interface. Information on the type of amine present in the oil is a prerequisite for estimating crude oils adhesion with fines.

Emulsion formation between crude oil and reservoir fines (O3& D1)

Furthermore these trends were examined for carbonate fines made from reservoir rock (Dan field). The carbonate fines of the reservoir rock were mixed with deionized water and thereafter O3 was added. The mixture was stirred and was allowed to attain equilibrium. Formation of oil emulsions took place in this case as well. Samples of the initial and the floating (final) oil were analyzed by GC and the compositions were plotted in a triangular diagram for graphical analysis (Figure 7). The GC analysis of the final oil shows that the hexadecylamine content was significantly diminished, indicating that hexadecylamine was the main component in emulsion formation. The content of C5 to C10 slightly increased in the final oil, indicating that the heavier fractions were selectively chosen for oil emulsion formation (Figure 7). The content of the lighter alkanes increased and hexadecylamine was completely depleted from the final oil in these experiments.

In previous SmW-EOR experiments it has been shown that reservoir rocks can behave differently from outcrops (or other model calcite) (Zahid et al. 2012b). So, experimental results obtained for model $CaCO_3$ (as shown in figure 2) was compared with those for reservoir $CaCO_3$ fines (as shown in figure 7c). With both reservoirs carbonate fines and model $CaCO_3$ similar kind of oil-emulsion formation took place. In both case we observe that hexadecylamine was completely diminished from the floating oil, indicating its active participation in emulsion formation. For both fines it is also observed that the floating oil in enriched with lighter alkane, indicating that hexadecylamine preferred to form emulsions with heavier alkanes. Thus, observed properties for model $CaCO_3$ fines (like alkane selectivity and active participation of hexadecylamine in emulsion formation) are properties which reproducible with reservoir fines.

Herein for all three systems: (1) Model $CaCO_3$-Designed Oil (as shown in Figure 2), (2) Model $CaCO_3$-Crude oil (as shown in Figure 7a) and (3) Reservoir $CaCO_3$-Crude oil (as shown in Figure 7c) it is observed that interaction of insoluble salt with insoluble oil leads to formation of water soluble oil emulsion. And patterns of oil emulsion observed with laboratory chemicals are reproducible with its reservoir analogs.

General observation and correlations

All these experiments indicate that oil emulsion formation can take place under many different reservoir conditions. The main criterion for emulsion formation from trapped oil is the accessibility of polar fractions in the crude oil and free mobile fines in the pore space. It is consistently observed that the short chain basic hydrocarbon do not contribute to oil emulsion formation to the same extent as longer chain basic hydrocarbons do. Around 0.94-0.95 fraction of the available hexadecylamine in (O1 and O3) contributed in emulsion formation, while only 0.5-0.55 fraction of the available heptylamine in (O2 and O4) contributed in the emulsion formation.

In all sulfate fines it was observed that there is no selectivity of any particular alkane in emulsion formation. While on the other hand in carbonate fines it was observed that light bases prefer to form oil emulsions with light alkanes and heavy bases prefer to form oil emulsions with heavy alkanes. These observations clearly indicate that the amount of oil emulsion formation significantly depends on the kind of bases available in the crude oil. Thus, oil with the same/similar total base number (TBN) may result in different amounts of emulsion formation, and thus leading to different oil recoveries. It is therefore suggested that the TBN of the crude oil alone cannot be used to estimate the oil's potential for emulsion formation and the exact amount of availability of each base must be known in order to predict the amount of oil emulsion formation potentially taking place. Inconsistent variation in oil recovery with changes in TBN (Suijkerbuijk et al. 2012; Zahid et al. 2010) could be related to the variation in the amount of emulsion formation. The results also showed that the observed pattern and conditions for oil emulsion formation was also replicated for reservoir fines with crude oil.

Oil emulsion formation takes place in the water phase due to interaction between insoluble salts and the polar components of the crude oil. Their properties are of great interest with respect to smart water flooding. The formation of mixed-wet mobile fines has been suggested to significantly enhance the displacement efficiency of residual oil during smart water flooding (Tang and Morrow et al. 1999). These results correlates well with the fundamental idea that oil emulsions can be formed by a buildup of a viscoelastic interface with low salinity flooded water (Moradi et al. 2011; Moradi et al. 2013; Wang and Alvardo, 2012; Alvardo et al. 2014). Oil emulsions formed in the pores can thus be a possible reason behind the observed EOR. Although there is not enough experimental evidence to prove that these water soluble oil emulsions contribute to SW-EOR the phenomenon needs to be considered for further experimental analysis. Besides wettability alteration, formation of fines due to changes in brine composition may have additional effects in SW-EOR. It also needs to be considered that there are several cases of fines formations in previously conducted experiments (Tang and Morrow et al. 1999; Zahid et al. 2010; Zahid et al. 2011). Emulsification of crude oil through interaction with fines can be a possible mechanism for EOR as in several cores, SW-EOR is only observed in cases where free mobile fines are available (Tang and Morrow et al. 1999).

The importance of fines has mostly been observed in sandstone reservoirs where there is a possibility of migration of clay fines during low salinity water flooding (with reduction in the thickness of the electric double layer).Thus there is a significant possibility that oil emulsion could be leading to increased oil recovery in sandstone reservoirs also. On the basis of experiments with chalk, high concentrations of Ca^{2+}, Mg^{2+}, and SO_4^{2-} are suggested to be the reason behind an observed oil recovery (Austad et al. 2005). Flooding the reservoir with high concentrations of Ca^{2+} and SO_4^{2-} can lead to the formation of sulfate fines such as $CaSO_4$ with very low solubility, a solubility that further decreases with an increase in temperature (Carlsberg, B. L. 1973). Proposed substitution of Ca^{2+} by Mg^{2+} (Austad et al. 2005; Zhang et al. 2007) further enhances the possibility of sulfate fines (precipitate) formation in the pore space. Thus even in chalk samples it is possible that fines based oil emulsion formation could be taking place, enhancing the displacement efficiency of the flooded water. These factors together suggest that there can be a significant correlation between fines based oil emulsion formation and observed oil recovery. Further studies in this area needs to be conducted to explore this correlation.

It is known that available fines form electric double layer on the pore surface due to their interaction with the NaCl brine available in the formation water (Tang and Morrow, 1999; Pu et al. 2010; Hadia et al. 2012; Ligthelm et al. 2009). The use of low salinity water flooding is suggested as a method to remove the electric double layer by detaching the fine particles from the mineral surface (Ligthelm et al. 2009). Migration of these mobile fines has mostly been associated with increasing the sweep efficiency of the flooding water by blocking the available pore throat (and thus decreases the permeability). But, researchers at British Petroleum have executed water flooding experiments where they saw little variation in end point relative permeability between high salinity and low salinity water floods, in both secondary and tertiary mode (Webb et al. 2008). But oil-emulsion formation due to interactions with fines may not necessarily lead to a decrease in permeability. It is therefore possible that the correlation observed between available mobile fines and oil recovery could be a result of oil emulsion formation as suggested by (Tang and Morrow et al. 1999). Tang and Morrow suggested that release of oil droplets from the mineral surface can take place, due to its interaction with the mobile fine. Herein the fines enhance the fluid-fluid interaction which can significantly increase the mobility of the oil (Tang and Morrow et al. 1999).Therefore it is suggested that fines can have two different behaviors.

1. Small mobile fines which can flow through the pore space can release trapped oil through emulsion formation. These fines can increase the adhesion between the flooded water and residue oil. Thus enhance the displacement efficiency of oil. Herein the role of mixed wet small fines was primarily suggested by Tang and Morrow 1999. But the proposed mechanism that mobile fines do carry trapped oil into flooded water phase was not demonstrated experimentally in previous studies. This, pre-

sented work contributes with supporting experimental evidence which show that insoluble fines can interact with insoluble oil and produce water soluble oil emulsions. These emulsion formation with small fines does not lead to additional decrease in relative permeability.

2. Migration of large fines can block the pore throat (Pu et al. 2010; Hadia et al. 2012). This alters the flow pattern of the flooded water, and force water to flow through upswept pores. It also affects the final oil recovery. But, migration of these large fines will lead to additional decrease in relative permeability. The conducted experimental studies in this work does not provide any supporting evidence to this mechanism, neither does it show any contradictions to it.

The study highlights the possibility that fines may have two different types of behaviors in the reservoir during water flooding and fine migration during low salinity brine injection may not necessarily lead to significant decrease in relative permeability of the coreplug.

Conclusion

Tang and Morrow had suggested (but not proved) that interaction of oil with fines can increase the displacement efficiency of oil as fines can bring trapped oil droplets to the mobile water phase. This study provides consistent and detailed experimental evidence that substantiate this claim. It was observed that insoluble fines can interact with insoluble crude oil in the presence of water and produce water soluble oil emulsions. This study provides a characterization of oil emulsion formation during interactions between hydrocarbon bases available in crude oil and diverse fines available at reservoir conditions.

1. All kinds of carbonates, sulfates, and clay fines used in these experiments promoted the formation of oil emulsions in the water.
2. Polar hydrocarbons must be available in the crude oil for any such emulsions to form.
3. The cations of the fines do not show any impact on the amount or composition of oil emulsion formation, while the anions have a prominent effect in the composition of the formed emulsion.
4. Carbonate fines show selectivity of alkanes during oil emulsion formation: with carbonate fines, light alkanes prefer to form emulsions with light bases while heavy alkanes prefer to form emulsions with heavy bases.
5. No alkane preference in emulsion formation was observed for sulfate fines or clay fines. These results together suggest that fines in the system can act as a major catalyst in increasing the oil-water interaction.
6. The observed patterns with model fines and design oil were replicated with reservoir fines and crude oil from the Dan field of the North Sea.
7. The oil emulsion formation actively takes place when heavier bases are present. This is irrespective of the kinds of fines available in the system.
8. Formation of fines (like $CaSO_4$) during high sulfate water flooding or release of carbonate or clay fines during low salinity water flooding or core fracturing can lead to emulsion formation.

In most previous studies it has been advocated that fines migration can increase the sweep efficiency of flooded water. But, this study suggests that existence of small mobile fines can also increase oil displacement through emulsion formation.

Acknowledgment

This article is a part of a research as part of the Smart Water project at the Center for Energy Resources Engineering (CERE). The authors acknowledge Maersk Oil, Dong Energy, and The Danish Energy Agency (EUDP) for funding the Smart Water project.

References

- Adahchour, M., Beens, J., & Brinkman, U. A. (2008). Recent developments in the application of comprehensive two-dimensional gas chromatography. *Journal of Chromatography A*, **1186**(1), 67-108.
- Akbar, M., Vissapragada, B., Alghamdi, A. H., Allen, D., Herron, M., Carnegie, A., Dutta, D., Olesen J. R., Chourasiya R. D., Logan, D., Stief, D., Netherwood R., Russell S. D., & Saxena, K. (2000). A snapshot of carbonate reservoir evaluation.*Oilfield Review*, **12**(4), 20-21.
- Alagic, E., Spildo, K., Skauge, A., & Solbakken, J. (2011). Effect of crude oil ageing on low salinity and low salinity surfactant flooding. *Journal of Petroleum science and Engineering*, *78*(2), 220-227.
- Alvarado, V., Moradi Bidhendi, M., Garcia-Olvera, G., Morin, B., & Oakey, J. S. (2014, April). Interfacial Visco-Elasticity of Crude Oil-Brine: An Alternative EOR Mechanism in Smart Waterflooding. In *SPE Improved Oil Recovery Symposium*. Society of Petroleum Engineers.
- Austad, T., Strand, S., Madland, M. V., Puntervold, T., & Korsnes, R. I. (2008). Seawater in chalk: An EOR and compaction fluid. *SPE Reservoir Evaluation & Engineering*, **11**(04), 648-654.
- Austad, T., Strand, S., Høgnesen, E. J., & Zhang, P. (2005). Seawater as IOR fluid in fractured chalk. SPE, 93000, 2-4.
- ASTM D2887-06, Standard Test Method for Boiling Range Distribution of Petroleum Fractions by Gas Chromatography, http://www.astm.org/DATABASE.CART/HISTORICAL/D2887-06.htm.

- Alvarado, V., Moradi Bidhendi, M., Garcia-Olvera, G., Morin, B., & Oakey, J. S. (2014, April). Interfacial Visco-Elasticity of Crude Oil-Brine: An Alternative EOR Mechanism in Smart Waterflooding. In *SPE Improved Oil Recovery Symposium*. Society of Petroleum Engineers.
- Bagci, S., Kok, M. V., & Turksoy, U. (2001). Effect of brine composition on oil recovery by waterflooding. *Petroleum science and technology*, **19**(3-4), 359-372.
- Blomberg, J., Schoenmakers, P. J., & Brinkman, U. A. (2002). Gas chromatographic methods for oil analysis. *Journal of Chromatography A*,**972**(2), 137-173.
- Bæk, M., Oil and Gas Production in Denmark 2013 and subsoil use http://www.ens.dk/sites/ens.dk/files/dokumenter/ publikationer/downloads/danmarks_olie-_og_gasproduktion_2013_uk.pdf
- Carlsberg, B. L. (1973, January). Solubility of calcium sulfate in brine. In *SPE Oilfield Chemistry Symposium*. Society of Petroleum Engineers.
- Chakravarty, K. H., Fosbøl, P. L., & Thomsen, K. (2015, April). Interactions of Fines with Oil and its Implication in Smart Water Flooding. In *SPE Bergen One Day Seminar*. Society of Petroleum Engineers.
- Chorn, L. G. (1984). Simulated Distillation of Petroleum Crude Oil by Gas Chromatography. Characterizing the Heptanes-Plus Fraction. *Journal of Chromatographic Science*, **22**(1), 17-21.
- Clementz, D. M. (1976). Interaction of petroleum heavy ends with montmorillonite. *Clays and clay minerals*, *24*(6), 312-319.
- Delshad M., Shalabi E. W., and Sepehrnoori K., (2013, April). Mechanisms Behind Low Salinity Water Flooding in Carbonate Reservoirs. In *SPE Western Regional & AAPG Pacific Section Meeting 2013 Joint Technical Conference*. Society of Petroleum Engineers.
- Demny, F. C., & Stewart, T. L. (1985). *U.S. Patent No. 4,543,191*. Washington, DC: U.S. Patent and Trademark Office.
- Dutriez, T., Courtiade, M., Thiébaut, D., Dulot, H., & Hennion, M. C. (2010). Improved hydrocarbons analysis of heavy petroleum fractions by high temperature comprehensive two-dimensional gas chromatography. *Fuel*, **89** (9), 2338-2345.
- Fernø, M. A., Grønsdal, R., Åsheim, J., Nyheim, A., Berge, M., & Graue, A. (2011). Use of Sulfate for Water Based Enhanced Oil Recovery during Spontaneous Imbibition in Chalk. *Energy & fuels*, **25**(4), 1697-1706.
- Fjelde, I. F., & Aasen, S. M. A. (2009, April). Improved spontaneous imbibition of water in reservoir chalks. In *15th European Symposium on Improved Oil Recovery*.
- Fogden, A., Kumar, M., Morrow, N. R., & Buckley, J. S. (2011). Mobilization of fine particles during flooding of sandstones and possible relations to enhanced oil recovery. *Energy & Fuels*, *25*(4), 1605-1616.
- Garrels, R. M., Thompson, M. E., & Siever, R. (1961). Control of carbonate solubility by carbonate complexes. *American Journal of Science*, **259**(1), 24-45.
- Gupta R., Smith G. G., Hu L., Willingham T., Cascio M. L. Shyeh J. J., &Harris C. R. (2011, January). Enhanced Waterflood for Carbonate Reservoirs-Impact of Injection Water Composition. In *SPE Middle East Oil and Gas Show and Conference*. Society of Petroleum Engineers.
- Hadia, N. J., Hansen, T., Tweheyo, M. T., & Torsæter, O. (2012). Influence of Crude Oil Components on Recovery by High and Low Salinity Waterflooding.*Energy & Fuels*, **26** (7), 4328-4335.
- Fabricius, I. L., Røgen, B., & Gommesen, L. (2007). How depositional texture and diagenesis control petrophysical and elastic properties of samples from five North Sea chalk fields. *Petroleum Geoscience*, **13**(1), 81-95.
- Jorgensen, L. N. (1992). Dan Field--Denmark Central Graben, Danish North Sea.
- Karoussi, O., & Hamouda, A. A. (2007). Imbibition of sulfate and magnesium ions into carbonate rocks at elevated temperatures and their influence on wettability alteration and oil recovery. *Energy & fuels*, **21**(4), 2138-2146.
- Kittrick, J. A. (1980). Gibbsite and kaolinite solubilities by immiscible displacement of equilibrium solutions. *Soil Science Society of America Journal*,**44**(1), 139-142.
- Lebedeva, E. V., & Fogden, A. (2011). Micro-CT and wettability analysis of oil recovery from sand packs and the effect of waterflood salinity and kaolinite.*Energy & Fuels*, **25** (12), 5683-5694.
- Ligthelm, D., Gronsveld, J., Hofman, J., Brussee, N., Marcelis, F., & Van Der Linde, H. (2009, June). Novel Waterflooding Strategy by Manipulation of Injection Brine Composition (SPE-119835). In *71st EAGE Conference & Exhibition*.
- McGuire, P. L., Chatham, J. R., Paskvan, F. K., Sommer, D., & Carini, F. (2005). Low Salinity Oil Recovery: An Exciting New EOR Opportunity for Alaska's North Slope. Paper SPE 93903 presented at the SPE Western Regional Meeting, Irvine, California, 30 March–1 April. *dx. doi. org/10.2118/93903-MS*.
- Moradi, M., Alvarado, V., & Huzurbazar, S. (2010). Effect of salinity on water-in-crude oil emulsion: evaluation through drop-size distribution proxy. *Energy & fuels*, **25** (1), 260-268.

- Moradi, M., Topchiy, E., Lehmann, T. E., & Alvarado, V. (2013). Impact of ionic strength on partitioning of naphthenic acids in water–crude oil systems–Determination through high-field NMR spectroscopy. *Fuel*, **112**, 236-248.
- Moradi, M., Kazempour, M., French, J. T., & Alvarado, V. (2014). Dynamic flow response of crude oil-in-water emulsion during flow through porous media. *Fuel*,**135**, 38-45.
- Parracello, V. P., Pizzinelli, C. S., Nobili, M., Masserano, F., Callegaro, C., Caschili, A., & Bartosek, M. (2013, June). Opportunity of enhanced oil recovery low salinity water injection: From experimental work to simulation study up to field proposal. In *Proceedings of the 75th EAGE Conference & Exhibition incorporating SPE EUROPEC, Society of Petroleum Engineers, London, United Kingdom*.
- Puntervold, T., Strand, S., & Austad, T. (2009). Coinjection of seawater and produced water to improve oil recovery from fractured North Sea chalk oil reservoirs. *Energy & fuels*, **23**(5), 2527-2536.
- Pu H., Yin P., & Morrow N. R. (2010, January). Low-salinity waterflooding and mineral dissolution. In *SPE Annual Technical Conference and Exhibition*. Society of Petroleum Engineers.
- Robertson, E. P. (2007, January). Low-salinity waterflooding to improve oil recovery-historical field evidence. In *SPE Annual Technical Conference and Exhibition*. Society of Petroleum Engineers.
- Saleh, A., Yamini, Y., Faraji, M., Rezaee, M., & Ghambarian, M. (2009). Ultrasound-assisted emulsification microextraction method based on applying low density organic solvents followed by gas chromatography analysis for the determination of polycyclic aromatic hydrocarbons in water samples. *Journal of Chromatography A*, **1216**(39), 6673-6679.
- Stewart, T. L. (1980). *U.S. Patent No. 4,184,952*. Washington, DC: U.S. Patent and Trademark Office.
- Strand, S., Høgnesen, E. J., & Austad, T. (2006). Wettability alteration of carbonates—Effects of potential determining ions (Ca^{2+} and SO_4^{2-}) and temperature. *Colloids and Surfaces A: Physicochemical and Engineering Aspects*, **275**(1), 1-10.
- Suijkerbuijk, B. M. J. M., Hofman, J. P., Ligthelm, D. J., Romanuka, J., Brussee, N., Van der Linde, H. A., & Marcelis, A. H. M. (2012, April). Fundamental investigations into wettability and low salinity flooding by parameter isolation. In *18th SPE IOR Symposium, Tulsa, Oklahoma, USA* (pp. 14-18).
- Tang, G. Q., & Morrow, N. R. (1999). Influence of brine composition and fines migration on crude oil/brine/rock interactions and oil recovery. *Journal of Petroleum Science and Engineering*, **24**(2), 99-111.
- Tweheyo, M. T., Zhang, P., & Austad, T. (2006, January). The effects of temperature and potential determining ions present in seawater on oil recovery from fractured carbonates. In *SPE/DOE Symposium on Improved Oil Recovery*. Society of Petroleum Engineers.
- Webb, K. J., Black, C. J. J., & Tjetland, G. (2005, November). A laboratory study investigating methods for improving oil recovery in carbonates. In*International Petroleum Technology Conference*. Doha, Qatar: International Petroleum Technology Conference.
- Webb, K., Lager, A., & Black, C. (2008, October). Comparison of high/low salinity water/oil relative permeability. In *International symposium of the society of core analysts, Abu Dhabi, UAE* (Vol. 29).
- Yildiz, H. O., Valat, M., & Morrow, N. R. (1999). Effect of brine composition on wettability and oil recovery of a Prudhoe Bay crude oil. *Journal of Canadian Petroleum Technology*, **38** (01).
- Zahid, A., Stenby, E., & Shapiro, A. (2010, June). Improved Oil Recovery in Chalk–Wettability Alteration or Something Else?(SPE-131300). In *72nd EAGE Conference & Exhibition*.
- Zahid, A., Sandersen, S. B., Stenby, E. H., von Solms, N., & Shapiro, A. (2011). Advanced waterflooding in chalk reservoirs: Understanding of underlying mechanisms. *Colloids and Surfaces A: Physicochemical and Engineering Aspects*, **389**(1), 281-290.
- Zahid, A., Shapiro, A. A., & Skauge, A. (2012a, January). Experimental Studies of Low Salinity Water Flooding Carbonate: A New Promising Approach. In *SPE EOR Conference at Oil and Gas West Asia*. Society of Petroleum Engineers.
- Zahid, A., Shapiro, A. A., Skauge, A., & Stenby, E. H. (2012b, June). Smart Waterflooding (High Sal/Low Sal) in Carbonate Reservoirs (SPE 154508). In*74th EAGE Conference & Exhibition*.
- Zhang, P., Tweheyo, M. T., & Austad, T. (2007). Wettability alteration and improved oil recovery by spontaneous imbibition of seawater into chalk: Impact of the potential determining ions Ca^{2+}, Mg^{2+}, and SO_4^{2-}. *Colloids and Surfaces A: Physicochemical and Engineering Aspects*, **301**(1), 199-208.
- Zhang, P., & Austad, T. (2006). Wettability and oil recovery from carbonates: Effects of temperature and potential determining ions. *Colloids and Surfaces A: Physicochemical and Engineering Aspects*, **279**(1), 179-187.

Table

Table 1: Different Carbonate, sulfate and clay fines used to study emulsion formations with different designed oils O1, O2, O3, and O4

Fines:				
Carbonates:	C1: $CaCO_3$	C2: $MgCO_3$	C3:Li_2CO_3	
Sulfates:	S1: $CaSO_4$	S2: $BaSO_4$	S3: $SrSO_4$	
Clay:	K1: Kaolinite			
Reservoir rock	D1: Carbonate fines from Dan field of North Sea			
Designed Oil:				
Oil O1	Hexane	Hexadecane	Hexadecylamine	
Oil O2	Hexane	Hexadecane	Heptylamine	
Oil O3	Crude oil	Hexadecylamine	Hexane	Hexadecane
Oil O4	Crude oil	Heptylamine	Hexane	Hexadecane

Figures

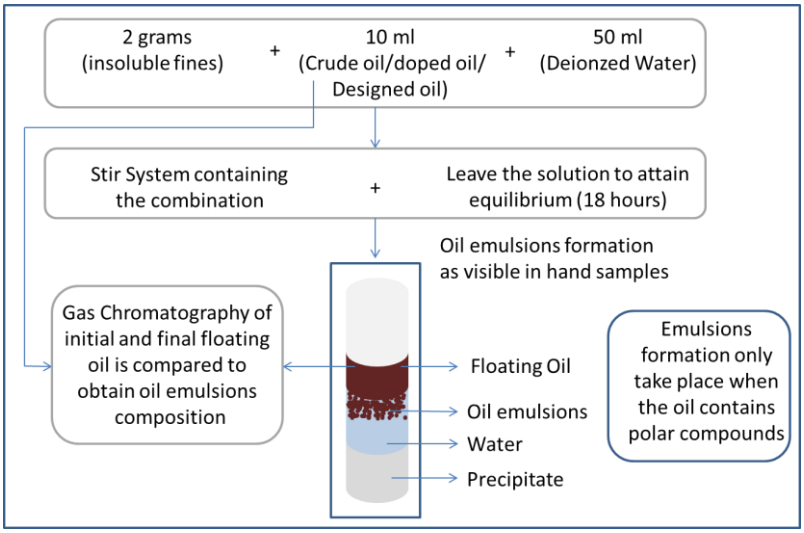


Figure 1: Schematic diagram of the experimental setup for emulsion formation.

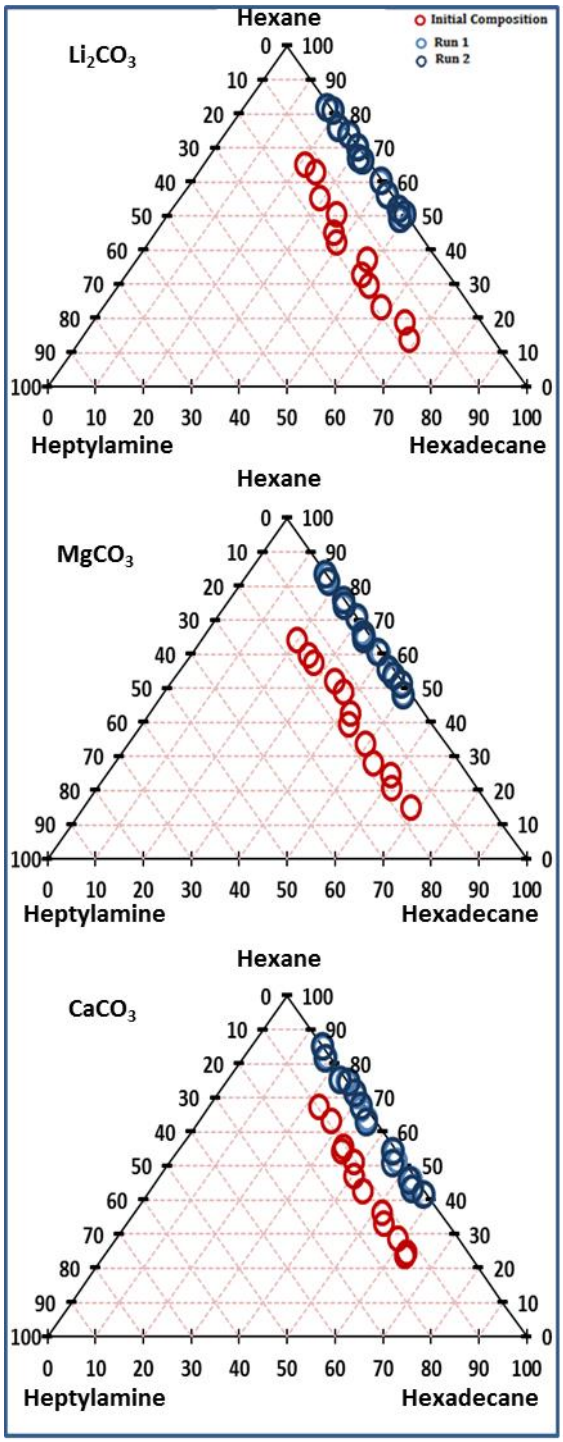


Figure 2: Representation of initial and final oil composition in (triangular diagram for hexane, hexadecane and hexadecylamine) for calcium, magnesium and lithium carbonate fines with oil O1. GC analysis of two samples of the final oil was conducted to ensure consistency as indicated by 'Run 1' and 'Run 2').

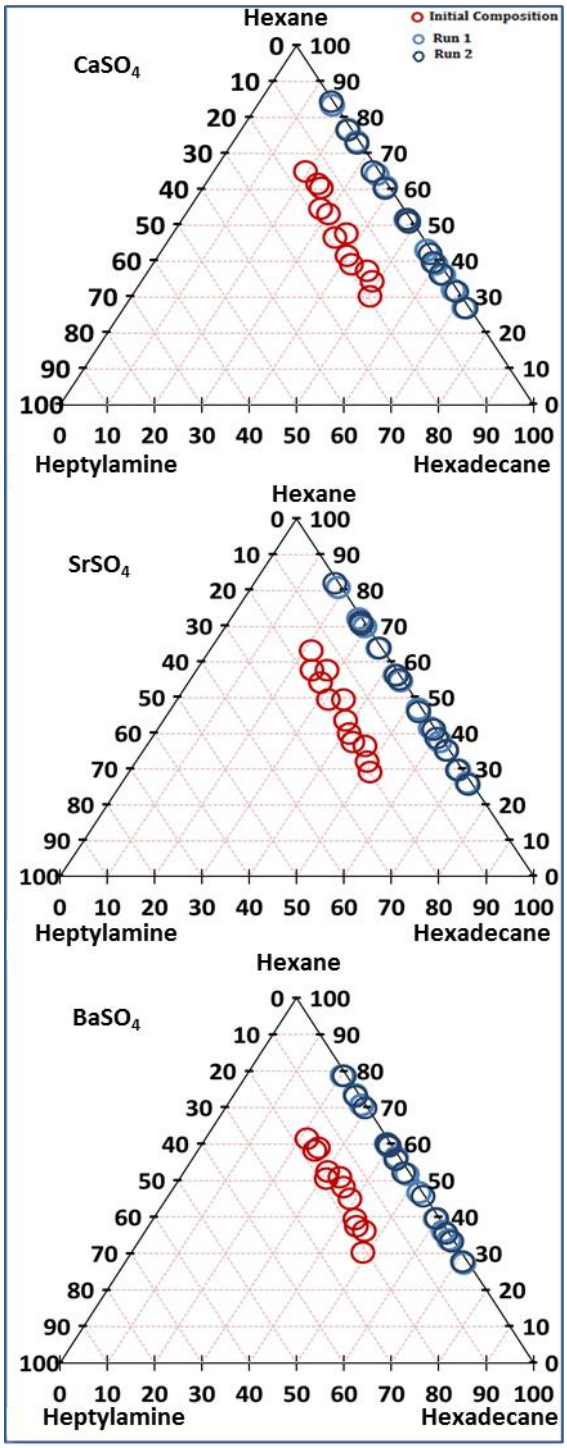


Figure 3: Representation of initial and final oil composition (triangular diagram with hexane, hexadecane and hexadecylamine) for calcium, barium and strontium sulfate fines with oil O2. GC analysis of two samples of the final oil was conducted to ensure consistency as indicated by 'Run 1' and 'Run 2').

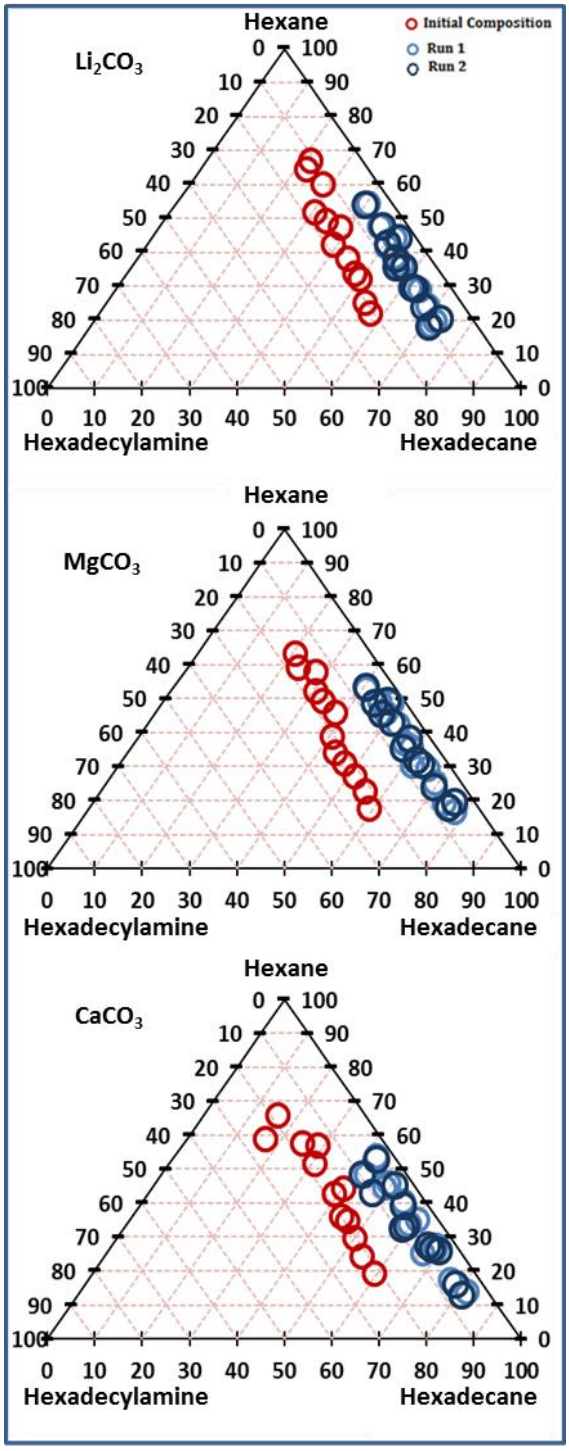


Figure 4: Heptylamine, hexane and hexadecane composition in the initial and final oil after emulsion formation with calcium, magnesium, and lithium carbonate fines with oil O2. GC analysis of two samples of the final oil was conducted to ensure consistency as indicated by 'Run 1' and 'Run 2').

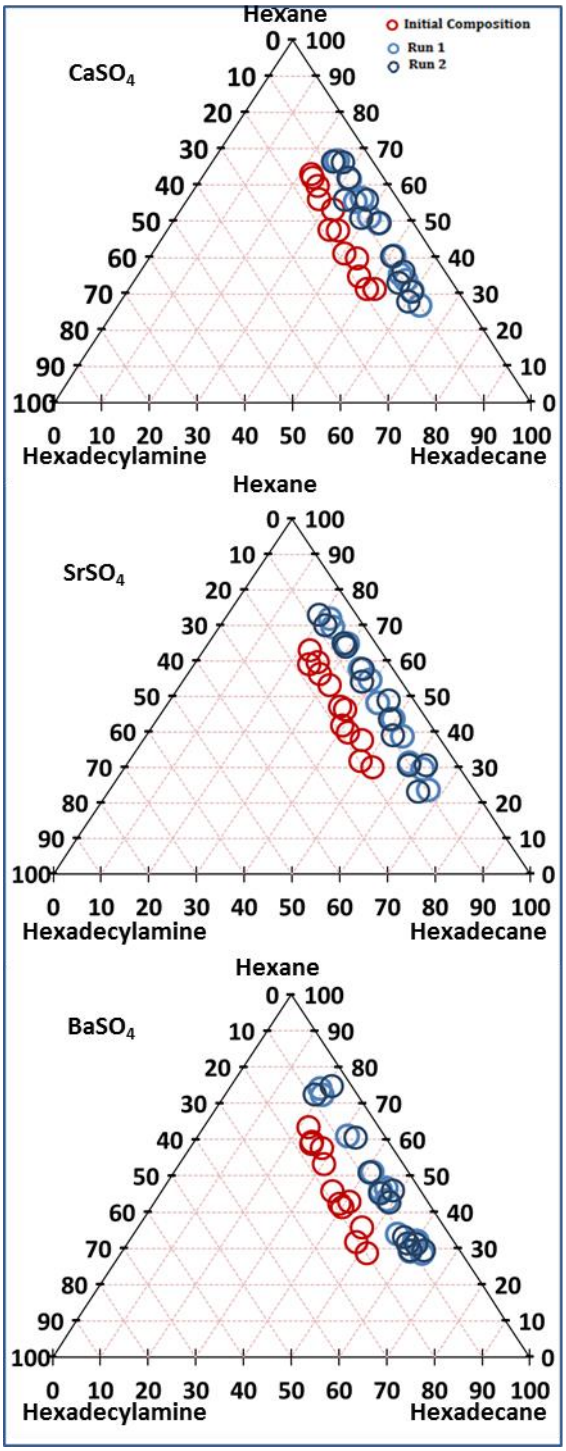


Figure 5: Heptylamine, hexane and hexadecane composition in the initial and floating oil after emulsions formations with calcium, strontium, and barium sulfate fines with Oil O2. GC analysis of two samples of the final oil was conducted to ensure consistency as indicated by 'Run 1' and 'Run 2').

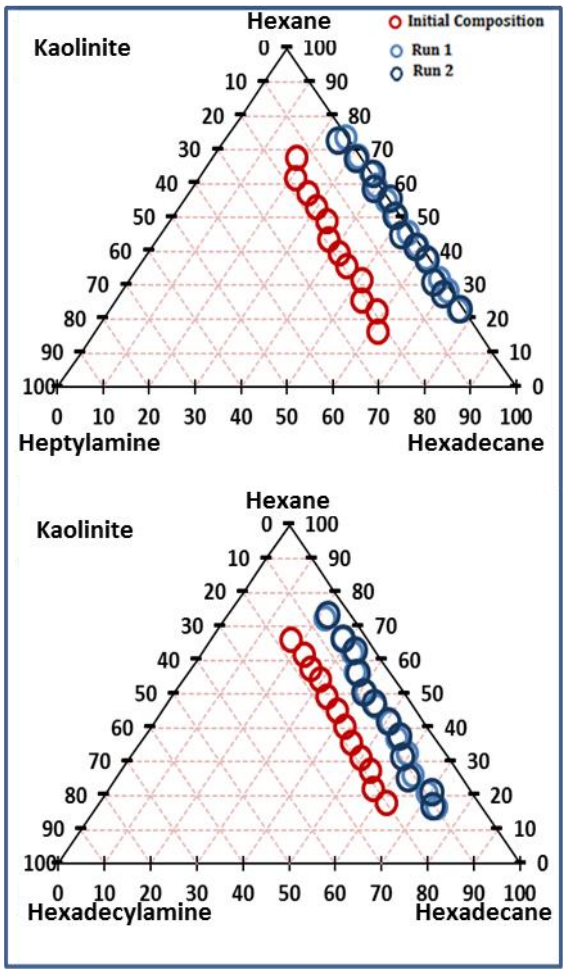


Figure 6: Representation of initial and floating oil composition in two runs (triangular diagram for hexane, hexadecane and base) for calcium, magnesium, and lithium carbonate fines with oils O1(with hexadecylamine) and O2(with heptylamine).Final oil experiments were repeated twice to ensure consistency(data represented : Run1 light blue, Run2 dark blue circles).

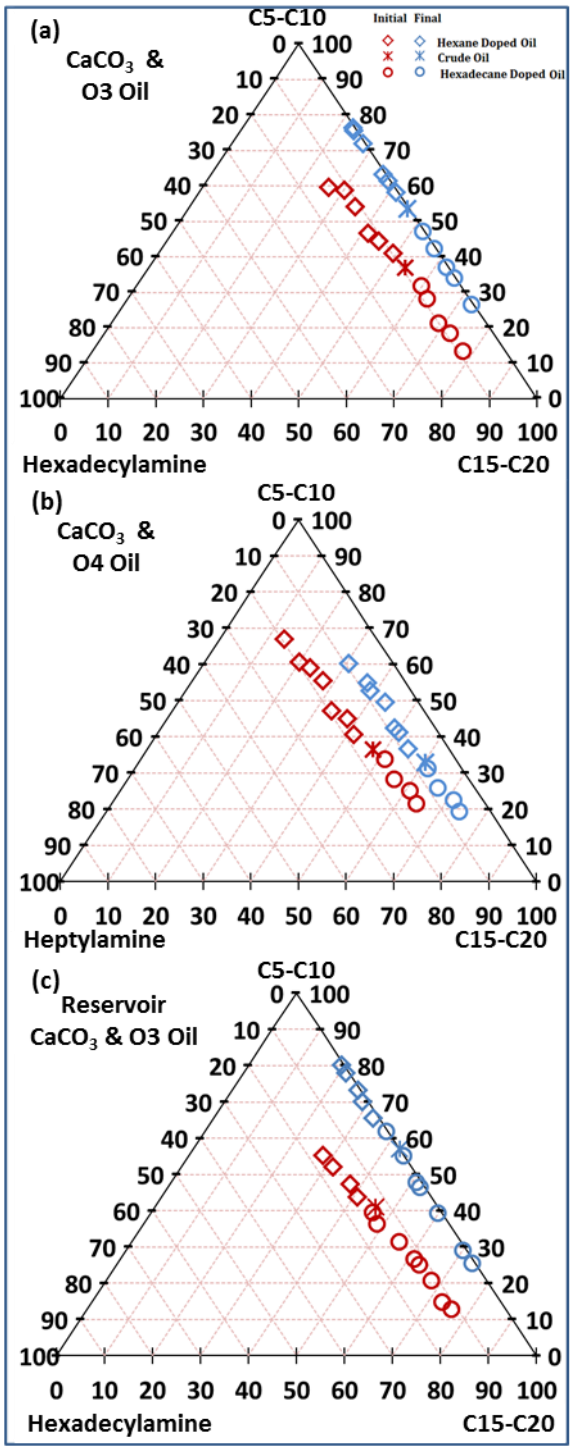


Figure 7: Representation of initial and floating oil composition in two runs (triangular diagram for C5-C10, C15-C20, and hexadecylamine/heptylamine) for calcium carbonate fines with oils O3 and O4.Fig(a) and (b) are emulsion formation with laboratory $CaCO_3$ while (c) emulsion formation with reservoir $CaCO_3$ from Dan field of Danish North Sea.

Paper IV

Chakravarty, K. H., Fosbøl, P. L., & Thomsen, K. (2015, August). Brine Crude Oil Interactions at the Oil-Water Interface. In *SPE Asia Pacific Enhanced Oil Recovery Conference*. Society of Petroleum Engineers.



SPE-174685-MS

Brine Crude Oil Interactions at the Oil-Water Interface

Krishna Hara Chakravarty, Philip Loldrup Fosbøl and Kaj Thomsen, Center for Energy Resources Engineering (CERE), Department of Chemical and Biochemical Engineering, Technical University of Denmark

Copyright 2015, Society of Petroleum Engineers

This paper was prepared for presentation at the SPE Enhanced Oil Recovery Conference held in Kuala Lumpur, Malaysia, 11–13 August 2015.

This paper was selected for presentation by an SPE program committee following review of information contained in an abstract submitted by the author(s). Contents of the paper have not been reviewed by the Society of Petroleum Engineers and are subject to correction by the author(s). The material does not necessarily reflect any position of the Society of Petroleum Engineers, its officers, or members. Electronic reproduction, distribution, or storage of any part of this paper without the written consent of the Society of Petroleum Engineers is prohibited. Permission to reproduce in print is restricted to an abstract of not more than 300 words; illustrations may not be copied. The abstract must contain conspicuous acknowledgment of SPE copyright.

Abstract

The impact of brine salinity and its ionic composition on oil displacement efficiency has been investigated extensively in recent years due to the potential of enhanced oil recovery (EOR). Wettability alterations through relative interactions at the mineral surface have been the basis of proposed mechanisms. The ion specific interaction between fines and polar fractions of crude oil at the oil-water interface has been less explored.

In this study the relative affinity between different ions and the oil surface was determined. The experiments prove the importance of Ca^{2+}, SO_4^{2-}, and HPO_4^{2-} ions in enhancing oil emulsion formation by increasing interactions between polar acids and brine solutions. The results propose the potential use of HPO_4^{2-} ions in reservoirs having inactive mineral surfaces.

The relative oil affinity of different ions including K^+, Na^+, Mg^{2+}, and Ca^{2+} (cations), and Cl^-, SO_4^{2-}, HPO_4^{2-}, and HCO_3^- (anions), were studied through gas chromatographic analysis. Crude oil from the North Sea was doped with various fractions of organic acids to mimic different polar behavior. Increased brine concentration showed up to 15% upsurge of polar fractions on the oil-water emulsion formation. During emulsion formation the relative interactions at the oil-water interface are proved to follow the Hofmeister series: $K^+<Na^+<Mg^{2+}<Ca^{2+}$. Beyond $CaCl_2$ concentrations of 0.08mol/l no additional acid participation in emulsion formation was observed. Among anions, SO_4^{2-} and HPO_4^{2-} showed optimum emulsion formation at 0.05 mol/l. The amount of emulsion formation showed significant dependency on the type of acid doped in oil. Experiments demonstrate that the brine solution can alter the micro forces at the oil-water interface, and this ion specific interaction leads to oil emulsion formation and thus reduces the interfacial viscoelasticity of the trapped oil. These results show significant correlation between oil emulsion formation and increased oil recovery.

Introduction

Smart water flooding has gradually developed into a possible enhanced oil recovery method, since the pioneering work by Tang and Morrow (1997), which showed that oil recovery, can be increased by changing the salinity of the flooded brine. Temperature, oil composition, brine composition, and aging affect oil recovery. Initial studies by Morrow and his group (Morrow et al. 1998) using varied salinity brines in the flooding water indicate that the low salinity brine change mineral wettability towards water wetness. A pioneering study by Morrow and his co-workers (Tang and Morrow et al. 1999) provided primary conditions for Smart Water-Enhanced Oil Recovery (SW-EOR), which includes: (1) availability of potential mobile fines of clay and carbonates, (2) desorption of crude oil from the mineral surface during water flooding and (3) initial water saturation. The study also proposed that mobile fines can release trapped oil from the mineral surface and enhance its mobility during water flooding (Tang and Morrow et al. 1999).

Significant investigative research has been conducted to understand this phenomenon, and several experiments have been conducted by altering the water chemistry of the flooding water (Yildiz et al. 1999; Fogden 2011; Lebedeva and Fogden 2011; Jerauld et al. 2006; Gupta et al. 2011; Delshad et al. 2013; Parracello et al. 2013; Robertson, 2007; Webb et al. 2004; McGuire et al. 2005; Alagic et al. 2011). Despite the significant development in simulation works and experimental studies, a controversy on what dominate smart water flooding based oil recovery has dawdled for several years. Proposed mechanisms that claimed to describe EOR through alteration in salinity include:

1) Mineral surface primary wettability alteration (Zhang et al. 2006; Zhang et al. 2007; Rivet et al. 2010; Yi and Sharma, 2012)
2) Interfacial tension (IFT) reduction, in-situ emulsification (McGuire et al. 2005; Vijapurapu and Rao, 2003)
3) Increasing sweep efficiency of flooded water through fines migration (Yi and Sharma, 2012; Fogden et al. 2011; Zekri et al, 2012; Nasralla and Nasr-El-Din 2011; Pu et al. 2010).

Carbonate rock shows significant wettability alteration (towards more water wetness) in the presence of magnesium, becoming more effective at higher temperatures (Chukwudeme and Hamouda 2009; Fathi et al. 2010; Fathi et al. 2011; Austad et al. 2011). For carbonate rock, maximum increase in oil recovery has been observed for sulphate enriched waterfloods (Chukwudeme and Hamouda 2009; Austad et al. 2011). High temperature has also been shown to have a positive effect on SW-EOR (Austad et al. 2011; Zahid et al. 2012a; Zahid et al. 2012b). The availability of soluble potential ions (Ca^{2+}, Mg^{2+} & SO_4^{2-}) in the flooded water has been proposed to be the primary reason for the observed wettability alteration. These studies (Chukwudeme and Hamouda 2009; Fathi et al. 2010; Fathi et al. 2011; Austad et al. 2011) do not specifically explain why the availability of fines is a primary requirement for obtaining successful EOR as previously shown (Morrow et al. 1999). Questions have been posed to whether wettability alteration is the main cause for low-salinity water flooding oil recovery (Kasmael and Rao 2014; Zahid et al. 2010).

In carbonate rocks, completely water wet core plugs have also shown increased oil recovery for increased sulphate concentration in the flooding water (Zahid el al. 2010). This is contrary to the previously proposed wettability alteration mechanism (Austad et al. 2011). It has also been shown that the effect of brine solution in oil recovery is significantly dependent on the composition of oil (Suijkerbuijk, et al. 2014). The formation of oil emulsions in the water phase is associated with a decrease in crude oil viscosity. This has been observed for sulphate enriched brines (Zahid et al. 2012b). Copious confirmation has shown that oil emulsions can be formed by a buildup of a viscoelastic interface with low salinity brine (Moradi et al. 2011; Moradi et al. 2013; Wang and Alvardo, 2012; Alvardo et al. 2014). Previously, it has also been shown that organic acids can play a significant role in the buildup of a viscoelastic brine-crude oil interface (Moradi et al. 2013). Herein, it has been shown that the formation of oil emulsion is associated with a reduction in the interfacial tension between reservoir oil and the flooded water. Comparative experiments (McGuire et al. 2005) have shown that when the oil is in contact with elevated-pH smart water, the polar fractions of the oil are saponified, which act as an emulsifying agent to bring the dispersed oil into the flooded water leading to low viscosity emulsion formation.

The studies by Zahid et al. 2012b; Moradi et al. 2011; Moradi et al. 2013; Wang and Alvardo, 2012; Alvardo et al. 2014; and McGuire et al. 2005 clearly show that formation of emulsions takes place during SW-EOR. Formation of these emulsions is highly useful in increasing the displacement efficiency of the oil (McGuire et al. 2005). The oil bound to the mineral surface has significantly higher rigidity and immobility as compared to the water soluble oil emulsions. The higher the degree of emulsion formation, the easier is the displacement of the oil and thus the higher is the oil production. On this basis, a set of experiments have been conducted to study the effect of different soluble brines in the oil emulsion formation. The amount of emulsion formation caused by each salt was individually analyzed. Herein both the salt type and salt concentration was varied. Two different sets of brines were used. In the first set of experiments, the type of cation was kept constant while the type of anion was varied. For the same cation (Na^+) the effects of different anions were independently studied. This includes the analysis of Cl^-, SO_4^{2-}, HPO_4^{2-}, and HCO_3^- ions (Table 1). Previously, in the water floods concentrations of Cl^- (Tang and Morrow 1997; Morrow et al. 1999), SO_4^{2-} (Chukwudeme and Hamouda 2009; Austad et al. 2011), and of HPO_4^{2-} (Gupta et al. 2011) have been shown to affect oil recovery. So the effect of these ions (Cl^-, SO_4^{2-}, and HPO_4^{2-}) in emulsion formation was considered. In the other set of experiments, the type of anion was kept constant and the type of cation was varied.

As indicated in Table 1, the effect of K^+, Na^+, Mg^{2+}, and Ca^{2+} ions in emulsion formation was studied. KCl was used as reference brine. Mg^{2+} and Ca^{2+} ions have shown their significance in SW-EOR (Austad et al. 2011). Thus, their influence on emulsion formation was also considered. The interactions of these brines with different sets of designed oil were studied. Specific organic acids can play a substantial role in emulsion formation (Moradi et al. 2013). Therefore, two sets of designed and doped oil were developed. The first set of designed oil consisted of crude oil doped with water soluble acids. The amounts of oil emulsion obtained for different brine solutions were measured. The second set of designed oil consisted of water insoluble acids and alkanes mixed in different combinations as presented in Table 1. The amounts of emulsion formation with these oil combinations were plotted in triangual diagrams. The aim of the study was to obtain the composition of the emulsion for different brine solutions in order to be able to calculate the amount of acid contributing to the emulsion formation. This emulsion formation pattern has thereafter been correlated to reported oil recovery patterns.

Experiment

Experimental Setup:

A simple experimental setup was developed (Figure 1) to study the conditions of the emulsion formation. First, 2 grams of the insoluble fines ($CaCO_3$(s)) were added to 10 mL of oil and 50 mL of a specific brine solution (Table 1). This system was stirred for one hour and the solution was kept in isolation for 18 hours to attain equilibrium. Subsequently it was observed that an emulsion was formed, as shown in Figure 1. A layer of water soluble oil emulsion was formed between the oil phase and the water phase. These emulsions were not observed in case of pure alkanes, probably due to the unavailability of a polar component. To further study the property of these oil emulsions, samples of oil were extracted from the floating fraction. This floating oil (final

oil) and the oil added to the system originally (initial oil) was analyzed by gas chromatography and the compositions of the two oils were determined. The obtained compositions were plotted in triangular diagrams so that any change in composition could be analyzed.

Gas chromatography analysis:
As per previous recommendations and applications (Blomberg et al. 2002; Adahchour et al. 2008; Dutriez et al. 2010), the ASTM D2887 method (Chorn et al. 1984) was used for compositional analysis of crude oil mixtures. Each sample was introduced through the front GC Injector. The acquisition method's instrument was Agilent 7890A, as previously used for alkane analysis (Dutriez et al. 2010; Saleh et. al.). The oven had an equilibrium time of 3 mins, with maximum temperature of 350 °C with an initial temperature of 40°C and was thereafter heated to 350°C in 4 mins. The runtime of each sample was 19.5 mins. A 1 µL front injector, with each injection volume 0.05 µL was used. After each analysis the injector was thrice washed with toluene with each sample volume of 0.8 µL. In the front inlet He gas had a pressure of 0.226 bar, a total flow rate of 42.9 mL min^{-1} and septum purge flow 3 mL min^{-1}. The inlet temperature initially was at 50°C, then raised from 200°C/min to 330°C for 5 min. Inlet in split mode had 2:1 ratio with split flow rate of 26.6 mL min^{-1}. The Agilent 125-10HB10 m x 530 µm x 2.65 µm column (ASTM D2887-06) was used. The outlet had an initial temperature of 40°C, and a pressure 0.226 bar with a flow rate of 13.3 mL min^{-1} and an average velocity of 96.52 cm/sec. The Front Detector FID was heated to 375 °C. A H_2 flow at 40 mL min^{-1}, and an air flow of 450 mL min^{-1}were used. The column used with Inventory: autoID-1, Model: 125-10HB and Manufacturer: Agilent, had Diameter: 530.00 µm, Length: 10.0 m, Film thickness: 2.65 µm, Void time: 0.173 min and maximum temperature: 350.0 °C. For each run the relative compositions of the oil components were calculated using Agilent simulated distillation. For all initial samples up to 5 repetitions was made, and the consistency in measured composition was more than 95%.

To analyze the effect of different brines in oil emulsions, two sets of brine solution and two sets of oil mixtures (Doped oil & Designed oil) were prepared.

Brine Solutions:

Two sets of brine were used.

1) In the first set (B1), the type of cation was kept constant and the type of anion was varied. This includes NaCl, Na_2SO_4 $NaHCO_3$ and Na_2HPO_4. The salts were obtained from Sigma-Aldrich (Product Number NaCl: 746398; Na_2SO_4: 239313; $NaHCO_3$: 792519; Na_2HPO_4: 795410). Sodium chloride was used as it is readily available in sea water and is the most used brine in all water flooding experiments (Tang and Morrow 1997; Morrow et al. 1999); while sulphate ions have proven to be a potential ion in enhanced oil recovery (Chukwudeme and Hamouda 2009; Austad et al. 2011). There is also indication that hydrogen phosphate ions participate in enhanced oil recovery (Gupta et al. 2011) so its influence on emulsion formation was also considered. $NaHCO_3$ was considered as the majority of chalk and lime stone reservoirs are composed of carbonates, free CO_2 leads to the formation of bicarbonates in the solution. The set of these four brines is important in respect to smart water oil recovery and thus its effect on emulsion formation was explored in a varied concentration range (from 0.01mol/l to 0.5mol/l).
2) In the other set of brines (B2), the anion type was kept constant and the cation type was varied. This includes KCl, NaCl, $MgCl_2$, and $CaCl_2$. The salts were obtained from Sigma-Aldrich (Product Number KCl: 746436; NaCl: 746398; $MgCl_2$: 449172; $CaCl_2$: 793639). KCl was used as reference brine. Variation in Na^+ concentration has been the basis of low salinity EOR water flooding experiments (Tang and Morrow 1997; Morrow et al. 1999); while Mg^{2+} has been shown to significantly alter the wettability of chalk surfaces (Chukwudeme and Hamouda 2009; Fathi et al. 2010; Fathi et al. 2011;). Ca^{2+} ions have also shown their potential in SW-EOR (Austad et al. 2011). Thus, the effects of K^+, Na^+, Mg^{2+}, and Ca^{2+} ions in emulsion formation were individually considered. The interaction of these brines was studied with the different sets of designed oil.

Doped Oil:

In the first set of experiments, crude oil was doped with water soluble acids. This includes three different acids (Table 1).

1) Oil TC1 was crude oil doped with acetic acid, which is completely miscible with water and the used brine.
2) TC2 was crude oil doped with different amounts of propanoic acid, which is also soluble in water.
3) TC3 was crude oil doped with valeric acid, which is soluble with a solubility of 4.97g/100 mL.

Several different compounds were present in the oils (TC1, TC2, and TC3). The concentration corresponding to each carbon number was calculated using the Agilent SimDist program. The ratio between the final and the initial concentration for each carbon number was plotted in Figure 2. For the initial oil, the acid peak area was obtained from the gas chromatogram and was plotted against acid wt%. A linear correlation was observed between the peak area and the acid wt% (Supplementary Figures 1 and 2). This linear correlation was used to obtain the acid concentration of the final oil. Further to confirm the obtained composition, 0.1 mL of N,O-Bis (trimethylsilyl)trifluoroacetamide (BSTFA) was added to the oil samples and the chromatographic analysis was repeated. BSTFA is a chemical compound that is used to derivatise labile groups such as carboxyl on other chemicals, with the

more stable trimethylsilyl group, which protects the labile group and allows the compound to be used for analytical purposes including gas chromatographic analysis (Stalling et al. 1998). As shown in Figure 3, sharp peaks for the acid samples were obtained and their corresponding concentrations were confirmed. The ASTM D2887 method ensured that the concentrations of hydrocarbons corresponding to each carbon number were obtained from its respective peaks in the gas chromatography plots. It is shown in Figures 4 and 5. Using this method the oil composition corresponding to each carbon number was obtained (up to C_{40}: hydrocarbon containing 40 carbon atoms).

Designed Oil:

In the second set of experiments, oils composed of well-defined alkanes and acids were prepared (Table 1).

1) Oil O1 contained hexane, hexadecane, and heptanoic acid in various fractions. The acid in oil sample O1 was a water insoluble, light acid. One fraction of the alkanes (hexane) was of similar length as the acid and the rest fraction (hexadecane) was a relatively heavy alkane.
2) Oil O2 contained hexane, hexadecane, and stearic acid. Stearic acid is completely insoluble in water. One fraction of the alkanes (hexadecane) was of similar length as the acid and the rest fraction (hexane) was a significantly lighter alkane.

Detailed compositional analysis was possible for the initial and final oil for O1 and O2 oil samples as each sample consisted of only three fractions. The composition of initial and final oil was determined and was represented in a triangular plot. The formation of oil emulsion is associated with a decrease in the acid concentration in the final oil. The percentage of acid that was depleted from the final oil was assumed to be contributing to the oil emulsion formation. The percentage of acid participating in the oil emulsion formation was clearly correlated with the increase in brine concentration. Figure 6 shows the observed pattern for acid participation in oil emulsion formation versus brine salinity. It has previously been documented that brine salinity and composition affect the efficiency of fines in interacting with crude oil (Nasralla, et al. 2014).

Best grade chemicals available were used for the fines and the organic compounds to avoid any error in the experiments. These experiments were conducted in coherence with the previous study for oil emulsion formation with deionized water and similar oil combinations (Chakravarty et al. 2015).

Result and Discussions
Interactions between crude oil (doped with soluble acids) and NaCl, $CaCl_2$ and Na_2SO_4 brines

In the first set of experiments NaCl, $CaCl_2$ and Na_2SO_4 brines (with Na^+ concentration of 0.1 mol/l) were prepared. A SO_4^{2-} concentration of 0.05mol/l is twice the average sea water SO_4^{2-} concentration. This enriched sulphate concentration (with respect to sea water) was selected because similar concentrations have shown to increase oil recovery significantly during smart water floods (Austad et al. 2011). Three different samples were prepared by adding a mixture containing TC1 oil and $CaCO_3$ fines to the three brine solutions. The samples were stirred and allowed to attain equilibrium. Emulsion formation took place in all three cases. Samples from the final oil (after emulsion formation) and the initial oil were taken for gas chromatographic analysis. Subsequently, the compositions of the final oil and the initial oil were determined. By comparing these compositions, it is clear that the final oil was depleted of heavier alkanes (alkanes beyond C_{10}). The ratio between the initial oil and final oil content for components corresponding to each carbon number is shown in Figure 2. The acid was completely absent in the final oil. Figure 3 shows the gas chromatogram of the final oil and the initial oil. To confirm these results, the oil was doped with 4 different concentrations of acids. As shown in Figure 3 the chromatographic experiments indicated that the acid was completely removed from the final oil. Since the used GC method is most suitable for alkane composition analysis a sharp peak was not obtained for the doped acids. Therefore, the GC samples were subsequently doped with BSTFA (to obtain sharp peak for the available acids as well). As shown in Figure 3, adding BSTFA confirmed the disappearance of acids from the final oil. Thus the acid was either dissolved in the available water or participated in emulsion formation. The amount of acid contributing to the emulsion formation could not be directly correlated to the amount of acid removed from the final oil as the amount of acid present in the brine solution was still unknown. The same set of experiments was conducted with TC2. In this experiment, the crude oil was doped with propanoic acid. The crude oil was doped with five different concentrations of propanoic acid (Supplementary Figure2). The final oil seemed to be enriched in light alkane and depleted of heavy alkane (as shown in Figure 4). The results remained the same irrespective of the selected brine. The acid content was reduced in the final oil for all the TC2 samples. But, the fraction of acid that participated in emulsion formation was not calculate able as the acid presence in the brine solution was still unknown. The same set of experiments was conducted for TC3 (i.e. valeric acid doped crude oil). Also in this case it was observed that in the final oil, the acid was completely removed. This indicated that the acid was either dissolved in the available brine solution or contributed to the emulsion formation. Gas chromatographic analysis after adding BSTFA to the oil sample confirmed the disappearance of valeric acid from the final oil. This is shown in Figure 3. Emulsion formation did take place and the concentration of lighter alkane was enhanced in the final oil (Figure 5). These results together suggest that as a general trend: lighter alkanes remain in the final oil and the heavier alkanes participate in the emulsion formation (Figure 2). It needs to be noted that the lighter acid became rapidly soluble in brine solutions, so the available acids for emulsion formation was relatively less compared to the heavier acids (already present in crude oil). It was previously shown that heavier alkanes prefer to form emulsion with heavier acids and that lighter alkanes prefer to form emulsion with lighter acids (Chakravarty et al. 2015). This is quite consistent with the current finding: the final oil contains

most of the lighter alkane and only a fraction of the heavier alkanes. This indicates that the heavier alkanes are participating in the emulsion formation along with the heavier (insoluble) acids present in the crude oil. While the lighter soluble acids mostly got dissolved in the brine solution and the lighter alkanes remained in the final oil.

The degree of participation of each acid in the emulsion formation was not determined in these experiments because of the presence of multiple acids in the doped oil. In order to determine how much acid participated in the emulsion formation, designed oil containing only a single acid was used thereafter. Furthermore, certain acids (particularly light acids) can dissolve in the brine instead of participating in the emulsion formation. So, insoluble acids were used in the second set of experiment.

Interactions between designed oil O1 (doped with heptanoic acid) and Cl^-, SO_4^{2-}, HPO_4^{2-}, and HCO_3^- (anions)

To determine the amount of acid participating in emulsion formation, designed oil containing only a single acid insoluble in brine solution was used. Selectivity of alkanes has previously been observed when carbonate fines were used for emulsion formation (Chakravarty et al. 2015). The presence of a single acid in the designed oil also helped to track any change in alkane selectivity during emulsion formation. By using a water insoluble acid, it was ensured that the acid would either be present in the oil fractions or participated in oil emulsion formation. Thus fraction of acid participation in emulsion formation could be precisely calculated.

The first oil set O1 is composed of hexane, hexadecane and heptanoic acid in different concentrations. The emulsion formation experiment was conducted for O1 with B1 (composed of different Na^+ brines including NaCl, Na_2SO_4 $NaHCO_3$ and Na_2HPO_4). Herein, since the Na^+ ion is present among the different solutions it was used to express the concentration of the brine solutions. The experiments were conducted for 12 different concentration of brine (between 0.01mol/l to 0.5mol/l). Through gas chromatography, the composition of initial oil and the final oil was analyzed. The amount of acid participation in emulsion formation was obtained by calculating the missing fraction of acid from the final oil (relative to the initial oil).

The contribution of acid in emulsion formation was plotted in Figure 6. It was observed that the emulsion formation was affected by the availability of brines in the system. For the different brine concentrations, the initial and final oil composition is shown in Figure **7**. In case of brine solutions containing NaCl (with concentration of 0.01 mol/l), the acid concentration in the final oil was only 55% of that in the initial oil. Thus indicating that around 45% of the heptanoic acid participated in emulsion formation (Figure 6). Subsequently with increase in the concentration of the brine, the acid concentration further diminished in the final oil. It signifies an increase in acid contribution in emulsion formation. It maximized (for Na^+ concentration of 0.1mol/l) with 51% of acid contributing in emulsion formation. As shown in Figure 6, increasing the concentration up to 0.5 mol/l did not lead to any additional acid contribution in emulsion formation. Thereafter the same set of experiments was repeated with $NaHCO_3$ solutions. It is observed that for an initial Na^+ concentration of 0.01 mol/l, 45% of the acid participated in emulsion formation. This participation increased up to 52% at a Na^+ concentration of 0.14mol/l (Figure 7). Further increasing the concentration to 0.5 mol/l reduced the acid participation to 46%, as some acid fractions returned to the final oil. With Na_2SO_4 brine solution it was observed that 47% of the acid participated in emulsion formation for an initial Na^+ concentration of 0.01mol/l (Figure 6). It increased significantly to 59 % for a brine solution with Na^+ concentration of 0.1mol/l and thereafter it remained constant. Acid participation in oil emulsion formation was 58 % for final brine concentrations of 0.5 mol/l. Subsequently in case of Na_2HPO_4 it was observed that the initial participation of acid in emulsion formation was around 46% for 0.01mol/l Na^+. The acid in the emulsion increased to 55 % at 0.1mol/l (Figure 7). Further increasing the concentration reduced the acid participation to 52% in 0.5mol/l (Figure 6). These results indicate that if mobile ions are present, they can interact with the polar oil fractions and cause emulsion formation. This is illustrated in figure 8a. Furthermore it indicates that increasing brine concentration initially increases the amount of emulsion formation by enhancing the amount of acid participation in the emulsion formation. Alteration in micro forces caused by interactions between brine and crude oil at the oil-water interface could be a possible reason for the initial rise in the emulsion formation. As previously suggested (Moradi et al. 2011; Moradi et al. 2013; Wang and Alvardo, 2012), formation of a viscoelastic layer might be taking place, by the interactions between the soluble ions and the oil-polar fractions. A schematic view is shown in Figure 8b. Herein SO_4^{2-} ion (at 0.1mol/l) followed by HPO_4^{2-} (0.08mol/l) (Figure 7) has proved to be the most effective ion in enhancing the amount of emulsion formation. Further increasing the concentration had a reverse effect in emulsion formation with HPO_4^{2-} while it remained unaltered for SO_4^{2-} ions. It is interesting to note that these results also correlate with water flooding experiments reported in the literature. It has been shown that SO_4^{2-} is a potential ion in enhanced oil recovery (Chukwudeme and Hamouda 2009; Austad et al. 2011). Previous experiments indicate that HPO_4^{2-} ions participate in enhanced oil recovery (Gupta et al. 2011) which is also supported by the experiments reported here.

Beyond the optimum concentration (which is specific for each brine), it is observed that the amount of oil emulsion does not further increase. At low salt concentration the mobile fines can interact with the polar fractions of the crude oil. But increasing the concentration can lead to an electric double layer formation on the fines surface (Nasralla, et al. 2014). As a result, fines coagulate and their participation in oil-emulsion formation reduces. This could be a possible reason, why no further oil-emulsion formation is observed with high concentration brine solutions. A schematic view of this is shown in Figure 8c.

Interactions between designed oil O1 (doped with heptanoic acid) and K^+, Na^+, Mg^{2+}, and Ca^{2+} (cations)

The same set of experiments was conducted with oil O1 and brine B2 (Table 1). In B2 brines, the anion type was kept constant and the cation type in the solutions was varied. This group of brines included KCl, NaCl, $MgCl_2$, and $CaCl_2$. Since the chloride ion

is present in all the different solutions its concentration was used to express the concentration of the brine solutions. The initial and final oil compositions shown in Figure 99 were obtained through gas chromatography. The missing fraction of acid in the final oil (relative to the initial oil) indicates the amount of acid participating in emulsion formation. Experiments conducted with KCl brine indicated that the acid fraction was reduced in the final oil. As shown in Figure 6, 45% of the acid contributed to emulsion formation for an aqueous solution of 0.01 mol/l KCl. The acid contribution to emulsion formation increased to 47% for a concentration of 0.14 mol/l (Figure 6). Further increasing the concentration to 0.5 mol/l reduced the acid participation to 43%. Formation of an electric double layer as previously suggested (Nasralla, et al. 2014) could be a possible reason for the observed decrease in emulsion formation. In case of brine solutions containing NaCl, it was noted that for concentrations of 0.01 mol/l, 45% of the heptanoic acid contributed to emulsion formation (Figure 99). Successively increasing the brine concentration increased the involvement of the acid in emulsion formation. The largest value was reached at 0.1mol/l with 51% of the acid contributing to emulsion formation. The obtained values are plotted in Figure 6. Increasing the concentration up to 0.5 mol/l did not lead to any additional emulsion formation. Subsequently with $MgCl_2$ brine solutions it was observed that 47% of the acid contributed to emulsion formation for Cl^-(aq) concentrations of 0.01mol/l (Figure 6). It increased significantly to 53% for brine solution of 0.12 mol/l and thereafter it started decreasing. Acid participation in oil emulsion formation was 50% for final brine concentrations of 0.5 mol/l. In case of 0.01 mol/l $CaCl_2$ solution it was also observed that the acid concentration was depleted in the final oil. 47% of the acid participated in emulsion formation. With an increase in brine concentration, the amount of acid present in the final oil was further diminished. The acid participation in emulsion formation significantly increased to 58% at 0.08mol/l (Figure 6). Further increase in the brine concentration reduced the acid participation to 56% at 0.5 mol/l. These results indicate that increasing brine concentration initially increases the amount of emulsion formation by enhancing the amount of acid participation in the emulsion formation (as shown in figure 8). The Ca^{2+} ion (at 0.08 mol/l) followed by Mg^{2+} (0.12 mol/l) has proved to be the most effective in enhancing the amount of emulsion formation (Figure 99). Further increasing the concentration had reverse effect on emulsion formation for both Mg^{2+} and Ca^{2+} ions. The importance of Mg^{2+} and Ca^{2+} ions is further highlighted: as the observed variation in emulsion formation correlate with previously reported SW-EOR water flooding experiments (Chukwudeme and Hamouda 2009; Austad et al. 2011). The Ca^{2+} concentration of 0.04mol/l (i.e. Cl^- concentration of 0.08 mol/l) is thrice the average Ca^{2+} concentration in sea water. Sea water enriched with similar concentrations of Ca^{2+} ion has been shown to enhance the oil recovery. The observed pattern of ion efficiency in emulsion formation was $K^+<Na^+<Mg^{2+}<Ca^{2+}$, which follows the Hofmeister series. It is interesting to note that previous interaction analysis between cations and organic molecules has also been shown to follow the same trend (Rimmen et al. 2014).

Interactions between designed oil O2 (doped with stearic acid) and Cl^-, SO_4^{2-}, HPO_4^{2-}, and HCO_3^- (anions)

An analogous set of experiments was conducted with the second oil, O2. Oil O2 was composed of hexane, hexadecane and stearic acid (Table 1). The interaction of oil O2 with NaCl, Na_2SO_4, $NaHCO_3$ and Na_2HPO_4 was analyzed (Figure 10). After oil O2 was stirred with brine and $CaCO_3$ fines, a gas chromatographic analysis of the final oil and the initial oil was conducted. Thereafter the participation of acid in the emulsion formation was determined for these different cases. In case of brine solution containing NaCl, 95% of the stearic acid participated in emulsion formation and only 5% of the acid was available in the final oil (Figure 10). With an increase in brine concentration, the amount of acid participation did not show any major variation. Na_2SO_4 brines gave similar results as 95.2% of the acid participated in emulsion formation for a brine concentration of 0.01 mol/l (concentration of Na^+). The brine concentration was increased to 0.5mol/l but no observable trend within the experimental accuracy was observed. The acid participation in emulsion formation for different brine concentrations is shown in Figure 10. Subsequently the same set of experiments was performed with Na_2HPO_4 and oil O2. In this case again it was observed that the stearic acid concentration was significantly diminished in the final oil indicating that it consistently contributed to emulsion formation. The acid contribution to emulsion formation for Na_2HPO_4 brine solution was 94.7% (Figure 10). With $NaHCO_3$ analogous results were achieved. 94.7% of the acid participated in emulsion formation and increasing the brine concentration to 0.5 mol/l did not result in any observable variation. The acid percentage in emulsion for different brine concentrations is shown in Figure 10. These results indicate that varying the concentration of these brines did not have any major effect. These results show that irrespective of the type of brine available in the solution, the polar components in the solution are keen to form oil emulsions. Heavier acids are significantly more probable of forming oil emulsions than lighter acids and emulsion formation is not affected by an increase or decrease in brine concentration. Previous studies have shown that the oil composition has significant effect in the utility of SW-EOR processes (Zahid et al. 2012; Austad et al. 2011; Moradi et al. 2013). Interestingly, the amount of emulsion formation also shows significant variation with change in the organic acids in the oil. Similar to SW-EOR water flooding experiments (Zahid et al. 2012; Austad et al. 2011) the significance of the ions also changes in emulsion formation with variation in the polar oil composition.

It has previously been shown that the adhesive force between the calcium ion and stearic acid is significantly higher than the corresponding force between the calcium ion and heptanoic acid. It was shown by the high contact angle for stearic acid doped oil (Jabbar et al. 2013). Higher adhesion between stearic acid and calcite has also been suggested in other studies as well (Milter et al. 1996; Rezaei Gomari. K. A. 2009). The observed significantly higher acid participation in emulsion formation for stearic acid (as compared to heptanoic acid) also indicates the greater adhesive force between calcite and stearic acid.

Interactions between designed oil O2 (doped with stearic acid) and K^+, Na^+, Mg^{2+} & Ca^{2+} (cations)

Subsequently the interaction of oil set O2 and brine set B2 (keeping the anion type constant and varying the cation in the solutions) was analyzed. The brine set B2 included KCl, NaCl, $MgCl_2$, and $CaCl_2$ salts. Since the chloride ion is the common anion, the chloride concentration was used to express the concentrations of these brine solutions. Emulsion formation experiments were conducted and initial and final oil compositions were analyzed (Figure 10). The participation of acid in the emulsion formation was determined for these different cases. Brine solutions containing KCl showed that 94.5% of the acid participated in the emulsion formation, while the acid was completely depleted from the final oil (Figure 10). Increasing the brine concentration to 0.5mol/l showed minor variations but no major trend was observed. Brine solutions containing NaCl, caused 95% of the stearic acid to participate in emulsion formation and only 5% of the acid was available in the final oil (Figure 10). With increase in concentration, the amount of acid participation did not show any major variation (Figure 10). Subsequently the same set of experiments was conducted with $MgCl_2$ and oil O2. In this case again it was observed that the stearic acid concentration was significantly diminished in the final oil indicating that it consistently contributed to emulsion formation. The acid contribution to emulsion formation with $MgCl_2$ brine solution was 94.8% (Figure 10). Increasing the brine concentration did not result in any variation in amount of emulsion formation. The experiment with $CaCl_2$ gave comparable results as 95.1% of the acid participated in emulsion formation and increasing the brine concentration to 0.5 mol/l showed no considerable variation. The amount of emulsion formation at different brine concentrations has been shown in Figure 10. The experiments collectively indicate that the different brines and their variation in concentration had no major effect on oil emulsion formation. These results further confirm that irrespective of the type of brine available in the solution, the polar components were keen to form oil emulsions. Thus, it indicates that the availability of heavier acids results in oil emulsion formation which is not affected by an increase or decrease in brine concentration.

Interaction between crude oil and fines leads to emulsion formation which releases the trapped oil from the mineral surface. An increase in emulsion formation results in a higher mobility of the oil and thus it enhances the displacement efficiency of the oil and finally increasing the oil recovery. According to these presumptions, the amount of emulsion formation is the basic property that governs the entire process. The results show that available brines can significantly affect the interaction between the fines and the crude oil. Two major trends were observed for the different experiments conducted with O1.

- For all different brine solutions it is observed that an initial increase in brine concentration increases the amount of emulsion formation. It has previously been shown that brine-polar hydrocarbon interactions can lead to formation of a viscoelastic interface, and this interface can enhance oil emulsion formation (Alvatdo et al. 2014). The observed increase in oil emulsion with increase in brine concentration; could be associated to such brine-polar hydrocarbon interactions. A representation is shown in figure 8a and b.
- No additional emulsion formation takes place beyond an optimum concentration. The optimum concentration was found to be brine specific. It has previously been suggested that at high brine concentration, the formation of electric double layers takes place on the fines surface (Nasralla, et al. 2014). As a result, the fines coagulate at the bottom and their interaction with the final oil becomes limited. The adhesion of fines towards the polar fraction is also reduced because of the formation of a thick electric double layer (Ligthelm et al. 2009). This could be the possible reason that no additional oil emulsion formation is observed beyond the optimum brine concentrations. Similar claims have previously been made in water flooding experiments (Nasralla, et al. 2014). A representation is shown in figure 8b and c.

Interestingly for systems with heptanoic acid, (Figure 6) the substantial increase in emulsion formation for SO_4^{2-}, Ca^{2+}, and Mg^{2+} ions show significant correlation with the observed EOR in smart water flooding experiments. (Austad et al. 2011; Zahid et al. 2012a; Zahid et al. 2012b).

Comparing the experiments conducted with O1 and O2 it is observed that the acid type can have a significant effect on the amount of emulsion formation. Experiments with O1 showed significant increase in emulsion formation with potential ions (SO_4^{2-}, Ca^{2+}, and Mg^{2+}); while no considerable trend was observed in the experiments conducted with O2. These results indicate that significances of brine in oil emulsion formation do not just depend on the total acid number of the oil; it also depends on the detailed composition of individual polar compounds. Therefore two acids with similar total acid number may behave significantly to the same brine variations. It is interesting to note that the efficiency of smart water flooding also is significantly dependent on the oil composition (Zahid et al. 2010), and oils with similar acid numbers have shown significantly different recovery fractions for the same brine concentrations (Austad et al. 2011). Thus significant coherence can be observed between the amount of oil recovery and emulsion formation. Additional studies need to be conducted to further scrutinize and establish these correlations.

Gupta et al. 2011 showed that phosphate ions can also be used for increasing oil recovery significantly. Up to 20% increase in oil recovery has been observed by injection of phosphate ions in the absence of sulphate ions. Here we also observe a significant increase in emulsion formation for sodium phosphate salts as well. This increase in emulsion formation with phosphate ions can also positively increase the displaceability of oil thus leading to the observed EOR. Therefore it is suggested that phosphate ions can also be used in increasing the displacement efficiency of residue oil by increasing the adhesion between the flooded water and trapped oil.

Conclusion

The study shows that water soluble oil emulsion formation takes place when insoluble fines interact with crude oil containing polar components. This can release the trapped oil and increase the mobility of the oil significantly. The brine concentration has a significant effect on the amount of oil emulsion formed.

- An increase in emulsion formation is observed with an initial increase in brine concentration. A buildup of a viscoelastic interface could be the possible reason.
- Beyond an optimum brine concentration, no further emulsion formation is observed. Hindrance in fines-polar oil adhesion because of formation of an electric double layer (by the salt ions) on the fines surface could be the possible reason for no further emulsion formation.
- Among anions $SO_4^{2-}$and HPO_4^{2-} can significantly enhance the oil emulsion formation.
- $Ca^{2+}$and Mg^{2+} are the most useful cations in increasing the amount of oil emulsion formation. The efficiency of cations in emulsion formation was shown to follow the Hofmeister series: $K^+<Na^+<Mg^{2+}<Ca^{2+}$
- The emulsion formation has shown to be significantly dependent on the oil composition. Stearic acid readily formed emulsions irrespective of the available ions in the brine solution, while heptanoic acid showed significant dependence on the brine composition.
- An interesting correlation was observed between the amount of emulsion formation and observed oil recovery previously reported in literature.

These results collectively suggest that HPO_4^{2-} can also be widely used in SW-EOR processes along with SO_4^{2-}, Ca^{2+}, and Mg^{2+} potential ions.

Acknowledgement
This paper is a part of a research study in smart water at the Center for Energy Resources Engineering (CERE). The authors acknowledge Maersk Oil, Dong Energy, and The Danish Energy Agency (EUDP) for funding the Smart Water project. We also thank Christian Schack Pedersen of Dong Energy for providing the BSTFA samples.

Reference

- Adahchour, M., Beens, J., & Brinkman, U. A. (2008). Recent developments in the application of comprehensive two-dimensional gas chromatography. *Journal of Chromatography A*, **1186**(1), 67-108.
- Alagic, Edin, et al. "Effect of crude oil ageing on low salinity and low salinity surfactant flooding." *Journal of Petroleum science and Engineering* **78**.2 (2011): 220-227.
- Alvarado, V., et al. (2014, April). Interfacial Visco-Elasticity of Crude Oil-Brine: An Alternative EOR Mechanism in Smart Waterflooding. In *SPE Improved Oil Recovery Symposium*. Society of Petroleum Engineers.
- Austad, T., Strand, S., Høgnesen, E. J., & Zhang, P. (2005, January). Seawater as IOR fluid in fractured chalk. In *SPE International Symposium on Oilfield Chemistry*. Society of Petroleum Engineers.
- ASTM D2887-06, Standard Test Method for Boiling Range Distribution of Petroleum Fractions by Gas Chromatography, http://www.astm.org/DATABASE.CART/HISTORICAL/D2887-06.htm.
- Blomberg, J., Schoenmakers, P. J., & Brinkman, U. A. (2002). Gas chromatographic methods for oil analysis. *Journal of Chromatography A*,**972**(2), 137-173.
- Chukwudeme, E. A., & Hamouda, A. A. (2009). Oil recovery from polar components (asphaltene and SA) treated chalk rocks by low salinity water and water containing SO_4^{2-} and Mg^{2+} at different temperatures. *Colloids and Surfaces A: Physicochemical and Engineering Aspects*, **336** (1), 174-182.
- Chakravarty et al. (2015) Interactions of Fines with Oil and its Implication in Smart Water Flooding In *SPE Bergen One Day Seminar*, Society of Petroleum Engineers
- Chorn, L. G. (1984). Simulated Distillation of Petroleum Crude Oil by Gas Chromatography. Characterizing the Heptanes-Plus Fraction. *Journal of Chromatographic Science*, **22**(1), 17-21.
- Delshad et al. (2013, April). Mechanisms Behind Low Salinity Water Flooding in Carbonate Reservoirs. In *SPE Western Regional & AAPG Pacific Section Meeting 2013 Joint Technical Conference*. Society of Petroleum Engineers.
- Dutriez, T., Courtiade, M., Thiébaut, D., Dulot, H., & Hennion, M. C. (2010). Improved hydrocarbons analysis of heavy petroleum fractions by high temperature comprehensive two-dimensional gas chromatography. *Fuel*, **89**(9), 2338-2345.
- Fathi, S. J., Austad, T., & Strand, S. (2010). "Smart Water" as a Wettability Modifier in Chalk: The Effect of Salinity and Ionic Composition. *Energy & fuels*,**24** (4), 2514-2519.
- Fathi, S. J., Austad, T., & Strand, S. (2011). Effect of water-extractable carboxylic acids in crude oil on wettability in carbonates. *Energy & Fuels*,**25** (6), 2587-2592.
- Fogden, A. (2011). Effect of Water Salinity and pH on the Wettability of a Model Substrate. *Energy & Fuels*, **25** (11), 5113-5125.
- Fogden, A., Kumar, M., Morrow, N. R., & Buckley, J. S. (2011). Mobilization of fine particles during flooding of sandstones and possible relations to enhanced oil recovery. *Energy & Fuels*, **25** (4), 1605-1616.
- Gupta et al. (2011, January). Enhanced Waterflood for Carbonate Reservoirs-Impact of Injection Water Composition. In *SPE Middle East Oil and Gas Show and Conference*. *Reservoir Evaluation & Engineering*, **11** (06), 1-000. Society of Petroleum Engineers.

- Jerauld, G. R., Webb, K. J., Lin, C. Y., & Seccombe, J. C. (2008). Modeling low-salinity waterflooding.
- Jabbar, M. Y., Al-Hashim, H. S., & Abdallah, W. (2013, May). Effect of brine composition on wettability alteration of carbonate rocks in the presence of polar compounds. In *SPE Saudi Arabia Section Technical Symposium and Exhibition*. Society of Petroleum Engineers.
- Kafili Kasmaei, A., & Rao, D. N. (2014, April). Is Wettability Alteration the Main Cause for Enhanced Recovery in Low-Salinity Waterflooding?. In *SPE Improved Oil Recovery Symposium*. Society of Petroleum Engineers.
- Ligthelm et al. (2009). Novel Waterflooding Strategy by Manipulation of Injection Brine Composition (SPE-119835). In *71st EAGE Conference & Exhibition*.
- Lebedeva, E. V., & Fogden, A. (2011). Micro-CT and wettability analysis of oil recovery from sand packs and the effect of waterflood salinity and kaolinite.*Energy & Fuels*, **25** (12), 5683-5694.
- McGuire et al. (2005). Low salinity oil recovery: an exciting new EOR opportunity for Alaska's North Slope. In *SPE Western Regional Meeting*. Society of Petroleum Engineers.
- Moradi, M., Alvarado, V., & Huzurbazar, S. (2010). Effect of salinity on water-in-crude oil emulsion: evaluation through drop-size distribution proxy. *Energy & fuels*, **25** (1), 260-268.
- Moradi, M., Topchiy, E., Lehmann, T. E., & Alvarado, V. (2013). Impact of ionic strength on partitioning of naphthenic acids in water–crude oil systems–Determination through high-field NMR spectroscopy. *Fuel*, **112**, 236-248.
- Moradi, M., Kazempour, M., French, J. T., & Alvarado, V. (2014). Dynamic flow response of crude oil-in-water emulsion during flow through porous media. *Fuel*,**135**, 38-45.
- Morrow, N. R., Tang, G. Q., Valat, M., & Xie, X. (1998). Prospects of improved oil recovery related to wettability and brine composition. *Journal of Petroleum Science and Engineering*, **20** (3), 267-276.
- Nasralla, R. A., & Nasr-El-Din, H. A. (2014). Double-Layer Expansion: Is It A Primary Mechanism of Improved Oil Recovery by Low-Salinity Waterflooding?. SPE Reservoir Evaluation & Engineering, (Preprint).
- Nasralla et al. (2011). Efficiency of oil Recovery by low salinity water flooding in sandstone reservoirs. In *SPE Western North American Region Meeting*. Society of Petroleum Engineers.
- Parracello et al. (2013) Opportunity of enhanced oil recovery low salinity water injection: From experimental work to simulation study up to field proposal. In *Proceedings of the 75th EAGE Conference & Exhibition incorporating SPE EUROPEC, Society of Petroleum Engineers, London, United Kingdom*.
- Pu et al. (2010). Low-salinity waterflooding and mineral dissolution. In *SPE Annual Technical Conference and Exhibition*. Society of Petroleum Engineers.
- Rimmen, M., Matthiesen, J., Bovet, N., Hassenkam, T., Pedersen, C. S., & Stipp, S. L. (2014). Interactions of Na+, K+, Mg2+, and Ca2+ with Benzene Self-Assembled Monolayers. *Langmuir*, **30** (30), 9115-9122.
- Rivet et al. (2010). A coreflood investigation of low-salinity enhanced oil recovery. In *SPE Annual Technical Conference and Exhibition*. Society of Petroleum Engineers.
- Robertson, E. P. (2007, January). Low-salinity waterflooding to improve oil recovery-historical field evidence. In *SPE Annual Technical Conference and Exhibition*. Society of Petroleum Engineers.
- Saleh, A., Yamini, Y., Faraji, M., Rezaee, M., & Ghambarian, M. (2009). Ultrasound-assisted emulsification microextraction method based on applying low density organic solvents followed by gas chromatography analysis for the determination of polycyclic aromatic hydrocarbons in water samples. *Journal of Chromatography A*, **1216**(39), 6673-6679.
- Stalling, D. L., Gehrke, C. W., & Zumwalt, R. W. (1968). A new silylation reagent for amino acids bis (trimethylsilyl) trifluoroacetamide (BSTFA).*Biochemical and biophysical research communications*, **31** (4), 616-622.
- Suijkerbuijk et al. (2014). Low Salinity Waterflooding at West-Salym: Laboratory Experiments and Field Forecasts. In *SPE Improved Oil Recovery Symposium*. Society of Petroleum Engineers.
- Tang, G. Q., & Morrow, N. R. (1997). *Salinity, Temperature, Oil Composition, and Oil Recovery by Waterflooding. SPE Res Eng* **12** (4)*: 269–276*. SPE-36680-PA.
- Tang, G. Q., & Morrow, N. R. (1999). Influence of brine composition and fines migration on crude oil/brine/rock interactions and oil recovery. *Journal of Petroleum Science and Engineering*, **24** (2), 99-111.
- Vijapurapu, C. S., & Rao, D. N. (2003, January). Effect of brine dilution and surfactant concentration on spreading and wettability. In *International Symposium on Oilfield Chemistry*. Society of Petroleum Engineers.
- Yi, Z., & Sarma, H. K. (2012, January). Improving Waterflood Recovery Efficiency in Carbonate Reservoirs through Salinity Variations and Ionic Exchanges: A Promising Low-Cost" Smart-Waterflood" Approach. In *Abu Dhabi International Petroleum Conference and Exhibition*. Society of Petroleum Engineers.
- Yildiz, H. O., Valat, M., & Morrow, N. R. (1999). Effect of brine composition on wettability and oil recovery of a Prudhoe Bay crude oil. *Journal of Canadian Petroleum Technology*, **38** (01).
- Wang, X., & Alvarado, V. (2012). Effects of Aqueous-Phase Salinity on Water-in-Crude Oil Emulsion Stability. *Journal of Dispersion Science and Technology*,**33** (2), 165-170.
- Webb et al. (2004, January). Low salinity oil recovery-log-inject-log. In *SPE/DOE Symposium on Improved Oil Recovery*. Society of Petroleum Engineers.
- Zahid et al. (2010). Improved Oil Recovery in Chalk: Wettability Alteration or Something Else?. In *SPE EUROPEC/EAGE Annual Conference and Exhibition*. Society of Petroleum Engineers.

- Zahid, A., Sandersen, S. B., Stenby, E. H., von Solms, N., & Shapiro, A. (2011). Advanced waterflooding in chalk reservoirs: Understanding of underlying mechanisms. *Colloids and Surfaces A: Physicochemical and Engineering Aspects*, **389**(1), 281-290.
- Zahid et al. (2012, January). Experimental Studies of Low Salinity Water Flooding Carbonate: A New Promising Approach. In *SPE EOR Conference at Oil and Gas West Asia*. Society of Petroleum Engineers.
- Zahid et al. (2012, January). Smart Waterflooding (High Sal/Low Sal) in Carbonate Reservoirs. In *SPE Europec/EAGE Annual Conference*. Society of Petroleum Engineers.
- Zekri et al. (2012). Effect of EOR technology on Wettability and Oil Recovery of Carbonate and Sandstone Formation. In *IPTC: Technology and Operational Excellence: Keys to Sustainable Global Energy*.
- Zhang, P., Tweheyo, M. T., & Austad, T. (2007). Wettability alteration and improved oil recovery by spontaneous imbibition of seawater into chalk: Impact of the potential determining ions Ca^{2+}, Mg^{2+}, and SO_4^{2-}. *Colloids and Surfaces A: Physicochemical and Engineering Aspects*, **301**(1), 199-208.
- Zhang, P., & Austad, T. (2006). Wettability and oil recovery from carbonates: Effects of temperature and potential determining ions. *Colloids and Surfaces A: Physicochemical and Engineering Aspects*, **279**(1), 179-187.

Tables

Table 1: Brines with constant anion type and constant cation type used to study emulsion formation with different doped oils TC1, TC2, TC3 and designed oils O1 & O2

Brines:				
Cation Constant (B1)	NaCl	Na_2SO_4	$NaHCO_3$	Na_2HPO_4
Anion Constant (B2)	KCl	NaCl	$MgCl_2$	$CaCl_2$
Doped Oil:				
TC1	Crude oil	Acetic acid		
TC2	Crude oil	Propanoic acid		
TC3	Crude oil	Valeric acid		
Designed Oil:				
Oil O1:	Hexane	Hexadecane	Stearic Acid	
Oil O2:	Hexane	Hexadecane	Heptanoic Acid	

Figures

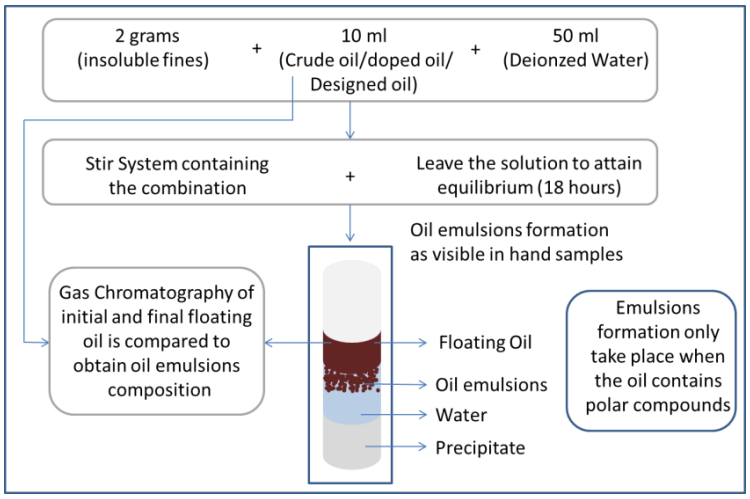


Figure 1 Schematic diagram of the experimental setup for emulsion formation.

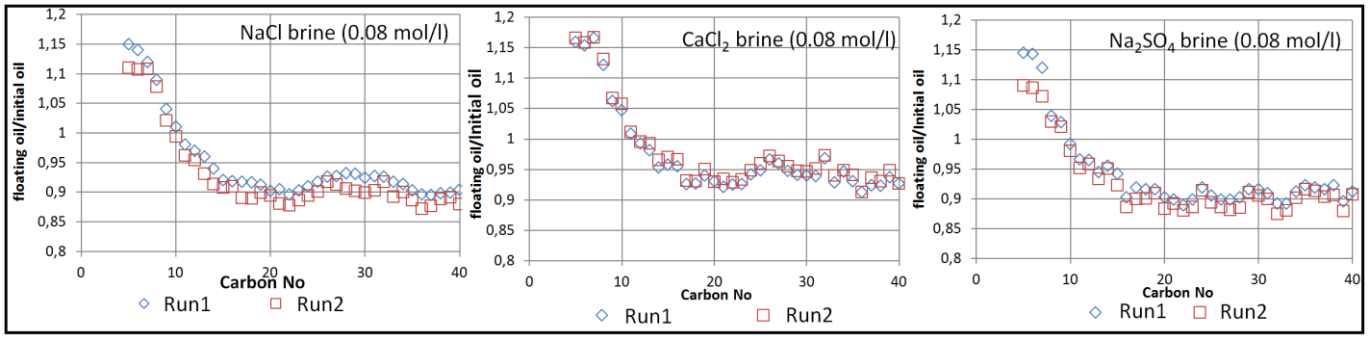


Figure 2: Ratio between the initial oil and final oil content for components corresponding to each carbon number. The concentrations were obtained through gas chromatographic analysis. Crude oil doped with acetic acid (TC1).

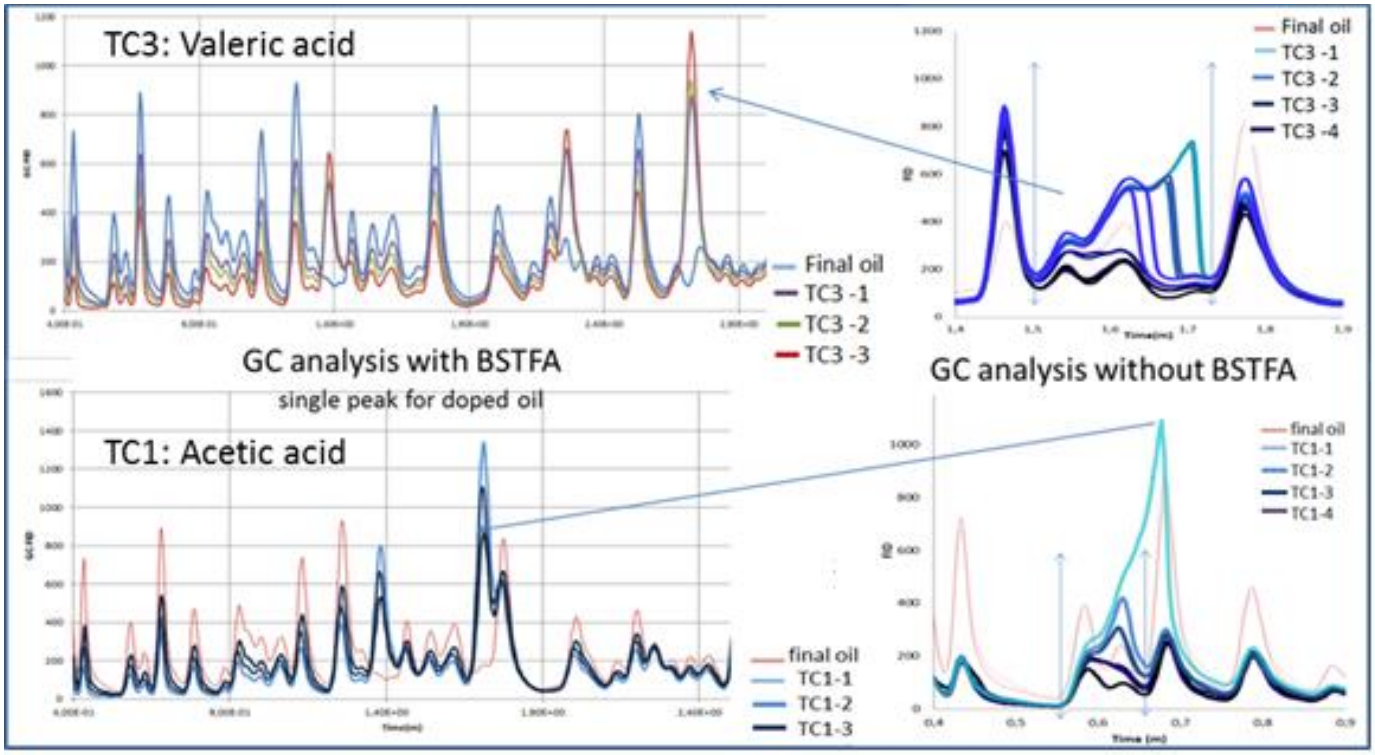


Figure 3: Gas Chromatographic analysis of the final oil (floating oil) and initial oil doped with different fractions of acetic acid and valeric acid. Adding BSTFA removes the multiple humps and produces a single distinguished peak, associated to specific acid (indicated by blue arrow). Disappearance of the acid from the final oil is confirmed by the GC analysis after adding BSTFA in the oil samples.

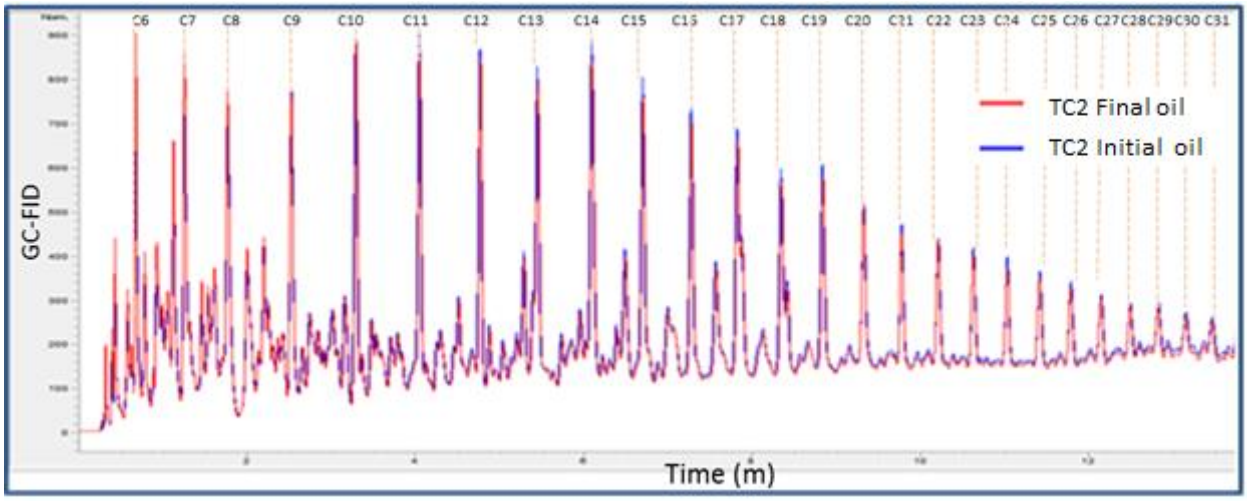


Figure 4: Gas chromatographic analysis of initial and final oil for crude oil TC2 (doped with Propanoic acid) and NaCl (0.08 mol/l) brine solution.

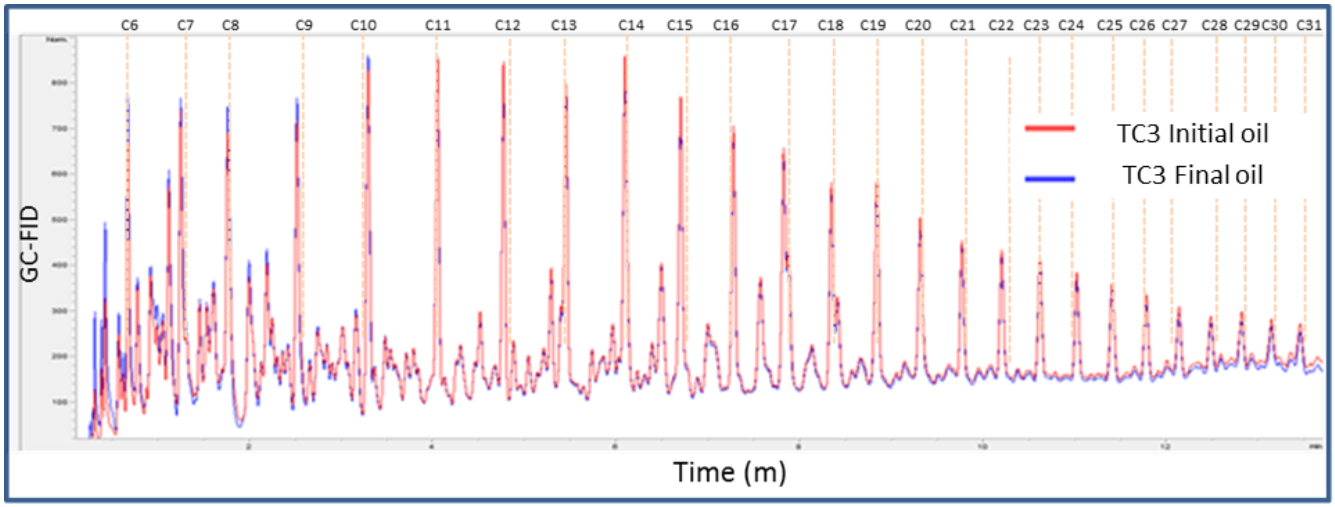


Figure 5 Gas chromatographic analysis of initial and final oil for TC3 (oil doped with Valeric acid) and $CaCl_2$ (0.01 mol/l) brine solution.

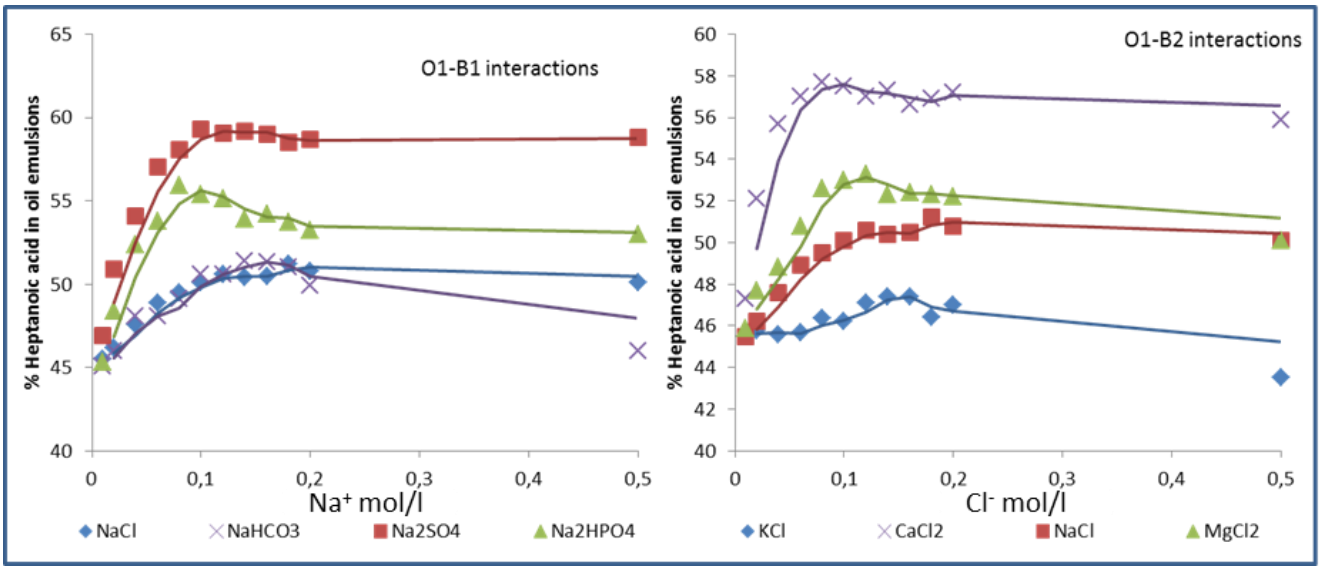


Figure 6: Percentage of heptanoic acid contributing to the oil emulsion formation for different brine concentrations. Left: Cation type constant: NaCl, Na_2SO_4 $NaHCO_3$ & Na_2HPO_4, (Na^+ (aq) represents the brine concentration). Right: Anion type constant: NaCl, KCl, $MgCl_2$, and $CaCl_2$ (Cl^-(aq) represents the brine concentration).

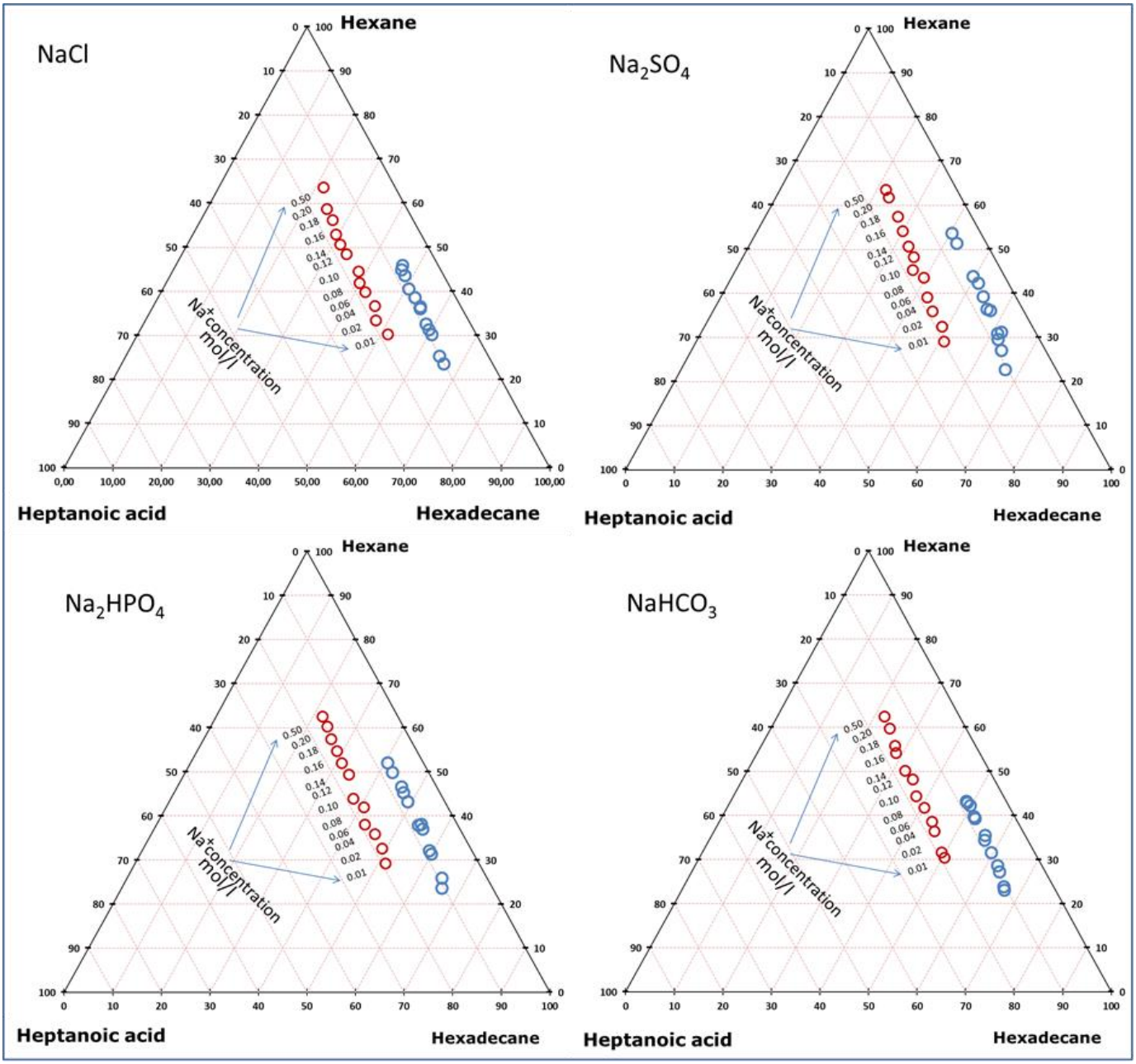


Figure 7: Representation of mass% of initial and final oil composition in triangular diagram (for hexane, hexadecane and heptanoic acid) for interaction of oil O1 with different brines with various concentrations expressed as mol/l of the common cation, Na^+.

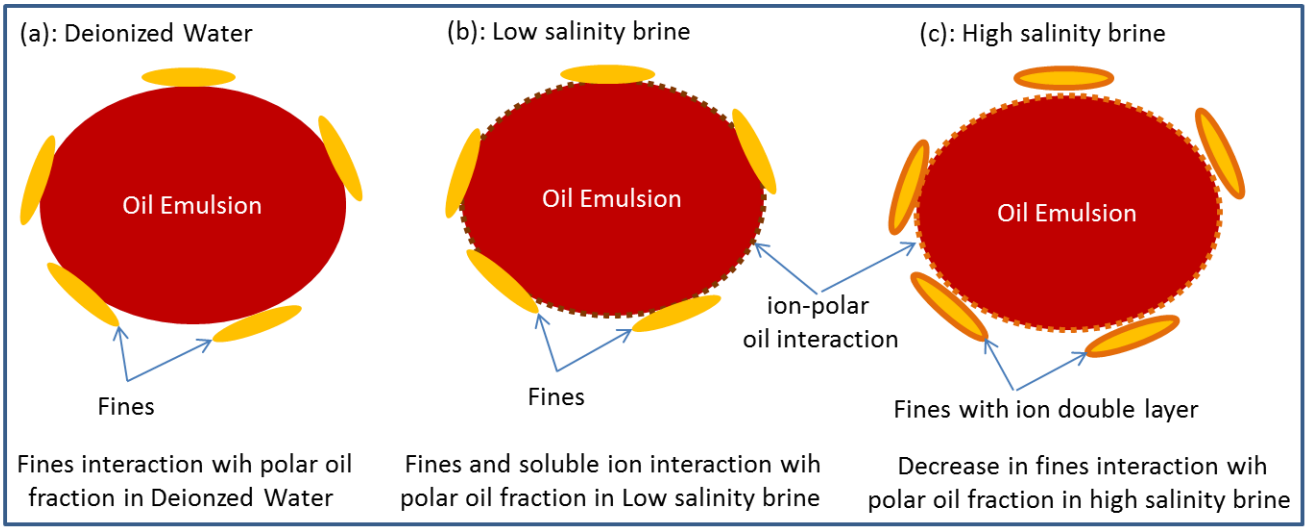


Figure 8: Schematic representation of interaction between soluble ions, insoluble fines and oil-polar fraction during emulsion formation: (a) shows perceived arrangement of emulsion due to interaction between fines and oil droplets, (b) & (c) shows formation of viscoelastic layer at the oil-water interface due to the interaction between soluble ions and oil-polar fraction. (c) Show decrease in fines adhesion towards oil emulsion because of electric double layer formation on fines (as previously suggested by Nasralla, et al. 2014).

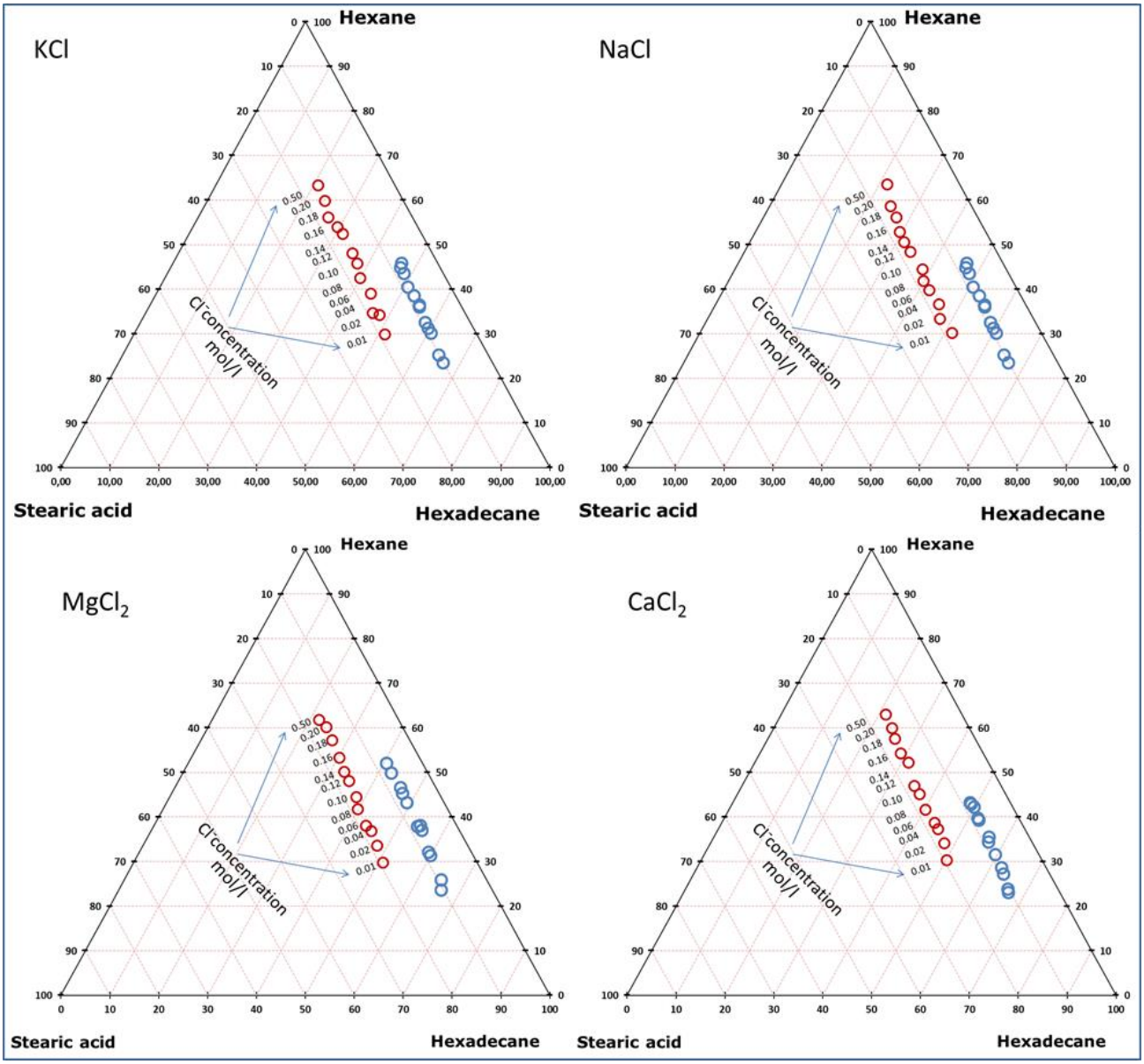


Figure 9:Representation of mass% of initial and final oil composition in triangular diagram (for hexane, hexadecane and heptanoic acid) for interaction of oil O1 with different brines with various concentrations expressed as mol/l of the common anion.

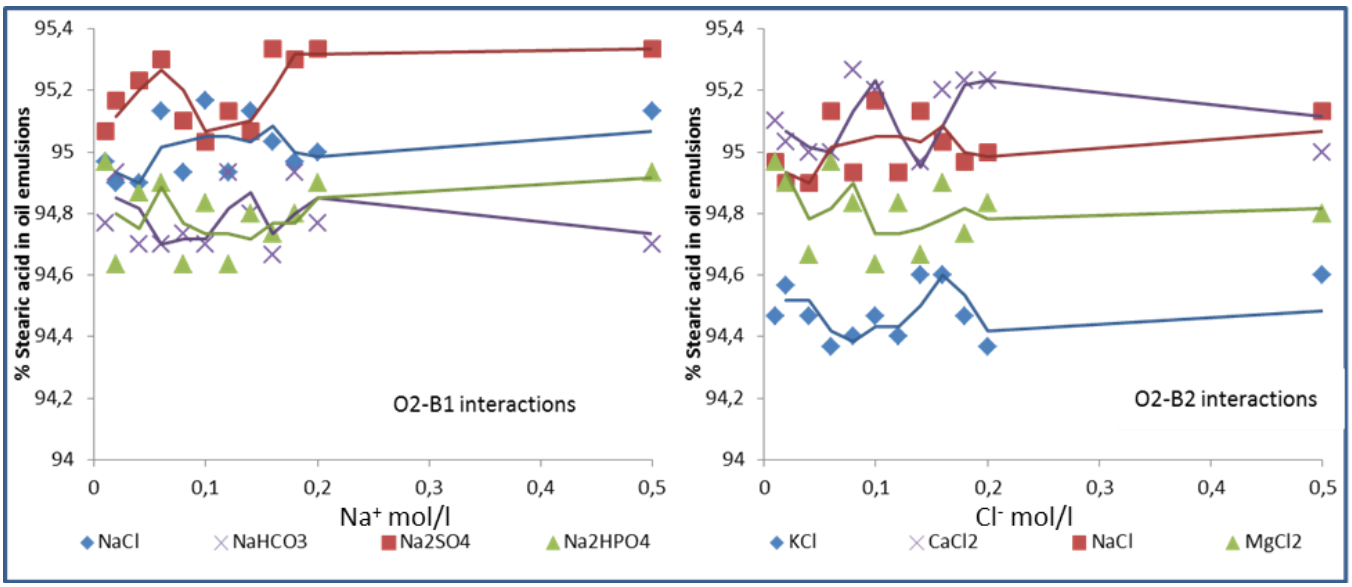
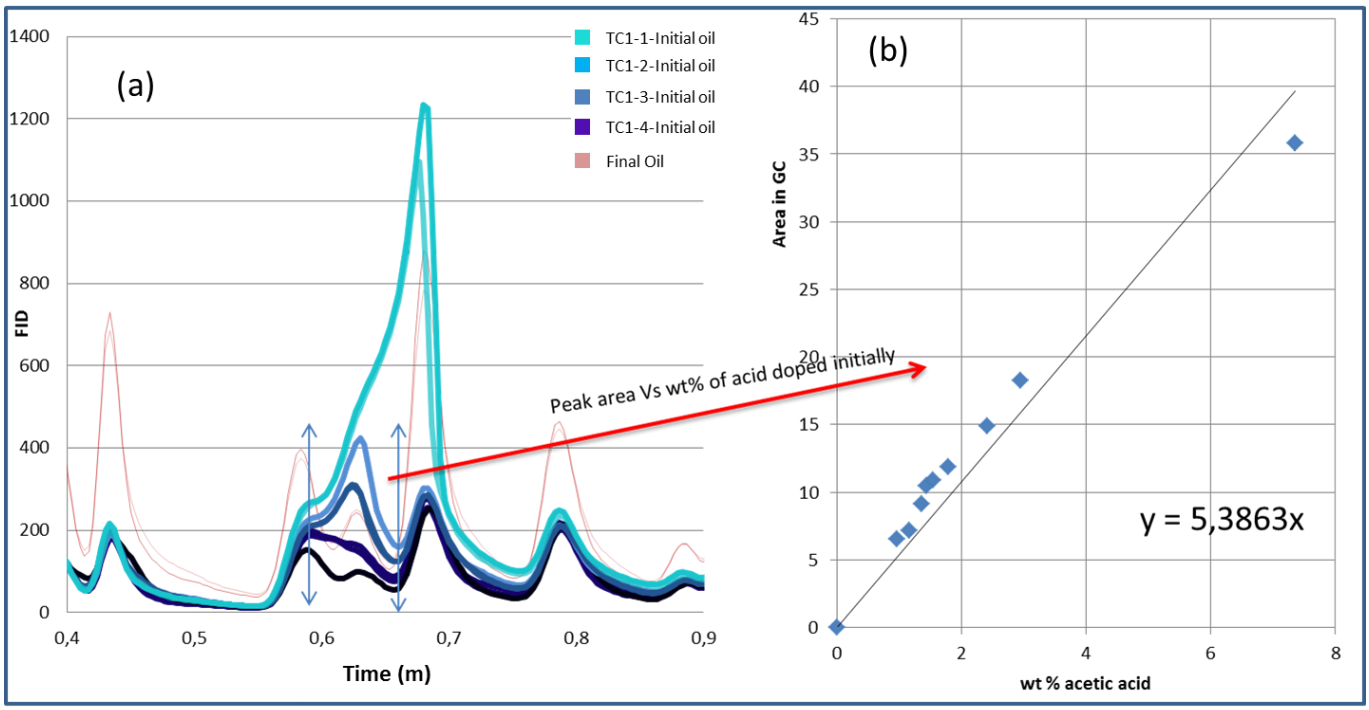
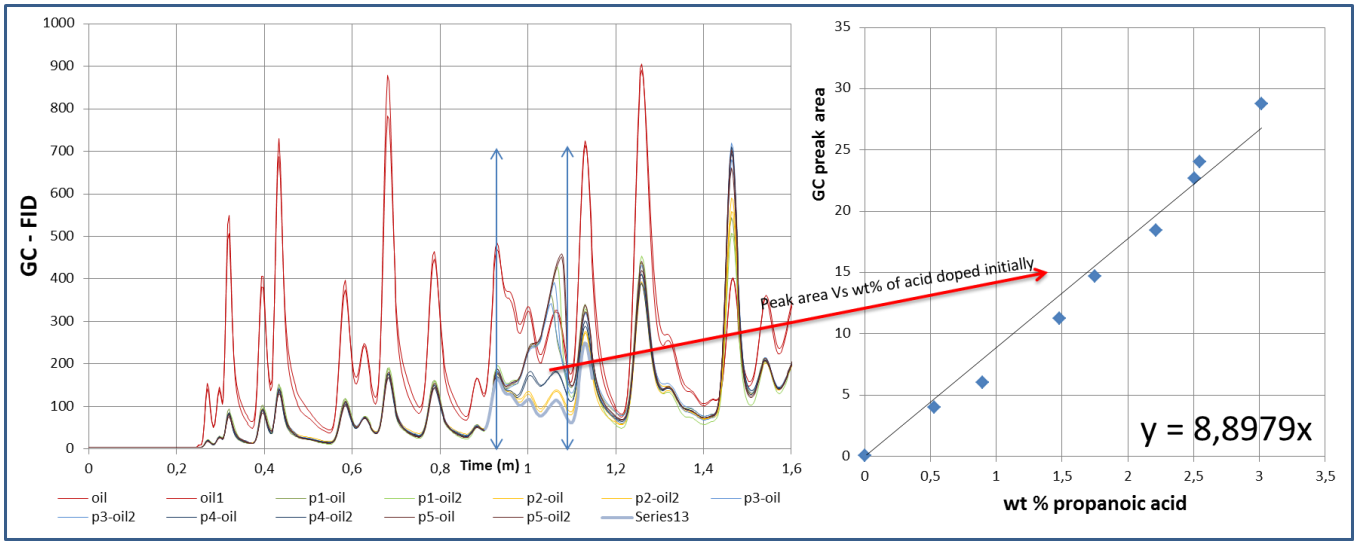


Figure 10: Percentage of stearic acid contribution to oil emulsion formation for different brine concentration: Cation type constant: NaCl, Na_2SO_4 $NaHCO_3$, and Na_2HPO_4, The brine composition is expressed as the concentration of the common ion, $Na^+(aq)$ and Anion type constant NaCl, KCl, $MgCl_2$, and $CaCl_2$ The brine composition is expressed as the concentration of the common ion, $Cl^-(aq)$.



Supplementary Figure1: (a) GC analysis of initial and final oil for crude oil doped with acetic acid in different concentration. GC-FID signal varies with changes in concentration but no clear peak is observed. The total area under chromatogram (between time 0.59 m and 0.66 m) was calculated and plotted against the wt % of acetic acid (indicated by red arrow) (b) shows consistent linear correlation between the area under chromatogram and wt% of acid doped in crude oil.



Supplementary Figure 2: (a) GC analysis of initial and final oil for crude oil doped with propanoic acid in different concentration. GC-FID signal varies with changes in concentration but no clear peak is observed. The total area under chromatogram (between time 0.92 m and 1.09 m) was calculated and plotted against the wt % of propanoic acid (indicated by red arrow) (b) shows consistent linear correlation between the area under chromatogram and wt% of acid doped in crude oil.

Paper V

Chakravarty, K. H., Fosbøl, P. L., & Thomsen, K. (2015, June). Importance of Fines in Smart Water Enhanced Oil Recovery (SmW-EOR) for Chalk Outcrops. In *EUROPEC 2015*. Society of Petroleum Engineers.

SPE-174334-MS

Importance of Fine in Smart Water Enhanced Oil Recovery (SmW-EOR) for Chalk Outcrop

Krishna Hara Chakravarty, Philip Loldrup Fosbøl and Kaj Thomsen, Center for Energy Resources Engineering (CERE), Department of Chemical and Biochemical Engineering, Technical University of Denmark

Copyright 2015, Society of Petroleum Engineers

This paper was prepared for presentation at the EUROPEC 2015 held in Madrid, Spain, 1–4 June 2015.

This paper was selected for presentation by an SPE program committee following review of information contained in an abstract submitted by the author. Contents of the paper have not been reviewed by the Society of Petroleum Engineers and are subject to correction by the author. The material does not necessarily reflect any position of the Society of Petroleum Engineers, its officers, or members. Electronic reproduction, distribution, or storage of any part of this paper without the written consent of the Society of Petroleum Engineers is prohibited. Permission to reproduce in print is restricted to an abstract of not more than 300 words; illustrations may not be copied. The abstract must contain conspicuous acknowledgment of SPE copyright.

Abstract

In SmW-EOR it is generally believed that precipitation of brines must be avoided since it can have a negative impact on the SmW sweep efficiency. Substitution of Mg^{2+} by Ca^{2+} on calcite surfaces (a well-accepted phenomenon) can change the brine concentration and enhance the possibility of solid formation also known as fines formation. Considering this phenomenon we analyze the possibility of fines formation and its influence in SmW-EOR.

To calculate the brine speciation and the amount of precipitate formed at different pressure and temperature conditions, we use the Extended UNIQUAC model for 61 SmW-EOR experiments reported in literature. Both the amount of available soluble SO_4^{2-} in the solution and the amount of $CaSO_4$ precipitation has been calculated and correlated with the corresponding oil recovery. Brine speciation after considering the substitution of Ca^{2+} by Mg^{2+} on chalk surfaces showed possible precipitation of $CaSO_4$ in most of the brine solutions. The amount of $CaSO_4$ precipitate formed increased with temperature and consequently the amount of dissolved SO_4^{2-} decreased. Increasing Ca^{2+}, Mg^{2+}, or SO_4^{2-} ion concentrations relative to their concentrations in Sea Water (SW) also enhanced the amount of precipitate formed. By increasing the NaCl concentration, the solubility of SO_4^{2-} and Ca^{2+} in SmW increased and the amount of precipitate formed decreased. The amount of precipitate formed in the pore space (after the substitution of Mg^{2+} on the calcite surface) was consistently correlated with the increased oil recovery observed in various experiments. In several cases, additional oil recovery did not correlate with the amount of soluble SO_4^{2-} present in the SmW at equilibrium. These results together suggest that substitution reaction on the mineral surface followed by solid fines formation is the fundamental reason behind the observed EOR. Furthermore it indicates that the previously thought main EOR mechanism of wettability alteration in chalks may not be the primary cause but an additional effect of SmW-EOR.

This study shows how the Extended UNIQUAC model can be used as a rigorous mathematical tool for understanding the SmW-EOR in chalk. It also quantitatively explains a series of previous experiments reported in the literature and shows the importance of fines formation in SmW-EOR, through correlation between modeling and experiments.

Introduction

Around half of the world's proven hydrocarbon reserves are in carbonate rock (Akbar et al. 2001). Carbonate reservoirs are mostly associated with a low permeability matrix, high fracture density and wettability ranging from mixed-wet to oil-wet rocks. The recovery of oil from underground reservoirs is a challenge. Consequently, numerous enhanced oil recovery (EOR) methods have been developed to increase the oil recovery. Through extensive research in the past decade smart water (SmW) flooding has been established as a possible EOR method for carbonate reservoirs. It is also known in the literature as LoSal (Zekri et al. 2011), Low salinity water injection, and Advanced Ion Management (Gupta et al. 2011).

Numerous laboratory experimental studies of water injection were carried out by Austad and co-workers at University of Stavanger. Diverse core plugs were used and they studied oil recovery as a function of temperature and brine composition (Strand et. al. 2006; Zhang et. al. 2007; Austad et. al. 2005). It was reported that SO_4^{2-}, Ca^{2+}, and Mg^{2+} are the potential determining ions for improving the oil recovery in chalk reservoirs. The desired temperatures must be above 70°C (Strand et. al. 2006; Zhang et. al. 2007; Zhang et. al. 2006a; Zhang et. al. 2006b; Austad et. al. 2005; Zhang et. al. 2006; Puntervold et. al. 2009). It has been reported that SO_4^{2-} ions must act together, with Ca^{2+} or Mg^{2+}, as introducing SO_4^{2-} with Na^{+} ions had an observable effect on the oil

recovery (Zhang et. al. 2006a). On the basis of the experimental results, wettability alteration was proposed to be a key reason for the improving oil recovery. The proposed EOR mechanism consists of two processes: (1) Substitution of calcium by magnesium on the calcite surface (2) followed by adsorption of sulfate ions on the mineral surface associated with the release of adsorbed carboxyl compound (thus making the surface more water wet). In the effluent water, a decrease in sulfate concentration shows that sulfate acts as a reagent in this process (Zhang et. al. 2007; Bagci et al. 2001).
In most of the reported studies, the importance of soluble Ca^{2+}, Mg^{2+} and SO_4^{2-} ions in brine solutions has been emphasized for obtaining enhanced oil recovery. The studies further suggest that available NaCl in the brine solution leads to formation of an electric double layer on the calcite surface (Fathi et al. 2010) which reduces accessibility of the potential ions to the mineral surfaces. Therefore selectively reducing NaCl concentration has shown to increase the oil recovery (Fathi et al. 2010). Furthermore in the same study instead of selectively reducing the NaCl concentration, experiments have been conducted by diluting the sea water significantly. Thus the concentration of the potential ions (i.e. Ca^{2+}, Mg^{2+} and SO_4^{2-}) also decreases and eventually leads to a lower oil recovery. Other spontaneous imbibition and water flooding experiments have shown to comply with this trend (Zhang et al. 2006b). The same study has suggested that a possible precipitation of $CaSO_4$ must be avoided as it can block the flow of the waterflood (Zhang et al. 2006b). It has been systematically shown that increasing the Ca^{2+} concentration in the injected brine can lead to a higher oil recovery (Zhang et al. 2006b). Reported experiments also show that available soluble SO_4^{2-} ions in the injected brine solutions have the most prominent effect in increasing oil recovery (Fathi et al. 2011). Amongst these publications, Stevns Klint outcrop chalk from Denmark was used in the majority of the reported experiments (Strand et. al. 2006; Fathi et al. 2010; Fathi et al. 2011; Zhang et al. 2006b). Spontaneous imbibition studies with limestone reservoir rocks also have shown significantly higher oil recovery for brines containing high sulfate concentrations (Strand et al. 2008).

Questions have been raised (Zahid et al. 2010); regarding the proposed wettability alteration model (Austad et. al. 2005). Completely water wet core plugs have also shown an increase in oil recovery with an increase in the SO_4^{2-} concentration of the injected brine (Zahid et al. 2010). Emulsification of oil and dissolution of rock were possible explanations for the observed EOR in completely water wet systems, but no concrete evidence of emulsion formation was provided. In another study, formation of oil emulsion was observed for brine solutions containing high concentration of sulfate ions. The phenomenon was even stronger at higher temperatures (Zahid et. al. 2011). But a correlation between the emulsion formation (Zahid et. al. 2011) and the observed oil recovery (Zahid et al. 2010) was not established. For carbonate reservoirs it has also been shown that an increase in SO_4^{2-} concentration is associated with oil recovery only up to an optimum concentration, beyond which no additional oil recovery is observed (Awolayo et al. 2014). No successful EOR for very high SO_4^{2-} concentration in the injected brine is in conflict with the proposed potential ion based wettability alteration model (Austad et. al. 2005). Successful EOR with completely water wet coreplugs and no EOR for very high SO_4^{2-} concentration represent points of fundamental disagreement with the wettability alteration mechanism. Collectively the cited results (Zahid et al. 2010; Zahid et. al. 2011; Awolayo et al. 2014) prove that the potential ions based wettability alteration mechanism is not applicable to all conditions.

In all of the above cited results; experiments with higher sulfate concentration in the injected brine has led to a higher oil recovery. In all of the cited experiments, it has been attempted to correlate the composition of the injected brines with the observed oil recovery. But in the proposed mechanism it is suggested that Mg^{2+} replaces Ca^{2+} from the mineral surfaces. Thus the Mg^{2+} concentration is decreased in the brine solution and the Ca^{2+} concentration is increased equivalently in the pore space. Thereby, the possibility of precipitation is significantly enhanced, particularly at higher temperatures. Ion substitution followed by electrolyte speciation thus leads to the formation of a new brine composition in the pore space. This new brine interacts with the crude oil in the pore space and alters its displacement efficiency. Therefore it is important to calculate the actual concentration of the brine in the pore space. The properties of this brine composition should be correlated with the reported oil recovery. This report contains the calculation of the brine composition in the pore space, using the Extended UNIQUAC model (Thomsen and Rasmussen 1999).

The Extended UNIQUAC model is a thermodynamic model for aqueous solutions of electrolytes and non-electrolytes (Thomsen and Rasmussen 1999). The optimized parameters of this model are based on a large amount of experimental data (Christensen and Thomsen 2003; Thomsen et al. 1996; García et al. 2006; García et al. 2005). The experimental basis of this model enables it to describe the phase behavior and the thermal properties of solutions containing electrolytes with great accuracy (García et al. 2005). Experimental data including solid-liquid equilibrium data as well as experimentally measured activity and osmotic coefficients from the open literature have been used to optimize the parameters. Thermal properties such as heat of dilution, heat of solution, and apparent molal heat capacity for salt solutions have also been used for the determination of model parameters. These properties can therefore also be reproduced by the model. In Figure 1, the calculated solid-liquid equilibrium curves for the ternary $CaSO_4 – Na_2SO_4 – H_2O$ system (at room temperature) and the binary $CaSO_4 – H_2O$ system (at elevated pressure and temperature conditions) are plotted along with experimental data from the open literature in order to demonstrate the accuracy of the model (García et al. 2005). In this work, the model was used to calculate phase equilibria related to the changes in brine concentration with change in temperature, pressure and interactions at mineral surfaces. Spontaneous imbibition and water flooding experiments from 5 different literature sources were examined in detail. The exact brine concentrations as reported in literature were used and all the calculations were conducted at the specified temperature and pressure conditions. Thereafter the composition and properties of the brine present in the pore space was obtained. Significant precipitation of $CaSO_4$ (or fines formation) was observed in the pore space form the different injected brines. Both the amount of soluble SO_4^{2-} present in the brine solution in the pore space and the corresponding amount of fines formation was correlated with the observed oil recovery. Studies with variation in brine composition, temperature, origin of core plug, origin of oil and wetness of the core plug were considered.

Calculation Method

The main model parameters of the Extended UNIQUAC model are the volume and surface area parameters (r- and q-parameters), which are determined on the basis of massive amounts of binary and ternary experimental data (Thomsen and Rasmussen 1999). Parameters for all ions used in smart water experiments have already been extensively optimized (Iliuta et al. 2000; Thomsen et al. 1996; García et al. 2005). The group of ions and neutral species includes H_2O, CO_2, Na^+, K^+, Mg^{2+}, Ca^{2+}, Ba^{2+}, H^+, Sr^{2+}, Cl^-, SO_4^{2-}, OH^-, CO_3^{2-} and HCO_3^-. The optimized r- and q-parameters are listed in table 1. The two individual parameters are specific to each species. In addition, each species pair has two additional parameters that describe the interaction between the species, which is assumed to have a linear temperature dependency. These species pair interaction parameters have also been previously optimized (Iliuta et al. 2000; Thomsen et al. 1996; García et al. 2005) and are listed in Table 2. The model predicts the behavior of multi component systems based on these unary and binary parameters. As the model parameters are based on binary and ternary data alone, the calculation of phase behavior in multi-component systems represents prediction by the model. In several calculations it has been shown that the Extended UNIQUAC model is capable of accurately representing multi-component systems with common ions covering a range of temperatures and ionic strengths that is large enough to represent all the conditions stated in laboratory and reservoir water flooding experiments.

The Extended UNIQUAC model was used for calculating the brine properties and the amount of precipitate formation for 61 different core flooding experiments. 61 core flooding experiments were taken from five different reports available in the literature. In these reports, the effect of each ion in SW-EOR has been extensively investigated. The detailed references are provided in Table 3.

As shown in Table 3, data set 1 includes 4 sub sections (1.1, 1.2, 1.3 and 1.4). This data set includes core plug no. 1 to 13 (Fathi et al. 2011). The effect of SO_4^{2-} and Ca^{2+} in oil recovery was reported for a variation in temperature and oil acid number. Spontaneous imbibition experiments were mostly conducted for brine solutions wherein NaCl was absent (Fathi et al. 2010). Based on the reported brine composition, we calculated the amount of precipitate and soluble SO_4^{2-} present in the pore space after ion substitution (Ca^{2+} by Mg^{2+}) on the mineral surface (as suggested by Austad et al. 2005). Detailed specifications of the reported experiments are summarized in Table 4. The amounts of $CaSO_4$ precipitate and SO_4^{2-} in solution calculated with the Extended UNIQUAC model are shown in Figure 2 and 3 along with the reported oil recovery. Data set 2 (Table 3) includes 3 sub sections (2.1, 2.2 and 2.3) (Fathi et al. 2011). This data set includes core plugs no. 14 to 25. The effect of dilution of sea water and variation in NaCl concentration in oil recovery was reported for different temperatures. The required experimental details are provided in Table 5. The corresponding amounts of fines formation and soluble SO_4^{2-} ion present in the solution was calculated at the stated pressure and temperature conditions. The calculated values are presented in Figure 4 and 5. The third data set consists of spontaneous imbibition experiments with limestone reservoirs. It embraces core plugs no 26 and 27 (Strand et al. 2008). The details of the experiments are summarized in table 6, while the calculated equilibrium composition is presented in Figure 6. Data set 4 includes 3 sub sections (4.1, 4.2 and 4.3). Core plugs number 26 to 41 are obtained from this report (Zhang et al. 2006b). In the presence of NaCl, a prominent and consistent increase in oil recovery was observed when increasing the Ca^{2+} concentration in the brine solutions (Zhang et al. 2006b). The corresponding amounts of fines formation and soluble SO_4^{2-} ion present in the solution was calculated at the specified pressure, temperature conditions. The experimental details are listed in Table 7, and the calculated values are presented in Figures 7 and 8. The last data set (5) consists of three sub-sections (5.1, 5.2 and 5.3) (Zahid et al. 2010). This data set includes core plugs no. 42 to 61. Water flooding experiments for completely water wet chalk have been documented in this study. Oils originating from various sources were used and the effect of SO_4^{2-} on oil recovery was studied (Zahid et al. 2010). The details of the experiments are summarized in table 8, 9 and 10, while the calculated speciation composition is presented in Figure 9, 10 and 11.

Results and Discussion

Data set 1 :(Fathi et al. 2011)

The first set of experiments includes an extensive spontaneous imbibition study of oil saturated chalk cores. (Fathi et al. 2011) In this study a total of 14 core samples from Stevns Klint chalk were examined with different brine solutions. In this report 4 different sets of experiments were documented. The experimental details are summarized in Table 3.

In the data subset 1.1 spontaneous imbibition into 4 oil-saturated chalk cores was conducted (core plug no 1-4) at 90°C using VB (formation water), SW (sea Water), and modified seawater: SW0NaCl and SW0NaCl-4SO_4^{2-} (Fathi et al. 2011). The total acid number of the used oil was 0.5 mg of KOH/g. The obtained oil recovery trend was: SW0NaCl-4SO_4^{2-} > SW0NaCl > SW > VB. The corresponding amounts of soluble SO_4^{2-} ion in the different brine solutions at 90°C were calculated using Extended UNIQUAC model. The possibility of fines formation because of precipitation of $CaSO_4$ was also calculated. As previously proposed (Austad et al. 2005) the change in brine composition because of substitution of Ca^{2+} by Mg^{2+} on calcite surface was included. The calculated amount of soluble SO_4^{2-} ion present in the different brine solutions showed the following trend: SW0NaCl-4SO_4^{2-} > SW > SW0NaCl > VB. The calculated amount of fines formation because of $CaSO_4$ precipitation revealed the trend: SW0NaCl-4SO_4^{2-} > SW0NaCl > SW > VB. The calculated values are shown in Figure 2. It is important to note that the amount of soluble SO_4^{2-} ion present in the brine solution only partially correlates with the observed oil recovery while the amount of fines formation taking place completely correlates with the observed oil recovery. The oil recovery observed for SW and SW0NaCl are two cases where the concentration of soluble SO_4^{2-} ion do not correlate to the observed oil recovery. Comparing SW with

SW0NaCl, it is observed that the decrease in NaCl concentration in the brine decreases the solubility of $CaSO_4$. Thus the amount of soluble SO_4^{2-} ion in the solution decreases and the amount of fines formation increases. This increase in fines formation completely correlates with the reported oil recovery.

In the data subset 1.2, spontaneous imbibition into 3 oil-saturated chalk cores (No. 5-7) was studied at 70°C using different imbibing fluids with different salinities and ionic compositions: SW, SW0NaCl and SW0NaCl-$4SO_4^{2-}$ (Fathi et al. 2011). The total acid number of the used oil was 0.5 mg of KOH/g. The obtained oil recovery trend was: SW0NaCl-$4SO_4^{2-}$ > SW0NaCl > SW. The corresponding amount of soluble SO_4^{2-} ion and insoluble $CaSO_4$ formation in the different brine solution was calculated at 70°C using the Extended UNIQUAC model. The calculated amount of soluble SO_4^{2-} ion present in the different brine solutions showed the following trend: SW0NaCl-$4SO_4^{2-}$ > SW > SW0NaCl; while $CaSO_4$ precipitation revealed the trend: SW0NaCl-$4SO_4^{2-}$ > SW0NaCl > SW. The calculated values are shown in Figure 2. It should be noted here that the amount of soluble SO_4^{2-} ion present in the brine solution does not correlate with the observed oil recovery; while the amount of fines formation taking place completely correlates with the observed oil recovery. For the experiments at 70°C, the comparison between SW and SW0NaCl shows the same trend. The solubility of $CaSO_4$ increases with increasing NaCl concentration (salting in). The amount of soluble SO_4^{2-} ion in the solution therefore decreases with decreasing NaCl concentration and the amount of fines formation increases. It further suggest that the amount of fines formation correlates better with the oil recovery trend than does the amount of soluble SO_4^{2-} for variations in imbibing fluid composition.

When comparing the two data subsets 1.1 and 1.2, it is seen that the amount of fines formation increases with an increase in temperature and the amount of soluble SO_4^{2-} decreases. As shown in Figure 2c and 2d. This is due to the solubility of $CaSO_4$ decreasing with increasing temperature as seen in Figure 1. This trend is observed for all the considered brines (including SW0NaCl-$4SO_4^{2-}$, SW0NaCl, and SW). Moreover for each of the three brines the amount of oil recovery observed at 90°C is higher than that at 70°C. As per reported results (Fathi at al. 2011) shown in Figure 2a and 2b. Thus, with variation in temperature the amount of fines formation entirely correlates with the corresponding oil recovery while the concentration of soluble SO_4^{2-} ion in the brine solution doesn't.

Thereafter in subset 1.3 and 1.4, the total acid number of the used oil was changed from 0.5 mg (used in data set 1.1 and 1.2) to 2.0 mg of KOH/g. In subset 1.3, spontaneous imbibition into 3 oil-saturated chalk cores (no. 8-10) at 120°C using different imbibing fluids with different salinities and ionic compositions: SW, SW0NaCl and SW0NaCl-$4SO_4^{2-}$ was conducted (Fathi et al. 2011). As stated in the report (Fathi et al. 2011) no major difference in oil recovery was observed between SW0NaCl-$4Ca^{2+}$ and SW0NaCl imbibing fluids but significantly high oil recovery was observed for SW0NaCl-$4SO_4^{2-}$. Thus the reported oil recovery trend was: SW0NaCl-$4SO_4^{2-}$ > SW0NaCl-$4Ca^{2+}$ ≈ SW0NaCl. The corresponding amounts of soluble SO_4^{2-} ion and insoluble $CaSO_4$ in the different brine solutions were calculated at 120°C using Extended UNIQUAC model. The calculated amounts of soluble SO_4^{2-} ion present in the different brine solutions and the corresponding amounts of $CaSO_4$ precipitation showed the same trend: SW0NaCl-$4SO_4^{2-}$ > SW0NaCl -4Ca ≈ SW0NaCl. The calculated values are shown in Figure 3. The observed oil recovery trend completely correlates with both the amount of fines formation and the concentration of soluble SO_4^{2-} in the different brine solutions. Removing NaCl from the solution decreases the solubility of $CaSO_4$ in the brine solution. Thus a significant fraction of the available SO_4^{2-} precipitates. Adding more Ca^{2+} to the solution (SW0NaCl-$4Ca^{2+}$) does not lead to any significant increase in fines formation as the available amount of SO_4^{2-} is constrained by the solubility limit for $CaSO_4$. Thus both, the amount of fines formed and the amount of soluble SO_4^{2-} present in the solution remains unaltered. Increasing SO_4^{2-} concentration in the brine leads to a significant increase in fines formation since substitution of Mg^{2+} by Ca^{2+} leads to increased availability of Ca^{2+} ion in the solution. It is suggested by Zhang et al. 2006b that Ca^{2+} plays a significant role in enhanced oil recovery. But comparing SW0NaCl and SW0NaCl-$4Ca^{2+}$ shows that in the absence of NaCl, even a major increase in Ca^{2+} concentration does not lead to a significant increase in oil recovery.

In the fourth subset, 1.4, spontaneous imbibition into 3 oil-saturated chalk cores (no. 11-13) at 100°C using different imbibing fluids with different salinities and ionic compositions: SW, SW0NaCl and SW0NaCl-$4SO_4^{2-}$ was reported (Fathi et al. 2011). The oil recovery trend reported in literature (Fathi et al. 2011) was: SW0NaCl-$4SO_4^{2-}$ > SW0NaCl -4Ca ≈ SW0NaCl. The calculated amounts of soluble SO_4^{2-} ion present in the different brine solutions and the corresponding amounts $CaSO_4$ precipitation show the same trend: SW0NaCl-$4SO_4^{2-}$ > SW0NaCl-$4Ca^{2+}$ ≈ SW0NaCl. The calculated values are shown in Figure 3. The observed oil recovery trend completely correlates with both the amounts of fines formation and the amounts of soluble SO_4^{2-} present in the different brine solutions. As previously observed at 120°C(in subset 1.3), the comparison between SW0NaCl and SW0NaCl-$4Ca^{2+}$ suggest that in the absence of NaCl, even a major increase in Ca^{2+} concentration does not lead to a significant increase in oil recovery.

Further comparing data subsets 1.3 and 1.4 it is indicated that with increase in temperature the amount of fines formation increases and the amount of soluble SO_4^{2-} decreases for all considered brines (including SW0NaCl-$4SO_4^{2-}$, SW0NaCl-$4Ca^{2+}$, SW0NaCl). The calculated values are shown in figure 3c and 3d. For each of the three brines the amount of oil recovery observed at 120°C is greater than that at 100°C. As per reported results (Fathi at al. 2011) shown in Figure 3a and 3b. With increase in temperature (from 100°C to 120°C) for each of the three brine solutions, the amount of oil recovery increased with the amount of fines formation, while the available soluble SO_4^{2-} ion in the brine solution decreased. Thus, in this case also it is evident that with variation

in temperature the amount of fines formation completely correlates with the corresponding oil recovery while the amount of soluble SO_4^{2-} ion in the brine solution doesn't.

Thus oil recovery correlates to fine formation for varied oil types with different acid number, and varied temperature conditions.

Data set 2: (Fathi et al. 2010)

The second set of experiments includes an extensive spontaneous imbibition study of oil saturated chalk cores (Fathi et al. 2010). In this study, a total of 12 core samples of Stevns Klint chalk were examined with different brine solutions. The effect in oil recovery because of change in NaCl concentration and brine salinity has been reported in the study. Three different sets of experiments were conducted as listed in Table 5.

In the first set, 2.1, spontaneous imbibition into 3 oil-saturated chalk cores (14-16) at 100°C using SW, SW0NaCl and SW4NaCl was conducted (Fathi et al. 2010). The reported oil recovery trend was: SW0NaCl > SW > SW4NaCl (Fathi et al. 2010). The corresponding amounts of fines formation and concentrations of soluble SO_4^{2-} ion in the different brine solutions at 100°C was calculated using the Extended UNIQUAC model. The calculated amount of soluble SO_4^{2-} ion present in the different brine solutions showed the following trend: SW4NaCl > SW > SW0NaCl. While $CaSO_4$ precipitation exhibited the trend: SW0NaCl > SW > SW4NaCl identical to the oil recovery trend. The calculated values are shown in Figure 4. The amount of soluble SO_4^{2-} present in the brine solution clearly does not correlate with the observed oil recovery trend; On the other hand, the amount of fines formation taking place completely correlates with the observed oil recovery. Increasing NaCl concentration in the brine solution significantly enhances the solubility of $CaSO_4$ in the brine solution and decreases the amount of fines formation. Thus with an increment in the NaCl concentration of the brine solution, the amount of available soluble SO_4^{2-} ion in the solution also increases. This set of results indicates that only the amount of fines formation match the oil recovery trend reported for variations in NaCl concentration.

In the second set, 2.2, spontaneous imbibition into 5 oil-saturated chalk cores (no. 17-21) at 120°C using different imbibing fluids with different salinities and ionic compositions (SW0NaCl, SW, SW4NaCl, dSW1600 (diluted sea water)) was reported (Fathi et al. 2010). Two core plugs were flooded with the diluted sea water (dSW1600). The described oil recovery trend was: SW0NaCl > SW> SW4NaCl > dSW1600 (Fathi et al. 2010). The calculated amounts of soluble SO_4^{2-} ion present in the different brine solutions showed the following trend: SW4NaCl > SW > SW0NaCl > dSW1600; while $CaSO_4$ precipitation revealed the trend: SW0NaCl > SW> SW4NaCl > dSW1600 (identical to the oil recovery trend). The calculated values are shown in Figure 4. The amount of soluble SO_4^{2-} ion present in the brine solution only partially correlate with the observed oil recovery; but the amount of fines formation taking place completely correlates with the observed oil recovery. Mismatch between oil recovery and soluble SO_4^{2-} trends for variation in NaCl concentration, is directly related to corresponding changes in $CaSO_4$ solubility, (as explained for data set 2.1). Decreasing the NaCl content in the brine solution (SW0NaCl) decreases the solubility of $CaSO_4$ in the brine solution, thus leading to increased fines formation. But diluting the sea water (dSW1600) does not have the same effect as decreasing the NaCl content. By diluting the sea water, the available concentration of Ca^{2+} and SO_4^{2-} ions in the solutions are also reduced, thus significantly reducing the possible amount of fines formation. With dSW1600 only $CaCO_3$ precipitation can take place as the $CaSO_4$ concentration remains within the solubility limits even after substitution of Ca^{2+} by Mg^{2+} on the mineral surface. By diluting the sea water, the amount of available Mg^{2+} in the solution was also diminished, so on substitution no major variation was observed in the brine composition. Thus a significant amount of oil recovery and fines formation is observed for SW0NaCl and a quite low oil recovery and fines formation is observed for dSW1600. It also suggest that fines formation better correlates with the oil recovery trend than does the amount of soluble SO_4^{2-} for different brine combinations.

In the third set, 2.3, spontaneous imbibition into 4 oil-saturated chalk cores (no. 22-25) at 110°C using different imbibing fluids with different salinities and ionic compositions (SW0NaCl,SW,dSW20000 and dSW10000) was reported (Fathi et al. 2010). The described oil recovery trend was: SW0NaCl > SW > dSW20000 > dSW10000 (Fathi et al. 2010). The calculated amount of soluble SO_4^{2-} ion present in the different brine solution showed the following trend: SW > dSW10000 > dSW20000 > SW0NaCl; while $CaSO_4$ precipitation revealed the trend: SW0NaCl > SW > dSW20000 > dSW10000. The calculated values are shown in Figure 5. Herein it is clearly observable that the amount of soluble SO_4^{2-} ion present in the brine solution does not correlate with the observed oil recovery, while the amount of fines formation completely correlates with the observed oil recovery. Diluted sea water solutions (dSW10000 and dSW20000) have higher concentrations of soluble SO_4^{2-} ion as compared to SW0NaCl at 110°C. But the observed oil recovery for diluted solutions is significantly less than for the SW0NaCl solution. On the other hand, the amount of fines formation for diluted solutions is significantly lower than that of SW0NaCl, which perfectly correlates with the observed oil recovery. In general it further indicates that the amount of fines formation is closely correlated with the corresponding oil recovery.

Further comparing the 3 subsets (data set: 2.1, 2.2 and 2.3); it is observed that imbibition experiments with SW0NaCl and SW brine was repeated at 100°C, 110°C and 120°C. The oil recoveries at different temperatures are shown in Figure 4a, 4b & 5a. For both of the bines (SW0NaCl and SW) the reported results clearly indicate that with increase in temperature the oil recovery increases. With the two brines the amount of oil recovery observed at 120°C is significantly higher than that at 110°C, which is higher than that at 100°C. It is shown in Figure 5b & 5c, that with increase in temperature the amount of fines formation increases

and the amount of amount of soluble SO_4^{2-} decreases for both of the considered brines (including SW0NaCl and SW). In this set of experiments also it is evident that with variation in temperature the amount of fines formation entirely correlates with the corresponding oil recovery while the soluble SO_4^{2-} ion in the brine solution doesn't.

Thus oil recovery perfectly correlates to fine formation for variation in salinity, NaCl concentration and temperature.

Data set 3:(Strand et al. 2008)

The third set of reported experiments includes spontaneous imbibition into core plugs from a limestone reservoir (Strand et al. 2008). The used limestone is of low porosity (25-30 %) compared to Stevns klint chalk (45-48 %). The effect of sulfate ion on oil recovery was reported in the study. Detailed specification is available in Table 6. Since this study showed that substitution of Ca^{2+} by Mg^{2+} takes place at the mineral surface for limestone reservoir rocks as well (more evidently at higher temperature) (Strand et al. 2008). So, in the speciation calculation the same was considered. The experiment was conducted at 120°C. In the first core (no. 26) SW followed by SW3S (with thrice SO_4^{2-}) was used as imbibing fluid. In the second core (no. 27) SW0S (without SO_4^{2-}) followed by SW3S was used as imbibing fluid. Later 1wt% of C12TAB was added to SW3S in both the core plugs (Strand et al. 2008). The reported results showed that high sulphate concentration in the imbibing fluid led to higher oil recovery. Comparing core number 26 and 27 it is observable that changing the brine composition from SW0S to SW3S (core no. 27) shows higher increment in oil recovery than changing the brine composition from SWS to SW3S(core no. 26). Thus the summarized oil recovery trend is: SW3S > SW > SW0S & SW0S→SW3S > SWS→SW3S. The results are shown in Figure 6a. This final oil recovery because of the three individual brines completely correlate to both, the amount of fines formation taking place and the amount of soluble SO_4^{2-} present in the brine solution, as both show the same trend : SW3S > SW > SW. The calculated values are shown in Figure 6b and 6d. But (as shown in Figure 6e), the amount of soluble SO_4^{2-} present in the brine mixture during alteration of brine composition does not correlate to the corresponding increment in oil recovery. As brine mixture of SWS and SW3S had higher soluble SO_4^{2-} concentration (but showed less increment in oil recovery) than brine mixture of SW0S and SW3S. On the other hand the amount of fines formation taking place during changing of brine composition perfectly correlate to the increment in oil recovery. As observable in Figure 6c the amount of fines formed during interaction between the SW0S and SW3S was significantly higher than that with SWS and SW3S. The calculations indicates that the amount of soluble SO_4^{2-} ion present in the brine solution did only partially correlate with the observed oil recovery; while the amount of fines formation completely correlated with the observed oil recovery. At 120°C, the brine SW3S-Mg (before Ca^{2+} by Mg^{2+}) leads to precipitation of $CaSO_4$ even before any mineral substitution takes place; thus shutting the pores. Adding 1wt% of C12TAB (sulfate adsorbent) may have adsorbed this additional sulfate. Using brines that naturally precipitate at reservoir condition may have an adverse effect on the oil recovery by shutting the pore throats. Having mobile fines formation in the pore space after mineral substitution is advocated for successful EOR (this avoids shutting the initial pore throats). Thus the amount of fines formation taking place within the pore needs to be considered. Overall in this set of experiments, the amount of fines formation in the pore space did correlate with the observed oil recovery for reservoir limestone rocks as well.

Data set 1 & 2 were obtained from Stevns Klint (Denmark) outcrop chalk samples with 45% porosity. Data set 3 were obtained from Middle East reservoir limestone samples with porosity of 25%. Comparing dataset 1, 2 and 3 it is observed that oil recovery completely correlates to fine formation for variation in porosity, origin and type of coreplug.

Data set 4: (Zhang et al. 2006b)

The fourth set of experiment includes an extensive spontaneous imbibition study of oil saturated chalk cores. (Zhang et al. 2006b). In this study a total of 14 core samples of Stevns Klint chalk were examined with different brine solutions. The typical effect of change in Ca concentration in the presence of NaCl was reported in the study. Effect of variation in composition of formation water in oil recovery was also studied. Three different sets of experiments were reported. Specifications of the experiments are listed in Table 7.

In the first set, 4.1, spontaneous imbibition into 5 oil-saturated chalk cores (no 28-32) was reported at 70°C using sea water modified with different Ca^{2+} concentration (Zhang et al. 2006b). It includes SW-0Ca, SW-½Ca, SW, SW-3Ca and SW-4Ca. The stated oil recovery trend was: SW-0Ca < SW-½Ca < SW < SW-3Ca < SW-4Ca. The corresponding amounts of fines formation and soluble SO_4^{2-} ion present in the different brine solutions at 70°C were calculated using the Extended UNIQUAC model. The calculated amounts of soluble SO_4^{2-} ion present in the different brine solution showed the following trend: SW-0Ca > SW-½Ca > SW > SW-3Ca > SW-4Ca. $CaSO_4$ precipitation exhibited the subsequent trend: SW-0Ca < SW-½Ca < SW < SW-3Ca < SW-4Ca. The calculated values are shown in Figure 7. Here it is clearly observable that the reported oil recovery is consistently correlated with the amount of fines formation. While the calculated soluble SO_4^{2-} present in the different brine solution shows exactly the opposite trend. With an increase in Ca^{2+} concentration, the amount of $CaSO_4$ precipitation increases, thus the amount of soluble SO_4^{2-} decreases. Thus only fine formation provides a match to the observed oil recovery.

In the second set, 4.2, spontaneous imbibition into 3 oil-saturated chalk cores (no 33-35) at 70°C (later elevated to 100 °C) using SW-0Ca, SW and SW-4Ca was described (Zhang et al. 2006b). The stated oil recovery trend was: SW-4Ca > SW >SW-0Ca both at 70°C and at 100°C. The corresponding amount of fines formation and soluble SO_4^{2-} ion present in the different brine solutions at 70°C was calculated. The amount of soluble SO_4^{2-} ion present in the different brine solutions showed the following trend: SW-0Ca > SW > SW-4Ca both at 70°C and at 100°C. While $CaSO_4$ precipitation exhibited the subsequent trend: SW-4Ca > SW > SW-0Ca both at 70°C and at 100°C. The calculated values are shown in Figure 7. Here it is clearly observable that the observed oil recovery is consistently correlated with the amount of fines formation. The calculated amount of soluble SO_4^{2-} present in the different brine solution shows exactly the opposite trend. An increase in temperature from 70°C to 100°C clearly shows a corresponding increase in oil recovery. This perfectly correlates with the increase in fines formation at elevated temperature. A clear mismatch was observed between oil recovery and the amount of soluble SO_4^{2-} present in the brine solutions, as the concentration of the soluble SO_4^{2-}consistently decreases with increase in temperature while the recovery increased for all three used brines.

In the third set, 4.3, spontaneous imbibition into 6 oil-saturated chalk cores (No 36-41) was reported at 70°C using combinations of 3 imbibing brines (SW-2S, SW, SW½S) and two formation brines (EF and EF-mod) (Zhang et al. 2006b). The stated oil recovery trend was: SW-2S (EF) > SW-2S (EF-mod) > SW (EF) > SW (EF-mod) > SW-½S (EF) > SW-½S (EF-mod). The calculated amount of soluble SO_4^{2-} ion present in the different brine solutions showed the following trend: SW-2S (EF-mod) > SW-2S (EF) > SW (EF) ≈ SW (EF-mod) > SW-½S (EF) ≈ SW-½S (EF-mod). While $CaSO_4$ precipitation exhibited the subsequent trend: SW-2S (EF) > SW-2S (EF-mod) > SW (EF) > SW (EF-mod) > SW-½S (EF) > SW-½S (EF-mod). The calculated values are shown in Figure 8. Here it is clearly observed that the oil recovery is consistently correlated with the amount of fines formation. No clear pattern is observed between the available soluble SO_4^{2-} concentration and the oil recovery. It is highlighted that none of the two formation brines (EF and EF-mod) showed any fines formation as no SO_4^{2-} was present in the two brines. On interaction with the imbibing water, fines formation took place. Mixing of the EF formation brine with the imbibing fluids showed higher fines formation than the corresponding mixing with EF-mod brine. The calculated values are shown in figure 8d and 8e. This perfectly correlates to the oil recovery pattern as EF formation water showed higher oil recovery pattern than the corresponding with EF-mod brine.

The previously proposed behavior of NaCl for smart water floods in chalk reservoir is the following (Fathi et al. 2010): The NaCl concentration is directly proportional to the thickness of the electric double layer on the mineral surface. The thickness of the electric double layer is inversely proportional with the accessibility of potential ions (Ca^{2+}, Mg^{2+} and SO_4^{2-}) to the mineral surface. The accessibility of the potential ions to the mineral surface is directly proportional with the oil recovery. Thus NaCl concentration is inversely correlated to oil recovery. Experiments indicating inverse correlation between NaCl concentration and oil recovery support the proposed mechanism (Fathi et al. 2010). Now according to this mechanism for SW0NaCl the thickness of the electric double layer on the calcite surface is significantly reduced. Thus it leads to higher accessibility of potential ions to the mineral surface and a significant impact of the available potential ions in the oil recovery. So the expected oil recovery for SW0NaCl-4Ca^{2+} should be significantly higher than that of SW0NaCl. But as reported in data set 1.3 and 1.4 (shown in figure 3a and 3b), the oil recovery for SW0NaCl-4Ca^{2+} is almost equivalent to the oil recovery for SW0NaCl (Fathi et al. 2011). It must be noted that in the SW0NaCl-4Ca^{2+} brine solution, the SO_4^{2-} ion was not absent. This indicates that Ca^{2+} did not have a significant effect on oil recovery even though it had high accessibility to the calcite surface because of absence of NaCl in the brine solution (as reported by Fathi et al. 2011).

Moreover according to the existing mechanism (Fathi et al. 2010), SW should lead to the formation of a thick electric double layer on the calcite surface. Thus it leads to a very low accessibility of potential ions to the mineral surface, which diminish the accessibility of potential ions to the mineral surface and thereby reduces the impact of potential ions on the oil recovery. So no major difference should be expected between the oil recovery obtained for SW-nCa and SW-(n-1) Ca (∀n = 1, 2, 3 and 4). While figures 6 and 7 clearly show that for SW-nCa, the Ca^{2+} ion has a prominent effect (Zhang et al. 2006b). But going by the accessibility to the mineral surface mechanism the SW0NaCl should show a more significant increase in oil recovery for an increase in the concentration of the potential ions (viz Ca^{2+}). But clearly that is not the case. A prominent and very consistent increase in oil recovery was observed for SW-nCa (Zhang et al. 2006b) and not for SW0NaCl-nCa (Fathi et al. 2010).

But oil recovery for the two data set perfectly correlate to the corresponding fine formation. Herein for sea water with no NaCl (SW0NaCl), an increase in Ca^{2+} concentration neither resulted in additional oil recovery nor additional fines formation (Fathi et al. 2010). As shown in Figure 3a and 3b. Since, SW0NaCl was associated with a significant decrease in $CaSO_4$ solubility, thus most of the available SO_4^{2-} had precipitated. Addition of Ca^{2+} to the solution did not lead to any additional fines formation. But (as shown in figure 7) in this case the presence of NaCl increased the solubility of $CaSO_4$ and precipitation increased only with a gradual increase in Ca^{2+} concentration. Furthermore the amount of fines formation through $CaSO_4$ precipitation is perfectly correlated with the corresponding oil recovery for variation in Ca concentration (for both SW-nCa (as shown in Figure 7) and SW0NaCl-nCa (as shown in Figure 3) brine combinations). It further establishes the consistency between calculated fines formation and observed oil recovery. And it also proves that Ca^{2+} ion cannot be directly correlated to oil recovery, as its effect is dependent on the overall brine composition and reservoir (pressure, temperature) conditions. Furthermore it shows that the inverse correlation between NaCl concentration and oil recovery should be attributed to alteration in $CaSO_4$ solubility with change in NaCl concentration and not to the formation electric double layer formation on the calcite surface.

Data set 5: (Zahid et al. 2010)

The fifth (5.0) set of experiments includes an extensive water flooding study with chalk core plugs (Zahid et al. 2010). In this study a total of 15 core samples from Stevns Klint outcrop chalk were examined with different brine solutions. Oils originating from Latin America, North Sea and Middle East were considered as described in this report. All the core plugs were kept completely water wet. Details of the experimental conditions are provided in Table 8, 9 and 10.

In the first set, 5.1, spontaneous imbibition into 4 water wet chalk cores (No 42-45) was reported. Oil from Latin America was introduced in all the core plugs. Experiments with the four core plugs were conducted at 40°C, 110°C, 110°C and 130°C respectively. SW0S was used as the initial brine for water flooding. Thereafter SW3S was introduced into the different core plugs (Zahid et al. 2010). The stated oil recovery trend was: SW0S→SW3S at 40° C < SW0S → SW3S at 110°C < SW0S → SW3S at 130° C (Zahid et al. 2010). The calculated amount of soluble SO_4^{2-} ion present in the different brine solution showed the following trend: SW0S → SW3S at 40° C > SW0S → SW3S at 110°C > SW0S → SW3S at 130° C. The $CaSO_4$ precipitation exhibited the subsequent trend: SW0S → SW3S at 40° C < SW0S → SW3S at 110°C < SW0S → SW3S at 130° C. The calculated values are shown in Figure 9. It clearly shows that the correlation between fines formation and oil recovery remained consistent for oil originating from Latin America. The amount of soluble SO_4^{2-} in the solution showed no correlation to the observed oil recovery. It is difficult to explain the increased oil recovery by using the wettability alteration mechanism as the system was initially completely water wet yet increasing SO_4^{2-} in the injected brine led to increment in oil recovery.

Polar hydrocarbons can be adsorbed on the mineral surface during aging. The adhesion between mobile fines and these adsorbed polar compounds can help in desorption and release of the immobile trapped oil. Formation of fine can increase the mobility of the oil by formation of water soluble oil emulsion (Chakravarty et al. 2015). This can lead to a more water wet state as observed in several experiments (Fathi et al. 2010a; Fathi et al. 2010b; Fathi et al. 2011). But, increase in displacement efficiency by fines based oil emulsion formation does not necessarily undergo wettability alteration and thus the phenomenon can be observed for completely water wet core plugs (as reported by Zahid et al. 2010). Thus the observed wettability alteration (Fathi et al. 2010a; Fathi et al. 2010b; Fathi et al. 2011) could be an effect and not a cause of SW-EOR.

In the second set 5.2, water flooding into 11 water wet chalk cores (No 46-57) was reported. The experiments were conducted at 110°C and 130°C, with three different brines (SW; SW0S and SW3S). Oil from Latin America, North Sea and Middle East was introduced into different core plugs (Zahid et al. 2010). The stated oil recovery trend was: SW0S < SW < SW3S & Oil Recovery at 110°C < Oil Recovery at 130°C. The reported oil recovery trend was consistent for oil samples from all three sources. The corresponding amounts of fines formation and soluble SO_4^{2-} ion present in the different brine solutions at 70°C was calculated using the Extended UNIQUAC model. The calculated amounts of soluble SO_4^{2-} ion present in the different brine solutions showed the following trend: SW0S < SW < SW3S & Oil Recovery at 110°C > Oil Recovery at 130°C. The amount of $CaSO_4$ precipitation exhibited the subsequent trend: SW0S < SW < SW3S & Oil Recovery at 110°C< Oil Recovery at 130°C. The calculated values are shown in Figure 10. Both the amounts of fines formation and the amounts of soluble SO_4^{2-} correlate well with the described oil recovery at constant temperature. But the increase in oil recovery with an increase in temperature only correlated with the corresponding fines formation. This indicated that irrespective of the source of oil used in water flooding experiments, the amount of fines formation better correlates with the oil recovery.

In the third set, 5.3, water flooding into 4 water wet chalk cores (No 58-61) was reported. The experiments were conducted at 40°C, 90°C and 110°C with two different brines (including SW and SW0S). SW0S was used as the initial brine for water flooding (Zahid et al. 2010). Thereafter SW was introduced into the different core plugs. The documented oil recovery trend was: SW0S → SW at 40° C < SW0S → SW at 90° C ≈ SW0S → SW at 90° C < SW0S → SW at 110° C. The calculated amount of soluble SO_4^{2-} ion present in the different brine solutions showed the following trend: SW0S → SW at 40° C > SW0S → SW at 90° C ≈ SW0S → SW at 90° C > SW0S → SW at 110° C. While $CaSO_4$ precipitation exhibited the subsequent trend: SW0S → SW at 40° C < SW0S → SW at 90°C ≈ SW0S → SW at 90° C < SW0S → SW at 110° C. The calculated values are shown in Figure 11. With an increase in temperature, a complete mismatch between the soluble SO_4^{2-} concentration and the observed oil recovery is seen. The amount of fines formation completely correlates with the observed oil recovery. These results were also obtained at completely water wet conditions. Thus it further suggests that the formation of fines based oil emulsions may have led to the increase in displacement efficiency of the residual oil. The significant correlation between the observed amounts of fines and the oil recovery supports the oil emulsion formation because of the adhesion between the formed mobile fines and the crude oil. Thus wettability alteration may not be a necessary condition for smart water EOR.

Conclusion:

In most previous core flooding studies, properties of the injected brines have been correlated with the observed oil recovery. But ion substitution on the mineral surface can change the composition and properties of the injected brine significantly. This study suggests that properties of the brine present in the pore space – after substitution - should be correlated with the reported oil recovery.

- Substitution of Ca^{2+} by Mg^{2+} can change the brine properties significantly and fines formation through possible precipitation of $CaSO_4$ is significantly enhanced.

- The amount of fines formation consistently correlates with the observed oil recovery for the studied 61 core flooding experiments.
- The amount of soluble SO_4^{2-} ions present in brine solutions is only partially correlated with the observed oil recovery.
- The study also indicates that the observed wettability alteration towards a more water wet state could be an effect and not the primary cause of SW-EOR.
- The Extended UNIQUAC model can be used as a very useful tool to exactly calculate the amount of fines formation for different brine combination for a diverse range of pressure and temperature conditions.

Acknowledgment
This article is a part of research study in smart water project and center for energy resource engineering. The authors acknowledge Maersk Oil, Dong Energy, and The Danish Energy Agency (EUDP) for funding the Smart Water project.

References

- Akbar, M., Vissapragada, B., Alghamdi, A. H., Allen, D., Herron, M., Carnegie, A., & Saxena, K. (2000). A snapshot of carbonate reservoir evaluation.*Oilfield Review*, **12** (4), 20-21.
- Austad, T., Strand, S., Høgnesen, E. J., & Zhang, P. (2005, January). Seawater as IOR fluid in fractured chalk. In *SPE International Symposium on Oilfield Chemistry*. Society of Petroleum Engineers.
- Awolayo, A., Sarma, H., & AlSumaiti, A. M. (2014, March). A Laboratory Study of Ionic Effect of Smart Water for Enhancing Oil Recovery in Carbonate Reservoirs. In SPE EOR Conference at Oil and Gas West Asia. Society of Petroleum Engineers.
- Bagci, S., Kok, M. V., & Turksoy, U. (2001). Effect of brine composition on oil recovery by waterflooding. *Petroleum science and technology*, **19**(3-4), 359-372.
- Chakravarty, K. H., Fosbøl, P. L., & Thomsen, K, (2015) Interactions of Fines with Oil and its Implication in Smart Water Flooding In *SPE Bergen One Day Seminar*, Society of Petroleum Engineers
- Christensen, S. G., & Thomsen, K. (2003). Modeling of vapor-liquid-solid equilibria in acidic aqueous solutions. *Industrial & engineering chemistry research*, **42** (18), 4260-4268.
- Thomsen, K., Rasmussen, P., & Gani, R. (1996). Correlation and prediction of thermal properties and phase behaviour for a class of aqueous electrolyte systems. *Chemical Engineering Science*, **51** (14), 3675-3683.
- Fathi, S. J., Austad, T., & Strand, S. (2010). "Smart Water" as a Wettability Modifier in Chalk: The Effect of Salinity and Ionic Composition. Energy & fuels, **24** (4), 2514-2519.
- Fathi, S. J., Austad, T., & Strand, S. (2011). Water-based enhanced oil recovery (EOR) by "smart water": Optimal ionic composition for EOR in carbonates. Energy & fuels, **25** (11), 5173-5179.
- García, A. V., Thomsen, K., & Stenby, E. H. (2006). Prediction of mineral scale formation in geothermal and oilfield operations using the Extended UNIQUAC model: Part II. Carbonate-scaling minerals. *Geothermics*, **35** (3), 239-284
- García, A. V., Thomsen, K., & Stenby, E. H. (2005). Prediction of mineral scale formation in geothermal and oilfield operations using the extended UNIQUAC model: part I. Sulfate scaling minerals. *Geothermics*, **34** (1), 61-97.
- Gupta, R., Griffin, P., Hu, L., Willingham, T. W., Cascio, M. L., Shyeh, J. J., & Harries, C. R. (2011). Enhanced waterflood for Middle East carbonate cores–impact of injection water composition. *paper SPE*, *142668*.
- Iliuta, M. C., Thomsen, K., & Rasmussen, P. (2000). Extended UNIQUAC model for correlation and prediction of vapour–liquid–solid equilibria in aqueous salt systems containing non-electrolytes. Part A. Methanol–water–salt systems. *Chemical Engineering Science*, **55** (14), 2673-2686.
- Puntervold, T., Strand, S., & Austad, T. (2009). Coinjection of seawater and produced water to improve oil recovery from fractured North Sea chalk oil reservoirs. *Energy & fuels*, **23**(5), 2527-2536.
- Strand, S., Austad, T., Puntervold, T., Høgnesen, E. J., Olsen, M., & Barstad, S. M. F. (2008). "Smart Water" for Oil Recovery from Fractured Limestone: A Preliminary Study. Energy & fuels, **22** (5), 3126-3133.
- Strand, S., Høgnesen, E. J., & Austad, T. (2006). Wettability alteration of carbonates—Effects of potential determining ions (Ca^{2+} and SO_4^{2-}) and temperature. *Colloids and Surfaces A: Physicochemical and Engineering Aspects*, **275**(1), 1-10.
- Thomsen, K., & Rasmussen, P. (1999). Modeling of vapor–liquid–solid equilibrium in gas–aqueous electrolyte systems. Chemical Engineering Science, 54 (12), 1787-1802.
- Zahid, A., Stenby, E. H., & Shapiro, A. A. (2010, June). Improved Oil Recovery in Chalk: Wettability Alteration or Something Else? (SPE-131300). SPE EUROPEC. In EAGE Annual Conference and Exhibition, Barcelona, Spain.

- Zahid, A., Sandersen, S. B., Stenby, E. H., von Solms, N., & Shapiro, A. (2011). Advanced waterflooding in chalk reservoirs: Understanding of underlying mechanisms. *Colloids and Surfaces A: Physicochemical and Engineering Aspects*, **389**(1), 281-290.
- Zekri, A. Y., Nasr, M. S., & Al-Arabai, Z. I. (2011, January). Effect of LoSal on Wettability and Oil Recovery of Carbonate and Sandstone Formation. In *International Petroleum Technology Conference*. International Petroleum Technology Conference.
- Zhang, P., & Austad, T. (2006). Wettability and oil recovery from carbonates: Effects of temperature and potential determining ions. *Colloids and Surfaces A: Physicochemical and Engineering Aspects*, **279**(1), 179-187a.
- Zhang, P., Tweheyo, M.T., Austad, T. (2006) Wettability alteration and improved oil recovery in chalk: The effect of calcium in the presence of sulfate. Energy and Fuels **20** (5), 2056-2062b
- Zhang, P., Tweheyo, M. T., & Austad, T. (2007). Wettability alteration and improved oil recovery by spontaneous imbibition of seawater into chalk: Impact of the potential determining ions Ca^{2+}, Mg^{2+}, and SO_4^{2-}. *Colloids and Surfaces A: Physicochemical and Engineering Aspects*, **301**(1), 199-208.

Tables:

Table 1: The optimized parameters (r and q) for different species in the Extended UNIQUAC model for calculating the speciation of different brine solutions. These parameters have been previously reported (Christensen and Thomsen 2003; García et al. 2006; García et al. 2005).

ion	r	q
H_2O	0,92	1,4
$CO_2(aq)$	0,74721	2,4496
Na^+	1,4034	1,199
K^+	2,2304	2,4306
Mg^{2+}	5,406	2,542
Ca^{2+}	3,87	1,48
Ba^{2+}	15,671	14,475
H+	0,13779	1E-16
Sr^{2+}	7,1446	12,894
Cl^-	10,386	10,197
SO_4^{2-}	12,794	12,444
OH^-	9,3973	8,8171
CO_3^{2-}	10,828	10,769
HCO_3^-	8,0756	8,6806

Table 2: The optimized interactions parameters for each pair of species used in the Extended UNIQUAC model for calculating the speciation of different brine solutions. These parameters have been previously reported (Christensen and Thomsen 2003; García et al. 2006; García et al. 2005).

	H_2O		CO_2(aq)		Na^+		K^+		Mg^{2+}		Ca^{2+}		Ba^{2+}		H^+		Sr^{2+}		Cl^-		SO_4^{2-}		OH^-		CO_3^{2-}		HCO_3^-	
	u0	ut	u0	ut	u0	ut	u0	ut	u0	ut	u0	ut	u0	ut	u0	ut	u0	ut	u0	ut	u0	ut	u0	ut	u0	ut	u0	ut
H_2O	0	0																										
CO_2(aq)	8,838	0,863	302,2	0,359																								
Na^+	733,3	0,487	172,4	-0,436	0	0																						
K^+	535	0,994	398,5	3,336	-46,19	0,119	0	0																				
Mg^{2+}	-2,043	-3,554	-581,8	-2,855	-70,96	1,339	-273,7	-1,079	0	0																		
Ca^{2+}	496,4	-8,065	2500	0	-100	-4,656	-275,6	-3,101	1	1	0	0																
Ba^{2+}	-0,379	0,582	2500	0	779,1	2,338	100	1	628,5	0	2500	0	0	0														
H^+	10000	0	1E+09	0	1E+09	0	1E+09	0	1E+09	0	1E+09	0	1E+09	0	0	0												
Sr^{2+}	543,1	1,274	-100,7	0	-103,9	-0,62	100	1	-400,6	-1,437	-402,8	-4,253	2500	0	1E+09	0	0	0										
Cl^-	1523	14,63	1613	15,02	1443	15,64	1465	15,33	2049	12,13	1806	11,14	1403	14,89	1E+09	0	1896	15,69	2215	14,44								
SO_4^{2-}	752,9	9,491	1942	4,79	845,1	11,68	913,8	12,28	1407	3,328	1258	50,45	2500	0	1E+09	0	2500	10	2036	12,41	1266	8,319						
OH^-	600,5	8,546	2500	0	1398	20,28	1806	27,28	736,4	0	164,6	3,608	2500	0	1E+09	0	2500	0	1896	13,63	1226	8,59	1563	5,617				
CO_3^{2-}	361,4	3,352	2500	0	548	3,782	1857	4,06	99	1	2500	0	2500	0	1E+09	0	2500	0	2725	5,727	1217	7,007	1588	2,75	1458	-1,345		
HCO_3^-	577,1	-0,388	526,3	-3,734	1102	1,829	967,8	1,26	99	1	2500	0	2500	0	1E+09	0	2500	0	1737	14,04	990,5	6,965	2500	0	800	1,724	771	-0,02

Table 3: The different data sets for which speciation calculations have been conducted.

Data set	Reference	Data subset	Core No	Figure No
1	Fathi et al. 2011	1.1	1-4	2a
		1.2	5-7	2b
		1.3	8-10	3a
		1.4	11-13	3b
2	Fathi et al. 2010	2.1	14-16	4a
		2.2	17-21	4b
		2.3	22-25	5a
3	Strand et al. 2008	3.0	26-27	6
4	Zhang et al. 2006b	4.1	28-32	7a
		4.2	33-35	7b
		4.3	36-41	8
5	Zahid et al. 2010	5.1	42-45	9
		5.2	46-57	10
		5.3	58-61	11

Table 4: Reported experiments and the corresponding results obtained for data set 1 (Fathi et al. 2011). It includes calculated trends in amounts of soluble SO_4^{2-} and fines formation for core no 1 to 13. Correlation between with oil recovery is highlighted in green, while mismatch is shown in pink.

Experiment data ref [1]					
No.	Figure No	Specification	Used brines	Observed trends	
1	Fig 1 a	4 brine T= 90°C TAN=0.5 mg of KOH/g Stevns klint chalk	SW0NaCl-4SO4		
2			SW0NaCl	Oil Recovery	SW0NaCl-4SO4 >SW0NaCl > SW > VB
3			SW	Fines formed	SW0NaCl-4SO4 >SW0NaCl > SW > VB
4			VB	SO42- in solution	SW0NaCl-4SO4 >SW >SW0NaCl > VB
	Fig 1b	3 brines T= 70° C TAN=0.5 mg of KOH/g Stevns klint chalk			
5			SW0NaCl-4SO4	Oil Recovery	SW0NaCl-4SO4 >SW0NaCl > SW
6			SW0NaCl	Fines formed	SW0NaCl-4SO4 >SW0NaCl > SW
7			SW	SO42- in solution	SW0NaCl-4SO4 >SW >SW0NaCl
	Fig 2a	3 brines T= 120° C TAN=2 mg of KOH/g Stevns klint chalk			
8			SW0NaCl-4SO4	Oil Recovery	SW0NaCl-4SO4>SW0NaCl -4Ca~SW0NaCl
9			SW0NaCl-4Ca	Fines formed	SW0NaCl-4SO4>SW0NaCl -4Ca~SW0NaCl
10			SW0NaCl	SO42- in solution	SW0NaCl-4SO4>SW0NaCl -4Ca~SW0NaCl
	Fig 2b	3 brines T= 100°C TAN=2 mg of KOH/g Stevns klint chalk			
11			SW0NaCl-4SO4	Oil Recovery	SW0NaCl-4SO4>SW0NaCl -4Ca~SW0NaCl
12			SW0NaCl-4Ca	Fines formed	SW0NaCl-4SO4>SW0NaCl -4Ca~SW0NaCl
13			SW0NaCl	SO42- in solution	SW0NaCl-4SO4>SW0NaCl -4Ca~SW0NaCl

Table 5: Reported experiments and the corresponding results obtained for data set 2 (Fathi et al. 2010). It includes calculated trends in amounts of soluble SO_4^{2-} and fines formation for core no 14 to 25. Correlation between with oil recovery is highlighted in green, while mismatch is shown in pink.

Data Set 2: (Fathi et al. 2010)					
No.	Data set & Figure No	Specification	Used brines	Observed trends	
	Data set: 2.1 Figure: 4a	3 brines T= 100° C Swi=10% Stevns klint chalk			
14			SW0NaCl	Oil Recovery	SW0NaCl>SW >SW4NaCl
15			SW	Fines formed	SW0NaCl>SW >SW4NaCl
16			SW4NaCl	SO_4^{2-} in solution	SW4NaCl>SW >SW0NaCl
17	Data set: 2.2 Figure: 4b	3 brines T= 120° C Swi=10% Stevns klint chalk	SW0NaCl		
18			SW		
19			SW4NaCl	Oil Recovery	SW0NaCl > SW >SW4NaCl>dSW 1600
20			dSW 1600	Fines formed	SW0NaCl > SW >SW4NaCl>dSW 1600
21			dSW 1600	SO_4^{2-} in solution	SW4NaCl> SW >SW0NaCl >dSW 1600
22	Data set: 2.3 Figure: 5a	3 brines T= 110° C Swi=10% Stevns klint chalk	XW0NaCl		
23			SW	Oil Recovery	SW0NaCl>SW>dSW20000>dSW10000
24			dSW20000	Fines formed	SW0NaCl>SW>dSW20000>dSW10000
25			dSW10000	SO_4^{2-} in solution	SW>dSW10000>dSW20000>SW0NaCl

Table 6: Reported experiments and corresponding results obtained for data set 3 (Strand et al. 2008). It includes calculated trends in amounts of soluble SO_4^{2-} and fines formation for core no 26 and 27. Correlation between with oil recovery is highlighted in green, while mismatch is shown in pink.

Data Set 3: (Strand et al. 2008)					
No.	Data set & Figure No	Specification	Used brines	Observed trends	
26a	Data set: 3.0 Figure: 6a	3 brines T= 120° C 2 coreplugs limestone reser-voir	SW0S		
27a			SW		
26-27			SW3S	Oil Recovery	SW3S>SW >SW0S & SW0S→SW3S > SWS→SW3S
26b			SW → SW3S	Fines formed	SW3S>SW >SW0S & SW0S→ SW3S > SWS→SW3S
27b			SW0S → SW3S	SO_4^{2-} in solution	SW3S>SW >SW0S & SW0S→ SW3S < SWS→SW3S

Table 7: Reported experiments and corresponding results obtained for data set 4 (Zhang et al. 2006b). It includes calculated trends in amounts of soluble SO_4^{2-} and fines formation for core no 28 to 41.

Data Set 4:(Zhang et al. 2006b)					
No.	Data set & Figure No	Specification	Used brines	Observed trends	
28	Data set: 4.1 Figure: 7a	3 brines T= 70°C Swi=10% Stevns klint chalk	SW-0Ca		
29			SW-½Ca		
30			SW	Oil Recovery	SW-0Ca < SW-½Ca < SW < SW-3Ca < SW-4Ca
31			SW-3Ca	Fines formed	SW-0Ca < SW-½Ca < SW < SW-3Ca < SW-4Ca
32			SW-4Ca	SO_4^{2-} in solution	SW-0Ca > SW-½Ca > SW > SW-3Ca > SW-4Ca
	Data set: 4.2 Figure: 7b	3 brines T= 70 & 100°C Swi=10% Stevns klint chalk			
33			SWX4Ca	Oil Recovery	SW-4Ca > SW > SW-0Ca at 70 °C & 100° C
34			SW	Fines formed	SW-4Ca > SW > SW-0Ca at 70° C & 100 °C
35			dSW 1600	SO_4^{2-} in solution	SW-0Ca > SW > SW-4Ca at 70 °C & 100° C
36	Data set: 4.3 Figure:	6 coreplugs 3 flooding brines T= 70°C	SW-2S (EF)	Oil Recovery Fines formed	SW-2S (EF)> SW-2S(EF-mod)> SW(EF) > SW(EF-mod) > SW-½S(EF) > SW-½S(EF-mod)
37			SW-2S (EF-mod)		

38	8a	2 formation brines Stevns klint chalk	SW (EF)	SO_4^{2-} in solution Oil Recovery	SW-2S (EF) > SW-2S(EF-mod) > SW(EF) > SW(EF-mod) > SW-½S(EF) > SW-½S(EF-mod)
39			SW (EF-mod)		
40			SW-½S (EF)	Fines formed	SW-2S(EF-mod) > SW-2S (EF) > SW(EF) ≈ SW(EF-mod) > SW-½S(EF) ≈ SW-½S(EF-mod)
41			SW-½S (EF-mod)		

Table 8: Reported experiments and corresponding results obtained for data set 5.1 (Zahid et al. 2010). It includes calculated trends in amounts of soluble SO_4^{2-} and fines formation for core no 42 to 45.

Data set 5: (Zahid et al. 2010)					
No.	Data set & Figure No	Specification	Used brines	Observed trends	
42	Data set: 5.1 Figure: 9a	2 brines T= 40, 110 & 130°C completely water-wet 4 Stevns klint chalk	SW0S	Oil Recovery	SW0S →SW3S at 40° C <SW0S →SW3S at 110° C < SW0S →SW3S at 130° C
43				Fines formed	SW0S →SW3S at 40° C <SW0S →SW3S at 110° C < SW0S →SW3S at 130° C
44			SW3S	SO_4^{2-} in solution	SW0S →SW3S at 40° C >SW0S →SW3S at 110° C > SW0S →SW3S at 130° C
45					

Table 9: Reported experiments and corresponding results obtained for data set 5.2 (Zahid et al. 2010). It includes calculated trends in amounts of soluble SO_4^{2-} and fines formation for core no 46 to 57.

Data set 5: (Zahid et al. 2010)					
No.	Data set & Figure No	Specification	Used brines	Observed trends	
46-49	Data set: 5.2 Figure: 10a-e	3 brines T= 110 & 130°C completely water-wet 5 Stevns klint chalk	SW0S;SW & SW3S	Oil Recovery (OR)	SW0S < SW < SW3S & OR at 110°C < OR at 130°C
50-51			SW0S; SW3S		
52-53			SW0S; SW3S	Fines formed(FF)	SW0S < SW <SW3S & FF at 110°C < FF at 130°C
54-55			SW0S; SW3S		
56-57			SW0S; SW3S	SO_4^{2-} in solu-tion(SS)	SW0S < SW< SW3S & SS at 130°C< SS at 110°C

Table 10: Reported experiments and corresponding results obtained for data set 5.2 (Zahid et al. 2010). It includes calculated trends in amounts of soluble SO_4^{2-} and fines formation for core no 58 to 61.

Data set 5: (Zahid et al. 2010)					
Sl No.	Data set & Figure No	Specification	Used brines	Observed trends	
58	Data set: 5.3 Figure: 11a-d	2 brines T= 40, 90 & 110°C completely water-wet 4 Stevns klint chalk	SW0S → SW at 40°C	Oil Recovery	SW0S →SW at 40° C <SW0S →SW at 90° C ≈SW0S →SW at 90° C <SW0S→SW at 110° C
59			SW0S →SW at 90°C	Fines formed	SW0S →SW at 40° C <SW0S →SW at 90° C ≈SW0S →SW at 90° C <SW0S→SW at 110° C
60			SW0S →SW at 40°C	SO_4^{2-} in solution	SW0S →SW at 40° C >SW0S →SW at 90° C ≈SW0S →SW at 90° C >SW0S→SW at 110° C
61			SW0S →SW @at 110°C		

Figures:

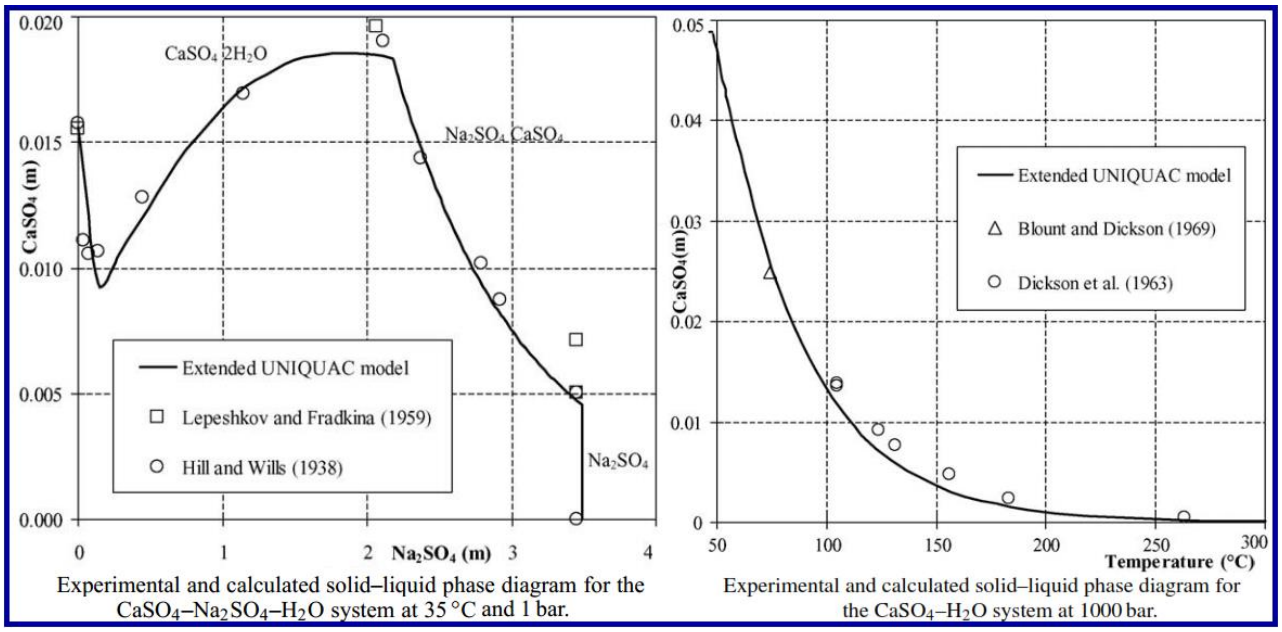


Figure 1: The accurate prediction of $CaSO_4$ precipitation at ambient and elevated pressures for single and multi-component systems. (García et al. 2005). The concentration unit on the axes is molality (mol/kg water).

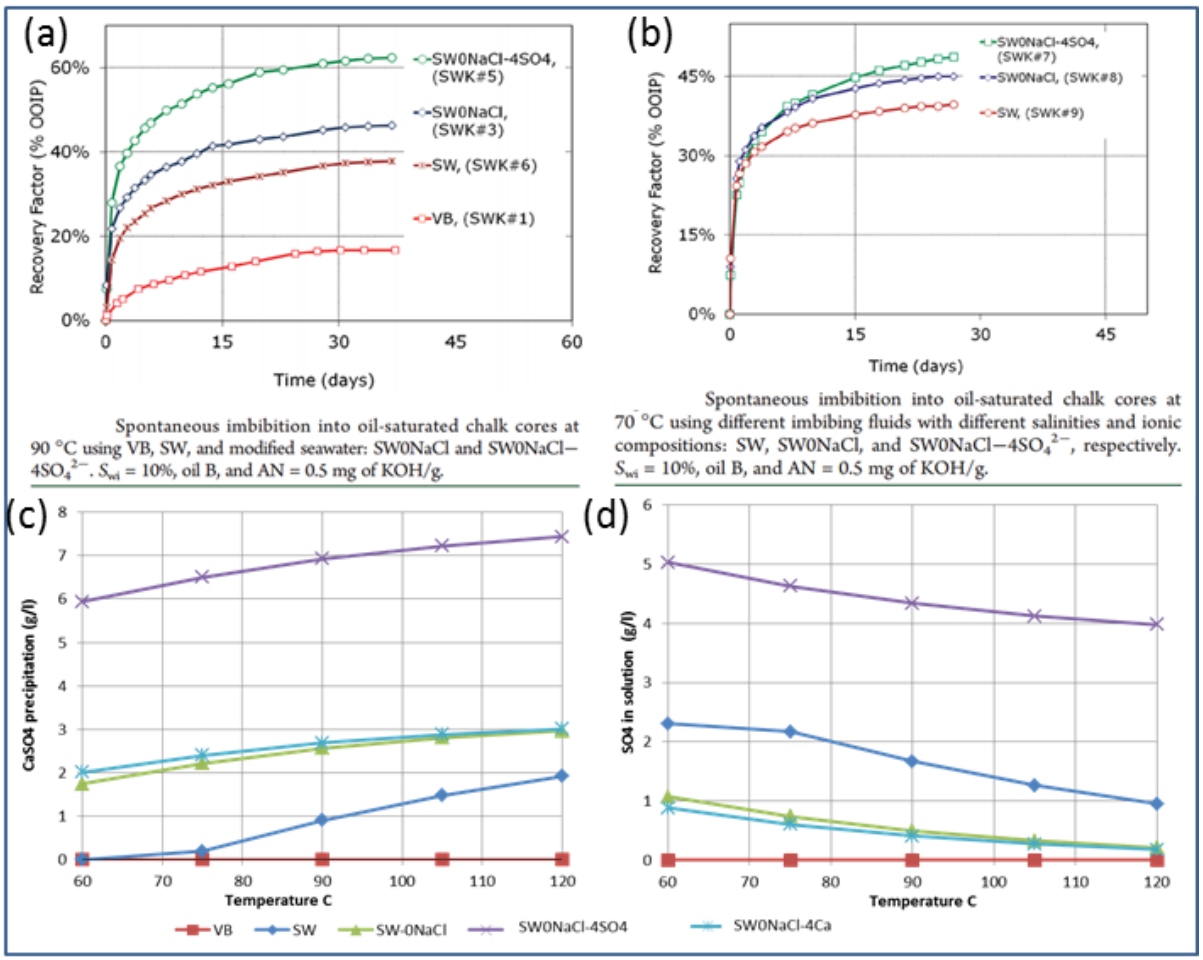
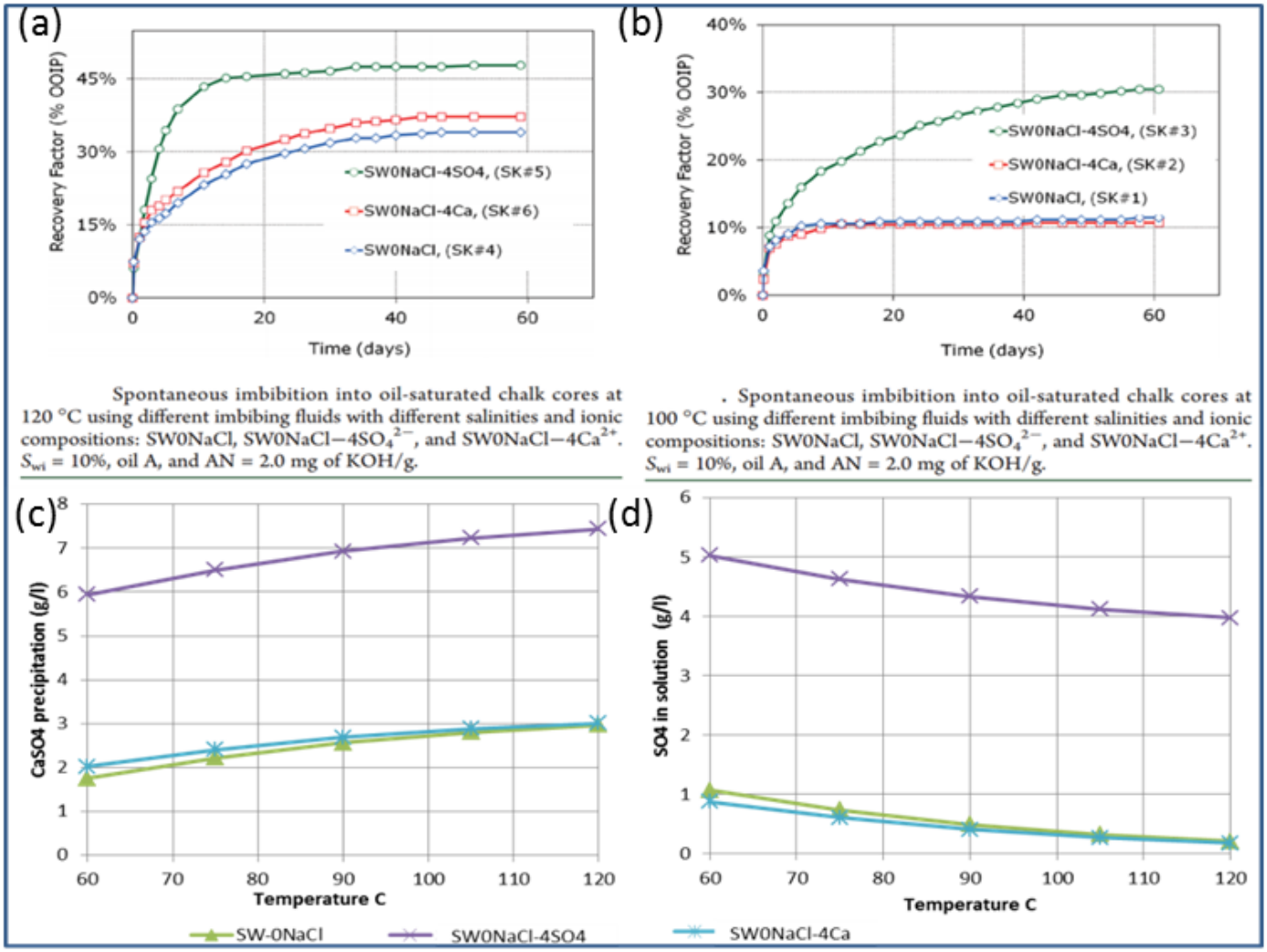


Figure 2 a&b: Spontaneous imbibition experiments (Fathi et al. 2011). c&d: The calculated amounts of $CaSO_4$ precipitation and soluble SO_4^{2-} in the solution for each of the different brines used. The reported values represent data set 1.1 & 1.2.



Spontaneous imbibition into oil-saturated chalk cores at 120 °C using different imbibing fluids with different salinities and ionic compositions: SW0NaCl, SW0NaCl−$4SO_4^{2-}$, and SW0NaCl−$4Ca^{2+}$. S_{wi} = 10%, oil A, and AN = 2.0 mg of KOH/g.

. Spontaneous imbibition into oil-saturated chalk cores at 100 °C using different imbibing fluids with different salinities and ionic compositions: SW0NaCl, SW0NaCl−$4SO_4^{2-}$, and SW0NaCl−$4Ca^{2+}$. S_{wi} = 10%, oil A, and AN = 2.0 mg of KOH/g.

Figure 3 a&b: Spontaneous imbibition experiments (Fathi et al. 2011). c&d: The calculated amounts of $CaSO_4$ precipitation and soluble SO_4^{2-} in the solution for each of the different brines used. The reported values represent data set 1.3 & 1.4.

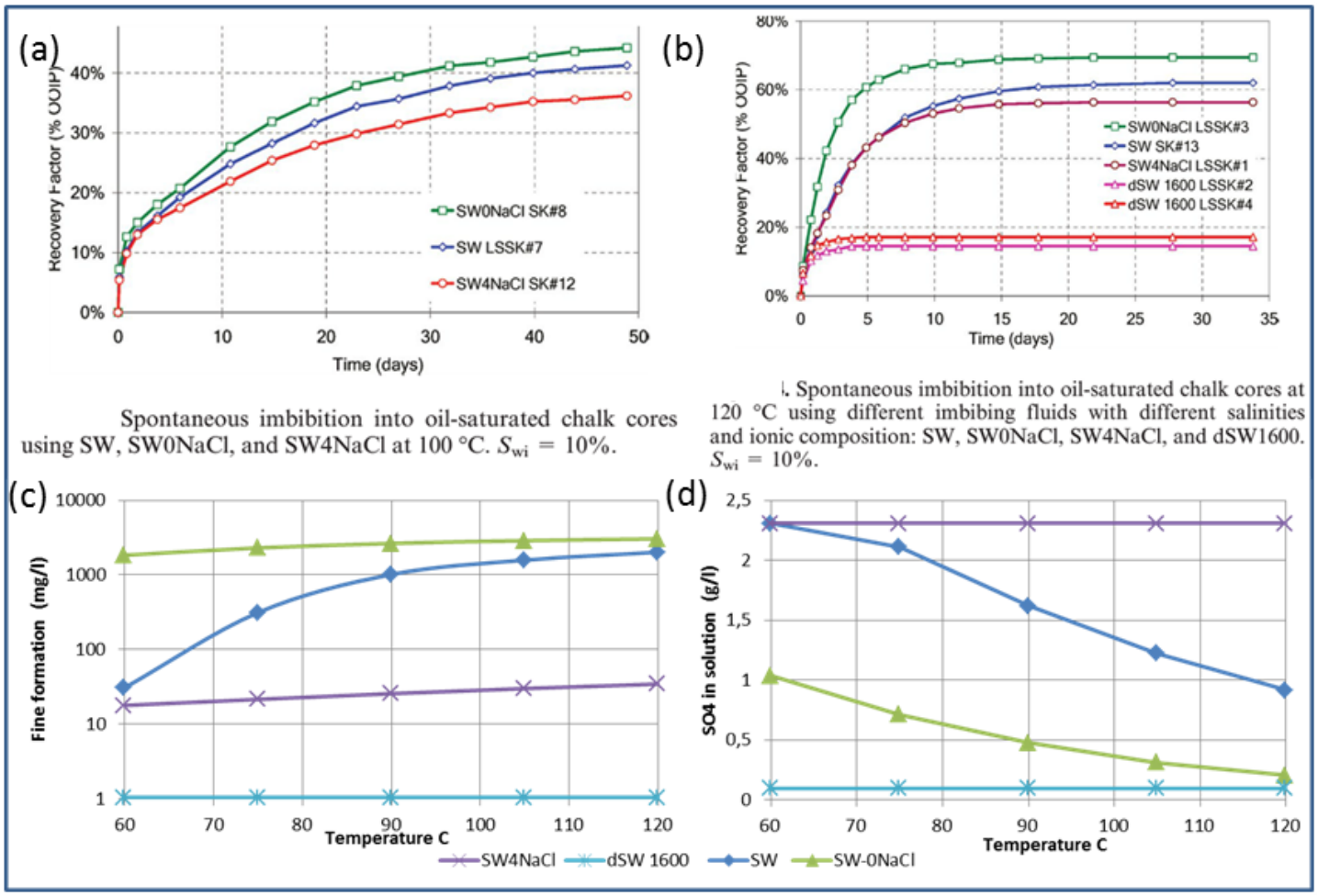


Figure 4 a&b: Spontaneous imbibition experiments (Fathi et al. 2010) c&d: The calculated amounts of fines formation and soluble SO_4^{2-} in the solutions for each of the different brines used. The reported values represent data set 2.1 & 2.2.

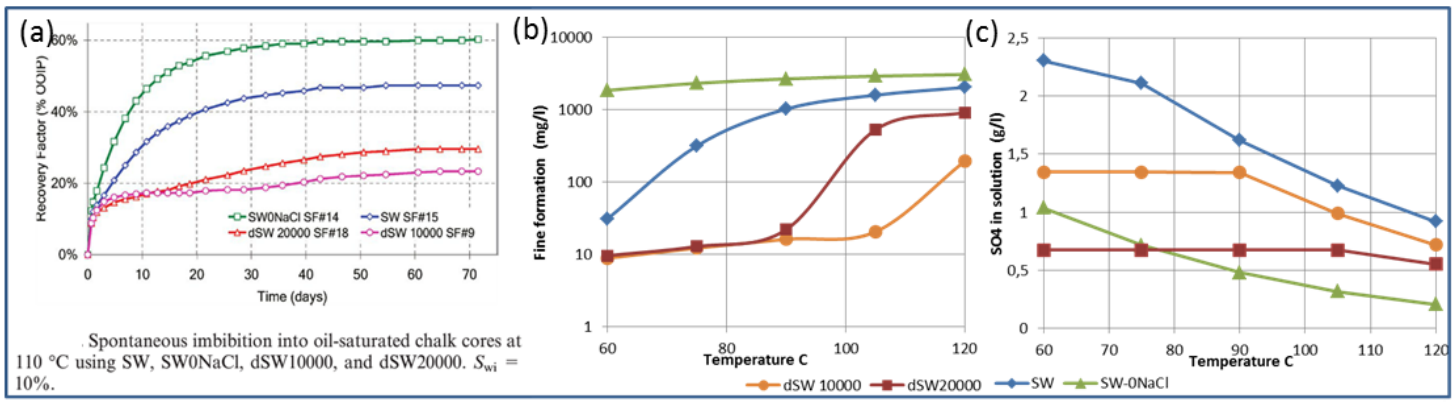


Figure 5a: Spontaneous imbibition experiments (Fathi et al. 2010) b&c: The calculated amounts of fines formation and soluble SO_4^{2-} in the solution for each of the different brines used. The reported values represent data set 2.3.

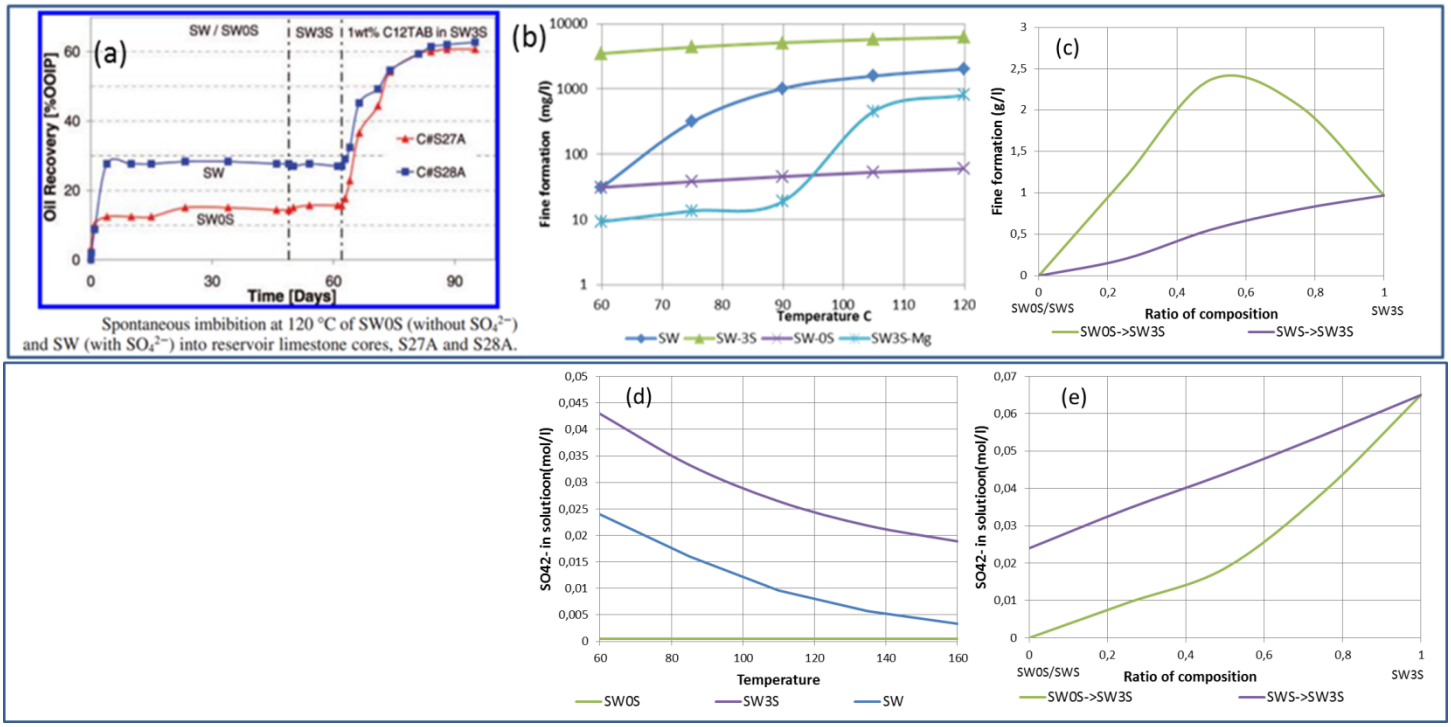


Figure 6a: Experiments with very low permeability limestone reservoir core plugs (Strand et al. 2005). b: The calculated amount of fines formation caused by the different brines used. (c) Amount of fines formation caused by the interaction between two successive imbibing fluids. (d) The calculated amounts of soluble SO_4^{2-} in the solutions for each of the different brines used. (c) Amount of soluble SO_4^{2-} present in the solutions for the mixture of two imbibing fluids. The reported values represent data set 3. SW3S-Mg represent the amount of precipitation of $CaSO_4$ before ion substitution (Ca^{2+} by Mg^{2+}) on the mineral surface.

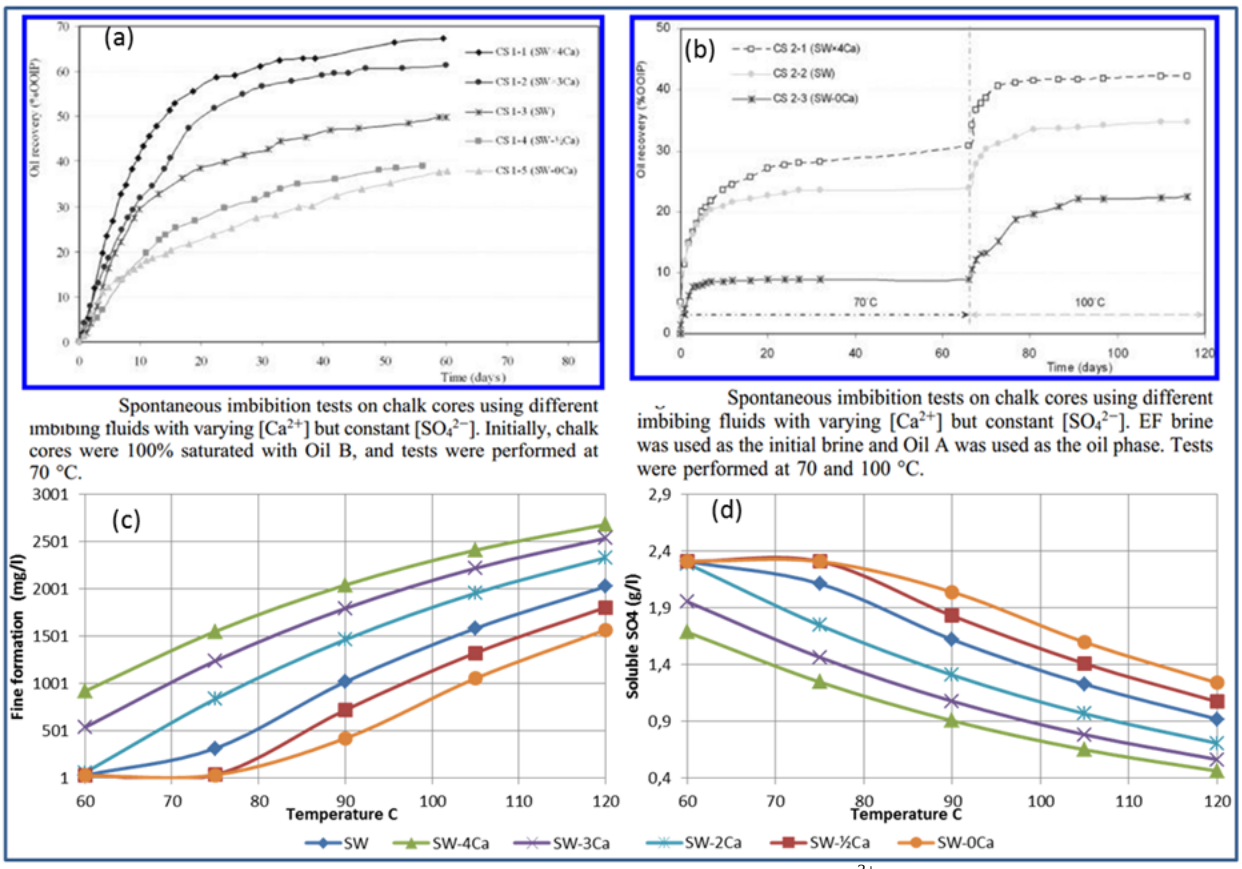


Figure 7a&b: Spontaneous imbibition experiments highlighting the importance of Ca^{2+} ion in the brine solution (Zhang et al. 2006b).c&d: The calculated amounts of $CaSO_4$ precipitation and soluble SO_4^{2-} in the solution for each of the different brines used. The reported values represent data set 4.1 and 4.2.

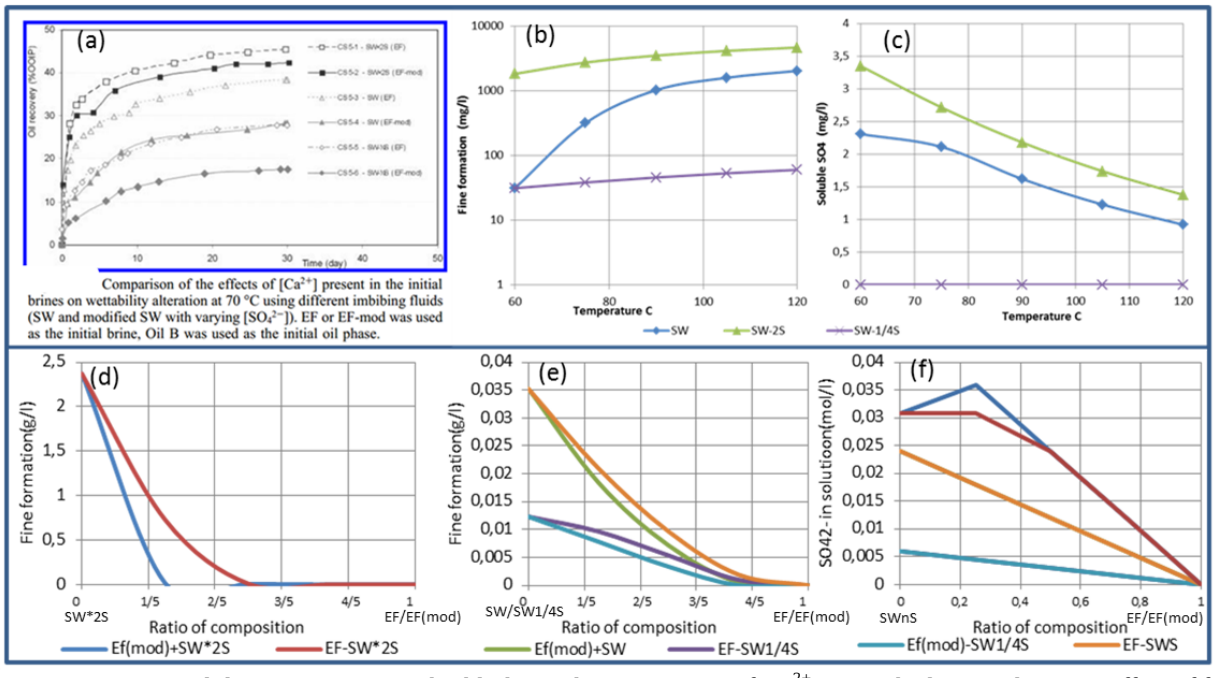


Figure 8a: Spontaneous imbibition experiments highlighting the importance of Ca^{2+} ion in the brine solution & effect of formation water in SmW-EOR (Zhang et al. 2006b) .b&c: The calculated amounts of $CaSO_4$ precipitation and soluble SO_4^{2-} in the solution for each of the different brines used. d&e: The calculated amount of fines formation during mixing of different amounts of formation water and injected water. (f) Soluble SO_4^{2-} in the solution during mixing of the formation water and imbibing fluid. The reported values represent data set 4.3.

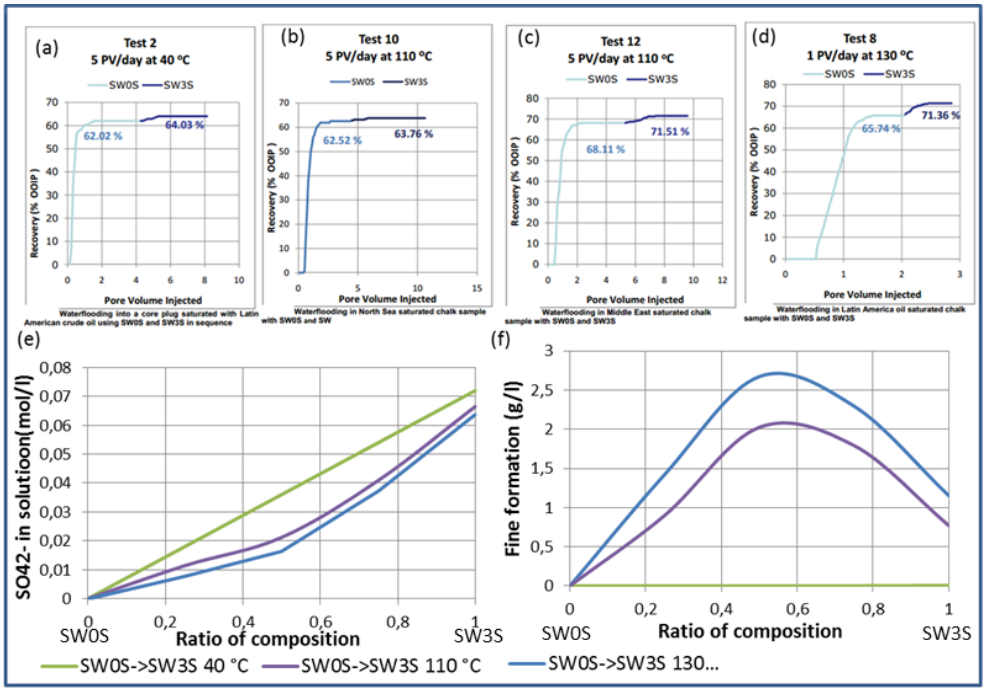


Figure 9a-d: Water flooding experiment with SW0S followed by SW3S for completely water-wet core plug (Zahid et al. 2010). e&f: The calculated amounts of SO_4^{2-} in solution and $CaSO_4$ precipitation during the mixing of two brines at different temperatures. This figure represents data set 5.1.

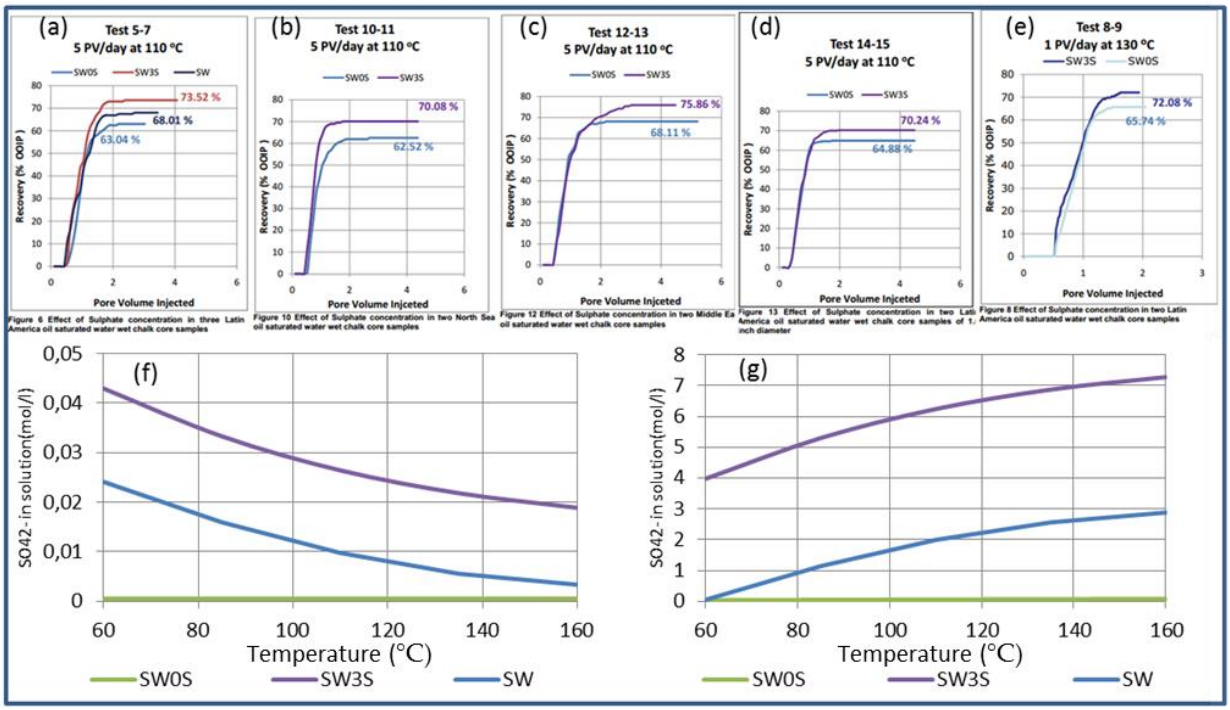


Figure 10a-e: Water flooding experiments with SW0S SW and SW3S for completely water-wet core plug with oil originating from varied sources (Zahid et al. 2010). f&g: The calculated amounts of SO_4^{2-} in solution and $CaSO_4$ precipitation for each of the different brines used. This figure represents data set 5.2.

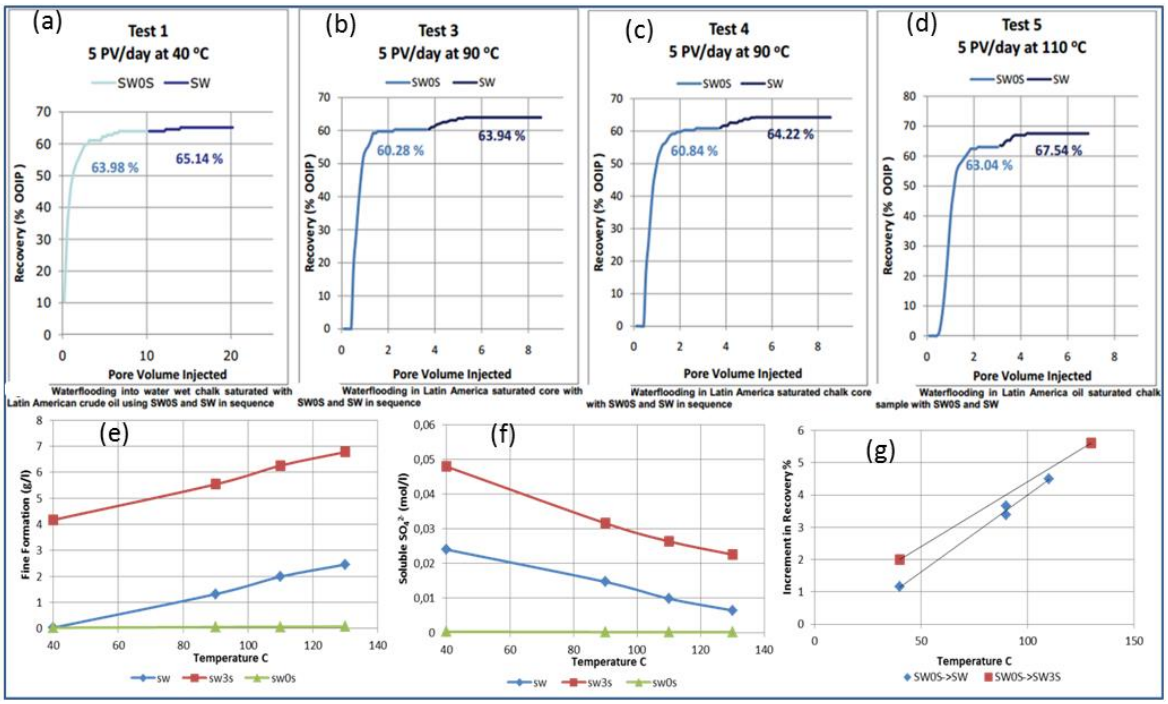


Figure 11a-d: Water flooding experiment with SW0S followed by SW for completely water-wet core plug (Zahid et al. 2010) .e&f: The calculated amounts of SO_4^{2-} in solution and $CaSO_4$ precipitation during the mixing of two brines at different temperatures. (g) The increment in recovery brine alteration from SW0S to SW at different temperatures. This figure represents data set 5.3.

Paper VI

Chakravarty, K. H., Fosbøl, P. L., & Thomsen, K. (2015, November). Fine Formation during brine-crude oil-calcite interaction in Smart Water flooding and its correlation to Enhanced Oil Recovery. In *SPE Annual Caspian Technical Conference & Exhibition*. Society of Petroleum Engineers.

SPE-177379-MS

Fine Formation during brine-crude oil-calcite interaction in Smart Water flooding and its correlation to Enhanced Oil Recovery

Krishna Hara Chakravarty, Philip Loldrup Fosbøl and Kaj Thomsen, Center for Energy Resources Engineering (CERE), Department of Chemical and Biochemical Engineering, Technical University of Denmark

Copyright 2015, Society of Petroleum Engineers

This paper was prepared for presentation at SPE Annual Caspian Technical Conference & Exhibition held in Baku, Azerbaijan, 4–6 November 2015.

This paper was selected for presentation by an SPE program committee following review of information contained in an abstract submitted by the author(s). Contents of the paper have not been reviewed by the Society of Petroleum Engineers and are subject to correction by the author(s). The material does not necessarily reflect any position of the Society of Petroleum Engineers, its officers, or members. Electronic reproduction, distribution, or storage of any part of this paper without the written consent of the Society of Petroleum Engineers is prohibited. Permission to reproduce in print is restricted to an abstract of not more than 300 words; illustrations may not be copied. The abstract must contain conspicuous acknowledgment of SPE copyright.

Abstract

Modified sea water has been shown to affect the oil recovery fraction considerably during secondary and tertiary waterfloods. Available soluble potential ions (i.e. Ca^{2+}, Mg^{2+} & SO_4^{2-}) in the interacting waterflood (ITW) are suggested to play a key role in increasing the displacement efficiency of oil. In previous studies, compositions of injected waterfloods (IJW) have been correlated to the observed oil recovery. This study highlights differences between IJW and ITW for different studies reported in literature.

To calculate the composition of ITW, the speciation calculation of IJW in contact with reservoir rock was conducted at the stated pressure and temperature conditions. The Extended UNIQUAC model was used because of its high accuracy and optimized parameters. The amounts of soluble ions in the ITW and the changes taking place due to dissolution/precipitation was calculated for 77 SmW-EOR experiments reported in literature.

The calculations showed that there can be significant amounts of fines formation in ITW during the use of different smart waterfloods. Fines formations were attributed to three primary causes. (1) Cation substitution on mineral surfaces. (2) Interaction between new IJW and existing brine in the pore space. (3) Variation in temperature and pressure conditions. Precipitation / dissolution of calcite, dolomite, and anhydrite created a significant difference between the IJW and ITW. The reservoir composition and NaCl concentration in IJW also play a significant role in possible fines formations. It was observed that the composition of soluble potential ions in ITW was significantly different from that in IJW. The amounts of soluble potential ions in ITW and the amounts of fines formation taking place was correlated to the observed oil recovery. The increased oil recovery observed in various experiments repeatedly correlated well with the amount of fines formed in the pore space. In several cases, the amount of soluble potential ions in the ITW did not correlate with the observed oil recovery. Experiments involving Caspian carbonate were also analyzed, and significant correlation between fines formation and oil recovery was observed. These results together suggest that fines formation can be used to explain both low salinity and smart water flooding experiments, and the two recovery processes may not necessarily have distinct mechanisms.

This study quantitatively explains a series of previous experiments reported in the literature and shows how fines formation can lead to major differences between the IJW and ITW. It also shows that fines formation previously unaccounted for can be precisely calculated at exact reservoir conditions using the Extended UNIQUAC model.

Introduction

Around 50% of petroleum reserves are in carbonate reservoir, in which production becomes uneconomical after production of 30% of the original oil in place (OOIP) (Akbar et al. 2001). High porosity, low permeability characterization of the carbonate reservoirs with initial wettability condition ranging from mixed-wet to oil-wet indicates the challenge of finding a sophisticated enhanced oil recovery (EOR) method. Among the different proposed EOR methods, smart water (SmW) flooding has been proven as a low cost, effective, non-toxic method.

Among the various ions, SO_4^{2-} , Ca^{2+}, and Mg^{2+} are reported as the potential ions for improving oil recovery throughout the laboratory observation of water flooding conducted by Austad and co-workers at University of Stavanger. The importance of SO_4^{2}

together with Ca^{2+} and Mg^{2+} is reported as injection of SO_4^{2-} alongside with Na^+ resulted in a major recovery reduction (Zhang et al. 2006a). Increase in oil recovery is more significant when temperature is above 70°C (Strand et al. 2006; Zhang et al. 2007; Zhang et al. 2006a; Zhang et al. 2006b; Austad et al. 2005; Zhang et al. 2006; Puntervold et al. 2009). Among the proposed physico-chemical mechanism, wettability alteration is identified as key factor for the improving oil recovery. This mechanism is through two processes: (1) Substitution of calcium by magnesium on the calcite surface (2) Change of wettability towards a more water-wet condition by adsorption of sulfate ions on the mineral surface correspondent with the release of adsorbed carboxyl compound. Decrease in sulfate concentration in effluent water, supports that it acts as a reagent in this process (Zhang et al. 2007; Bagci et al. 2001).

Diluting sea water (reducing potential ions concentration) resulted in lower oil recovery (Fathi et al. 2010). Other spontaneous imbibition and waterflooding experiments certified the trend (Zhang et al. 2010b). Same study also suggested that possible precipitation of $CaSO_4$ can block the flow and must be prohibited (Zhang et al. 2010b). Contributing effect of the increase in Ca^{2+} concentration on oil recovery was also concluded (Zhang et al. 2010b). Importance of potential ions in brine solution has been concluded in most of the reported studies. Among the potential ions, sulfate is reported to have the most prominent effect on oil recovery (Fathi et al. 2011). Available NaCl in the brine leads to formation of an electric double layer on the calcite surface (Fathi et al. 2010) which inhibits the accessibility of the determining ions to the rock surface. It explains the effect of NaCl concentration on oil recovery reduction. Similarly, selective reduction of NaCl concentration is shown to increase the oil recovery (Fathi et al. 2010). Stevns Klint outcrops chalk from Denmark was used is majority of the discussed experiments (Strand et al. 2006; Fathi et al. 2010; Fathi et al. 2011; Zhang et al. 2006b). High concentration of sulfate resulted in higher oil recovery also in the spontaneous imbibition experiments with limestone reservoir rocks (Strand et al. 2008).

Wettability alteration mechanism (Austad et al. 2005) was doubted (Zahid et al. 2010) as increase in SO_4^{2-} concentration of injection brine increased oil recovery in completely water-wet coreplugs (Zahid et al. 2010). In the same study, dissolution of rock and emulsification of oil were mentioned as the possible mechanisms. However, concrete evidence of emulsification formation was not provided. Formation of oil emulsion was observed in another study for high concentrations of sulfate, which increased by the increase in temperature (Zahid et al. 2011). Formation of oil emulsion (Zahid et al. 2011) did not establish a correlation with the observed oil recovery (Zahid et al. 2010). Furthermore, a maximum sulfate concentration for carbonate coreplugs have been reported, from which no further increase in oil recovery was observed (Awolayo et al. 2014). No increase in oil recovery for very high sulfate concentration (Awolayo et al. 2014) coupled with a successful EOR with completely water wet coreplugs (Zahid et al. 2010; Zahid et al. 2015) are in contradiction with the proposed potential ion based wettability alteration model (Austad et al. 2005), thus indicate that it is not applicable to all conditions.

Establishment of a correlation between injection brine composition and the observed oil recovery was attempted in the cited studies. However, new brine forms in the pore space due to substitution of Ca^{2+} on the rock surface by Mg^{2+} from the injection brine. The proposed mechanism suggested that Mg^{2+} decreases and Ca^{2+} increases equivalently in the pore space. Thereby, the possibility of precipitation significantly enhances with the increase in temperature. Reported oil recovery should be correlated with the real time properties of brine in pore space. This report contains the calculation of the brine composition in the pore space, using Extended UNIQUAC model (Thomsen and Rasmussen 1999).

The Extended UNIQUAC model is a thermodynamic model for aqueous solutions of electrolytes and non-electrolytes (Thomsen and Rasmussen 1999). The optimized parameters of this model are based on a large amount of experimental data (Christensen and Thomsen 2003; Thomsen et al. 1996; García et al. 2006; García et al. 2005). Including solid-liquid equilibrium data, experimentally measured activity, and osmotic coefficients as well as thermal properties such as heat of dilution, heat of solution, and apparent molal heat capacity for salt solutions. The optimized parameters enable the model to accurately predict the phase behavior and thermal properties of solutions containing electrolytes (García et al. 2005). Experimental data from the open literature and calculated solid-liquid equilibrium curves for the ternary $CaSO_4 – Na_2SO_4 – H_2O$ system (at room temperature) and the binary $CaSO_4 – H_2O$ system (at elevated pressure and temperature conditions) are brought in Figure 1 to illustrate the accuracy of the model (García et al. 2005). In this study, the exact brine properties and experimental condition (temperature and pressure) of spontaneous imbibition and water flooding experiments have been extracted from 5 different literature sources. Thereafter the evolution of brine concentrations with the change in temperature, pressure, and mineral interactions were calculated by the model. For different injection brines, precipitation of $CaSO_4$ (or fines formation) was observed. Fine formation correspondent to available amount of SO_4^{2-} in the brine solution in the pore space was correlated with the observed oil recovery. Similar trends have been observed for various studies with variation in brine composition, temperature, coreplug properties, oil specification, and wetness of the coreplugs.

Calculation method

In this study the group of ions and neutral species including H_2O, CO_2, Na^+, K^+, Mg^{2+}, Ca^{2+}, Ba^{2+}, H^+, Sr^{2+}, Cl^-, SO_4^{2-}, OH^-, CO_3^{2-} and HCO_3^- have been investigated. For each individual species, volume and area parameters (r- and q- parameters) are the main parameters of the Extended UNIQUAC model. For each pair of species, two additional parameters are used to describe their interaction. The additional parameters are assumed to have a linear temperature dependency. Massive amount of binary and ternary experimental data have been used to optimize the main parameters for each individual ion (Iliuta et al. 2000; Thomsen et al. 1996;

García et al. 2005), and species pair interaction parameters (Iliuta et al. 2000; Thomsen et al. 1996; García et al. 2005). The parameters are brought in Table 1, and Table 2, respectively. Extended UNIQUAC model has shown promising results in predicting multi-component systems with a wide range of temperature and ionic strength which covers all the spontaneous imbibition and water flooding experimental conditions.

Brine properties in the pore space and the amount of precipitate formation for 61 different water flooding experiments have been calculated using the Extended UNIQUAC model. Water flooding data have been extracted from five different reports available in the literature, which are listed in Table 3. For each individual experiment, the effect of each ion in Sw-EOR has been extensively investigated.

Results:

Data set 1: (Zhang et al. 2006)

In the first set of experiment, ion selective spontaneous imbibition study of oil saturated chalk cores was reported (Fathi et al. 2011). In this study a total of 4 core samples from Stevns Klint chalk were examined with different brine solutions. The spontaneous imbibition experiment was first conducted 70 °C for all core plugs later it was increased to 100°C and 130°C. Modified sea water without Ca^{2+} and/or Mg^{2+} was initially used as imbibing fluid, and later on Mg^{2+} or Ca^{2+} was added with a concentration equivalent to Seawater. First the final oil recovery at 130°C was analysed. The corresponding amount of fine formation and presence of soluble ions were calculated for the given brine concentrations by Zhang et al. 2006a. The obtained values for are represented in Figure 1. The observed oil recovery of trend is in this experiment is the following: SW0X4S+Mg > SW0+Mg > SW0X2S+Ca> SW0X0S+Mg. While using Extended UNIQUAC model the calculated amount of Soluble $SO_4^{2-}$and the total available potential ions show the same trend: SW0X4S+Mg > SW0X2S+Ca> SW0+Mg>SW0X0S+Mg. While the total amount of supersaturating present in solution show the subsequent trend: SW0X4S+Mg > SW0+Mg > SW0X2S+Ca> SW0X0S+Mg. Thus in this case we can clearly observe that the observed oil recovery only partially correlates to either the total potential ion or the amount of soluble SO_4^{2-} present in the interacting brine; while the amount of expected fine formation perfectly correlates to the observed oil recovery. So at 130 °C the calculated fine formation and the observed oil recovery perfectly correlate.

Secondly at 100 °C (initial) in the different used brines only SO_4^{2-} was present in different concentrations. And since SO_4^{2-} is soluble with Na^+; so there is no expected fine formation. And since there is no presence of Ca^{2+} or Mg^{2+} so there is no possibility of ion substitution or sulphate precipitation. Thus it perfectly correlated to the fact that: for varying concentration of SO_4^{2-} in absence of Mg^{2+} or Ca^{2+} no variation in oil recovery is observed. So the absence of variation of oil recovery for variation in SO_4^{2-} is also in complete congruence to the expected amount of fine formation. Thereafter it is observed that introducing Ca^{2+} or Mg^{2+} in the system can lead to fine formation during the interaction of two brines. i.e. when Ca^{2+} is injected in the pore space where there is brine containing SO_4^{2-} then the interaction of the injected Ca^{2+} rich brine with SO_4^{2-} containing brine can lead to fine formation. It must be noted change in brine speciation because of ion substitution, interaction of two injected brine, variation in temperature and pressure are different parameters that can cause fine formation. Thus injecting Ca^{2+} alone into brine containing SO_4^{2-} ion can lead to fine formation because of the interaction of the two brines. In the calculation it is also observed that injection of cation (Ca^{2+} or Mg^{2+}) leads to fine formation in all four cases, this is in congruence to the observed increase in oil recovery. The calculation at 100°C is represented in Figure 2. In this case also the observed oil recovery pattern: SW0X4S+Mg > SW0+Mg > SW0X2S+Ca> SW0X0S+Mg perfectly correlates with the calculated fine formation trend: SW0X4S+Mg > SW0+Mg > SW0X2S+Ca> SW0X0S+Mg. Furthermore with increase in temperature the solubility of $CaSO_4$ decreases. This leads to higher fine formation at elevated temperature. Thus the amount of available soluble SO_4^{2-} and the total available soluble potential ions consistently decreases. This is also observable in the calculated values as shown in Figure 3. Consistently with increase in temperature both the amount of Soluble SO_4^{2-} and the total amount of available potential fines decreases. While the amount of super saturation increases in both cases. The oil recovery also showed a significant increase for these brines with increase in temperature. Thus these results also indicate a good correlation between the oil recovery and fine formation, while soluble ions show the opposite trend.

Additionally it is interesting to note that for core plug CM-2(SWX2S+Ca) increasing temperature did not lead to a significant increase in oil recovery. Although a small increase in oil recovery was observed. The calculated amount of fine formation also shows the same trend. In this case we observe only a small increase in amount of saturation for the given brine composition. While the decrease in soluble SO_4^{2-} and total potential ions with increase in temperature clearly show a mismatch to the observed increase in oil recovery. Moreover it is interesting to note that in case of SW0+Mg(core plug: CM-1) and SW0X4S+Mg (core plug : CM-4) significant increase in oil recovery was observed (with increase in temperature from 100°C to 130°C). The calculated amount of fine formation also showed significant increase. While a considerable drop in soluble amounts of SO_4^{2-} and total potential ions was observed. Thus the amount of increase in oil recovery also correlates to the corresponding increase in fine formation as shown in Figure 3. While in case of CM-2(SWX2S+Ca) an increase in oil recovery was observed but the increment was significantly less compared to the other two core plugs. Similar results were obtained for fine formation. Herein increase in fine formation was observable, but the amount of increase in fine formation was significantly less than that observed for SW0+Mg or SW0X4S+Mg. As shown in Figure 4, it is clearly observable that only a minute increase in fine formation takes place, this perfectly correlates to the observed oil recovery. While it is also observed that the amount of soluble SO_4^{2-} and total potential ions

present in this system remains almost constant at elevated temperature. This also shows a contradiction as high amount of soluble ions is retained at elevated temperature, but is not associated with major increase in oil recovery. While as shown in Figure 2 in case if SW0+Mg(core plug: CM-1) significant decrease in concentration of soluble ions is observed, while massive increase in oil recovery is observed. Thus not only the amount of oil recovery but also the amount of increase in oil recovery correlates to the amount of fine formation. And the increment in oil recovery for these cases (CM-2 & CM-1) shows an inverse correlation between oil recovery and the amount of soluble ions. These results further highlight the observed correlation between amount of fine formation and increased oil recovery (Chakravarty et al. 2015).

Therefore significant increase in oil recovery for SW0+Mg (core plug: CM-1) and SW0X4S+Mg (core plug: CM-4) while minute increase in oil recovery in case of CM-2(SWX2S+Ca) (i.e. Ca^{2+} in absence of Mg^{2+}) also perfectly correlates for to the fine formation. As with increase in temperature significant increase in fine formation is observed for the brines containing Mg^{2+} i.e. SW0+Mg (core plug: CM-1) and SW0X4S+Mg (core plug: CM-4)), while only a minute increase in fine formation is observed for brine containing Ca^{2+} (i.e. CM-2(SWX2S+Ca)). While there is no observable correlation to explain the amount of increase in oil recovery from the soluble SO_4^{2-} or total soluble potential ion stand point. As massive decrease in the soluble ion concentration is estimated in core plug (CM-1) which shows significant increase in oil recovery. And only minute increase in oil recovery is observed (CM-3) when the amount of soluble potential ions is almost unaffected.

Data set 2: (Puntervold et al. 2007)

The Second (2.0) set of experiments includes an extensive water flooding study with chalk core plugs (Puntervold et al. 2007). In this study a total of 8 core samples from Stevns Klint outcrop chalk were examined with different brine solutions. Designed oil with varied total acid number and total base number was used in these experiments. The effect of acid number and base number in SW-EOR was meticulously studied.

In the data subset 2.1 (shown in Figure 5a) spontaneous imbibition experiment into 4 oil-saturated chalk cores was conducted at 70°C for chalk core plugs with water saturation of 30-50%. Imbibition of four different brines (SSW/US, SSW, SSW2S and SSW4S) with different sulphate concentration was conducted in all four core plugs. The four coreplug contained oil with different proportions of acid and base numbers. The obtained oil recovery trend for all four coreplug was: SSW4S> SSW2S> SSW> SSW/US. The corresponding amounts of soluble SO_4^{2-} ion in the different brine solutions at 70°C were calculated using Extended UNIQUAC model. The possibility of fines formation because of precipitation of $CaSO_4$ was also calculated. As previously proposed (Austad et al. 2005) the change in brine composition because of substitution of Ca^{2+} by Mg^{2+} on calcite surface was included. The calculated amount of soluble SO_4^{2-} ion present in the different brine solutions and the amount of fine formation taking place both showed the following trend: SSW4S> SSW2S> SSW> SSW/US. The calculated values are shown in Figure 5c and 5d. It is important to note that not only the amount of soluble SO_4^{2-} ion present in the brine solution correlates with the observed oil recovery but also the fine formation taking place correlates to the oil recovery.

In the data subset 2.2 (shown in Figure 5b) spontaneous imbibition experiment into 4 oil-saturated chalk cores was conducted at 70°C for chalk core plugs with water saturation of 10-20%. Imbibition of four different brines (SSW/US, SSW, SSW2S and SSW4S) with different sulphate concentration was conducted in all four core plugs. The four coreplug contained oil with different proportions of acid and base numbers. The obtained oil recovery trend for all four coreplug was: SSW4S> SSW2S> SSW> SSW/US. The corresponding amounts of soluble SO_4^{2-} ion in the different brine solutions at 70°C were calculated using Extended UNIQUAC model. The possibility of fines formation because of precipitation of $CaSO_4$ was also calculated. As previously proposed (Austad et al. 2005) the change in brine composition because of substitution of Ca^{2+} by Mg^{2+} on calcite surface was included. The calculated amount of soluble SO_4^{2-} ion present in the different brine solutions and the amount of fine formation taking place both showed the following trend: SSW4S> SSW2S> SSW> SSW/US. The calculated values are shown in Figure 5c and 5d. It is important to note that for low water saturation also both the amount of soluble SO_4^{2-} ion present in the brine solution and the amount of fine formation taking place correlates to the oil recovery.

Data set 3: (Kazankapov et al. 2007)

The third set of experiments includes an extensive spontaneous imbibition study of oil saturated chalk cores (Kazankapov et al. 2007). In this study a total of 4 core samples from Stevns Klint chalk were examined with different brine solutions. Herein, spontaneous imbibition into 4 oil-saturated chalk cores was conducted at 90°C using VB (formation water), SW (sea Water), and modified seawater: SW0NaCl and SW0NaCl-4SO_4^{2-} (Kazankapov et al. 2007). The total acid number of the used oil was 0.5 mg of KOH/g. The obtained oil recovery trend was: SW0NaCl-4SO_4^{2-} > SW0NaCl > SW > VB. The corresponding amounts of soluble SO_4^{2-} ion in the different brine solutions at 90°C were calculated using Extended UNIQUAC model. The possibility of fines formation because of precipitation of $CaSO_4$ was also calculated. As previously proposed (Austad et al. 2005) the change in brine composition because of substitution of Ca^{2+} by Mg^{2+} on calcite surface was included. The calculated amount of soluble SO_4^{2-} ion present in the different brine solutions showed the following trend: SW0NaCl-4SO_4^{2-} > SW > SW0NaCl > VB. The calculated amount of fines formation because of $CaSO_4$ precipitation revealed the trend: SW0NaCl-4SO_4^{2-} > SW0NaCl > SW > VB. The calculated values are shown in Figure 6. It is important to note that the amount of soluble SO_4^{2-} ion present in the brine solution only partially correlates with the observed oil recovery while the amount of fines formation taking place completely correlates

with the observed oil recovery. The oil recovery observed for SW and SW0NaCl are two cases where the concentration of soluble SO_4^{2-} ion do not correlate to the observed oil recovery. Comparing SW with SW0NaCl, it is observed that the decrease in NaCl concentration in the brine decreases the solubility of $CaSO_4$. Thus the amount of soluble SO_4^{2-} ion in the solution decreases and the amount of fines formation increases. This increase in fines formation completely correlates with the reported oil recovery.

Data set 4: (Awolayo et al. 2014)

The fourth set of experiments includes water flooding of oil wet limestone cores (Awolayo et al. 2014). In this study 3 core samples from Middle East limestone reservoirs were examined with different brine combinations. Herein, in the 3 core plugs the following series of brine injection was conducted: Core Plug 1: FW→SW→SW#0.5S; Core Plug 2: FW→SW→SW#4S; Core Plug 3: FW→SW#2S→SW#4S→SW#8S. Herein SW#nS indicate sea water with n times SO_4^{2-} concentration. The core flooding experiment was conducted at 110°C and 206 bars. For each of the three fore flooding experiments the corresponding amounts of soluble SO_4^{2-} ion in the different brine solutions at 110°C and 206 bars were calculated using Extended UNIQUAC model. The possibility of fines formation because of precipitation of $CaSO_4$ was also calculated. As previously proposed (Austad et al. 2005) the change in brine composition because of substitution of Ca^{2+} by Mg^{2+} on calcite surface was included.

In core plug 1; 75.5% of OOIP was produced during FW injection, subsequently injection of SW showed 6.86% increment in oil production. But thereafter injection of SW#0.5S did not produce any additional oil recovery. As shown in Figure 7 the calculated amount of soluble SO_4^{2-} ion present showed the following trend: FW>SW0.5S~SW while amount of fines formation because of $CaSO_4$ precipitation revealed the trend: FW>SW0.5S>SW. Herein thus no increase in oil production during injection of SW#0.5S after flooding with SW can be correlated to both the soluble fraction as well the insoluble fine fraction, as the amount of soluble , as the amount of soluble SO_4^{2-} and insoluble $CaSO_4$(s) reduced when SW0.5S was injected. The calculated values are shown in Figure 7.In core plug 2; 71.1% of OOIP was produced during FW injection, subsequently injection of SW showed 5.7% increment in oil production; thereafter injection of SW#4S produced 3.1% additional oil recovery. As shown in Figure 7 the calculated amount of soluble SO_4^{2-} ion and insoluble fine formation showed the following trend: FW>SW>SW#4S. Thus continued increase in oil production during both injections of SW and SW#4S correlates to the amount of fine formation and amount of soluble SO_4^{2-} ion present in the coreplug. In core plug 3; 66.6% of OOIP was produced during FW injection, subsequently injection of SW#2S showed 2.89% increment in oil production; thereafter injection of SW#4S produced 5.71% additional oil recovery. But subsequently injection of SW#8S produced only 1.11% additional oil recovery. As shown in Figure 7 the calculated amount of soluble SO_4^{2-} showed the following trend: FW>SW#2S >SW#4S>>SW#8S while amount of fines formation because of $CaSO_4$ precipitation revealed the trend: FW>SW#2S >SW#4S~SW#8S. Herein the amount of soluble sulphate was significantly higher for SW#8S as compare to SW#4S, but no major increase in oil production was observed. While the amount of fine formation in the core plug for SW#8S was marginally greater than SW#4S. Thus Observed minor increase in oil recovery during injection SW#8S after being flooded with SW#4S perfectly correlates to the fine formation, and not to the amount of soluble SO_4^{2-} ion present in the coreplug. Overall in this study it was concluded that SW#4S was the most suitable brine composition for optimum oil recovery. Herein among the compared brines the amount of fine formation taking place for SW#4S also showed an optimum behavior beyond which further increasing sulphate concentration did not lead to major increase in fine formation or oil recovery. Thus increase in fines formation (and corresponding emulsification of oil) completely correlates with the reported oil recovery.

Data set 5: (Zhang and Austad 2006)

The fifth set of experiments includes spontaneous imbibition into oil-saturated Stevns Klint out crop chalk core plugs (Zhang and Austad 2006). In this study 16 core samples where studied at 70°C, 100°C and 130°C and two different types of oil having acid number 0.55 and 2.07 mgKOH/g was used. Herein the 5 core plugs was flooded each at 70°C, 100°C and 130°C with different with the following brines: SSW-0S, SSW-½S, SSW, SSW-2S and SSW-4S. At 100°C an additional experiment was conducted with SSW-3S brine. The observed oil recovery trend was: SSW-US < SSW-½S < SSW < SSW-2S <SSW-3S < SSW-4S at all three different temperatures. Herein at major increase in oil production was observed for initial increase in sulphate concentration. i.e. from SSW-0S to SSW-2S, increment by 38 % of OOIP was observed; while further increase sulphate concentration (i.e. from SSW-2S to SSW-4S) showed only increment by 6% of OOIP (as shown in figure 8). The corresponding amount of soluble SO_4^{2-}, total soluble potential ions, precipitation on injection and insoluble fine formation was calculated at reservoir condition. The same oil (with acid number 2.07 mg KOH/g) and same imbibing conditions was used 100°C to 130°C for the experiments, thus direct correlation between the two sets of experiments can be conducted; while different crude oil with acid number 0.55 mg KOH/g was used.

The amount of soluble SO_4^{2-} in the pore space was also calculated at the experimental condition and was plotted in Figure 8.Herein it is observable that the amount of soluble SO_4^{2-} for all different brines decreases with increase in temperature. But, the oil production has been consistently increasing during change in temperature from 100°C to 130°C for all the respective brines. Thus (considering the effect of temperature) soluble SO_4^{2-} show negative correlation to oil production; which is contrary to the proposed wettability alteration mechanism (Strand et al. 2008). Furthermore with increase in injection brine SO_4^{2-} concertation the amount of soluble sulphate also increase in the pore space as shown in figure 8. This shows good correlation to the observed in-

crease in oil production with increase in injection brine SO_4^{2-} composition. But major increase in oil production tokes place during initial increase in SO_4^{2-} composition of the injection brine (i.e. from SSW-0S to SSW-2S) and only minor increment take place thereafter (i.e. form SSW-2S to SSW-4S). While no such trend in observed for soluble SO_4^{2-} concentration in reservoir condition. Essentially prominent increase in soluble SO_4^{2-} concentration in reservoir condition (particularly at 130°C) is observed for increase in injection brine concentration from SSW-2S to SSW-4S; which is opposite to the reported oil recovery pattern.

This shows that the injection brine composition and the brine composition in the reservoir are not same. The reported increase in oil production is for increase in SO_4^{2-} composition of injection brine at ambient condition. But the interacting brine in the pore space at the imbibing condition no longer have the same brine/ SO_4^{2-} composition because of major change in brine speciation following alteration in pressure temperature condition and mineral substitution on calcite surface.

The calculated amount of total soluble potential ions showed a steady decrease for increasing sulphate concentration beyond that in sea water (i.e. SSW) (as shown in figure 8). Particularly for SSW-2S a consistent decrease in total soluble potential ions was observable for all at all three temperatures. With increase temperature to 130°C this decrease in sulphate concentration for increase in SO4 concentration in injection brine became more prominent. Further increasing sulphate concentration beyond SSW-2S showed a consistent increase in reservoir total soluble potential ions composition. But in the oil production no such decrease in oil production is observed for SSW-2S as compare to SSW at any temperature. Therefore oil production show no consistent correlation to total potential ions as previously proposed (Strand et al. 2008). In fact the observed oil recovery shows a major increase in oil production from SSW-0S to SSW-2S (following an increment by 38 % of OOIP) and thereafter from shows a relatively minor increase (form SSW-2S to SSW-4S by 6% of OOIP). Thus major increase in oil production can be observed even when the total soluble potential ions in the pore space decreases. And steady increase in total soluble potential ions (i.e. from SSW-2S to SSW-4S) may not necessarily lead major increase in oil recovery. Thus the total soluble potential ions do not correlate to reported oil productions for the conducted spontaneous imbibition study.

Furthermore the amount of precipitation taking place on injection due to changes in pressure and temperature condition (from ambient condition to imbibing experimental condition) was calculated using Extended UNIQUAC model. As shown in figure 8 it was observed that significant precipitation was taking place on injection of SW4S, SW3S and SW2S at 130°C, and SW3S and SW4S at 100°C. The amount of precipitation formation also increased with increase in the SO_4^{2-} composition of the injection brine at both 130°C and 100°C. Although formation of precipitation has been recommended to be avoided (Stand et al. 2008), yet herein with increase oil recovery is observed with precipitating brines. Furthermore for the precipitating brines the observed oil recovery trend is: SW4S at 130°C> SW3S at 130°C > SW2S at 130°C> SW4S at 100°C> SW3S at 100°C. The amount of precipitation taking place is also of the following trend: SW4S at 130°C> SW3S at 130°C > SW2S at 130°C> SW4S at 100°C> SW3S at 100°C. Thus the expected negative correlation is observed between precipitation amount and oil recovery. But precipitation also does not show a complete correlation to oil production as for the experiments at 70°C there is no observed precipitation on injection, yet there is a consistent increase in oil production for increase in the SO_4^{2-} composition of the injection brine. Furthermore at higher temperatures major increase in oil production takes place for initial increase in sulphate concentration i.e from SSW-0S to SSW-2S. But, none of these brines show any precipitation on injection at the imbibing conditions. Thus significant increase in oil recovery can take place for precipitating brines, and no direct negative correlation between precipitation and oil recovery is observed. But, in the reported study major variation in oil recovery can takes place even when no precipitation takes place, thus precipitation cannot be the driving mechanism.

The amount of fine formation taking place in the coreplug was also calculated the different imbibition experiment and was plotted in Figure 8. The amount of fines consistently increased with increase in SO_4^{2-} concentration on the injection brine, correspondingly the oil production also increased with increase in SO_4^{2-} concentration on the injection brine for all core flooding experiments conducted at different respective temperatures. With increase in temperature both the amount of fine formation and oil production shows steady increase for all imbibing brines. At higher temperature (130°C) major increase in fine formation is observed from SSW-0S to SSW-2S, thereafter precipitation on injection start taking place and relative minor increase is fine formation is observed from SSW-2S to SSW-4S. The oil production also show major increase in production during initial increase in SO_4^{2-} composition of the injection brine (i.e. from SSW-0S to SSW-2S), while minor increase is reported thereafter (form SSW-2S to SSW-4S). This shows that over variation in injection sulphate composition and imbibition temperature, the amount of oil trend and the amount of oil production show a good consistent correlation to the corresponding amount of fine formation taking place after ion substitution. No other brine property show similar consistent correlation. Thus fine based emulsification (Chakravarty et al. 2015a; Chakravarty et al. 2015b) may have possibly caused the observed increase in oil recovery.

Data set 6: (Strand et al. 2003)

The sixth set of experiments includes spontaneous imbibition study of oil saturated chalk cores (Strand et al. 2003). In this study 3 core samples from Stevns Klint chalk were examined with different SO_4^{2-} concentration but in combination with cationic C_{12}TAB emulsifying. Herein, spontaneous imbibition into 3 oil-saturated chalk cores was conducted using SW1.7S (sea water with C_{12}TAB and 1.7 g/l sulphate); SW0.4S (sea water with C_{12}TAB and 0.4 g/l sulphate); and SW0.07S (sea water with C_{12}TAB and 0.07 g/l sulphate). The total acid number of the used oil was 1.04 mg of KOH/g. The obtained oil recovery trend was: SW1.7S> SW0.4S> SW0.07S. The corresponding amounts of soluble SO_4^{2-} ion in the different brine solutions at were calculated using

Extended UNIQUAC model. The possibility of fines formation because of precipitation of $CaSO_4$ was also calculated. As previously proposed (Austad et al. 2005) the change in brine composition because of substitution of Ca^{2+} by Mg^{2+} on calcite surface was included. Both the calculated amount of soluble SO_4^{2-} ion present in the different brine solutions and amount of fines formation because of $CaSO_4$ precipitation revealed the following trend: SW1.7S> SW0.4S> SW0.07S. Thus when amount of fine formation correlates to oil recovery, when smart water EOR is implemented along with other EOR technologies, viz. cationic surfactant. Therefore the effect of fines-based emulsification in EOR is also observable in Mixed EOR studies.

Data set 7: (Fernø et al. 2011)

The seventh set of experiment includes spontaneous imbibition study of oil saturated chalk cores from three different sources including Stevns Klint, Rørdal Chalk (Denmark), and Niobrara Chalk (US) (Fernø et al. 2011). In this study 32 core samples was water flooded with different wettability and water compositions at 130°C.

In the first experiment spontaneous imbibition into 6 unaged coreplugs were conducted. Herein 2 coreplugs each from Stevns Klint, Rørdal, and Niobrara Chalk was used. 3 coreplugs (on from each pair) was flooded with SW-0S and the rest three with SW-4S. To maintain complete water wetness decane was used as for oil saturation, thus the injection oil has no polar fractions. The Sulphate enriched showed no increase in oil production for water wet decane oil for all three core plugs. The conducted Extended UNIQUAC calculation show that SW-4S led to significant fine formation and precipitation. But the used oil (decane) did not contain any polar fraction; therefore fine interaction with oil shall not lead to any emulsification of residue oil (as previously observed Chakravarty et al. 2015a). So no increase in oil production for non-polar decane perfectly correlates to no fine based emulsification of residue oil for variation in sulphate concentration.

In the second set of spontaneous imbibition experiment 26 aged coreplugs including Stevns Klint (13 core plugs), Rørdal (6 core plugs) and Niobrara (7 core plugs) was reported. Imbibition of SW-0S and SW-4S was conducted into various coreplugs with varying wettability. Herein the core plugs were oil flooded with crude oil at constant differential pressure (2bar/cm) at 80°C. At irreducible water saturation the flow of oil injection was reduced to $1.5cm^3/h$ and continuous injection of polar fraction containing crude oil injection was continued during the aging process. This provided ample amount time and polar fraction to get adsorbed on the mineral surface. After aging 5 PV decane was injected into the coreplug to avoid asphaltene precipitation. Thus before imbibition the coreplug contained majority if decane with mineral adsorbed polar fractions of crude oil. Thus the amount of adsorption of polar fraction from the initially injected crude oil affected the final wettability of coreplug (for core preparation processes). So core plugs with lower water wettability had higher fraction of polar oil initial adsorbed on the mineral surface.

Imbibition experiments with Stevns Klint chalk showed prominent influence of mineral wettability on oil production during imbibition of different sulphate brines. Core plugs with mixed wet Stevns Klint chalk showed an average increase in 6% of OOIP for imbibition of SW-4S (when compared to the corresponding oil recovery fir SW-0S). While completely oil wet core plugs showed an average increase in 20% of OOIP for imbibition of SW-4S (when compared to the corresponding oil recovery fir SW-0S). Oil wet coreplugs ($0.08 < I_w < 0.2$) ensures that formation water did not have access to the mineral surface and mineral substitution had not taken place during aging process, thus on imbibition of SW-4S into coreplug ion substitution on the entire pore surface is possible. Thus the amount of possible ion substitution for oil wet coreplugs is relatively greater. While mixed wet coreplugs ($I_w > 0.2$) already has a considerable fraction of the mineral surface which has been in contact with the Mg containing formation brine. Thus during aging (in absence of SO_4^{2-}) a fraction of ion substitution may have already take place. Therefore initial wettability determines fraction of mineral surface available for ion substitution during smart water imbibition. This in turn affects the corresponding amount of supersaturation of brine after ion substitution on the mineral surface. Figure 10 shows the amount of fine formation taking place for different extent of ion substitution on the calcite surface. Thus the strongly oil wet core plugs may provide significantly higher fractions of (virgin calcite) surfaces where ion substitution could have taken place spontaneous imbibition.

Similar spontaneous imbibition experiment was conducted for coreplugs from Rørdal (6 core plugs) and Niobrara (7 core plugs) chalks. It was observed that SW-4S did not show any major increase in oil productions (as compared to their SW-0S analogs) irrespective of variation in initial mineral wettability. As shown in Figure 10, the used brines where significantly supersaturated at the imbibition conditions. Thus significant amount of precipitation do take place irrespective of extend of ion substitution taking place inside the coreplug. Thus effective fine formation is the total amount of fine formation taking place inside the coreplug minus the amount taking place on injection. Therefore the fine formation in the pore space only becomes dominant when at least 20% of the injected brine undergoes ion substitution. And extent of ion substitution has shown to be significantly coreplug dependent; viz. Advanced Ion Management (AIM) studies show that Middle East coreplugs undergo 7.54% Mg^{2+} ion substitution (Gupta et al. 2011; Vo et al. 2012) while other Middle East coreplugs have shown 50% Mg^{2+} ion substitution (Shariatpanahi et al. 2010). Therefore it is possible that Rørdal and Niobrara core plugs may have had less than 20% Mg^{2+}/ Ca^{2+} ions substitution could have taken place. Thus no observed increase in oil recovery was observed for SW-4S for Rødral and Niobrara while prominent

increase oil production (by 20% of OOIP) in Stevns Klint chalk was observed. Nevertheless further analysis of extent of ion substitution for Rødral and Niobrara chalks shall be required to scrutinize this possibility.

Data Set 8: (Hognesen et al. 2005)

The 8th data set of experiment includes spontaneous imbibition study of Stevns Klint at 90°C, 110°C and 130°C using SSW-US (sea water without SO_4^{2-}) , SSW (sea water) and SSW-3S (sea water with 3 times SO_4^{2-}) (Hognesen et al. 2005). In the first two experiments first coreplugs where imbibed with SSW-US for 8 days and thereafter SSW-3S was used as the imbibing fluid. Both coreplugs initially produced 11% of OOIP, while imbibing with SSW-3S led to production of 60% OOIP at 130°C. The corresponding amount of fine formation was calculated using Extended UNIQUAC model. Herein as shown in figure 11; it was Extended UNIQUAC calculation showed that the amount of fine formulation taking place after ion substitution for SSW-US was 0.06g/l while for SSW-3S was 6.1 g/l. Thus the observed major increase in oil recovery is coherent with significant increase in fine formation as well. In the second set two core plugs was imbibed with the following brines pattern at 110°C: SSW-US (8 days); SSW (17 days); SSW3S (15 days). Both coreplugs showed reproducible similar production profile. The oil production amount was: SSW-US 8% of OOIP; SSW 15% of OOIP; SSW-3S 25% of OOIP. The Extended UNIQUAC calculation corresponding show that the amount of fine formation taking place in the coreplug after ion substitution at 110°C was: SSW-US 0.05g/l; SSW 1.6g/l; SSW-3S; 5.4g/l. Therefore a steady increase in fine formation for a corresponding increase in oil recovery was observed. In the third set two core plugs was imbibed with the same brines pattern at 90°C. The reported oil production amount was: SSW-US 7% of OOIP; SSW 13% of OOIP; SSW-3S 20% of OOIP. As shown in figure 11 the Extended UNIQUAC calculation showed the amount of fine formation for the brines in the pore space at 90°C was: SSW-US 0.04g/l; SSW 0.8g/l; SSW-3S; 5.4g/l. Hence increment in oil recovery shows reproducible correlation to the amount of fine formation taking place in the coreplug following ions substitution in the mineral surface. Furthermore it must be noted that the amount of oil production taking place consistently increased with increased in temperature from 20% of OOIP for SSW-3S at 90°C to 61% of OOIP for SSW-3S at 130°C. Correspondingly the amount of fine formation also increased with increase in temperature and injection brine SO_4^{2-} concentration. But as shown in figure 11 e and f, the amount of soluble SO_4^{2-} consistently decreased with increase in the coreplug temperature. Thus only fine formation taking place in the coreplug after ions substitution shows consistent correlation to the observed oil recovery. Furthermore the fine formation in the coreplug is around 2g/l to 6g/l depending upon temperature and injection brine SO_4^{2-} concertation. The amount of soluble sulphate present in the coreplug after ion substitution is also around 0.8g/l to 4g/l. Thus the amount of fine formation is comparable to the soluble fraction and thus formation of these fines is not negligible and cannot be ignored.

Data Set 9: (Yi and Sarma 2005)

The 9th data set of smart waterflooding experiment into Middle East limestone coreplug has been studied (Yi and Sarma 2005). Herein reservoir coreplugs with average porosity of 25% and low permeability of 1.3mD was used for water flooding. The coreplug was flooded with Ca^{2+} rich formation brine for 4 PV; thereafter SW was injected for 2.5 PV and finally $CaMg4SO_4$ i.e. four times enriched SO_4^{2-} was flooded for 3.5 PV. Injection FW showed oil production of 68.43 %OOIP, thereafter injection of SW showed increment in oil production by 7.47% of OOIP and finally $CaMg4SO_4$ showed an increment of oil production by 18.66 %OOIP at 120°C. The correspond amount of fine formation and precipitation was calculated at 120°C using Extended UNIQUAC model. The amount of fine formation taking place was: FW 0 g/l; SW 3.5 g/l and CaMg4SO4 8.91 g/l. While the amount of precipitation taking place was: FW 0 g/l; SW 0 g/l and CaMg4SO4 1.14 g/l. This shows that increase in oil recovery during flooding of SW and thereafter major increase in oil recovery during flooding of CaMg4SO4 shows a direct correlation to the amount fine formation. As significantly high amount of fine formation and oil production takes place on injection of CaMg4SO4 brine in the reservoir. Furthermore CaMg4SO4 shows considerable amount of precipitation formation on injection. No precipitation is observed during increase in oil production following injection of SW but significant increase in oil recovery is observed when precipitation with CaMg4SO4 takes place. Thus no direct correlation between precipitation and oil production can be made. But this also shows that precipitating supersaturated brines may not necessarily choke coreplugs and always have an adverse effect (as previously proposed Tweheyo et al. 2006). And a (on injection) precipitating brine can cause significant increase in oil production if the fine formation taking place in the coreplug is dominant over the injection precipitation.

Conclusion:

In most previous core flooding studies, properties of the injected brines have been correlated with the observed oil recovery. But ion substitution on the mineral surface can change the composition and properties of the injected brine significantly. This study suggests that properties of the brine present in the pore space – after substitution - should be correlated with the reported oil recovery.

1. No selective increase in oil recovery for the brines for variation in SO_4^{2-} (in absence of Ca^{2+} or Mg^{2+}) perfectly correlates to the fine formation as no precipitation of $CaSO_4$ can be obtained.
2. Secondly increase in oil recovery with injection of cations is also explained by the fine formation mechanism. Selective injection of Ca^{2+} (in absence of Mg^{2+}) in SO_4^{2-} containing brine leads to fine formation during the interaction of the injected brine with the existing brine.

3. The observed oil recovery trend at 100 °C after injection of cation perfectly correlates to the amount of fine formation taking place due to the interaction between the two.
4. Furthermore the final oil recovery observed at 130 °C also correlates to the calculated amount of fine formation at the same temperature pressure condition; while amount of Soluble SO_4^{2-} present in the injecting brine only partially correlates to the observed oil recovery.
5. Moreover the increase in oil recovery with increase in temperature also correlates the increase in fine formation, while the opposite trend is observed for amount of soluble $S0_4^{2-}$ and total potential ions present in the interacting brine.

References

- Akbar, M., Vissapragada, B., Alghamdi, A. H., Allen, D., Herron, M., Carnegie, A., & Saxena, K. (2000). A snapshot of carbonate reservoir evaluation.*Oilfield Review*, **12** (4), 20-21.
- Austad, T., Strand, S., Høgnesen, E. J., & Zhang, P. (2005, January). Seawater as IOR fluid in fractured chalk. In *SPE International Symposium on Oilfield Chemistry*. Society of Petroleum Engineers.
- Awolayo, A., Sarma, H., & AlSumaiti, A. M. (2014, March). A Laboratory Study of Ionic Effect of Smart Water for Enhancing Oil Recovery in Carbonate Reservoirs. In SPE EOR Conference at Oil and Gas West Asia. Society of Petroleum Engineers.
- Bagci, S., Kok, M. V., & Turksoy, U. (2001). Effect of brine composition on oil recovery by waterflooding. *Petroleum science and technology*, **19**(3-4), 359-372.
- Chakravarty, K. H., Fosbøl, P. L., & Thomsen, K, (2015) Interactions of Fines with Oil and its Implication in Smart Water Flooding In *SPE Bergen One Day Seminar*, Society of Petroleum Engineers
- Christensen, S. G., & Thomsen, K. (2003). Modeling of vapor-liquid-solid equilibria in acidic aqueous solutions. *Industrial & engineering chemistry research*, **42** (18), 4260-4268.
- Thomsen, K., Rasmussen, P., & Gani, R. (1996). Correlation and prediction of thermal properties and phase behaviour for a class of aqueous electrolyte systems. *Chemical Engineering Science*, **51** (14), 3675-3683.
- Fathi, S. J., Austad, T., & Strand, S. (2010). "Smart Water" as a Wettability Modifier in Chalk: The Effect of Salinity and Ionic Composition. Energy & fuels, **24** (4), 2514-2519.
- Fathi, S. J., Austad, T., & Strand, S. (2011). Water-based enhanced oil recovery (EOR) by "smart water": Optimal ionic composition for EOR in carbonates. Energy & fuels, **25** (11), 5173-5179.
- García, A. V., Thomsen, K., & Stenby, E. H. (2006). Prediction of mineral scale formation in geothermal and oilfield operations using the Extended UNIQUAC model: Part II. Carbonate-scaling minerals. *Geothermics*, **35** (3), 239-284
- García, A. V., Thomsen, K., & Stenby, E. H. (2005). Prediction of mineral scale formation in geothermal and oilfield operations using the extended UNIQUAC model: part I. Sulfate scaling minerals. *Geothermics*, **34** (1), 61-97.
- Gupta, R., Griffin, P., Hu, L., Willingham, T. W., Cascio, M. L., Shyeh, J. J., & Harries, C. R. (2011). Enhanced waterflood for Middle East carbonate cores–impact of injection water composition. *paper SPE*, *142668*.
- Hognesen, E. J., Strand, S., & Austad, T. (2005, January). Waterflooding of preferential oil-wet carbonates: Oil recovery related to reservoir temperature and brine composition. In *SPE Europec/EAGE Annual Conference*. Society of Petroleum Engineers.
- Iliuta, M. C., Thomsen, K., & Rasmussen, P. (2000). Extended UNIQUAC model for correlation and prediction of vapour–liquid–solid equilibria in aqueous salt systems containing non-electrolytes. Part A. Methanol–water–salt systems. *Chemical Engineering Science*, **55** (14), 2673-2686.
- Kazankapov, N. (2014, October). Enhanced Oil Recovery in Caspian Carbonates with" Smart Water". In *SPE Russian Oil and Gas Exploration & Production Technical Conference and Exhibition*. Society of Petroleum Engineers.
- Puntervold, T., Strand, S., & Austad, T. (2009). Coinjection of seawater and produced water to improve oil recovery from fractured North Sea chalk oil reservoirs. *Energy & fuels*, **23**(5), 2527-2536.
- Puntervold, T., Strand, S., & Austad, T. (2007). Water flooding of carbonate reservoirs: Effects of a model base and natural crude oil bases on chalk wettability. Energy & fuels, 21(3), 1606-1616.
- Shariatpanahi, S. F., Strand, S., & Austad, T. (2010). Evaluation of Water-Based Enhanced Oil Recovery (EOR) by Wettability Alteration in a Low-Permeable Fractured Limestone Oil Reservoir. *Energy & Fuels*, *24*(11), 5997-6008.
- Strand, S., Austad, T., Puntervold, T., Høgnesen, E. J., Olsen, M., & Barstad, S. M. F. (2008). "Smart Water" for Oil Recovery from Fractured Limestone: A Preliminary Study. Energy & fuels, **22** (5), 3126-3133.
- Strand, S., Høgnesen, E. J., & Austad, T. (2006). Wettability alteration of carbonates—Effects of potential determining ions (Ca^{2+} and SO_4^{2-}) and temperature. *Colloids and Surfaces A: Physicochemical and Engineering Aspects*, **275**(1), 1-10.
- Thomsen, K., & Rasmussen, P. (1999). Modeling of vapor–liquid–solid equilibrium in gas–aqueous electrolyte systems. Chemical Engineering Science, 54 (12), 1787-1802.
- Tweheyo, M. T., Zhang, P., & Austad, T. (2006, January). The effects of temperature and potential determining ions present in seawater on oil recovery from fractured carbonates. In *SPE/DOE Symposium on Improved Oil Recovery*. Society of Petroleum Engineers.

- Vo, L. T., Gupta, R., & Hehmeyer, O. J. (2012, January). Ion chromatography analysis of advanced ion management carbonate coreflood experiments. In *Abu Dhabi International Petroleum Conference and Exhibition*. Society of Petroleum Engineers.
- Yi, Z., & Sarma, H. K. (2012, January). Improving Waterflood Recovery Efficiency in Carbonate Reservoirs through Salinity Variations and Ionic Exchanges: A Promising Low-Cost" Smart-Waterflood" Approach. In *Abu Dhabi International Petroleum Conference and Exhibition*. Society of Petroleum Engineers.
- Zahid, A., Stenby, E. H., & Shapiro, A. A. (2010, June). Improved Oil Recovery in Chalk: Wettability Alteration or Something Else? (SPE-131300). SPE EUROPEC. In EAGE Annual Conference and Exhibition, Barcelona, Spain.
- Zahid, A., Sandersen, S. B., Stenby, E. H., von Solms, N., & Shapiro, A. (2011). Advanced waterflooding in chalk reservoirs: Understanding of underlying mechanisms. *Colloids and Surfaces A: Physicochemical and Engineering Aspects*, **389**(1), 281-290.
- Zekri, A. Y., Nasr, M. S., & Al-Arabai, Z. I. (2011, January). Effect of LoSal on Wettability and Oil Recovery of Carbonate and Sandstone Formation. In *International Petroleum Technology Conference*. International Petroleum Technology Conference.
- Zhang, P., & Austad, T. (2006). Wettability and oil recovery from carbonates: Effects of temperature and potential determining ions. *Colloids and Surfaces A: Physicochemical and Engineering Aspects*, **279**(1), 179-187a.
- Zhang, P., Tweheyo, M.T., Austad, T. (2006) Wettability alteration and improved oil recovery in chalk: The effect of calcium in the presence of sulfate. Energy and Fuels **20** (5), 2056-2062b
- Zhang, P., Tweheyo, M. T., & Austad, T. (2007). Wettability alteration and improved oil recovery by spontaneous imbibition of seawater into chalk: Impact of the potential determining ions Ca^{2+}, Mg^{2+}, and SO_4^{2-}. *Colloids and Surfaces A: Physicochemical and Engineering Aspects*, **301**(1), 199-208.

Tables:

Table 1: The optimized parameters (r and q) for different species in the Extended UNIQUAC model for calculating the speciation of different brine solutions. These parameters have been previously reported (Christensen and Thomsen 2003; García et al. 2006; García et al. 2005).

ion	r	q
H_2O	0,92	1,4
$CO_2(aq)$	0,74721	2,4496
Na^+	1,4034	1,199
K^+	2,2304	2,4306
Mg^{2+}	5,406	2,542
Ca^{2+}	3,87	1,48
Ba^{2+}	15,671	14,475
H+	0,13779	1E-16
Sr^{2+}	7,1446	12,894
Cl^-	10,386	10,197
SO_4^{2-}	12,794	12,444
OH^-	9,3973	8,8171
CO_3^{2-}	10,828	10,769
HCO_3^-	8,0756	8,6806

Table 2: The optimized interactions parameters for each pair of species used in the Extended UNIQUAC model for calculating the speciation of different brine solutions. These parameters have been previously reported (Christensen and Thomsen 2003; García et al. 2006; García et al. 2005).

	H_2O		CO_2(aq)		Na^+		K^+		Mg^{2+}		Ca^{2+}		Ba^{2+}		H^+		Sr^{2+}		Cl^-		SO_4^{2-}		OH^-		CO_3^{2-}		HCO_3^-	
	u0	ut	u0	ut	u0	ut	u0	ut	u0	ut	u0	ut	u0	ut	u0	ut	u0	ut	u0	ut	u0	ut	u0	ut	u0	ut	u0	ut
H_2O	0	0																										
CO_2(aq)	8,838	0,863	302,2	0,359																								
Na^+	733,3	0,487	172,4	-0,436	0	0																						
K^+	535	0,994	398,5	3,336	-46,19	0,119	0	0																				
Mg^{2+}	-2,043	-3,554	-581,8	-2,855	-70,96	1,339	-273,7	-1,079	0	0																		
Ca^{2+}	496,4	-8,065	2500	0	-100	-4,656	-275,6	-3,101	1	0	0																	
Ba^{2+}	-0,379	0,582	2500	0	779,1	2,338	100	1	628,5	0	2500	0	0	0														
H^+	10000	0	1E+09	0	1E+09	0	1E+09	0	1E+09	0	1E+09	0	1E+09	0	0	0												
Sr^{2+}	543,1	1,274	-100,7	0	-103,9	-0,62	100	1	-400,6	-1,437	-402,8	-4,253	2500	0	1E+09	0	0	0										
Cl^-	1523	14,63	1613	15,02	1443	15,64	1465	15,33	2049	12,13	1806	11,14	1403	14,89	1E+09	0	1896	15,69	2215	14,44								
SO_4^{2-}	752,9	9,491	1942	4,79	845,1	11,68	913,8	12,28	1407	3,328	1258	50,45	2500	0	1E+09	0	2500	10	2036	12,41	1266	8,319						
OH^-	600,5	8,546	2500	0	1398	20,28	1806	27,28	736,4	0	164,6	3,608	2500	0	1E+09	0	2500	0	1896	13,63	1226	8,59	1563	5,617				
CO_3^{2-}	361,4	3,352	2500	0	548	3,782	1857	4,06	99	1	2500	0	2500	0	1E+09	0	2500	0	2725	5,727	1217	7,007	1588	2,75	1458	-1,345		
HCO_3^-	577,1	-0,388	526,3	-3,734	1102	1,829	967,8	1,26	99	1	2500	0	2500	0	1E+09	0	2500	0	1737	14,04	990,5	6,965	2500	0	800	1,724	771	-0,02

Figures:

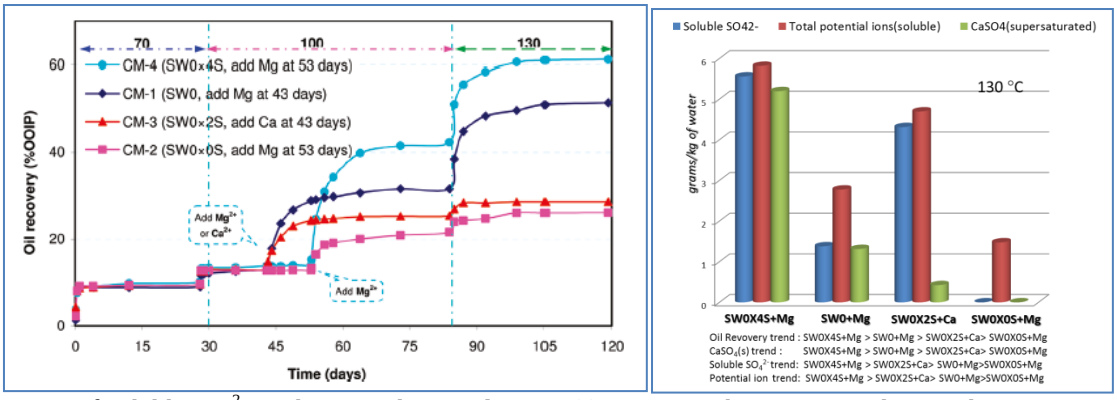


Figure 1:Amount of Soluble SO_4^{2-},total potential ion and $CaSO_4$(s) present in the interacting brine solution at 130 °C. The observed oil recovery perfectly correlated to the amount of fine formation, while only partial correlation is observed with Soluble SO_4^{2-} or total potential ion.

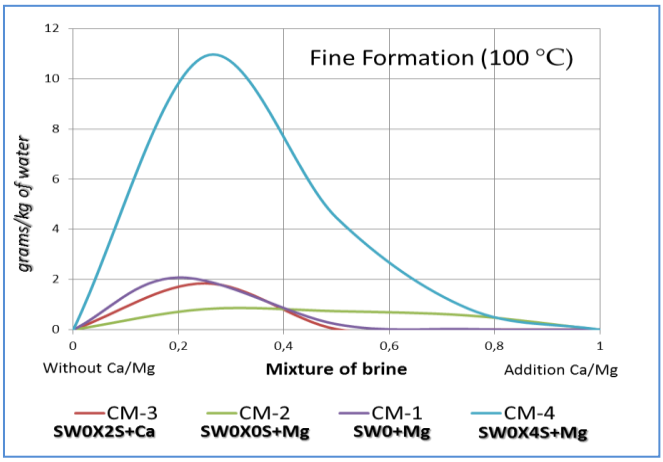


Figure 2:Amount of fine formation taking place at 100°C during interaction of the inject cations(Ca^{2+} or Mg^{2+}) with the existing brines (including SW0X2S , SW0X0S, SW0+Mg, SW0X4S+Mg). The exact same concentrations have been used as stated by Zhang et al. 2006.

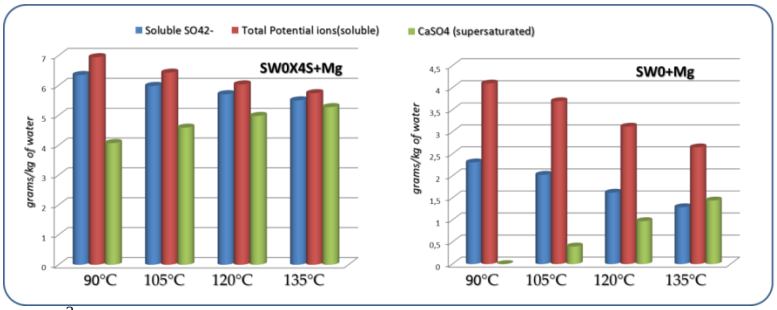


Figure 3: Amount of Soluble SO_4^{2-}, total potential ion and $CaSO_4$(s) present in the interacting brine solution at different temperatures. Significant increase in fine formation and decrease in amount of Soluble SO_4^{2-}, total potential ion is observed in SW0X4S+Mg and SW0+Mg. The exact same concentrations have been used as stated by Zhang et al. 2006.

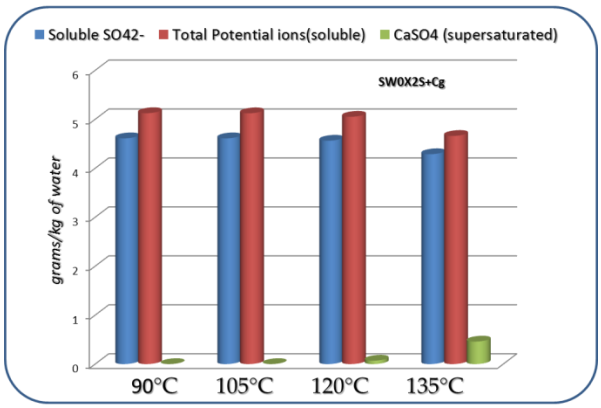


Figure 4: Amount of Soluble SO_4^{2-}, total potential ion and $CaSO_4$(s) present in the interacting brine solution at different temperatures. Only minute increase in fine formation is observed in SW0X2S+Ca while no major variation is observed in the amount of Soluble SO_4^{2-}, total potential ion present in the solution. The exact same concentrations have been used as stated by Zhang et al. 2006.

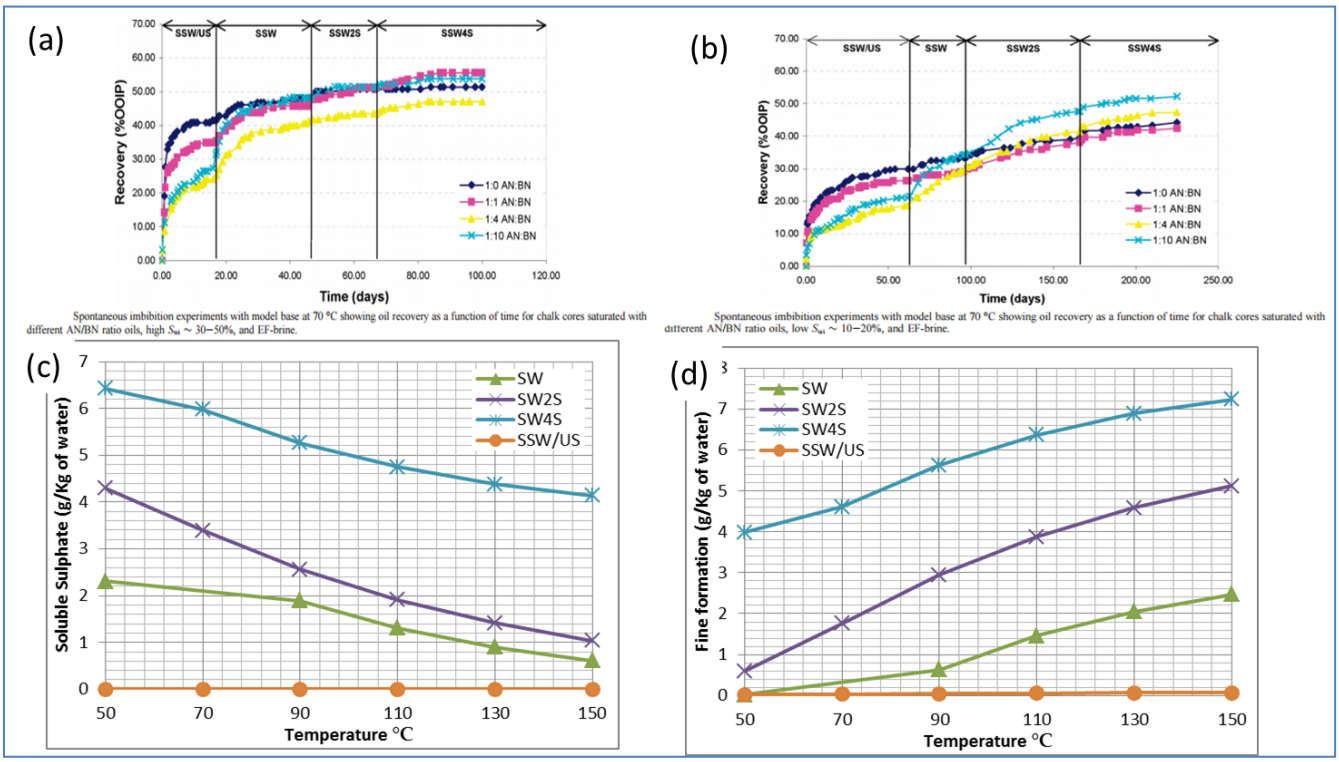


Figure 5 a&b: Spontaneous imbibition experiments (Puntervold et al. 2007) c&d: The calculated amounts of fines formation and soluble SO_4^{2-} in the solutions for each of the different brines used.

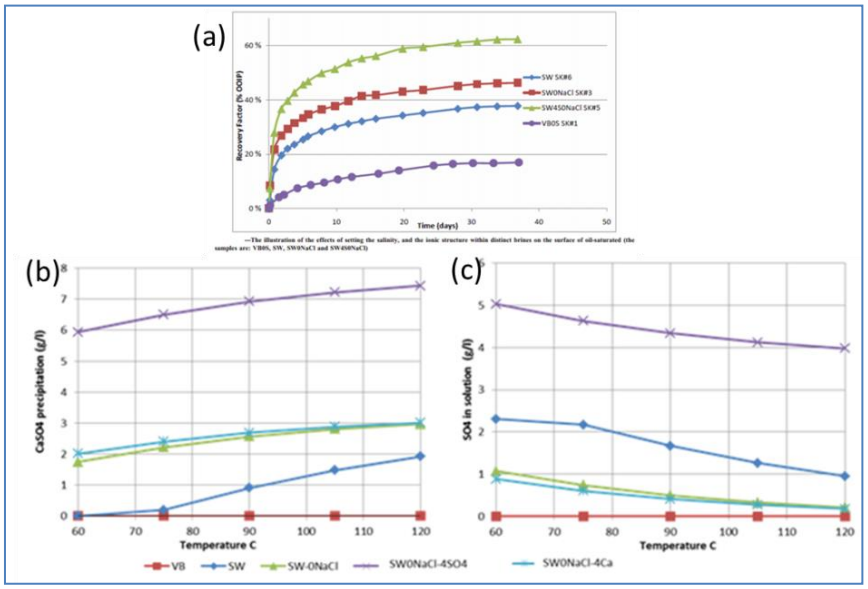


Figure 6 a: Spontaneous imbibition experiments (Kazankapov et al. 2007) b&c: The calculated amounts of fines formation and soluble SO_4^{2-} in the solutions for each of the different brines used.

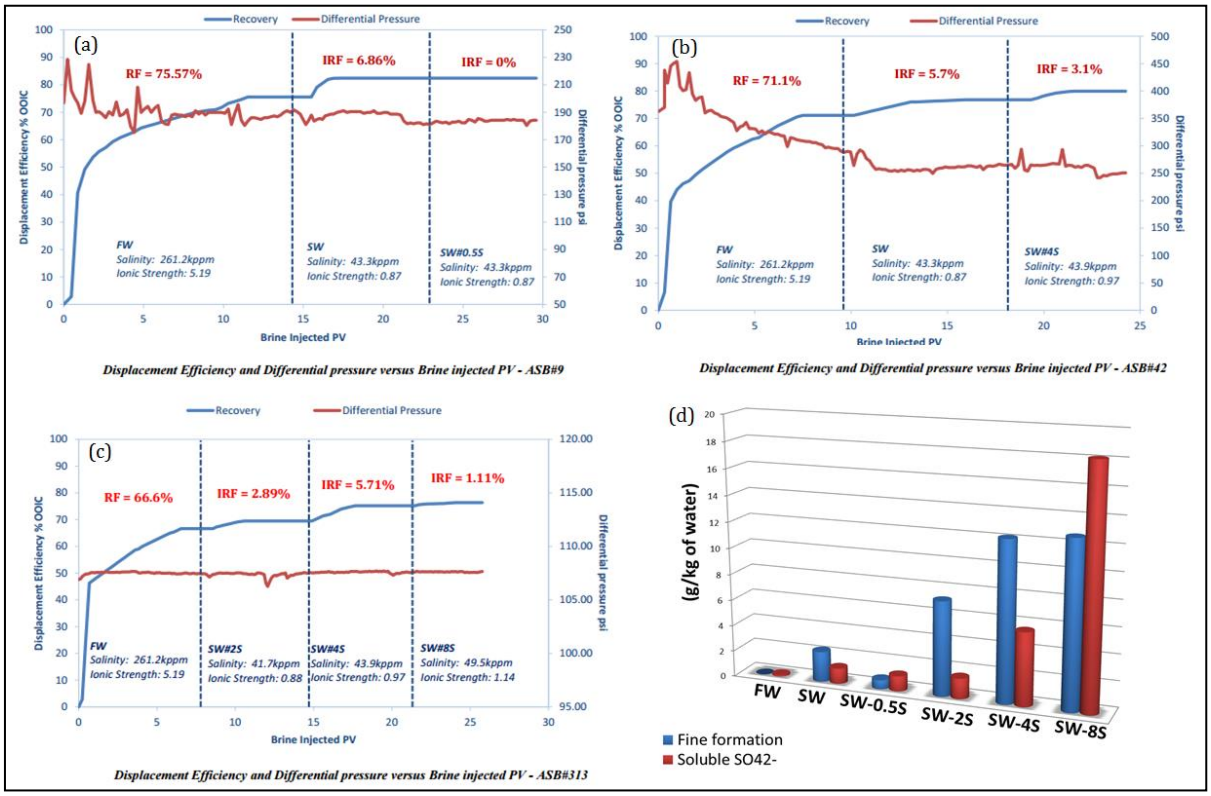


Figure 7 a-c: SW-4S showing the optimum increment in oil recovery during water flooding experiment into lime stone reservoirs coreplugs from Middle East. (Awolayo et al. 2014) d: The calculated amounts of fines formation and soluble SO_4^{2-} in the solutions for each of the different brines used also showing optimum amount of fine formation for SW4S and no additional fine formation for SW-8S.

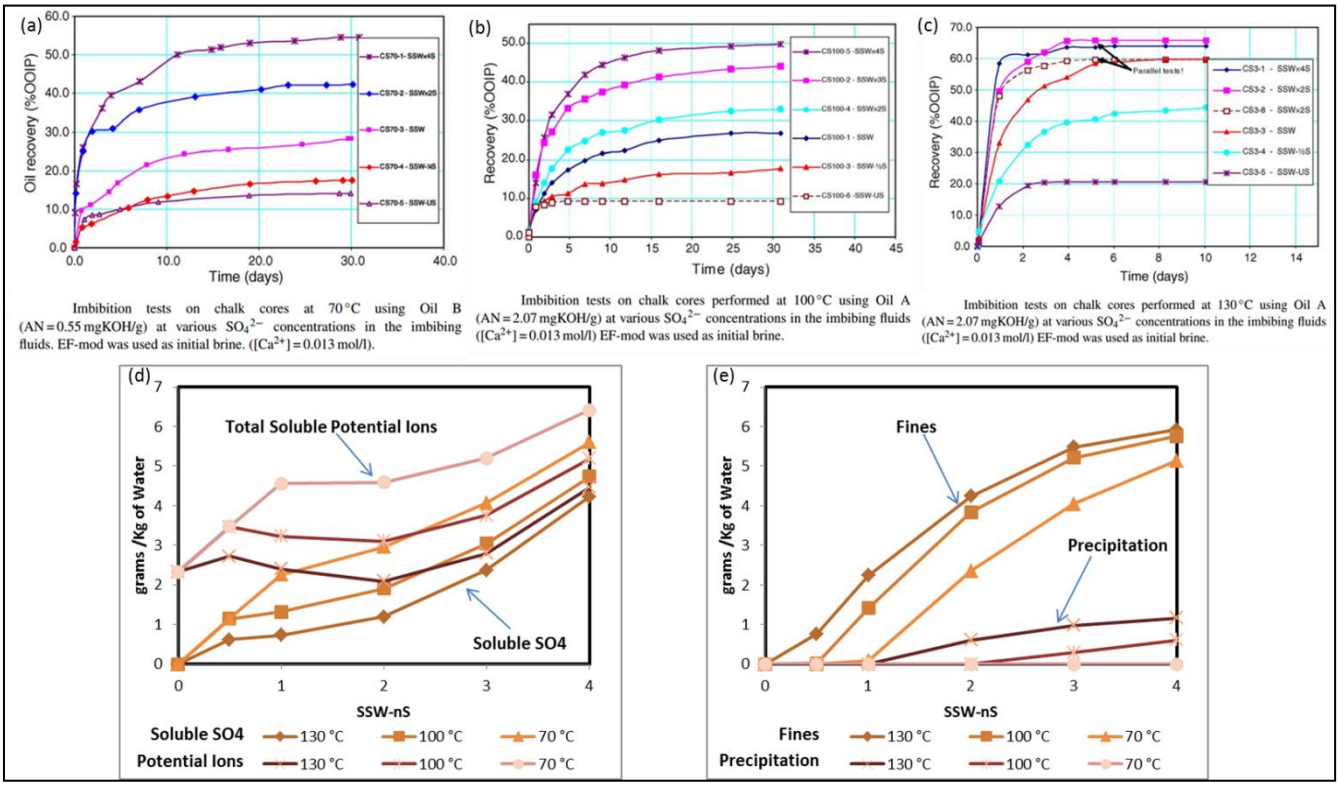


Figure 8: Reported spontaneous imbibition experiments (Zhang and Austad) b&c: The calculated amounts of fines formation, soluble SO_4^{2-} , precipitation and total soluble potential ions in the solutions for each of the different brines used at 70°C, 100°C and 130°C.

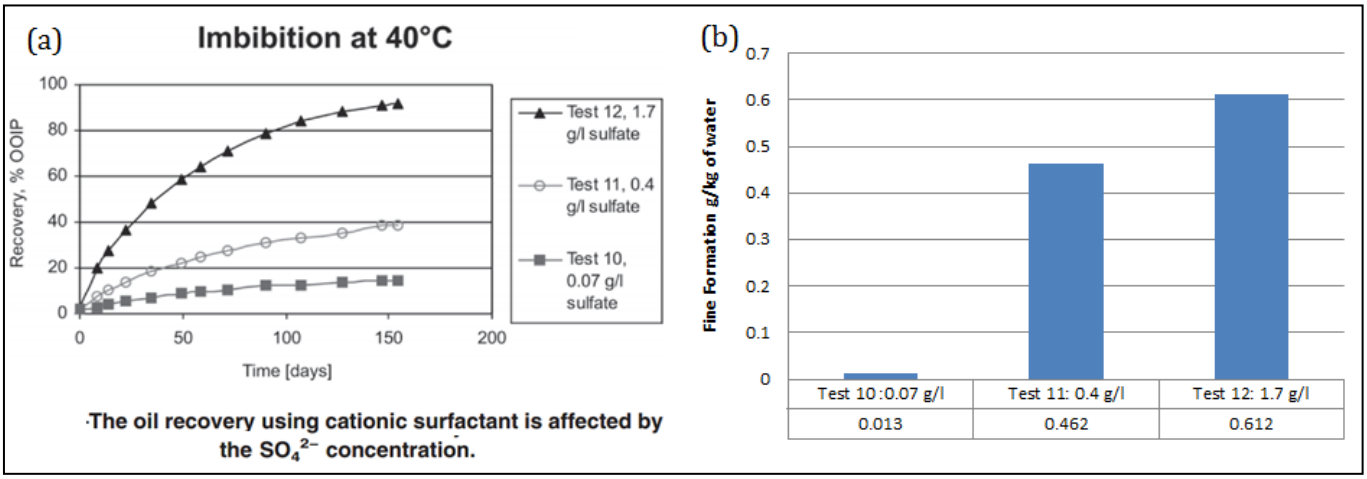


Figure 9 a: Spontaneous imbibition experiments for different concentration of sulphate in presence of surfactant (Strand et al. 2003) b: The calculated amounts of fines formation and soluble SO_4^{2-} in the solutions for each of the different brines used.

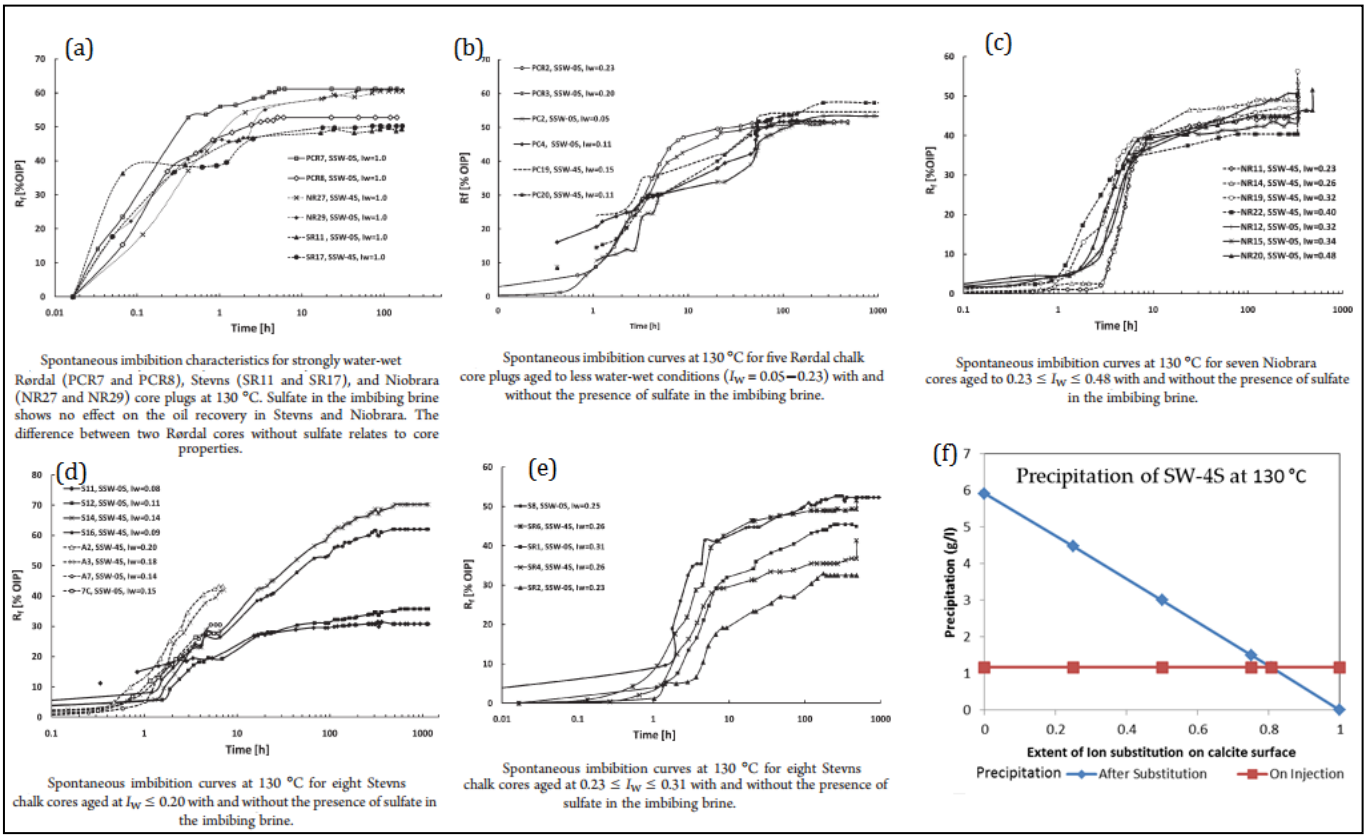


Figure 10: (a-e) Spontaneous imbibition into Stevns Klint, Rørdal, and Niobrara Chalks at 130°C using SW-0S and SW-4S for coreplugs with varied mineral wettability and aging conditions. (f) Amount of precipitation on injection and after ion substitution for different extent of ion substitution on the calcite surface for SW-4S brine at 130°C calculated using Extended UNIQUAC Model.

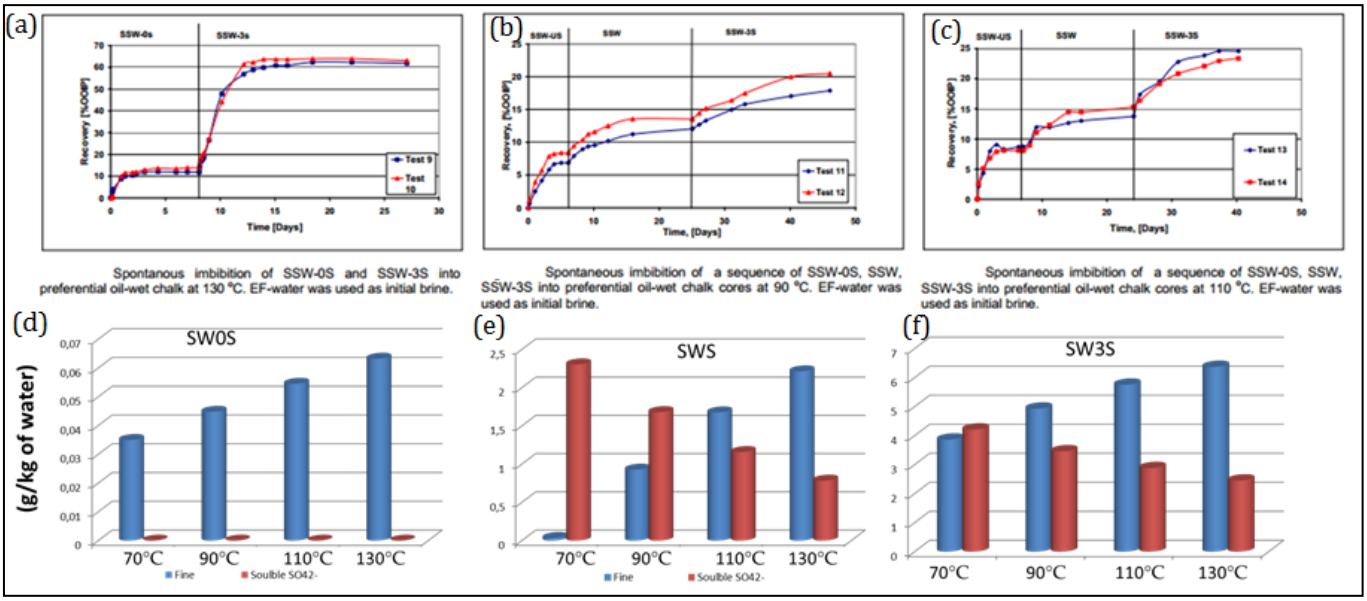


Figure 11: (a-c) Spontaneous imbibition into Stevns Klint, 90, 110 and 130°C using SSW-US, SSW and SSW-3S as imbibing brines. (d-f) Amount of fine formation and soluble SO_4^{2-} present at the imbibing condition after ion substitution in the coreplug calculated using Extended UNIQUAC Model.

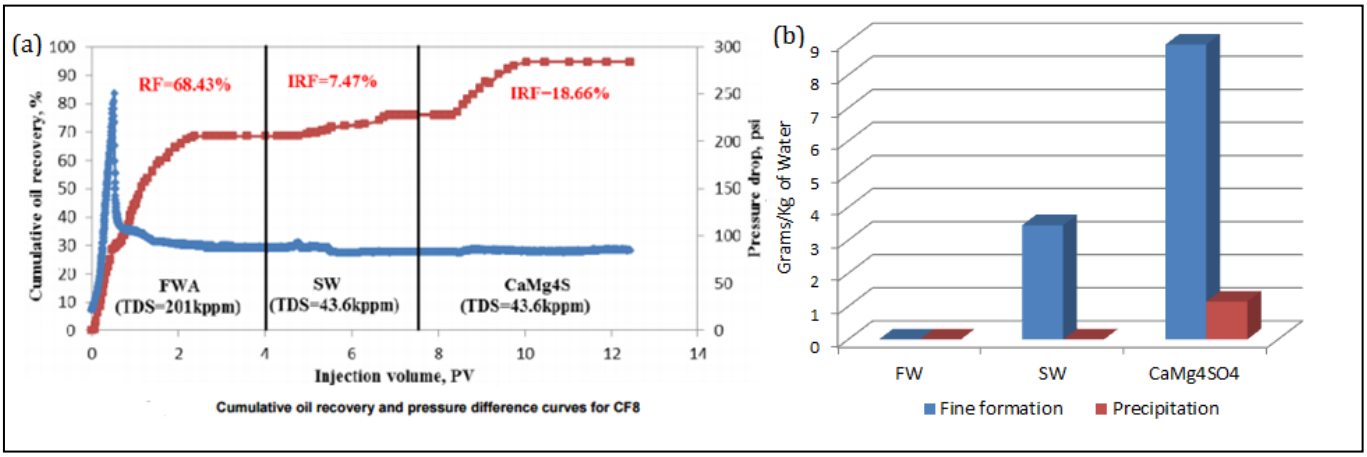


Figure 11: (a) Oil production profile for smart water flooding with FW, SW and CaMg4SO4 brines into Middle East reservoir coreplugs at 120°C. (b) Calculated amount of fine formation and precipitation taking place in the coreplug using Extended UNIQUAC Model.

Paper VII

Chakravarty, K. H., Fosbøl, P. L., & Thomsen, K. (2015, November). Significance of Fines and their Correlation to Reported Oil Recovery. In *Abu Dhabi International Petroleum Exhibition and Conference*. Society of Petroleum Engineers.

SPE-177711-MS

Significance of fines and their correlation to reported oil recovery

Krishna Hara Chakravarty, Philip Loldrup Fosbøl and Kaj Thomsen, Center for Energy Resources Engineering (CERE), Department of Chemical and Biochemical Engineering, Technical University of Denmark

Copyright 2015, Society of Petroleum Engineers

This paper was prepared for presentation at the Abu Dhabi International Petroleum Exhibition and Conference held in Abu Dhabi, UAE, 9–12 November 2015.

This paper was selected for presentation by an SPE program committee following review of information contained in an abstract submitted by the author(s). Contents of the paper have not been reviewed by the Society of Petroleum Engineers and are subject to correction by the author(s). The material does not necessarily reflect any position of the Society of Petroleum Engineers, its officers, or members. Electronic reproduction, distribution, or storage of any part of this paper without the written consent of the Society of Petroleum Engineers is prohibited. Permission to reproduce in print is restricted to an abstract of not more than 300 words; illustrations may not be copied. The abstract must contain conspicuous acknowledgment of SPE copyright.

Abstract

Condensation, vaporization and volumetric changes are well-studied phenomena that create differences between the properties of oil at reservoir and surface condition. But similar changes in effluent brine properties have not received the same attention. This study attempts to analyze variations in properties of the effluent brine at reservoir and surface conditions.

Various research groups have conducted water flooding experiments. Concentrations of the effluent brines have been reported. In this study speciation properties of these brines have been reanalyzed. The Extended UNIQUAC Model was used to precisely compute the brine speciation. Calculations was conducted both at surface and reservoir (pressure, temperature) conditions. Possible release of fines that remained unaccounted for in previous studies was explored.

The calculation at high temperature and pressure showed that during water flooding, significant amounts of fines were released from the core plug. But with a decrease in temperature and pressure (i.e. at surface condition) these produced fines got dissolved in the effluent water. Thus the produced fines were no longer observable at room temperature. A significant increase in the solubility of anhydrite with decrease in temperature is found to be the principal reason for the dissolution of produced fines. The previously unaccounted fines were observed for the following types of experiments:

- Rock Type: Chalk, Limestone and Dolostone
- Coreplug Type: Outcrop and Reservoir Coreplug
- Flooding Type: Spontaneous imbibition and water flooding experiment
- EOR Strategy: Low salinity, Smart waterfloods and Advanced Ion Management
- Rock Origin: Middle East, North Sea and United States

Furthermore a good correlation was observed between the amount of produced fines and the reported amount of oil recovery. Herein it was observed that production of fines increased significantly when the composition of injected brine was significantly altered. The interaction between the injected brines and the existing brine could have led to formation of mobile fines. This trend was found congruent with incrementing oil recovery.

The calculations show that brine speciation at reservoir condition is significantly different from that at surface conditions. During EOR waterfloods significant amounts of fines are produced which are closely correlated with the increments in oil recovery. These produced fines have previously been unaccounted for. The Extended UNIQUAC model can be used to accurately calculate the amounts of these fines.

Introduction:

The properties of oil at reservoir conditions is significantly different from that at surface conditions with change in pressure and temperature, condensation of gases vaporization of oil crystallization of asphaltene and volumetric changes of oil can take place (Pernyeszi et al. 1998; Betancourt et al. 2008; Kriz et al. 2005; Venkatesan et al. 2003). Based on extensive research of enormous field data, these phenomena have been studied in detail (Akbar et al. 2001; Venkatesan et al. 2003). But along with recovered oil,

significant amount of formation and injected brine also moves from reservoir to surface (ambient) condition which has not received similar attention. Furthermore, even in laboratory coreplug experiment (which mimics reservoir behavior) the variation in brine properties due to changes in pressure temperature conditions has not received much attention. During tertiary (enhanced) oil recovery the effluent brine can play a dominant role particularly when the salinity and composition of the injection brine is varied significantly (Zhang et al 2006; Zhang et al 2007; Zahid et al 2010; Austad et al 2005; Puntervold et al. 2009; Gupta et al. 2012; Strand et al 2008; Strand et al. 2006). There are three general enhanced oil recovery methods involving variation in composition and salinity of injected brine. These include low salinity brine injection (Zahid et al. 2011; Austad et al 2011; Romanuka et al. 2012; Pu et al. 2010) smart water enhanced oil recovery (Austad et al 2005; Zhang et al. 2006; Zahid et al. 2010) and advanced ion management (Gupta et al. 2011; Gupta et al. 2015; Vo et al 2012).

Low salinity brine injection involves an increase in oil recovery by injecting dilute sea water (Zahid et al. 2011; Austad et al 2011; Romanuka et al. 2012; Pu et al. 2010). For carbonate rock, dissolution of calcite and/or anhydrite is proposed to be the primary reason behind the observed enhanced oil recovery (Pu et al 2010; Morrow et al 2011; Romanuka et al. 2012). Some research studies show that dissolution of anhydrite increases the amount of soluble Ca^{2+} and SO_4^{2-} present in the brine solution (Austad et al. 2011). This increase in concentration of soluble ion causes changes in mineral surface wettability towards more water wetness and thereby increases oil recovery (Romanuka et al. 2012; Austad et al. 2011). According to this mechanism, precipitation of salts must be avoided as it can completely block the water flow (Austad et al. 2012). These studies recommend that presence of anhydrite and its dissolution must take place (Austad et al. 2011). There is disagreement to the proposed mechanism as it is suggested that dissolution of any mineral salt, calcite or anhydrite can have effect on reservoir permeability (McGurie et al. 2005; Zahid et al. 2012). Thus, it can in turn increase the sweep efficiency of the flooded water by forcing the water to move away from the preferential flow path and thereby increase the oil recovery (Pu et al. 2010; McGurie et al. 2005; Zahid et al. 2012). Observed successful EOR for coreplugs containing no anhydrite minerals; support the claim that: dissolution of any mineral can support EOR for Low salinity brine injection with carbonate rocks (Zahid et al. 2012).

Smart water enhanced oil recovery suggest that instead of decreasing the overall salinity of brine by diluting the solution, selectively decreasing the concentration of Na^+ and Cl^- ions can also increase the amount of production (Austad et al. 2005; Zhang et al. 2007). Based on several meticulous experiment the study suggests that increasing the fraction of potential ions (i.e. Ca^{2+},Mg^{2+} and SO_4^{2-}) can increase the oil recovery (Austad et al 2005; Zhang et al. 2006; Zhang et al. 2007; Strand et al. 2006; Strand et al. 2008; Fathi et al. 2010; Fathi et al 2010). The proposed mechanism consists of two major parts. (1): Injected Mg^{2+} substitutes Ca^{2+} from the mineral surface. (2) Soluble SO_4^{2-} is adsorbed on the mineral surface by replacing polar hydrocarbons (Austad et al 2008). This makes the mineral surface more water wet and increases the mobility of residual oil. It is further suggested that precipitation of anhydride must be avoided during this process (Strand et al. 2008; Fathi et al. 2010; Fathi et al 2010).The proposed mechanism states that injection of smart water should necessarily increase the water wettability for obtaining EOR (Austad et al 2008). But contrary to the proposed mechanism observed EOR for completely water wet system remain as an unexplained phenomenon (Zahid et al. 2010). Significant amount of precipitation /fines formation can take place after ion substitution has taken place on the mineral surface (Chakravarty et al. 2015a; Chakravarty et al. 2015b). According to the proposed mechanism, these fines should cause hindrance in oil displacement but it shows good consistent co-relation to the reported oil recovery (Chakravarty et al. 2015b).

Advanced ion management is the third method which applies variation in salt salinity and composition for obtaining increase in oil recovery (Gupta et al. 2015; Gupta et al. 2012; Vo et al. 2012). Herein it has been shown that instead of using just SO_4^{2-} ions, using PO_4^{3-} and /or BO_3^{3-} can also increase the oil production (Gupta et al. 2012; Vo et al. 2012). The study also shows that neither SO_4^{2-} nor Ca^{2+}/Mg^{2+} is necessary for obtaining an increase in oil production. The study also recommends that neither mineral dissolution/precipitation nor soluble ion based wettability alteration can explain various EOR experiments (Gupta et al. 2015).

Clearly in all three enhanced oil recovery technique both the amount of soluble ions and the amount of insoluble supersaturated salt play a certain role in the interpretation of the data and obtaining the fundamental mechanism associated with this phenomenon. During these water flooding experiments (Vo et al. 2012; Chandrasekhar et al. 2013; Awolayo et al. 2014; Shariatpanahi et al. 2010; RezaeiDoust et al. 2009) the composition of the effluent has been calculated at ambient concentration and this composition has been there after co-related with the observed oil recovery. But the effluent that came out of the core plug was transferred from elevated pressure /temperature to ambient conditions which could have significantly altered its speciation properties. In this report, therefore we calculate the brine speciation both in reservoir condition, using extended UNIQUAC model (Thomsen and Rasmussen 1999).

The extended UNIQUAC model is an optimized thermodynamic model for aqueous solution of electrolytes and non- electrolytes (Thomsen and Rasmussen 1999). All required parameters in the model for the ions in concern have been optimized using a large amount of experimental data accumulated from various sources (Christensen and Thomsen 2003; Thomsen et al. 1996; Garcia et al. 2005; Garcia et al. 2006). The vast experimental basis of this model enables it to describe the phase behavior and the thermal properties of solution containing electrolytes with great accuracy (Garcia et al 2005). Along with solid–liquid equilibrium data over diverse pressure temperature conditions, activity and osmotic coefficients from open literature have been used to optimize the parameters. Moreover thermal properties including heat of dissolution, heat of solution and apparent molal heat capacity of salt solution have also been used for determining model parameters. And thus these properties are also reproducible by the model. In

Figure 1, the calculated solid-liquid equilibrium curves for the ternary $CaSO_4$–Na_2SO_4–H_2O system (at room temperature) and the binary $CaSO_4$–H_2O system (at elevated pressure and temperature conditions) are plotted along with experimental data from the open literature in order to demonstrate the accuracy of the model (García et al. 2005). In this work, the model was used to calculate phase equilibria related to the changes in brine concentration with change in temperature, pressure and interactions at mineral surfaces.

Spontaneous imbibition and water flooding experiments from 6 different literature sources were examined in detail. The exact effluent brine concentrations as reported in literature were used and all the calculations were conducted at the specified temperature and pressure conditions. Thereafter the composition and properties of the brine present in the pore space was obtained at the flooding condition. It was consistently observed that the effluent brine at reservoir conditions contained significant amounts of insoluble salts (or mobile fine), which with decrease in temperature became soluble in effluent vials at room temperature. Both the amount of soluble SO_4^{2-} present in the brine solution in the pore space and the corresponding amount of fines formation was correlated with the observed oil recovery. This study establishes a clear speciation difference between the produced brine at water flooding condition and the effluent brine at ambient conditions. Studies with variation in brine composition, temperature, and origin of core plug, and origin of oil core plug were considered.

Calculation Method

The main model parameters of the Extended UNIQUAC model are the volume and surface area parameters (r- and q-parameters), which are determined on the basis of massive amounts of binary and ternary experimental data (Thomsen and Rasmussen 1999). Parameters for all ions used in smart water experiments have already been extensively optimized (Iliuta et al. 2000; Thomsen et al. 1996; García et al. 2005). The group of ions and neutral species includes H_2O, CO_2, Na^+, K^+, Mg^{2+}, Ca^{2+}, Ba^{2+}, H^+, Sr^{2+}, Cl^-, SO_4^{2-}, OH^-, CO_3^{2-} and HCO_3^-. The optimized r- and q-parameters are listed in table 1. The two individual parameters are specific to each species. In addition, each species pair has two additional parameters that describe the interaction between the species, which is assumed to have a linear temperature dependency. These species pair interaction parameters have also been previously optimized (Iliuta et al. 2000; Thomsen et al. 1996; García et al. 2005) and are listed in Table 2. The model predicts the behavior of multi component systems based on these unary and binary parameters. As the model parameters are based on binary and ternary data alone, the calculation of phase behavior in multi-component systems represents prediction by the model. In several calculations it has been shown that the Extended UNIQUAC model is capable of accurately representing multi-component systems with common ions covering a range of temperatures and ionic strengths that is large enough to represent all the conditions stated in laboratory and reservoir water flooding experiments.

The Extended UNIQUAC model was used for calculating the effluent brine properties both at reservoir and at ambient conditions for core flooding experiments from 7 different literature sources. In this report the brine speciation in the water flooding condition and its co-relation to the oil recovery has been extensively investigated the detailed references are provided in Table 3.

As shown in table 3, data set 1 includes analysis of spontaneous imbibition experiment conducted with North Sea chalk using smart water enhanced oil recovery method (SW-EOR). Large amount of literature study with North Sea chalks are based on SW-EOR. So, analyzing its brine speciation in reservoir condition is important. The data set 2 includes effluent analysis of limestone reservoir core plugs originating from the carbonate reservoirs of Middle East. Properties and oil recovery pattern of outcrops are known to be different from their reservoir analysis. Thus, calculating effluent brine composition at reservoir condition is equally important for reservoir core plugs. Furthermore Smart water spontaneous imbibition experiment for chalk originating from North Sea has shown significantly different behavior than these from United States. Therefore analyzing the effluent brine concentration for chalk originating from United States was also conducted at reservoir conditions. The data set 3 in the experiment highlights this analysis. Huge amounts of limestone in the Middle East are also great potential of smart water EOR. Thus, data set 4 included water flooding experiments conducted for reservoir limestone using SW-EOR method. The brine speciation at reservoir conditions was calculated both the amount of supersaturation and the amount of fine formation were co-related to the oil recovery. Other than SW-EOR method low salinity brine injection is another equally promising EOR strategy. Therefore in data set 5 effluent concentrations for low salinity brine injection was analyzed. Water flooding experiment with US carbonate rock was used. First, high salinity formation water was injected, thereafter sea water, twice diluted sea water, 10 times diluted sea water, and 20 times diluted sea water was followed. Advanced ion management is the third EOR strategy (AIM-EOR) where variation in salinity and composition of sea water is applied during brine injection. Effluent brine speciation for AIM-EOR was also calculated at flooding condition. Data set 6 includes Aim –EOR analysis for water flooding at 70 °C. Here the amount of insoluble ions present in the effluent was co-related to the recovered oil.

Results:

Data Set 1: (**RezaeiDoust et al. 2009)**

Spontaneous imbibition experiments with outcrop chalk from Stevns Klint chalk from Denmark were conducted in this study (RezaeiDoust et al. 2009). The experiments were conducted at 130°C and 18 bars, and the obtained effluent concentration and corresponding increase in Ca^{2+} ion reported. The solubility of $CaSO_4$ is very low and it further decreases with increase in tempera-

ture. The additional Ca^{2+} production due to cation substitution may have led to supersaturation of the effluent brine at experimental conditions. Speciation calculation both at experimental conditions and at ambient condition were performed using Extended UNIQUAC model. As shown in figure 2, it was observed that the effluent brines were significantly supersaturated and up to 440 mg of anhydrite was present at reservoir conditions. Throughout the experiment around 205 to 300 mg of anhydrite was continuously produced for every kg of water. This is a significant fraction of brine as only 520 mg of Ca^{2+}/ per kg of water was introduced into the core plug (RezaeiDoust et al. 2009).This observed supersaturated fraction of anhydrite cannot be neglected. Furthermore calculating the brine speciation at room temperature showed no anhydrite super saturation. This is shown in figure 2. The recorded brine composition showed no insoluble anhydrite fraction in any of these different effluent samples. This indicates that when the brine was produced from the core plug (i.e. at high pressure, high temperature) it contained a significant fraction of insoluble salt. These insoluble salts there after became soluble with decrease in temperature. Thus, no precipitate was observed at room temperature (RezaeiDoust et al. 2009). As shown in figure 1, the solubility of anhydride decreases significantly with an increase in temperature. It is therefore possible that cation substitution on the calcite surface has produced an additional amount of Ca^{2+} in the pore space. This additional Ca^{2+} in the pore space made the brine super saturated. The additional insoluble salts got dissolved with the decrease in temperature after being produced. This clearly shows that the speciation of effluent brine at reservoir condition is significantly different from that at room temperature. Effluent brine properties should therefore be calculated at reservoir conditions after obtaining its composition.

Data Set 2: (Shariatpanahi et al. 2010)

In the second dataset, water flooding experiment for limestone reservoir was analyzed over different pressure and temperature conditions. Herein waster flooding with 3 different coreplug was studied at 110°C, 130°C and 150°C respectively (Shariatpanahi et al. 2010). Unlike Data Set 1 (where outcrop chalk coreplugs were used) herein limestone reservoir coreplugs were used. Reservoir core plugs are known to have low permeability, thus possible super saturation may cause blockage in the pore throat This may affect the flow of injected water (Shariatpanahi et al. 2010).

In the first core the effluent concentration was analyzed at the experimental conditions of 110 °C and 10 bars. Conducting the brine speciation calculating using Extended UNIQUAC model showed that the brine was highly supersaturated at experimental conditions. Here in with increase in Pore Volume injection the substitution of Mg^{2+} by Ca^{2+}consistently increased and this additional Ca^{2+} in the pore space made the brine solution supersaturated 398 mg grams of anhydrite/kg of water was observable after 2.25 PVI Ca^{2+}/ Mg^{2+} substitution optimized at 1.5 PVI and as shown in figure 3. There after 330 to 350 mg of anhydrite super saturation was observed consistently for every kg of water. The injected brine contained 520 mg of Ca^{2+} ions (0.013 mol of Ca^{2+}) (Shariatpanahi et al. 2010). In spite of the significant insoluble fraction of anhydrite (i.e.350 mg) no supersaturation of anhydrite was observed at room temperature. Different samples corresponding to different PVI consistently showed no fraction of insoluble salts at 25 °C. This shows that during water flooding in low permeability limestones a considerable fraction of insoluble salts can be formed. After cat-ion substitution this fraction can become more prominent. Correspondingly the amount of $CaSO_4$ (s) formation also consistently increased the cat-ion substitution optimized at 1.35 PVI and correspondingly around 1130 mg of insoluble anhydrite was observable for each kg of water since on 520 mg of Ca^{2+} is injected in the core plug. A brine speciation calculation at 25 °C shows no super saturation of insoluble anhydrite. It indicates that the insoluble salt fraction present at reservoir conditions became soluble with decrease in temperature and thus no precipitation was reported in the effluent vials.

In the second coreplug of dataset 2 waterflooding into limestone core plugs was conducted at 130°C. Therefore for the reported brine composition, speciation was back calculated at 130°C and 10 bars (Shariatpanahi et al. 2010). The Extended UNIQUAC calculation showed that at 130°C significant amount of insoluble salts (or mobile fines) was present in the brine at experimental condition. Herein again with increase in PVI the cation substitution of Ca^{2+} by Mg^{2+} became more prominent. And as shown in Figure 4; through the speciation calculation, it is observable that correspondingly the amount of insoluble $CaSO_4$ salt also increased. The cation substitution optimized at 1.35 PVI, and correspondingly around 1139 mg of insoluble anhydrite was observable for each kg of water. Since only 520 mg of Ca^{2+} is injected in the coreplug so these insoluble anhydrite fraction (of 1130 mg/kg of water) becomes an important fraction of the effluent brine. Thus its effect cannot be neglected during calculation or during interpretation. As shown in figure4b, brine speciation calculation at 25°C shows no supersaturation. It indicates that insoluble salt fraction present in reservoir became soluble with decrease in temperature and thus no precipitation was reported from the effluent vials.

Comparing the experiments at 110°C and 130°C it is observable that the amount of mobile insoluble salt fines formed during flooding at 130°C (i.e. 1130 mg/kg water) is significantly greater than that at 110°C (with 330 mg/kg of water). And since the injection brine composition was same for the two experiments, thus the soluble ions present in the coreplug decreased significantly with increase in flooding temperature. And it is known that oil recovery factor increases significantly with increase in temperature (Austad et al. 2005; Fathi et al. 2010; Strand et al. 2006). These observations put together shows that the amount of mobile fines formation correlates to oil recovery while amount of soluble ions doesn't. Thus it supports previously observed correlation fine-recovery correlation from injection brine (Chakravarty et al. 2015b).

The third reservoir limestone core plug was flooded at 150 °C (Shariatpanahi et al. 2010). There in again the brine speciation of the effluent was calculated at reservoir conditions. It was observed that the reported brine composition was significantly supersat-

urated at 150 °C (Shariatpanahi et al. 2010). Here in again it was observed that with substitution of Ca^{2+} by Mg^{2+} around 1120 mg of mobile fines was formed for each kg of water. Since, on 520 grams of $Ca^{2+}$is injected for every kg of water so, this 1120 mg of insoluble anhydride formation cannot be ignored. The obtained amount of insoluble ions is quite comparable to the amount of insoluble anhydride present in the core-plug. Furthermore it is observed that the sulphate concentration continuously decrease with increases in PVI. It is attributed to precipitation in the core-plug. The amount of precipitation in the core plug can be calculated by bring a mass balance between the injected and the output brine. Figure 5 shows the proportion of insoluble salt (fines) that remained that remained in the core plug and the fraction that flowed through the core plug and was recorded in the effluent. This clearly shows the amount of precipitation is not equal to the amount of insoluble salt (fines) present in the core plug and only a fraction of the total insoluble salt is actually precipitated. As shown in figure 5c, the amount of precipitation (or static fines) and the amount of moveable insoluble salts (or the mobile fines) are quite comparable to each other and thus, neither can be neglected. The proportion of static and mobile fines formation taking place will heavily depend on composition of injected brine and on the temperature of water flooding. The brine speciation properties were also calculated at room temperature using extended UNIQUAC model. It was observed that the reported brine composition was completely soluble at room temperature and thus no precipitation was observable in the effluent vials (Shariatpanahi et al. 2010).

This effluent brine analysis shows that a fraction of insoluble salt (or mobile fines) can flow with the flooded water. And thus on flowing through the porous medium it can be observable from the effluent brine. But with decrease in temperature the effluent brines become soluble and thus is not observable in room temperature comparing of data set 1 and 2. It is observed that these mobile fines can not only be obtained for high permeable chalk out crop but also for low permeable limestone reservoir core plugs.

Data Set 3: (Chandrasekhar et al. 2013)

In data set 3 smart water enhanced oil recovery with US carbonates was analyzed (Chandrasekhar et al. 2013). Reservoir core plug used in the water flooding experiment was composed of lime stone and dolomites grains. Here in sulphate enrich brine was injected into the core plug (Chandrasekhar et al. 2013). The recorded brine composition was calculated both at experimental condition (130°C & 18 bars). As shown in figure 6b, at experimental condition the effluent brine was significantly supersaturated up to 3.5 grams of anhydride fines was calculated during 0.64 PVI. This high amount of fine formation is primarily because the formation water present in the core plug was rich in Ca^{2+} ion. It when interacts with SO_4^{2-}enriched brine injection formed mobile fines which is observable in the speciation calculation. Once the Ca^{2+} formation water was removed the amount of mobile fines also decreased there after around 3.38 PVI a sudden increase in effluent fines was observed and 112 grams of anhydrite fines was released from the core plug at the high pressure high temperature condition (figure 6). It is interesting to note that at the same specific point the rate of oil production suddenly increased on further continuing the water flooding both the rate of oil production and the amount of mobile fines gradually decreased. This shows a clear and consistent co-relation between the amount of oil recovery and the amount of mobile fine formation.

Furthermore the amount of static fines present in the core plug was also calculated and herein it was observed a significant amount of static fine formation did take place. This, reproves the point previously observed in set 2 that all insoluble salt do not form precipitation (static fines) and a large fraction can flow through the pores medium and thus found in the effluent vials. Moreover it is observed that static fines formation take place at 2.93 PVI and gradually increases beyond the mobile fines composition at 5.92 PVI (Figure 6). It is also observable that with increase in amount of static fine formation the oil recovery consistently decreases. Thus, it is observed that mobile fines have a direct co-relation while static fines have an inverse co-relation to oil recovery.

The brine speciation for the reported brine (Chandrasekhar et al. 2013) was also calculated at room temperature and it was observed that the no supersaturation was observed at room temperature. Therefore the mobile fines produced from reservoir must have becomes soluble at room temperature and thus, no precipitation was observed. This study shows that for core plugs containing both lime stone and dolomite. It is possible that in soluble salt fractions can flow through the porous medium. These insoluble salts (or mobile fines) show direct co-relation to the rate of oil productions.

Data Set 4: (Awolayo et al. 2014)

In data set 4 lime stone reservoir core plugs was flooded with 3 different brines of varied SO_4^{2-} concentration (Awolayo et al. 2014). For first 10 PV, high salinity formation water was introduced. Thereafter for the following 8 PV normal sea water was injected and for the final 7 PV Sea water with four times sulphate was injected (Awolayo et al. 2014). The reported effluent concentration corresponding to each PVI was used to back calculate the brine speciation in reservoir condition. It was observed that during injection of Sea water Ca^{2+} increased significantly because of cation substitution. This increase in Calcium concentration made the effluent supersaturated as previously observed. In the experimental conditions at 120°C around 980 mg of anhydrite fine was found in the effluent for every kg of water. This amount is a considerable fraction as in the injected sea water on 510 grams of Ca^{2+} ion was present. Furthermore when the injection brine was replaced from SW to SW4S, the amount of insoluble mobile fines present in the effluent also increased. And up to 2.3 grams of insoluble anhydrite fines were observed in the effluent at the reservoir conditions. During injection of SW4S the oil recovery also increased significantly. As observable from figure 7, the increase

in oil recovery shows a direct correlation to the amount of fine formation taking place. The brine speciation at room temperature was also calculated using Extended UNIQUAC Model. It was observed that none of the effluent samples had any insoluble salt fractions present (as shown in Figure 7). Thus no precipitate was observed in the effluent vials (Awolayo et al. 2014). All mobile fines must have got dissolved as solubility of anhydrite increase significantly with decrease in temperature.

Data Set 4 (Awolayo et al. 2014) and Data set 2 (Shariatpanahi et al. 2010) both where experiments based on reservoir limestone core plugs. The two set of studies was independently conducted by different research groups. But, in both the studies the effluent concentration recorded at ambient concentration was directly correlated to the oil recovery. And thereby the mobile fines formed in high pressure high temperature respective experimental conditions was ignored as for both data set the effluent samples remain completely soluble at room temperature.

Data Set 5:(Chandrasekhar et al. 2013)

Other than Smart Water EOR, Low Salinity brine injection is another useful EOR strategy where the salinity of injection brine is reduced to alter oil displaceability. In Dataset 5 Low salinity EOR experiment was analyzed for reservoir limestone core plug (Chandrasekhar et al. 2013). Herein in the coreplug 13 PV of Sea Water was injected. Thereafter for the next 25 PV diluted sea water with half salinity was injected. And subsequently 10 times and 20 times diluted sea water injection was followed (Chandrasekhar et al. 2013). The effluent concentration throughout the water flooding was reported in literature. Brine speciation property for the reported effluent brine was calculated at experimental conditions. Herein, as shown in Figure 8 Extended UNIQUAC calculations showed that during Sea water injection there was significant amount of insoluble salts present in the experimental conditions. During 1st 2 PV the mobile fine formation was up to 2.3 grams per kg water. Herein the injected seawater contained only 521 mg of Ca^{2+} ion per kg of water. This indicates that the mobile fines formed the dominant fraction of the reported effluent brine. The amount of insoluble mobile fines forming in the first two PV was significantly higher (2.3 grams/kg of water) than the water flooding thereafter (1.1 grams per kg of water flooding). The majority of the oil production also took place during these two pore volume of SW injection. The rate of oil production significantly slowed down thereafter. This shows that the amount of mobile fine formation taking place shows a direct correlation to the amount of mobile fines present in the effluent brine. Thereafter using mass balance the amount of static fine formation taking place in the coreplug was calculated. It gradually increased from 0.13 gram/kg of water (at 1.82 PV) to 0.5 gram/kg of water (at 3.82 PV), and remained consistent thereafter. And corresponding to the same 3.82 PVI the rate of oil production stated gradually decreasing. This shows that static fines have a consistent negative influence in oil production. The brine speciation at room temperature was also calculated using Extended UNIQUAC Model. It was observed that none of the effluent samples had any insoluble salt fractions present. Thus no precipitate was observed in the effluent vials. All mobile fines must have got dissolved as solubility of anhydrite increase significantly with decrease in temperature. Thereafter the sea water was replaced with half salinity brine solution. The effluent concentration during the diluted water flooding was reported(Chandrasekhar et al. 2013).. Brine speciation property for the reported effluent brine was calculated at experimental conditions. It was observed that up to 0.7 grams of mobile fines formation was present at elevated pressure temperature conditions. Herein also majority of fine production was observable during brine replacement. It was associated with a responsive increase in oil production. The Extended UNIQUAC calculations showed that after completion of 13 PVI the amount of mobile fine present in the effluent sample decreased significantly and so did the rate of oil production. But, the sudden increase in oil recovery production during 21 PV could not be correlated to mobile fine, as associated data 21 PV was not reported in the effluent brine. Subsequently 10 times diluted brine was injected in the coreplug. Herein the brine speciation calculation was conducted for the reported oil recovery. And it was observed that the initial effluent samples where contained insoluble salts at reservoir conditions. 0.18 grams of fines/kg of water was observed during brine alteration. After a few vials the mobile fine concertation decreased and no additional fines was observed. The reported oil recovery also showed the same trend as during initial brine alteration a small increase in oil production by 2.1% of OOIP was observed. Thereafter from 40 to 45 PVI further continuing injection did not produce any additional oil. Brine speciation was calculated at room temperature as well and no insoluble salt fraction was observable. Finally 20 times diluted sea water was injected into the coreplug (Chandrasekhar et al. 2013) and it was observed that no additional oil recovery was observed. Calculating the brine speciation at reservoir condition also showed no mobile fine formation. The overall oil production and fine formation for different brine injections is reported in Figure 8. Herein it is observable that the increase in oil recovery for the first three brines correlates to associated fine formation at exactly same PV of brine injection. This shows that amount of mobile fines in the effluent directly correlates to the produced. These results show that during low salinity brine injection also formation of mobile and static fines are possible. And these fines so good direct correlation to the rate of oil production. And with decrease in temperature these fines becomes soluble and thus is not observable as precipitate in the effluent.

Data Set 6: (Vo et al. 2012)

The third EOR strategy which uses variation of salinity and composition of injection brine is Advanced Ion Management (Gupta et al 2012; Vo et al. 2012). This AIM-EOR water flooding analysis was conducted with Middle East Limestone reservoir coreplug. In the first water flooding experiment, a Ca^{2+} rich formation water was injected for 27 PV and thereafter Seawater with 4 times SO_4^{2-} was introduced for the following 28 PV (Vo et al. 2012). Herein significant increase in oil recovery was observed during the 1st two PV of Ca^{2+} rich formation water injections. Subsequently the recovery rate slowed down until 27 PV. Between 27 and 30 PV a quick increase in oil production by 10% of OOIP took place. The rate of production thereafter slowed down sig-

nificantly for the next 25 PV of high SO_4^{2-} injection. The brine composition of the effluent water was reported for the 1st 50 PVI. Effluent brine speciation calculation for AIM-EOR was also calculated at experimental condition (of 70°C and 103.4 bars) using Extended UNIQUAC model. As shown in figure 9 the brine speciation calculation showed that for the initial 2 PV the effluent brine contained significant amount of insoluble salts in high pressure high temperature conditions. Existence of high concentration Ca^{2+} along with an increased concentration of SO_4^{2-} for the first two pore volume could be the possible reason. The SO_4^{2-} concentration after the first two PV decreased significantly and thus the amount of insoluble fines present in the solution also decreased significantly. Furthermore an increase in oil recovery took place when the Ca^{2+} rich formation water was replaced with SO_4^{2-} enriched sea water. Herein the interaction of the two brines made the flooded water significantly supersaturated. Herein from 27 to 30 PV existence of both Ca^{2+} and SO_4^{2-} allowed the formation of mobile fines. Thereafter the amount of Ca^{2+} injection reduced significantly and the corresponding amount of insoluble salt present in experimental conditions also reduced accordingly. Herein it is interesting to note that high during 1st 2 PVI and during brine replacement i.e. from 27 to 30 PVI, both the rate of oil production (Vo et al. 2012) and amount of fine formation was considerably high. While the water flooding between 2 PV to 26 PV and 30 PV to 50 PV both the rate of oil production and amount of insoluble mobile fines present in reservoir was quiet low. This shows a direct correlation between oil production and presence of mobiles in reservoir conditions. Subsequently the brine speciation calculation was also conducted at room temperature and it was observed that the brine did not contain any supersaturation of anhydrite fines at room temperature and thus no precipitate was observable in the effluent vials.

In the 2nd water flooding experiment, a Ca^{2+} rich formation water was injected for 9 PV and thereafter Seawater with 4 times SO_4^{2-} was introduced for the following 9 PV (Vo et al. 2012). Herein significant increase in oil recovery (to 50% of OOIP) was observed during the 1st 2 PV of Ca^{2+} rich formation water injections (Vo et al. 2012). Subsequently no considerable oil recovery was observable for the following 7 PV of Ca^{2+} rich formation brine injection. Between 9 and 10 PV a quick increase in oil production by 5% of OOIP took place. No additional oil recovery was observed on further continuing the injection SO_4^{2-} enriched brine for 9 PV (Vo et al. 2012). The brine composition of the effluent water was reported for the 1st for all 18PV of brine injection. Effluent brine speciation calculation for AIM-EOR was also calculated at experimental condition (of 120°C and 344.7 bars) using Extended UNIQUAC model. As shown in figure 10 the back calculating the brine speciation calculation at 120°C and 344.7 bars, showed that for the initial 2 PV the effluent brine contained significant (200 mg/kg of water) insoluble salts. Existence of high concentration Ca^{2+} along with an increased concentration of SO_4^{2-} for the first two pore volume could be the possible reason. The SO_4^{2-} concentration after the first two PV decreased significantly and thus the amount of insoluble fines present in the solution also decreased significantly. And continued injection of Ca^{2+} for the next 7 PV did not produce any additional fines. Thereafter an increase in fine formation took place when the Ca^{2+} rich formation water was replaced with SO_4^{2-} enriched sea water. Herein the interaction of the two brines made the flooded water significantly supersaturated. Herein from 9 to 10 PV existence of both Ca^{2+} and SO_4^{2-} allowed the formation of mobile fines and up to 350 mg of anhydrite fines was formed for each kg of water. Thereafter the amount of Ca^{2+} injection reduced significantly and the corresponding amount of insoluble salt present in experimental conditions also reduced completely. And no calculating the brine speciation showed no additional insoluble salt formation at flooded condition. Herein it is interesting to note that high during 1st 2 PVI and during brine replacement i.e. from 9 to 10 PVI, both the rate of oil production (Vo et al. 2012) and amount of fine formation was considerably high (up to 350 mg/kg of water). While the water flooding between 2 PV to 8 PV and 10 PV to 18 PV both the rate of oil production (Vo et al. 2012) and amount of insoluble mobile fines present in reservoir was zero. This shows a direct correlation between oil production and presence of mobiles in reservoir conditions for high pressure high temperature water flooding as well. Subsequently the brine speciation calculation was also conducted at room temperature and it was observed that the brine did not contain any supersaturation of anhydrite fines at room temperature and thus no precipitate was observable in the effluent vials.

This analysis shows that during water flooding with AIM-EOR strategy it is possible that mobile insoluble fines can form due to interaction between two brines. Amount of insoluble mobile salts found back by calculating brine speciation at flooded condition shows a direct correlation to the corresponding rate of oil production.

Discussion:

In all of these reported experiments (Vo et al. 2012; Chandrasekhar et al. 2013; Awolayo et al. 2014; Shariatpanahi et al. 2010; RezaeiDoust et al. 2009) during interpretation the observed effluent brine composition has been directly correlated to the correspondingly produced oil. But this brine speciation calculation shows that the recorded effluent at room temperature can contain significant of insoluble salts. This implies that only a fraction of reported composition of the effluent brine was in form of soluble ions in the reservoir condition. And therefore for correlating the soluble ions to oil recovery; soluble fraction of potential ions (i.e. SO_4^{2-}, Ca^{2+} and Mg^{2+}) must be first calculated at reservoir condition and thereafter any interpretation be made. Herein the pressure and temperature in which the water flooding is conducted plays a curtail role as solubility of anhydrite is significantly dependent on pressure temperature variations at near reservoir conditions. Furthermore brine composition variation based EOR is suggested to have a prominent role with increase in flooding temperature (Austad et al 2005; Faith et al. 2011). With increase in temperature the amount of insoluble mobile salts present in the effluent also increases significantly. Thereby obtaining a proper distinction between the soluble fraction and insoluble fraction becomes even more important for EOR implementation in high temperature reservoirs.

After the brine is released from the core plug and it moves through the pipes into the effluent sample, the pressure and the temperature of the effluent decreases, thereby the solubility of fines also increases. This makes the brines soluble at room temperature, and thus neither Extended UNIQUAC calculation shows any possibility of anhydrite formation nor any precipitate is observe in the effluent vials(Vo et al. 2012; Chandrasekhar et al. 2013; Awolayo et al. 2014; Shariatpanahi et al. 2010; RezaeiDoust et al. 2009). And therefore distinction between insoluble mobile salt fraction and soluble ions cannot be directly from the effluent vials and after obtaining its composition back calculating its speciation at flooding condition is very critical.

For many carbonate coreplug it has been established that the injected Mg^{2+} can replace Ca^{2+} from the calcite surface. This produces significantly increases the concentration of Ca^{2+} in pore space. As observable in Figure 1-4 and 7, enriched Ca^{2+} concentration with associated decrease in Mg^{2+} composition indicates the occurrence of ion substitution on mineral surface. The additional Ca^{2+} released as virtue of ion substitution makes the SO_4^{2-} brine in pore space supersaturated. This leads a formation of insoluble salts fraction. But these insoluble salts must not be treated equivalent to precipitate as the insoluble salts and able to move through the porous network and are thus observable in the effluent analysis. Therefore a fraction of brine which should precipitate in the porous coreplug, actually flows through it and is thus observable when brine speciation calculation is conducted for effluent brines at flooded conditions. A fraction of expected precipitate which is insoluble yet can flow through the porous network and be observable from the effluent analysis has been termed as mobile fines. Other than cation substitution mobile fines can form when brine replacement takes place. As observable in Figure 9 and 10 the two injected brines where individually completely soluble in the flooding temperature, and correspondingly in the effluent no insoluble fines formation was observable at flooding conditions. But, when a Ca^{2+} enriched formation water interacts with SO_4^{2-} enriched brine then formation of mobile fines can take place. Thus on speciation calculation mobile fines where observable only for 2 PV exactly when the brine replacement took place.

Moreover as shown in Figure 5, 6 and 7 it is important to note that all insoluble salts formed in the coreplug flows through the porous network and is observable in the effluent. A considerable fraction of the expected precipitate does remain in the coreplug and is termed as static fines. Only these static fines can block the pore throats and/or alter the water flow pattern. Amount of static fines and the amount of mobile fines forming during water flooding is significantly dependent on both pressure temperature conditions of water flooding and the composition of the injected brine. As observable figure 5 and 6 considerable amount of both static fines and mobile fine can be formed during water flooding and therefore neither can ignored. Thus the total expected precipitation can be divided into static fine (which is obtained by mass balance between injected and effluent ions) and mobile fines (which is obtained by calculating effluent brine speciation in flooding condition using Extended UNIQUAC calculation).

Conclusion:

In most previous core flooding studies, properties of the effluent brines have been correlated with the observed oil recovery. But Extended UNIQUAC calculation shows that the produced brine from the coreplug (i.e. at the elevated experimental pressure temperature condition) has contains significant amount of insoluble salts. And as the temperature of the produced brine decreases these insoluble salts get dissolved, thus no precipitation is observed in the effluent vials at ambient temperature.

Release of Ca^{2+} ion in the pore space following ion substitution on the mineral surface can change the composition and properties of the injected brine significantly. This forms the basis of mobile fine formation in the coreplug. Moreover mobile fine are also produced due to interaction between two brines, during replacement of brine in injected water flood. Mobile fines released from coreplug which become soluble at room temperature are treated as soluble effluent brine during interpretation in all reported studies. Thus actual amount of soluble ion produced from the core plug at experimental conditions, is less than its observed composition in room temperature and is mistakenly overestimated. Also only a fraction of the total expected precipitation actually precipitates in the coreplug, and thus precipitation can also be overestimated. This precipitating fraction (or static fines) can be obtained by mass balance and is highly dependent on flooding conditions. The amount of mobile fines formation taking place consistently correlates with the observed oil recovery for various limestone, dolostone and chalk coreplug flooded at flooded over a temperature range from 70°C to 150°C. While the amount of static fine formation shows an inverse correlation to the oil production rate.

Accurate modelling tool like Extended UNIQUAC model should be used to calculate the exact amount of mobile fines and the amount of soluble ions present in the produced water at the flooded conditions. And this calculated brine speciation should be thereafter used for interpretation or correlation to recovered oil.

References:

- Akbar, M., Vissapragada, B., Alghamdi, A. H., Allen, D., Herron, M., Carnegie, A., & Saxena, K. (2000). A snapshot of carbonate reservoir evaluation.Oilfield Review, 12 (4), 20-21.
- Austad, T., Strand, S., Høgnesen, E. J., & Zhang, P. (2005, January). Seawater as IOR fluid in fractured chalk. In SPE International Symposium on Oilfield Chemistry. Society of Petroleum Engineers.
- Austad, T., Shariatpanahi, S. F., Strand, S., Black, C. J. J., & Webb, K. J. (2011). Conditions for a low-salinity enhanced oil recovery (EOR) effect in carbonate oil reservoirs. Energy & fuels, 26(1), 569-575.

- Awolayo, A., Sarma, H., & AlSumaiti, A. M. (2014, March). A Laboratory Study of Ionic Effect of Smart Water for Enhancing Oil Recovery in Carbonate Reservoirs. In SPE EOR Conference at Oil and Gas West Asia. Society of Petroleum Engineers.
- Bagci, S., Kok, M. V., & Turksoy, U. (2001). Effect of brine composition on oil recovery by waterflooding. Petroleum science and technology, 19(3-4), 359-372.
- Betancourt, S. S., Ventura, G. T., Pomerantz, A. E., Viloria, O., Dubost, F. X., Zuo, J.,& Mullins, O. C. (2008). Nanoaggregates of Asphaltenes in a Reservoir Crude Oil and Reservoir Connectivity†. Energy & Fuels, 23(3), 1178-1188.
- Chakravarty, K. H., Fosbøl, P. L., & Thomsen, K, (2015) Interactions of Fines with Oil and its Implication in Smart Water Flooding In SPE Bergen One Day Seminar, Society of Petroleum Engineers
- Chakravarty, K. H., Fosbøl, P. L., & Thomsen, K. (2015, June). Importance of Fines in Smart Water Enhanced Oil Recovery (SmW-EOR) for Chalk Outcrops. In EUROPEC 2015. Society of Petroleum Engineers.
- Christensen, S. G., & Thomsen, K. (2003). Modeling of vapor-liquid-solid equilibria in acidic aqueous solutions. Industrial & engineering chemistry research, 42 (18), 4260-4268.
- Thomsen, K., Rasmussen, P., & Gani, R. (1996). Correlation and prediction of thermal properties and phase behaviour for a class of aqueous electrolyte systems. Chemical Engineering Science, 51 (14), 3675-3683.
- Fathi, S. J., Austad, T., & Strand, S. (2010). "Smart Water" as a Wettability Modifier in Chalk: The Effect of Salinity and Ionic Composition. Energy & fuels, 24 (4), 2514-2519.
- Fathi, S. J., Austad, T., & Strand, S. (2011). Water-based enhanced oil recovery (EOR) by "smart water": Optimal ionic composition for EOR in carbonates. Energy & fuels, 25 (11), 5173-5179.
- García, M. D. C., & Carbognani, L. (2001). Asphaltene-paraffin structural interactions. Effect on crude oil stability. Energy & Fuels, 15(5), 1021-1027.
- García, A. V., Thomsen, K., & Stenby, E. H. (2006). Prediction of mineral scale formation in geothermal and oilfield operations using the Extended UNIQUAC model: Part II. Carbonate-scaling minerals. Geothermics, 35 (3), 239-284
- García, A. V., Thomsen, K., & Stenby, E. H. (2005). Prediction of mineral scale formation in geothermal and oilfield operations using the extended UNIQUAC model: part I. Sulfate scaling minerals. Geothermics, 34 (1), 61-97.
- Gupta, R., Griffin, P., Hu, L., Willingham, T. W., Cascio, M. L., Shyeh, J. J., & Harries, C. R. (2011). Enhanced waterflood for Middle East carbonate cores–impact of injection water composition. paper SPE, 142668.
- Gupta, R., Lu, P., Glotzbach, R., & Hehmeyer, O. (2015). A Novel, Field-Representative Enhanced-Oil-Recovery Coreflood Method. SPE Journal.
- Iliuta, M. C., Thomsen, K., & Rasmussen, P. (2000). Extended UNIQUAC model for correlation and prediction of vapour–liquid–solid equilibria in aqueous salt systems containing non-electrolytes. Part A. Methanol–water–salt systems. Chemical Engineering Science, 55 (14), 2673-2686.
- Kriz, P., & Andersen, S. I. (2005). Effect of asphaltenes on crude oil wax crystallization. Energy & fuels, 19(3), 948-953.
- Morrow, N., & Buckley, J. (2011). Improved oil recovery by low-salinity waterflooding. Journal of Petroleum Technology, 63(05), 106-112.
- McGuire, P. L., Chatham, J. R., Paskvan, F. K., Sommer, D. M., & Carini, F. H. (2005, January). Low salinity oil recovery: An exciting new EOR opportunity for Alaska's North Slope. In SPE Western Regional Meeting. Society of Petroleum Engineers.
- Pernyeszi, T., Patzko, A., Berkesi, O., & Dékány, I. (1998). Asphaltene adsorption on clays and crude oil reservoir rocks. Colloids and Surfaces A: Physicochemical and Engineering Aspects, 137(1), 373-384.
- Puntervold, T., Strand, S., & Austad, T. (2009). Coinjection of seawater and produced water to improve oil recovery from fractured North Sea chalk oil reservoirs. Energy & fuels, 23(5), 2527-2536.
- Pu, H., Xie, X., Yin, P., & Morrow, N. R. (2010, January). Low-salinity waterflooding and mineral dissolution. In SPE Annual Technical Conference and Exhibition. Society of Petroleum Engineers.
- RezaeiDoust, A., Puntervold, T., Strand, S., & Austad, T. (2009). Smart water as wettability modifier in carbonate and sandstone: A discussion of similarities/differences in the chemical mechanisms. Energy & fuels, 23(9), 4479-4485.
- Romanuka, J., Hofman, J., Ligthelm, D. J., Suijkerbuijk, B., Marcelis, F., Oedai, S., ... & Austad, T. (2012, January). Low salinity EOR in carbonates. In SPE Improved Oil Recovery Symposium. Society of Petroleum Engineers.
- Shariatpanahi, S. F., Strand, S., & Austad, T. (2010). Evaluation of Water-Based Enhanced Oil Recovery (EOR) by Wettability Alteration in a Low-Permeable Fractured Limestone Oil Reservoir. Energy & Fuels, 24(11), 5997-6008.
- Strand, S., Austad, T., Puntervold, T., Høgnesen, E. J., Olsen, M., & Barstad, S. M. F. (2008). "Smart Water" for Oil Recovery from Fractured Limestone: A Preliminary Study. Energy & fuels, 22 (5), 3126-3133.
- Strand, S., Høgnesen, E. J., & Austad, T. (2006). Wettability alteration of carbonates—Effects of potential determining ions (Ca2+ and SO42−) and temperature. Colloids and Surfaces A: Physicochemical and Engineering Aspects, 275(1), 1-10.
- Thomsen, K., & Rasmussen, P. (1999). Modeling of vapor–liquid–solid equilibrium in gas–aqueous electrolyte systems. Chemical Engineering Science, 54 (12), 1787-1802.
- Venkatesan, R., Östlund, J. A., Chawla, H., Wattana, P., Nydén, M., & Fogler, H. S. (2003). The effect of asphaltenes on the gelation of waxy oils. Energy & fuels, 17(6), 1630-1640.

- Vo, L. T., Gupta, R., & Hehmeyer, O. J. (2012, January). Ion chromatography analysis of advanced ion management carbonate coreflood experiments. InAbu Dhabi International Petroleum Conference and Exhibition. Society of Petroleum Engineers.
- Zahid, A., Stenby, E. H., & Shapiro, A. A. (2010, June). Improved Oil Recovery in Chalk: Wettability Alteration or Something Else? (SPE-131300). SPE EUROPEC. In EAGE Annual Conference and Exhibition, Barcelona, Spain.
- Zahid, A., Sandersen, S. B., Stenby, E. H., von Solms, N., & Shapiro, A. (2011). Advanced waterflooding in chalk reservoirs: Understanding of underlying mechanisms. Colloids and Surfaces A: Physicochemical and Engineering Aspects, 389(1), 281-290.
- Zekri, A. Y., Nasr, M. S., & Al-Arabai, Z. I. (2011, January). Effect of LoSal on Wettability and Oil Recovery of Carbonate and Sandstone Formation. In International Petroleum Technology Conference. International Petroleum Technology Conference.
- Zhang, P., Tweheyo, M.T., Austad, T. (2006) Wettability alteration and improved oil recovery in chalk: The effect of calcium in the presence of sulfate. Energy and Fuels 20 (5), 2056-2062b
- Zhang, P., Tweheyo, M. T., & Austad, T. (2007). Wettability alteration and improved oil recovery by spontaneous imbibition of seawater into chalk: Impact of the potential determining ions Ca2+, Mg2+, and SO42−. Colloids and Surfaces A: Physicochemical and Engineering Aspects, 301(1), 199-208.

Tables:

Table 1: The optimized parameters (r and q) for different species in the Extended UNIQUAC model for calculating the speciation of different brine solutions. These parameters have been previously reported (Christensen and Thomsen 2003; García et al. 2006; García et al. 2005).

ion	r	q
H_2O	0,92	1,4
$CO_2(aq)$	0,74721	2,4496
Na^+	1,4034	1,199
K^+	2,2304	2,4306
Mg^{2+}	5,406	2,542
Ca^{2+}	3,87	1,48
Ba^{2+}	15,671	14,475
H+	0,13779	1E-16
Sr^{2+}	7,1446	12,894
Cl^-	10,386	10,197
SO_4^{2-}	12,794	12,444
OH^-	9,3973	8,8171
CO_3^{2-}	10,828	10,769
HCO_3^-	8,0756	8,6806

Table 2: The optimized interactions parameters for each pair of species used in the Extended UNIQUAC model for calculating the speciation of different brine solutions. These parameters have been previously reported (Christensen and Thomsen 2003; García et al. 2006; García et al. 2005).

	H_2O		CO_2(aq)		Na^+		K^+		Mg^{2+}		Ca^{2+}		Ba^{2+}		H^+		Sr^{2+}		Cl^-		SO_4^{2-}		OH^-		CO_3^{2-}		HCO_3^-	
	u0	ut	u0	ut	u0	ut	u0	ut	u0	ut	u0	ut	u0	ut	u0	ut	u0	ut	u0	ut	u0	ut	u0	ut	u0	ut	u0	ut
H_2O	0	0																										
CO_2(aq)	8,838	0,863	302,2	0,359																								
Na^+	733,3	0,487	172,4	-0,436	0	0																						
K^+	535	0,994	398,5	3,336	-46,19	0,119	0	0																				
Mg^{2+}	-2,043	-3,554	-581,8	-2,855	-70,96	1,339	-273,7	-1,079	0	0																		
Ca^{2+}	496,4	-8,065	2500	0	-100	-4,656	-275,6	-3,101	1	0	0	0																
Ba^{2+}	-0,379	0,582	2500	0	779,1	2,338	100	1	628,5	0	2500	0	0	0														
H^+	10000	0	1E+09	0	1E+09	0	1E+09	0	1E+09	0	1E+09	0	1E+09	0	0	0												
Sr^{2+}	543,1	1,274	-100,7	0	-103,9	-0,62	100	1	-400,6	-1,437	-402,8	-4,253	2500	0	1E+09	0	0	0										
Cl^-	1523	14,63	1613	15,02	1443	15,64	1465	15,33	2049	12,13	1806	11,14	1403	14,89	1E+09	0	1896	15,69	2215	14,44								
SO_4^{2-}	752,9	9,491	1942	4,79	845,1	11,68	913,8	12,28	1407	3,328	1258	50,45	2500	0	1E+09	0	2500	10	2036	12,41	1266	8,319						
OH^-	600,5	8,546	2500	0	1398	20,28	1806	27,28	736,4	0	164,6	3,608	2500	0	1E+09	0	2500	0	1896	13,63	1226	8,59	1563	5,617				
CO_3^{2-}	361,4	3,352	2500	0	548	3,782	1857	4,06	99	1	2500	0	2500	0	1E+09	0	2500	0	2725	5,727	1217	7,007	1588	2,75	1458	-1,345		
HCO_3^-	577,1	-0,388	526,3	-3,734	1102	1,829	967,8	1,26	99	1	2500	0	2500	0	1E+09	0	2500	0	1737	14,04	990,5	6,965	2500	0	800	1,724	771	-0,02

Table 3: The different data sets for which speciation calculations have been conducted.

Data Set	Coreplug Type	Origin	EOR	Methodology	Reference
1	Chalk	North Sea Chalk	Smart Water	Spontaneous Imbibition	RezaeiDoust et al. 2009
2	Chalk	North Sea Chalk	Smart Water	Water Flooding	Shariatpanahi et al. 2010
3	Chalk	US chalk	Smart Water	Water Flooding	Chandrasekhar et al. 2013
4	Limestone	Middle East	Smart Water	Water Flooding	Awolayo et al. 2014
5	Chalk	US chalk	Low Salinity brine	Water Flooding	Chandrasekhar et al. 2013
6	Chalk	US chalk	AIM	Water Flooding	Vo et al. 2012

Figures:

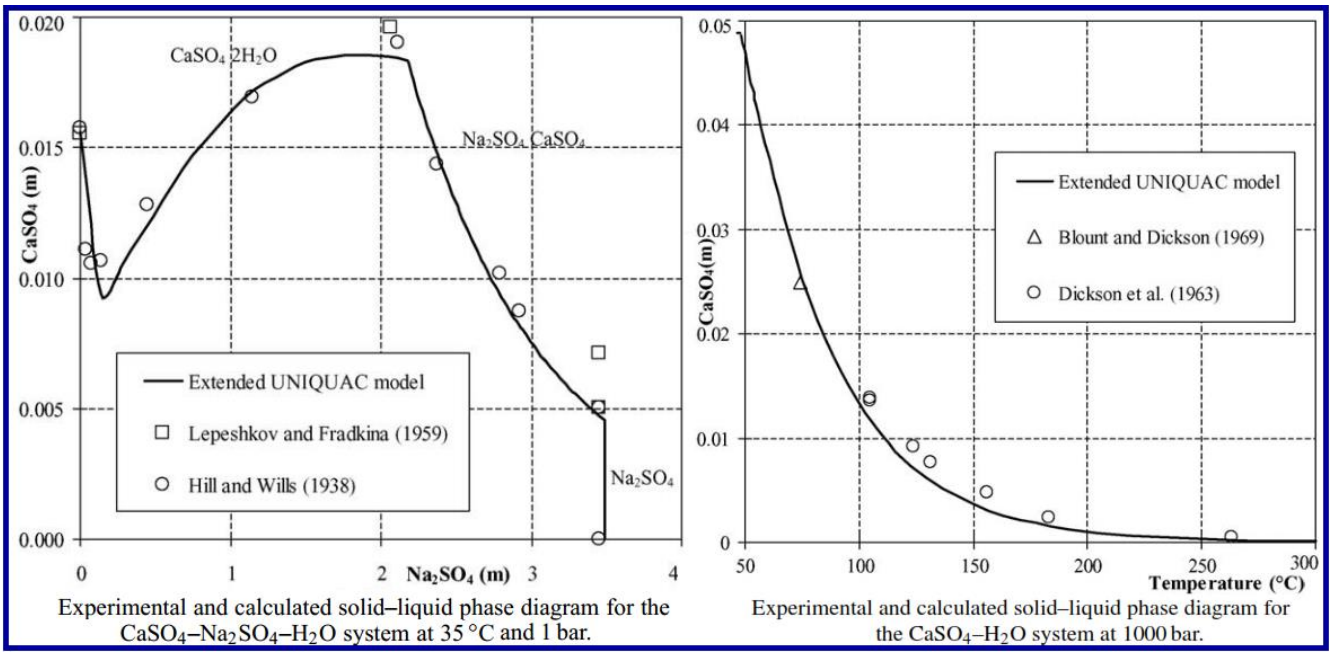


Figure 1: The accurate prediction of $CaSO_4$ precipitation at ambient and elevated pressures for single and multi-component systems. (García et al. 2005). The concentration unit on the axes is molality (mol/kg water).

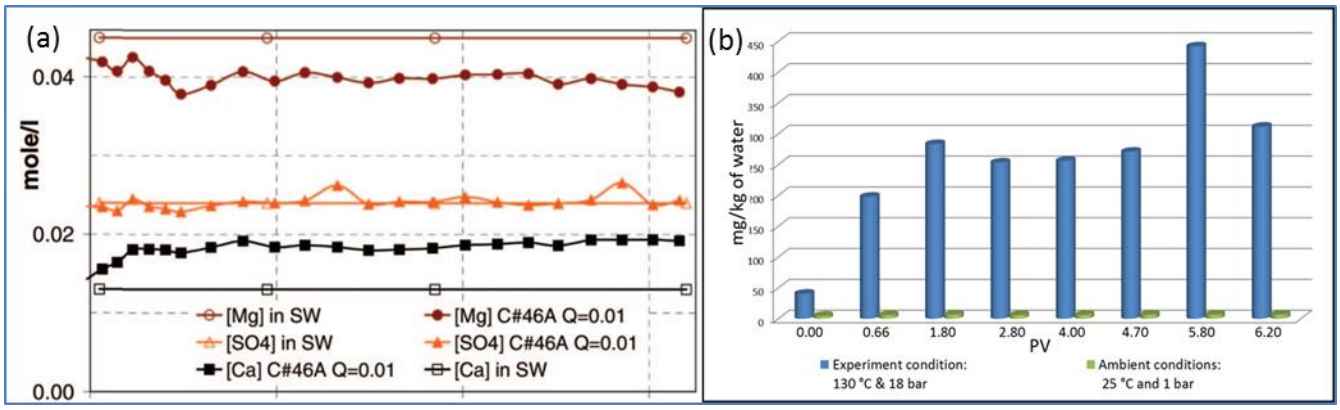


Figure 2 a: Effluent brine from spontaneous imbibition experiments (RezaeiDoust et al. 2009).b: The calculated amounts of $CaSO_4$ precipitation at experimental and ambient conditions. The reported values represent data set 1.

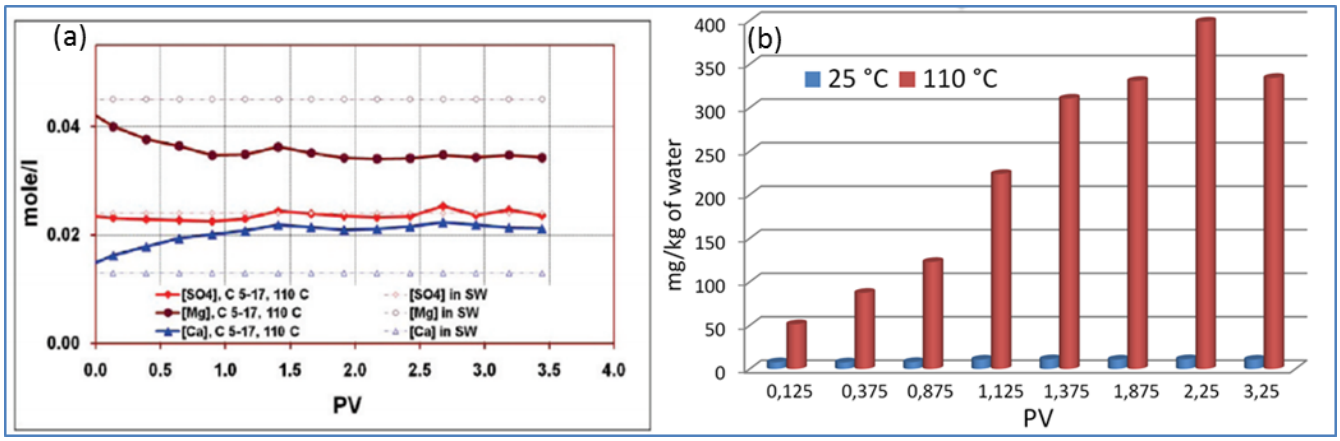


Figure 3a: Effluent brine from waterflooding experiment at 110°C (Shariatpanahi et al. 2010).b: The calculated amounts of $CaSO_4$ precipitation at experimental and ambient conditions. The reported values represent data set 2.

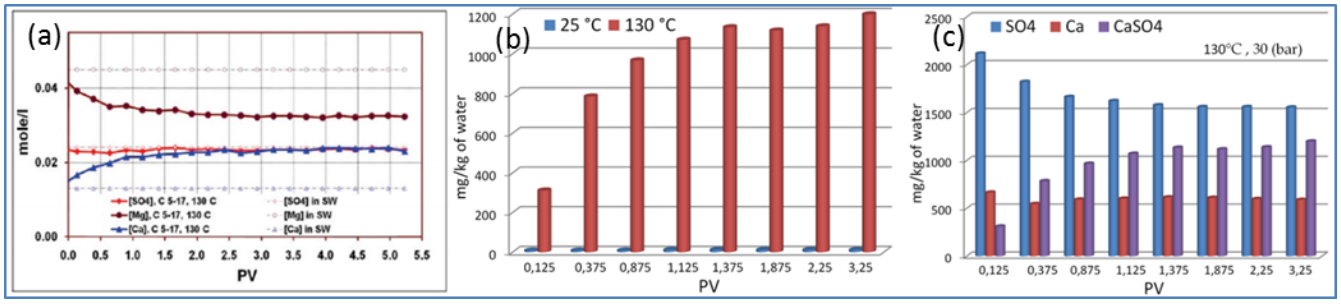


Figure 4 a: Effluent brine from waterflooding experiment at 130°C (Shariatpanahi et al. 2010).b: The calculated amounts of $CaSO_4$ precipitation at experimental and ambient conditions. c The calculated amount of soluble ions and insoluble salts produced from the coreplug at the flooding condition. The reported values represent data set 2.

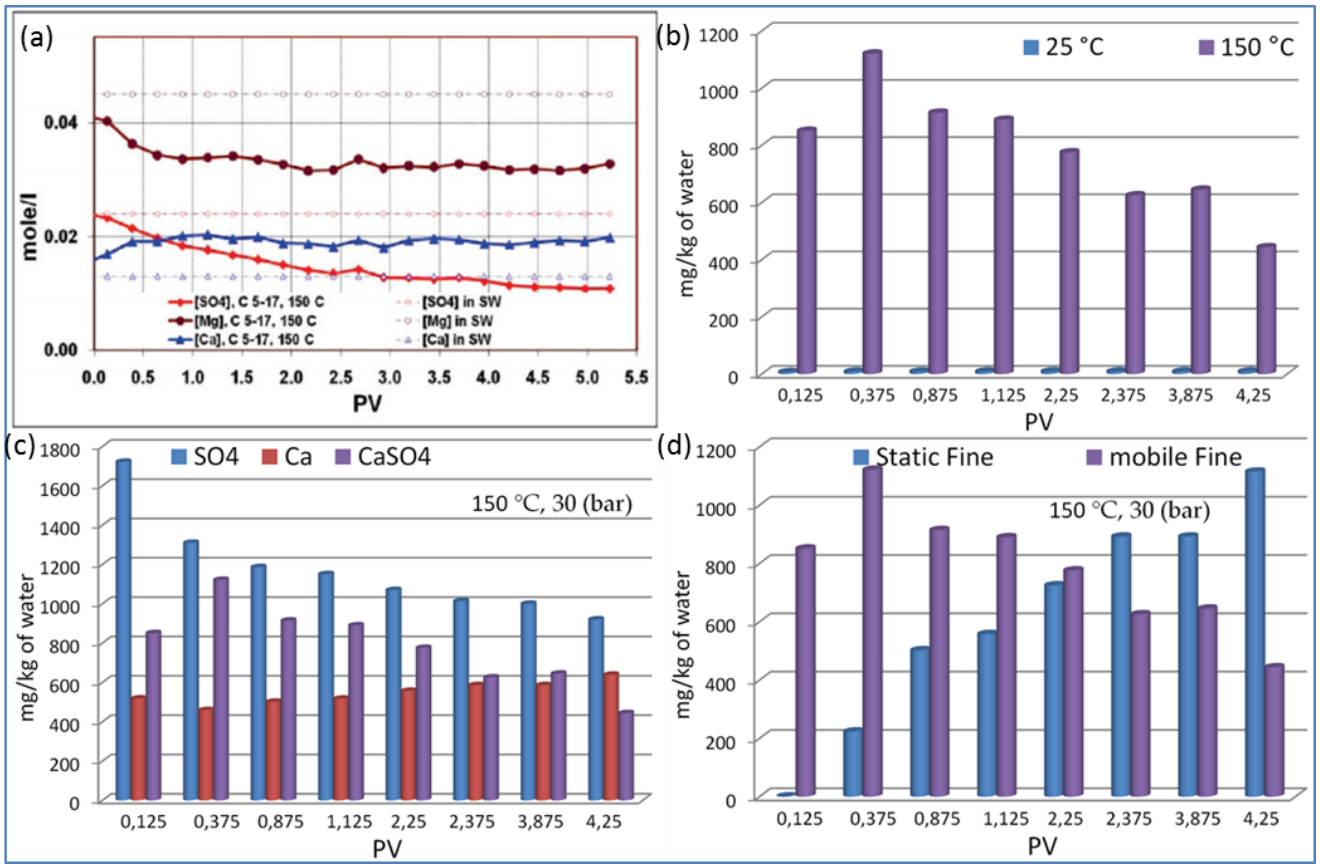


Figure 5 a: Effluent brine from waterflooding experiment at 150°C (Shariatpanahi et al. 2010).b: The calculated amounts of $CaSO_4$ precipitation at experimental and ambient conditions. c: The calculated amount of soluble ions and insoluble salts produced from the coreplug at the flooding condition. d: Amount of insoluble salts produced in the effluent (mobile fines), and amount of insoluble sat that precipitated in the coreplug (static fine). The reported values represent data set 2.

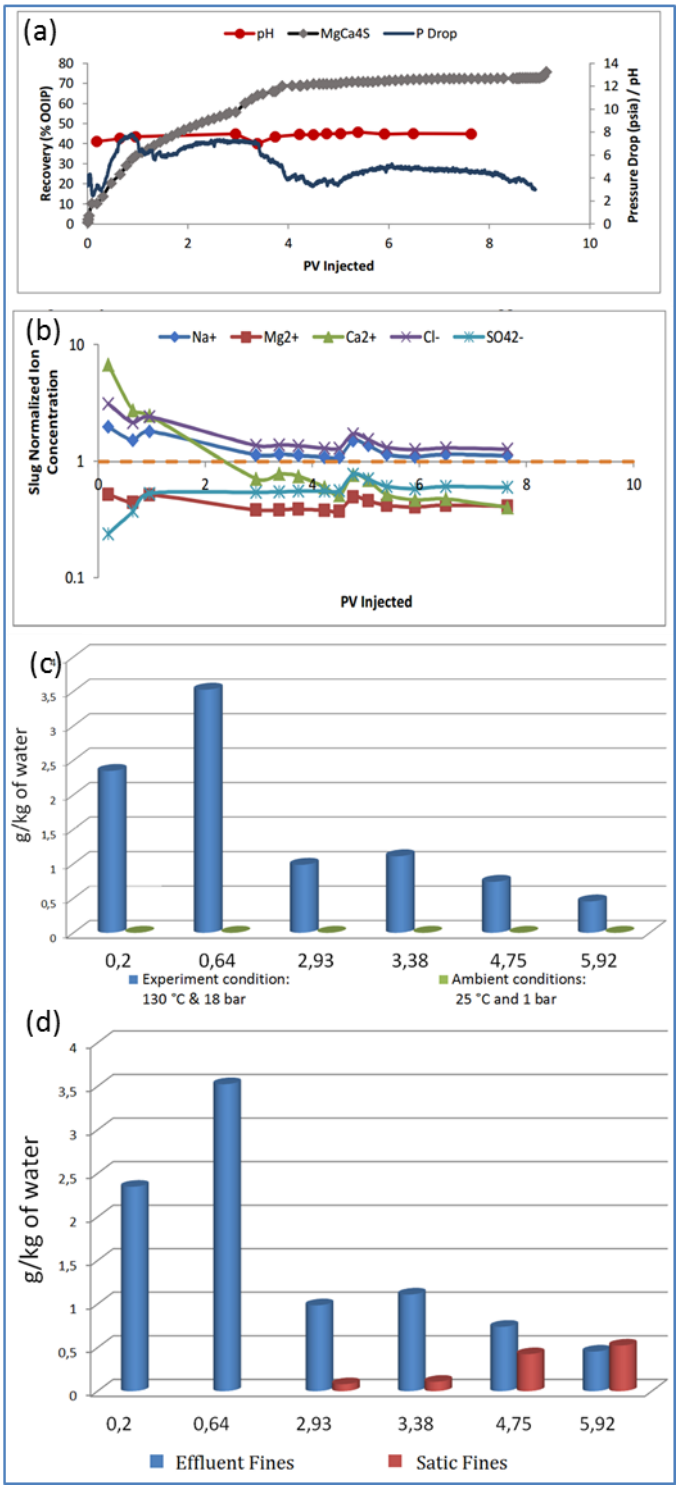


Figure 6 a &b: Reported oil recovery and Effluent brine from waterflooding experiment (Chandrasekhar et al. 2013).c: The calculated amounts of $CaSO_4$ precipitation at experimental and ambient conditions. d: The calculated amount of soluble ions and insoluble salts produced from the coreplug at the flooding condition. The reported values represent data set 3.

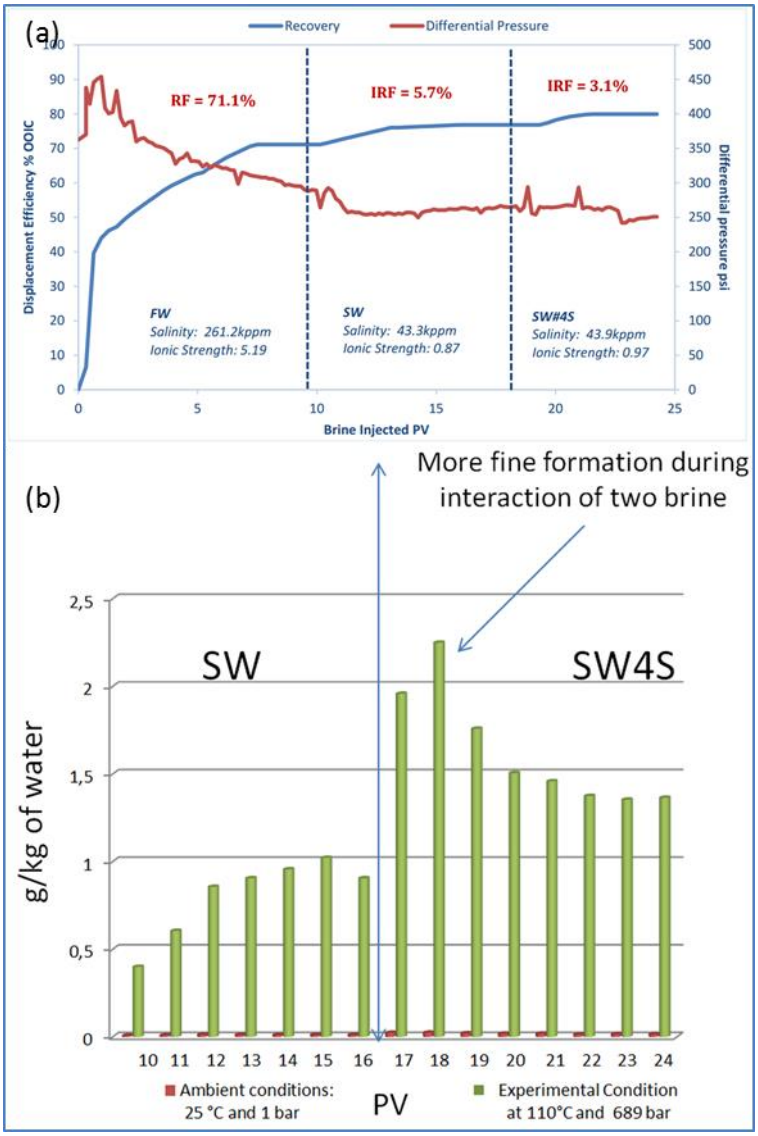


Figure 7 a: Reported oil recovery for smart waterflooding experiment US carbonates (Awolayo et al. 2014). b: The calculated amounts of $CaSO_4$ precipitation at experimental and ambient conditions. The reported values represent data set 4.

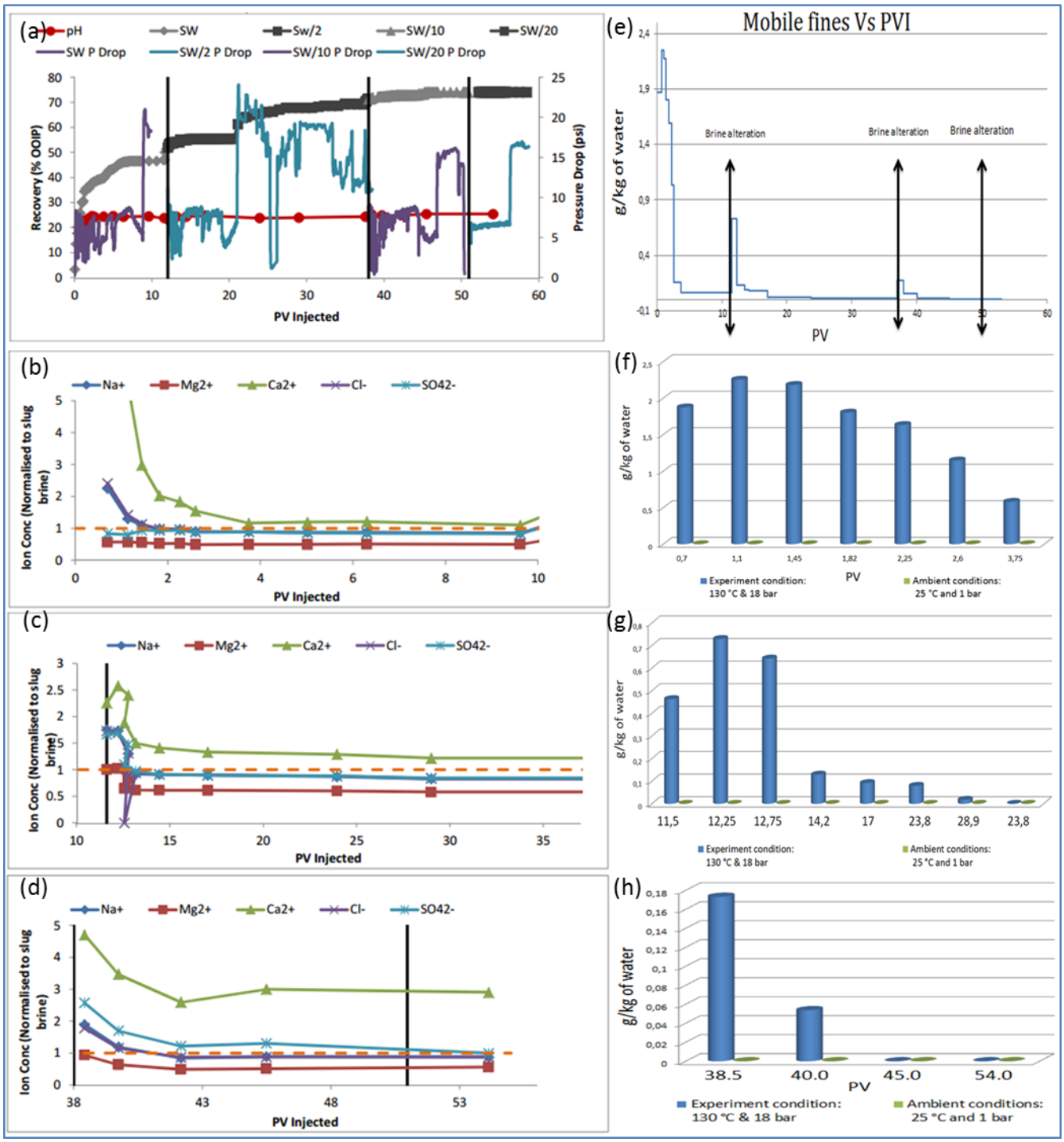


Figure 8 a-d: Reported oil recovery and effluent brine composition for low salinity brine flooding (Chandrasekhar et al. 2013). e-h: The calculated amounts of $CaSO_4$ precipitation at experimental and ambient conditions. The reported values represent data set 5.

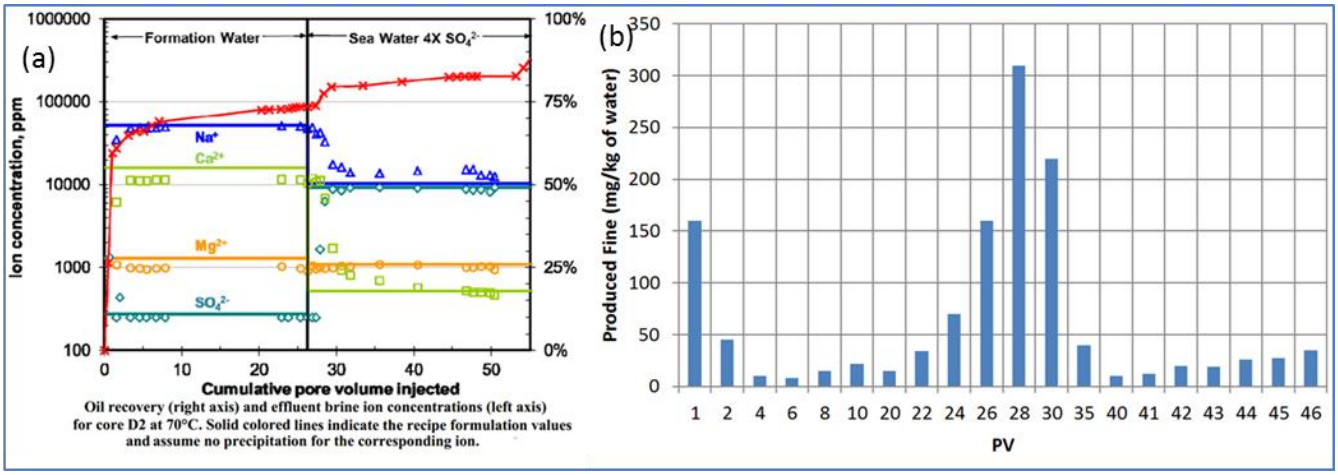


Figure 9 a: Reported oil recovery and effluent brine composition for Advanced Ion Management at (Vo et al. 2012). b: The calculated amounts of $CaSO_4$ precipitation at experimental and ambient conditions. The reported values represent data set 6.

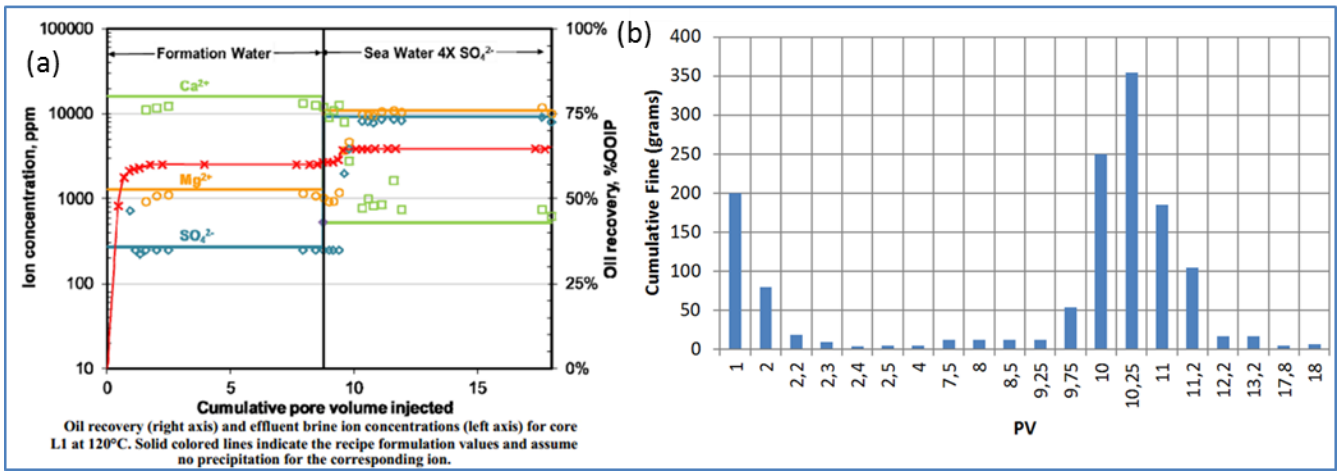


Figure 10 a: Reported oil recovery and effluent brine composition for Advanced Ion Management at (Vo et al. 2012). b: The calculated amounts of $CaSO_4$ precipitation at experimental and ambient conditions. The reported values represent data set 6.

Paper VIII

Chakravarty, K. H., & Thomsen, K. (2015, November). Formation of Anhydrite Due to Interaction Between Water Soluble CO_2 (aq) and Calcite Mineral During Enhanced Oil Recovery. In *SPE Oil & Gas India Conference and Exhibition*. Society of Petroleum Engineers.

SPE-178137-MS

Formation of Anhydrite due to interaction between water soluble CO_2(aq) and calcite mineral during Enhanced Oil Recovery

Krishna Hara Chakravarty, Philip Loldrup Fosbøl and Kaj Thomsen, Center for Energy Resources Engineering (CERE), Department of Chemical and Biochemical Engineering, Technical University of Denmark

Copyright 2015, Society of Petroleum Engineers

This paper was prepared for presentation at the SPE Oil and Gas India Conference and Exhibition held in Mumbai, India, 24–26 November 2015.

This paper was selected for presentation by an SPE program committee following review of information contained in an abstract submitted by the author(s). Contents of the paper have not been reviewed by the Society of Petroleum Engineers and are subject to correction by the author(s). The material does not necessarily reflect any position of the Society of Petroleum Engineers, its officers, or members. Electronic reproduction, distribution, or storage of any part of this paper without the written consent of the Society of Petroleum Engineers is prohibited. Permission to reproduce in print is restricted to an abstract of not more than 300 words; illustrations may not be copied. The abstract must contain conspicuous acknowledgment of SPE copyright.

Abstract

In the Low Salinity based EOR method, formation and migration of fines have proved to have profound effect on the displacement efficiency of residual oil. Salinity variations of injected brines have also been shown to affect oil recovery for WAG-CO_2 processes. But the effect of fines in EOR during LSWAG-CO_2 has not been studied previously. This study explores the possibility of fines formation during CO_2 injection and attempts to understand its implication in EOR.

In this study, we use the Extended UNIQUAC model to calculate the possibility of fines formation during CO_2 injection. Detailed simulations were conducted over a temperature range of 50°C to 250°C and a pressure range of 5 bars to 500 bars. The amounts of fines formation taking place for different LSWAG-CO_2 processes were correlated to the described oil recovery. It is observed that significant amounts of fines formation can take place during CO_2 injection in limestone reservoirs. At reservoir conditions, a considerable fraction of the injected CO_2 becomes soluble in sea water. This dissolved CO_2 causes dissolution of $CaCO_3$ from the mineral surface and releases Ca^{2+} ions into the pore space. Excess Ca^{2+} ions form anhydrite ($CaSO_4$) fines with the available SO_4^{2-} ions. The salinity and composition of brines present in pore space shows direct correlation with the amount of fines produced during CO_2 injection. With increase in temperature and pressure, the amount fines formation increased significantly.

The described oil recovery for different LSWAG injections showed a consistent correlation with the amounts of fines formation taking place in the pore space. The amount of mineral dissolution taking place was also precisely calculated using the Extended UNIQUAC model. Good correlation was also observed between calculated amounts of mineral dissolution and the observed increase in permeability. This study suggests that CO_2 injection in carbonate reservoir can have two distinct effects.

1. CO_2 miscible with oil can decrease oil viscosity, thus increase oil displacement.
2. CO_2 dissolved in water causes fines formation following dissolution of $CaCO_3$ .These fines can alter sweep efficiency by blocking pore throats and also increase oil displacement through its emulsification.

Injection of CO_2 leads to fines formation at most reservoir conditions. The formation of anhydrite fines have been neglected in previous studies. The amount of fines formation taking place shows significant correlation with the EOR obtained from LSWAG injection. The Extended UNIQUAC model can be used to precisely calculate both the amount of mineral dissolution and the amounts of fines formation taking place during CO_2 injection over varied pressure and temperature conditions.

Introduction:

WAG injection is the alternating use of waterflooding and gas injection, the two standard secondary oil recovery method. This combination is a well-known EOR method in which alternating rounds of water and gas are injected to enhance the sweep efficiency and thereby produce the residual oil (Christensen et al. 1998; Rogers et al. 2000; Yip et al 2015). Herein CO2 gas can be injected to reduce the viscosity of the residue oil; thus causing oil swelling. And CO2 injection also increases the relative permeability, thus promoting mobilization of trapped oil through the rock porous network. Due to the low gas density, the unfavorable high mobility ratio eventually decreases the sweep efficiency. Thus, subsequently the injection of CO2 is replaced by injection of sea water which further improves the macroscopic sweep efficiency. This combination of CO2 gas and sea water injection is recurrent until the rate of residue oil production decreases below a profitable level. Total increase in oil recovery during WAG EOR flooding is not substantial, since the average increase in residue oil production is only 5-10% of OOIP (Christensen et al. 1998;

Rogers et al. 2000; Yip et al 2015). Christensen et al. presented a comprehensive literature review of the WAG processes in about 59 fields and commented on several severe problems which caused the decrease in displacement efficiency when performing WAG-CO_2 injection. The fundamental challenges with WAG injection are the water and gas breakthrough and decrease in effectivity (Christensen et al. 1998; Gorell et al. 2001) due to challenges such as viscous variabilities/ fingering, gravity separation, through high permeability streaks zone.

For more than a century now, waterflooding has been consistently and widely implemented as the most beneficial method to accomplish the dual objectives of upkeeping reservoir pressure as well as water driven displacement of oil from the injector wells to the producer wells. In the mid-1990s, the concept of the impacts of brine composition variation on the residue oil production was introduced in the papers by Jadhunandan and Morrow 1995. And Yildiz and Morrow 1996 began to shift the industry's attention towards considering adjusting the ion composition and salinity of the injected fluid in order to produce an enhanced oil recovery. Sea water, chemically altered in composition, was thereafter termed as "smart water" (Strand et al. 2005). Subsequently, several meticulous studies have been conducted in order to further understand this phenomenon fundamentally (RezaeiDoust et al 2009; Fadili 2009; Fathi et al. 2011; Awolayo et al 2014; Yousef et al 2012). There have been several evidences from the various research laboratories that reduction in the salinity of sea water leads to higher oil production. The founding work by Tang and Morrow 1999 showed an improvement in the residue oil production efficiency when the salinity of the injection brine was reduced from 15,000 to 1,500 ppm. Following the extensive laboratory studies using core plugs, several larger scale implementation has also been conducted including single-well tests (Lager et al. 2006; McGuire et al. 2005; Hyatt et al 2005) and full field trials simulation study (Seccombe et al. 2008). Here the effect of Smart Water has also consistently demonstrated the potential of low-salinity waterflooding to improve residue oil production (Lager et al. 2006; McGuire et al. 2005; Hyatt et al 2005). Webb et al. 2005 described a decrease in the residual oil saturation, S_{or} as the salinity of the injection brine is altered from 100 to 20 % and finally 5 % of the salinity of the initial formation water. It is universally accepted that altering the brine composition and its salinity can increase the recovery fractions both in sandstone and carbonate reservoirs (Yildiz et al. 1999; Fogden 2011; Lebedeva and Fogden 2011; Gupta et al. 2011; Delshad et al. 2013; Parracello et al. 2013; Robertson, 2007; McGuire et al. 2005; Alagic et al. 2011; Webb et al. 2005; Karoussi et al. 2007; Zhang et al. 2007). Different methods have been suggested for potential EOR, but no clear mechanism for this technology has been universally accepted. There are several extensive investigation programs established to understand the scientific basis (Austad et al. 2005; Zahid et al. 2010; Gupta et al. 2011; Alvardo et al. 2014). SmW-EOR experiments with different outcrops and reservoir coreplug sample have shown significant increase in oil production for variation in composition and salinity of injected brine (Strand et al. 2006; Zhang et al. 2007; Austad et al. 2005; Bagci et al. 2001). Wettability alteration (Strand et al. 2006; Zhang et al. 2007; Austad et al. 2005) mineral dissolution (Pu et al. 2010; Yousef et al. 2011) and emulsification (Moradi et al. 2011; Moradi et al. 2013; Wang and Alvardo, 2012; Alvardo et al. 2014) are different mechanism that have been proposed to explain this phenomenon. But no general consensus has been established. According to the available literature, there are selective analyses concerning the applicability of Smart water in WAG CO2 processes (Yip et al. 2015; Kulkarni and Rao 2005). Kulkarni and Rao reported the impact of brine composition on the tertiary residue oil production through a laboratory study using 5 % and 0.5815 % NaCl reservoir brine during WAG. Herein it was concluded that WAG recoveries are exceedingly reliant on the salinity and composition of the injected brine. Jiang et al. 2010 further went on to show that the type of oil used had a major impact on the amount of additional oil production.

A substitute CO_2 injection strategy is carbonated (CO_2-enriched) water injection (CWI). In CWI, CO_2 is dissolved in the sea water (or modified sea water) before it is introduced into the reservoir. Instead of having a gaseous alternate liquid single phase, carbonated water ensures increased sweep efficiency. CO_2 is uniformly dispersed in the reservoir as the injected carbonated water mixes with the in situ water and retards CO_2 breakthrough, eventually improving sweep efficiency (Kechut et al. 2015; Sohrabiet al. 2009). This CO_2 injection strategy can possibly diminish meager sweep efficiency, which is one of the key limitations of orthodox constant CO_2 injection or WAG processes. It is also predominantly beneficial for watered-out oil reservoirs in which high water saturation unfavorably affects the CO_2 injection performance. Likewise, if the in situ oil is miscible with CO_2, carbonated water injection could result in noteworthy oil swelling, as in direct CO_2 injection (Sohrabi et al. 2009) despite only a fraction of the content of the injected fluid being CO_2. Thus CWI is another process which can not only increase the residue oil production, but also serve as an injection scheme for storing CO_2 in depleting oil reservoirs. The high solubility of CO_2 in the water phase is favorable for CO_2 storage. The risk of buoyancy-driven leak is lowered as the carbonated brine has much higher density than the oil (Hebach et al. 2004) and will move towards the bottom of the reservoir.

Clearly, in both CO_2 EOR methods, the available CO_2 in the reservoir can interact with the water present in reservoir. This interaction during the WAG process or the CWI process will lead to a new brine speciation. The amount of soluble ions and the amount of insoluble supersaturated salt play an important role in the interpretation of the data and in obtaining the fundamental mechanism associated with this phenomenon. When different smart water interacts with calcite surfaces in the presence of CO_2 dissolution of calcite from the mineral surface can occur. Dissolution of calcite from the mineral surface can enhance the pore space with Ca^{2+}. This additional Ca^{2+} in the pore space can interact with the SO_4^{2-} present in sea water and form insoluble anhydrite. Both dissolution of $CaCO_3$ and formation of insoluble anhydrite can affect the permeability of the coreplug. Thus accurately calculating the brine speciation of various smart waters in the presence of soluble CO_2 (aq) is very important. In this report, we calculate the brine speciation at reservoir conditions for different amounts of aqueous CO_2 in variedly modified sea water, using extended UNIQUAC model (Thomsen and Rasmussen 1999).

The extended UNIQUAC model is a thermodynamic model for aqueous solution of electrolytes and non- electrolytes (Thomsen and Rasmussen 1999). The parameters of this model have been optimized over a large amount of laboratory data (Christensen and Thomsen 2003; Thomsen et al. 1996; Garcia et al. 2005 ; Garcia et al. 2006). The experimental basis of this model enables it to describe the phase behavior and the thermal properties of solution containing electrolytes with great accuracy (Garcia et al 2005). Along with solid – liquid equilibrium data over diverse pressure temperature conditions, activity and osmotic co-efficient from the open literature have been used to optimize the parameters. Additionally, thermal properties including heat of dissolution, heat of solution and apparent molal heat capacity of salt solution have also been used for determining model parameters. And thus, these properties are also reproducible by the model. In Figure 1, the calculated solid-liquid equilibrium curves for the ternary $CaSO_4$ – Na_2SO_4 – H_2O system (at room temperature) and the binary $CaSO_4$ – H_2O system (at elevated pressure and temperature conditions) are plotted along with laboratory data from the open literature in order to demonstrate the accuracy of the model. Furthermore as shown in Figure 2, for systems including different salt solutions in water, the accurate amount of soluble CO_2(aq) can also be calculated using Extended UNIQUAC model over varied pressure and temperature conditions (García et al. 2005). In this work, the model was used to calculate phase equilibria related to the changes in brine concentration with change in temperature, pressure and interactions at mineral surfaces.

Calculation Method & Results

The main model parameters of the Extended UNIQUAC model are the volume and surface area parameters (r- and q-parameters), which are determined on the basis of massive amounts of binary and ternary laboratory data (Thomsen and Rasmussen 1999). Parameters for all ions used in smart water experiments have already been extensively optimized (Iliuta et al. 2000; Thomsen et al. 1996; García et al. 2005). The group of ions and neutral species includes H_2O, CO_2, Na^+, K^+, Mg^{2+}, Ca^{2+}, Ba^{2+}, H^+, Sr^{2+}, Cl^-, SO_4^{2-}, OH^-, CO_3^{2-} and HCO_3^-. The optimized r- and q-parameters are listed in table 1. The two individual parameters are specific to each species. In addition, each species pair has two additional parameters that describe the interaction between the species, which is assumed to have a linear temperature dependency. These species pair interaction parameters have also been previously optimized (Iliuta et al. 2000; Thomsen et al. 1996; García et al. 2005) and are listed in Table 2. The model predicts the behavior of multi component systems based on these unary and binary parameters. As the model parameters are based on binary and ternary data alone, the calculation of phase behavior in multi-component systems represents prediction by the model. In several calculations it has been shown that the Extended UNIQUAC model is capable of accurately representing multi-component systems with common ions covering a range of temperatures and ionic strengths that is large enough to represent all the conditions stated in laboratory and reservoir water flooding experiments.

Temperature variation effect on $CaCO_3$ and $CaSO_4$

Brine speciation was calculated at various different temperatures between 100 and 150 °C and at a pressure of 200 bars. Standard Sea water with the composition as stated in Austad et al. 2008 (0.45 m Na^+ ; 0.045 m Mg^{2+} ; 0.013 Ca^{2+}; 0.024 m SO_4^{2-} and 0.581 m Cl^-) was used in all calculations. Standard sea water with four different amounts of dissolved CO_2 was studied. It included 1 mol/kg, 0.5mol/kg, 0.1mol/kg and no dissolved CO_2. In previous studies it has been shown experimentally that at reservoir pressure (of 200 bars), 1.12 mol (1.0 mol) of CO_2 /kg of water are soluble in 1.09 m NaCl at 150°C (Takenouchi & Kennedy, 1965). An increase in CO_2 solubility is observed for a decrease in salinity (Prutton & Savage, 1945; Takenouchi & Kennedy, 1965; Rumpf et al. 1994). Standard sea water typically contains 0.45 m of Na^+ (Austad et al. 2009). Thus, it must have the capacity to dissolve more than 1.12 mol CO_2 /kg of water. The analysis done in this study was within the saturation limits for CO_2(aq). Several other studies also have shown that up to 2 mol of CO_2 per kg of water can be dissolved at temperatures between 100°C and 150°C and at pressures between 1 bars to 100 bars in standard sea water (Rumpf et al. 1994; García et al. 2005; Duan & Sun et al. 2003).

Basic brine speciation calculation shows that significant dissolution of $CaCO_3$ takes place from the mineral surface. Sea water containing small fraction of dissolved CO_2(aq) (i.e. 0.1 mol / per kg of water) can significantly alter brine speciation at reservoir condition and can lead to calcite dissolution at 130°C. With increase in temperature a gradual decrease in amount of precipitation was observed from 1.2 grams of $CaCO_3$ at 100°C to 0.7 grams of $CaCO_3$ at 150°C (As shown in Figure 3). For 0.5 m CO_2(aq) the amount of dissolution further increased to 2.5 grams of $CaCO_3$ at 100°C. It gradually decreased to 1.8 grams of $CaCO_3$ at 150°C (As shown in Figure 3). While for 1.0 m CO_2(aq) the amount of dissolution further increased to 3.5 grams of $CaCO_3$ at 100°C. It gradually decreased to 2.65 grams of $CaCO_3$ at 150°C (As shown in Figure 3). This shows that compared to temperature, the amount of CO_2 has a major effect in the increase in calcite dissolution. The higher the concentration of available soluble CO_2, the higher is the amount of dissolved mineral ions. Sea water typically contains only 520 mg of Ca^{2+} per kg of water. The release of additional 1 to 3 grams of Calcium carbonate in the pore space completely changes the composition of the water in the pore space. The sparingly soluble $CaSO_4$ reaches beyond its saturation limit and thus makes the solution supersaturated with $CaSO_4$. This amount of insoluble $CaSO_4$ present in the pore space was also calculated. It was observed that a significant amount of insoluble anhydrite can be formed following the dissolution of $CaCO_3$.

Sea water containing small fraction of dissolved CO_2 (aq) (i.e. 0.1 mol / per kg of water) can lead to significant amount of insoluble $CaSO_4$ formation at 130 °C and beyond. Up to 0.5 grams of insoluble $CaSO_4$ can form when the reservoir temperature is 150 °C. For 0.5 m CO_2(aq) this amount of insoluble anhydrite formation further increased to 0.7 grams of $CaSO_4$ at 100°C (As shown in Figure 3). With increase in temperature further increase in $CaSO_4$ formation was observed (to 1.8 m at 150°C), even though the

amount of calcite dissolution decreased. The decrease in the solubility of $CaSO_4$ with increase in temperature is expected to be the primary cause. For 1.0 m CO_2 (aq) the amount of insoluble anhydrite formation further increased to 2.8 grams of $CaSO_4$ at 100°C (As shown in Figure 3). It gradually increases to 2.6 grams of $CaSO_4$ at 150°C. This formation of anhydrite following the dissolution of calcite is in equally comparable amounts. Furthermore it is observed that the amount of anhydrite formation is significantly affected by both temperature and the amount of CO_2 present in the solution.

The dissolution of anhydrite has previously been observed in several studies and is well described in literature. But the associated anhydrite formation may not be visible in effluent vials after waterflooding at room temperature as anhydrite solubility increase significantly with a decrease in temperature.

Na variation effect on $CaCO_3$ and $CaSO_4$

In low Salinity and Smart Water are EOR techniques it is recommended to decrease the concentration of NaCl before sea water injection (Austad et al. 2005; Zhang et al. 2006). Use of Low salinity WAG CO_2 processes has also been considered. In various previous studies, a reduction of Na^+ ion concentration (from 0.45 mol/kg of water to 0.045 mol/kg) of water has been shown to increase the residue oil production. Up to 20 % dilution of sea water has been shown to result in an increase in displacement efficiency of the oil. When these low NaCl brines contain dissolved CO_2, the brine interaction with carbonate mineral surfaces can change significantly. NaCl depleted sea water with four different amounts of dissolved CO_2 were studied. It included 1 mol/kg, 0.5 mol/kg, 0.1 mol/kg and no dissolved CO_2. Brine speciation calculations were done for sea water with various concentrations of NaCl at a reservoir pressure of 200 bars and a temperature of 130°C. It was observed that in the absence of dissolved CO_2, no major dissolution of $CaCO_3$ took place, irrespective of the variation in NaCl concentration. .

A brine solution containing a small fraction of 0.1 m CO_2(aq) solution can significantly alter dissolution at various NaCl concentrations. For 0.45 m Na^+, 0.8 grams of $CaCO_3$ gets dissolved for each kg of water (As shown in Figure 4). Reducing the Na^+ concentration 10 times showed no major variation in the amount of $CaCO_3$ dissolution and 0.74 grams of calcite got dissolved for a brine solution containing 0.045 m of Na^+ ions. For 0.5 m CO_2(aq) this amount of dissolution further increased to 2.1 grams of $CaCO_3$ with 0.45 m Na^+ ions in the brine solution. It gradually decreased to 1.5 grams of $CaCO_3$ at 0.045 m Na^+ (As shown in Figure 4). With 1.0 m CO_2(aq) the amount of dissolution further increased to 2.9 grams of $CaCO_3$ at 0.45 m Na^+ ions in the brine solution (As shown in Figure 4). It gradually decreased to 1.95 grams of $CaCO_3$ at 0.045 m Na^+ (As shown in Figure 4).

This shows that compared to the Na^+ concentration, the amount of CO_2 has a major effect, increasing the calcite dissolution. Higher concentrations of dissolved CO_2 results in higher amounts of mineral ions dissolved from the reservoir rock. Decreasing the salinity of NaCl decreases the amount of $CaCO_3$ dissolution slightly. The effect of the Na^+ concentration on the dissolution of $CaCO_3$ is prominent for solutions containing higher concentrations of dissolved CO_2 in the water. As, for 0.1 m CO_2 no major variation in dissolution was observed for variation in Na^+ ion concentration.

Normal synthetic sea water with reduced Na^+ content shows formation of insoluble anhydrite salts at reservoir conditions. 10 times reduction of the Na^+ ion concentration in sea water results in up to 1.2 grams of $CaSO_4$ formation for each kg of water (at 130 °C and 200 bar). This anhydrite formation significantly reduces with increase in Na^+, and no insoluble fines are formed beyond 0.32 m Na^+ in absence of dissolved CO_2 (As shown in Figure 4). This shows that unlike dissolution of $CaCO_3$, formation of $CaSO_4$ significantly depend on the amount of Na^+ ions present in the pore space. Brine solution containing small fraction of 0.1 m CO_2(aq) can lead to significant amount of insoluble $CaSO_4$ formation at 0,045 m Na^+ (As shown in Figure 4). A 0.1 m CO_2 (aq) brine solution can result in up to 1.8 grams of $CaSO_4$ becoming insoluble when the reservoir contains reduced (0.045 m) concentration of Na^+. Increasing the concentration of Na^+ in the brine solution shows a consistent decrease in amount of anhydrite formation and at 0.45 m Na^+ no $CaSO_4$ supersaturation is observed. For 0.5 m CO_2(aq) the amount of insoluble anhydrite formation further increased to 2.6 grams of $CaSO_4$ at 0.045 Na^+ concentrations. With increase in Na^+ concentration a steady decrease in $CaSO_4$ formation was observed (to 1.4 g at 0.45 m Na^+). While for 1.0 m CO_2(aq) the amount of insoluble anhydrite formation further increased to 2.9 grams of $CaSO_4$ at 0.045 m Na^+ (As shown in Figure 4). It gradually decreased to 2.3 grams of $CaSO_4$ at 0.45 m Na^+. With increase in amount of dissolved CO_2(aq), the effect of Na^+ concentration on formation of anhydrite is gradually reduced. At 0.1 m CO_2, variation of the Na^+ concentration had a major impact on anhydrite formation. This impact decreased with increase in CO_2 (aq) concentration. The exact opposite was observed during $CaCO_3$ dissolution.

Furthermore it is observed that the amount of anhydrite formation is significantly affected by both Na^+ ion concentration and the amount of CO_2 present in the solution; while the amount of $CaCO_3$ is primarily related to the amount of dissolved CO_2 present in the solution.

Ca variation effect on $CaCO_3$ and $CaSO_4$

In smart water EOR studies with both North Sea chalks and Middle East lime stones it has been established that increasing the Ca^{2+} concentration can enhance residue oil production significantly (Austad et al. 2005; Zhang et al. 2006). Injection of Ca^{2+} rich brine along with CO_2 in WAG processes has also been considered. Normal synthetic sea water contains 0.013 m Ca^{2+} ion, studies by increasing this concentration to twice of four times have previously been considered in the literature. Thus, studying the variation in $CaCO_3$ dissolution and $CaSO_4$ formation due to variation in Ca^{2+} ion concentration is equally important. When the high

concentration Ca^{2+} brine solution gets a fraction of dissolved CO_2, its brine speciation with carbonates mineral surface can change significantly. Here Ca^{2+} enriched sea water with four different amounts of soluble CO_2 was studied. It included 1 mol/kg, 0.5 mol/kg, 0.1 mol/kg and no dissolved CO_2.

It was observed that in the absence of dissolved CO_2, no major dissolution of $CaCO_3$ took place, irrespective of the variation in Ca^{2+} concentration (from 0.013 m Ca^{2+} to 0.026 m Ca^{2+}). But a brine solution containing a small fraction of 0.1 m CO_2(aq) can significantly alter the dissolution that took place for various Ca^{2+} concentrations. For 0.013 m Ca^{2+} 0.8 grams of $CaCO_3$ gets dissolved for each kg of water. Increasing the Ca^{2+} concentration to 0.026 m showed no major variation in amount of $CaCO_3$ dissolution and 0.74 grams of calcite got dissolved (as shown in Figure 5). For 0.5 m CO_2(aq), the amount of dissolution further increased to 2.1 grams of $CaCO_3$ at 0.013 m Ca^{2+} ions in the brine solution. It gradually decreased to 1.6 grams of $CaCO_3$ at 0.026 m Ca^{2+}. For 1.0 m CO_2(aq), the amount of dissolution further increased to 2.9 grams of $CaCO_3$ at 0.013 m Ca^{2+} ions in the brine solution. It gradually decreased to 2.2 grams of $CaCO_3$ at 0.026 m Ca^{2+} (as shown in Figure 5).

This shows that compared to the Ca^{2+} concentration, the amount of dissolved CO_2 has a major effect on calcite dissolution. The higher the concentration of available dissolved CO_2, the higher is the amount of dissolved mineral ions. Increasing the concentration of Ca^{2+} decreases the amount of $CaCO_3$ dissolution. The effect of Ca^{2+} concentration on dissolution is $CaCO_3$ is prominent for solutions containing high concentration of dissolved CO_2 in the water. As, for 0.1 m CO_2 no major variation in dissolution was observed for variation in Ca^{2+} ion concentration.

The sea water typically contains only 520 mg of Ca^{2+} per kg of water and the release of additional up to 3 grams of $CaCO_3$ in the pore space completely changes the composition of the water in the pore space. The sparingly soluble $CaSO_4$ reaches beyond its saturation limit and thus makes the solution supersaturated with $CaSO_4$. This amount of insoluble $CaSO_4$ present in the pore space was also calculated. It was observed that a significant amount of insoluble anhydrite can be formed following the dissolution of $CaCO_3$.

Normal synthetic sea water itself does not show formation of any insoluble of anhydrite salts in reservoir conditions even for enriched Ca^{2+} concentration. Brine solutions containing a small fraction of 0.1 m CO_2(aq) can lead to significant amount of insoluble $CaSO_4$ formation at 0.026 m Ca^{2+}. For 0.1 m CO_2 (aq) brine solution, up to 0.7 grams of $CaSO_4$ can become insoluble when the reservoir contains 0.026 m Ca^{2+}. Decreasing the concentration of Ca^{2+} in the brine solution shows a consistent decrease in amount of anhydrite formation and at 0.013 m Ca^{2+} no $CaSO_4$ supersaturation is observed. For 0.5 m CO_2(aq) this amount of insoluble anhydrite formation further increased to 1.7 grams of $CaSO_4$ at 0.026 Ca^{2+} concertation. With increase in Ca^{2+} concentration a steady decrease in $CaSO_4$ formation was observed (to 1.3 grams at 0.013 m Ca^{2+}). While for 1.0 m CO_2 (aq) the amount of insoluble anhydrite formation further increased to 2.5 grams of $CaSO_4$ at for 0.026 m Ca^{2+} (as shown in Figure 5). It gradually decreased to 2.3 grams of $CaSO_4$ at 0.013 m Ca^{2+}. It is observable that unlike dissolution of $CaCO_3$ formation of $CaSO_4$ is significantly affected by variation in Ca^{2+} ion concentration. With increase in amount of dissolved CO_2 (aq) the effect of Ca^{2+} concentration on formation of anhydrite is gradually reduced. As at 0.1 m CO_2 Ca^{2+} concentration variation showed major impact in anhydrite dissolution. And this impact decreased with increase in CO_2 (aq) concentration.

This formation of anhydrite following the dissolution of calcite is in equally comparable amounts for variation in Ca^{2+} concentration and thus neither can be ignored. Furthermore it is observed that amount of anhydrite formation is significantly affected by both Ca^{2+} ion concentration and the amount of CO_2 present in the solution; the amount of $CaCO_3$ dissolution is primarily related to the amount of dissolved CO_2 present in the solution.

SO_4^{2-} variation effect on $CaCO_3$ and $CaSO_4$

In smart water EOR studies with both North Sea chalks and Middle East lime stones it has been established that increasing the amount of SO_4^{2-} concentration can enhance residue oil production significantly (Austad et al. 2008; Zhang et al. 2006). Injection of SO_4^{2-} rich brine along with CO_2 in WAG processes has also been considered. Normal synthetic sea water contains 0.024 m SO_4^{2-} ion. Studies of increasing this concentration to twice of four times have been previously considered in the literature. Thus studying variation in amount of $CaCO_3$ dissolution and $CaSO_4$ formation due to variation in SO_4^{2-} ion concentration is equally important. When this high concentration SO_4^{2-} brine solution is mixed with CO_2, its interaction with the carbonate mineral surface can change significantly. Here SO_4^{2-} enriched sea water with four different amounts of dissolved CO_2 was studied.

It was observed that in the absence of dissolved CO_2, no major dissolution of $CaCO_3$ took place irrespective of the variation in SO_4^{2-} concentration (from 0.024 m SO_4^{2-} to 0.048 m SO_4^{2-}). The corresponding brine solution containing a small fraction of 0.1 m CO_2 (aq) is significantly better for carbonate dissolution for various SO_4^{2} concentrations. For 0.024 m SO_4^{2-} 0.9 grams of $CaCO_3$ gets dissolved for each kg of water. Increasing the SO_4^{2-} concentration to 0.048 m showed a slight increase in amount of $CaCO_3$ dissolution and 1.12 grams of calcite got dissolved (as shown in Figure 6). For 0.5 m CO_2(aq) this amount of dissolution further increased to 2.1 grams of $CaCO_3$ at 0.024 m SO_4^{2-} ions in the brine solution. It gradually increased to 2.6 grams of $CaCO_3$ at 0.048 m SO_4^{2-}. For 1.0 m CO_2 (aq) the amount of dissolution further increased to 2.8 grams of $CaCO_3$ at 0.024 m SO_4^{2-} ions in the brine solution. It gradually increased to 3.7 grams of $CaCO_3$ at 0.048 m SO_4^{2-}(as shown in Figure 6).

This shows that both the amount of SO_4^{2-} ion concentration the amount of CO_2 has a major effect in increase in calcite dissolution. Normal synthetic sea water itself does not show formation of insoluble anhydrite salts at reservoir conditions, even with enriched SO_4^2 concentration. Brine solutions containing a small fraction of 0.1 m CO_2 (aq) can lead to significant amount of insoluble $CaSO_4$ formation at 0.024 m SO_4^{2-}. For 0.1 m CO_2 (aq) brine solution up to 0.8 grams of $CaSO_4$ can become insoluble when the reservoir contains enriched (0.024 m) concentration of SO_4^{2-}. Increasing the concentration of SO_4^{2-} in the brine solution shows a consistent increase in amount of anhydrite formation and at 0.048 m SO_4^{2-} 1.6 gram $CaSO_4$ supersaturation is observed. For 0.5 m CO_2 (aq) the amount of insoluble anhydrite formation further increased to 3.1 grams of $CaSO_4$ at 0.024 m SO_4^{2-} concertation. With increase in SO_4^2 concentration a steady increase in $CaSO_4$ formation was observed (to 3.8 grams at 0.048 m SO_4^{2-}). While for 1.0 m CO_2 (aq) the amount of insoluble anhydrite formation further increased to 4.5 grams of $CaSO_4$ at for 0.024 m SO_4^{2-}(as shown in Figure 6). It gradually increased to 5.6 grams of $CaSO_4$ at 0.048 m SO_4^{2-}. It is observable that like dissolution of $CaCO_3$, formation of $CaSO_4$ is significantly affected by variation in SO_4^{2-} ions. With increase in amount of dissolved CO_2(aq) the effect of SO_4^{2-} concentration on formation of anhydrite gradually also increased.

The amount of anhydrite fine formation is consistently comparable to the amount of dissolved calcite. Thus formation of these in soluble anhydrites can have a major impact in the relative permeability of the reservoir. Furthermore it is observed that the amount of calcite dissolution and anhydrite formation is significantly affected by both SO_4^{2-} ion concentration and the amount of CO_2 present in the solution.

Discussion

Previously, the effect of salinity and composition variations has been studied for WAG-CO_2 processes. It has been shown that increasing the injected Ca^{2+} from 0.002mol/L to 0.02mol/L can increase the oil production by 1.2% of OOIP (Dang et al. 2014). In this study we also observed that with a similar increase of Ca^{2+} concentration the amount of anhydrite fine formation also increases by 0.5 g/kg of water (as shown in figure 5). Moreover, the amount of dissolution of $CaCO_3$ showed a minor decrease with increase in Ca^{2+} concentration in the injected water. This shows that for carbonate reservoirs during injection of carbonated water an increase in amount of Ca^{2+} can produce higher fraction of anhydrite formation, which shows direct correlation to the observed oil recovery. And dissolution of calcite shows no direct correlation to the observed oil recovery.

In the same study (Dang et al. 2014) it was observed that if the concentration of Na^+ is reduced from 0.45 mol/L to 0.045 mol/L, the corresponding oil production increases 5.1% of OOIP (i.e. from 69.3% oil recovery to 74.4% oil recovery). As shown in figure 4, the amount of anhydrite production also increases with and decrease in the Na^+ concentration of the injected water. When Na^+ concentration is reduced 10 times, anhydrite formation increases by 1.7 g/kg of water for 0.1 mol of dissolved CO_2 at 130°C and 200 bars. Moreover the amount of dissolution of $CaCO_3$ showed a significant decrease with decrease in Na^+ concentration of the injected water. This also shows that with a decrease in Na concentration both oil recovery and anhydrite fine formation increases. Furthermore an inverse correlation between calcite dissolution and oil recovery is observed. Variation of HCO_3^- in the injected water has also been previously studied (Dang et al. 2014). It has been observed that with an increase in HCO_3^- concentration (from 0.002 m to 0.02 m) a consistent decrease in oil recovery by 2.7 % of OOIP is observed. The Extended UNIQUAC calculation was conducted for the same compositions at 130°C and 200 bars. As shown in Figure 7, it was observed that for varying concentration of dissolved CO_2 the amount of calcite dissolution and the amount of anhydrite formation both showed consistent decrease with increase in HCO_3^-. For 10 times increase in HCO_3^- concentration both calcite dissolution and anhydrite formation decreased by 0.5 grams/kg of water. This shows that for variation in HCO_3^- both calcite dissolution and anhydrite fine formation correlates to the observed oil recovery. This shows that during CO_2 WAG processes implementation, the formation of anhydrite fines show a consistent correlation to the observed oil recovery and reducing composition of all ions may not be necessary for carbonate reservoirs.

The Extended UNIQUAC modeling show that the reported oil recovery has a direct correlation with the amount of anhydrite fines formation taking place in the coreplug. It has previously been shown that fines can increase adhesion between oil and water by emulsification of residue oil (Chakravarty et al. 2015). The emulsification only takes place when the crude oil contains polar fractions (Chakravarty et al. 2015). It has also previously been shown that crude oil must contain polar acids for successful implementation of CO_2 based WAG processes (Dang et al. 2014). Therefore, it is possible that interaction between insoluble anhydrite fines and polar acids may be responsible behind increased oil displacement in CO_2 based WAG processes. Nevertheless more supporting evidence is required to prove the correlation.

The effect of brine composition alteration has also been studied with CWI (Shorabi et al. 2011). Core flooding experiments with two different brine compositions was conducted. The first brine had 10,000 ppm salinity, containing 0.8 wt% sodium chloride (NaCl) and 0.2 wt% calcium chloride hexahydrate ($CaCl_2 \cdot 6H_2O$). The second brine used was of relatively higher salinity representing seawater. It contained 2.6 wt% of sodium chloride (NaCl) and 0.6 wt% of calcium chloride hexahydrate ($CaCl_2 \cdot 6H2O$) with overall salinity of 35,380 ppm (Shorabi et al. 2011). The carbonated water flooding showed that for low salinity brine the increment in oil recovery was 6.6 % of PV while for higher salinity the increment in oil recovery was 11.9 % of PV (Shorabi et al. 2011). The extended UNIQUAC modeling at the same conditions show that the total amount of calcium sulphate fines formation taking place was 0.7 grams/kg of water and 1.2 grams/ kg of water for the first and the second brines respectively. This shows that

the amount of fines formation taking place directly correlates to the reported oil recovery. And the exact composition of brines is needed for obtaining the amount of fine formation taking place in the coreplug.

The reservoir mineral wetting state or wettability has been extensively reported to influence the residue oil displacement during EOR mechanisms. Oil and water composition, the mineralogy of the rock, the initial water saturation, and the temperature are various factors that affect mineral wettability (Buckley et al. 1989; Buckley and Liu 1998). Previously carbonated water injection into both mixed wet and water wet coreplugs have been conducted (Sohrabi et al. 2011). Herein core flooding with CWI at 38 °C and 2000 psi showed that for the mixed wet coreplug, the increment in oil recovery from CWI took place earlier than in the water wet coreplugs. This shows that an efficient displacement in CWI is observed for mixed wet coreplugs, but wettability alteration is not necessary for the same. The Extended UNIQUAC calculations show that the used carbonated water can lead to dissolution of calcite; which in turn leads to $CaSO_4.2H_2O(s)$ (gypsum) fines formation in the coreplug. It has been shown previously that displacement of oil can be enhanced for mixed wet coreplugs by its interaction with mobile fines (Tang and Morrow 1999). Therefore the observed efficient oil displacement for mixed wet coreplugs could be related to the formation of $CaSO_4.2H_2O$ fines in the coreplug.

These analyses show that the amount of fines formation shows good initial correlation to the reported oil recovery for dissolved CO_2 injection during WAG and CWI processes. To establish this correlation further, analysis needs to be conducted on reported oil recovery that involves variation in sea water salinity and injection of CO_2.

Conclusion:

During WAG and CWI the EOR processes dissolved CO_2 present in water interact with the carbonate rock and cause dissolution of calcium carbonate. This produces additional Ca^{2+} ions in the pore space. These additional Ca^{2+} ions lead to formation of insoluble $CaSO_4$ fines. The formation of this $CaSO_4$ salt is significantly dependent on the amount of soluble CO_2 present in the brine solution. Availability of even small amount of 0.1 m CO_2 (aq) in sea water can significantly influence both the amount of calcite dissolution and the amount of anhydrite formation.

- Different carbonated sea water solutions show that with an increase in temperature the amount of $CaCO_3$ dissolution consistently decreases, while the amount of $CaSO_4$ formation shows a steady increase. Both temperature and amount of dissolved CO_2 can alter the speciation significantly.
- Reducing the NaCl concentration of the brine solution results in a consistent increase in anhydrite formation. Available dissolved CO_2(aq) further enhances the amount of anhydrite formation. The $CaCO_3$ dissolution is not much affected by changes in the NaCl composition of the brine solution.
- Sea water with enriched Ca^{2+} concentration enhanced the amount of anhydrite formation and reduced the amount of calcite dissolution. The amount of dissolved CO_2 (aq) present in the coreplug have the most impact on the amount of dissolution and super saturation.
- Sea water with enriched SO_4^{2-} concentration enhanced both the amount of anhydrite formation and the amount of calcite dissolution. Herein both SO_4^{2-} concentration and amount of soluble CO_2 show significant effect in speciation salt formations.
- In all of these studies the amount of $CaCO_3$ dissolution and the amount of $CaSO_4$ formation was completely comparable and thus none of them can be ignored.

The dissolution and formation of salts can alter the relative permeability and preferential flow paths significantly.

References:

- Alvarado, V., Moradi Bidhendi, M., Garcia-Olvera, G., Morin, B., & Oakey, J. S. (2014, April). Interfacial Visco-Elasticity of Crude Oil-Brine: An Alternative EOR Mechanism in Smart Waterflooding. In *SPE Improved Oil Recovery Symposium*. Society of Petroleum Engineers.
- Austad, T., Strand, S., Madland, M. V., Puntervold, T., & Korsnes, R. I. (2008). Seawater in chalk: An EOR and compaction fluid. *SPE Reservoir Evaluation & Engineering*, **11**(04), 648-654.
- Awolayo, A., Sarma, H., &AlSumaiti, A. M. (2014, March). A Laboratory Study of Ionic Effect of Smart Water for Enhancing Oil Recovery in Carbonate Reservoirs. In SPE EOR Conference at Oil and Gas West Asia. Society of Petroleum Engineers.
- Christensen, J. R., Stenby, E. H., &Skauge, A. (1998, January). Review of WAG field experience. In International Petroleum Conference and Exhibition of Mexico. Society of Petroleum Engineers.
- Dang, C. T., Nghiem, L. X., Chen, Z., Nguyen, N. T., & Nguyen, Q. P. (2014, April). CO2 Low Salinity Water Alternating Gas: A New Promising Approach for Enhanced Oil Recovery. In *SPE Improved Oil Recovery Symposium*. Society of Petroleum Engineers.

- Fadili, A., Kristensen, M. R., & Moreno, J. (2009, January). Smart integrated chemical EOR simulation. In International Petroleum Technology Conference. International Petroleum Technology Conference.
- Fathi, S. J., Austad, T., & Strand, S. (2011). Water-based enhanced oil recovery (EOR) by "smart water": Optimal ionic composition for EOR in carbonates. Energy &fuels, 25(11), 5173-5179.
- García, A. V., Thomsen, K., &Stenby, E. H. (2006). Prediction of mineral scale formation in geothermal and oilfield operations using the Extended UNIQUAC model: Part II. Carbonate-scaling minerals. Geothermics, 35(3), 239-284.
- García, A. V., Thomsen, K., &Stenby, E. H. (2005). Prediction of mineral scale formation in geothermal and oilfield operations using the extended UNIQUAC model: part I. Sulfate scaling minerals. Geothermics, 34(1), 61-97.
- Gorell, S., & Bassett, R. (2001, January). Trends in Reservoir Simulation: Big Models, Scalable Models? Will you please make up Your Mind?. In SPE Annual Technical Conference and Exhibition. Society of Petroleum Engineers.
- Gupta R., Smith G. G., Hu L., Willingham T., Cascio M. L. Shyeh J. J., &Harris C. R. (2011, January). Enhanced Waterflood for Carbonate Reservoirs-Impact of Injection Water Composition. In *SPE Middle East Oil and Gas Show and Conference*. Society of Petroleum Engineers.
- Hebach, A., Oberhof, A., &Dahmen, N. (2004). Density of water+ carbon dioxide at elevated pressures: measurements and correlation. Journal of Chemical & Engineering Data, 49(4), 950-953.
- Hyatt, J. H., & Hutchison, D. A. (2005, January). Enhanced oil recovery in east Texas. In SPE Middle East Oil and Gas Show and Conference. Society of Petroleum Engineers.
- Jadhunandan, P. P., & Morrow, N. R. (1995). Effect of wettability on waterflood recovery for crude-oil/brine/rock systems. SPE reservoir engineering, 10(01), 40-46.
- Jiang, H., Nuryaningsih, L., &Adidharma, H. (2010, January). The effect of salinity of injection brine on water alternating gas performance in tertiary miscible carbon dioxide flooding: experimental study. In SPE Western Regional Meeting. Society of Petroleum Engineers.
- Kechut, N. I., Jamiolahmady, M., &Sohrabi, M. (2011). Numerical simulation of experimental carbonated water injection (CWI) for improved oil recovery and CO 2 storage. Journal of Petroleum Science and Engineering, 77(1), 111-120.
- Kulkarni, M. M., & Rao, D. N. (2005). Experimental investigation of miscible and immiscible Water-Alternating-Gas (WAG) process performance. Journal of Petroleum Science and Engineering, 48(1), 1-20.
- Lager, A., Webb, K. J., Black, C. J. J., Singleton, M., &Sorbie, K. S. (2008). Low Salinity Oil Recovery-An Experimental Investigation1. Petrophysics, 49(01).
- McGuire, P. L., Chatman, J. R., Paskvan, F. K., Sommer, D. M., &Carini, F. H. (2005). Low Salinity Oil Recovery: An Exciting New EOR Opportunity for Alaska's North Slope, paper SPE 93903 presented at 2005 SPE Western Regional Meeting. Irvine, Ca.
- Moradi, M., Alvarado, V., & Huzurbazar, S. (2010). Effect of salinity on water-in-crude oil emulsion: evaluation through drop-size distribution proxy. *Energy & fuels*, **25** (1), 260-268.
- Moradi, M., Kazempour, M., French, J. T., & Alvarado, V. (2014). Dynamic flow response of crude oil-in-water emulsion during flow through porous media. *Fuel*,**135**, 38-45.
- Pu H., Yin P., & Morrow N. R. (2010, January). Low-salinity waterflooding and mineral dissolution. In *SPE Annual Technical Conference and Exhibition*. Society of Petroleum Engineers.
- RezaeiDoust, A., Puntervold, T., Strand, S., & Austad, T. (2009). Smart water as wettability modifier in carbonate and sandstone: A discussion of similarities/differences in the chemical mechanisms. Energy &fuels, 23(9), 4479-4485.
- Rogers, J. D., &Grigg, R. B. (2000, January). A literature analysis of the WAG injectivity abnormalities in the CO2 process. In SPE/DOE Improved Oil Recovery Symposium. Society of Petroleum Engineers.
- Rumpf, B., Nicolaisen, H., Öcal, C., & Maurer, G. (1994). Solubility of carbon dioxide in aqueous solutions of sodium chloride: experimental results and correlation. *Journal of Solution Chemistry*, *23*(3), 431-448.
- Sohrabi, M., Riazi, M., Jamiolahmady, M., Ireland, S., & Brown, C. (2009). Mechanisms of oil recovery by carbonated water injection, SCA2009-26. In International Symposium of the Society of Core Analysis.
- Seccombe, J. C., Lager, A., Webb, K. J., Jerauld, G., &Fueg, E. (2008, January). Improving Wateflood Recovery: LoSalTM EOR Field Evaluation. In SPE Symposium on Improved Oil Recovery. Society of Petroleum Engineers.
- Strand, S., Austad, T., Puntervold, T., Høgnesen, E. J., Olsen, M., &Barstad, S. M. F. (2008). "Smart water" for oil recovery from fractured limestone: a preliminary study. Energy &fuels, 22(5), 3126-3133.
- Thomsen, K., Rasmussen, P., & Gani, R. (1996). Correlation and prediction of thermal properties and phase behaviour for a class of aqueous electrolyte systems. Chemical Engineering Science, 51(14), 3675-3683.

- Thomsen, K., & Rasmussen, P. (1999). Modeling of vapor–liquid–solid equilibrium in gas–aqueous electrolyte systems. Chemical Engineering Science, 54(12), 1787-1802.
- Webb, K. J., Black, C. J. J., &Tjetland, G. (2005, January). A laboratory study investigating methods for improving oil recovery in carbonates. In International Petroleum Technology Conference. International Petroleum Technology Conference.
- Yan, W., &Stenby, E. H. (2009, January). The influence of CO2 solubility in brine on CO2 flooding simulation. In SPE Annual Technical Conference and Exhibition. Society of Petroleum Engineers.
- Yildiz, H. O., & Morrow, N. R. (1996). Effect of brine composition on recovery of Moutray crude oil by waterflooding. Journal of Petroleum science and Engineering, 14(3), 159-168.
- Yip, P. M., &Alta'ee, A. F. (2015). Simulation Study of the Effect of Smart Water on Relative Permeability During WAG-CO2 Injection for Light Oil Reservoir. In ICIPEG 2014 (pp. 109-120). Springer Singapore.
- Yousef, A. A., Liu, J., Blanchard, G., Al-Saleh, S., Al-Zahrani, T., Al-Zahrani, R., & Al-Mulhim, N. (2012, October). Smartwater flooding: industry's first field test in carbonate reservoirs. In Proceedings of the SPE Annual Technical Conference and Exhibition (pp. 8-10).
- Zhang, P., & Austad, T. (2006). Wettability and oil recovery from carbonates: Effects of temperature and potential determining ions. *Colloids and Surfaces A: Physicochemical and Engineering Aspects*, **279**(1), 179-187.

Tables:

Table 1: The optimized parameters (r and q) for different species in the Extended UNIQUAC model for calculating the speciation of different brine solutions. These parameters have been previously described (Christensen and Thomsen 2003; García et al. 2006; García et al. 2005).

ion	r	q
H_2O	0,92	1,4
$CO_2(aq)$	0,74721	2,4496
Na^+	1,4034	1,199
K^+	2,2304	2,4306
Mg^{2+}	5,406	2,542
Ca^{2+}	3,87	1,48
Ba^{2+}	15,671	14,475
H+	0,13779	1E-16
Sr^{2+}	7,1446	12,894
Cl^-	10,386	10,197
SO_4^{2-}	12,794	12,444
OH^-	9,3973	8,8171
CO_3^{2-}	10,828	10,769
HCO_3^-	8,0756	8,6806

Table 2: The optimized interactions parameters for each pair of species used in the Extended UNIQUAC model for calculating the speciation of different brine solutions. These parameters have been previously described (Christensen and Thomsen 2003; García et al. 2006; García et al. 2005).

	H_2O		CO_2(aq)		Na^+		K^+		Mg^{2+}		Ca^{2+}		Ba^{2+}		H^+		Sr^{2+}		Cl^-		SO_4^{2-}		OH^-		CO_3^{2-}		HCO_3^-	
	u0	ut	u0	ut	u0	ut	u0	ut	u0	ut	u0	ut	u0	ut	u0	ut	u0	ut	u0	ut	u0	ut	u0	ut	u0	ut	u0	ut
H_2O	0	0																										
CO_2(aq)	8,838	0,863	302,2	0,359																								
Na^+	733,3	0,487	172,4	-0,436	0	0																						
K^+	535	0,994	398,5	3,336	-46,19	0,119	0	0																				
Mg^{2+}	-2,043	-3,554	-581,8	-2,855	-70,96	1,339	-273,7	-1,079	0	0																		
Ca^{2+}	496,4	-8,065	2500	0	-100	-4,656	-275,6	-3,101	1	0	0																	
Ba^{2+}	-0,379	0,582	2500	0	779,1	2,338	100	1	628,5	0	2500	0	0	0														
H^+	10000	0	1E+09	0	1E+09	0	1E+09	0	1E+09	0	1E+09	0	1E+09	0	0	0												
Sr^{2+}	543,1	1,274	-100,7	0	-103,9	-0,62	100	1	-400,6	-1,437	-402,8	-4,253	2500	0	1E+09	0	0	0										
Cl^-	1523	14,63	1613	15,02	1443	15,64	1465	15,33	2049	12,13	1806	11,14	1403	14,89	1E+09	0	1896	15,69	2215	14,44								
SO_4^{2-}	752,9	9,491	1942	4,79	845,1	11,68	913,8	12,28	1407	3,328	1258	50,45	2500	0	1E+09	0	2500	10	2036	12,41	1266	8,319						
OH^-	600,5	8,546	2500	0	1398	20,28	1806	27,28	736,4	0	164,6	3,608	2500	0	1E+09	0	2500	0	1896	13,63	1226	8,59	1563	5,617				
CO_3^{2-}	361,4	3,352	2500	0	548	3,782	1857	4,06	99	1	2500	0	2500	0	1E+09	0	2500	0	2725	5,727	1217	7,007	1588	2,75	1458	-1,345		
HCO_3^-	577,1	-0,388	526,3	-3,734	1102	1,829	967,8	1,26	99	1	2500	0	2500	0	1E+09	0	2500	0	1737	14,04	990,5	6,965	2500	0	800	1,724	771	-0,02

Figures:

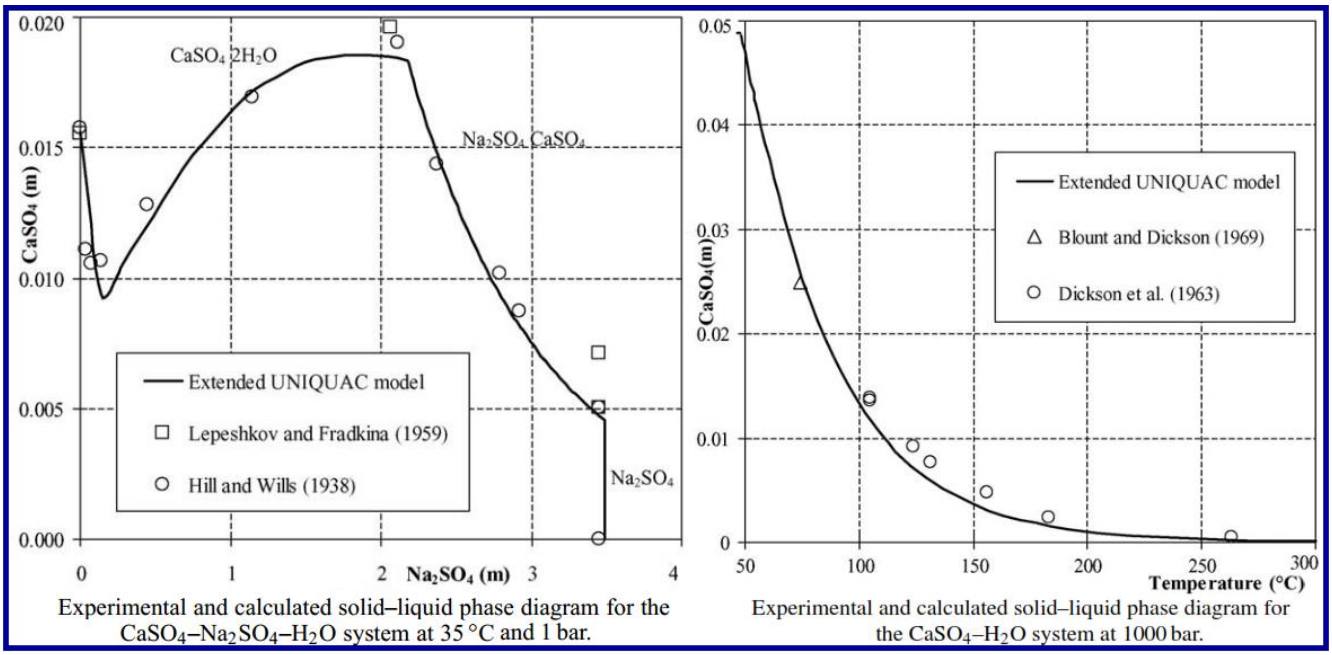


Figure 1: The accurate prediction of $CaSO_4$ precipitation at ambient and elevated pressures for single and multi-component systems. (García et al. 2005). The concentration unit on the axes is molality (mol/kg water).

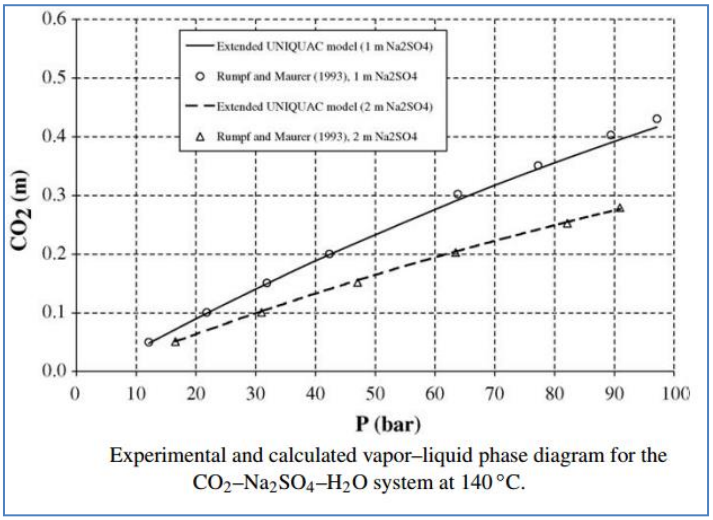


Figure 2: The accurate prediction of CO_2 solubility elevated pressures for multi-component systems. (García et al. 2006). The concentration unit on the axes is molality (mol/kg water).

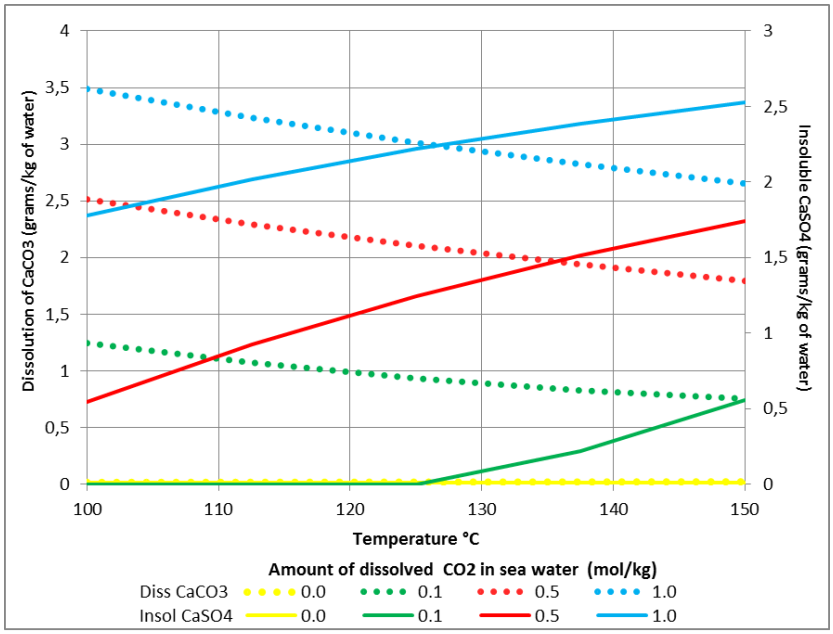


Figure 3: Amount of $CaCO_3$ dissolution calculated using Extended UNIQUAC model at various temperatures (from 100°C to 150°C) is plotted in dotted lines. Amount of insoluble $CaSO_4$ formed following the dissolution $CaCO_3$ is calculated plotted in bold lines. Color code indicates different concertation of soluble CO_2 present in the brine solution.

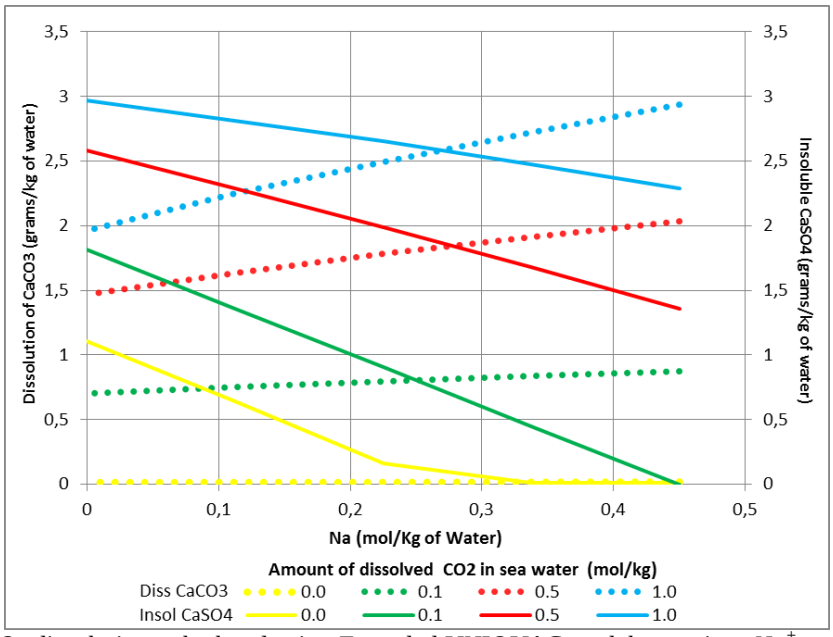


Figure 4: Amount of $CaCO_3$ dissolution calculated using Extended UNIQUAC model at various Na^+ concentration (from 0.045 m Na^+ to 0.45 Na^+) is plotted in dotted lines. Amount of insoluble $CaSO_4$ formed following the dissolution $CaCO_3$ is calculated plotted in bold lines. Color code indicates different concertation of soluble CO_2 present in the brine solution. Brine speciation calculation is done at 130 °C and 200 bars.

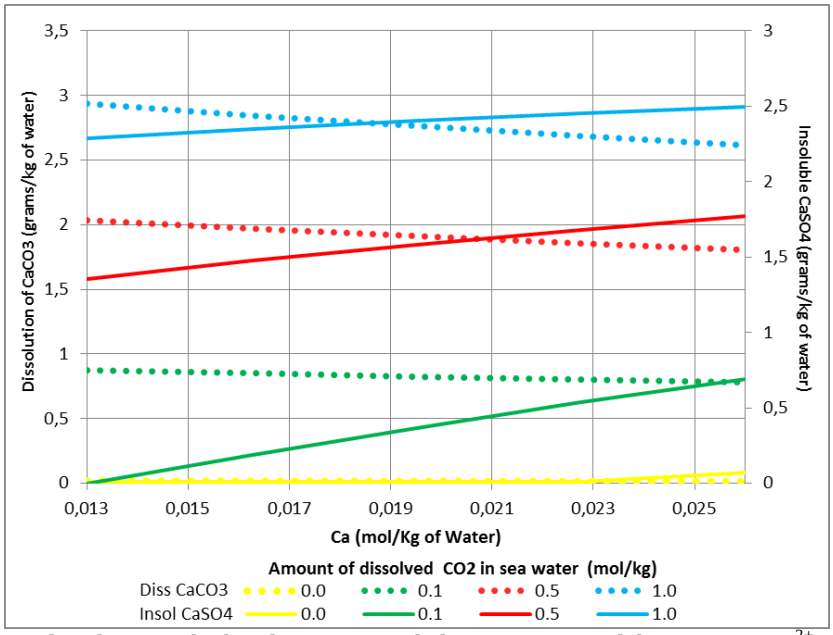


Figure 5: Amount of $CaCO_3$ dissolution calculated using Extended UNIQUAC model at various Ca^{2+} concentration (from 0.013 m Ca^{2+} to 0.026 Ca^{2+}) is plotted in dotted lines. Amount of insoluble $CaSO_4$ formed following the dissolution $CaCO_3$ is calculated plotted in bold lines. Color code indicates different concertation of soluble CO_2 present in the brine solution. Brine speciation calculation is done at 130 °C and 200 bars.

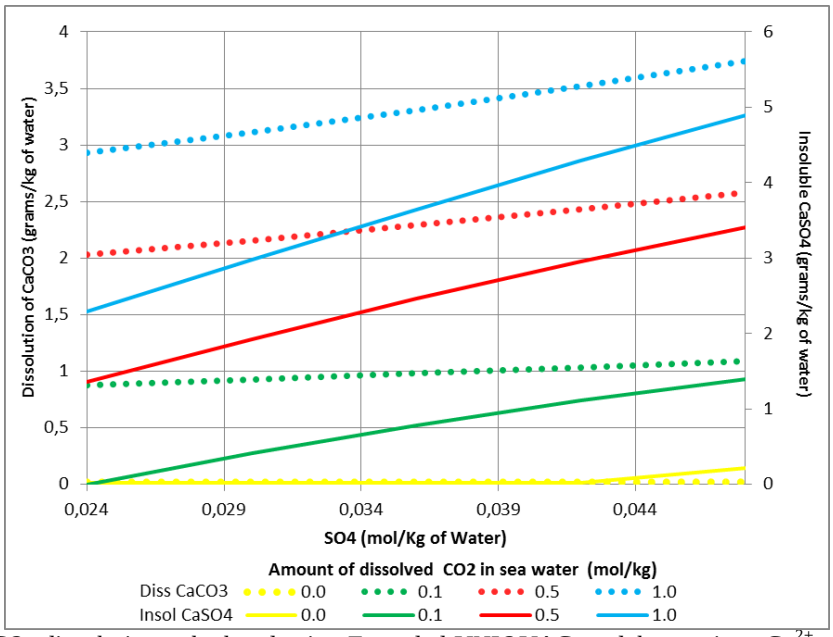


Figure 6: Amount of $CaCO_3$ dissolution calculated using Extended UNIQUAC model at various Ca^{2+} concentration (from 0.024 m SO_4^{2-} to 0.026 mSO_4^{2-}) is plotted in dotted lines. Amount of insoluble $CaSO_4$ formed following the dissolution $CaCO_3$ is calculated plotted in bold lines. Color code indicates different concertation of soluble CO_2 present in the brine solution. Brine speciation calculation is done at 130 °C and 200 bars.

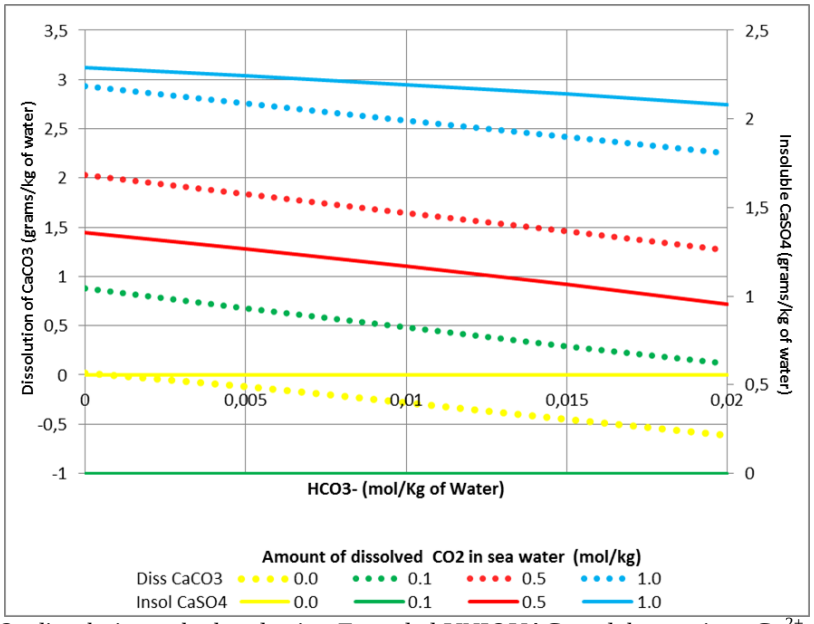


Figure 7: Amount of $CaCO_3$ dissolution calculated using Extended UNIQUAC model at various Ca^{2+} concentration (from 0.001 m HCO_3^- to 0.02 mHCO_3^-) is plotted in dotted lines. Amount of insoluble $CaSO_4$ formed following the dissolution $CaCO_3$ is calculated plotted in bold lines. Color code indicates different concertation of soluble CO_2 present in the brine solution. Brine speciation calculation is done at 130 °C and 200 bars. Negative values of dissolution indicate precipitation of Calcite.

Paper IX

Modeling of salt solubility and dissolution during smart water flooding for carbonate reservoir

Chakravarty, K. H., Fosbøl, P. L., & Thomsen, K. (2016) Modeling of salt solubility and dissolution during smart water flooding for carbonate reservoir. ***Journal of Petroleum Science and Engineering (To be submitted)***

Abstract:
Alteration of the composition of sea water for injection in chalk reservoirs has developed into a potential enhanced oil recovery method. The proposed wettability alteration mechanism suggests that a high fraction of potential ions (i.e. Ca^{2+}; Mg^{2+} and SO_4^{2-}) should be used and insoluble salt precipitation must be avoided for optimum oil production. But based on Extended UNIQUAC calculations it has been found that significant amounts of insoluble fines formation of anhydrite ($CaSO_4$) are formed from brines reported in literature. A consistent, direct correlation between the amount of insoluble fines and the observed oil recovery has also been established by analyzing various flooding and imbibition experiments. In this study, the distinction between the formation of insoluble fines and salt precipitation during injection into core plugs for smart water flooding is made. It is shown through examples that for highly precipitating brines, the oil production shows a one-to-one correlation with the amount of fines formation. Furthermore, this study differentiates between the speciation properties of injected brine at ambient conditions and at reservoir conditions. It is shown that most recommended brines are supersaturated at reservoir conditions and will cause major precipitation during injection in reservoirs.

Introduction:
In most oil fields 10-15% of the original oil in place (OOIP) is produced during primary oil recovery and thereafter sea water is injected into the reservoirs (Tang and Morrow 1997). This method of sea water injection into the reservoirs has been extensively used over the last century and is known as secondary oil recovery. Through extensive research in the past two decades it has been observed that instead of only injecting sea water, brines with modified composition and salinity can significantly increase the oil production (Tang and Morrow 1997; RezaeiDoust et al. 2009; Fathi et al. 2011; Strand et al. 2006; Yousef et al. 2012; Yousef et al. 2011; .Awolayo et al. 2014; Morrow and Buckley 2011; Al Shalabi et al. 2014; Alvarado et al. 2014; Zahid et al. 2012; Chakravarty et al. 2015). This observation has gradually developed into a potential and enhanced oil recovery process. In this process, the concentration of selective ions like Na^+ and Cl^- are reduced while the concentrations of certain ions are increased (Ca^{2+}; Mg^{2+} and SO_4^{2-}) to increase the oil production significantly (RezaeiDoust et al. 2009; Fathi et al. 2011; Strand et al. 2008).
In the first systemic study, diluted sea water was injected into Berea sandstone core plugs and it was observed that 10 times dilution of sea water can increase oil production by 10-15% of OOIP (Tang and Morrow 1997). Thereafter, in 2006 it was observed that in case of carbonate rock, selectively removing NaCl from the sea water instead of diluting it, can significantly enhance oil recovery. Removing all ions was not necessary (Strand et al. 2006). It was observed that further increasing the concentration of Ca^{2+}, Mg^{2+} and SO_4^{2-} ions can positively influence the oil displacement (RezaeiDoust et al. 2009; Fathi et al. 2011; Strand et al. 2008). This increase in oil recovery with increase in concentration of divalent ions was termed as smart water flooding (RezaeiDoust et al. 2009). This study has been established through various meticulous water flooding experiments and spontaneous imbibition experiments (RezaeiDoust et al. 2009; Fathi et al. 2011; Strand et al. 2006; Yousef et al. 2012; Yousef et al. 2011; Awolayo et al. 2014). In most of the smart water experiments chalk outcrops from Stevns Klint (Denmark) have been used (Fathi et al. 2011; Strand et al. 2006). Thereafter, low salinity water flooding (i.e. flooding with diluted sea water) has also been studied and a considerable increase in oil recovery has been observed (Al Shalabi et al. 2014; Zahid et al. 2012). In certain carbonate reservoirs, the applicability of low salinity water floods has been debated (Austad et al. 2011). Nevertheless these high potential and low salinity brines have been suggested for increasing the oil production in the oil reservoirs (Puntervold et al. 2014; Puntervold et al. 2015).
In all of the analyzed experiments, there has been a general flooding system which has been followed (Tang and Morrow 1997; Strand et al. 2006). Modified sea water is injected into core plugs which are kept at a high pressure and high temperature condition. This injected water removes the existing oil from the pore space. The produced oil and the water are collected in effluent samples as observable in figure 1. Before the brine is injected into the injection pipes, no change in composition of brine takes place. After the brine is injected into the core plug, it interacts with the mineral surface and residue oil. Several processes like adsorption (Zhang et al. 2006), desorption (RezaeiDoust et al. 2009), precipitation (Zhang et al. 2006; Tweheyo et al. 2006) and dissolution (Yousef et al. 2012) can take place during this interaction. These processes can alter the brine composition in the core plug. But, once the brine is released from the core plug, again no compositional change take place in the effluent pipes. Thus, all compositional change in injected brine can only takes place within the core plug. The core plug is universally considered as the only region where brine properties can be altered (Tang and Morrow 1997; Strand et al. 2006).

But the brines in the injection tubes are at room temperature, and the temperature gradually increases to reservoir conditions during the injection into the core plug. This variation in pressure and temperature can significantly change the brine properties, particularly its equilibrium speciation (Chakravarty et al. 2015a). Similarly, the speciation of the produced effluent brine can also be altered as it moves from the reservoir to ambient conditions. In most previous studies, the produced brine and the effluent brine are assumed to be the same with no compositional change (Chakravarty et al. 2015b). But a possible change in this brine speciation has not been previously considered. Using Extended UNIQUAC model (Thomsen and Rasmussen 1999) it has been observed that the produced brine contains significant amounts of insoluble salt. These amounts are directly proportional to the amount of oil production (Chakravarty et al. 2015b). Similarly, the injection brine in the holding cylinders and the brine at reservoir conditions are assume to be the same, because no compositional change apparently takes place. But possible changes in brine properties, particularly brine speciation can take place before injection into the core plug.

Based on various smart water flooding and imbibition experiments the concluding recommendation for North Sea chalk reservoirs at 130 °C given by Puntervold et al. 2014 and Puntervold et al. 2015 is that: Selectively remove 90% of NaCl from the sea water for optimum increase in oil recovery. Spontaneous imbibition experiments with Stevns Klint outcrop chalk support and substanti-

ate this as a consistent increase in oil recovery is observed for a decrease in NaCl concentration. It has been shown that spontaneous imbibition experiments at 90ºC can produce around 42% of OOIP with normal sea water; while up to 51% of OOIP is produced when NaCl is selectively removed from sea water (Puntervold et al. 2014). Furthermore, it has been shown that removing NaCl and selectively increasing the concentration of SO_4^{2-} ions in the injection brine, the oil recovery can be further increased. As shown in figure 2, sea water without sodium chloride and four times the sulfate concentration of sea water produces 62% of OOIP when spontaneous imbibition experiment was conducted under similar conditions (Puntervold et al. 2015).

By conducting reverse osmosis of sea water, low salinity brines can easily be obtained for large scale field implementation. Selectively removing NaCl from sea water on the other hand becomes a major challenge employing both nano filtration and reverse osmosis in parallel (Yousef and Ayirala 2014). This makes the process much more costly and energy consuming. In order to possibly avoid this costly and energy consuming process, this study aims to conduct a detailed analysis of possible changes in brine speciation during injection as the brine moves from room temperature to reservoir conditions.

It has also been shown that increasing the Ca^{2+} concentration to four times of that in sea water, can significantly increase the oil production at 70ºC and 100ºC (Zhang et al. 2006; Tweheyo et al. 2006). But at 130 ºC this Ca^{2+} enriched brine does not result in increased oil production when compared to sea water (Tweheyo et al. 2006). It is suggested that high concentration of Ca^{2+} causes precipitation of the injected brine due to anhydrite formation. Therefore it is recommended that the brine has an optimum temperature beyond which its efficiency starts decreasing when compared to synthetic sea water (Tweheyo et al. 2006). So, in comparison to sea water, Ca^{2+} enriched brine can cause more oil production up to 100 ºC; but not at 130 ºC as precipitation of anhydrite chokes the flow of oil (Zhang et al. 2006; Tweheyo et al. 2006).

Based on these studies, two recommendations have been made (RezaeiDoust et al. 2009):

1. High concentration of potential ions i.e. Ca^{2+}, Mg^{2+} and SO_4^{2-} ions should be used
2. Any salt precipitation during smart water floods must be avoided.

On the basis of the above study the brines recommended for injection in reservoirs are SW0NaCl (sea water with no NaCl), SW0NaCl-2SO4 (sea water without NaCl and twice SO_4^{2-}), SW0NaCl-3SO4 (sea water without NaCl and thrice SO_4^{2-}) and SW0NaCl-4SO4 (sea water without NaCl and 4 times SO_4^{2-}) (Puntervold et al. 2014). At high temperature other brine compositions such as, SWnSO4 (sea water with n times SO_4^{2-} ∀ n= 2, 3, 4 and 8 (Fathi et al. 2011;Awolayo et al. 2014)), SWnCa (sea water with n times Ca^{2+} ∀ n= 2, 3 and 4 (Zhang et al. 2006)); SW2Ca4SO4 (Sea water with twice Ca^{2+} and 4 times SO_4^{2-} (RezaeiDoust et al. 2009)); SW2Mg (sea water with twice Mg^{2+}(RezaeiDoust et al. 2009)) have also shown increase in oil production for chalk and limestone core plugs. This study aims to explore if any possible precipitation can take place with these recommended brines in high temperature core plugs. The study further attempts to understand its implications during implementation in reservoir conditions.

Calculations and Results

Brine Speciation of SW0NaCl-nSO4

Calculations were conducted using Extended UNIQUAC model (Thomsen and Rasmussen 1999) for modeling SW0NaCl-nSO4 (∀ n= 1, 2, 3 and 4) at reservoir conditions at the Ekofisk field (as recommended for injection (Puntervold et al. 2014)). Calculations were conducted over a pressure range from 1 to 600 bar. Spontaneous imbibition process are typically conducted at 10 to 50 bar (Fathi et al. 2011; Puntervold et al. 2014) while reservoirs conditions can go up to 400 bar (Stokka et al. 2005). The brine properties were calculated over a temperature range from 120ºC to 140ºC. The temperature of North Sea chalk reservoirs is typically 130ºC (Stokka et al. 2005; Puntervold et al. 2014). Local variation in temperature may cause a variation by plus/minus 10ºC (Stokka et al. 2005). Calculations were therefore done in the temperature range from 120 to 140 ºC.

Extended UNIQUAC SW0NaCl-4SO4 Speciation

Through Extended UNIQUAC speciation calculation it was observed that SW0NaCl-4SO4 is supersaturated at Ekofisk field conditions. If enough time is available for nucleation and crystal growth, a fraction of the brine will precipitate at 130 °C as shown in figure 3. The brine is super saturated at 10-50 bar (experimental conditions) as well as at 400 bar (reservoir conditions). It was observed that for all local variation in temperature i.e. 120 ºC to 140 ºC the brine was supersaturated and a significant amount of precipitation would take place (Figure 3). It must be noted that this precipitation of SW0NaCl-4SO4 is a property of the brine alone and it will take place irrespective of variations in crude oil composition or mineral lithology.

Furthermore it has been shown in literature (RezaeiDoust et al. 2009) that injection of Mg^{2+} into chalk reservoirs causes mineral substitution as Ca^{2+} ions from the mineral surface is replaced by the flooded Mg^{2+}. Thus, following ion substitution, Ca^{2+} concentration further increases in the pore space (Chakravarty et al. 2015a). The pore brine composition changes significantly as observable from the effluent composition (Shariatpanahi et al. 2010). A new speciation calculation for the changed pore brine was performed using the Extended UNIQUAC model. As shown in figure 3, it was observed that the amount of soluble SO_4^{2-} and Ca^{2+} in the pore space decreased significantly due to precipitation of $CaSO_4$(s) in the pore space after ion substitution.

Extended UNIQUAC SW0NaCl-3SO4 Speciation

Speciation properties of SW0Na-3SO4 was also calculated at reservoir conditions (120 to 140ºC and 1 to 600 bar) using the Extended UNIQUAC model. As shown in figure 4, it was observed that the injected brine was supersaturated at reservoir conditions and provided enough time it will cause precipitation. This precipitation can take place near the injection point or in the injection pipe depending upon the kinetics of brine nucleation.

Furthermore, when the brine enters the reservoir, ion substitution on the mineral surface takes place (RezaeiDoust et al. 2009). This additional Ca^{2+} production from the pore space changes the brine properties and thus, causes the possibility of further precipitation. It was observed that a significant amount of the remaining soluble salt forms anhydrite fines because of the increase in Ca^{2+}. It was observed that only 1.2 grams of sulfate per kg of water was soluble at the reservoir conditions after ion substitution, while around 5.8 grams of sulfate per kg of water was initially injected (figure 4). This shows that the majority of the sulfate ion injected into the core plug becomes insoluble and forms precipitate at reservoir conditions. The proposed brine SW0NaCl-3SO4 is therefore supersaturated at both the experimental and the reservoir conditions. Therefore using SW0NaCl-3SO4 (Puntervold et al. 2015) and avoiding precipitation (Tweheyo et al. 2006) are two contradictory statements which cannot be maintained simultaneously.

Extended UNIQUAC SW0NaCl-2SO4 Speciation

Furthermore, properties of sea water with double sulfate content was calculated at reservoir conditions for temperature variation from 120 ºC to 140 ºC and pressures ranging from 1 to 600 bar using Extended UNIQUAC model. It was observed that SW0NaCl-2SO4 also becomes supersaturated at reservoir conditions. As shown in Figure 5, a significant fraction of salt from the injected brine will form precipitate at Ekofisk conditions. It was also observed that when the brine enters into the reservoir, it undergoes mineral substitution (as previously stated (RezaeiDoust et al. 2009)), which produces more Ca^{2+} in the pore space. This additional Ca^{2+} in the pore space further causes precipitation of anhydrite salt and the sulfate concentration in the reservoir decreases significantly. With SW0NaCl-2SO4, 4.6 g of sulfate is injected for each kg water and less than 0.5 gm sulfate reservoir remains soluble at the reservoir conditions (as observable in figure 5). This shows that the majority of the injected sulfate ions become insoluble when the brine enters into the reservoir.

Extended UNIQUAC SW0NaCl Speciation

Finally, sea water without sodium chloride with no additional sulfate was analyzed by Extended UNIQUAC calculation. In this case it was observed that for conditions at Ekofisk field, SW0NaCl also forms precipitate at reservoir conditions (as shown in figure 6). Thus, injecting sea water with no sodium chloride can result in precipitation during injection. Only a fraction of the injected SO_4^{2-} and Ca^{2+} ions remains soluble at reservoir conditions. If precipitation takes place in the injection pipe or in the reservoir (near the injection point) depends on the grain nucleation kinetics. Furthermore, when Mg^{2+} ions of the injection brine interacts with the mineral surface of chalk, Mg^{2+} replaces Ca^{2+} from the surface and releases Ca^{2+} to the pore space. This causes formation of anhydrite salt – a fact that has not been reported previously. In this case 2.3 g sulfate was injected into the reservoir (for SW0NaCl) and less than 0.25 gm of sulfate remains soluble in the reservoir (as shown in figure 6). This shows that the majority of soluble sulfate becomes insoluble due to formation of anhydrite fines.

It must be noted that the precipitation of $CaSO_4$ from the recommended brine SW0NaCl-nSO4 in the Ekofisk field (Puntervold et al. 2015) is exclusively a property of the brine, and it will take place irrespective of variations in crude oil composition or mineral lithology. This precipitation is independent of associated smart water flooding mechanisms. Regardless of which mechanism causes SW-EOR, the precipitation of $CaSO_4$ on injection of SW0NaCl-nSO4 into the core plug should be considered, as it is a brine property, independent of any associated interaction with the mineral or oil. The precipitate can form in the injection pipe or near the injection point, once its nucleation kinetics becomes favorable. These calculation show that there are the two kinds of precipitation that can take place due to the injection of SW0Na-nSO4 in core plugs or in reservoirs.

1. Precipitation at the injection point can take place simply because the recommended brine becomes supersaturated at reservoir conditions. The brine remains supersaturated over variations of temperature and pressure in the range of Ekofisk field conditions.
2. More precipitation can take place when the brine is injected into the reservoir, due to ion substitution on the mineral surface.

This analysis clearly shows that precipitation will take place from the recommended brines. Using the recommended brines (Puntervold et al. 2015) and avoiding precipitation (Tweheyo et al. 2006, Zhang et al. 2006) cannot be simultaneously attained.

Furthermore speciation calculations for other similar brines were conducted at imbibition experiment conditions (25 bar and 130ºC) and at Ekofisk field conditions (at 400 bar and 130 ºC). As shown in Figure 7 it was observed that when spontaneous imbibition experiments are conducted at high temperature, most of the studied brines (SWnSO4; SWnCa; SW2Ca4SO4 (Fathi et al. 2011;Awolayo et al. 2014; Zhang et al. 2006; RezaeiDoust et al. 2009)) did form significant amounts of precipitation on injection. This amount of precipitation was significantly enhanced after the Mg^{2+}/Ca^{2+} substitution at reservoir conditions. All of these brines did form precipitate at both Ekofisk field conditions and at the conditions of the imbibition experiments. This is shown in figure 7 and 8. It is observed that the use of high potential ions (RezaeiDoust et al. 2009) and avoiding precipitation (RezaeiDoust et al. 2009) cannot be simultaneously attained for the suggested brines.

Optimum brine composition to avoid precipitation

The composition of the optimum brine with a high fraction of potential ions but with no precipitation of salts was determined at 130 ºC and 200 bar. There are three major ways of obtaining a high fraction of potential ions from sea water.

1. Reducing the sodium chloride concentration (Puntervold et al. 2014): Extended UNIQUAC calculation show that no precipitation is observed up to 42% removal of NaCl from sea water at 130 ºC and 200 bar. Further reducing the NaCl concentration makes the brine supersaturated and anhydrite starts precipitating. So, removing 90% of the NaCl from sea water will cause precipitation. At this reservoir condition, 58% of the NaCl content must be kept in the injected brine in order to avoid any precipitation during injection.
2. Increasing the SO_4^{2-} concentration (Fathi et al. 2011): The optimum concentration was determined such that the fraction of potential ion was maximized but precipitation was avoided. In this case it was observed that increasing the SO_4^{2-} concentration of sea water up to 83% can increase the potential ion fraction while ensuring that no precipitation takes place at 120 ºC and 200 bar. Increasing the sulfate ion concentration beyond 83% will cause precipitation of anhydrite fines on the injection. Thus, the recommended brines consisting of sea water with twice the sulfate of sea water or four times the sulfate of sea water are not suitable as they will precipitate at reservoir conditions.
3. Increasing divalent cation concentration (Tweheyo et al. 2006): The degree to which the cation concentration can be increased without precipitation on injection was determined. It was found that if the Ca^{2+} fraction was increased more than 19%, it will start causing precipitation. Thus injecting sea water with four times the Ca^{2+} will cause $CaSO_4$ precipitation 130 ºC and 200 bar.

These calculations show the optimum concentrations up to which the potential ion fractions can be increased without precipitation takes place. Previously, it has been recommended that the use of maximum amounts of potential ions with no associated precipitation leads to most oil production. So with the injection of NaCl depleted sea water, maximum oil production should take place when 42% of NaCl is removed from sea water. Further removal of NaCl leads to precipitation on injection, which according to previous studies will adversely affect oil mobility and decrease oil production. The optimum oil production by imbibition of NaCl depleted sea water should take place with a brine containing 58% of the NaCl in sea water. But according to the imbibition experiments (as shown in figure 2) there is no optimum oil production while reducing the NaCl concentration (Puntervold et al. 2014). And when 42% of sodium chloride is removed from sea water, the oil production graph does not show any optimum concentration. This shows a fundamental disagreement between the observed oil recovery (Puntervold et al. 2014) and the proposed potential ion based wettability alteration mechanism (RezaeiDoust et al. 2009). Another brine property must be identified which shows a direct correlation to oil production.

Brine Properties at Reservoir Conditions

Various possible brine properties should be calculated at reservoir conditions and be correlated to the observed oil recovery in order to find the property which can consistently be correlated to the observed oil recovery. The Extended UNIQUAC model was used to calculate various brine properties, which have previously been considered responsible for SW-EOR. These include: (1) the total amount of potential ions (RezaeiDoust et al. 2009), (2) the total amount of soluble SO_4^{2-} (Zhang et al. 2006) (3) the total precipitation on injection (Tweheyo et al. 2006) and (4) the total effective fine formation (Chakravarty et al. 2015a) (i.e. the total amount of precipitation taking place inside the core plug minus the amount precipitation on the injection). The calculation was conducted over temperatures ranging from 50 to 170 °C and from pressures ranging from 1 to 600 bar. All properties were calculated for SW0NaCl (since it has been recommended for injection in North Sea reservoirs (Puntervold et al. 2014)) and SW2Ca brines (since it is known that Ca enriched brines form precipitate at elevated pressure and temperature conditions (Tweheyo et al. 2006)).

Properties of SW0NaCl at reservoir conditions

The properties of sea water depleted of sodium chloride were calculated at various pressure and temperature conditions and were plotted in Figure 9—13. It was observed that for SW0NaCl fines started forming at 70 °C. The amount of fines formation gradually increased up to 130ºC. On further increase in temperature (up to 170 °C) a minor decrease in the amount of fines formation was

observed. Figure 9 also shows that the amount of fines formation depends on both pressure and temperature. It has been shown in literature that brines have an optimum temperature beyond which their efficiency in oil production decreases. (Tweheyo et al. 2006). The amount of fines formation shows a similar trend with a continuous increase with temperature until a certain temperature (which is selective to each brine) beyond which the amount of fines formation decreases (Figure 9).

The amount of soluble sulfate was also calculated and plotted in Figure 9. It was observed that the amount of soluble sulfate was highest at 50 °C and with increase in temperature, the amount of soluble sulfate consistently decreased irrespective of a variation in pressure At lower pressure, the amount of soluble sulfate was significantly higher (Figure 9). Therefore the amount of soluble sulfate in the reservoir consistently decrease with increase in temperature while the amount of oil recovery is known to increase with the temperature (Fathi et al 2011; Strand et al. 2006; Zahid et al. 2006) in the oil reservoir. Consequently, the soluble sulfate shows a negative correlation to the oil production for SW0NaCl.

Furthermore, the amount of precipitation taking place on injection was calculated at various temperature and pressure conditions (Figure 9). It was observed that the amount of precipitation consistently increase with an increase in temperature. At reservoir conditions of 130 ºC and 400 bar there was a significant amount of precipitation which could not be avoided (as highlighted by yellow circle in Figure 9) .This shows that the amount of precipitation taking place in the core plugs consistently increases with temperature. Each brine is known to have an optimum temperature beyond which its efficiency in oil recovery decreases (Zahid et al. 2006; Tweheyo et al. 2006). But the total amount of precipitation taking place consistently increased, and no optimum temperature was seen. Therefore the amount of precipitation also does not correlate to the oil recovery.

The amount of total potential ions available in the core plug was also calculated at various temperature and pressure conditions (Figure 9). It was observed that beyond 70 °C there was a steady decrease in concentration for an increase in temperature. It is known that oil recovery increases significantly with temperature from 70 °C to 130 °C (Fathi et al 2011; Strand et al. 2006; Zahid et al. 2006) while the total amount of potential ions showed a consistent decrease with increase in temperature (Figure 9). This shows that the total amount of potential ions does not correlate to the oil recovery.

Among the four available parameters, only the amount of fines formation taking place in the core plug showed an increase with increase in temperature. The fines formation also go through an optimum, beyond which the amount of fines formation start decreasing. This perfectly correlates to the pattern for oil production observed during temperature variance (Zahid et al. 2006; Tweheyo et al. 2006).

Furthermore, it is known that Ca^{2+}/Mg^{2+} substitution depends on temperature (RezaeiDoust et al. 2009). Brine speciation was performed considering the previously reported temperature dependence of Ca^{2+}/Mg^{2+} ion substitution for Stevns Klint chalk (RezaeiDoust et al. 2009). As shown in figure 10, it was observed that fines formation is even taking place at high pressure and temperature used for mimicking reservoir conditions. Between 70 and 130 °C the amount of fines formation drastically increases. On further increase of temperature, the amount of fines formation decreased even more(figure 10). This shows that an optimum behavior is found when both pressure and temperature dependence of the kinetics of mineral substitution is considered (figure 10). The amount of soluble sulfate was also calculated and plotted in figure 10. It was observed that the concentration of soluble SO_4^{2-} ions decreased with an increase in temperature. This decrease became even more drastic after considering the temperature dependence of mineral substitution (as observable in figure 10).

This shows that among the various properties only fines formation correlates to the oil recovery production pattern for SW0NaCl.

Reservoir properties of SW2Ca

Properties of sea water with twice Ca^{2+} was also evaluated at temperatures from 60 to 180 °C and pressures from 1 to 600 bar. The Extended UNIQUAC calculations are plotted in figure 11 and show a gradual increase in the amount of fines formation with increase in temperature beyond 80 °C. It was observed that for SW2Ca the amount of fines formation also showed an optimum behavior. As shown in figure 11 the optimum amount of fines formation showed both pressure and temperature dependence. At 400 bar, the optimum fine formation was observed at 135°C.

The total amount of soluble ions for SW2Ca was calculated at various temperature and pressure conditions. It was observed that the amount of soluble salts decreased with increase in temperature. At 130 °C and 400 bar, more than 50% of the soluble salt had precipitated (figure 11). It is known that oil production increases from 70 to 100 °C for Ca^{2+} enriched sea water (as shown in figure 14 (Tweheyo et al. 2006)). But the amount of soluble sulfate significantly decreases. This shows that the amount of oil recovery and the amount of soluble sulfate cannot be directly correlated.

The amount of precipitation was calculated at various pressure and temperature conditions. It was observed that above 100 °C, sea water with Ca^{2+} also causes precipitation on injection (as presented in figure 11). This precipitation can take place in the injection pipe near the injection point or in the core plug. This study showed that at reservoir conditions of 130 ºC and 400 bar, precipitation takes place consistently. Furthermore the precipitation consistently increases with increase of temperature above 100 °C and no optimum temperature is observed (figure 11); The amount of precipitate thus does not show the same trend with temperature as observed for the oil recovery.

The amount of total soluble potential ions for SW2Ca was calculated at various temperature and pressure conditions. It was observed that the total amount of potential ions consistently decreased at temperatures above 100 °C. This trend continued up to 180 ºC (as plotted in figure 11). This shows that the total amount of potential ions gradually decrease which is opposite to the observed oil recovery trend. Thus, the amount of potential ions cannot be directly correlated to the observed oil recovery.

The speciation calculation shows that the total amount of fines is the only property for SW2Ca which initially increases with an increase in temperature. Beyond a certain optimum temperature the production of fines gradually decreases. This is the same trend as is observed for the oil production (Tweheyo et al. 2006; Zhang et al. 2006).

It is known that the substitution of Ca^{2+} with Mg^{2+} is temperature dependent. This has previously been calculated for Stevns Klint chalk (RezaeiDoust et al. 2009). Considering this temperature dependent ion substitution process, the amount of fines formation was calculated at various temperature and pressure conditions. As shown in figure 12 it was observed that the amount of fines formation sharply increased with increase in temperature (beyond 90 °C). And as shown in figure 12 an evident optimum temperature (of 150 °C) was observed. Above this temperature the amount of fine formation decreased. A calculation was also performed considering the temperature dependence of mineral substitution. The calculated amount of fines formation and soluble sulfate was also plotted in figure 12. It is observed that the concentration of soluble sulfate ions drastically decreased above 90 °C. It is known that oil recovery also decrease with increase in temperature. Thus, only the amount of fines formation can be correlated to the observed oil recovery for SW2Ca.

Fines correlation to oil recovery

From this calculation we can try to correlate the oil production when using sea water depleted for NaCl (as shown in figure 1 (Puntervold et al. 2014)). It is observed that the amount of fines formation taking place at 90 °C for sea water with low NaCl content consistently correlates to the observed oil recovery. As both the amount of fines formation and the amount of oil recovery consistently increases with decrease in NaCl concentration at 90 °C (as indicated by the green line in figure 13). With variation in temperature, the amount of fines formation vs NaCl fraction significantly changes. It is observed that removing all of the NaCl content leads to maximum amount of fine formation above 110 ºC. At 130 ºC, the amount of fines formation taking place is optimum when only 56% of NaCl is removed from water. This shows that the experiment conducted at 90 ºC (Puntervold et al. 2014) completely correlates to the amount of fines formation but the conclusion made at 90ºC is not analogous to the Ekofisk field at 130 ºC (figure 13). Thus, removing 90% of NaCl may not give the most suitable brine composition for the recommended field.

Fines formation is the only property which gradually increases with temperature and beyond a specific temperature decreases. Based on these studies it can be concluded that the amount of fines formation after substitution directly correlates to the oil recovery. Furthermore, from these calculations it can be concluded that the amount of fines formation has significant temperature and pressure dependence as seen in figure 13. Thus studies at 90 ºC may not be directly correlated to a reservoir at 130 °C.

Precipitation vs fines formation

Previously it has been recorded that precipitation must be avoided during SW-EOR during both core flooding and reservoir condition (RezaeiDoust et al. 2009; Tweheyo et al. 2006; Zhang et al. 2006). But the calculations shown in figures 3-13 clearly show that significant precipitation takes place on injection and after ion substitution. Therefore, the role of fines in SW-EOR should be studied for experiments wherein precipitation has been observed as an adverse phenomenon to oil production (Tweheyo et al. 2006; Zhang et al. 2006). And correspondingly avoiding precipitation has been adviced for SW-EOR studies (Tweheyo et al. 2006).

The recommendation of avoiding precipitation is based on spontaneous imbibition experiments wherein three different brines were used as imbibing fluids including SW0Ca (sea water with no calcium); SW (normal sea water) and SW4Ca (sea water with 4 times Ca^{2+}) (Tweheyo et al. 2006). It was observed that at 70 °C and at 100 °C SW4Ca produce maximum oil recovery. The oil recovery trend both at 70 °C and 100 °C was SW0Ca<SW<SW4Ca (as shown in figure 14). This showed that at lower temperature, increasing the Ca^{2+} concentration did increase the oil recovery. When a similar experiment was conducted at a higher temperature (of 130 °C) SW4Ca produced the least amount of oil recovery. The oil recovery trend at 130 °C was SW4Ca<SW0Ca<SW (as shown in figure 14). In that study it was concluded that SW4Ca produces less oil due to the precipitation of anhydrite salt. Based on this experiment it was concluded that the precipitation of $CaSO_4$ must be avoided for EOR (Tweheyo et al. 2006).

The solubility of these brines at imbibing conditions was calculated using the Extended UNIQUAC model (as shown in figure 14). It is observed that the amount of soluble ions for SW4Ca decreases from 70 ºC to 130 ºC Both the amount of soluble potential ions present on injection and after mineral substitution show a steady decrease with increase in temperature. The amount of soluble potential ions decrease while the oil recovery is shown to consistently increase with increase in temperature from 70 °C to 130 ºC (figure 14). This shows that the amount of soluble potential ions does not correlate to the oil recovery for SW4Ca. In case of SW (from 70 ºC to 130 ºC) there is no precipitation on injection. After substitution there is significant precipitation which causes the amount of soluble potential ions in the pore space to decrease with increase in temperature. Here again an inverse relation between oil production and total soluble potential ions is observed (figure 14). Furthermore the same property is observed for SW0Ca. No

precipitation takes place on injection but after substitution with increase in temperature the amount of soluble ions decreases in the pore space. An inverse relation between oil production and total soluble potential ions is again observed as the oil production for SW0Ca continues to increase with increase in temperature (figure 14). This shows that the effect of temperature for the stated experiment cannot be explained using soluble potential ions.

The amount of precipitation was calculated for all the three brines at 70 °C, 100 °C and 130 °C. It was observed that SW4Ca did form significant amounts of precipitate at 130 °C. This has also been claimed in the literature (Tweheyo et al. 2006). But among the rest of brine/temperature combinations, maximum precipitation takes place for SW4Ca at 100 °C (figure 14). Since precipitation is suggested to have an adverse effect on oil production, SW4Ca at 100 °C should not have produced higher oil recovery than normal sea water. Nevertheless SW4Ca at 100 ºC and 70 °C did produce the maximum amount of oil production (when compared to SW and SW0Ca at the respective temperatures) (figure 14). As observable in this figure, this result is reproducible over two different experiments. This shows that even though up to 100 °C maximum precipitation takes place for SW4Ca, yet a significant, high oil production is observed. While at 130 ºC the highest precipitation on injection takes place for SW4Ca, yet it shows the least oil production. So, it can be concluded in case of high precipitation that there can be high oil production but high precipitation does not always guarantee a high oil production.

Thus, precipitation does not show any consistent direct correlation with increase in oil production over variation in temperature.

The study shows that oil recovery with smart water has an optimum temperature behavior; beyond this temperature its efficiency in oil production decreases (compared to sea water). The total amount of fines formation taking place in the reservoir (i.e. the amount of precipitate forming in the reservoir after substitution minus amount of precipitate taking place on injection) was calculated and is shown in (figure 14). At 70ºC SW4Ca the oil recovery trend at 70 ºC was SW0Ca<SW<SW4Ca. The same oil recovery trend was observed at 100ºC. Both at 70 ºC and at 100 ºC the observed fine formation trend is also the same: SW0Ca<SW<SW4Ca (as shown in figure 14). At 70 ºC the amount of precipitation taking place at the core plug dominated. Thus, the amount of fines formation taking place in the reservoir decreased. For SW4Ca an increase in temperature (to 130 ºC) led to a decrease in the amount of fines formation; The problem was that the majority of the precipitation took place on injection. Thus, at 130 ºC the amount of fines formation taking place decreased as compared to SW or SW0Ca. Thus, at 130ºC the amount of fines formation trend was SW4Ca<SW0Ca<SW. The oil recovery trend at 130ºC also was SW4Ca<SW0Ca<SW (as shown in figure 14).

This shows that for variation in temperature, pressure and brine compositions neither the precipitation on injection nor the amount of soluble ion can be correlated to the oil production. Only the amount of fines formation taking place inside the core plug can be correlated to the reported oil production (Tweheyo et al. 2006). Thus, fines formation is the only brine phenomenon that has an optimum temperature behavior similar to the observed oil production pattern for highly precipitating brines.

There has been another similar experiment which shows the possible effects of anhydrite precipitation for Ca^{2+} enriched brine (Tweheyo et al. 2006). As shown in figure 15; herein two similar imbibition experiments were conducted at 40, 70, 100 and 130 °C .In the first core plug, Ekofisk formation brine (EF) was used as formation brine and SW4Ca used as the imbibing fluid. In the second case EF-¼Ca (Ekofisk formation brine with ¼ Ca^{2+}) was used as the formation brine and SW (sea water) used as the imbibing fluid. As shown in figure 15, the amount of oil production showed the following pattern: SW-4Ca at 40 °C < SW at 40 °C < SW at 70 °C < SW-4Ca at 70 °C < SW at 100 °C < SW-4Ca at 100 °C < SW-4Ca at 130 °C < SW-4Ca at 130 °C (figure 15). Based on Extended UNIQUAC model calculations, the amount of fines formation taking place was also calculated and the amount of fines formation taking place was of the following pattern: SW-4Ca at 40 °C < SW at 40 °C < SW at 70 °C < SW-4Ca at 70 °C < SW at 100 °C < SW-4Ca at 100 °C < SW-4Ca at 130 °C < SW-4Ca at 130 °C (figure 15). This shows that an exact one-to-one correlation is observed between the amount of fines formation and the amount of oil recovery. Thus, it shows that the amount of fines formation taking place inside the core plug consistently correlates to the amount of oil recovery for core plugs wherein significant precipitation is observed.

Discussion

These studies (figure 3-15) clearly show that precipitation and fines formation are numerically different properties of the injected brine. The practical implementation of the two (precipitation and fines formation) needs to be understood at reservoir scale.

Precipitation can take place in the injection pipe or initial region of the core plug near the injection point. All it requires are suitable temperature and pressure conditions and enough time for the grain nucleation kinetics to develop. During continuous flooding, the supersaturated injection brine shall pass through the same path. All injected brine will undergo the same kinetics over time. Thus, in the same region near the injection point the brine will consistently cause precipitation. Fines formation doesn't take place at one specific region since fines formation is based on Mg^{2+} and Ca^{2+} substitution. Once fines formation has taken place at a specific surface, the specific surface becomes saturated with Mg^{2+} and thus further substitution cannot take place. Thus further fines cannot be produced from the same surface. Thus, continuous flooding through the same pore space does not consistently result in any changes in the brine speciation and correspondingly does not cause any fine formation in the pore space. Each time brine interaction with a new surface is required for fines formation. This fines formation can be caused by the following conditions:

1. A new surface can be activated when the sweep efficiency is blocked by the initial precipitation. Thus, the brine is forced to flow through new pores where Mg^{2+} substitution has not taken place. After ion substitution, the brine speciation is altered and fines formation takes place.
2. When wettability alteration takes place (to more water wetness (RezaeiDoust et al. 2009)), the flooded mineral surface becomes more water wet. This excess of new water wet surface in the flooding region can also cause mineral substitution which can be followed by new brine speciation in the pore space.
3. Fines formation can be caused due to interaction between two brines (Chakravarty et al. 2015a) .i.e. when one injection brine is replaced by another, the mixing of the two brines can further cause fines formation. The interaction between formation water and modified sea water can also cause fines formation.
4. Variation in pore space pressure and temperature can also change the brine speciation and cause further fines formation. Experimentally it has been observed in various studies where the core plug temperature has been varied (Tweheyo et al. 2006; RezaeiDoust et al. 2009) and correspondingly fines formation takes place (as shown in figure 14 and 15)
5. Injection of soluble gases like CO_2 can also affect the solubility of brines in pore space and cause fines formation (Chakravarty et al 2015c).

Thus fines formation takes place inside the core plug and not selectively at the injection point. It always takes place in a new region and access to new surface is required for additional fines formation. Furthermore neither sweep efficiency (Yi and Sarma 2012) nor wettability alteration mechanism (RezaeiDoust et al. 2009) are contradictory to fines formation as fine formation is supported through both causes. Therefore wettability alteration to higher water wetness is beneficial for fines formation and corresponding oil production but not necessarily at all. So, successful EOR observed for SW3S (Sea Water with 3 times SO4) can be correlated to fines formation for completely water wet core plugs (Zahid et al. 2010; Chakravarty et al. 2015a). Similarly an increase in sweep efficiency can also enhance the possibility of additional fines formation. Cation substitution through both wettability alteration and increase in sweep efficiency are supportive to additional fines formation by providing new surfaces or ion substitution followed by brine speciation alteration and eventually leading to mobile fines formation.

Conclusion

Based on the above analysis, the following conclusion can be made: suggested brines including Sw0NaCl are supersaturated at reservoir conditions for the Ekofisk field and given enough time at reservoir condition anhydrite will precipitate from it. Thus (1) using high fraction of potential ions and (2) avoiding precipitation during flooding/imbibition (i.e. the two section of the proposed wettability alteration model) are contrary and cannot be simultaneously achieved for recommended brine. The brine composition in the pore space is altered after cation substitution on the mineral surface. This causes additional insoluble salt formation which directly correlates to the oil recovery. Experimental results explained by the wettability alteration mechanism can also be explained by the amount of fines formation. Salt precipitation and fines formation are practically different phenomena. Precipitation is likely to take place at a specific region near the injection point; fines formation takes place in a different region each time.

References:

- Al Shalabi, E. W., Sepehrnoori, K., & Delshad, M. (2014). Mechanisms behind low salinity water injection in carbonate reservoirs. *Fuel*, *121*, 11-19.
- Alvarado, V., Moradi Bidhendi, M., Garcia-Olvera, G., Morin, B., & Oakey, J. S. (2014, April). Interfacial visco-elasticity of crude oil-brine: An alternative EOR mechanism in smart waterflooding. In *SPE Improved Oil Recovery Symposium*. Society of Petroleum Engineers.
- Austad, T., Shariatpanahi, S. F., Strand, S., Black, C. J. J., & Webb, K. J. (2011). Conditions for a low-salinity enhanced oil recovery (EOR) effect in carbonate oil reservoirs. *Energy & fuels*, *26*(1), 569-575.
- Awolayo, A., Sarma, H., & AlSumaiti, A. M. (2014, March). A laboratory study of ionic effect of smart water for enhancing oil recovery in carbonate reservoirs. In *SPE EOR Conference at Oil and Gas West Asia*. Society of Petroleum Engineers.
- Chakravarty, K. H., Fosbøl, P. L., & Thomsen, K. (2015a, June). Importance of Fines in Smart Water Enhanced Oil Recovery (SmW-EOR) for Chalk Outcrops. In *EUROPEC 2015*. Society of Petroleum Engineers.
- Chakravarty, K. H., Fosbøl, P. L., & Thomsen, K. (2015b, November). Significance of Fines and their Correlation to Reported Oil Recovery. In *Abu Dhabi International Petroleum Exhibition and Conference*. Society of Petroleum Engineers.
- Chakravarty, K. H., & Thomsen, K. (2015c, November). Formation of Anhydrite Due to Interaction Between Water Soluble CO 2 (aq) and Calcite Mineral During Enhanced Oil Recovery. In *SPE Oil & Gas India Conference and Exhibition*. Society of Petroleum Engineers.
- Fathi, S. J., Austad, T., & Strand, S. (2011). Water-based enhanced oil recovery (EOR) by "smart water": Optimal ionic composition for EOR in carbonates. *Energy & fuels*, *25*(11), 5173-5179.

- Morrow, N., & Buckley, J. (2011). Improved oil recovery by low-salinity waterflooding. *Journal of Petroleum Technology*, *63*(05), 106-112.
- Puntervold, T., Strand, S., Ellouz, R., & Austad, T. (2014, December). Why is it Possible to Produce Oil from the Ekofisk Field for Another 40 Years?. In*International Petroleum Technology Conference*. International Petroleum Technology Conference.
- Puntervold, T., Strand, S., Ellouz, R., & Austad, T. (2015). Modified seawater as a smart EOR fluid in chalk. *Journal of Petroleum Science and Engineering*, *133*, 440-443.
- RezaeiDoust, A., Puntervold, T., Strand, S., & Austad, T. (2009). Smart water as wettability modifier in carbonate and sandstone: A discussion of similarities/differences in the chemical mechanisms. *Energy & fuels*, *23*(9), 4479-4485.
- Shariatpanahi, S. F., Strand, S., & Austad, T. (2010). Evaluation of Water-Based Enhanced Oil Recovery (EOR) by Wettability Alteration in a Low-Permeable Fractured Limestone Oil Reservoir. *Energy & Fuels*, *24*(11), 5997-6008.
- Stokka, S., Oesthus, A., & Frangeul, J. (2005, January). Evaluation of air injection as an IOR method for the Giant Ekofisk Chalk Field. In *SPE International Improved Oil Recovery Conference in Asia Pacific*. Society of Petroleum Engineers.
- Strand, S., Austad, T., Puntervold, T., Høgnesen, E. J., Olsen, M., & Bartad, S. M. F. (2008). "Smart water" for oil recovery from fractured limestone: a preliminary study. *Energy & fuels*, *22*(5), 3126-3133.
- Strand, S., Høgnesen, E. J., & Austad, T. (2006). Wettability alteration of carbonates—Effects of potential determining ions (Ca 2+ and SO 4 2−) and temperature. *Colloids and Surfaces A: Physicochemical and Engineering Aspects*, *275*(1), 1-10.
- Strand, S., Høgnesen, E. J., & Austad, T. (2006). Wettability alteration of carbonates—Effects of potential determining ions (Ca 2+ and SO 4 2−) and temperature. *Colloids and Surfaces A: Physicochemical and Engineering Aspects*, *275*(1), 1-10.
- Tang, G. Q., & Morrow, N. R. (1997). Salinity, temperature, oil composition, and oil recovery by waterflooding. *SPE Reservoir Engineering*, *12*(04), 269-276.
- Thomsen, K., & Rasmussen, P. (1999). Modeling of vapor–liquid–solid equilibrium in gas–aqueous electrolyte systems. *Chemical Engineering Science*, *54*(12), 1787-1802.
- Tweheyo, M. T., Zhang, P., & Austad, T. (2006, January). The effects of temperature and potential determining ions present in seawater on oil recovery from fractured carbonates. In *SPE/DOE Symposium on Improved Oil Recovery*. Society of Petroleum Engineers.
- Yi, Z., & Sarma, H. K. (2012, January). Improving Waterflood Recovery Efficiency in Carbonate Reservoirs through Salinity Variations and Ionic Exchanges: A Promising Low-Cost" Smart-Waterflood" Approach. In *Abu Dhabi International Petroleum Conference and Exhibition*. Society of Petroleum Engineers.
- Yousef, A. A., & Ayirala, S. C. (2014, April). A novel water ionic composition optimization technology for SmartWater flooding application in carbonate reservoirs. In *SPE Improved Oil Recovery Symposium*. Society of Petroleum Engineers.
- Yousef, A. A., Al-Saleh, S., & Al-Jawfi, M. S. (2012, January). Improved/enhanced oil recovery from carbonate reservoirs by tuning injection water salinity and ionic content. In *SPE Improved Oil Recovery Symposium*. Society of Petroleum Engineers.
- Yousef, A. A., Al-Salehsalah, S. H., & Al-Jawfi, M. S. (2011, January). New recovery method for carbonate reservoirs through tuning the injection water salinity: smart waterflooding. In *SPE EUROPEC/EAGE Annual Conference and Exhibition*. Society of Petroleum Engineers.
- Zahid, A., Stenby, E. H., & Shapiro, A. A. (2010, January). Improved Oil Recovery in Chalk: Wettability Alteration or Something Else?. In *Spe Europec/eage Annual Conference and Exhibition*. Society of Petroleum Engineers.
- Zahid, A., Stenby, E. H., & Shapiro, A. A. (2012, January). Smart Waterflooding (High Sal/Low Sal) in Carbonate Reservoirs. In *SPE Europec/EAGE Annual Conference*. Society of Petroleum Engineers.
- Zhang, P., Tweheyo, M. T., & Austad, T. (2006). Wettability alteration and improved oil recovery in chalk: The effect of calcium in the presence of sulfate. *Energy & fuels*, *20*(5), 2056-2062.

Figures:

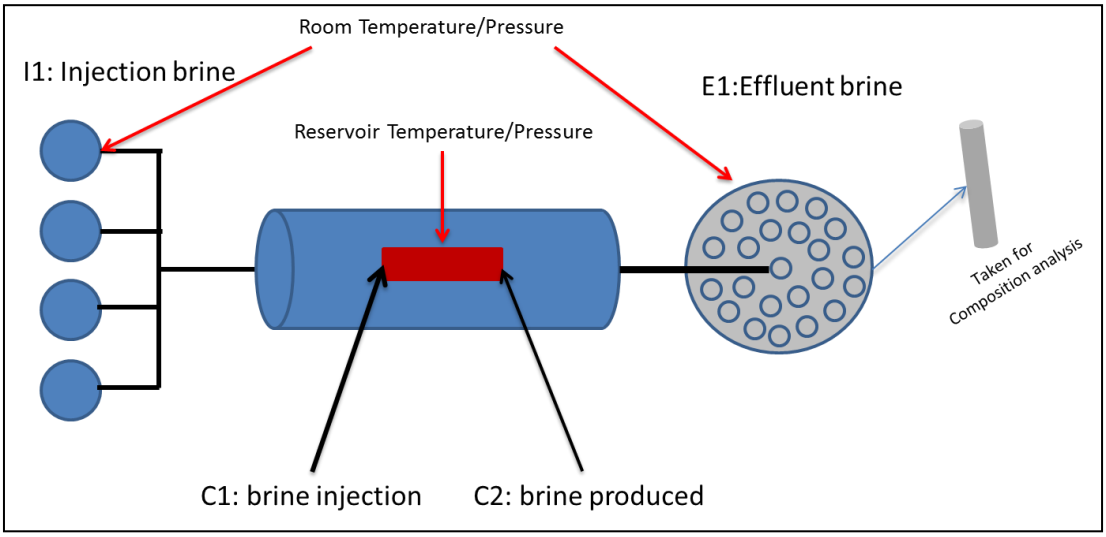


Figure 1: Schematic representation of water flooding setup. No compositional change before C1 or after C2. Adsorption/ desorption/ precipitation/ dissolution all takes place between C1 and C2; only pressure and temperature changes after C2 or C1. So speciation of brine can change between I1 and C1 or C2 and E1.

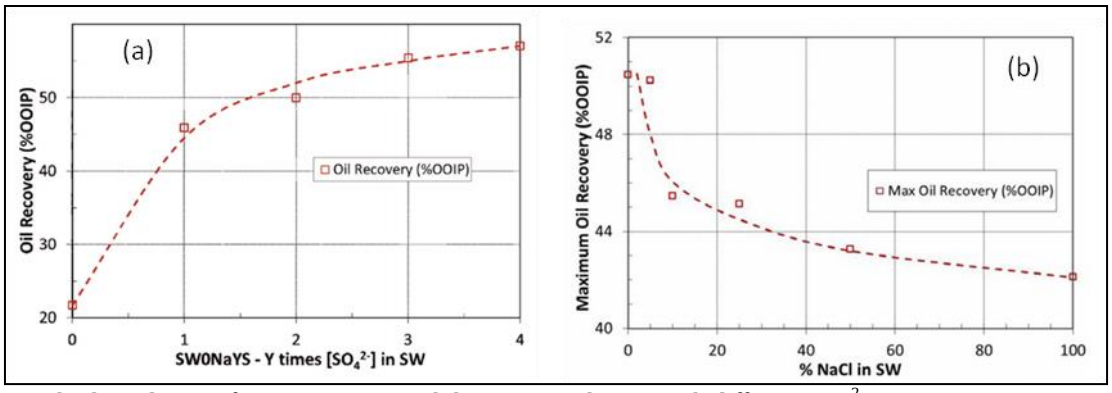


Figure 2: (a) Final oil production for spontaneous imbibition using brines with different SO_4^{2-} concentrations in sea water without NaCl at 90 °C for Stevns Klint chalk. (b) Final oil production for spontaneous imbibition of sea water decreasing NaCl concentration at 90 °C for Stevns Klint chalk (Puntervold et al. 2015).

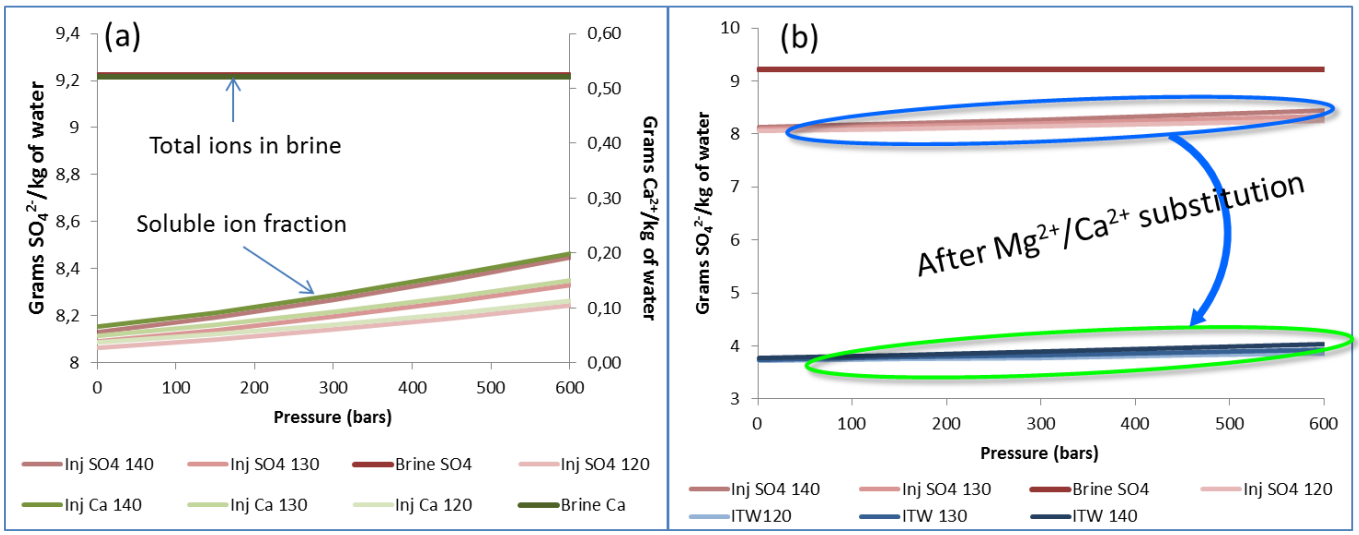


Figure 3: Solubility fraction of recommended brine, SW0NaCl-4SO4 (Puntervold et al. 2015) at Ekofisk conditions on injection (a) and after ion substitution (b). Significant decrease in soluble fraction indicates major precipitation during both the steps.

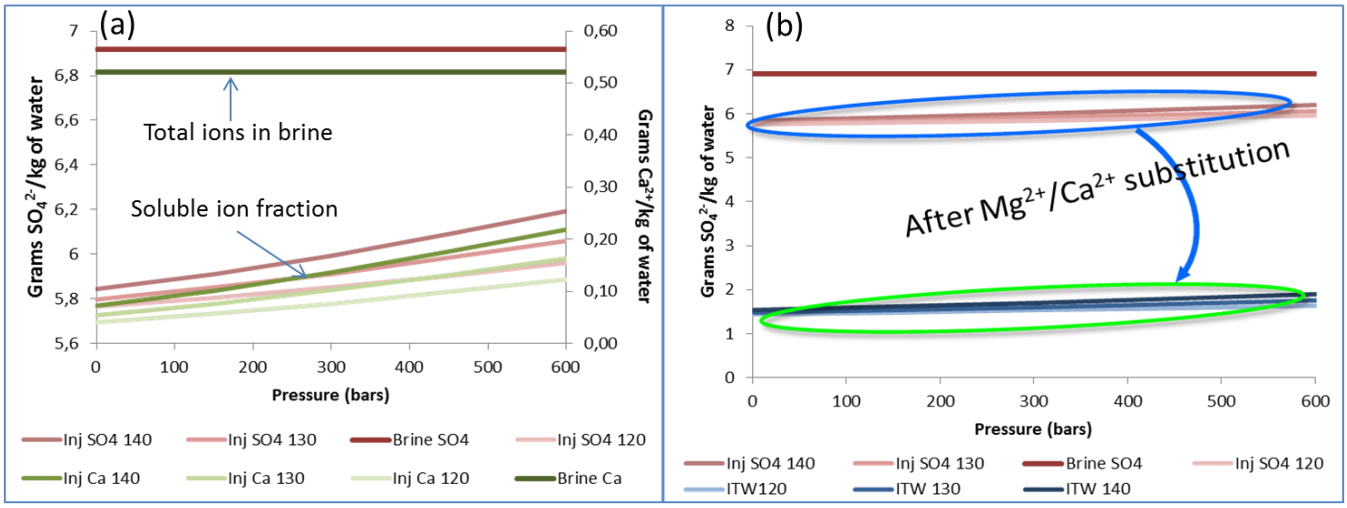


Figure 4: Solubility fraction of recommended brine, SW0NaCl-3SO4 (Puntervold et al. 2015) at Ekofisk conditions on injection (a) and after ion substitution (b). Significant decrease in soluble fraction indicates major precipitation during both the steps.

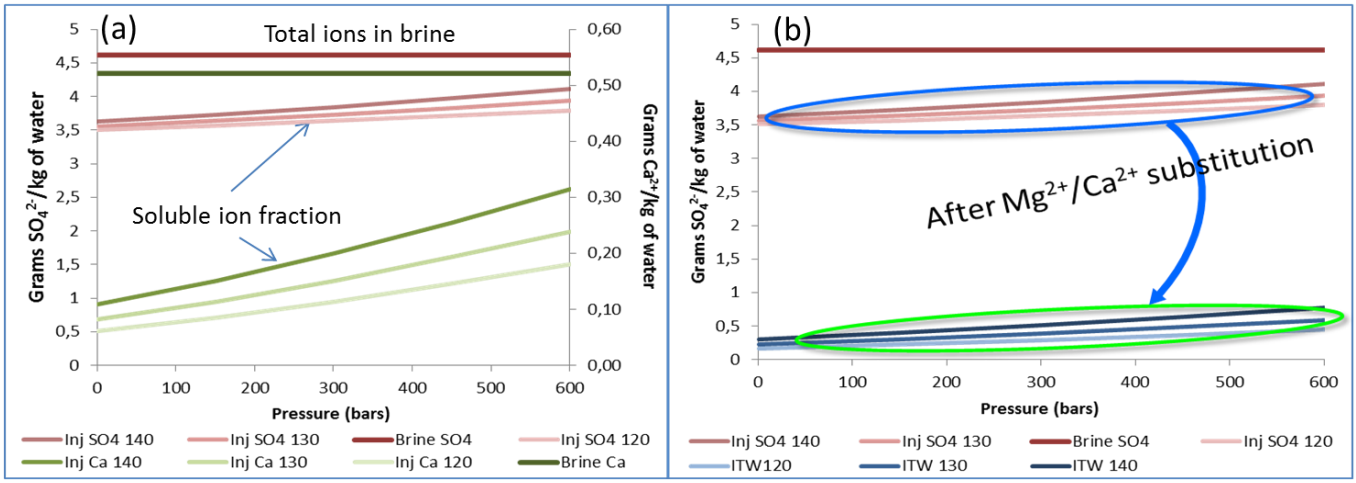


Figure 5: Solubility fraction of recommended brine, SW0NaCl-2SO4 (Puntervold et al. 2015) at Ekofisk conditions on injection (a) and after ion substitution (b). Significant decrease in soluble fraction indicates major precipitation during both the steps.

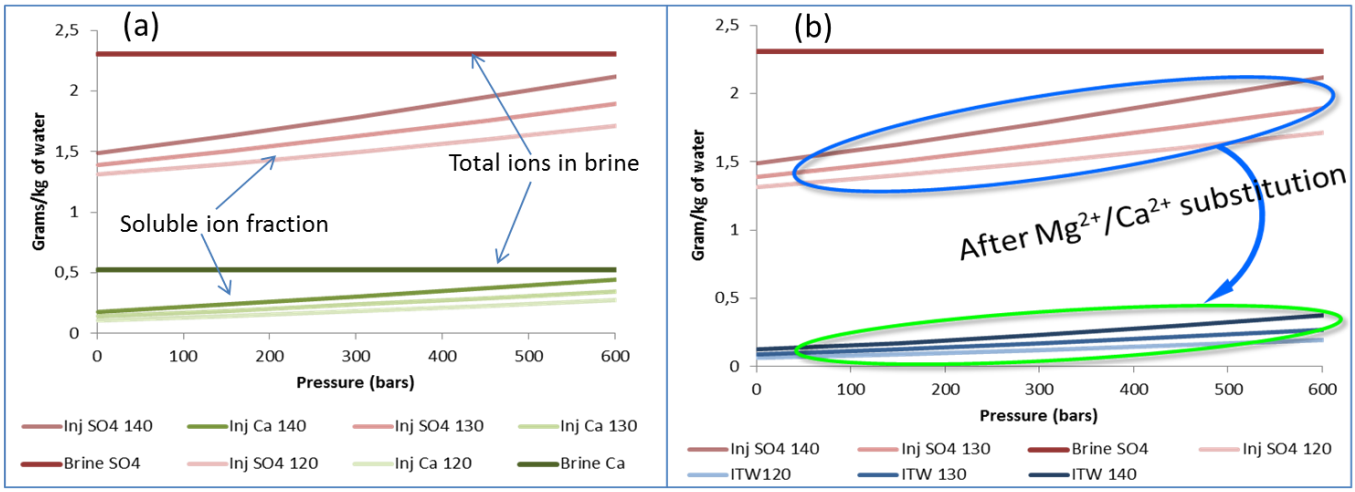


Figure 6: Solubility fraction of recommended brine, SW0NaCl (Puntervold et al. 2015) at Ekofisk conditions on injection (a) and after ion substitution (b). Significant decrease in soluble fraction indicates major precipitation during both the steps, thus use of SW0NaCl and avoiding precipitation are not simultaneously possible.

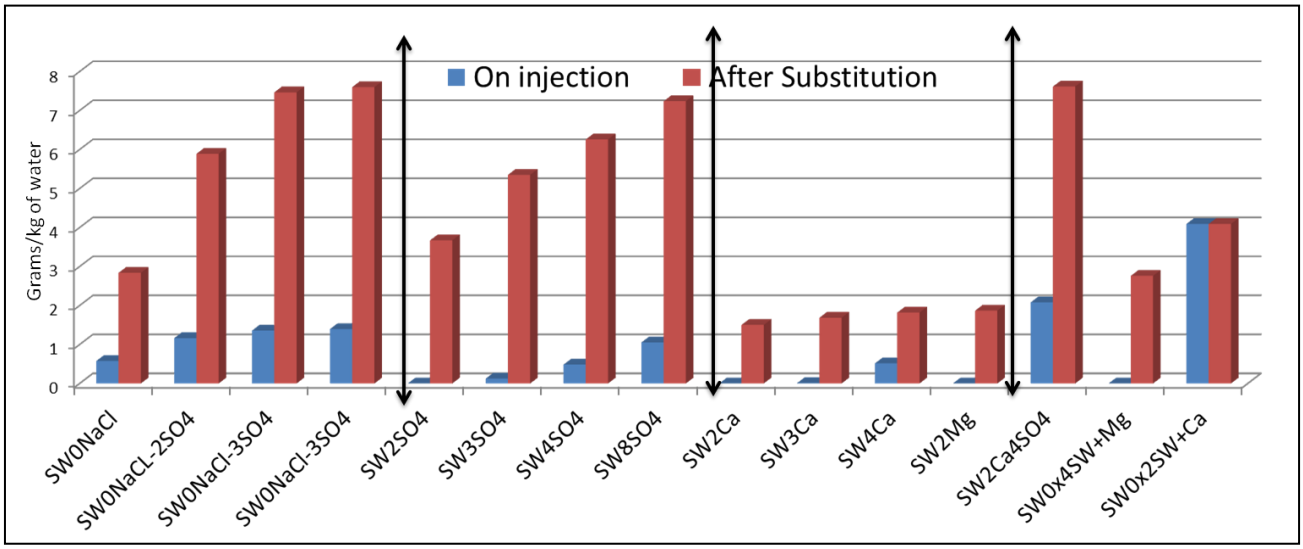


Figure 7: Amount of precipitation on injection and after ion substitution at Ekofisk conditions (400 bar) for various commonly recommended smart waters (Fathi et al. 2011; Awolayo et al. 2014; Zhang et al. 2006; RezaeiDoust et al. 2009). Significant increase in precipitation takes place after ion substitution for most studied brines.

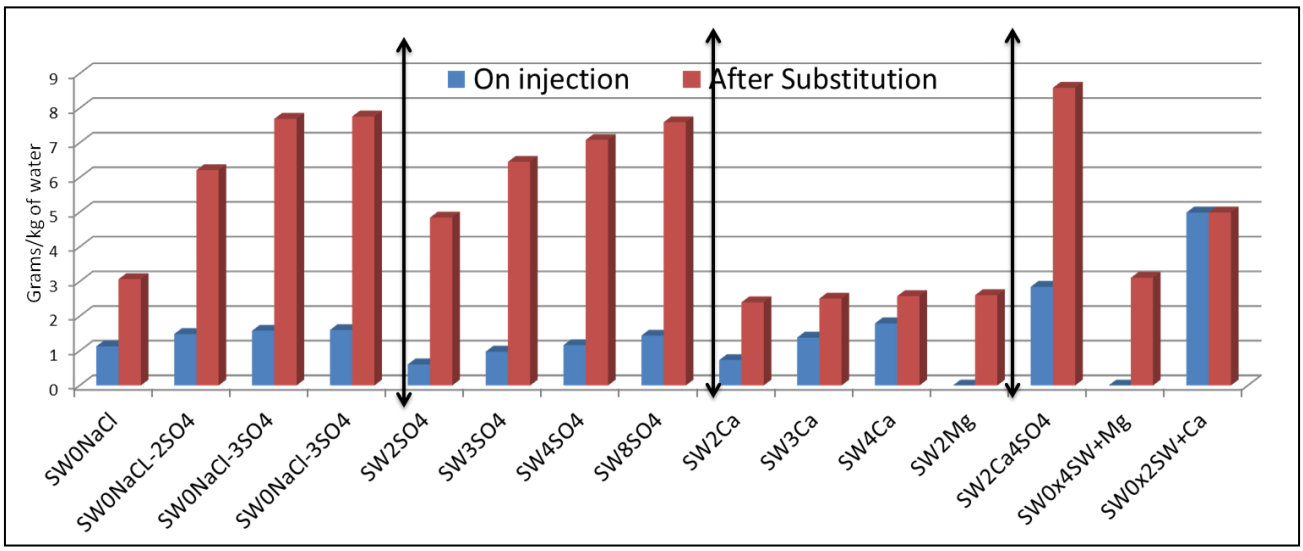


Figure 8: Amount of precipitation on injection and after ion substitution at experimental conditions (20 bar) for various commonly recommended smart waters (Fathi et al. 2011; Awolayo et al. 2014; Zhang et al. 2006; RezaeiDoust et al. 2009). Significant increase in precipitation takes place after ion substitution for most studied brines.

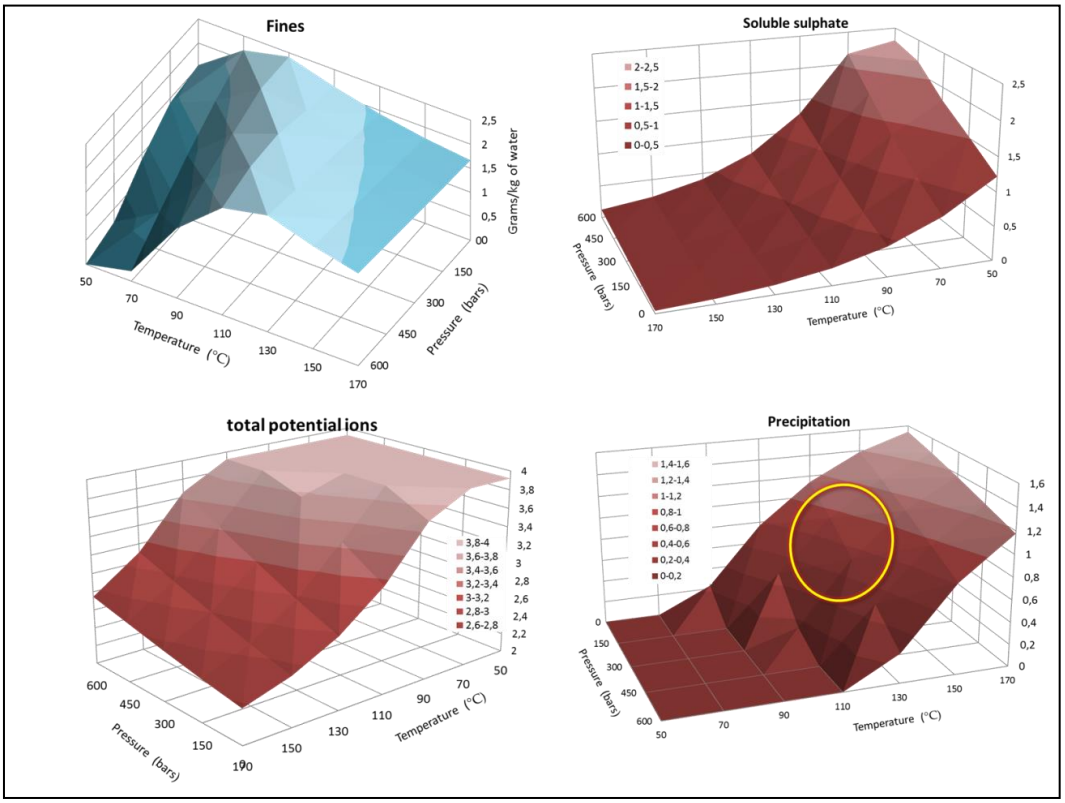


Figure 9: Speciation calculation for SW0NaCl at 50 to 170 °C and 1 to 600 bar, and the corresponding amount of fines formation; Soluble SO_4^{2-}, total potential ion and precipitation (in gram/kg of water) taking place during smart water flood. The yellow circle indicates that significant precipitation takes place at Ekofisk conditions.

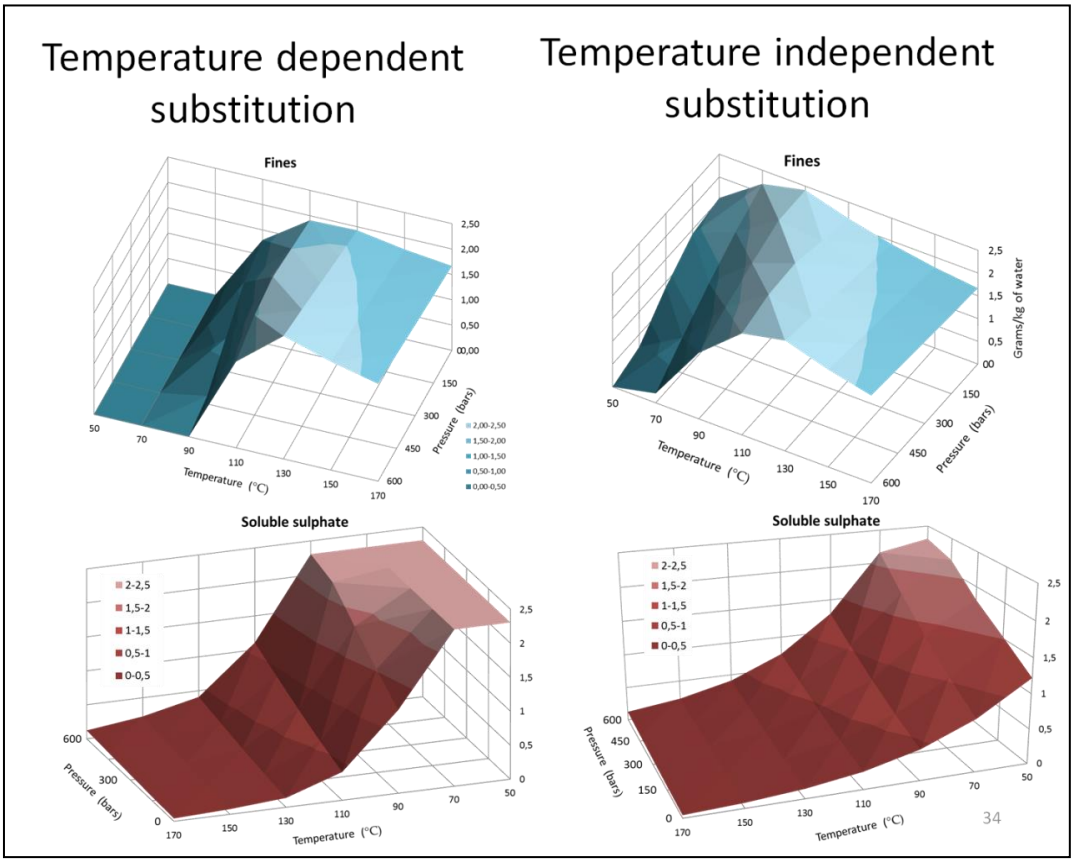


Figure 10: Speciation calculation for SW0NaCl at 50 to 170 °C and 1 to 600 bar and the corresponding amount of fines formation; Soluble SO_4^{2-}, (in gram/kg of water) for temperature dependent (RezaeiDoust et al. 2009) and temperature independent ion substitution. Temperature dependent ion substitution show a more prominent increase in fines formation with temperature.

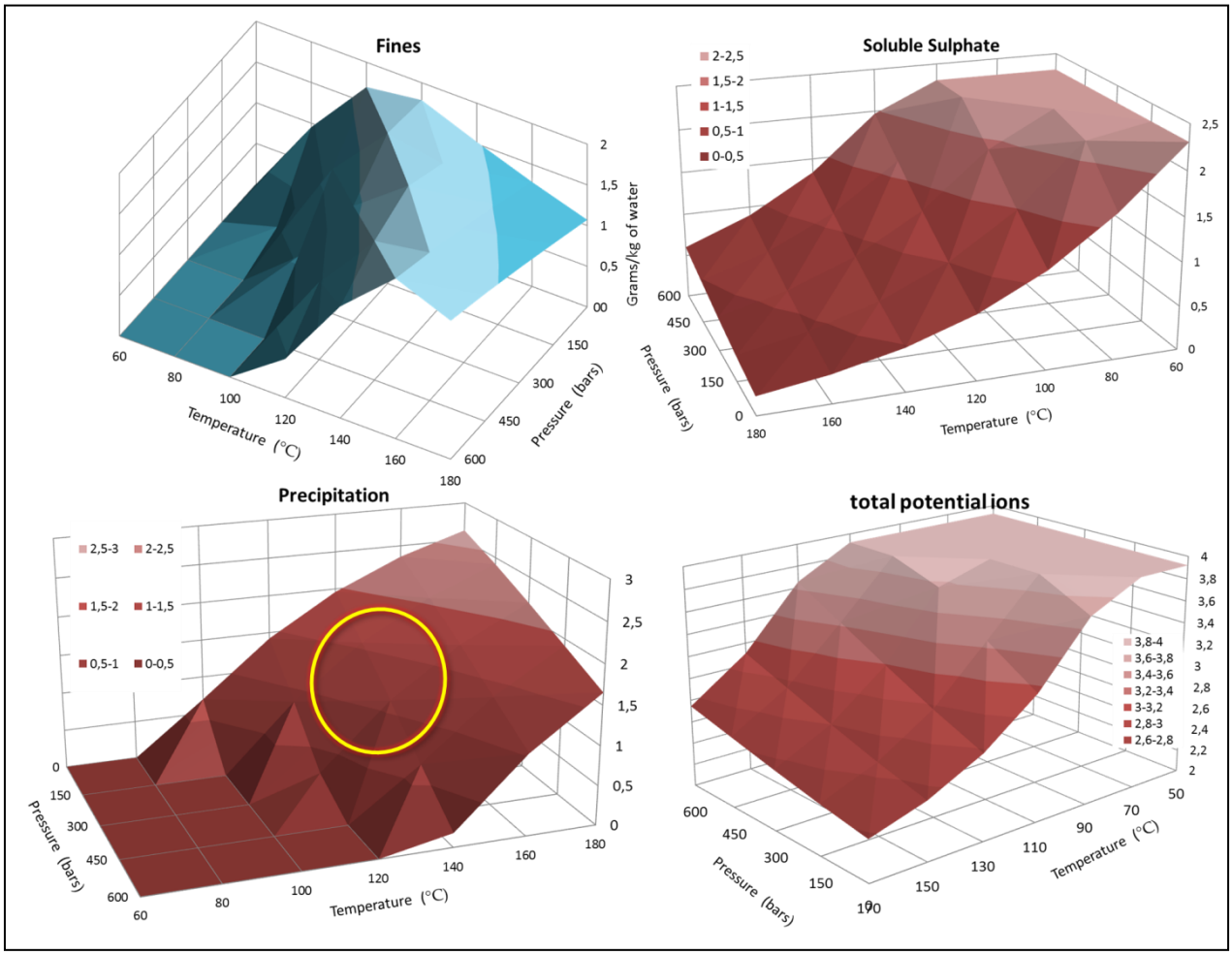


Figure 11: Speciation calculation for SW2Ca at 60 to 180 °C and 1 to 600 bar and the corresponding amount of fines formation; Soluble SO_4^{2-}, total potential ion and precipitation (in gram/kg of water) taking place during smart water flooding. The yellow circle indicates that significant precipitation takes place at Ekofisk conditions during injection.

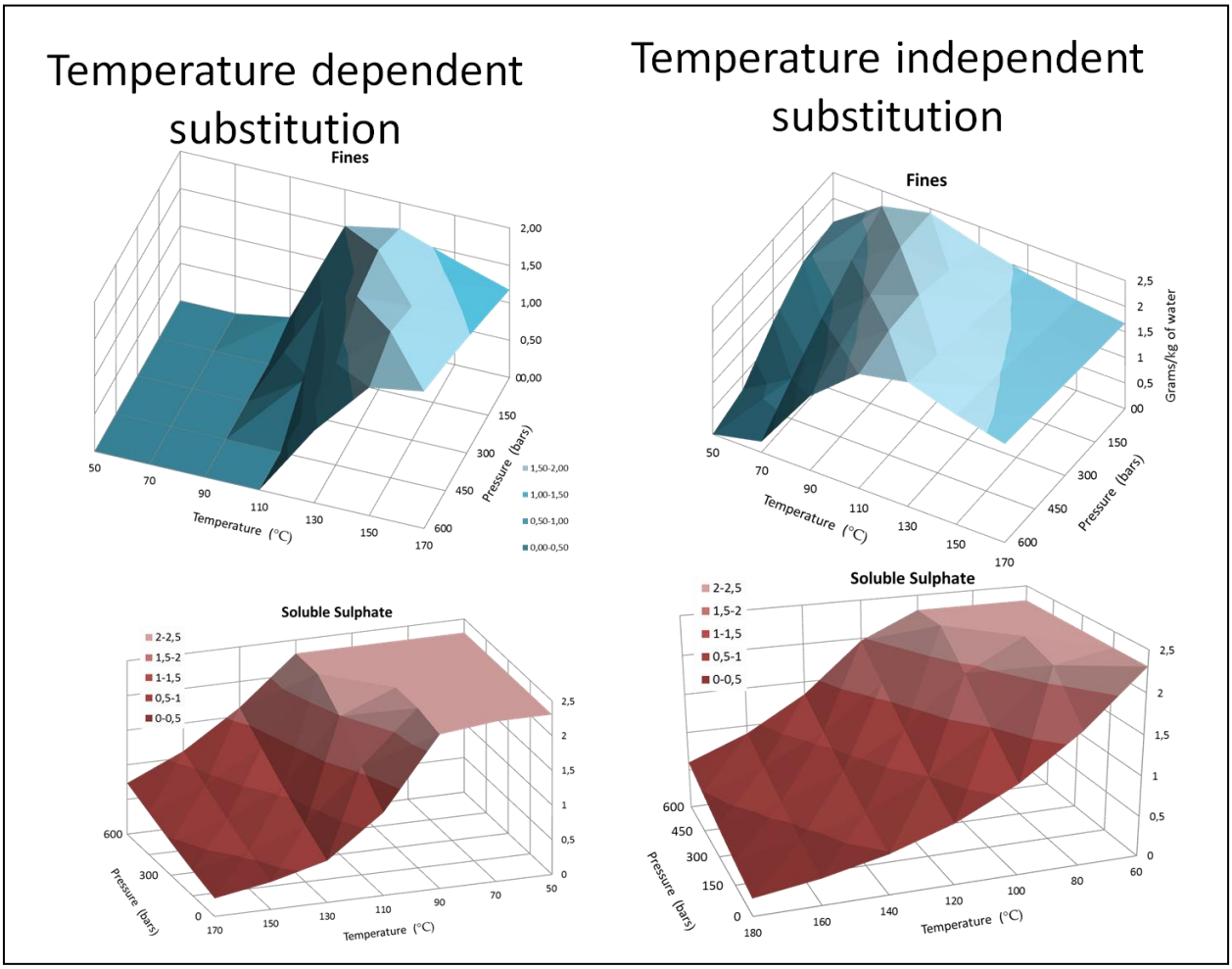


Figure 12: Speciation calculation for SW2Ca for 60 °C to 180 °C and 1 bar to 600 bar and corresponding amount of fine formation; Soluble SO_4^{2-}, (in grams/kg of water) for temperature dependent (RezaeiDoust et al. 2009) and temperature independent ion substitution. Temperature dependent ion substitution show more prominent increase in fine formation.

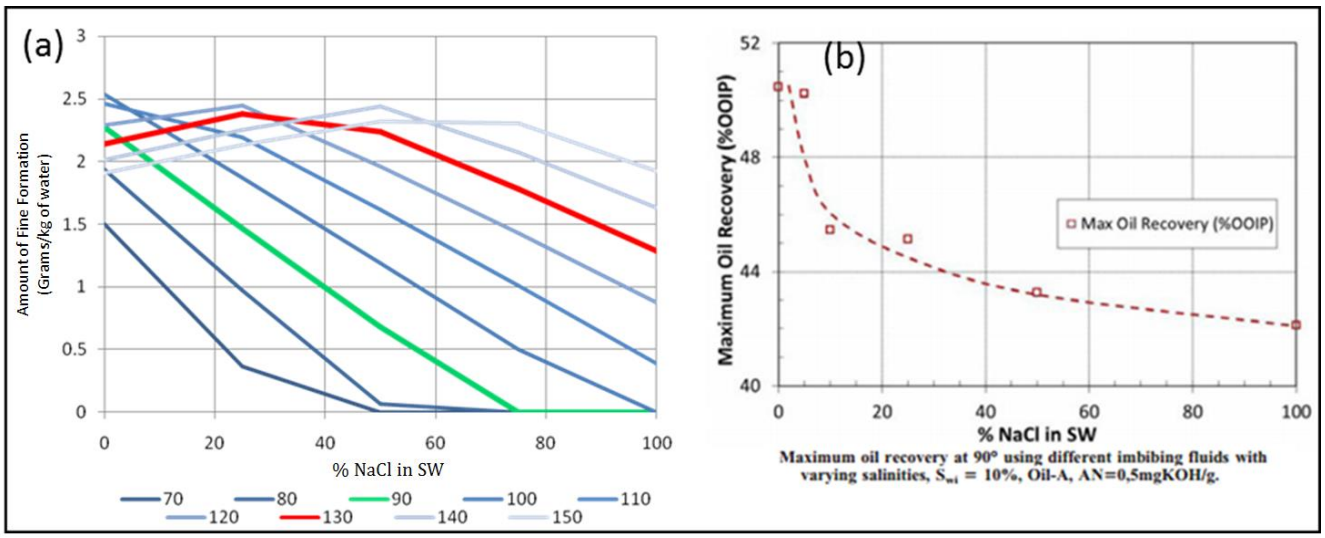


Figure 13: (a) Amount of fines formation taking place at different temperatures for sea water with decreased NaCl concentration; (b) Reported oil recovery for variation in NaCl concentration from sea water during spontaneous imbibition at 90 °C. At 90 °C both the amount of fines formation and the amount of oil recovery show steady increase with decrease in NaCl concentration. But this pattern is not observed beyond 110 °C.

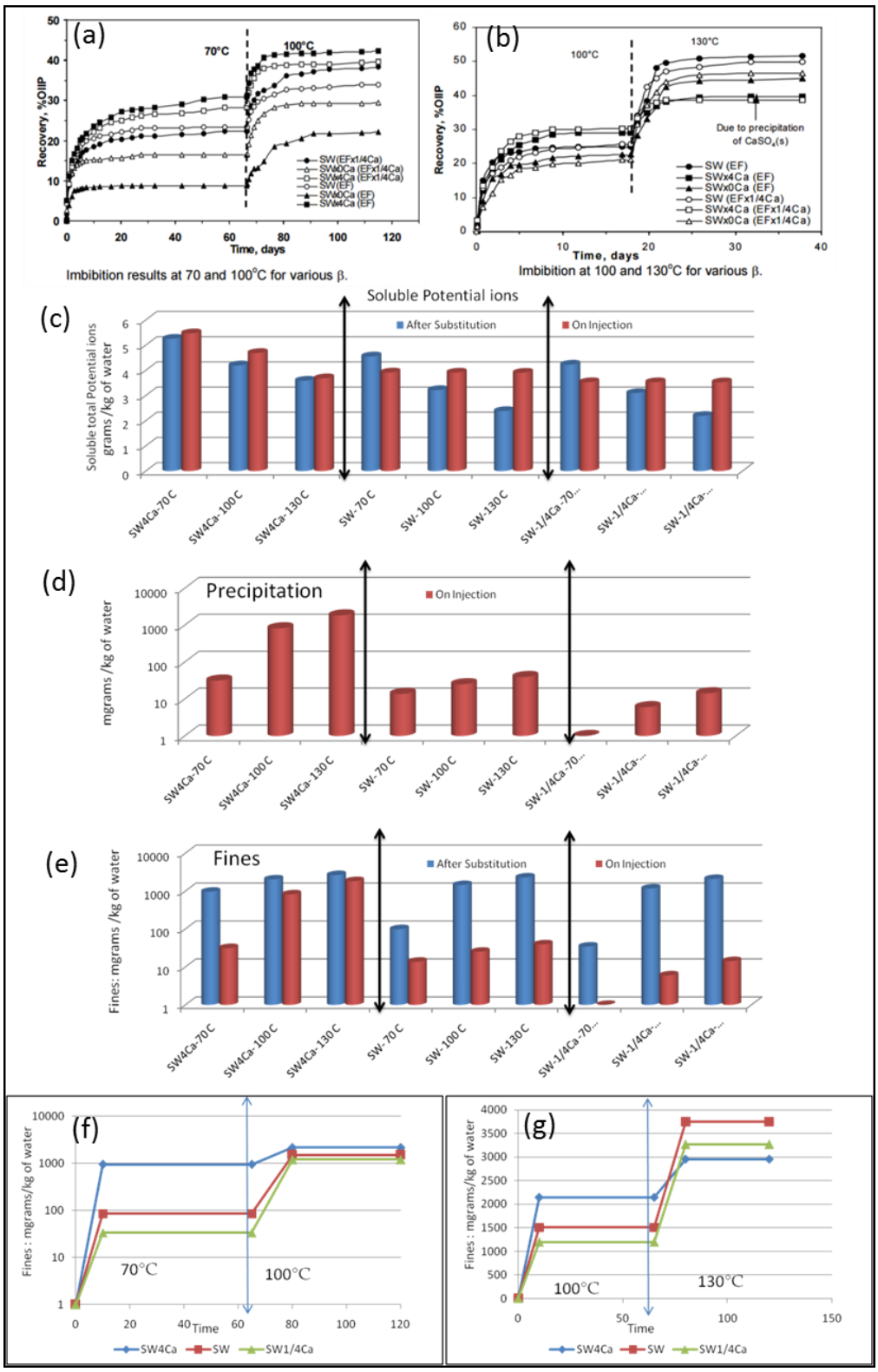


Figure 14: (a-b) Oil production for spontaneous imbibition of SW0Ca, SW and SW4Ca at 70 °C, 100 °C and 130 °C (Tweheyo et al. 2006). (c) Amount of soluble SO_4^{2-} present on injection and after ion substitution (d) Amount of precipitation on injection. (e) Amount of insoluble salts on injection and after ion substitution for the different core plugs. (f) and (g) show amount of fines formation corresponding to the reported oil recovery in (a) and (b). Both fines formation and oil recovery show the same trend (SW0Ca<SW<SW4Ca 70 °C & 100 °C and SW4Ca< SW0Ca<SW at 130 °C).

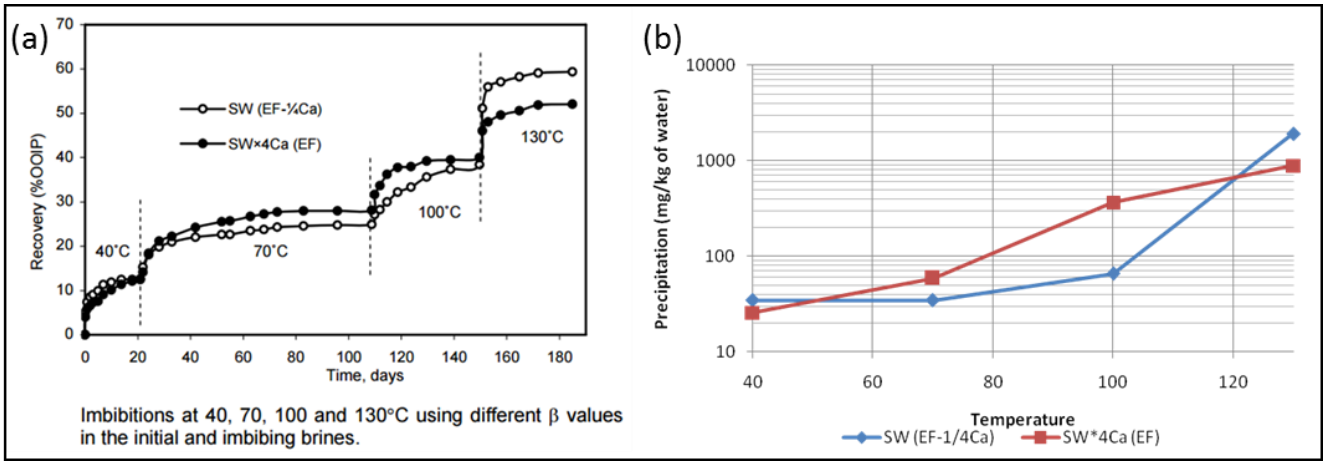


Figure 15: (a) Oil production for spontaneous imbibition of SW (EF-¼Ca) and SW-4Ca (EF) at 40, 70, 100, and 130 °C. (b) Corresponding amount of fines formation for imbibition of SW (EF-¼Ca) and SW-4Ca (EF) at 40 °C, 70 °C, 100 °C and 130 °C. The amount of fines formation and the amount of oil recovery show same trend: SW-4Ca at 40 °C < SW at 40 °C < SW at 70 °C < SW-4Ca at 70 °C < SW at 100 °C < SW-4Ca at 100 °C < SW-4Ca at 130 °C < SW-4Ca at 130 °C.

Paper X

Ahkami, M., Chakravarty, K. H., Xiarchos, I., Thomsen, K., & Fosbøl, P. L., (2016), April Determining Optimum Aging Time Using Novel Core Flooding Equipment. In *SPE Bergen One Day Seminar*. Society of Petroleum Engineers.

SPE-180054-MS

Determining Optimum Aging Time Using Novel Core Flooding Equipment

Mehrdad Ahkami, Krishna Hara Chakravarty, Ioannis Xiarchos, Kaj Thomsen, Philip Loldrup Fosbøl; Center for Energy Resources Engineering (CERE), Technical University of Denmark (DTU)

Copyright 2016, Society of Petroleum Engineers

This paper was prepared for presentation at the SPE Bergen One Day Seminar held in Bergen, Norway, 20 April 2016.

This paper was selected for presentation by an SPE program committee following review of information contained in an abstract submitted by the author(s). Contents of the paper have not been reviewed by the Society of Petroleum Engineers and are subject to correction by the author(s). The material does not necessarily reflect any position of the Society of Petroleum Engineers, its officers, or members. Electronic reproduction, distribution, or storage of any part of this paper without the written consent of the Society of Petroleum Engineers is prohibited. Permission to reproduce in print is restricted to an abstract of not more than 300 words; illustrations may not be copied. The abstract must contain conspicuous acknowledgment of SPE copyright.

Abstract

New methods for enhanced oil recovery are typically developed using core flooding techniques. Establishing reservoir conditions is essential before the experimental campaign commences. The realistic oil-rock wettability can be obtained through optimum aging of the core. Aging time is affected by temperature, crude oil, formation brine, and coreplug lithology. Minimum time can significantly reduce the experimental cost while insufficient aging time can result in false conclusions.

Real-time online resistivity measurements of coreplugs are presented and a novel method is introduced for determining the optimum aging time regardless of variations in crude oil, rock, and brine properties. State of the art core flooding equipment has been developed that can be used for consistently determining the resistivity of the coreplug during aging and waterflooding using advanced data acquisition software. In the proposed equipment, independent axial and sleeve pressure can be applied to mimic stresses at reservoir conditions. 10 coreplugs (four sandstones and six chalk samples) from the North Sea have been aged for more than 408 days in total and more than 29000 resistivity data points have been measured to consistently investigate the change of wettability during aging.At 60°C and 100 bars a homogeneous sandstone coreplug attained optimized wettability after 5 days, a heterogeneous coreplug required 30 days of aging. Chalk coreplugs needed 45 days of aging. This shows that coreplugs originating from the same field, when aged at equivalent conditions can have significantly different aging times because of minor variations in the coreplug properties. No fixed aging time can be recommended on the other hand a method is recommended which can determine the extent of aging. Coreplug aging patterns were studied for variation in pressure (20 to 130 bar) and temperature (60 to 130°C). Based on these experiments an algorithm has been developed which distinguishes the effect of wettability alteration, pressure, and temperature on coreplug resistivity.

This study highlights the use of hydraulic oil to avoid release of fluids in the effluent pipes during the aging process. Furthermore, the described multiple monitoring devices are useful in detecting any experimental error that may have occurred during mounting of the coreplug in the core holder. Thus imperfect waterflooding which can otherwise produce misleading data can be avoided. The presented equipment can instantly and continuously calculate the mineral wettability throughout the aging process at any pressure, temperature condition and for any combination of rock and crude oil. Thus, using the stated core flooding equipment can not only decrease the cost and time of doing aging and waterflooding studies but can also significantly increase the accuracy in conducting core flooding experiments.

Introduction

Decreasing oil production rate throughout the recent years has highlighted the need for sophisticated enhanced oil recovery (EOR) methods. Core waterflooding experiments have been used to innovate, understand and explore the applicability of EOR methods in different types of hydrocarbon reservoirs(Thakur 1991). Migration of fines(Yuan & Shapiro 2011), dissolution of mineral(Emberley et al. 2004), salting-in effect(Austad et al. 2010),double layer effect(Nasralla & Nasr-el-din 2012), oil emulsification,(Farajzadeh et al. 2012) and mineral wettability alteration(Standnes & Austad 2000) are some of the commonly referred physico-chemical mechanisms which contribute to increase is oil recovery during various EOR practices. Among these mentioned mechanisms, change of rock surface wettability towards a more water wet condition is a prominent mechanism in various EOR studies including; smart waterflooding(Austad et al. 2005; Vledder et al. 2010); Surfactants flooding (Standnes & Austad 2000; Standnes & Austad 2003; Salehi et al. 2008; Kumar et al. 2008); CO_2 gas injection (Chiquet et al. 2007); (Kewen & Abbas 2000); ZrO_2 nanofluid flooding (Karimi et al. 2012). The reliability of core flooding experiments depends on the establishment of initial rock wettability similar to that at reservoir conditions. Aging of coreplug is widely used to ensure this

initial wettability condition. The aging time, and correspondingly established mineral wettability condition has a prominent effect on final oil recovery. Final oil recovery for similar waterflooding experiments changed from 50% of OOIP to less than 20% of OOIP when the aging time was increased from zero to 31 days (Graue et al. 1999). Optimum aging duration is needed to reach the realistic wettability condition. It depends on experimental properties such as crude oil, coreplug, and temperature(Dia et al. 1991; Graue et al. 2002; Graue et al. 1999; Yildiz et al. 1999). Traditionally, the aging assessments were based on try and error methods, in which the coreplugs were aged for different time intervals and specific properties such as the Amott index has been used as an indication of rock surface wettability condition(Zhou et al. 1995; Zhou et al. 1996) or oil recovery(Morrow et al. 1998). In these experiments it is crucial to determine the optimum aging time. This is the basis for coreplug waterflooding experiments.

Lack of a consistent method of wettability investigation has caused a discussion in the literature. Some examples of contradiction between different aging times and the effect of experimental parameter on aging efficiency are presented in the following. Thereafter in this study a consistent, reliable, and reproducible method for wettability investigation is introduced. This method can be assisted to distinguish the optimum aging time of each coreplug to increase the reliability of waterflooding experiments.

Aging time

Contradiction in proposed aging time is reflected in different studies. Initial aging studies with Rørdal and Dania chalk coreplugs from Ålborg, Denmark showed that 14 days of aging was the optimum time. This was found using the Amott index which showed no major variation in mineral wettability in the following 16 days(Graue et al. 1999). Mineral wettability for three different coreplugs was stabilized after two weeks of aging. Thereafter, in another similar study, measurement of Amott index for chalk coreplugs from Rørdal, near Ålborg in Denmark, in static and dynamic aging experiments were conducted. It was concluded that 10 days is the optimum aging time, and further aging shows no variation in coreplug properties(Fernø et al. 2010). Oil recovery was also correlated with the change in wettability condition of coreplugs in similar studies. Oil recovery after spontaneous imbibition of four coreplugs from Stevns Klint chalk from Sealand, Denmark showed that 35 days is sufficient time for aging(Yu et al. 2009). In this study, two coreplugs were aged for 35 days and two others were aged for 100 days. The rate of oil production and the final oil recovery were similar for both sets of coreplugs, thus suggesting that additional aging had no effect on coreplug properties. In a similar study, spontaneous imbibition into 3 chalk coreplugs from Stevns Klint outcrop chalk was studied. Based on the production profile from these outcrops it was claimed that 21 days of aging was sufficient to ensure optimum mineral wettability for mimicking initial reservoir conditions (Puntervold et al. 2007). In this study the only variation in the coreplug conditions was the aging time as they were aged for two, four, and eight weeks respectively. These studies collectively indicate that aging up to 4-8 weeks must be sufficient for all coreplugs, but in another study (Dia et al. 1991), two coreplugs were aged for 180 days and their wettability index were measured at different time intervals. A change of wettability index was reported even after 136 days of aging. Thus the presented studies propose different aging times which are significantly different in specific cases. This complexity can be explained by the variation in coreplug, crude oil, and temperature in the experiments(Dia et al. 1991; Graue et al. 2002; Graue et al. 1999; Yildiz et al. 1999). The effects of each of the mentioned factors are explained individually in the following.

Aging temperature

The effect of aging temperature on wettability condition of coreplugs is documented in the literature. Increase in temperature during aging experiments is reported to change the wettability condition of coreplug towards a more oil wet condition (Dia et al. 1991). In this study, wettability index and water saturation of the coreplug after one day of aging and with varying temperatures were reported. It was shown that an increase in temperature from 20 °C to about 100 °C resulted in a consistent decrease in wettability index of water from more than 0.8 to less than 0.1. In another study(Yildiz et al. 1999), two coreplugs were aged at 25 °C and the other two coreplugs were aged at 80 °C. Thereafter spontaneous imbibition tests were conducted using 2 different imbibing brines. The coreplugs which were aged at 80 °C had relatively lower oil recovery which was produced in considerably longer time interval (more than 12 days). Brine variations showed less than 10% change in oil production while aging temperature showed more than 20% change in oil recovery. Thus, the effect of aging temperature had significantly higher influence on oil production than the imbibing brine. It was interpreted that aging at higher temperatures made the coreplugs significantly more oil wet and that brine variation had only minor influence on mineral wettability. In a similar study (Zhou et al. 1995), 22 coreplugs were used to investigate the effect of aging temperature on coreplugs with varying aging time. It was concluded that oil recovery decreases with the increase in temperature and aging time. Effect of temperature on oil recovery is consistent for all the aging times. In their study (Zhou et al. 1995), 6 coreplugs were aged in the range of 0 – 48 hours at 25 °C, and another 5 coreplugs were aged with the same time range at 80 °C. The experiment was re-conducted with a different crude oil type but with a similar number of coreplugs and similar time and temperature sets. The results were consistent for both oil types and in all the aging time range. These studies collectively show that aging temperature has a prominent effect on mineral wettability and oil production.

Coreplug and crude oil properties

Coreplug properties have shown the potential to affect the wettability condition of rock surface after aging (Graue et al. 1999). Herein two rounds of spontaneous imbibition experiments were conducted on six different coreplugs. Coreplugs were non-aged in the first round of experiments while they were aged for 14 days in the second round. The difference in oil recovery between aged and non-aged condition varies significantly for different core types. For instance, aging decreased oil production (from more than 30% to less than 5%) for the Dania chalk coreplugs from Ålborg, Denmark, while it remained unchanged for Bentheimer sandstone coreplugs from Germany. Crude oil properties also affect the wettability condition of rock surface after aging

experiments. In the same study (Graue et al. 1999), six coreplugs were saturated with two types of refined oils and one type of crude oil. Half of them were aged for 8, and 16 weeks while the others were not aged. End time water saturation after 1000 hours of spontaneous imbibition illustrated that the effect of aging on oil displacement was not the same for different oil samples. End time saturation decreased about 0.3 for the coreplugs with crude oil while it decreased less than 0.05 for the samples with the other oil types. Since saturating oil is the only variation in the imbibition experiment, it was concluded that crude oil type plays an important role in aging condition. In a similar study (Graue et al. 2002), six similar coreplugs aged with old barrel and new barrel oils from the same field were studied. Spontaneous imbibition experiments were conducted for 1000 hours. Around 10% variation in end time water saturation was observed between new barrel and old barrel condition of same crude oil. The presented studies indicate that a suggestion for a specific set of coreplug and crude oil cannot be generalized for other types of coreplugs. And each crude oil has its own unique rate of wettability alteration during aging into a specific coreplug. In the presented study, all the samples were saturated with identical crude oil, thus the effect of crude oil variation on wettability condition of coreplugs after aging is excluded and other parameters are the matter of investigation.

Coreplug resistivity measurement as a way to investigate rock surface wettability

The importance of the initial reservoir wettability condition prior to core waterflooding experiments was previously presented in the introduction. It requires sufficient aging time which is unique for each set of coreplug, crude oil, and experimental temperature. Determination of this unique time requires a consistent way of observing and measuring wettability. Coreplug resistivity is shown to be affected by water saturation and rock surface wettability (Sweeney & Jennings 1956). In this same study, resistivity measurement of 25carbonate coreplugs with porosity range of 0.11 to 0.31, dolomization range of 10 to 75 %, and different cementation level varied from poor to strong were conducted. It was concluded that change of resistivity in a stable condition and in constant water saturation during aging experiments reflects the change of wettability condition of rock surface. Resistivity measurement was used previously in core waterflooding experiments (Gamage & Thyne 2011) and aging experiments with low confining pressure (Pairoys et al. 2011).

In this work, novel equipment was developed to measure the resistivity of the coreplug under static condition of constant water saturation. Thereafter, a consistent, reproducible, and reliable method is established to correlate resistivity of coreplugs with its wettability condition. Different regions of resistivity change are introduced to distinguish the effect of wettability alteration and the effect of external parameters. Through resistivity monitoring during coreplug aging this study provides the opportunity to determine the optimum aging time, unique to each core flooding experiment without need of additional experimentation.

Equipment and experiments

The developed core flooding equipment is shown in Figure 1, which consists of three major sections: a. Injection brine section (which is shown in a red box); b. Core holder section; c. Data acquisition unit (which is shown in a green box). The injection brine section was designed for the waterflooding experiments and was not used in the aging experiments of this work, thereafter it will not be explained in the following.

Core holder section

The Hassler steel core holder can maintain a coreplug with the dimension up to 30cm of length and 1½" of diameter. The core placement procedure is illustrated in Figure 2. After mounting the coreplug, the core holder should be placed horizontally and be connected to five connection vessels.

These connections are: axial and radial pressures, the brine injection line, heating connection, and the connection for electric wires. Applying different axial and radial pressures on the coreplug simulates the reservoir condition where the minerals are exposed to different stresses (Schade 1974). This distinction has not been implemented in previous waterflooding experiments (Zahid et al. 2012). Radial or confining pressure simulates the overburden pressure on the coreplug while axial pressure is crucial to maintain a thorough contact between the core and the data acquisition plates plus mimic the pressure coming from the sides in the reservoir. A back pressure regulator (BPR) is connected to the core outlet to simulate the pore pressure by setting the outlet pressure for the experiment (Zhang et al. 2000). The injection brine vessel is connected to the two ends of the coreplug (inlet and outlet) and is capable of operating at pressures up to 700 bars and temperatures up to 150°C. Pressure transducers are installed in the inlet, outlet, axial, radial, and back pressure regulator to monitor the flow and pressure condition of the experiment. In this study the outlet condition was closed by a manual valve to maintain static conditions.Two sides of the core holder are connected to electrical heat supply units and the temperature is measured by thermocouples to provide a uniform and stable temperature in the coreplug. Temperature variation tests illustrated that the temperature variation in the coreplug is less than 1°C gradient when the temperature was increased to 130°C. Note, temperature is claimed to have a major effect on the petrophysical properties and oil productions (Rezaeidoust et al. 2009). An oscilloscope is connected to the two ends of the coreholder by electric wires. These wires transmit the spikes generated from the oscilloscope into the electrical and seismic sensor in one end of the coreplug and receive them from the other end of the coreplug. The oscilloscope is monitored and controlled by the Labview™ 8.6 software. Detailed description and engineering drawing of the moveable head assembly and the pressure sleeve are shown in Figure 3 and Figure 4, respectively.

Data acquisition unit

All the connections of the Hassler type core holder are connected to a single acquisition center, which is controlled by an in-house data acquisition system. It records pressures, temperature, electrical resistance and sound velocity measurement. The system is based on National Instruments Labview^{TM} 8.6 (Wang & Zhou 2012) which acquires, records, and plots data for further analysis. In-house Sound Wave software is used to process the oscilloscope signals passed through the coreplug to produce its sound velocity and electrical resistivity during aging experiments. As it is shown in section 3 of Figure 2, an insulating plastic plug is implemented between essential metal pieces in the core holder to prevent the electric signal from flowing through the body of the core holder. Thus the resistivity path is through the coreplug and the obtained resistivity is due to the coreplug, not the surrounding metal. For constant water saturation, pressure, and temperature, the variation in resistivity is known to be correlated with the rock surface wettability(Sweeney & Jennings 1956).

Coreplug preparation

Ten coreplugs including 4 sandstone and 6 chalk samples were investigated.(specifications in Table 1) These coreplugs are from different origins and different depths with varying lithology, heterogeneity, porosity, permeability and initial water saturation (Table 2). All the coreplugs were initially CT-scanned to obtain information about the possible heterogeneities or fractures. Thereafter they were cleaned by flooding with toluene and with ethanol. Cleaned coreplugs were dried in an oven at 90 ºC and their porosity and permeability were measured (Katika et al. 2016). The recorded petrophysical properties of samples are coherent with previous reports (Fabricius et al. 2007). Thereafter they were water flooded at 40 ºC at an injection rate of 0.2 ml/min. They were consequently water flooded with crude oil for 5 pore volumes (PV), and with similar injection rate, to obtain irreducible water saturation.

Sandstone coreplugs

Four sandstone coreplugs were taken from North Sea. The coreplugs are S1, S2, S3, and S4. All the coreplugs had similar physical properties such as length, diameter, and porosity (Table 2). Their heterogeneity is reflected in their permeability values where permeability of S3 and S2 is considerably higher than S4 and S1. In addition, S1 had the highest water saturation around 0.6 while it was in the range of 0.32 to 0.45 for the other samples.

Chalk coreplugs

The coreplugs were originated from North Sea. The chalk coreplugs consisted of around 98% of calcite and their dolomite or anhydrate content is negligible. C1 and C2 were used in the high temperature aging experiments. They were identical in different aspects such as dimensions, porosity, and water saturation (Table 2). The remaining 4 coreplugs including C3, C4, C5, and C6 were used for low temperature aging experiments. The diameter of the coreplugs is similar while the C3 is slightly shorter in length. The porosity of the coreplugs is in the range of 0.34 to 0.4 and their water saturation is around 0.05 (as reported in Katika et al. 2016) (Table 2). All the samples were chosen with the similar physical and petrophysical properties to minimize the effect of core properties on resistivity measurement analysis.

Crude oil

Crude oil from North Sea, with the viscosity of 8.83 cp, was used to saturate the coreplugs. Its acid number and base number were 0.09 and 2.44 (mg KOH/g oil), which were measured using modified version of ASTM D2896 for the base number titration and ASTM D664 for the acid numbers titration (Fan & Buckley 2006).SARA analysis of the crude oil illustrated that crude oil contained 0.3 % asphaltene. These data are shown in Table 3.

Aging

Aging experiments were conducted at different temperatures, pressures and durations (Table 1). Six chalk coreplugs were aged at two different temperatures and pressures. The first group consisted of two coreplugs which were aged at 130 °C and confining pressure of 90 bar. The remaining four samples were aged at 60 °C and a confining pressure of 100 bar. Sandstone cores were also aged at 60 °C and 100 bars. Resistivity acquisition interval varies from 1 to 30 minute(s). A smaller acquisition interval is helpful to achieve a higher resolution of the wettability change while a longer time interval reduces the computational difficulties of resistivity determination. Herein all the suggested aging times are calculated with pressurizing from the beginning of the experiment. Resistivity values were multiplied by the coreplug surface area and were divided by the coreplug length to cancel out the effect of coreplug length and cross section surface area. Thus, the reported values in this study have the unit of $\Omega \cdot m$.

Results and discussion

The variation in resistivity of the coreplug during aging experiments shows a specific behavior and is regardless of core properties and experimental conditions. Thus, resistivity variation can be divided into three main regions. Determination of these regions is crucial in order to distinguish the effect of wettability modification and external parameters on resistivity. Resistivity evolution of coreplug S4 is chosen to illustrate these regions. The duration of each region differs for different coreplugs but the pattern of resistivity change is the same for all of the coreplugs. The first region is the transient zone, in which resistivity is affected by the increase in temperature and pressure (this zone starts from the beginning of the experiment until 0.8 day in Figure 5). Resistivity decreases with the increase in pressure and temperature while the effect of temperature is more significant than the effect of pressure (Figure 5). The rate of resistivity decrease is proportional to the rate of pressure and temperature increase. Associated changes in coreplug properties for sudden variations in pressure and temperature have also been reported (Hjelmeland & Larrondo

1986). Second region (this region is correspondent to the time 0.8 to 1.1 days in Figure 6) starts right after the initial decrease of resistivity in the transient zone. In this region, resistivity slightly increases until it reaches a stable position (resistivity condition after 1.1 days in Figure 6). This position is the unique initial resistivity point for the specific set of coreplug, crude oil, temperature, and pressure. Third region starts after the second region and continues until the end of experiment (this region is from the time 1.1 until 21 days in Figure 7). This region reflects a slight decrease in resistivity of the coreplug. Effect of surrounding parameters such as pressure and temperature is excluded in this region, thus change in resistivity can be correlated with the change of rock wettability. The decrease in rate of resistivity is sharper in the early stages of this region while it gradually stabilizes in the later stages (Figure 7). Stabilization of resistivity indicates that rock surface wettability has reached an equilibrium condition.

These studies have illustrated the capability of this method to produce significantly high amount of data by which rock surface wettability can be investigated consistently. It highlights the advantage of this method in comparison with traditional methods where each experiment can produce limited data points. In addition, this method determines the optimum aging time, thus it ensures the accuracy of further waterflooding experiments. Real time determination of the unique aging time for each set of coreplug, crude oil, and temperature (without waterflooding or other destructive method) eliminates the need of additional experiments and will save time, experimental expenditures, and complexities of the experiment.

Lower temperature chalk samples

In three coreplugs, including C4, C3, and C6, the initial resistivity was in the range of 180 – 200 $\Omega \cdot m$. However, the optimum aging time for these samples was not identical. Coreplug C6 was aged for more than 100 days (Figure 8). Its resistivity sharply decreased with the increase in temperature and confining pressure. This sharp decrease was followed by a smooth increase, from which the fluctuations in pressure did not reflect major effect on the resistivity. The decrease in the resistivity values from this point can be correlated to the change in rock surface wettability. Resistivity was stabilized after 20 days of aging but the sharp decrease in resistivity after 40 days of aging indicates that the aging time should be more than 40 days for this coreplug. Resistivity remained stable in the next 60 days with minor variation related to the temperature. Coreplug C3 reflected the same behavior as C6. It was stabilized after 20 days until the 40th day in which the resistivity suddenly decreased. No other considerable change in resistivity was observed in the next days (Figure 9). There was a gap in the early stages of the experiment due to a problem in the recording software. The effect of pressure on resistivity measurements was investigated in coreplug C4. Confining pressure increased to 100 bar initially. Thereafter the pressures were kept constant to enable the coreplug to reach the stable condition. From this point, the confining pressure increased gradually from 100 to 150 bar during 50 days. The decrease in resistivity was correlated with the increase in pressure but the decrease rate was lower in later stages of the experiment (Figure 10). It is probably due to decreasing effect of wettability change on resistivity measurement overtime. It also can be concluded that variation in pressure affects the resistivity measurement even after 60 days. Therefore the pressure should be kept constant during aging experiments to exclude the effect of temperature and pressure. Finally, coreplug C5 was aged for about 40 days. In this experiment the resistivity was considerably higher than other coreplugs, although all of them have similar properties. It can be explained by a failure in core mounting because the sensors were not completely attached to the core. The delay in the increase of axial pressure in comparison with radial pressure can be the reason for this failure (Figure 11). Thus the axial pressure should remain higher than radial pressure during the entire experiment.

Sandstone samples

Four sandstone coreplugs S1, S2, S3, and S4 were all aged for different time intervals. They returned a resistivity behavior which is similar to the already discussed chalk patterns of resistivity change. For the studied sandstone samples, the resistivity is lower than the corresponding resistivity of chalk coreplugs. The low resistivity of sandstone coreplugs can be explained by their higher water saturation(Sweeney & Jennings 1956). The optimum aging time was not identical for all samples but in this study it was less than the aging time for chalk coreplugs. The optimum aging time for S3, S4, and S2 were between 5 and 7 days (Figure 12-14).Coreplug S1 was used to investigate the effect of varying pressure on the resistivity measurement. The results were similar to the low temperature chalk sample C4. The variation in resistivity values are correlated with the change in pressure. The effect of pressure on resistivity was observed even after 30 days of aging; however its effect decreased over time (Figure 15). It can be explained as the effect of wettability is excluded in the later stages of the experiment.It must be noted that all the three coreplugs originate from same field in North Sea, they all contained the same brine and crude oil saturation. All lithological properties of the coreplugs where quite similar; yet significant differences were observed in the optimum time for the different coreplugs.

Elevated temperature chalk samples

This experimental section includes the coreplugs C1 and C2. As shown in Figure 16 it is observed that for coreplugs aged at 130°C a sharp decrease of resistivity after the increase of pressure and temperature was continued until very low resistivity values were obtained (Figure 16). These low resistivity values and the continued decreasing trend in coreplug resistivity are in contradiction with the established pattern of resistivity change. This behavior raised doubt about the electric current path during aging experiments of chalk samples at elevated temperatures. Further investigations illustrated that a fraction of the formation fluid flowed back into the plastic head isolating the metal core holder from the coreplug. This short-circuited the resistivity measurement through the metal casing. In order to overcome the shortcut issue, hydraulic oil was put in the outlet end of the coreplugs in later experiments. This prevents the core liquids from flowing out of the coreplug and consequently ensures the

correct resistivity path. This observation highlights the role of resistivity measurement in investigation of proper core mounting and aging experimental condition.

Conclusion

The developed core flooding equipment shows that a change in wettability results in a change of the resistivity of the coreplug. Therefore resistivity measurement is a novel way to assess the aging experiments. It has been also observed that the optimum aging time is unique for each set of coreplug, crude oil and experimental conditions.

- A new method was developed, by which a consistent, real time, and reproducible way of wettability alteration monitoring is provided.
- A pattern has been established which explains the different regions of resistivity change during aging. The duration of each individual region differs for different coreplugs but the pattern of resistivity change is independent of coreplug and experimental conditions.
- The presented method provides a high resolution of wettability alteration monitoring, by which the optimum aging time for each individual set of coreplug, crude oil, temperature, and pressure can be determined.
- Determination of optimum aging time eliminates the need for additional aging experiments prior to core waterflooding experiments. It also increases the accuracy and reliability of the waterflooding experiments.
- Resistivity measurements of high temperature chalk aging indicate that coreplug liquid might flow out of coreplug during the aging experiments.
- Hydraulic oil has shown the potential to solve the outflow of liquids from coreplug.
- Increase in pressure and temperature affects the resistivity measurements. Therefore their effect should be excluded from total results.

References:

- Austad, T. et al., 2005. Seawater as IOR Fluid in Fractured Chalk. 2005 SPE International Symposium on Oilfield Chemistry, (3), pp.1–10.
- Austad, T., Rezaei Doust, A. & Puntervold, T., 2010. Chemical Mechanism of Low Salinity Water Flooding in Sandstone Reservoirs. IEA EOR Workshop & Symposium, pp.1–18.
- Chiquet, P., Broseta, D. & Thibeau, S., 2007. Wettability alteration of caprock minerals by carbon dioxide. Geofluids, 7(2), pp.112–122.
- Dia, D. et al., 1991. Control of Core wettability with crude oil. Proceedings of SPE International Symposium on Oilfield Chemistry, pp.401–409. Available at: http://www.spe.org/elibrary/servlet/spepreview?id=00021041.
- Emberley, S. et al., 2004. Geochemical monitoring of fluid-rock interaction and CO2 storage at the Weyburn CO2-injection enhanced oil recovery site, Saskatchewan, Canada. Energy, 29(9-10), pp.1393–1401.
- Fabricius, I.L., Røgen, B. & Gommesen, L., 2007. How depositional texture and diagenesis control petrophysical and elastic properties of samples from five North Sea chalk fields. Petroleum Geoscience, 13(1), pp.81–95.
- Fan, T. & Buckley, J.S., 2006. SQ-95. , pp.1–6.
- Farajzadeh, R. et al., 2012. Foam–oil interaction in porous media: Implications for foam assisted enhanced oil recovery. Advances in colloid and interface science, 183, pp.1–13.
- Fernø, M. a. et al., 2010. Dynamic laboratory wettability alteration. Energy and Fuels, 24(7), pp.3950–3958.
- Gamage, P. & Thyne, G., 2011. Comparison of Oil Recovery by Low Salinity Waterflooding in Secondary and Tertiary Recovery Modes. Spe 147375.
- Graue, a. et al., 2002. Alteration of wettability and wettability heterogeneity. Journal of Petroleum Science and Engineering, 33(1-3), pp.3–17.
- Graue, A. et al., 1999. Systematic wettability alteration by aging sandstone and carbonate rock in crude oil. Journal of Petroleum Science and Engineering, 24(2-4), pp.85–97.
- Hjelmeland, O.S. & Larrondo, L.E., 1986. Experimental investigation of the effects of temperature, pressure, and crude oil composition on interfacial properties. SPE Reservoir Engineering, 1(04), pp.321–328.
- Karimi, A. et al., 2012. Wettability alteration in carbonates using zirconium oxide nanofluids: EOR implications. Energy & Fuels, 26(2), pp.1028–1036.
- Katika, K. et al., Wettability of chalk and and argillaceous sandstones assessed from T1/T2 ratio. 78th EAGE Conference & Exhibition, 30 May – 2 June 2016, Vienna, Austria.
- Kewen, L. & Abbas, F., 2000. Experimental study of wettability alteration to preferential gas-wetting in porous media and its effects. SPE Reservoir Evaluation & Engineering, 3(02), pp.139–149.
- Kumar, K., Dao, E. & Mohanty, K., 2008. Atomic Force Microscopy Study of Wettability Alteration by Surfactants. SPE Journal, 13(2), pp.2–5.
- Morrow, N.R. et al., 1998. Prospects of improved oil recovery related to wettability and brine composition. Journal of Petroleum science and Engineering, 20(3), pp.267–276.
- Nasralla, R. a & Nasr-el-din, H. a, 2012. Double-Layer Expansion: Is It A Primary Mechanism of Improved Oil Recovery by

Low-Salinity Waterflooding? Eighteenth SPE Improved Oil Recovery Symposium, (2008), pp.1–17.
- Puntervold, T., Strand, S. & Austad, T., 2007. Water flooding of carbonate reservoirs: Effects of a model base and natural crude oil bases on chalk wettability. Energy and Fuels, 21(3), pp.1606–1616.
- Rezaeidoust, a. et al., 2009. Smart water as wettability modifier in carbonate and sandstone: A discussion of similarities/differences in the chemical mechanisms. Energy and Fuels, 23(9), pp.4479–4485.
- Salehi, M., Johnson, S.J. & Liang, J.-T., 2008. Mechanistic study of wettability alteration using surfactants with applications in naturally fractured reservoirs. Langmuir, 24(24), pp.14099–14107.
- Schade, W.H. and U.K. and K.R. and E., 1974. Investigation of a cylindrical, axially blown, high-pressure arc. Journal of Physics D: Applied Physics, 7(4), p.607. Available at: http://stacks.iop.org/0022-3727/7/i=4/a=315.
- Standnes, D.C. & Austad, T., 2003. Wettability alteration in carbonates: Interaction between cationic surfactant and carboxylates as a key factor in wettability alteration from oil-wet to water-wet conditions. Colloids and Surfaces A: Physicochemical and Engineering Aspects, 216(1-3), pp.243–259.
- Standnes, D.C. & Austad, T., 2000. Wettability alteration in chalk 2. Mechanism for wettability alteration from oil-wet to water-wet using surfactants. Journal of Petroleum Science and Engineering, 28(3), pp.123–143.
- Standnes, D.C. & Austad, T., 2000. Wettability alteration in chalk: 1. Preparation of core material and oil properties. Journal of Petroleum Science and Engineering, 28(3), pp.111–121.
- Sweeney, B.Y.S.A. & Jennings, H.Y., 1956. Effect of Wettabiliti ' on the Electrical Resistivity of Carboxate Rock Fro31 a Petroleu3I Reservoir. Production, 1225(6), p.1956.
- Thakur, G.C., 1991. Waterflood surveillance Techniques - A Reservoir Management Approach. Journal of Petroleum Technology, 43(10).
- Vledder, P. et al., 2010. Low Salinity Water Flooding: Proof of Wettability Alteration On A Field Wide Scale. Proceedings of SPE Improved Oil Recovery Symposium, (Lil), pp.1–10. Available at: http://www.onepetro.org/mslib/servlet/onepetropreview?id=SPE-129564-MS&soc=SPE.
- WANG, J. & ZHOU, Q., 2012. Design of a Temperature Monitoring System Based on DS18B20 and LabVIEW [J]. Research and Exploration in Laboratory, 3, p.17.
- Yildiz, H., Valat, M. & Morrow, N., 1999. Effect of Brine Composition On Wettability And Oil Recovery of a Prudhoe Bay Crude Oil. Journal of Canadian Petroleum Technology, 38(1). Available at: https://www.onepetro.org/journal-paper/PETSOC-99-01-02.
- Yu, L. et al., 2009. Spontaneous imbibition of seawater into preferentially oil-wet chalk cores - Experiments and simulations. Journal of Petroleum Science and Engineering, 66(3-4), pp.171–179. Available at: http://dx.doi.org/10.1016/j.petrol.2009.02.008.
- Yuan, H. & Shapiro, A. a., 2011. Induced migration of fines during waterflooding in communicating layer-cake reservoirs. Journal of Petroleum Science and Engineering, 78(3-4), pp.618–626. Available at: http://linkinghub.elsevier.com/retrieve/pii/S0920410511001938.
- Zahid, A., Shapiro, A. & Resources, E., 2012. SPE 155625 Experimental Studies of Low Salinity Water Flooding in Carbonate Reservoirs : A New Promising Approach. Chemical Analysis.
- Zhang, Y. et al., 2000. New and Effective Foam Flooding To Recover Oil in Heterogeneous Reservoir. 2000 SPE/DOE Improved Oil Recovery Symposium.
- Zhou, X. et al., 1995. The Effect of Crude-Oil Aging Time and Temperature on the Rate of Water Imbibition and Long-Term Recovery by Imbibition. SPE Formation Evaluation, 10(4), pp.259–265.
- Zhou, X., Morrow, N.R. & Ma, S., 1996. Interrelationship of wettability, initial water saturation, aging time, and oil recovery by spontaneous imbibition and waterflooding. In SPE/DOE Improved Oil Recovery Symposium. Society of Petroleum Engineers.

Tables:

Table 1: Aging duration and number of measured resistivity points for the different coreplugs

Coreplug ID	Aging time (day)	Number of resistivity measured points	Temperature (°C)	Pressure (bar)
D4H	14.5	625	60	100
D3H	20.4	1000	60	100
D7H	20.5	1026	60	100
D13H	37.1	2580	60	100
N3X9H	45	2370	60	100
N1X4H	70	4605	60	100
N1X11H	100	3374	60	100
N3X17V	38	2125	60	100
M1X10H	31	2665	130	90
M1X12H	32	9375	130	90

Table 2: Physical properties of the copreplugs (Katika et al. 2016), (PhD dissertation of Konstantina Katika, Technical University of Denmark).

Coreplug ID	Length (mm)	Diameter (mm)	Porosity	Permeability (mDa)	Water Saturation
D-3H	49.43	38.21	0.30	94.00	0.46
D-4H	50.61	38.23	0.32	156.00	0.33
D-7H	49.46	38.05	0.33	130.00	0.34
D-13H	49.12	38.07	0.31	65.00	0.67
N3X9H	70.66	38.38	0.34-0.35	4.16-6.07	0.05-0.02
N3X17V	74.63	38.38	0.34-0.35	4.16-6.07	0.05-0.02
N3X4H	74.56	38.34	0.34-0.35	4.16-6.07	0.05-0.02
N1X11H	74.76	38.41	0.34-0.35	4.16-6.07	0.05-0.02
M1X12	74.44	38.50			
M1X10	74.96	38.56			

Table 3: Crude oil Properties

Crude Oil	Acid Number	Base Number	Asphaltene	Viscosity
North Sea	(mg KOH/g oil)	(mg KOH/g oil)	(%)	(cp)
	0.09	2.44	0.3	8.83

Figures:

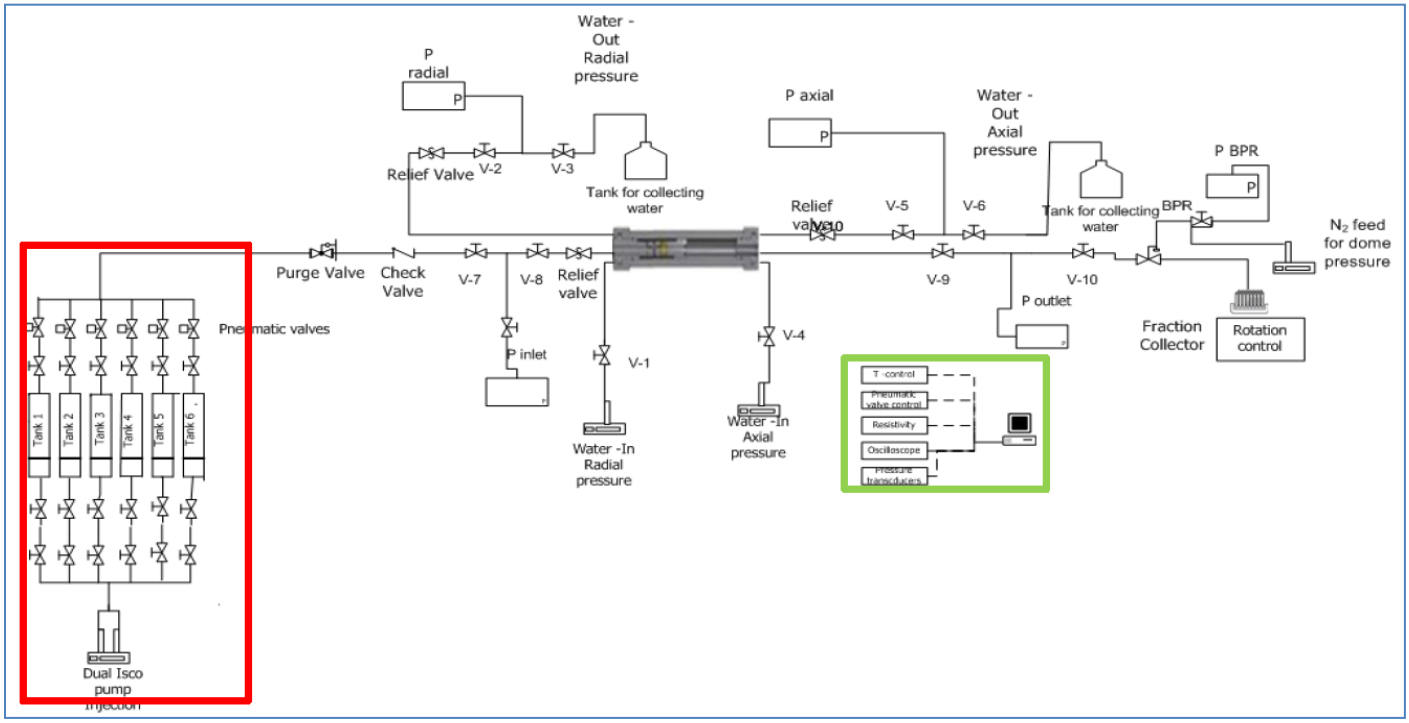


Figure 1: Overview of multiple sensors enables automated core flooding and aging setup.

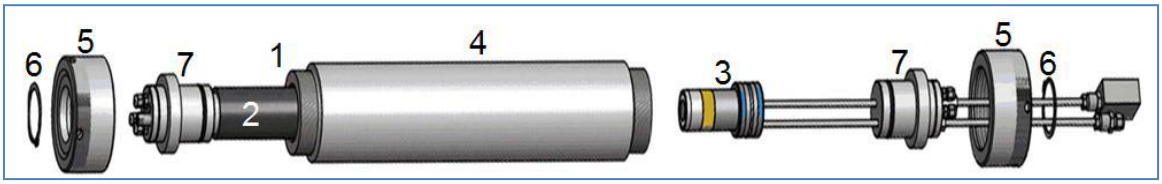


Figure 2: Illustration of the various sections of the core holder wherein the coreplug is first placed in a rubber hose (1) and then connected to a fixed head assembly (2) and a movable head assembly (3) into the pressure sleeve (4). Two union nuts (5) and retaining rings (6) keep the shafts (7) locked in the closed position.

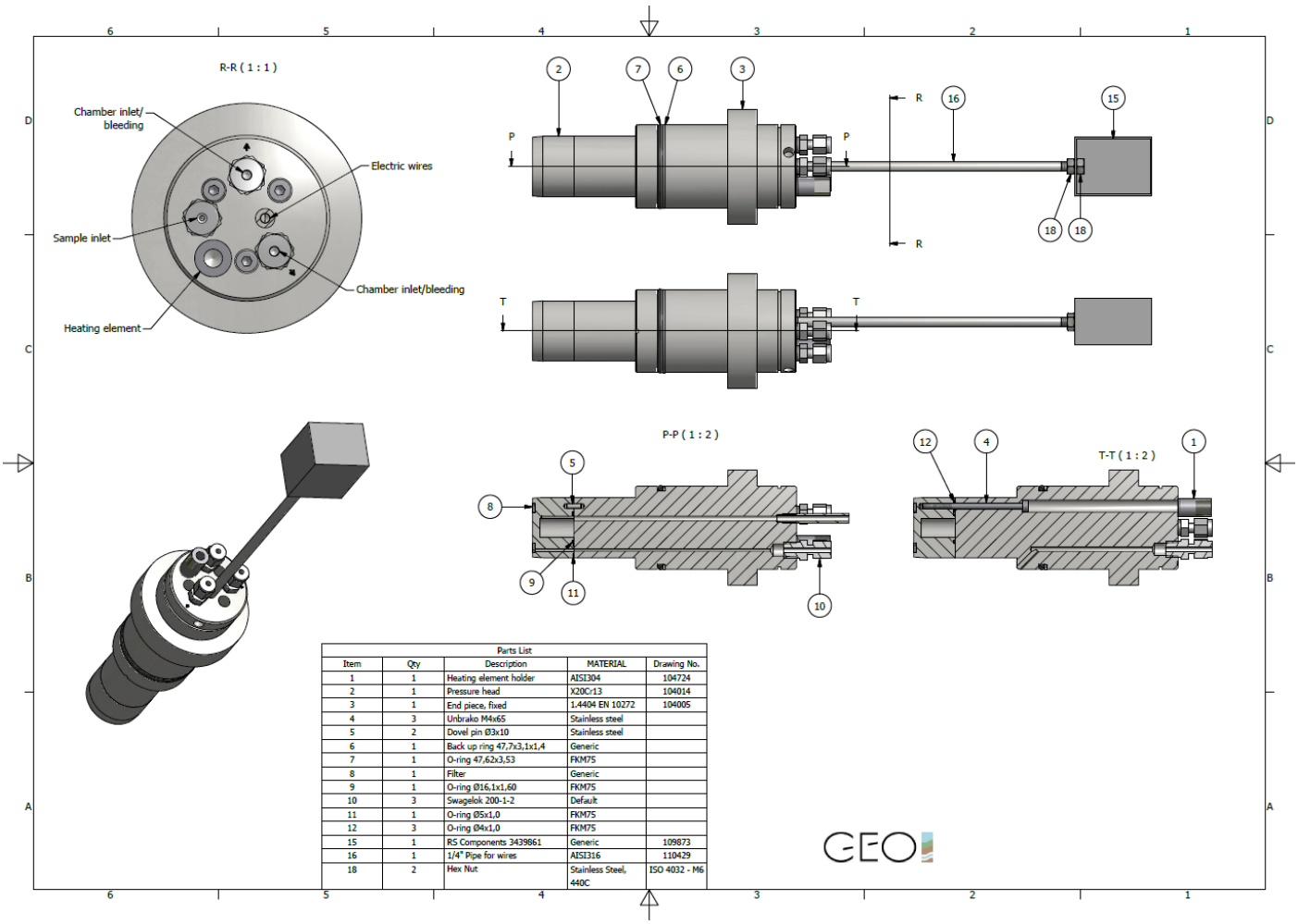


Figure 38: Engineering drawing of effluent head to the core holder. It includes the top view, the 3D structure and the different cross sectional view. The heating element and the electric connection to the oscilloscope are depicted in its top view.

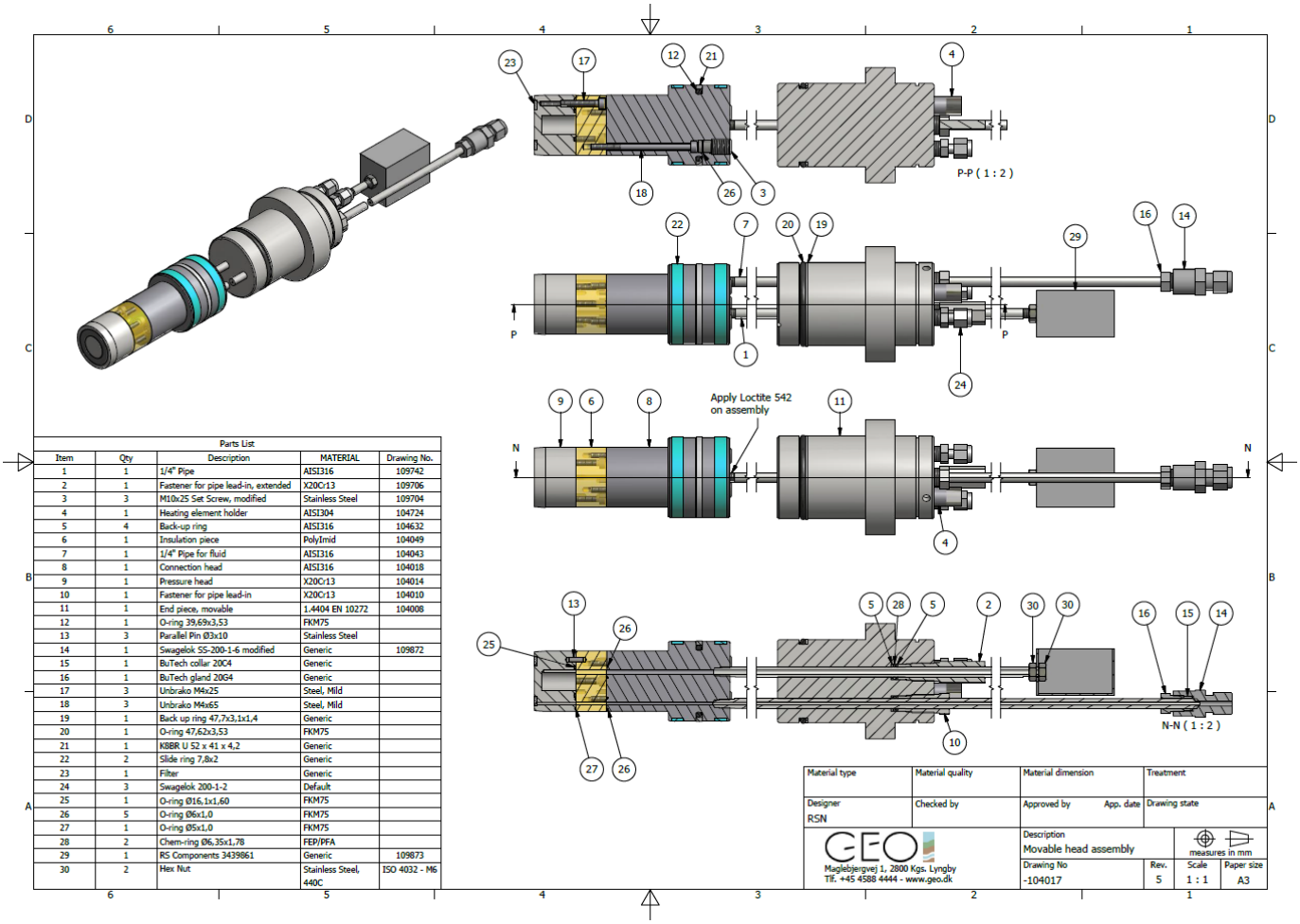


Figure 49: Engineering drawing of injection head to the core holder. It includes the top view, the 3D structure and the different cross sectional view. The yellow region represents the insulating plastic enabling measurement of the coreplug resistivity during aging.

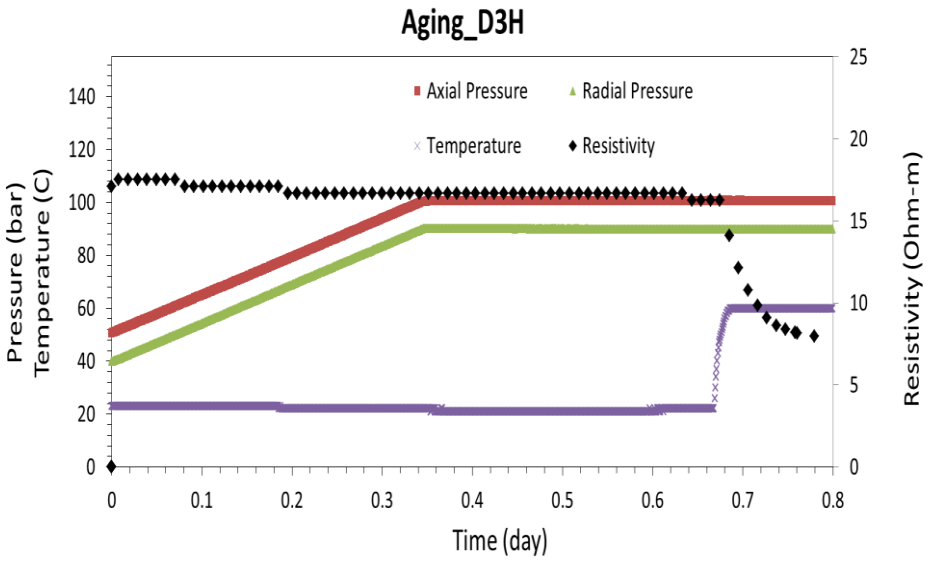


Figure 510: Transient zone, where resistivity values decreases with the increase in pressure and temperature.

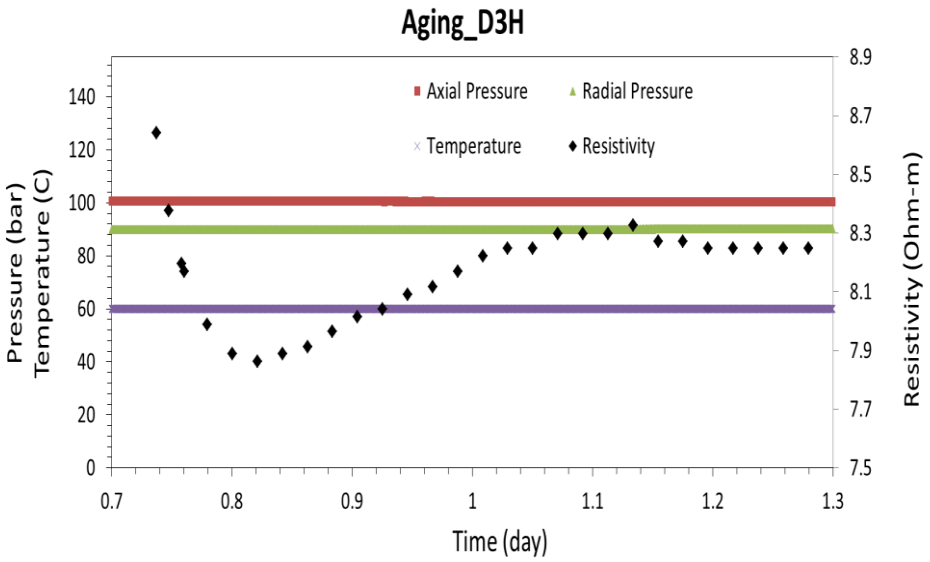


Figure 611: Increase in resistivity values after the initial decrease (transient zone) to reach the initial condition which is unique for each set of coreplug, crude oil, temperature, and pressure.

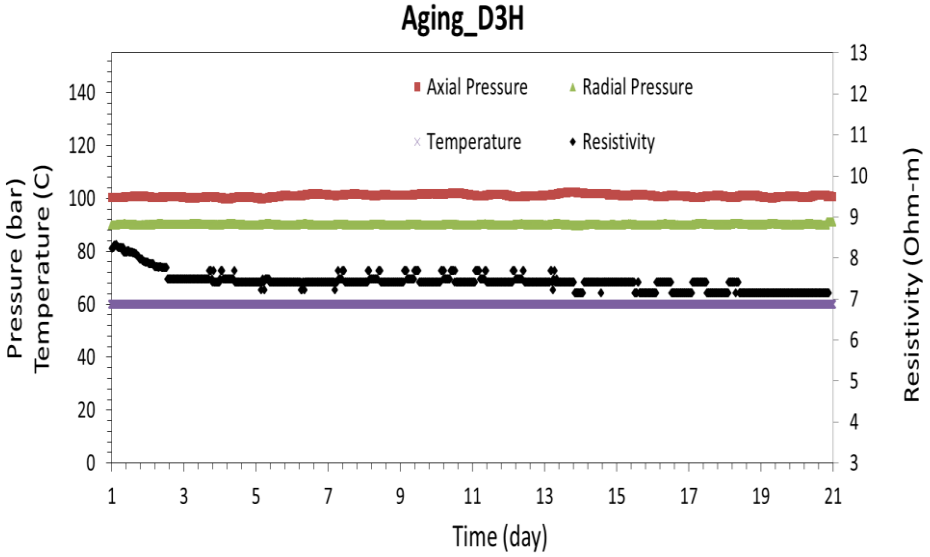


Figure 712: Slight decrease of resistivity after the initial point. This decrease is sharper in the early days. Change in resistivity values can be correlated with the change in rock surface wettability.

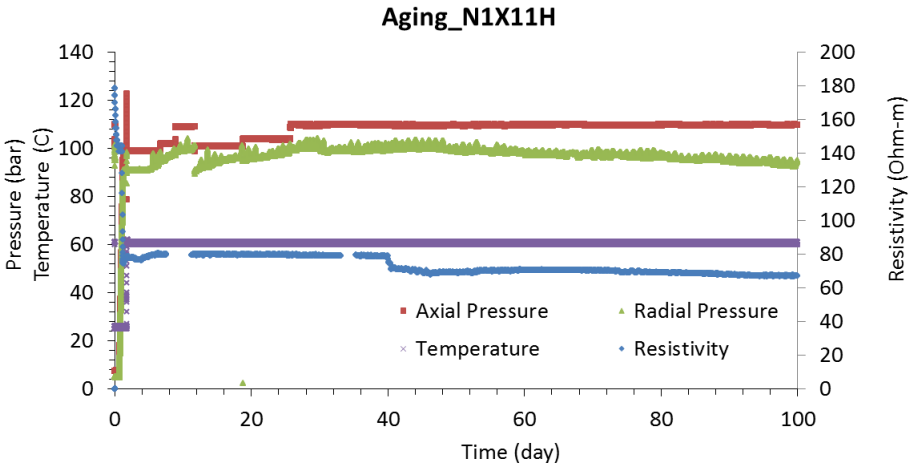


Figure 813: Aging of N1X11H. Resistivity was stabilized after 20 days but showed a sudden decrease after 40 days. No further decrease was observed after 40 days.

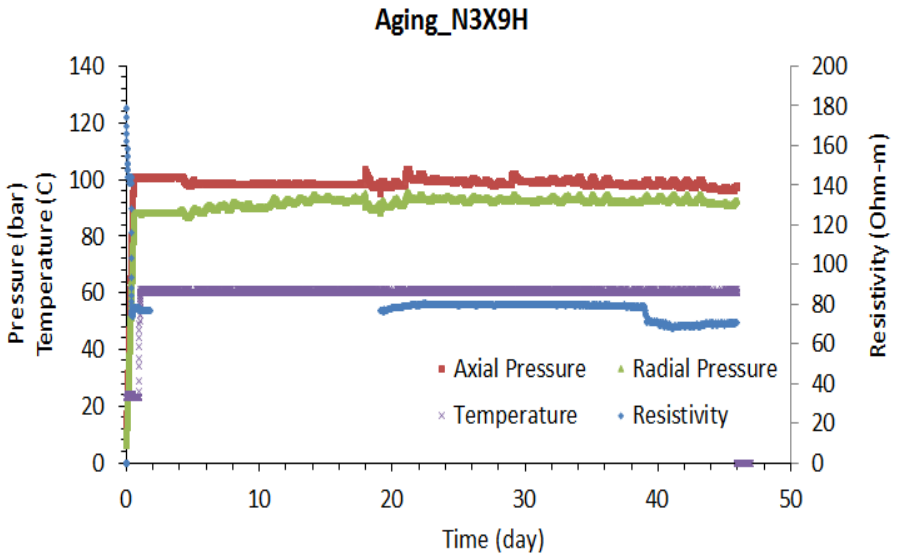


Figure 914: N3X9H aging experiment. Resistivity was stabilized after 20 days but showed a sudden decrease after 40 days. It remained unchanged afterwards.

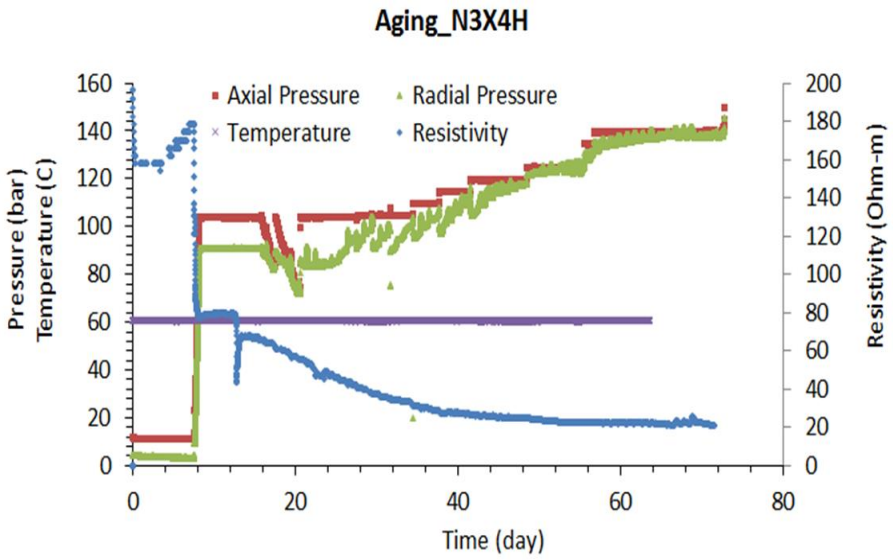


Figure 10: N3X4H aging experiment. Resistivity decreased with the increase in pressure. This decrease was continued even after 60 days.

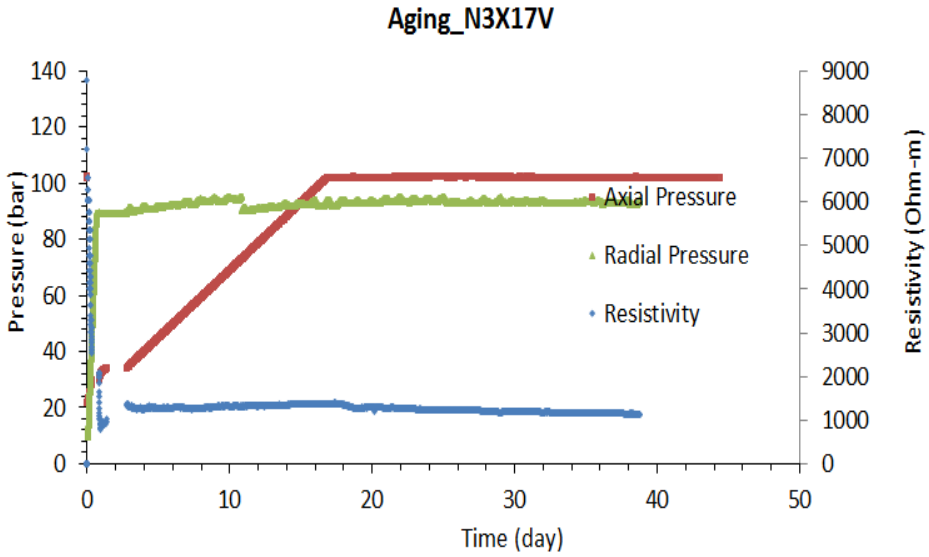


Figure 1115: N3X17V aging experiment. High resistivity values are caused by improper attachment of coreplug and the recording sensors. The sequence in the increase of axial and radial pressure is the possible explanation for this problem.

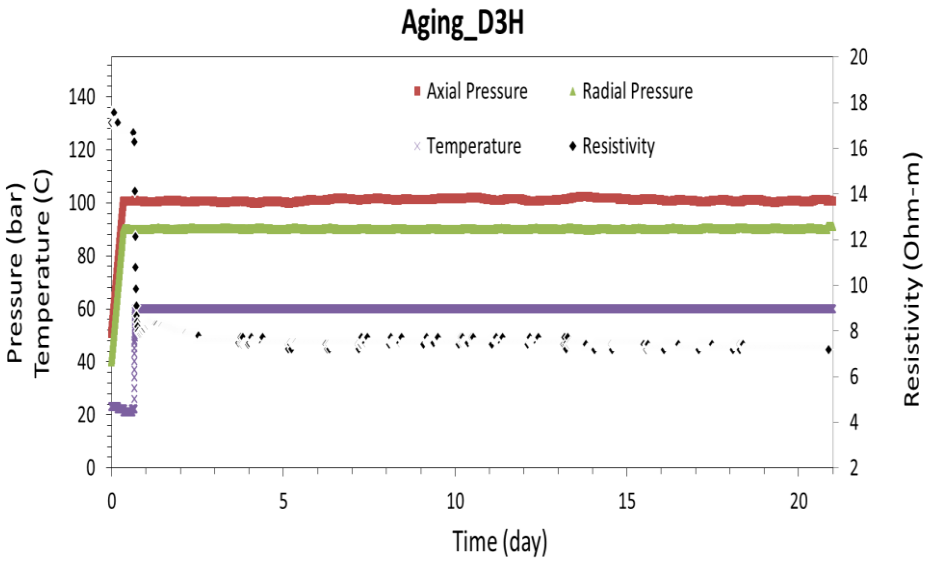


Figure 1216: Aging experiment D3H.

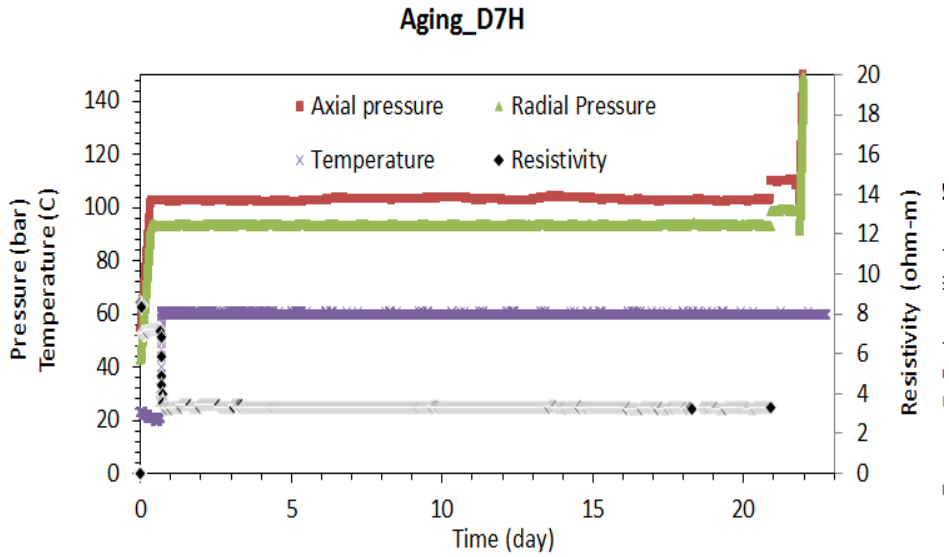


Figure 13: Aging experiment D7H.

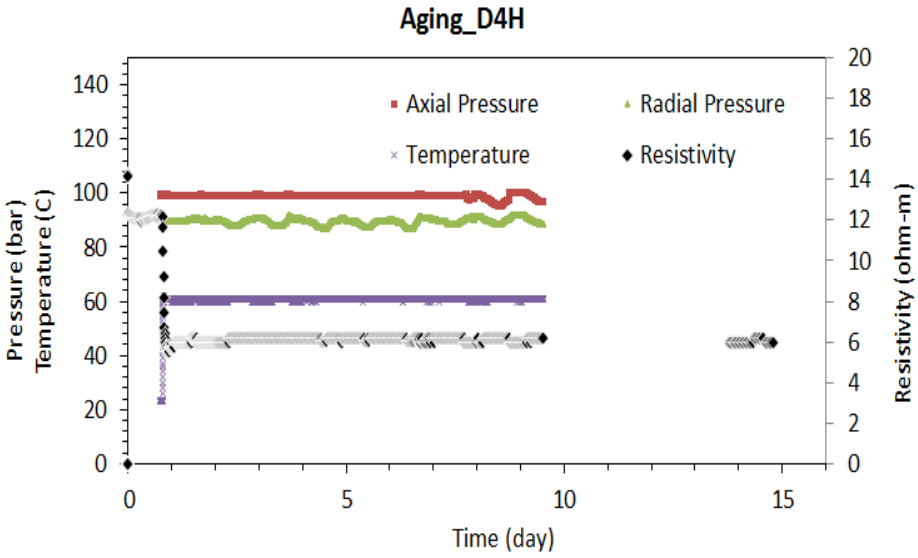


Figure 14: Aging experiment D4H.

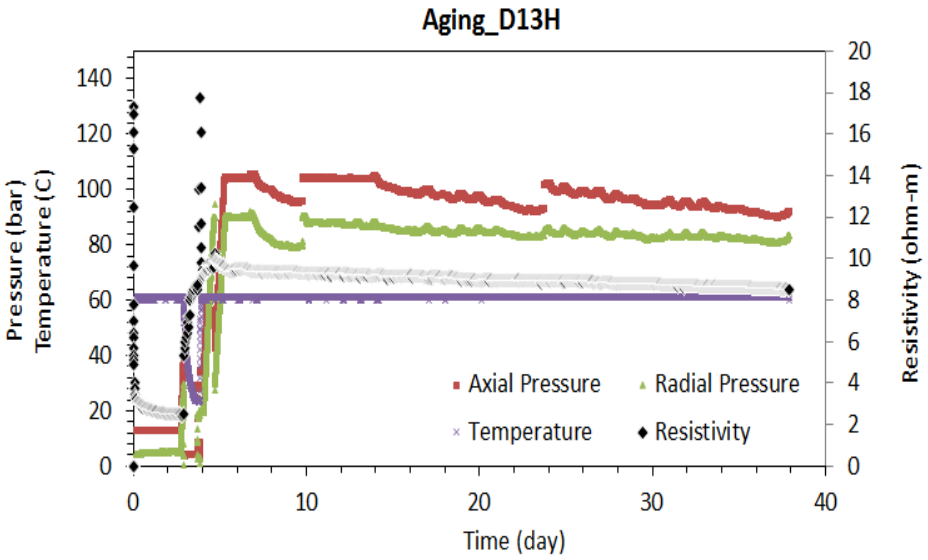


Figure 15: Aging experiment D13H.

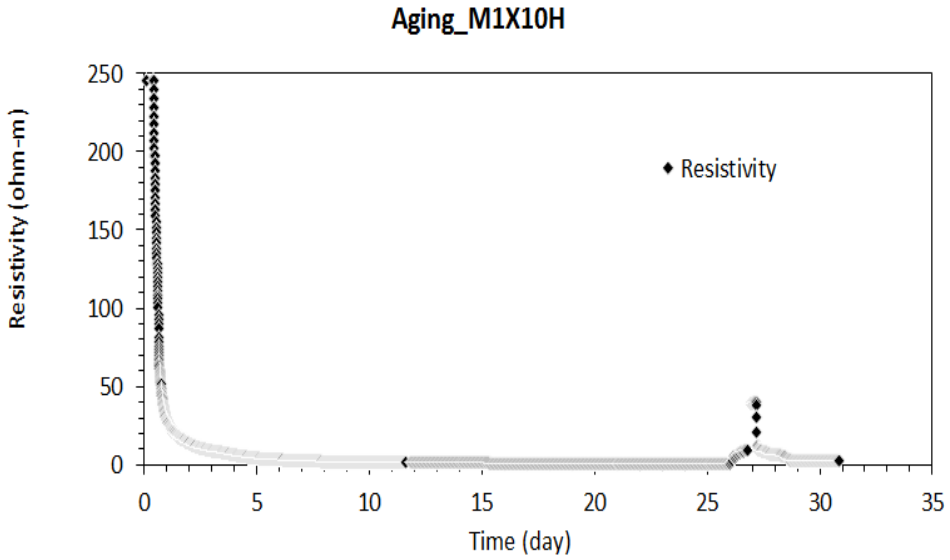


Figure 16: Very low resistivity values which are caused by the outflowing coreplug fluids. It resulted in a shortcut in the currency path.

Paper XI

Effect of injection of Sodium salts in Smart Water-Enhanced Oil Recovery (SmW-EOR): A case study from the North Sea

---

Chakravarty, K. H., Ahkami, M., Xiarchos, I., Fosbøl, P. L., & Thomsen, K. (2016) Effect of pause in brine injection during Smart Water-Enhanced Oil Recovery (SmW-EOR) for low temperature chalks: A case study from North Sea. ***Journal of Petroleum Science and Engineering*** **(Draft Manuscript: To be submitted)**

Abstract
Modifying the chemistry of injection water has proven to increase oil recovery from core plugs made from chalk outcrops and from reservoir rocks. In smart water flooding, several potential ions (including Ca^{2+}, Mg^{2+}, SO_4^{2-}, PO_4^{3-}, BO_3^{3-}, etc) have been considered for EOR. Investigations focusing on the particular effect of the sodium ion in SmW-EOR have not previously been published. This study includes core flooding experiments followed by thermodynamic modeling to explore the effect of sodium ion in EOR.

Water flooding experiments at 130 °C were conducted on reservoir chalk with varying concentrations of NaCl and Na_2SO_4. The amount of recovered oil was measured using radioactive tracer and was thereafter correlated to the effluent brine concentrations obtained using ICP-OES.

It was observed that alteration of the type or concentration of sodium salts basically did not have any major influence on the oil recovery during continuous injections. But pausing the water flood and resuming injecting the same brine showed consistent increase in oil production by up to 5.1 % of OOIP. Effluent water analysis also indicated that possible $CaCO_3$ fines formation could have taken place during the pause in water flooding. Against the common notion, these results indicate that the availability of high concentrations of SO_4^{2-} ions in the solutions may not always be beneficial in obtaining EOR. Contrasting to the universal belief, this study shows that SmW-EOR can be obtained without direct use of Ca^{2+}, Mg^{2+}, PO_4^{3-}, or $B_4O_7^{2-}$ ions. Thereafter, it also clearly proves that through a smart flow scheme, NaCl brine can also be used for enhanced oil recovery. And since NaCl brine is readily available in seawater, its proper management can be exceedingly beneficial in reservoir performance.

Introduction:
Around 50% of the word hydrocarbon production is from carbonate chalk reservoirs (Akbar et al. 2001). The total oil recoveries from these reservoirs are often less than 40% of the original oil in place (OOIP) (Akbar et al. 2001). This calls for development of innovative enhanced oil recovery methods which can increase the recovery fraction from the matured fields. SmW-EOR is a newly developing low cost non–toxic EOR method (Webb et al. 2005; Karoussi et al. 2007; Fjelde et al. 2009; Strand et al. 2006; Tweheyo et al. 2006; Zhang et al. 2007). It is universally accepted that altering the brine composition and its salinity can increase the recovery fractions both in sandstone and carbonate reservoirs (Yildiz et al. 1999; Fogden 2011; Lebedeva and Fogden 2011; Gupta et al. 2011; Delshad et al. 2013; Parracello et al. 2013; Robertson, 2007; McGuire et al. 2005; Alagic et al. 2011; Webb et al. 2005; Karoussi et al. 2007; Zhang et al. 2007). Different methods have been suggested for potential EOR, but no clear mechanism for this technology has been universally accepted. Several extensive investigation programs have been established in order to understand the scientific basis (Austad et al. 2008; Zahid et al. 2010; Gupta et al. 2011; Alvardo et al. 2014).

Austad and his co-workers have conducted a series of scrupulous experiments to understand this phenomenon (Strand et al. 2006; Zhang et al. 2007; Austad et al. 2008; Zhang et al. 2006; Puntervold et al. 2009). Herein wettability alteration (towards more water wetness) has been suggested to be the primary reason behind the observed increase in oil recovery (Puntervold et al. 2009). Water wetness is achieved by using brines with high concentrations of potential ions (including SO_4^{2-}, Ca^{2+} and Mg^{2+}). It has been suggested that SO_4^{2-} must be injected along with Ca^{2+}/Mg^{2+} ions. The injection of different concentrations of NaCl and Na_2SO_4 have been claimed to have no effect on oil recovery. Furthermore it has been suggested that precipitation must be avoided during SmW-EOR. The decrease in sulfate concentration in the effluent water shows that sulfate acts as a reagent in this process (Zhang et al. 2007). In most studies, the importance of soluble Ca^{2+}, Mg^{2+} and SO_4^{2-} ions in brine solutions has been recognized as the reason for obtaining enhanced oil recovery. The majority of these studies have been conducted with Stevns Klint outcrop cores from Denmark (Austad et al. 2005; Zhang et al. 2006; Puntervold et al. 2009).

Questions have been raised on this wettability alteration mechanism (Zahid et al. 2011; Zahid et al. 2012a; Zahid et al. 2012b; Gupta et al. 2011; Alvardo et al. 2014ba). Successful SmW-EOR has been observed for completely water wet cores (Zahid et al. 2010) as a significant increase in oil recovery was observed by injecting SO_4^{2-} enhanced sea water. This observation is contrary to the proposed wettability alteration mechanism (Austad et al. 2005). According to the wettability alteration mechanism, an increase in oil recovery should be a result of increased water wetness in the core plug (Austad et al. 2005). But injection of brines with high concentration of SO_4^{2-} has shown no corresponding increase in water wetness (Zahid et al. 2010), yet this type of core flooding results in increased oil recovery. Emulsification of oil and dissolution/attrition of rock were suggested to be the possible reasons for the observed EOR in completely water wet systems, but no detailed mechanism was provided. A series of published studies in recent years also show that oil emulsions can be formed by a buildup of a viscoelastic interface with low salinity flooded water (Moradi et al. 2011; Moradi et al. 2013; Alvardo et al. 2014). Furthermore, for high SO_4^{2-} brines significant increase in oil recovery has been observed with Stevns Klint outcrops chalks but no such recovery has been observed with reservoir core plugs (Zahid et al. 2011). Spontaneous imbibition experiments using SO_4^{2-} enriched brine have shown no increase in oil recovery for Rørdal chalk (Denmark) and Niobara chalk (USA) formations (Fernø et al. 2011). Experiments have also shown that high concentration sulphate is not necessary for SmW-EOR, and increased oil recovery can be obtained in absence of SO_4^{2-} ions (Gupta et al. 2011). Collectively, wettability alteration (Strand et al. 2006; Zhang et al. 2007; Austad et al. 2005) mineral dissolution/attrition (Pu et al. 2010;Yousef et al. 2011) and emulsification (Moradi et al. 2011; Moradi et al. 2013; Alvarado et al. 2014b) are different mechanisms that have been proposed to explain this phenomenon. But no general consensus has been established.

These results clearly show that there is no universally accepted understanding or mechanism associated to SmW-EOR. In order to understand the effect of individual ions in SmW-EOR, we performed a study where only brines containing NaCl and Na_2SO_4 in different concentrations were injected. Reservoir core plugs have been shown to behave differently from outcrop cores (Zahid et al. 2011). Variation in oil type has also been shown to have a prominent effect in oil production (Zahid et al. 2012). Reservoir core plugs from the Dan field of the North Sea were used along with oil generated from the same field. Both temperature and pressure of the core plug has been shown to affect the oil production (Austad et al. 2005; Zhang et al. 2006). The specific reservoir conditions of 130 $^{\circ}$C and 400 bar pressure were applied during the water flooding. Different possible monitoring methods are available. Collectively, the aim of this study is to understand the effect of sodium salts in reservoir core plugs from the Dan field. During low salinity water flooding, pausing and resumption of the injection of the same brine has been shown to increase oil production considerably (Alvarado et al. 2014b). Several pauses of different lengths was therefore introduced into the waterflood to study the effect of individual ions during pauses in waterfloods.

Experimental Details:

Core plug

Two core plugs originating 6400 ft below the sea surface from the Dan field of Danish North Sea were provided by Maersk Oil for this study. An XRD analysis showed that the core plugs contained around 98% wt of calcite mineral. No major fraction of dolomite or anhydrite was observed in the XRD analysis. The initial porosity of the core plugs was 27% and the calculated gas permeability was around 1 mD. The CT images (Figure 1) showed that both core plugs were very homogeneous with consistent and similar CT numbers variation. These measured properties of the core plug are consistent with previous reports (Fabricius et al. 2007; Jorgensen 1992). Both core plugs used in the experiments have very similar petro-physical properties and are of the same origin. The core plugs have an average specific surface area of 0.97 m^2 /gas determined by BET analysis. The detailed properties of the core plug used in this study are gives in Table 1 and 2.

Crude oil

Crude oil from the North Sea was used in this study. Acid and base numbers of the crude oil were measured using Metrohm 702 SM Titrino by the methods developed by Fan and Buckley (modified version of ASTM, D2896 for the base number titration of ASTM D664 for the acid numbers titration Fan and Buckley et al. 2006). The SARA analysis of the oil also has been previously conducted. The obtained specification of the properties is given in Table 3. [^{14}C] radiotracer was purchased by Perkin Elmer in the chemical form of stearic acid ($CH_3(CH_2)_{16}{}^{14}COOH$). It was delivered in the form of 1.25 ml solution of ^{14}C stearic acid dissolved in toluene (7.4 MBq/ml). This amount was used to mark one liter of North Sea crude oil (density = 0.845 g/cm^3). The tracer doped crude oil was injected into the core plug to obtain irreducible water saturation. The weight of the core plug at each step was recorded and is recorded in Table 4.

Core preparation

First the core plug was CT-scanned in its dry form to obtain the initial density variation in the core plug (Figure 1). This gave the information about any major heterogeneity or fracture that may affect the flow of injected water. The core plug was thereafter flooded with toluene until the effluent was colorless, and then flooded with ethanol. After cleaning, the core plugs were dried in an oven at 90 ºC to constant weight. The core plug properties were thereafter measured. This included the porosity, permeability and sound velocity of the cleaned core plug. This provided information about the initial core plug properties. Subsequently, formation water (FW: Na^+: 22866; Ca^{2+}: 1244; Mg^{2+}: 226; K^+: 175; Cl^-: 38383 mg/l) was injected into the core plug at 40°C at an injection rate of 0.2 ml/min. Sound velocity, electric resistivity and CT-scanning were performed to obtain the properties of the core plug after initial water saturation. Successively, five pore volumes (PV) of crude oil were injected at the rate of 0.2 ml/min to ensure that irreducible water saturation was achieved. Then the petro-physical properties were again recorded. These oil saturated core plugs were thereafter left for aging for three weeks. It has been previously shown that aging from 2, 4 and 8 weeks does not have any major impact on the final oil recovery (Puntervold et al. 2007), so 2 weeks of aging was assumed to be enough for water and oil to reach a near equilibrium state.

The prepared core plug was thereafter used for water flooding. 4 different brines as listed in table 5 were injected into the core plug and the produced fluid was collected in the effluent tubes. Images of the effluent samples were taken for calculating the amount of oil production. Brine samples from effluent tubes were taken for brine concentration analysis using ICP-OES. The oil production volume was thereafter again calculated using the scintillation method for radioactive stearic acid ($CH_3(CH_2)_{16}{}^{14}COOH$) tracers (Sugiharto et al. 2009).

Smart Waterflooding

In the core flooding experiment four different brines have been used as listed in Table 5. Na-Lq1 contained 0.6 m NaCl; this is equivalent to the North Sea water composition, which is presently being injected in the Dan field (Bæk et al. 2013). Thereafter in Na-Lq2 the Na^+ concentration was kept constant and Cl^- ion was replaced with SO_4^{2-} ion. In liquid 3 also the Na^+ concentrations was kept constant and equal proportions of both NaCl and Na_2SO_4 were added. The salinity of liquid was significantly enhanced only for Na-Lq4. Herein a significant fraction of Na_2SO_4 (0.75 mol/l) was added to the existing NaCl solution in Na-Lq1. Na-Lq4 precisely replicates the impact of SO_4^{2-} enriched high saline sea water in SmW-EOR processes. The density and viscosity of these

brines was calculated at room temperature and is reported in Table 6. In this study neither Ca^{2+} nor Mg^{2+} were used; according to the previous study (Austad et al. 2008) no additional oil recovery should be observed on variation in the concentration of Na salts.

Injection Sequence

In the two core flooding experiments the same brines were injected in different sequences. In the first core flooding (core M1X12H) Na-Lq1 was used initially, as it mimics the presently sea water flooded state of the Dan field reservoir. At regular intervals, the flooding was paused thrice for different time intervals and injection of Na-Lq1 was resumed each time. This ensured ample time for kinetics of any possible reaction to take place. 25 PV of Na-Lq1 were injected in total. Subsequently, 15 PV of Na-Lq2 were injected. The flooding with Na-Lq2 was paused once and then resumed. The oil production did not increase after 40 PV of brine injection. Following the same series of injections in the second core plug (M1X10H), first Na-Lq2 was injected. Subsequently Na-Lq3, Na-Lq4 and Na-Lq1 were injected into M1X10H. During each of the brine injections, the water flooding was paused regularly to ensure ample time for kinetics of any possible reaction. Otherwise, the flow rate was kept constant at 0.2 ml/min throughout the waterflood. In both core plugs finally deionized water was injected into the core plug. This is to ensure ejection of any mobile oil that may otherwise remain in the core plug or in the equipment. The flooding test was conducted continuously at 130 $^{\circ}C$ with an axial pressure of 400 bar and a radial pressure of 390 bar. A back pressure of 350 bar was used to rear the formation of air pressure drop across the core plug. The CT-scan of the core plug was also conducted after the flooding was completed to trace any heterogeneity that might have developed (Figure 1).

Chemical analysis

Effluent was collected at constant time intervals using a fractional collector. The effluent samples were analyzed for Na^{+}, Ca^{2+}, Mg^{2+}, SO_4^{2-}, and CO_3^{3-} with ICP-OES acquired from Agilent 7700s.. Each sample was diluted with nitric acid (with 99% purity). Three different dilutions of 10 times, 100 times and 1000 times were performed in order to meet the concentration limit of the equipment for every brine. Each brine analysis was repeated 5 times and more than 95% consistency was achieved in the obtained brine composition. The obtained brine composition at room temperature was used to calculate the brine speciation at reservoir conditions using extended UNIQUAC model. The volume and surface area parameters (r- and q-parameters) are the main model parameters of the Extended UNIQUAC model, which have been previously determined based of massive amounts of binary and ternary experimental data (Thomsen and Rasmussen 1999). Ion specific interaction parameters for ions relevant to smart water core flooding experiments have been extensively optimized (Iliuta et al. 2000; Thomsen et al. 1996; García et al. 2005). The group of ions and neutral species includes H_2O, CO_2, Na^{+}, K^{+}, Mg^{2+}, Ca^{2+}, Ba^{2+}, H^{+}, Sr^{2+}, Cl^{-}, SO_4^{2-}, OH^{-}, CO_3^{2-} and HCO_3^{-}. The two individual parameters are specific to each species. In addition, each species pair has two additional parameters that describe the interaction between the species, which is assumed to have a linear temperature dependency. The model can be used to accurately calculate brine speciation at flooding conditions.

Results:

In Core plug M1X12H Na-Lq1 was first injected for 10.31 PV at a rate of 0.2 ml/min. 62.37% of the OOIP was produced due to the injection of Na-Lq1. 25% of OOIP was produced before the initial water break through (as shown in Figure 2). The axial and radial pressures remained consistent around 400 bar and 390 bar (see supplementary figure 1). Following the initial water break through, the pressure difference across the core plug gradually decreased from 20 bar to 4 bar. Thereafter, the injection of brine was stopped at 10.31 PV for 36.83 hours to ensure adequate period for adsorption or dissolution/attrition of potential ions and salts. The injection of Na-Lq1 was resumed at the same rate of 0.2 ml/min and an additional 2.89% of OOIP was produced within 0.4 PV of brine injection (Figure 2). On further injection, no additional increase in oil recovery was observed. As observable from the results of the ICP-OES analysis in Figure 3, Ca^{2+} and CO_3^{2-} concentrations in the effluent samples also significantly increased after the pause. This indicated that the pause in waterflooding allowed dissolution/attrition of calcite from the core plug. As observable from figure 2, injection of Na-Lq1 was continued for 2.1 PV and no major oil recovery was observed. The brine injection was thereafter stopped at 12.41 PV, for a relatively short period of 16.41 hours. Resumption of Lq1-Na injection led to an additional production of 0.63% of the OOIP within the first 0.5 PV of brine injection. During the same PV the concentration of Ca^{2+} and CO_3^{2-} in the effluent brine also increased (Figure 3). Further continuing injection of 8 PV did not result in any major oil production. A small fraction of oil was continuously produced in the effluent though. An additional 1% of OOIP was produced during this 8 PV of brine injection (Figure 2). Small amounts of Ca^{2+} and CO_3^{2-} ions were released during these 8 PV, but no significant increase in Ca^{2+} or CO_3^{2-} concentration was observed in the effluent brine (Figure 3). Subsequently, the flooding was again stopped for 58.23 mins, to further facilitate dissolution/attrition from the mineral surface. Resumption of Na-Lq1 injection at the same steady rate of 0.2 ml/min showed a significant increase in oil production by 1.46% of the OOIP within the first 0.35PV of brine injection. Calculating the effluent brine concentration during the same period showed a sudden rise in both Ca^{2+} and CO_3^{2-} ions, further indicating dissolution/attrition of calcite mineral. Injection with the same brine was continued for 4.35 PV (i.e. from 20.96 PV to 25.31 PV); no major oil production or calcite dissolution/attrition was observed during this injection. A minor fraction of oil (0.68% of OOIP) was continuously produced. The injection was thereafter stopped for 62.23 hours and a new brine, Na-Lq2 was subsequently injected at the same rate of 0.2 ml/min for 8.62 PV (from 25.52 to 34.21 PVI). The axial and radial pressures remained consistent around 400 bar and 390 bar, and the pressure difference across the core plug also remained consistent around 4 bar. Injection of Na-Lq2 showed a similar trend and an additional 0.76% of OOIP was produced in the first 3.02 PV (i.e. 25.52 to 28.54 PV) with observable dissolution/attrition of calcite. Further continuing injection of Na-Lq2 did not lead to any major oil production and only 0.14% of OOIP was additionally produced. Both amount and rate of oil production for Na-Lq2

was significantly less that that observed during resumption of Lq1-Na injection. No significant amounts of Ca^{2+} or CO_3^{2-} were produced in the effluent. The brine injection was thereafter stopped for 72 hours. Subsequently injection of Na-Lq2 was resumed for 0.52 PV which led to a quick increase in oil production by 0.5% of OOIP within 0.22 PV (Figure 2). After a total injection of 34.8 PV, further injection was stopped twice at quick intervals for 72 hours. Thereafter continuing injection with the same brine for 4.84 PV produced an additional recovery of 1.01% of OOIP. Thereafter further continuing injection did not produce any additional oil recovery. Finally Na-Lq3 was injected into the same core plug for 10 PV at the same rate of 0.2 ml/min but no additional oil recovery was observed. It is possible that most of the displaceable oil had been produced from the core plug. To further analyze the effect of sodium salts in oil production, a similar flooding was continued in a similar reservoir core plug M1X10H.

In Core plug M1X10H first Lq2-Na was injected for 5 PV at a rate of 0.2 ml/min. 41.46 % of the OOIP was produced due to injection of Na-Lq2 brine. 25% of OOIP was produced before initial water break through (Figure 4). The axial and radial pressures remained consistent around 400 bar and 390 bar (Supplementary Figure 2). Following the initial water break through the pressure difference across the core plug gradually decreased from 20 bar to 6 bar. The injection of Na-Lq2 was stopped for 15 hours after 3.99 PVI. Resumption of Lq2-Na injection did not show any major change in oil recovery rate. During injection of Lq2, a nominal fraction of Ca^{2+} was observable in the effluent and no possible dissolution/attrition of calcite is observable from the effluent composition in Figure 5. Thereafter Na-Lq3 was injected in the core plug at the same rate of 0.2 ml/min for 5.35 PV (i.e. from 5.00 to 10.35 PV). The axial and radial pressures remained consistent around 400 bar and 390 bar, and the pressure difference across the core plug also remained consistent around 5.8 bar. During injection of Na-Lq3 a consistent increase in oil recovery was observed and an additional amount of 1.7 % of OOIP was produced (Figure 4). While injecting Lq3, no major increase in Ca^{2+} or CO_3^{2-} was observed in the effluent. Pausing the water flooding also did not lead to any considerable dissolution/attrition of calcite. The injection of Na-Lq3 was stopped for 16 hours after 8.42 PVI. Reinjection of brine Lq3-Na did not show any major change in oil recovery rate. Moreover with Lq3 also no considerable dissolution/attrition of calcite was observed. Subsequently Na-Lq4 was injected in the core plug at the same rate of 0.2 ml/min for 5.21 PV (i.e. from 10.35 to 15.56 PV). The axial and radial pressures remained consistent around 400 bar and 390 bar, and the pressure difference across the core plug also remained consistent around 6 bar (see supplementary figure 2). During initial injection of brine Na-Lq4, no observable major increase in oil recovery is observed. In line with previous brines the injection of Na-Lq4 was stopped for 16 hours after 13.58 PVI. But unlike previous brines, resumption of the injection of brine Na-Lq4 showed an observable increase in the rate of oil production. 0.54% of OOIP was additionally produced during injection of brine Na-Lq4. Along with the increase in oil production (Figure 4) the Ca^{2+} concentration in the effluent also correspondingly increased. Finally, Na-Lq1 was injected into the core plug. The axial and radial pressures did not remain consistent and a noticeable decrease by 3-5 bar was observed on both radial and axial pressures. The pressure difference across the core plug also showed major fluctuations and increase up to 25 bar, which otherwise remained consistent at 6 bar (see supplementary figure 2). During injection of Na-Lq1 a consistent increase in oil recovery was observed and an additional amount of 1.33 % of OOIP was produced. After a total injection of 17.82 PV, further injection was stopped twice at short intervals for 17.75 hours. Thereafter continuing injection with the same brine for 3.08 PV (i.e. from 17.82 to 20.9 PV) produced an additional recovery of 0.57% of OOIP. Na-Lq1 injection into the core plug led to a significantly release of both Ca^{2+} and CO_3^{2-} ions in the effluent (Figure 5). The CT-scan of the core plug after flooding (Figure 1) shows a major fracture in M1X10H. The observed pressure variation (Supplementary Figure 2) and the exceptional release of Ca^{2+} and CO_3^{2-} ions in the effluent (Figure 5) indicate that the fracture may have taken place during Na-Lq1 injection at 18 PVI. Finally, deionized water was injected which did not lead to any additional oil recovery. 44.31% of the OOIP was ultimately recovered.

Discussion:

In previous SmW-EOR studies it has been stated that variation in the concentration of Na salts does not directly influence oil recovery (Austad et al. 2008). Na^+ and Cl^- ions present in the core plug forms electric double layer on calcite surfaces which limit the interaction between potential ions (Ca^{2+}, Mg^{2+} and SO_4^{2-}) and the mineral surface (Puntervold et al. 2009). Removing NaCl is therefore recommended for increasing the efficiency of potential ions in mineral wettability alteration. And it has been proposed that the presence of Ca^{2+} and/or Mg^{2+} is necessary for SO_4^{2-} ions to replace adsorbed carboxyl (polar) from the mineral surface. But in the conducted core flooding experiment neither Mg^{2+} nor Ca^{2+} was injected into the core plug. Variation in NaCl or Na_2SO_4 should not have any effect on the oil recovery. In core plug M1X12H when Na-Lq1 was injected there was no source of SO_4^{2-} ions in the pore space, neither the formation water nor the injected water contained any SO_4^{2-} ions. The XRD analysis also showed that the majority of the core plug was composed of carbonate minerals and no anhydrite was observed. The effluent brine composition also showed a prominent increase in Ca^{2+} and CO_3^{2-} concentration; while no SO_4^{2-} ions was observed during Na-Lq1 flooding (as observable in Figure 3). This shows that the pore space of the chalk core plug M1X12H remained SO_4^{2-} deficient. The presence of SO_4^{2-} ions (along with Ca^{2+} and/or Mg^{2+}) has been termed necessary for SmW-EOR. But in this study, pause and resumption of Na-Lq1 injection shows a consistent increment in oil recovery three consecutive times (with EOR of 5.1% of OOIP), even though no sulphate was present in the injection brine or in the pore space. This clearly shows that divalent cation based SO_4^{2-} adsorption with carboxyl ion desorption (wettability alteration to more water wet state) cannot explain the observed increment in oil recovery. Reinjection (after pause) showed significant increase in Ca^{2+} and CO_3^{2-} concentrations in the effluent (around 9.2 mmol/kg of water in Figure 3). The solubility of calcite at 130 °C and 400 bar was calculated using Extended UNIQUAC model and it was observed that only 0.93 mmol of calcite/kg of water is soluble at the flooding conditions. Therefore the effluent brine composition was significantly beyond the solubility limit of calcite at reservoir/flooding condition. When additional ions (from mineral salts present in the core plug) are produced in the effluent tubes, then these additional ions are assumed to be produced because of dissolution of mineral salts into the pore space (Romanuka et al. 2012). Correspondingly, during analysis these additional ions (ob-

served in effluent) are treated as soluble ions present in the coreplug. Therefore even if dissolution of salts from all pore surfaces (in the coreplug) had concurrently taken place into the corresponding pore space; then also the maximum amount of Ca^{2+} and CO_3^{2-} that would have been released and subsequently been observed in the effluent should be 0.93 mmol/kg of water (i.e. calcite solubility in Na-Lq1 at reservoir condition). But herein we observed that the effluent brine composition (7-9 mmol/kg of water) is significantly beyond the solubility limit (0.093 mmol/kg of water) at reservoir condition. Thus the observed increment in Ca^{2+} and CO_3^{2-} concentration cannot be explained as dissolution of calcite and hence the dissolution of calcite mechanism cannot be used to explain this observed increment in oil recovery.

The observed concentrations of Ca^{2+} and CO_3^{2-} in the effluent (around 9.2 mmol/kg of water) show that insoluble $CaCO_3$ was produced into the pore space from the mineral grain (as neither Ca^{2+} nor CO_3^{2-} was injected into the core plug). This insoluble calcite must be small fine particles as they pass through the small pore throats in the low permeability (0.816 mD) chalk and was observed in the effluent. CT-Scan of M1X12H also shows no major alteration in coreplug heterogeneity. Thus these fines were not released because of a fracture in the core plug (Figure 1). The CT-scan study did not provide enough resolution to distinguish between (mineral contained) grains space volume and (fluid contained) pore space volume. Else the exact location of release of these fine insoluble particles from the core plug could have been identified. This release in calcite fines was observed when ample time was provided for interaction at the mineral surface by pausing the water flood. During Na-Lq1 injection in M1X12H the amount of calcite fines production on reinjection showed direct correlation to the pause interval. The long pauses in water flood of 36.63 (with EOR of 2.89 % of OOIP) and 58.23 (with EOR of 1.46% of OOIP) hours showed corresponding increment in effluent concentration by Ca^{2+}: 9.23 mmol/l; CO_3^{2-}: 6.57 mmol/l and Ca^{2+}: 9.13 mmol/l; CO_3^{2-}: 9.07 mmol/l respectively (Figure 5). While the short pause in brine injection of 16.41 hours (with EOR of 0.63% of OOIP) showed increment in effluent concentration by Ca^{2+}: 6.08 mmol/l; CO_3^{2-}: 4.73 mmol/l. Thus this release of insoluble particles from the mineral grains into the pore space or (mineral attrition) took place during pause in water flooding along with corresponding increment in oil recovery. While during continuous flooding of Na-Lq1 neither any prominent increment in oil recovery was observed nor attrition based fine production was observed. Changing brine composition into Na-lq2 after a long pause of 62.23 hours (with minor EOR: 0.68% of OOIP) led to a minor increment in effluent concentration by Ca^{2+}: 2.81 mmol/l; CO_3^{2-}: 4.78 mmol/l (Figure 5). Thus, a change in brine composition affect both the increment in oil recovery (after pause) and the amount of attrition based fine formation. Pause/reinjection during water flooding in M1X10H with Na-Lq2 and Na-Lq3 showed no increment in oil recovery or attrition based fine formation (as no major increment in effluent Ca^{2+} and CO_3^{2-} concentration was observed). Shifting to Na-lq4 also did not produce any additional oil recovery but on reinjection, (after pause) a noticeable increase in oil production rate with associated calcite attrition was observed (effluent Ca^{2+} concentration: 18.73 mmol/kg of water). This correlation between an increment in oil recovery and the amount of fine formation was also observed after pause and reinjection of Na-Lq4 at 17.8 PVI. This shows that NaCl rich brines like Na-Lq1 and Na-Lq4, both can cause a noticeable increment in the rate of oil production and attrition based fine formation. Na_2SO_4 brines lead to attrition based oil recovery on pause and reinjection, but the amount of oil recovery remains less than that observed with NaCl rich brines like Na-Lq1 and Na-Lq4. Throughout the waterfloods no increase in oil recovery with associated selective decrease in effluent SO_4^{2-} concentration (indicative of SO_4^{2-} adsorption with desorption of carboxyl polar crude oil fraction) was observed. This is contrary to the proposed wettability alteration mechanism (Austad et al. 2008).

This shows that the pause and reinjection strategy for increment in oil production through attrition based fine formation is most evidently observed during Na-Lq1 injection. Further studies are required to document the same.

Conclusion:

SmW-EOR experiments were successfully conducted with chalk core plugs from the Dan field reservoir of the North Sea. The following conclusions were made from the conducted experiments at 130 °C.

- Successful SmW-EOR can be achieved without direct injection of Ca^{2+}, Mg^{2+}, PO_4^{3-} and $B_4O_7^{2-}$. Smart variation in composition of Na salts can result in an increase in oil production.
- Analysis of effluent brines at reservoir conditions show a consistent release of insoluble $CaCO_3$ from the core plugs. This must be a result of attrition of the calcite mineral. The amount of insoluble $CaCO_3$ is directly correlated to the amount of produced oil.
- Multiple pauses and reinjections of Na-Lq1 produced additional 5.1 % of OOIP. Injection of Na-Lq2 did not show any major increment in oil recovery.
- Adsorption of soluble potential ions (with associated desorption of polar carboxyl fraction of oil) was not observed, as there was no measurable decrease in effluent SO_4^{2-} concentration with associated EOR.

Traditionally, increasing the injection rate of brine has been shown to increase the oil production. But this study shows that pausing the waterflood and resuming injection of the same brine can enhance the oil production significantly.

References:

- Akbar, M., Vissapragada, B., Alghamdi, A. H., Allen, D., Herron, M., Carnegie, A., Dutta, D., Olesen J. R., Chourasiya R. D., Logan, D., Stief, D., Netherwood R., Russell S. D., & Saxena, K. (2000). A snapshot of carbonate reservoir evaluation.Oilfield Review, 12(4), 20-21.

- Alagic, E., Spildo, K., Skauge, A., & Solbakken, J. (2011). Effect of crude oil ageing on low salinity and low salinity surfactant flooding. Journal of Petroleum science and Engineering, 78(2), 220-227.
- Alvarado, V., Garcia-Olvera, G., Hoyer, P., & Lehmann, T. E. (2014a, October). Impact of polar components on crude oil-water interfacial film formation: A mechanisms for low-salinity waterflooding. In *SPE Annual Technical Conference and Exhibition*. Society of Petroleum Engineers.
- Alvarado, V., Moradi Bidhendi, M., Garcia-Olvera, G., Morin, B., & Oakey, J. S. (2014b, April). Interfacial Visco-Elasticity of Crude Oil-Brine: An Alternative EOR Mechanism in Smart Waterflooding. In SPE Improved Oil Recovery Symposium. Society of Petroleum Engineers.
- Austad, T., Strand, S., Høgnesen, E. J., & Zhang, P. (2005). Seawater as IOR fluid in fractured chalk. SPE, 93000, 2-4.
- Austad, T., Strand, S., Madland, M. V., Puntervold, T., & Korsnes, R. I. (2008). Seawater in chalk: An EOR and compaction fluid. SPE Reservoir Evaluation & Engineering, 11(04), 648-654.
- Bæk, M., Oil and Gas Production in Denmark 2013 and subsoil use http://www.ens.dk/sites/ens.dk/files/dokumenter/publikationer/downloads/danmarks_olie-_og_gasproduktion_2013_uk.pdf
- Delshad M., Shalabi E. W., and Sepehrnoori K., (2013, April). Mechanisms Behind Low Salinity Water Flooding in Carbonate Reservoirs. In SPE Western Regional & AAPG Pacific Section Meeting 2013 Joint Technical Conference. Society of Petroleum Engineers.
- Fabricius, I. L., Røgen, B., & Gommesen, L. (2007). How depositional texture and diagenesis control petrophysical and elastic properties of samples from five North Sea chalk fields. Petroleum Geoscience, 13(1), 81-95.
- Fan, T., & Buckley, J. S. (2006, January). Acid number measurements revisited. In *SPE/DOE Symposium on Improved Oil Recovery*. Society of Petroleum Engineers.
- Fernø, M. A., Grønsdal, R., Åsheim, J., Nyheim, A., Berge, M., & Graue, A. (2011). Use of Sulfate for Water Based Enhanced Oil Recovery during Spontaneous Imbibition in Chalk. Energy & fuels, 25(4), 1697-1706.
- Fjelde, I. F., & Aasen, S. M. A. (2009, April). Improved spontaneous imbibition of water in reservoir chalks. In 15th European Symposium on Improved Oil Recovery.
- Fogden, A., Kumar, M., Morrow, N. R., & Buckley, J. S. (2011). Mobilization of fine particles during flooding of sandstones and possible relations to enhanced oil recovery. Energy & Fuels, 25(4), 1605-1616.
- García, A. V., Thomsen, K., & Stenby, E. H. (2005). Prediction of mineral scale formation in geothermal and oilfield operations using the extended UNIQUAC model: part I. Sulfate scaling minerals. *Geothermics*, **34** (1), 61-97.
- García, A. V., Thomsen, K., & Stenby, E. H. (2006). Prediction of mineral scale formation in geothermal and oilfield operations using the Extended UNIQUAC model: Part II. Carbonate-scaling minerals. *Geothermics*, **35** (3), 239-284
- Gupta R., Smith G. G., Hu L., Willingham T., Cascio M. L. Shyeh J. J., &Harris C. R. (2011, January). Enhanced Waterflood for Carbonate Reservoirs-Impact of Injection Water Composition. In SPE Middle East Oil and Gas Show and Conference. Society of Petroleum Engineers.
- Gupta, R., Griffin, P., Hu, L., Willingham, T. W., Cascio, M. L., Shyeh, J. J., & Harries, C. R. (2011). Enhanced waterflood for Middle East carbonate cores–impact of injection water composition. *paper SPE, 142668*.
- Iliuta, M. C., Thomsen, K., & Rasmussen, P. (2000). Extended UNIQUAC model for correlation and prediction of vapour–liquid–solid equilibria in aqueous salt systems containing non-electrolytes. Part A. Methanol–water–salt systems. *Chemical Engineering Science*, **55** (14), 2673-2686.
- Jorgensen, L. N. (1992). Dan Field--Denmark Central Graben, Danish North Sea.
- Karoussi, O., & Hamouda, A. A. (2007). Imbibition of sulfate and magnesium ions into carbonate rocks at elevated temperatures and their influence on wettability alteration and oil recovery. Energy & fuels, 21(4), 2138-2146.
- Lebedeva, E. V., and Fogden, A. (2011). Micro-CT and wettability analysis of oil recovery from sand packs and the effect of waterflood salinity and kaolinite.Energy & Fuels, 25 (12), 5683-5694.
- McGuire, P. L., Chatham, J. R., Paskvan, F. K., Sommer, D., & Carini, F. (2005). Low Salinity Oil Recovery: An Exciting New EOR Opportunity for Alaska's North Slope. Paper SPE 93903 presented at the SPE Western Regional Meeting, Irvine, California, 30 March–1 April. dx. doi. org/10.2118/93903-MS.
- Moradi, M., Alvarado, V., & Huzurbazar, S. (2010). Effect of salinity on water-in-crude oil emulsion: evaluation through drop-size distribution proxy. Energy & fuels, 25 (1), 260-268.
- Moradi, M., Topchiy, E., Lehmann, T. E., & Alvarado, V. (2013). Impact of ionic strength on partitioning of naphthenic acids in water–crude oil systems–Determination through high-field NMR spectroscopy. Fuel, 112, 236-248.
- Parracello, V. P., Pizzinelli, C. S., Nobili, M., Masserano, F., Callegaro, C., Caschili, A., & Bartosek, M. (2013, June). Opportunity of enhanced oil recovery low salinity water injection: From experimental work to simulation study up to field pro-

posal. In Proceedings of the 75th EAGE Conference & Exhibition incorporating SPE EUROPEC, Society of Petroleum Engineers, London, United Kingdom.

- Pu H., Yin P., & Morrow N. R. (2010, January). Low-salinity waterflooding and mineral dissolution. In SPE Annual Technical Conference and Exhibition. Society of Petroleum Engineers.
- Puntervold, T., Strand, S., & Austad, T. (2007). Water flooding of carbonate reservoirs: Effects of a model base and natural crude oil bases on chalk wettability. Energy & fuels, 21(3), 1606-1616.
- Puntervold, T., Strand, S., & Austad, T. (2009). Coinjection of seawater and produced water to improve oil recovery from fractured North Sea chalk oil reservoirs. Energy & fuels, 23(5), 2527-2536.
- Robertson, E. P. (2007, January). Low-salinity waterflooding to improve oil recovery-historical field evidence. In SPE Annual Technical Conference and Exhibition. Society of Petroleum Engineers.
- Romanuka, J., Hofman, J., Ligthelm, D. J., Suijkerbuijk, B., Marcelis, F., Oedai, S., & Austad, T. (2012, January). Low salinity EOR in carbonates. In *SPE Improved Oil Recovery Symposium*. Society of Petroleum Engineers.
- Strand, S., Høgnesen, E. J., & Austad, T. (2006). Wettability alteration of carbonates—Effects of potential determining ions (Ca2+ and SO42−) and temperature. Colloids and Surfaces A: Physicochemical and Engineering Aspects, 275(1), 1-10.
- Sugiharto, S., Su'ud, Z., Kurniadi, R., Wibisono, W., & Abidin, Z. (2009). Radiotracer method for residence time distribution study in multiphase flow system. Applied Radiation and isotopes, 67(7), 1445-1448.
- Thomsen, K., Rasmussen, P., & Gani, R. (1996). Correlation and prediction of thermal properties and phase behaviour for a class of aqueous electrolyte systems. *Chemical Engineering Science*, **51** (14), 3675-3683.
- Thomsen, K., Rasmussen, P., & Gani, R. (1996). Correlation and prediction of thermal properties and phase behaviour for a class of aqueous electrolyte systems. *Chemical Engineering Science*, **51** (14), 3675-3683.
- Tweheyo, M. T., Zhang, P., & Austad, T. (2006, January). The effects of temperature and potential determining ions present in seawater on oil recovery from fractured carbonates. In SPE/DOE Symposium on Improved Oil Recovery. Society of Petroleum Engineers.
- Webb, K. J., Black, C. J. J., & Tjetland, G. (2005, November). A laboratory study investigating methods for improving oil recovery in carbonates. InInternational Petroleum Technology Conference. Doha, Qatar: International Petroleum Technology Conference.
- Yildiz, H. O., Valat, M., & Morrow, N. R. (1999). Effect of brine composition on wettability and oil recovery of a Prudhoe Bay crude oil. Journal of Canadian Petroleum Technology, 38 (01).
- Yousef, A. A., Al-Saleh, S. H., Al-Kaabi, A., & Al-Jawfi, M. S. (2011). Laboratory investigation of the impact of injection-water salinity and ionic content on oil recovery from carbonate reservoirs. SPE Reservoir Evaluation & Engineering, 14(05), 578-593.
- Zahid, A., Sandersen, S. B., Stenby, E. H., von Solms, N., & Shapiro, A. (2011). Advanced waterflooding in chalk reservoirs: Understanding of underlying mechanisms. Colloids and Surfaces A: Physicochemical and Engineering Aspects, 389(1), 281-290.
- Zahid, A., Shapiro, A. A., & Skauge, A. (2012a, January). Experimental Studies of Low Salinity Water Flooding Carbonate: A New Promising Approach. In SPE EOR Conference at Oil and Gas West Asia. Society of Petroleum Engineers.
- Zahid, A., Shapiro, A. A., Skauge, A., & Stenby, E. H. (2012b, June). Smart Waterflooding (High Sal/Low Sal) in Carbonate Reservoirs (SPE 154508). In74th EAGE Conference & Exhibition.
- Zahid, A., Stenby, E., & Shapiro, A. (2010, June). Improved Oil Recovery in Chalk–Wettability Alteration or Something Else?(SPE-131300). In 72nd EAGE Conference & Exhibition.
- Zhang, P., & Austad, T. (2006). Wettability and oil recovery from carbonates: Effects of temperature and potential determining ions. Colloids and Surfaces A: Physicochemical and Engineering Aspects, 279(1), 179-187.
- Zhang, P., Tweheyo, M. T., & Austad, T. (2007). Wettability alteration and improved oil recovery by spontaneous imbibition of seawater into chalk: Impact of the potential determining ions Ca2+, Mg2+, and SO42−. Colloids and Surfaces A: Physicochemical and Engineering Aspects, 301(1), 199-208.

Tables:

Table 1: Core plug initial properties

Core plug	Length	Diameter	Porosity	Permeability	Density	Pore Volume
	mm	mm		mD	g/cm^3	cm^3
M1X12H	74.44	38.50	0.26	0.816	2.71	22.56
M1X10H	74.96	38.56	0.25	1.047	2.714	22.2

Table 2: Irreducible water saturation and oil saturation properties

Core plug	S_{wir}	S_o	Specific Surface area	Carbonate
			(m^2/g)	(wt %)
M1X12H	0.083	0.917	0.97	97.8
M1X10H	0.073	0.927	0.97	99.4

Table 3: North Sea crude oil properties

Crude Oil	Acid Number	Base Number	Asphaltene	Viscosity
North Sea	(mg KOH/g oil)	(mg KOH/g oil)	(%)	(cp)
	0.09	2.44	0.3	8.83

Table 4: Recorded weight of core plugs at different stages of water flooding

Weight of core plug (g)	Dry	Water saturated	Oil Saturated	After Flooding
M1X12H	173.89	196.29	193.34	196.90
M1X10H	176.43	198.98	195.79	197.59

Table 5: 4 Different sodium salt combinations used in the water flooding.

mol/Kg H_2O	NaCl	Na_2SO_4	Total Na^+
Na-Lq1	0.6	0.0	0.6
Na-Lq2	0.0	0.3	0.6
Na-Lq3	0.3	0.15	0.6
Na-Lq4	0.6	0.75	2.15

Table 6: Density and viscosity of the injection brines at ambient conditions

Ambient condition	FW	Na-Lq1	Na-Lq2	Na-Lq3	Na-Lq4
Density(g/cm3)	1.0628	1.035	1.042	1.038	1.141
Viscosity (cp)					

Table 7: Sequence of brine injection in the two core plugs

M1X12H	FW	Na-Lq1	Na-Lq2		

M1X10H	FW	Na-Lq2	Na-Lq3	Na-Lq4	Na-Lq1

Figures:

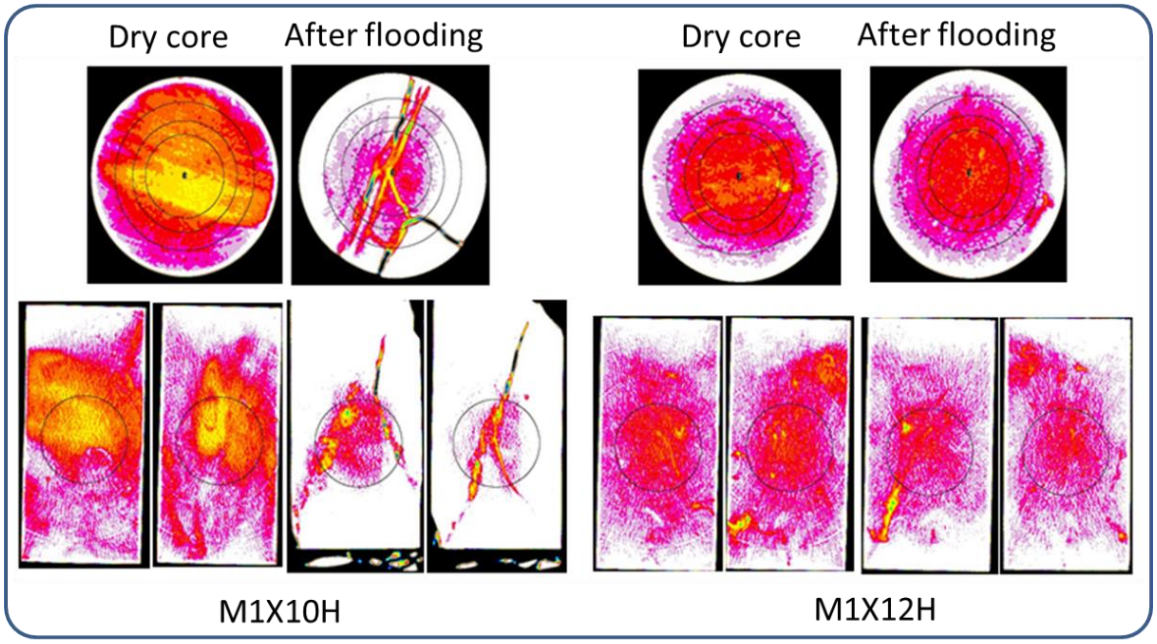


Figure 1: CT-scan of core plug M1X10H and M1X12H for initial dry core and after water flooding. Changes in homogeneity due to possible fracture are clearly observable in M1X10H.

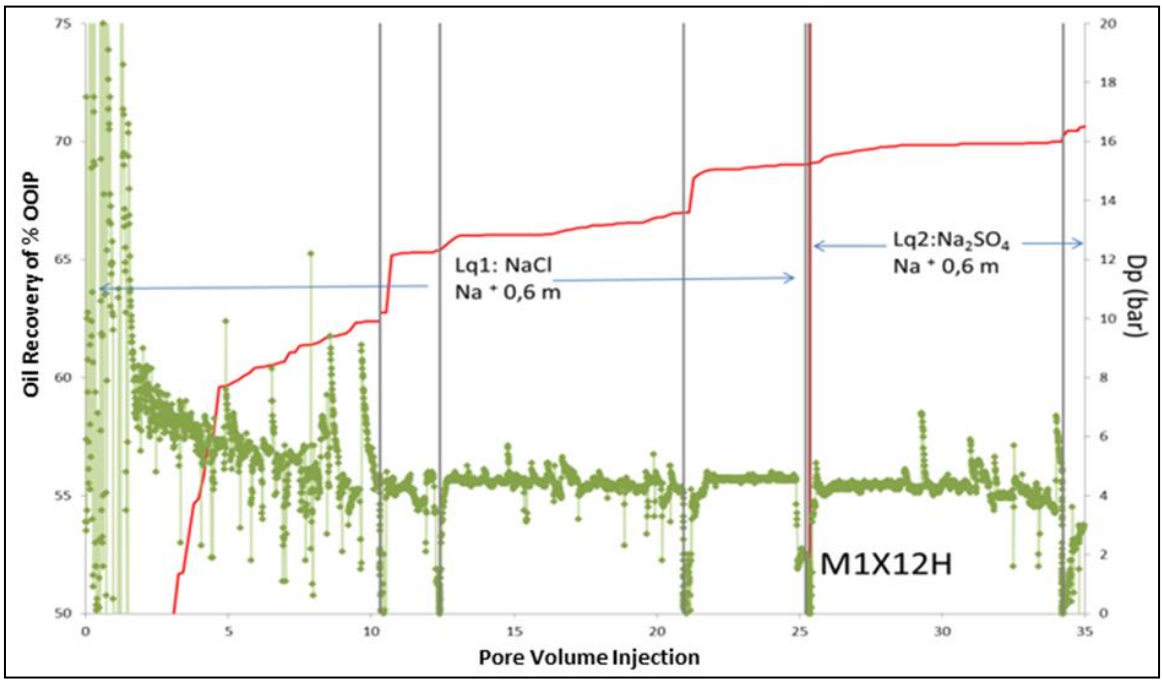


Figure 2: Differential pressure across the core plug and % oil recovery of the OOIP versus PV of brine injected into M1X12H

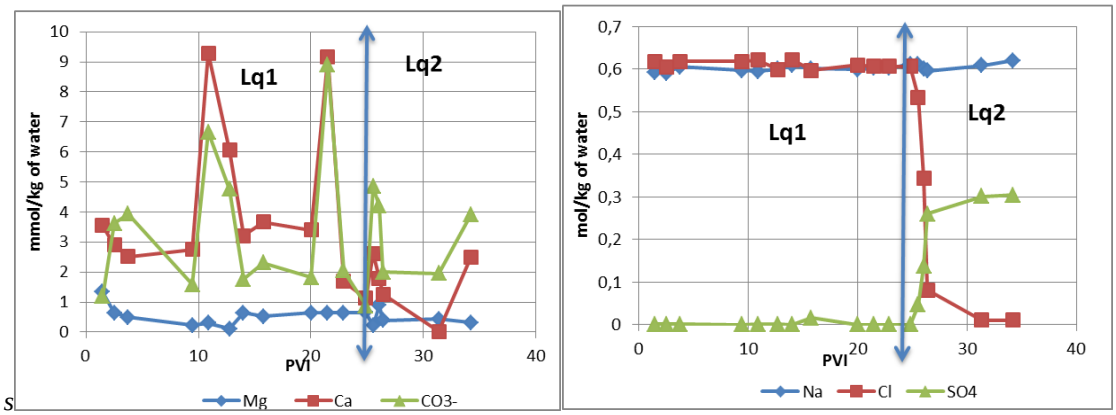


Figure 3: Effluent brine composition for M1X12H obtained by ICP-OES analysis

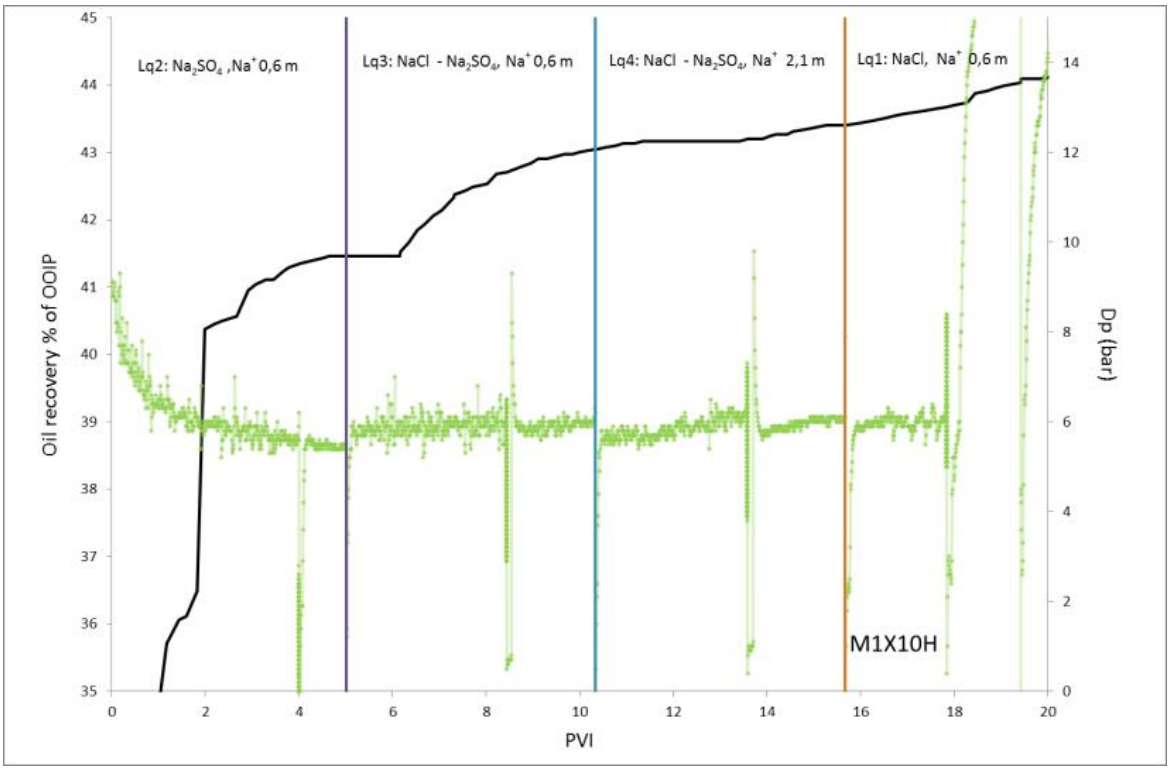


Figure 4: Differential pressure across the core plug and % oil recovery of the OOIP versus PV brine injected into M1X10H

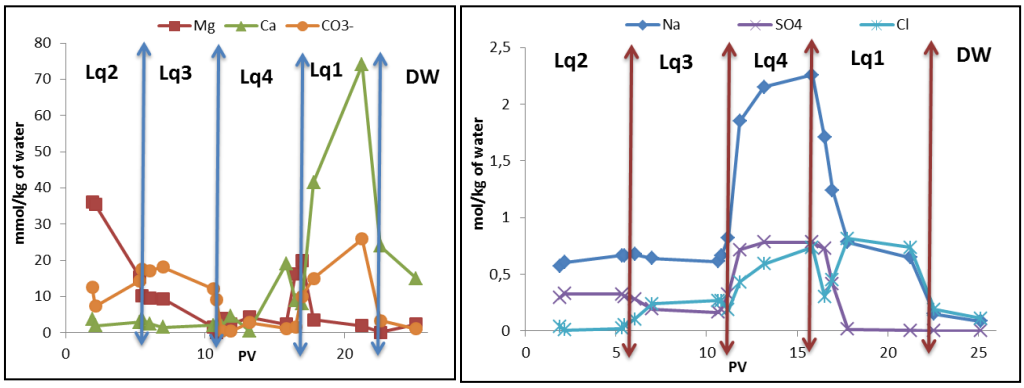
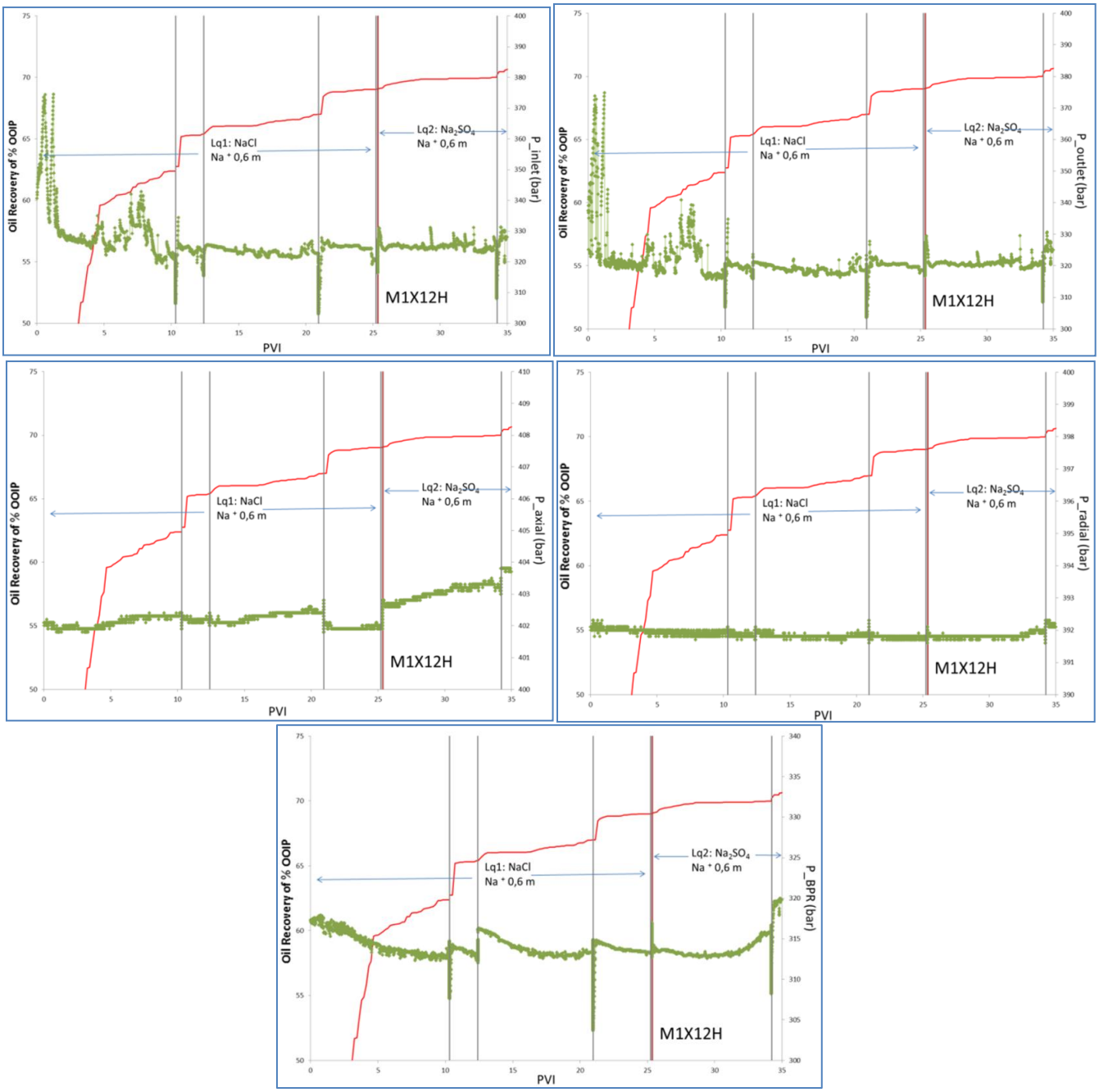
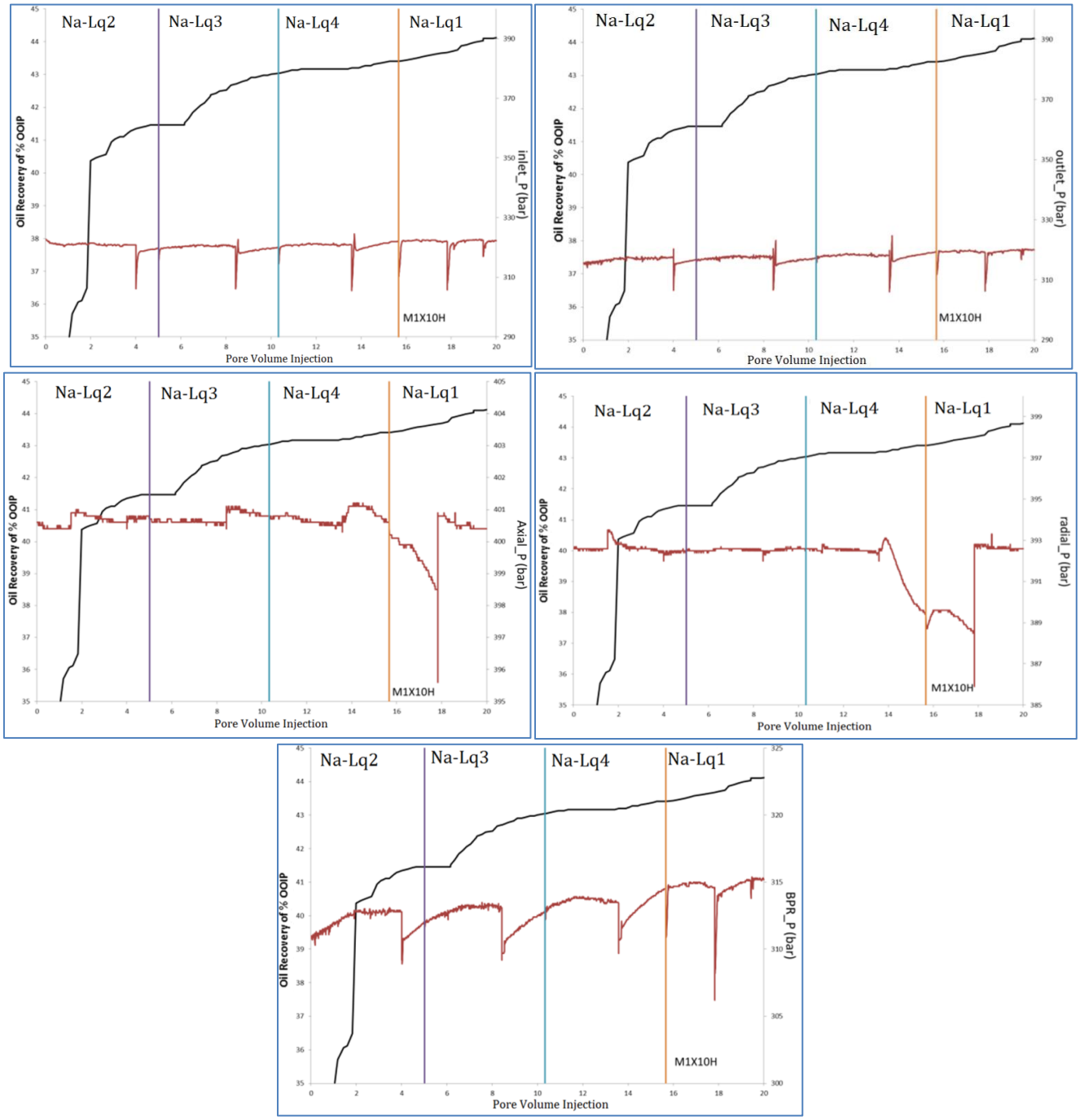


Figure 5: Effluent brine composition for M1X10H obtained by ICP-OES analysis

Supplementary Figure:



Supplementary Figure 1: Inlet, outlet, axial, radial and back pressure across the core plug and % oil recovery of the OOIP versus PV brine injected into M1X12H



Supplementary Figure 2: Inlet, outlet, axial, radial and back pressure across the core plug and % oil recovery of the OOIP versus PV brine injected into M1X10H

Paper XI: Supplementary Information: Condition for use of Liquid Scintillation method in calculating oil volumes

Method:
Liquid scintillation (LSC) method can be used to determine the oil volume by mixing the oil sample with scintillation liquid. The energy of the radioactive decay is then transferred to the scintillation liquid and converted to photons. By counting the photons using a photon multiplier tube (PMT), the activity of radionuclides is measured (L'Annunziata et al., 2012). This is performed in a dedicated scintillation counter. In liquid scintillation counting, molecular species present in the sample interfere with the process of energy transfer generated by the beta particle by pathways that do not involve light emission (chemical quenching). Also, the sample may interfere with light transmission after the conversion of this energy into light by the scintillator if the sample fluoresce or absorb light in the range of the wavelength emitted from the scintillator. This process is known as external or color quenching (Rogers and Moran, 1966).

According L'Annunziata et al., 2012 and Rogers and Moran, 1966, the internal standard method is the most accurate method to compensate for quenching (L'Annunziata et al., 2012; Rogers and Moran, 1966). The internal standard method consists of the following steps for each radioactive crude oil sample:

1. First step is to measure the photon count per minute (CPM) generated for the original samples after scintillation liquid is added.
2. Then the samples are removed from the liquid scintillation analyzer and as an internal standard (IS) a known radionuclide (^{14}C in our case) is added and thoroughly mixed in each sample.
3. For these samples the generated photon count per minute ($CPM_{(st)}$) is recalculated using the PMT. The difference between CPM and $CPM_{(st)}$ reflects the IS under the quenching effect.
4. Dividing this value by actual IS value returns the counting efficiency (CE) factor. CE is an indication of quenching effect. Dividing CPM by CE corrects the effect of quenching on oil radioactive measurements and returns disintegrations per minute (DPM) value.
5. The calculated DPM is linearly correlated with the oil volume in the sample (Figure 1).

$$CPM_{(st)} - CPM = IS_{(quenching)}$$

$$\frac{IS_{(quenching)}}{IS} = CE$$

$$\frac{CPM}{CE} = DPM$$

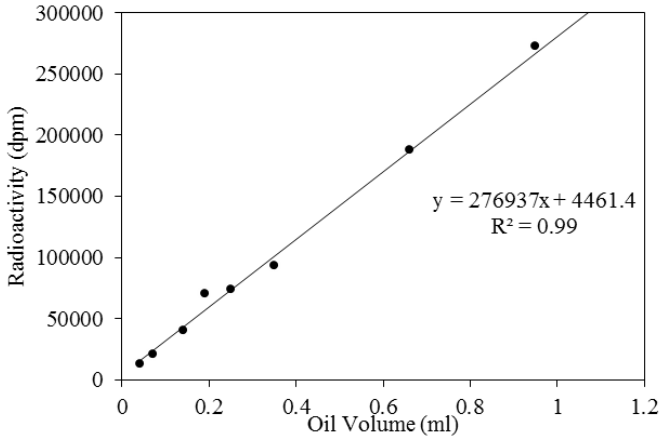


Figure 1: Linear correlation between radioactive DPM and oil volume

Challenges with large oil volumes:
The amount of scintillation liquid should be high enough to include all the radioactive energy. However due to limited room in the liquid containers (Figure 2), limited volume of scintillation liquid can be added to high amounts of oil. Higher amounts of oil

production take place in the early stages of water flooding. In which, a variation in scintillation method is observed in the conducted analysis for smart water flooding. This variation is reflected in the CE (negative) values and consequently on DPM and calculated oil volume. Oil amount decreases in later stages of water flooding, positive values of CE (between 0 and 1) indicates that the scintillation method is reliable for smaller amounts of oil. It brings the question about the threshold by which the LSC method should be used. The following calculations are brought to find out the threshold which is physically logical and is independent of the visual analyses.

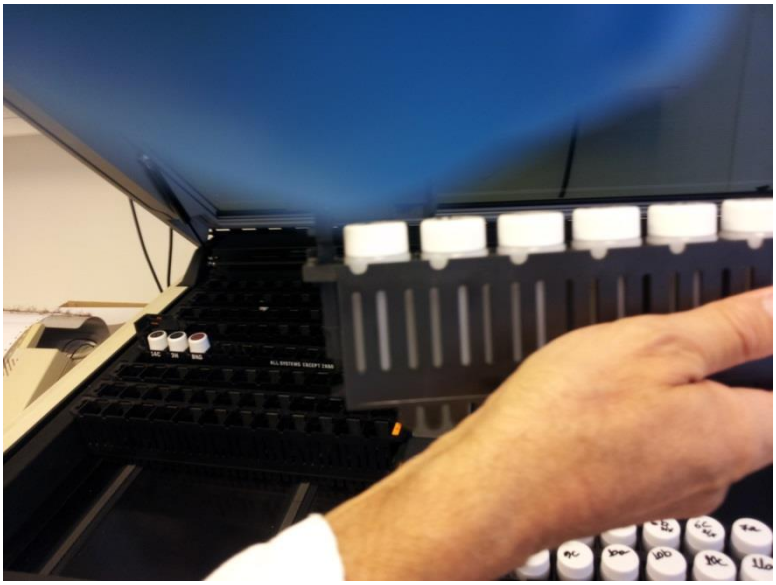


Figure 2: liquid containers in LSC experiments

Solution:
During the experiment equal amount of scintillation liquid is added to the samples in both steps of the experiment. This amount is high enough to include the radioactive radiations from IS. It is assumed that IS radiative emission is the maximum value which can be converted to photons by scintillation liquid. In other words, oil radiation should be less than IS to be completely observable by scintillation liquid.

Both CPM and $CPM_{(st)}$ are affected by quenching and thus they should be compared with the IS measurement under the same quenching condition. In the above stated method it is assumed that the quenching is similar in both experimental steps and both CPM an $CPM_{(st)}$ have the same counting efficiency. Thereafter IS is the difference between $CPM_{(st)}$ and CPM. Its value should be greater than CPM to ensure that all the radiations by oil is converted into photons and observed by the detection tools.

$$\text{Oil radiation} \prec \text{Internal standard}$$

$$CPM \prec CPM_{(st)} - CPM$$

$$\frac{CPM_{(st)} - CPM}{CPM} \succ 1$$

Radioactive data has been previously measured for predetermined volumes of oil. It was then used to establish the standard curve (Figure 1). The error analyses for the available data indicates that absolute error in the oil volume measurement drastically increases when the value of $(CPM_{st} - CPM)/(CPM)$ become less than 1. On the other hand, absolute error for the values higher than 1.47 remain within an acceptable range (Figure 3). Based on the presented results, this method is proposed to investigate the reliability of the LSC method for the available samples. This method investigates if all the emitted oil radioactive data has been detected by the detector. It is independent of any visual analyses and is applicable for all the available samples. LSC is a reliable method for oil volume estimation, using bigger liquid containers and adding more scintillation liquids will enable it to accurately measure higher volumes of oil.

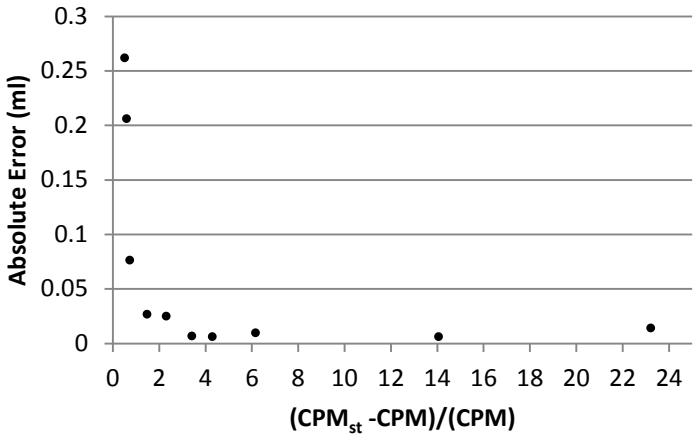


Figure 3: Absolute error in oil volume estimations using scintillation vs. (CPM_{st} -CPM)/(CPM). Absolute error increases significantly for (CPM_{st} -CPM)/(CPM) vales less than 1.47.

Conclusion:

This shows that the experimental error in predicting oil volumes using LSC is dependent on the internal standard and quenching effect due to the dark colored oil. The absolute error in oil volume prediction increases significantly with decrease in (CPM_{st} -CPM)/(CPM) and this error becomes more than 0.05 ml for LSC measurements with (CPM_{st} -CPM)/(CPM) vales of less than 1.47. Image analysis also has a similar error range, therefore for these particular values image analysis is also used for producing cumulative oil recovery plots for conducted water flooding experiments.

References

- L'Annunziata, M. F. (Ed.). (2012). *Handbook of radioactivity analysis*. Academic Press.
- Rogers, A. W., & Moran, J. F. (1966). Evaluation of quench correction in liquid scintillation counting by internal, automatic external, and channels' ratio standardization methods. *Analytical biochemistry*, *16*(2), 206-219.

Paper XII

Effect of pause in brine injection during Smart Water-Enhanced Oil Recovery (SmW-EOR) for low temperature chalks: A case study from North Sea

Chakravarty, K. H., Ahkami, M., Xiarchos, I., Fosbøl, P. L., & Thomsen, K. (2016) Effect of pause in brine injection during Smart Water-Enhanced Oil Recovery (SmW-EOR) for low temperature chalks: A case study from North Sea. ***Journal of Petroleum Science and Engineering*** **(Draft Manuscript: To be submitted)**

Abstract
Smart Water (SmW) flooding has received much attention recently as an Enhanced Oil Recovery (EOR) technique. Experiments have been performed on different formations and crude oils in order to identify the mechanism behind the observed increment in oil recovery. The majority of the studies recommend implementation of SmW-EOR in reservoirs with a temperature greater than 100°C. However, there is enormous potential of increasing oil production in low temperature reservoirs. Development of innovative brines that can lead to successful EOR in low temperature reservoir has received much less attention. This development poses a big challenge, especially for carbonate oil reservoirs.

In this paper, we explore the potential of using SmW as an injection fluid for EOR from low temperature (60°C) carbonate reservoirs. The water flooding experiments showed that SmW-EOR can be successfully implemented for low temperature reservoirs as well. Up to 77.58% of the OOIP can be recovered using innovative SmW-EOR methods. The obtained results show that an additional 17. 8% increase in oil recovery can be obtained by smart alteration of the concentrations of Mg salts combined with the introduction of multiple pauses in water flooding. Contrary to the general belief it was observed that SmW-EOR can be obtained just by varying the concentration of sodium salts. The injection of Mg^{2+} or Ca^{2+} ions is not necessary in all SmW recovery processes. Variation in the concentrations of sodium salts showed an increase in oil recovery by 9.6% of OOIP. Similar variation with magnesium salts with multiple pauses during injection showed an increase in oil recovery by 17.8 and 11.7% of OOIP. Core flooding experiments at 60 °C were compared to previously reported flooding experiments at 130 °C. It was observed that the injection of Na_2SO_4 brine with multiple pauses in water flooding produced an additional 4.4% of OOIP at 60°C compared to that at 130 °C. This observed increment in oil recovery for all 4 flooding campaigns show consistent correlation to attrition based calcite fines formation during reinjection(after pause) of smart water floods.

The results show that multiple pauses based SmW-EOR is a possible injection strategy that can enhance oil production from low temperature reservoirs significantly. Thus fines based SmW-EOR can be potentially considered for implementation in significantly many more oil fields than estimated previously.

Introduction:
Water flooding has been consistently termed the most effective method for recovering oil from various reservoirs. Various benefits of using water floods are: (1) Light to medium gravity oil can be displaced by injection of water; (2) In oil bearing porous networks water can be relatively easily injected; (3) high availability and low cost of water is also a major benefit; and (4) Low initial capital and operating cost makes injection of water economically favorable compared to other EOR methods (Yousef et al. 2012). But consistent water flooding in most carbonate reservoirs often leads to oil production of less than 40% of the original oil in place (OOIP) (Akbar et al. 2001). Thus innovative variation of traditional water flooding is required so that it can increase the recovery fraction from the matured fields. SmW-EOR is a newly developing low cost non–toxic EOR method (Webb et al. 2005; Karoussi et al. 2007; Fjelde et al. 2009; Strand et al. 2006). Through various reports in literature, consensus has been achieved that altering brine composition and salinity can increase the recovery fractions both in sandstone and carbonate reservoirs (Yildiz et al. 1999; Fogden 2011; Lebedeva and Fogden 2011; Gupta et al. 2011; Delshad et al. 2013; Parracello et al. 2013; Robertson, 2007; McGuire et al. 2005; Alagic et al. 2011; Webb et al. 2005; Karoussi et al. 2007; Zhang et al. 2007). Various research groups have recommended different mechanisms to explain the observed increase in oil production for brine variations, but no clear mechanism for this technology has been universally accepted and several extensive investigation programs have been established to understand the scientific basis (Austad et al. 2008; Zahid et al. 2010; Gupta et al. 2011; Alvardo et al. 2014).

A series of meticulous experiments to fundamentally understand this phenomenon has been conducted by Austad and his coworkers (Strand et al. 2006; Zhang et al. 2007; Austad et al. 2008; Zhang et al. 2006; Puntervold et al. 2009). Based on these studies it has been recommended that increased water wetness is achieved by using high concentration of potential ions (including SO_4^{2-}, Ca^{2+} and Mg^{2+}) in the brine solution. SO_4^{2-} ions along with Ca^{2+} and/or Mg^{2+} ions can cause desorption of adsorbed carboxyl groups from the mineral surface, which can in turn increase the residue oil mobility by making the system more water wet. Use of sodium salts are believed to have no direct influence on oil production and sodium ions are termed as non-active ions (Zhang et al. 2007). Reducing their concentration enhances the effectiveness of the potential ions. Moreover, precipitation must be avoided during SmW-EOR as it can choke the core plug and adversely affect the oil production. Collectively in most studies, the importance of soluble Ca^{2+}, Mg^{2+} and SO_4^{2-} ions has been substantiated. A vast fraction of these studies have been conducted with Stevns Klint outcrop cores from Denmark (Austad et al. 2005; Zhang et al. 2006; Puntervold et al. 2009); but similar pattern of oil production has also been observed for Middle East carbonates as well (Strand et al. 2006; Yi and Sarma 2012).

Other experimental studies show fundamental differences to the proposed wettability alteration mechanism (Zahid et al. 2011; Zahid et al. 2012a; Zahid et al. 2012b; Gupta et al. 2011; Alvardo et al. 2014). Observed successful SmW-EOR with SO_4^{2-} enriched brines for completely water wet cores (Zahid et al. 2010) is contrary to the proposed wettability alteration mechanism (Austad et al. 2005). Emulsification of oil and dissolution of rock were suggested to be the possible reasons for the observed EOR in completely water wet systems, but no detailed mechanism was provided. High SO_4^{2-} brines have shown a prominent increase in oil recovery for Stevns Klint outcrops chalks but similar experiments with North Sea reservoir core plugs have shown no additional oil production (Zahid et al. 2011). Spontaneous imbibition experiments using SO_4^{2-} enriched brine have shown no increase in oil recovery for Rørdal chalk (Denmark) and Niobrara chalk (USA) formations. The SO_4^{2-} effect for Stevns Klint chalk

has been shown to be significantly dependent on the initial mineral wettability (Fernø et al. 2011). Imbibition of Niobrara chalk with SO_4^{2-} enriched brine led to increased water wetness but no corresponding increase in oil recovery was observed. This observation remains fundamentally contradictory to the theory of wettability based (Austad et al. 2008) EOR. It has been observed that an increased oil recovery can be obtained in the absence of SO_4^{2-} ions. This also proves that desorption of carboxyl ions following SO_4^{2-} adsorption is not necessarily the fundamental mechanism (Gupta et al. 2011). Further studies have shown that oil emulsions can be formed by a buildup of a viscoelastic interface (Moradi et al. 2011; Moradi et al. 2013; Wang and Alvardo, 2012; Alvarado et al. 2014a). Collectively, wettability alteration (Strand et al. 2006; Zhang et al. 2007; Austad et al. 2005) mineral dissolution (Pu et al. 2010;Yousef et al. 2011), and emulsification (Moradi et al. 2011; Moradi et al. 2013; Wang and Alvarado, 2012; Alvarado et al. 2014b) are different mechanisms that have been proposed to explain this phenomenon of SmW-EOR for carbonates.

This observed increase in oil production for variation in the composition of the injection brine has been consistently reported for high temperature carbonates (typically beyond 100°C) (Yildiz et al. 1999; Fogden 2011; Lebedeva and Fogden 2011; Austad et al. 2008). Experiments have been conducted over a range of temperatures from 70°C to 150°C (Strand et al. 2008). The optimum oil production takes place at 130°C for most recommended brines (Austad et al. 2008; Zahid et al. 2010). But not all oil reservoirs have a temperature of 130°C, and various water flooded low temperature reservoirs exist (Grabowski et al. 2005; Helgeson et al. 1993; Hubert et al. 2012; Nasr-El-Din et al. 2002; Nazina et al. 2013a; Nazina et al. 2013b; Sydansk 1982; Voordouw et al. 1996). And because of economic limitations, the temperature of these reservoirs cannot be altered significantly. Several carbonate oil reservoirs have much lower temperature than the optimal condition for SmW-EOR (Nasr-El-Din et al. 2002; Grabowski et al. 2005; Levitt et al. 2006; Santanna et al. 2009; Hirasaki et al. 2008). These low temperature reservoirs also possess similar challenges as the final oil production remains less than 50% of OOIP (Santanna et al. 2009; Hirasaki et al. 2008).

Injection of SW-3S (i.e. sea water with 3 times SO_4^{2-}) into low temperature (40°C) chalk core plugs has only shown a minor increase of 1% in oil production (Zahid et al. 2010). Thus the injection of the recommended SO_4^{2-} enriched brine at high temperature SmW-EOR (Strand et al. 2008) is not equally efficient in low temperature reservoirs. This further calls for the development of new SmW compositions suitable for increasing oil recovery at low temperature conditions. Previously EOR for low temperature reservoirs have been addressed using surfactant (Hirasaki et al. 2008) and microbes (Brown 2010) injection. These methods have also shown promising results, but SmW-EOR provides the possibility of using unique non-toxic, low cost solution. Analyzing the applicability of SmW-EOR in low temperature reservoirs is therefore important.

In their experiments (Austad et al. 2005; Gupta et al. 2011; Yildiz et al. 1999; Fogden 2011; Fernø et al. 2011) the concentrations of various ions including Ca^{2+}; Mg^{2+}; Ba^{2+}; Na^{+}; K^{+}; SO_4^{2-}; Cl^{-}; PO_4^{3-} and $B_4O_7^{2-}$ have been varied for preparation of different injection brines. All of these injection brines contained a combination of multiple salts; an analysis of the effect of individual salts therefore remains less explored. Water flooding with brines containing specific salts need to be performed in order to evaluate the effect of each salt. The overall aim of the conducted core flooding experiment is to develop a SmW-EOR method for low temperature (60°C) carbonate reservoirs. Four different carbonate core samples from the Gorm field of the Danish North Sea were water flooded. In two core plugs, the individual effect of Na^{+} salts in the absence of Ca^{2+} and Mg^{2+} was analyzed. In two other core plugs, the effect of Mg^{2+} salts in the absence of Na^{+} and Mg^{2+} was analyzed. Pausing and resumption in the injection of the same brine has been shown to increase oil production during low salinity water flooding (Alvarado et al. 2014a). Water flooding with several pauses of different lengths was performed to study the effect of individual ions during pauses in waterfloods. The observed oil production along with the effluent brine composition was used to understand the potential for EOR for low temperature chalk core plugs.

Experimental Details:

Core Plugs

Four chalk core plugs (N3X9H, N3X17V, N3X4H and N3X11H) with similar length and diameter were used in the experiments. All the samples in this study are from the Tor formation of the Gorm field in the Danish North Sea and were provided by Maersk Oil. The core plugs had similar physical properties such as length, diameter, permeability, and porosity. Detailed petrophysical properties of the core plugs are reported in Table 1 and 2. The initial density of the dry core plugs was of the range of 2.68 – 2.71 g/cm^3. The initial porosity of the samples was 36-40%. Unlike standard Stevns Klint outcrop chalk widely used in the literature (Zahid et al. 2010; Strand et al. 2008, Fernø et al. 2011) for SmW-EOR studies, these core plugs where not highly permeable, with average gas permeability of 3.59-4.12 mD. The specific surface was measured by BET analyses, which are 1.41, 0.92, 1.39 and 1.3 m^2/g for N3X9H, N3X17V, N3X4H and N3X11H respectively. All used core plugs appeared homogenous and no major fractures could be observed from the obtained CT-scan analysis of the core plugs (Figure 1-4). Dissolution of dolomite can influence oil production (Austad et al. 2011) so XRD analysis of the core was conducted and it was observed that around 94-97 wt% of the core grains was carbonate and no considerable amount of anhydrite was observed in the chalk samples.

Crude oil

The origin of the oil has been shown to considerably influence the oil/brine interactions (Zahid et al. 2011) and the final oil recovery (Zahid et al. 2010) during smart water studies. Oil originating from the North Sea field was used in the water flooding experiments conducted. This enabled us to mimic reservoir conditions of the North Sea. SARA analysis of the crude oil was conducted; and the crude oil had a viscosity of 8.83 cp and it contained 0.3% of asphaltene. Acid and base numbers were measured by

Metrohm 702 SM Titrino using the method developed by Fan and Buckley (modified version of ASTM D2896 for the base number titration and ASTM D664 for the acid numbers titration). The oil properties are reported in Table 3. Since heavy oil fractions behave differently in water floods (Liu et al. 2006), the fractional carbon content in the oil was analyzed using GC-MS and both the mass fraction and mole fraction corresponding to each carbon number is reported in Figure 5. The GC-MS analysis showed it was a light oil with a very small of heavy oil fraction (C40-C57: 4.46 mole%; C57+: 2.19 mole %). To accurate calculate the quantity of the oil from effluent samples the crude oil was marked by [^{14}C] radio tracer (as previously recommended (Bjørnstad et al. 1994). Radio tracer was provided by Perkin Elmer in the chemical form of stearic acid ($CH_3(CH_2)_{16}{}^{14}COOH$) (Sugiharto et al. 2009). Each one liter of North Sea crude oil was marked by 1.25 ml of solution, containing ^{14}C stearic acid in toluene (7.4 MBq/ml). The doped crude oil was used to saturate the core plugs.

Core preparation

All the four core plugs were CT/scanned in their dry form to determine the variation in heterogeneity or fracture by measuring initial density. They were sequentially flooded with toluene and ethanol to ensure the thorough cleaning of the core plugs. To allow evaporation of the injected fluids the cleaned core plugs were thereafter dried at 90 ºC until a constant weight of the samples was achieved. The initial core properties of the cleaned core plugs were measured and are reported in Table 1 and 4. The core plugs were water flooded with formation water (FW: Na^+:13500; Ca^{2+}:1244; Mg^{2+}:23; K^+:360; Cl^-:18225 mg/l) at 40 ºC with an injection rate of 0.2 ml/min. The weights of the water saturated core plugs were measured and are reported in Table 4. Successively, 5 pore volumes (PV) of crude oil were injected at the rate of 0.2 ml/min to displace the FW in the core plug. The weights of the core plugs with the irreducible water saturation were measured. In order to attain equilibrium brine and oil interaction with the mineral surface, more than 2 weeks of aging was allowed as recommended (Puntervold et al. 2007). The aging temperature has been shown to influence mineral wettability and oil production considerably (Shariatpanahi et al. 2011) so the core plugs where both aged and flooded at 60°C. These aged core plugs were used for the water flooding experiments.

Smart waterflood

Two sets of brines were used in the core flooding experiments (Table 5). The produced fluid was collected in the effluent tubes. The amount of produced oil in each tube was measured by image analysis and by using the liquid scintillation method.

The first brine set was tagged as sodium campaign including: *Na-Lq1*, *Na-Lq2*, *Na-Lq3* and *Na-Lq4*. *Na-Lq1* contained 0.6 m NaCl, which represents the North Sea water composition currently being injected in the Gorm field. Cl^- was substituted by SO_4^{2-} in *Na-Lq2*, while the Na^+ concentration was kept constant. Keeping the Na^+ concentration constant, *Na-Lq3* contained 0.3 m NaCl and 0.15 m Na_2SO_4. *Na- Lq4* was prepared by using high concentration of Na_2SO_4 (0.75 m) and NaCl (0.6 m) to represent the high saline North Sea brine enriched by SO_4^{2-}.

The second brine set is tagged as magnesium campaign including: *Mg/Lq1*, *Mg/Lq2*, *Mg/Lq3*, *Mg/Lq4*, and *Mg/Lq5*. *Mg-Lq1* contained 0.3 m $MgCl_2$ which replicates the impact of Mg^{2+} enriched brine in the absence of SO_4^{2-}. Cl^- was replaced by SO_4^{2-} in *Mg-Lq2*, while the Mg^{2+} concentration was kept constant. *Mg-Lq3* contained $MgCl_2$ (0.3 m) and $MgSO_4$ (0.15 m). Finally, *Mg-Lq4* consisted of $MgCl_2$ (0.3 m) and $MgSO_4$ (0.75 m) which replicates the impact of high concentration of SO_4^{2-} and Mg^{2+}. *d10MgLq1* (0.06 m) represents diluted sea water. Deionized water (DIW) was also injected in both sodium and magnesium campaigns. The density of the discussed brines was measured at room temperature and is shown in Table 6.

The total ion concentration and anion composition of the magnesium campaign was exactly the same as was used in the sodium campaign. As reported in Table 5, the replacement of sodium by magnesium was the only alteration between the two sets of injection brines.

Injection sequence

The four sandstone core plugs were divided into two groups. Each group was water flooded with the same brine set, but with different injection sequences (Table 7). N3X4H and N3X11H were water flooded in the sodium campaign. N3X4H was initially water flooded with *Na-Lq1* for 23.06 (PV) to simulate the reservoir conditions. Pause and resumption of the injection of the same brine has been shown to alter oil production considerably in low salinity water flooding (Alvarado et al. 2014b); Multiple pauses in brine injection were therefore made to study the effect of pausing extensively. Pause lengths from 1 hours to 380 hours were applied at different PVI. Pause and reinjection was continued until no additional oil was recovered with reinjection of *Na-Lq1* brine. Water flooding was followed with *Na-Lq2*, *Na-Lq3*, and *Na-Lq4* for 13.9, 9.36, and 13.41 PV, respectively. Several pauses in water flooding were introduced during each of the three brine injections to study brine specific effects of pause/reinjection during water flooding. In N3X11H the injection sequence was altered and flooding was initiated with *Na-Lq2* for 12.23 PV, with three major pauses in the flooding. The injection was continued with *Na-Lq3* and *Na-Lq4*, and *Na-Lq1* for 14.01, 12.21, 2.87 PV, respectively. Pauses were introduced at regular intervals during the brine injections to study the effect of individual brines on pause in water floods.

N3X17 and N3X9H were water flooded in the magnesium campaign. N3X9H was initially water flooded with *Mg-Lq1* for 20.3 PV with 3 major pauses in the waterflood. Thereafter it was water flooded with *Mg-Lq2*, and *Mg-Lq3* for 19.57, and 8.28 PV, respectively. Flooding was stopped thereafter because of a significant increase in injection and differential pressures. The pressure increase was related to clogging associated with debris from corrosion on the purge valve in the injection line. In N3X17V the

injection sequence was altered and flooding was initiated with *Mg-Lq2* for 24.37 PV, thereafter *Mg-Lq3, Mg-Lq4*, and *Mg-Lq1* were injected for 8.28, 15.15 and 13.68 PV. Finally deionized water was injected for 11.33 PV to produce ions that may have formed electric double layers on the mineral surface. Throughout the experiments, the flooding was paused at regular intervals to provide sufficient time for crude oil – brine – rock interactions. All the experiments were conducted at 60 °C with a radial pressure of 390 bar, an axial pressure of 400 bar, and a back pressure of 300 bar to simulate the reservoir condition. Core plugs weight and CT-scan images were recorded after flooding to distinguish any possible modification in core properties (Detailed data are presented in Table 4 and Figure 1-4).

Chemical Analysis

Collected effluents were analyzed with ICP-OES acquired from Agilent 7700s. Nitric acid was used to dilute the samples for 10, 100, and 1000 times to determine the concentration limit of the equipment. The brines were analyzed for 5 times to ensure the consistency of the experiments. The brine compositions were determined with more than 95% consistency. Concentrations of various relevant ions including Na^+, Ca^{2+}, Mg^{2+}, SO_4^{2-}, CO_3^{3-} were determined at constant intervals in PVI. The effluent concentrations are reported for the four core plugs in Figures 6-9.

Results and Discussion

N3X4H core plug

To mimic the water flooding condition after injection of sea water N3X4H was initially flooded with *Na-Lq1* for 23.6 PVI. The oil recovery profile is plotted in Figure 10 and a detailed pressure profile is reported in Supplementary Figure 1. After production of 40.78% of OOIP in 1.25 PVI, the production rate decreased considerably for the following 0.6 PVI of brine injection and no observable oil was produced. The water flooding with *Na-Lq1* was correspondingly paused and resumed after 43 hrs. Reinjection (after pause) considerably increased the production rate. A 24% increase of OOIP produced was observed over 2.6 PVI (from 1.7 to 4.3 PVI) of *Na-Lq1* injection. In the effluent brine (as observable in figure 6) 68.47 mmol/kg of Ca per Kg of water and 49.41 mmol/kg of CO_3^{2-} per kg of water was produced on reinjection of *Na-Lq1* at 3.1 PVI. This shows that pause/ reinjection of brine led to release of $CaCO_3$ from the calcite from the mineral surface. The solubility of $CaCO_3$ in *Na-Lq1* was also calculated using Extended UNIQUAC model and it was observed that only 0.78 mmol/kg water is soluble at the flooding conditions (60°C and 400 bar). Thus the additional Ca^{2+} stemmed from attrition and not from dissolution of $CaCO_3$ from the mineral surface. Additional oil production following the pause was associated with the release of insoluble fine calcite particles by attrition of the mineral surface. Further brine injection led to a decrease in rate of oil production for 0.8 PVI (from 4.3 to 5.1 PVI). At 4.9 PVI the effluent brine composition was analyzed and it was observed that the Ca^{2+} and CO_3^{2-} concentration 0.65 and 0.49 mmol/kg of water respectively. The Ca^{2+} and CO_3^{2-} concentrations were within the calcite solubility limit of 0.78 mmol/kg water (at flooding conditions of 60°C and 400 bar as calculated from Extended UNIQUAC model). Thus, no attrition and production of fines was taking place during continued injection Na-*Lq1* between 4.3 and 5.1 PVI. The observed Ca^{2+} and CO_3^{2-} concentrations during reinjection after pause was considerably greater (with Ca: 56.19 mmol/kg and CO_3^{2-} 40.15 mmol/kg). Thus, after the pause, an initial increment in oil recovery and in fines production was observed, but after additional flooding, a decrease in fine production and in oil production rate was observed.

Since the production rate had considerably decreased, the flooding was paused for 18 hours and *Na-Lq1* was reinjected. Reinjection led to a quick increase in brine production of 1.6 % of OOIP in 0.5 PVI (from 5.1 to 5.6 PVI). At 5.3 PVI the effluent brine composition was analyzed and it was observed that the Ca^{2+} and CO_3^{2-} concentration was 50.5 and 41.5 mmol/kg of water respectively; which was significantly beyond the calcite solubility limits. Thus during reinjection (following the 18 hours pause) both oil and fine production considerably increased. But production rate dropped on further brine injection for 1.4 PVI. The effluent brine at 6.01 PVI produced 0.88 and 0.54 mmol/l of Ca^{2+} and CO_3^{2-}. This indicated that there was no additional calcite fines production during continued injection.

On observing an increment in oil recovery, the subsequent pause length was increased to 73 hrs. Reinjection led to an additional oil production of 6.61% of OOIP over 1.6 PVI. Thereafter, the rate of oil production declined again and an 18 hours pause (at 9.1 PVI) was made. During the high oil production the effluent concentration (at 7.06 PVI) of Ca^{2+} and CO_3^{2-} was 78.7 and 64.17 mmol/kg respectively. Further continued injection again decreased the effluent Ca^{2+} and CO_3^{2-} concentration to 2.08 and 1.55 mmol/l. This indicated that fines and oil production are only observed for a short time after a pause in the water flood. Subsequent brine injection after (the 18 hours pause) led to oil production of 3.69% of OOIP in 2.38 PVI. Further continued flooding did not produce any noticeable additional oil recovery. Again, fines production because of mineral attrition (Ca^{2+}: 22.1 mmol/l and CO_3^{2-} 15.9 mmol/l) was found associated with an increment in oil recovery at 9.52 PVI. At 10.05 PVI neither oil production nor attrition of fines (Ca^{2+}: 0.93 mmol/l and CO_3^{2-} 0.52 mmol/l) was observed.

Several pauses of varied intervals including; 79 hours (at 14.02 PVI); 3.1 hours (at 16.27 PVI); 10 hours (at 18.83 PVI); 382 hours (at 21.11 PVI) and 90 hours (at 23.25 PVI) were introduced to further increase the oil production. But varied pause lengths from 3.5 hours to 382 hours and continued reinjection of *Na-Lq1* did not produce any additional oil recovery. Thus pause/reinjection led to production of 77.58% of OOIP in 11.63 PVI and 7 pauses of varied intervals. Five pauses/reinjections of varied lengths over the following 12 PVI (11.6 to 23.6 PVI) did not produce any additional oil recovery. Reinjection of brine at 14.16 PVI showed mineral attrition (Ca^{2+}: 34.5 mmol/l and CO_3^{2-} 23.2 mmol/l) but no increment in oil recovery was observed. Since a considerable

fraction of oil (77.58% of OOIP) had already been produced from the core plug, no increment in oil recovery after fines formation could be observed. This can be associated with the lack of available residue oil in the flooded region.

Subsequently, the experiment was continued with the injection of *Na-Lq2*. Seven pauses of different lengths (17 hours to 376 hours) were introduced to explore the effect of pause between brine injections. No additional oil was observed after 13.9 PV (from 23.6 to 38.5 PVI) of injection. During brine alteration also an increment in effluent Ca^{2+} and CO_3^{2-} concentration was observed (Ca^{2+}: 40.25 mmol/l and CO_3^{2-} 22.3 mmol/l). Lack of availability of residue oil could be the associated reason for not observing an increment in oil recovery after fines production. The effluent brine composition through the different pauses in brine injection was also recorded (figure 6), but no considerable additional calcite was produced. Thus in the associated pauses with water flooding using *Na-Lq2* neither oil production nor attrition based fine formation was observed.

Thereafter the third Na brine (*Na-Lq3*) was injected into the core plug. Two pauses (19.3 hours at 40.3 PVI and 12 hours at 43.3 PVI) and reinjection of *Na-Lq3* was performed while flooding was continued 9.3 PV (from 38.5 to 47.8 PVI). No additional oil production was observed due to brine change or pause in brine injection. Furthermore the effluent brine showed no increment in Ca^{2+} and CO_3^{2-} concentration; thus indicating no more attrition based fine formation took place during these pauses. Finally, *Na-Lq4* was injected for 13.41 PV. No additional oil was observed in this step. At 49.6 PVI an increment in effluent Ca^{2+} and CO_3^{2-} concentration was observed (Ca^{2+}: 50.75 mmol/l and CO_3^{2-} 28.14 mmol/l) indicating attrition.

This core flooding experiment shows that pause and resumption of injection can cause increments in oil recovery. The additional oil production could be caused by attrition based calcite fine formation. Multiple pauses in brine injection can considerably increase the oil production with use of different sodium salts. Furthermore, a consistent correlation between fines formation and oil recovery has been observed through core flooding.

N3X11H core plug

N3X11H was initially flooded with *Na-Lq2* to investigate the initial oil recovery with sodium sulfate. The oil recovery profile is plotted in Figure 11 and a detailed pressure profile is reported in Supplementary Figure 2, while the effluent brine composition is shown in figure 7. Herein *Na-Lq2* was injected for 12.23 PV and oil recovery was stabilized after 3.4 PVI at 55.68% of OOIP. In N3X4H several pauses/reinjections led to no oil production for further brine injection. So in this case only three pauses/reinjections were introduced at regular intervals when the oil production rate had considerably decreased and no visible noticeable oil was produced for over 2 PVI of brine injection. The first pause of 24 hours at 6.5 PVI led to an oil production of 0.5% of OOIP in the subsequent 0.6 PVI of brine injection. Because of the insignificant amount of oil produced after 24 hours of pause, the length of the second pause was increased to 95 hrs. Reinjection of *Na-Lq2* led to increment in OOIP by 2.13% over 1 PVI (10 PVI to 11 PVI). The third pause of 111hrs was held at 12.23 PV and thereafter *Na-Lq3* was injected, which led to an increment in oil production of 1.91 % OOIP over 1.2 PVI (from 12.2 PVI to 13.4 PVI). Reinjection after the three pauses led to a considerable increment in calcite concentration in the effluent. After Pause 1 at 7.09 PVI the concentrations were Ca^{2+}: 35.6 mmol/l and CO_3^{2-}: 15.5 mmol/l. After Pause 2 at 10.63 PVI the concentrations were Ca^{2+}: 61.33 mmol/l and CO_3^{2-}: 29.35 mmol/l. After Pause 3 at 12.65 PVI the concentrations were Ca^{2+}: 71.67 mmol/l and CO_3^{2-}: 36.30 mmol/l. The solubility of $CaCO_3$ in *Na-Lq2* and *Na-Lq3* was calculated using Extended UNIQUAC model and it was observed that at the flooding conditions (60°C and 400 bar) only 0.98 mmol Ca^{2+} and 0.88 mmol CO_3^{2-} per kg water is soluble. This indicates that the increment in oil recovery in each of the three pauses was assisted by the attrition of calcite and production of fines during the corresponding PVI of water flooding into the core plugs. The Ca^{2+} and CO_3^{2-} concentrations for all other effluent samples during continued flooding of *Na-Lq2* were around 1-0.2 mmol/l. Thus no major attrition based fine formation took place during continued water flooding. This indicates that the attrition of calcite and production of fines was only observed after pause/reinjection of flooding water into the core plugs. With *Na-Lq3,* a 1 hours pause was introduced at 19.28 PVI, which led to a minor oil production of 0.5% of OOIP. The effluent brine analysis showed that again fine production because of mineral attrition (Ca^{2+}: 12.1 mmol/l and CO_3^{2-} 10.6 mmol/l) was associated with the increment in oil recovery at 19.43 PVI.

Thereafter *Na-Lq3* was replaced by *Na-Lq4* following a pause of 3.1 hours at 26.42 PVI. Waterflooding over 2 PV (after the pause) led to additional oil production of 0.3% of OOIP. At 26.65 PVI the effluent concentration was Ca^{2+}: 35.98 mmol/l and CO_3^{2-} 25.55 mmol/l; while according to the Extended UNIQUAC model the calcite solubility in *Na-Lq4* at flooding conditions was found to be 1.82 mmol/l. This indicates that attrition based fines production was also observed during increment in oil recovery after pause and injection of *Na-Lq4*. Finally *Na-Lq1* was injected for 2.87 PVI and no additional oil production was observed.

These core flooding experiments showed that various alterations in composition of sodium salts can cause an increase in oil production. The increment in oil production after a pause does not seem to be specific for any particular brine composition. The increment in oil recovery observed with *Na-Lq1* in N3X4H was actually considerably greater (24% of OOIP after 43 hours pause) than that observed with other brine combinations. This could be a coincidence. Subsequently it was observed that pauses in water flooding decreases the differential pressure across the core plug as observable in Figure 10. Subsequent reinjection again establishes the differential pressure across the core plugs ensuring a consistent flow through pore space. Thus, a pause in water flooding causes an alteration in core plug differential pressure (as observable in figure 10). To distinguish the effect of pause in waterflooding from variations in differential pressure, the inlet pressure was selectively reduced thrice (at 32.17, 35.27 and 38.47 PVI) for N3X11H. The obtained differential pressure profile mimics the observed pattern during various pauses. But these variation in inlet

pressure profile for both *Na-Lq4* (at 32.17 and 35.27 PVI) and *Na-Lq1* (at 38.47 PVI) did not produce any additional oil recovery. This further indicated that the increase in oil recovery observed should be correlated to the length of the pauses and not just to the associated pressure variations. The effluent brine concentration during these pressure variations at 32.34, 35.91 and 38.91 PVI was also calculated. No fines formation or major increment in Ca^{2+} and CO_3^{2-} concentrations was observed. This further shows that both attrition based fines formation and increment in oil production should be correlated to the pause in water floods and not the corresponding pressure variations.

N3X9H Core plug

First injection step for N3X9H was injection of *Mg-Lq1* (Table 5). It was injected for 20.1 PVI and oil recovery was stabilized at 53.75% after 2.8 PVI. The oil recovery profile is plotted in Figure 12 and a detailed pressure profile is reported in Supplementary Figure 3, while the effluent brine composition is shown in figure 8. During initial brine injection for 1.5 PV a considerable amounts (53.7 mmol/kg of water) of Ca^{2+} was produced in the effluent. Although 300 mmol Mg^{2+}/kg of water were injected, the effluent Mg^{2+} concentration was considerably lower. This indicates that Mg^{2+}/Ca^{2+} ion substitution took place on injection of Mg containing brine into the core plugs (as previously discussed (Austad et al. 2008)). But after 1.5 PV of brine injection, the Ca^{2+} concentration in the effluent decreased significantly to less than 14.18mmol/kg. This indicates that further injection (beyond 1.5 PV) did not lead to further ion substitution. The increment in effluent Ca^{2+} concentration during the first 1.5 PVI of brine injection cannot be associated with mineral attrition because herein no associated upsurge in CO_3^{2-} concentration was recorded (as the CO_3^{2-} concentration remained less than 1 mmol/kg).

With the continuation of flooding three pauses were held. At 9.46 PVI a 122hrs pause was introduced and reinjection of *Mg-Lq1* led to an increment in oil production by 2.6% of OOIP in the following 1.5 PVI. A second pause of 627 hours was held at 17.25 PVI. This pause led to an increase in oil production by 1.81% in the succeeding 0.75 PVI. The third pause was 16 hours at 20.08 PVI, but on reinjection no additional oil recovery was seen. Reinjection after the first two pauses led to a considerable increment in calcite concentration in the effluent: After Pause 1 at 9.61 PVI the concentrations were: Ca^{2+}:81.4 mmol/l and CO_3^{2-}: 29.6 mmol/l. After Pause 2 at 17.31 PVI the concentrations were: Ca^{2+}:21.56 mmol/l and CO_3^{2-}: 18.24 mmol/l. After Pause 3 at 20.14 PVI there was no major increment in Ca^{2+} and CO_3^{2-} concentrations (Ca^{2+}:1.43 mmol/l and CO_3^{2-}: 0.65 mmol/l). The solubility of calcite in *Mg-Lq1* was also calculated at the flooding conditions of 60°C and 400 bar and it was observed that only 0.3 mmol/kg was soluble. Thus, the produced brine at flooding conditions contained a significant fraction of insoluble fines released from the core plug. Majority of the attrition based fines formation took place only after pause and reinjection of *Mg-Lq1* as the effluent CO_3^{2-} concentration at other times remained less than 1 mmol/kg. Reinjection of brine after first (at 9.46 PVI) and second pause (at 17.25 PVI) pause in water flooding also showed a decrease in Mg^{2+} concentration in the effluent; thus indicating a fraction of the increment in Ca^{2+} concentration is associated with ion substitution at the calcite surface.

Afterwards, *Mg-Lq2* was injected for 20.01 PVI (from 20.08 to 40.09 PVI) with three pauses during flooding. A small pause of 5 hours led to a minute increment in oil production by 0.1% of OOIP in the following 0.3 PVI. Thereafter, a second pause of 14.7 hours was held. This led to a noticeable increment in oil production by 1.68% of OOIP during the next 2.5 PVI (from 29.4 to 31.9). Finally a pause of 58 hours in brine injection was introduced at 35.21 PV, which led to an increment in oil production of 0.9% of OOIP in 1.5 PVI. The solubility of $CaCO_3$ in Mg-*Lq2* was also calculated using Extended UNIQUAC model and it was observed that at the flooding conditions (60°C and 400 bar) only 0.03mmol/kg was water soluble. So, the second pause of 14.7 hours was associated with attrition based fines formation; as effluent concentration was increased to 31.35 mmol/kg for Ca^{2+} and 8.12 mmol/kg for CO_3^{2-} while calcite solubility is 0.03 mmol/kg of water for *Mg-Lq2*. The third pause at 35.21 PVI for 58 hours was also associated with attrition of calcite as effluent brine concentration was Ca^{2+}: 40.56 mmol/l and CO_3^{2-}: 19.54 mmol/l. No major increase in effluent Ca^{2+} and CO_3^{2-} concentrations was observed on reinjection after the initial small pause of 5 hours at 25.1 PVI. Thus attrition based fine formation and increment in oil recovery was observed only for second and the third pause in water flooding with *Mg-Lq2*; while the first pause showed neither increment in oil recovery nor any attrition based fine production. Reinjection of brine after second and third pause in waterfloods also showed a decrease in Mg^{2+} concentration in the effluent; thus indicating a fraction of the increment in Ca^{2+} concentration is associated with ion substitution from the calcite surface. During continuous flooding between 25.1 PVI and 29.6 PVI, the effluent Ca^{2+} concentration remained less than 1 mmol/kg, indicating no Mg^{2+}/Ca^{2+} ion substitution. Thus ion substitution only took place when the water flooding was paused. During reinjection, a decrease in Mg^{2+} with corresponding increase in Ca^{2+} is observable. Finally *Mg-Lq3* was injected after a pause of 16 hours but no additional oil production was observed. Due to debris from corrosion on the purge valve in the injection line at 42.51 PVI, the inlet pressure and the differential pressure increased considerably. Flooding was subsequently stopped at 48.43 PVI; and no additional oil recovery or fine production was observed during this period.

This coreflooding experiment further shows that attrition based fines formation is well correlated to the amount of oil recovery for magnesium salts as well. An increment in oil production by 10.6% of OOIP can be observed during injection of magnesium brines of varying composition with repeated pauses and resumptions of brine injection. Furthermore, two types of ion substitution were observed.

1. For the initial 1.5 PVI, ion substitution is observed during continuous flooding, which corresponds to 0.92 monolayers of mineral Ca^{2+} release into the effluent. The formation water contained 1244 mg/l of Ca^{2+}; so it is possible that a layer of Ca^{2+} got adsorbed on the mineral surface. And on injection of Mg^{2+} containing brine these adsorbed Ca^{2+} ions (from the

calcite surface) may have been replaced by Mg^{2+} ions. Thus only adsorption (of Mg^{2+}) and desorption (of Ca^{2+}) of ions took place. The mineral crystal lattice remained unaltered (as shown in through DFT calculations (Chakravarty et al. 2015)).

2. Furthermore, during all four major pauses and reinjections, a consistent increase in Ca^{2+} concentration and a corresponding decrease in effluent Mg^{2+} concentration, compared to the concentrations of the injected brine, was observed. Thus, additional ion substitution did take place. Continued flooding before and after these pauses did not show such variation in effluent composition. This shows that ion substitution only took place when ample time was provided for the brine to replace Ca^{2+} from the mineral. Throughout the water flood, no Ca^{2+} ions were injected and already 0.92 monolayer of mineral surface adsorbed Ca^{2+} was produced during the initial 1.5 PV of brine injection. Thus, this additional Mg^{2+}/Ca^{2+} ion substitution must have taken place on the crystal lattice leading to the formation of dolomite (as discussed based on previous experiments (Austad et al. 2008) and shown through DFT calculations (Karimi et al. 2015). The brine concentrations of all effluent vials were not analyzed, but the available data shows that at least 2.41 monolayers of calcite was replaced totally during the different pauses in water floods.

Thus ion substitution can take place both from the adsorbed ions on the mineral surface and by alteration in the calcite crystal lattice. The rate of brine injection plays a dominant role in both of the processes.

N3X17V Core plug

The N3X17V core plug was water flooded in the magnesium campaign starting with injection of *Mg-Lq2* for 23.06 PV. The oil recovery profile is plotted in Figure 13 and a detailed pressure profile is reported in Supplementary Figure 3, while the effluent brine composition is shown in figure 9. After the initial water breakthrough and 54.1% (of OOIP) oil production, the rate of oil production started decreasing. The effluent brine contained 53.48 mmol of Ca^{2+} per kg of water for 1.3 PVI of brine injection. This indicated Mg^{2+}/Ca^{2+} substitution, as a corresponding decrease in effluent Mg^{2+} concentration was also observed. Subsequently, brine injection was paused for 13 hours to allow further attrition of $CaCO_3$ and Mg^{2+}/Ca^{2+} ion substitution to take place on the mineral surface. Reinjection of *Mg-Lq2* led to an additional 2.5% of OOIP in 1.3 PV. A decline in production rate was thereafter observed and no major oil production was observed for the subsequent 8 PV of brine injection. During reinjection, the effluent Ca^{2+} concentration was 42.3 mmol/kg of water, the Mg concentration also decreased compared to the injection concentration from 0.3mol/kg to 0.27mol/kg. Thus both calcite attrition and dolomite formation (because of Mg^{2+}/Ca^{2+} lattice substitution) must have taken place during the pause in brine injection. The effluent Ca^{2+} concentration during the 8 PV of brine injection (with no major oil production) was 2.34mmol/kg while the Mg^{2+} concentration was 0.3mol/kg. During continuous brine injection, there was neither any attrition of calcite nor any ions substitution from the mineral lattice taking place. Consequently, a second pause of 125 hours was introduced at 15.4 PV; reinjection of *Mg-Lq2* led significant increase in oil recovery by 3.8% of OOIP within 1.4 PVI. The effluent concentrations were Ca^{2+}: 42.83 mmol/kg and Mg^{2+}: 0.274mol/kg. The effluent Ca^{2+} concentration was significantly above the calcite solubility limit for *Mg-Lq2* (which is 0.03mmol/kg at the flooding conditions). This indicates that both calcite attrition and dolomite formation (because of Mg^{2+}/Ca^{2+} lattice substitution) must have taken place during the pause in brine injection. Continued brine injection further diminished the effluent Ca^{2+} concentration to 3.86 mmol/kg. The third pause of 49 hours was introduced at 21.6 PVI. In the following reinjection for 2.9 PVI, 4.35 % OOIP was produced. Injection was continued after 645 hours pause, by injecting *Mg-Lq3* for 8.28 PV; which initially produced 1.6% OOIP within 1.8 PVI. The corresponding effluent brine showed significant attrition (Ca^{2+}: 43.56 mmol/kg and CO_3^{2-} mmol/kg) which is far above the solubility limit of calcite. The Mg^{2+} concentration in the effluent brine during reinjection was 32.7 mmol/kg of water less than the injected 300mmol/kg of water. Therefore, ion substitution obviously took place during the pause in water flooding. Further continued injection led to a decline in the rate of oil recovery and no major increment in oil recovery was observed for continued flooding for 8 PV. Three pauses of 304 hours (at 26.15 PVI), 73 hours (at 29.8 PVI) and 45 hours (at 30.44 PVI) were introduced in order to further enhance the oil production, but no major increment in oil production was observed. The Ca^{2+} concentration remained below 2 mmol/kg of water throughout the injection of *Mg-Lq3*. This shows that the injection of *Mg-Lq3* neither resulted in an increment in oil recovery nor any fine formation during the different pauses in water flooding. Thereafter *Mg-Lq4* was injected for 15.01 PV. The initial brine alteration did not produce any additional oil recovery, but following a pause of 2.3hrs (at 39.02 PVI) an increment in oil production by 1.2% of OOIP with 0.8 PVI of brine injection was observed. The effluent Ca^{2+} concentration (after the pause) increased to 28.56 mmol/kg and a corresponding decrease in Mg concentration was observed. Thus an increment in oil recovery took place, together with attrition based fine formation. Thereafter, *Mg-Lq1* and deionized water was injected for 13.68 and 11.33 PVI after 3.1 hours of pause, but no additional oil production was observed.

Multiple pauses (of lengths up to 645 hrs) introduced during Mg-*Lq3* flooding did not produce any noticeable additional oil recovery. During the subsequent injection of *Mg-Lq4*, a small pause of 2.3 hours led to a noticeable increment in oil production. This indicates that brine composition is determining for the effect of pausing the injection. This coreflooding experiment further shows that attrition based fine formation is well correlated to the oil recovery for magnesium brines as well. An increment in oil production by 17.8% of OOIP was observed by injecting magnesium brines of varied composition with repeated pauses and reinjections in the water floods. Furthermore the two types of ion substitution including: (1) substitution of the adsorbed ions from the mineral surface and (2) substitution by alteration in the calcite crystal lattice have been distinctively observed at different sections of the water flooding.

Comparative Discussion

In all four core floods, the effluent brine at the flooding conditions was supersaturated when there was an associated increment in oil recovery. This shows that the amount of calcite released from the mineral surface during the pause was greater than the solubility limit. Thus attrition of calcite (Flamant et al. 1990) and mobile calcite fines formation had taken place during the pause in waterflood. Availability of Ca^{2+} and CO_3^{2-} in effluent samples have been previously interpreted as dissolution of calcite from the mineral grains because of different brine injections (Pu et al. 2010;Yousef et al. 2011). Anhydrite containing core plugs have also shown an increment in effluent Ca^{2+} and SO_4^{2-} concentration during low salinity brine injection (Romanuka et al. 2012). It has been interpreted as dissolution of anhydrite because of decrease in salinity. The observed additional ions in the effluent samples at room temperature have been directly related to the dissolution of corresponding salts (Ca^{2+} and CO_3^{2-} for calcite dissolution and Ca^{2+} and SO_4^{2-} for anhydrite dissolution). But the speciation of the effluent brine composition at the high pressure and temperature conditions during the flooding needs to be considered to differentiate between attrition and brine speciation at flooding conditions. Figure 14 shows effluent brine composition for water flooding Stevns Klint outcrop chalk with 0.657 M NaCl (Megawati et al. 2015). Considerable concentration, 2-5 mmol/l of Ca^{2+} was consistently produced for 14 PVI of NaCl injections. Calculations using the Extended UNIQUAC model at the flooding conditions of 50°C and 130°C showed that all effluent brines with concentrations from 1 mmol/l to 5 mmol/l had considerable amounts of insoluble calcite. Less than 30% of the calcite reported in the effluent brine was soluble at the reservoir conditions. This shows that the reported brine was significantly supersaturated at reservoir conditions. The majority of the additionally released Ca^{2+} was therefore associated with attrition based fine formation and not dissolution of calcite in the injected smart water flood. Both attrition and dissolution will affect the permeability and alter the sweep efficiency of the flooded water. But insoluble fines can adhere to oil and support in mobilizing trapped residue oil (Tang and Morrow 1999, Chakravarty et al. 2015a). Figure 15 shows effluent brine compositions from the study of Romanuka et al. (2012) on low salinity brine injection in dolostone core plugs containing anhydrite. The recorded brine composition was also calculated at the experimental conditions using the Extended UNIQUAC model. It was observed that the SO_4^{2-} concentrations (in the effluent brines) was more than 2.5 times the value at the solubility limit of $CaSO_4$ at 85°C and 30 bar (experimental conditions). Thus, the observed increment in Ca^{2+} and SO_4^{2-} concentration is associated with attrition of anhydrite grains and not dissolution. The concentration in the produced water is significantly above the solubility limit for anhydrite. Therefore, the effluent brine composition recorded at room temperature should not be directly correlated to dissolution of core plug minerals. Instead, the reported composition and the speciation at experimental conditions should be back calculated to obtain the exact properties of the brine produced from the core plug during SmW-EOR experiments.

The net increment in oil recovery for injection of magnesium brines of varying composition was 17.8% of OOIP for the N3X17V core plug and 11.7% of OOIP for the N3X9H core plug. In both water floods pauses at regular intervals were introduced. The observed increment in oil recovery with *Mg-Lq2* as the first brine injected (in the N3X17V core plug with EOR of 15.8% of OOIP) was considerable higher than that for *Mg-Lq1* as the first brine injected (into the N3X9H core plug with EOR of 7.1% of OOIP). Thus, also *Mg-Lq2* as the second brine injected (in the N3X9H core plug with EOR of 4.6% of OOIP) was considerably better than the produced oil recovery with *Mg-Lq3* as the second brine injected (in N3X17V with EOR of 0.4% of OOIP). Thus, the increment in oil recovery was most significant for *Mg-Lq2* as previously shown (Austad et al. 2008). Adsorption of SO_4^{2-} ions followed by desorption of carboxyl polar fractions from the mineral surface was expected to lead to an increment in oil recovery during continuous water flooding with soluble Mg^{2+} and SO_4^{2-} ions. But unlike previous recommendation during continued flooding with available soluble Mg^{2+} and SO_4^{2-} ions did not lead to any increment in oil recovery and EOR is only observed after pause and reinjection of *Mg-Lq2*. Replacing SO_4^{2-} absent brine (*Mg-Lq1* in N3X9H) with high SO_4^{2-} brine *Mg-Lq2* showed no increment in oil recovery. This proves that injection of soluble Mg^{2+} and SO_4^{2-} ions alone does not cause an increment in oil recovery. During a pause in *Mg-Lq2* injection, the ion substitution and fine formation took place, and thereafter reinjection led to an increment in oil recovery. Thus formation of fines after the pause is the only parameter that shows consistent correlation to oil recovery. Moreover, the expected adsorption of SO_4^{2-} (Austad et al. 2008) should have led to a corresponding selective decrease in effluent SO_4^{2-} concentration, but no such selective decrease in effluent SO_4^{2-} composition during increment in oil recovery was observed. This further shows that soluble SO_4^{2-} does not consistently correlate to the observed SmW-EOR.

In the two sodium brine core floodings, pauses of different lengths were introduced. The number of pauses introduced for the N3X4H core plug was considerable larger than that in N3X11H as the effect of pauses was not well understood beforehand. An increment in oil recovery between the two cases can therefore not be directly compared. But 73 hours pause of *Na-Lq1* injection (in the N3X4H core plug led to an EOR of 6.61% of OOIP). It was significantly more than was achieved with 95 hours pause of *Na-Lq2* injection (in N3X11H core plug, which led to an EOR of 2.31% of OOIP). Thus in the sodium campaigns, the increment in oil recovery was more prominently observed when pauses were held during Na-*Lq1* injection (N3X4H core plug). Pauses in *Na-Lq2* injection (as the first injection brine in N3X11H core plug) did not show corresponding equivalent increment in oil recovery. Moreover, at high temperature (130°C) exactly similar water floods with same flooding campaign also showed consistent increment in oil recovery following multiple pauses in *Na-Lq1* brine injection (with collective EOR of 5.1% of OOIP) (Paper 10: Figure 2, Chakravarty et al. 2016 (to be submitted)). While no increment in oil recovery was observed when pauses in water flooding were introduced during injection of *Na-Lq2* as the first brine (core plug M1X10H Paper 10: Figure 4, Chakravarty et al. 2016 (to be submitted). Thus the observed increment in oil recovery for low temperature chalks is congruent to previous similar studies with high temperature chalks.

Comparing the Mg campaign with the Na campaign it is observed that when multiple pauses are introduced, a distinct benefit of using Mg salts is not observed (as previously expected for high temperature chalks (Austad et al. 2008). Nevertheless two distinctive differences between the two campaigns are observed.

1. Pause in sodium brines injection causes attrition of calcite fines from the mineral surface. Magnesium brines cause both attrition of calcite and substitution of Ca^{2+} ions from the mineral lattice. Thus correspondingly the strength of the grains is alerted (due to the smaller size of Mg^{2+} ions over Ca^{2+} ions). After flooding, CT-scan images along the radial sections of the core plugs from the Mg campaigns show grain dissociation from the core plug's mineral grains matrix. This was observed in both of the Mg campaigns and no such detachments of grains were observed during the Na campaign (Figure 1-2), even at similar high temperature flooding (Paper 10: Figure 1, Chakravarty et al. 2016 (to be submitted)).
2. Pause and reinjection of brine with SO_4^{2-} was more productive in producing oil and attrition based fines in the Mg campaign, while Cl^- proved more efficient in the Na campaign. The exact reason behind this difference between the two campaigns remains a topic to be further researched. But in both cases, pauses and reinjection of brines produced fines in an amount with consistent correlation to oil recovery.

Ion substitution on calcite surfaces has been debated in the literature. Water flooding with 5-10 PV/day into Middle East core plugs showed around 7.54% (with a maximum of 16.98%) of Mg^{2+} to substitute Ca^{2+} from the mineral surface (Gupta et al. 2011; Vo et al. 2012). Another study with Middle East core plugs have consistently shown 50% Mg^{2+} substitution for 12 PV when the brine injection rate was controlled at 1 PV/day (Shariatpanahi et al. 2010). In Stevns Klint Chalk up to 100% of the lattice surface Ca^{2+} has been shown to be substituted consistently by Mg^{2+} injection (Austad et al. 2008). Zahid et al. 2012 observed no substitution of ions when reservoir chalk from the Dan field was flooded at 2 PV/day. Since no additional Ca^{2+} was observable in the effluent solution. In this study both magnesium campaigns show that only with North sea reservoir chalks surface ion substitution takes place when the brine is injected at 0.2 PV/day. Addition ion substitution only takes place when flooding is paused and ample time is provided. Continuous flooding at 2 PV/day does not cause any substitution from the mineral lattice (similar to previously observed with Dan field chalk (Zahid et al. 2012b)). Thus the rate of brine injection plays a prominent role in ion substitution and the extent of ion substitution taking place is dependent on the origin of the core plug. So the optimum rate of ion substitution must be identified for each reservoir formation, so that ion substitution can be effectively conducted during Smart water floods.

During water flooding experiments, unrecorded pauses of a few hours can take place while brine composition is being altered during smart water flooding. The subsequent injection of new brine after the pause may lead to an increment in oil recovery as reported in various water flooding studies. This increase in oil recovery is likely to be interpreted as an effect of brine alteration, and the effect of small pauses are ignored. But this study shows that pauses in water flooding can cause an increment in oil recovery irrespective of changes in brine alteration. Therefore, the rate of brine injection and pause in brine injection is an important phenomenon which can affect the oil production pattern significantly and should be considered during interpretation of water flood studies.

Conclusion

Four different reservoir chalk core plugs were successfully flooded at 60 °C using different sodium and magnesium brines. Brine composition variation and multiple pauses/resumptions of injection showed an increment in oil recovery of N3X17V by 17.8% of OOIP. Among sodium salts: NaCl, and among magnesium salts. $MgSO_4$ was found to be most effective in enhancing oil production during reinjection after pauses in water floods. Formation of fines because of attrition of calcite showed consistent correlation to increment in oil recovery over various pauses and reinjections of brines. Adsorption of soluble potential ions (with associated desorption of polar carboxyl fraction of oil) was not observed, as there was no SO_4^{2-} selective decrease in effluent SO_4^{2-} concentration. This study also shows that high Ca^{2+} and CO_3^{2-}/SO_4^{2-} in the effluent brine at ambient conditions should not be directly associated to dissolution of calcite/anhydrite. Instead the speciation of the effluent brine composition should be back calculated to flooding conditions and the fraction of mineral attrition particles present in the effluent brine should be identified. Furthermore effluent brine composition during Mg flooding clearly shows that both substitution of adsorbed ions from the mineral surface and the substitution of ions from the mineral lattice can take place. But the latter requires ample time for the substitution kinetics to be observable in the effluent composition.

References:

- Akbar, M., Vissapragada, B., Alghamdi, A. H., Allen, D., Herron, M., Carnegie, A., Dutta, D., Olesen J. R., Chourasiya R. D., Logan, D., Stief, D., Netherwood R., Russell S. D., & Saxena, K. (2000). A snapshot of carbonate reservoir evaluation.Oilfield Review, 12(4), 20-21.
- Alagic, E., Spildo, K., Skauge, A., & Solbakken, J. (2011). Effect of crude oil ageing on low salinity and low salinity surfactant flooding. Journal of Petroleum science and Engineering, 78(2), 220-227.
- Alvarado, V., Garcia-Olvera, G., Hoyer, P., & Lehmann, T. E. (2014a, October). Impact of polar components on crude oil-water interfacial film formation: A mechanisms for low-salinity waterflooding. In *SPE Annual Technical Conference and Exhibition*. Society of Petroleum Engineers.

- Alvarado, V., Moradi Bidhendi, M., Garcia-Olvera, G., Morin, B., & Oakey, J. S. (2014b, April). Interfacial Visco-Elasticity of Crude Oil-Brine: An Alternative EOR Mechanism in Smart Waterflooding. In SPE Improved Oil Recovery Symposium. Society of Petroleum Engineers.
- Austad, T., Shariatpanahi, S. F., Strand, S., Black, C. J. J., & Webb, K. J. (2011). Conditions for a low-salinity enhanced oil recovery (EOR) effect in carbonate oil reservoirs. *Energy & fuels*, *26*(1), 569-575.
- Austad, T., Strand, S., Høgnesen, E. J., & Zhang, P. (2005). Seawater as IOR fluid in fractured chalk. SPE, 93000, 2-4.
- Austad, T., Strand, S., Madland, M. V., Puntervold, T., & Korsnes, R. I. (2008). Seawater in chalk: An EOR and compaction fluid. SPE Reservoir Evaluation & Engineering, 11(04), 648-654.
- Bjørnstad, T., Haugen, O. B., & Hundere, I. A. (1994). Dynamic behavior of radio-labelled water tracer candidates for chalk reservoirs. *Journal of Petroleum Science and Engineering*, *10*(3), 223-238.
- Brown, L. R. (2010). Microbial enhanced oil recovery (MEOR). *Current opinion in Microbiology*, *13*(3), 316-320.
- Chakravarty, K. H., Ahkami, M., Xiarchos, I.; Katika, K., Fabricius, I.L., Shapiro, A., Stenby, E.H., Fosbøl, P.L., & Thomsen, K. (2016). Effect of injection of Sodium salts in Smart Water-Enhanced Oil Recovery (SmW-EOR): A case study from the North Sea. Journal of Canadian Petroleum Technology(to be submitted)
- Chakravarty, K. H., Fosbøl, P. L., & Thomsen, K. (2015a, June). Interactions of Fines with Base Fractions of Oil and its Implication in Smart Water Flooding. In *EUROPEC 2015*. Society of Petroleum Engineers.
- Chakravarty, K. H., Fosbøl, P. L., & Thomsen, K. (2015b, November). Significance of Fines and their Correlation to Reported Oil Recovery. In *Abu Dhabi International Petroleum Exhibition and Conference*. Society of Petroleum Engineers.
- Delshad M., Shalabi E. W., and Sepehrnoori K., (2013, April). Mechanisms Behind Low Salinity Water Flooding in Carbonate Reservoirs. In SPE Western Regional & AAPG Pacific Section Meeting 2013 Joint Technical Conference. Society of Petroleum Engineers.
- Fan, T., & Buckley, J. S. (2006, January). Acid number measurements revisited. In *SPE/DOE Symposium on Improved Oil Recovery*. Society of Petroleum Engineers.
- Fernø, M. A., Grønsdal, R., Åsheim, J., Nyheim, A., Berge, M., & Graue, A. (2011). Use of Sulfate for Water Based Enhanced Oil Recovery during Spontaneous Imbibition in Chalk. Energy & fuels, 25(4), 1697-1706.
- Fjelde, I. F., & Aasen, S. M. A. (2009, April). Improved spontaneous imbibition of water in reservoir chalks. In 15th European Symposium on Improved Oil Recovery.
- Flamant, G., Chraibi, M. A., Vallbona, G., & Bertrand, C. (1990). Decarbonation and attrition of calcite in a plasma spouted bed reactor. *Le Journal de Physique Colloques*, *51*(C5), C5-27.
- Fogden, A., Kumar, M., Morrow, N. R., & Buckley, J. S. (2011). Mobilization of fine particles during flooding of sandstones and possible relations to enhanced oil recovery. Energy & Fuels, 25(4), 1605-1616.
- Grabowski, A., Nercessian, O., Fayolle, F., Blanchet, D., & Jeanthon, C. (2005). Microbial diversity in production waters of a low-temperature biodegraded oil reservoir. *FEMS Microbiology Ecology*, *54*(3), 427-443.
- Gupta R., Smith G. G., Hu L., Willingham T., Cascio M. L. Shyeh J. J., &Harris C. R. (2011, January). Enhanced Waterflood for Carbonate Reservoirs-Impact of Injection Water Composition. In SPE Middle East Oil and Gas Show and Conference. Society of Petroleum Engineers.
- Helgeson, H. C., Knox, A. M., Owens, C. E., & Shock, E. L. (1993). Petroleum, oil field waters, and authigenic mineral assemblages Are they in metastable equilibrium in hydrocarbon reservoirs. *Geochimica et Cosmochimica Acta*, *57*(14), 3295-3339.
- Hirasaki, G. J., Miller, C. A., & Puerto, M. (2008, January). Recent advances in surfactant EOR. In *SPE Annual Technical Conference and Exhibition*. Society of Petroleum Engineers.
- Hubert, C. R., Oldenburg, T. B., Fustic, M., Gray, N. D., Larter, S. R., Penn, K., & Voordouw, G. (2012). Massive dominance of Epsilonproteobacteria in formation waters from a Canadian oil sands reservoir containing severely biodegraded oil. *Environmental microbiology*, *14*(2), 387-404.
- Karoussi, O., & Hamouda, A. A. (2007). Imbibition of sulfate and magnesium ions into carbonate rocks at elevated temperatures and their influence on wettability alteration and oil recovery. Energy & fuels, 21(4), 2138-2146.
- Lebedeva, E. V., & Fogden, A. (2011). Micro-CT and wettability analysis of oil recovery from sand packs and the effect of waterflood salinity and kaolinite.Energy & Fuels, 25 (12), 5683-5694.
- Levitt, D., Jackson, A., Heinson, C., Britton, L. N., Malik, T., Dwarakanath, V., & Pope, G. A. (2006, January). Identification and evaluation of high-performance EOR surfactants. In *SPE/DOE Symposium on Improved Oil Recovery*. Society of Petroleum Engineers.

- Liu, Q., Dong, M., Yue, X., & Hou, J. (2006). Synergy of alkali and surfactant in emulsification of heavy oil in brine. *Colloids and Surfaces A: Physicochemical and Engineering Aspects*, *273*(1), 219-228.
- McGuire, P. L., Chatham, J. R., Paskvan, F. K., Sommer, D., & Carini, F. (2005). Low Salinity Oil Recovery: An Exciting New EOR Opportunity for Alaska's North Slope. Paper SPE 93903 presented at the SPE Western Regional Meeting, Irvine, California, 30 March–1 April. dx. doi. org/10.2118/93903-MS.
- Megawati, M., Madland, M. V., & Hiorth, A. (2015). Mechanical and physical behavior of high-porosity chalks exposed to chemical perturbation. *Journal of Petroleum Science and Engineering*, *133*, 313-327.
- Moradi, M., Alvarado, V., & Huzurbazar, S. (2010). Effect of salinity on water-in-crude oil emulsion: evaluation through drop-size distribution proxy. Energy & fuels, 25 (1), 260-268.
- Moradi, M., Topchiy, E., Lehmann, T. E., & Alvarado, V. (2013). Impact of ionic strength on partitioning of naphthenic acids in water–crude oil systems–Determination through high-field NMR spectroscopy. Fuel, 112, 236-248.
- Nasr-El-Din, H. A., Lynn, J. D., Hashem, M. K., & Bitar, G. (2002, January). Field Application of a Novel Emulsified Scale Inhibitor System to Mitigate Calcium Carbonate Scale in a Low Temperature, Low Pressure Sandstone Reservoir in Saudi Arabia. In *SPE Annual Technical Conference and Exhibition*. Society of Petroleum Engineers.
- Nazina, T. N., Pavlova, N. K., Tatarkin, Y. V., Shestakova, N. M., Babich, T. L., Sokolova, D. S., & Belyaev, S. S. (2013a). Microorganisms of the carbonate petroleum reservoir 302 of the Romashkinskoe oilfield and their biotechnological potential. *Microbiology*, *82*(2), 190-200.
- Nazina, T. N., Shestakova, N. M., Pavlova, N. K., Tatarkin, Y. V., Ivoilov, V. S., Khisametdinov, M. R., & Belyaev, S. S. (2013). Functional and phylogenetic microbial diversity in formation waters of a low-temperature carbonate petroleum reservoir. *International Biodeterioration & Biodegradation*, *81*, 71-81.
- Parracello, V. P., Pizzinelli, C. S., Nobili, M., Masserano, F., Callegaro, C., Caschili, A., & Bartosek, M. (2013, June). Opportunity of enhanced oil recovery low salinity water injection: From experimental work to simulation study up to field proposal. In Proceedings of the 75th EAGE Conference & Exhibition incorporating SPE EUROPEC, Society of Petroleum Engineers, London, United Kingdom.
- Pu H., Yin P., & Morrow N. R. (2010, January). Low-salinity waterflooding and mineral dissolution. In SPE Annual Technical Conference and Exhibition. Society of Petroleum Engineers.
- Puntervold, T., Strand, S., & Austad, T. (2007). Water flooding of carbonate reservoirs: Effects of a model base and natural crude oil bases on chalk wettability. *Energy & fuels*, *21*(3), 1606-1616.,
- Puntervold, T., Strand, S., & Austad, T. (2009). Coinjection of seawater and produced water to improve oil recovery from fractured North Sea chalk oil reservoirs. Energy & fuels, 23(5), 2527-2536.
- Robertson, E. P. (2007, January). Low-salinity waterflooding to improve oil recovery-historical field evidence. In SPE Annual Technical Conference and Exhibition. Society of Petroleum Engineers.
- Romanuka, J., Hofman, J., Ligthelm, D. J., Suijkerbuijk, B., Marcelis, F., Oedai, S & Austad, T. (2012, January). Low salinity EOR in carbonates. In *SPE Improved Oil Recovery Symposium*. Society of Petroleum Engineers.
- Santanna, V. C., Curbelo, F. D. S., Dantas, T. C., Neto, A. D., Albuquerque, H. S., & Garnica, A. I. C. (2009). Microemulsion flooding for enhanced oil recovery. *Journal of Petroleum Science and Engineering*, *66*(3), 117-120.
- Shariatpanahi, S. F., Strand, S., & Austad, T. (2011). Initial wetting properties of carbonate oil reservoirs: effect of the temperature and presence of sulfate in formation water. *Energy & Fuels*, *25*(7), 3021-3028.
- Strand, S., Austad, T., Puntervold, T., Høgnesen, E. J., Olsen, M., & Barstad, S. M. F. (2008). "Smart water" for oil recovery from fractured limestone: a preliminary study. *Energy & fuels*, *22*(5), 3126-3133.
- Strand, S., Høgnesen, E. J., & Austad, T. (2006). Wettability alteration of carbonates—Effects of potential determining ions (Ca2+ and SO42−) and temperature. Colloids and Surfaces A: Physicochemical and Engineering Aspects, 275(1), 1-10.
- Sugiharto, S., Su'ud, Z., Kurniadi, R., Wibisono, W., & Abidin, Z. (2009). Radiotracer method for residence time distribution study in multiphase flow system. Applied Radiation and isotopes, 67(7), 1445-1448.
- Sydansk, R. D. (1982). Elevated-Temperature Caustic/Sandstone Interaction: Implications for Improving Oil Recovery (includes associated papers 11348 and 11548). *Society of Petroleum Engineers Journal*, *22*(04), 453-462.
- Voordouw, G., Armstrong, S. M., Reimer, M. F., Fouts, B., Telang, A. J., Shen, Y., & Gevertz, D. (1996). Characterization of 16S rRNA genes from oil field microbial communities indicates the presence of a variety of sulfate-reducing, fermentative, and sulfide-oxidizing bacteria. *Applied and Environmental Microbiology*, *62*(5), 1623-1629.
- Webb, K. J., Black, C. J. J., & Tjetland, G. (2005, November). A laboratory study investigating methods for improving oil recovery in carbonates. In International Petroleum Technology Conference. Doha, Qatar: International Petroleum Technology Conference.

- Yildiz, H. O., Valat, M., & Morrow, N. R. (1999). Effect of brine composition on wettability and oil recovery of a Prudhoe Bay crude oil. Journal of Canadian Petroleum Technology, 38 (01).
- Yousef, A. A., Al-Saleh, S. H., Al-Kaabi, A., & Al-Jawfi, M. S. (2011). Laboratory investigation of the impact of injection-water salinity and ionic content on oil recovery from carbonate reservoirs. SPE Reservoir Evaluation & Engineering, 14(05), 578-593.
- Yousef, A. A., Al-Saleh, S., & Al-Jawfi, M. S. (2012, January). Improved/enhanced oil recovery from carbonate reservoirs by tuning injection water salinity and ionic content. In *SPE Improved Oil Recovery Symposium*. Society of Petroleum Engineers.
- Zahid, A., Sandersen, S. B., Stenby, E. H., von Solms, N., & Shapiro, A. (2011). Advanced waterflooding in chalk reservoirs: Understanding of underlying mechanisms. Colloids and Surfaces A: Physicochemical and Engineering Aspects, 389(1), 281-290.
- Zahid, A., Shapiro, A. A., & Skauge, A. (2012a, January). Experimental Studies of Low Salinity Water Flooding Carbonate: A New Promising Approach. In SPE EOR Conference at Oil and Gas West Asia. Society of Petroleum Engineers.
- Zahid, A., Shapiro, A. A., Skauge, A., & Stenby, E. H. (2012b, June). Smart Waterflooding (High Sal/Low Sal) in Carbonate Reservoirs (SPE 154508). In74th EAGE Conference & Exhibition.
- Zahid, A., Stenby, E., & Shapiro, A. (2010, June). Improved Oil Recovery in Chalk–Wettability Alteration or Something Else?(SPE-131300). In 72nd EAGE Conference & Exhibition.
- Zhang, P., & Austad, T. (2006). Wettability and oil recovery from carbonates: Effects of temperature and potential determining ions. Colloids and Surfaces A: Physicochemical and Engineering Aspects, 279(1), 179-187.
- Zhang, P., Tweheyo, M. T., & Austad, T. (2007). Wettability alteration and improved oil recovery by spontaneous imbibition of seawater into chalk: Impact of the potential determining ions Ca^{2+}, Mg^{2+}, and SO_4^{2-}. Colloids and Surfaces A: Physicochemical and Engineering Aspects, 301(1), 199-208.

Tables

Table 1: Initial petrophysical properties of flooded chalk core plugs

Core plug	Length	Diameter	Porosity	Permeability	Density	Pore Volume	Depth
	mm	mm		mD	g/cm3	cm3	(m)
N3X9H	70.66	38.38	0.36	3.59	2.70	29.63	6901
N3X17V	74.63	38.38	0.34	3.77	2.68	29.86	7033
N3 X4H	74.56	38.34	0.40	4.75	2.71	34.77	6877
N3X11H	74.76	38.41	0.3598	4.124	2.69	31.52	6915

Table 2: Irreducible water saturation and oil saturation properties

Core plug	S_{wir}	S_{oil}	BET Sp Surf	Carbonate
			(m^2/g)	(wt%)
N3X9H	0.05	0.95	1.41	94.83
N3X17V	0.05	0.95	0.92	97.02
N3X4H	0.04	0.96	1.39	97.8
N3X11H	0.05	0.95	1.3	97

Table 3: North Sea Crude Oil Properties

Crude Oil	Acid Number	Base Number	Asphaltene	Viscosity
North Sea	(mg KOH/g oil)	(mg KOH/g oil)	(%)	(cp)
	0.09	2.44	0.3	8.83

Table 4: Recorded weight of core plugs at different stages of water flooding

Weight of core plug(g)	Dry	Water saturated	Oil Saturated	After Flooding
N3X9H	143.20	172.33	168.73	162.78
N3X17V	154.62	184.12	180.48	177.45
N3X4H	141.82	176.16	171.44	155.60
N3X11H	151.45	182.39	178.50	178.07

Table 5: Composition of 4 different Na salt combinations and 4 different Mg salt combinations used in the water flooding

Na brines mol/kg H_2O	NaCl	Na_2SO_4	Total ions	Mg brines mol/kg H_20	$MgCl_2$	$MgSO_4$	Total ions
Na-Lq1	0.6	0	1.2	*Mg-Lq1*	0.3	0	1.2
Na-Lq2	0	0.3	1.2	*Mg-Lq2*	0	0.3	1.2
Na-Lq3	0.3	0.15	1.2	*Mg-Lq3*	0.15	0.15	1.2
Na-Lq4	0.6	0.75	4.2	*Mg-Lq4*	0.3	0.75	4.2

Table 6: Density and Viscosity of the injection brines at ambient conditions

Na salts	*FW*	*Na-Lq1*	*Na-Lq2*	*Na-Lq3*	*Na-Lq4*	*d10NaLq1*
Density(g/cm3)	1.063	1.035	1.043	1.039	1.142	1.003
Viscosity (cp)						
Mg Salts		Mg-Lq1	Mg-Lq2	Mg-Lq3	MgLq4	d10MgLq1
Density(g/cm3)		1.029	1.036	1.032	1.119	1.003
Viscosity (cp)						

Table 7: Sequence of brine injection in the four green sand core plugs

Core plug	Injection sequence				
N3X9H-Mg	*FW*	*Mg-Lq1*	*Mg-Lq2*	*Mg-Lq3*	
N3X17V-Mg	*FW*	*Mg-Lq2*	*Mg-Lq3*	*Mg-Lq4*	*Mg-Lq1*
N3X4H	*FW*	*Na-Lq1*	*Na-Lq2*	*Na-Lq3*	*Na-Lq4*
N3X11H-Na	*FW*	*Na-Lq2*	*Na-Lq3*	*Na-Lq4*	*Na-Lq1*

Figures

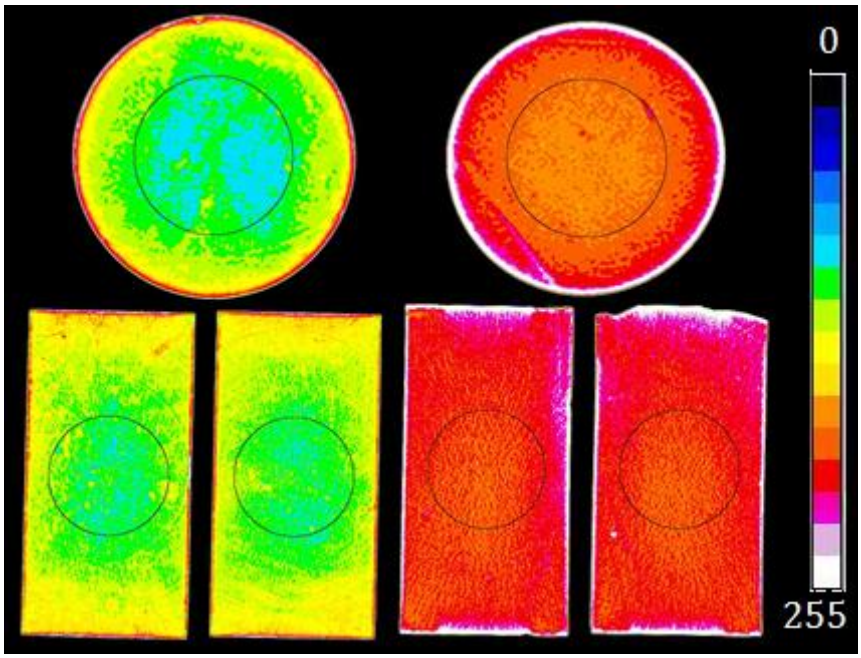


Figure 1: CT-Scan along axial and perpendicular radial sections of core plug for initial dry and after water flooding of N3X4H core plug.

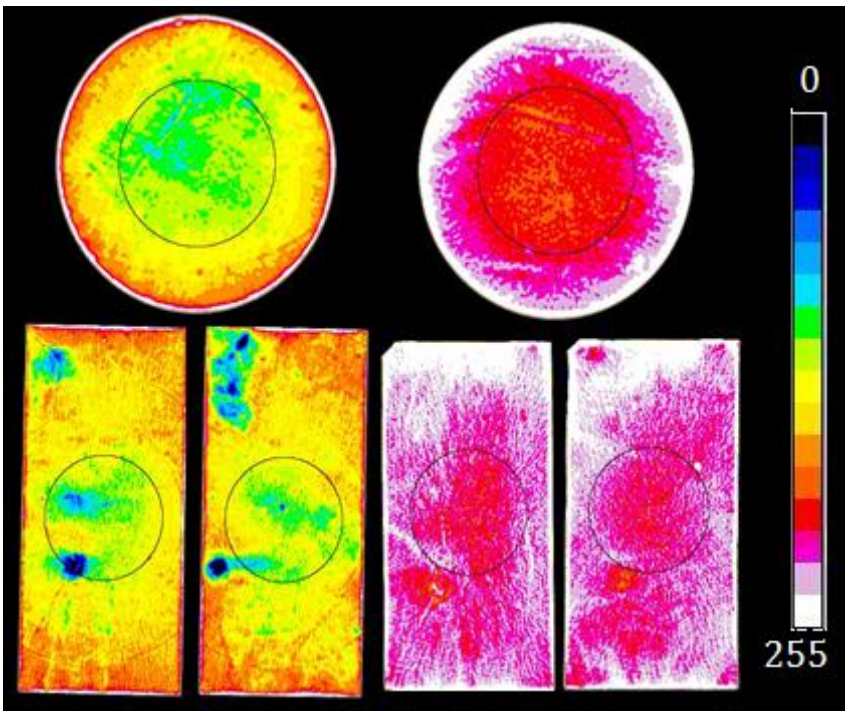


Figure 2: CT-Scan along axial and perpendicular radial sections of core plug for initial dry and after water flooding of N3X11H core plug.

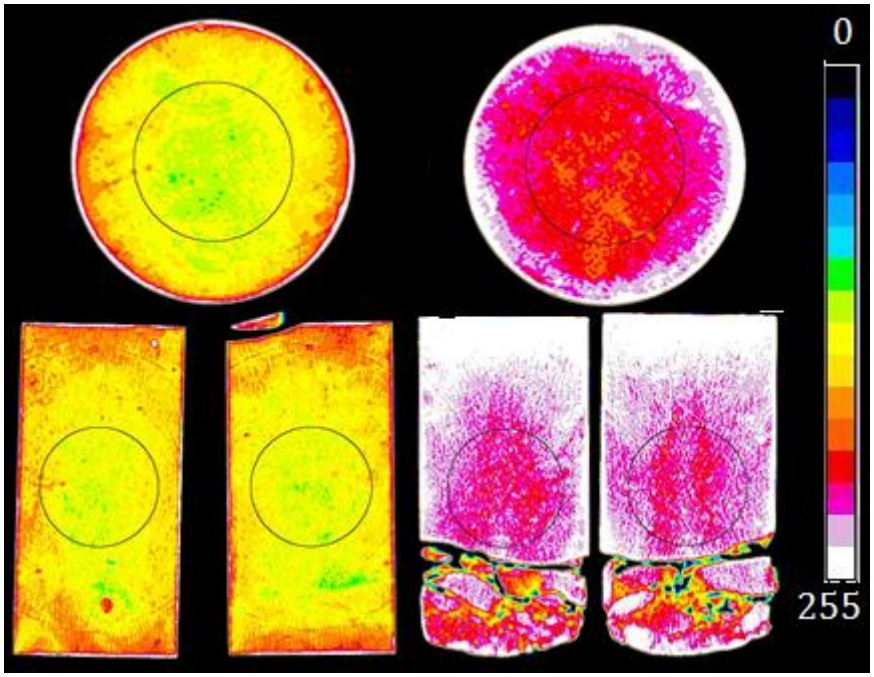


Figure 3: CT-Scan along axial and perpendicular radial sections of core plugs at different stages of water flooding N3X9H core plug.

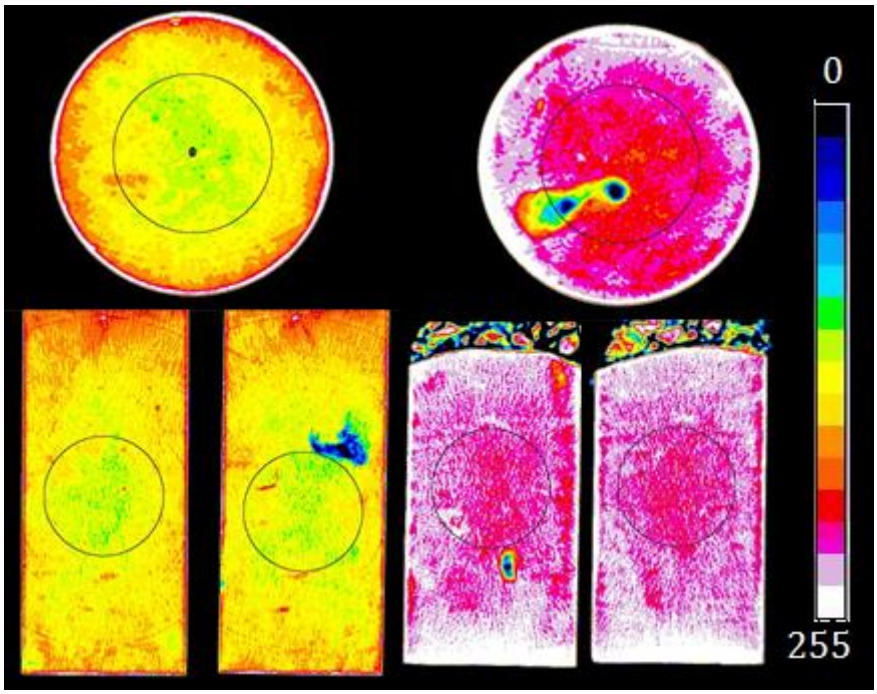


Figure 4: CT-Scan along axial and perpendicular radial sections of core plug for initial dry and after water flooding of N3X17V core plug.

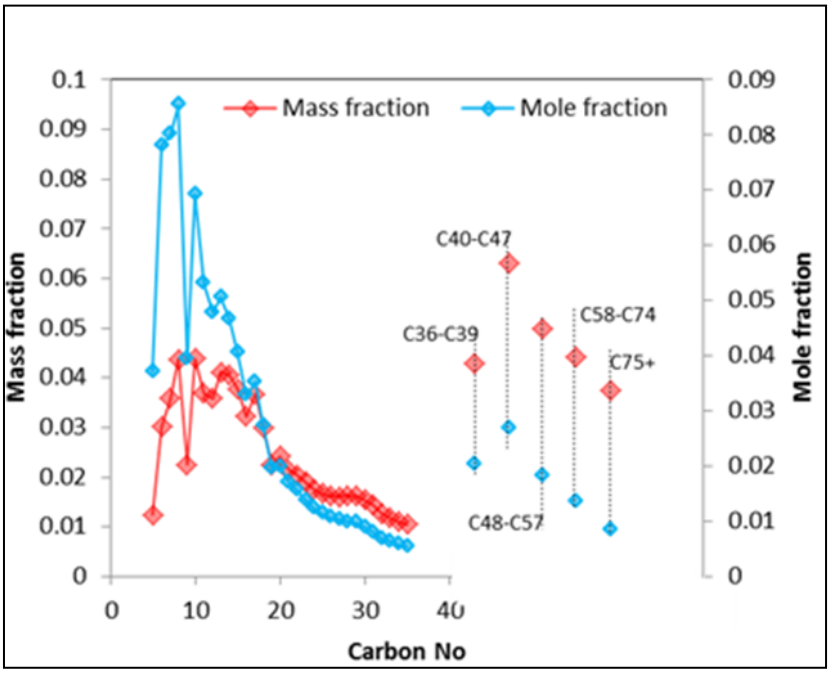


Figure 5: Fractional composition of crude oil used for core flooding studies.

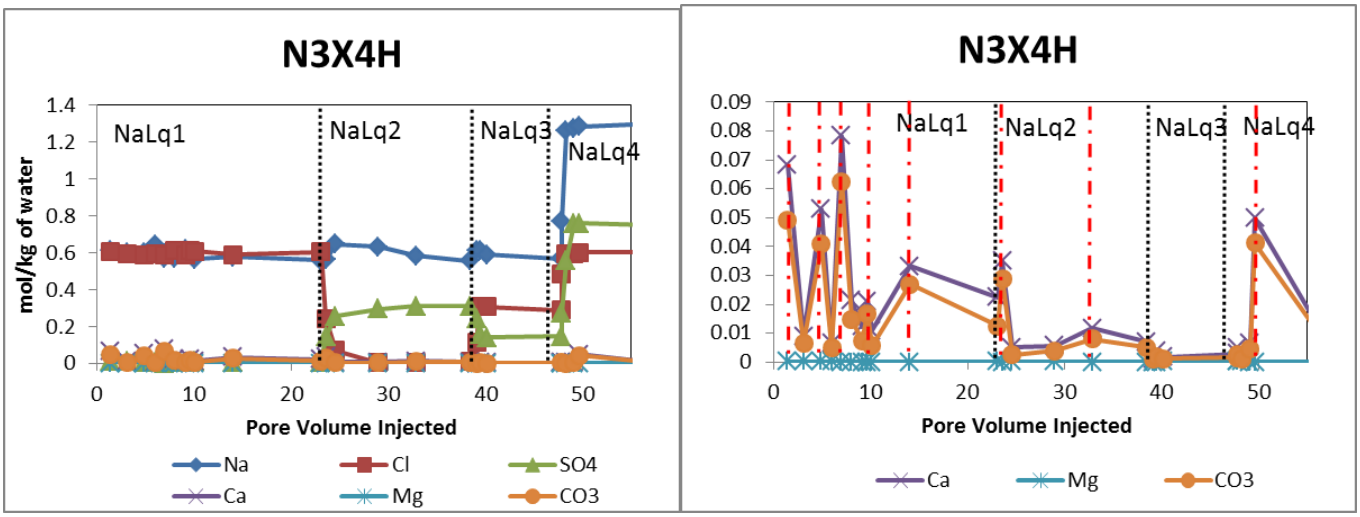


Figure 6: Composition of effluent brines vs pore volume injection for injection of different sodium salts into the N3X4H core plug. Red lines indicate PVI when the brine injection was paused and it led to attrition of $CaCO_3$ from the mineral surface.

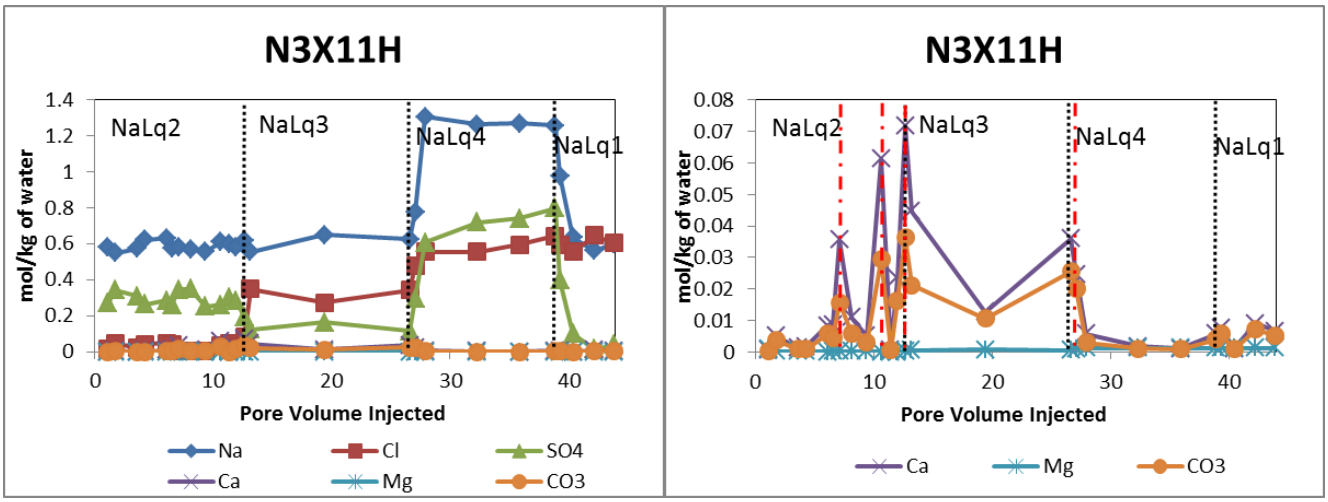


Figure 7: Composition of effluent brines vs pore volume injection for injection of different sodium salts into the N3X11H core plug. Red lines indicate PVI when the brine injection was paused and it led to attrition of $CaCO_3$ from the mineral surface.

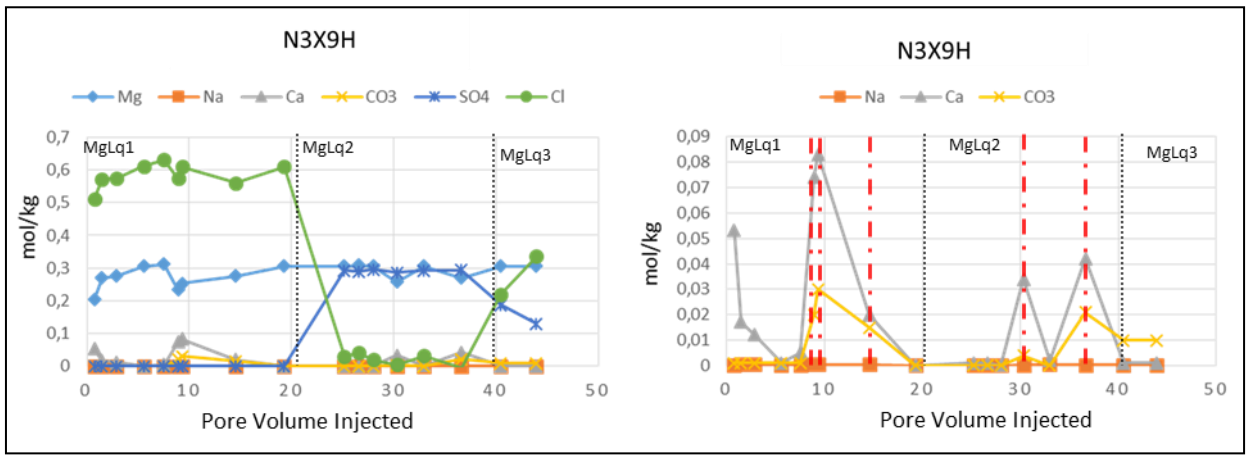


Figure 8: Composition of effluent brine vs pore volume injection for injection of different magnesium brines into the N3X9H core plug. Red lines indicate PVI when the brine injection was paused and it led to attrition of $CaCO_3$ from the mineral surface.

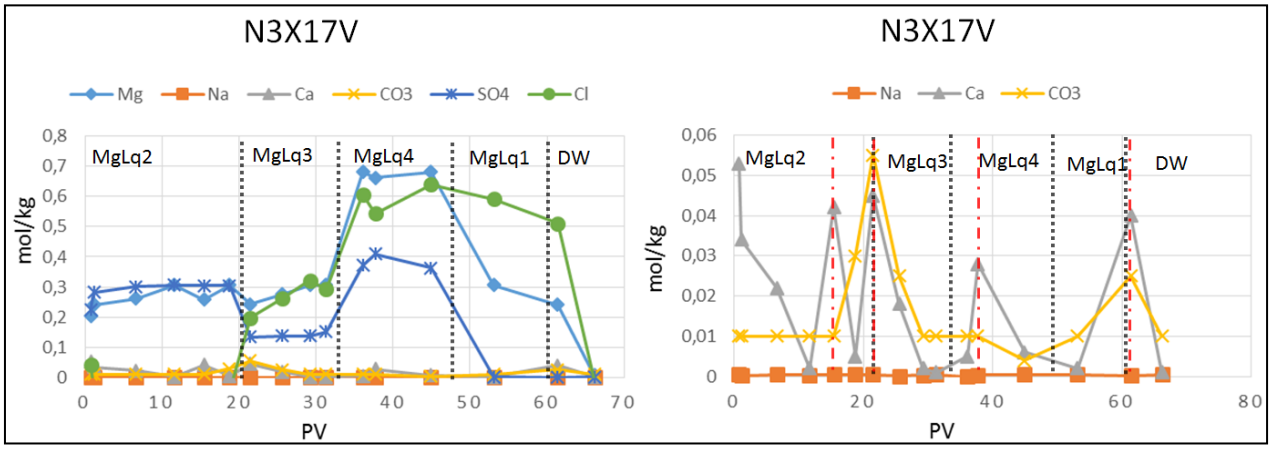


Figure 9: Composition of effluent brines vs pore volume injection for injection of different magnesium brines into the N3X17V core plug. Red lines indicate PVI when the brine injection was paused and it led to attrition of $CaCO_3$ from the mineral surface.

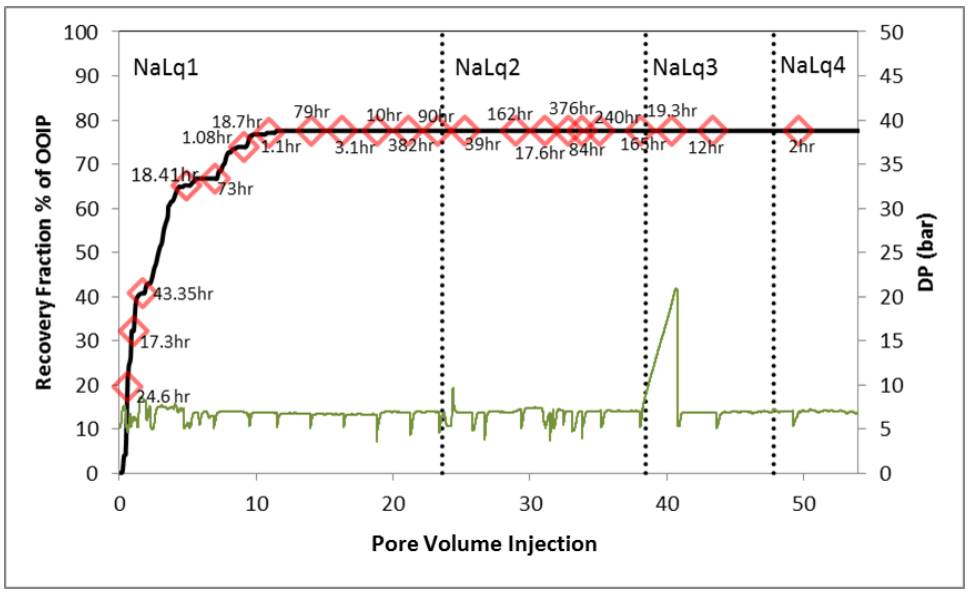


Figure 10: Observed oil recovery and differential pressure across the core plug vs PV sodium brine injection for the N3X4H core plug.

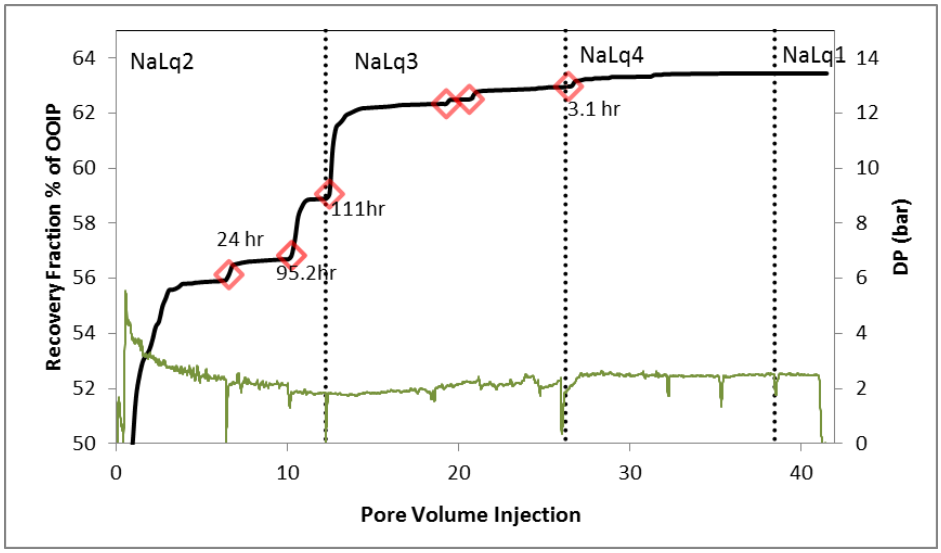


Figure 11: Observed oil recovery and differential pressure across the core plug vs PV sodium brine injection for the N3X11H core plug.

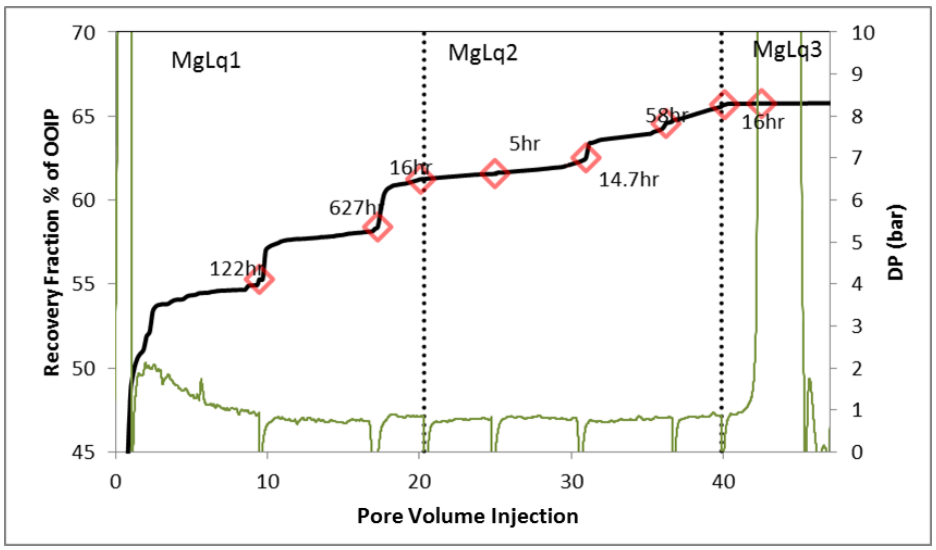


Figure 12: Observed oil recovery and differential pressure across the core plug vs PV magnesium brine injection for the N3X9H core plug.

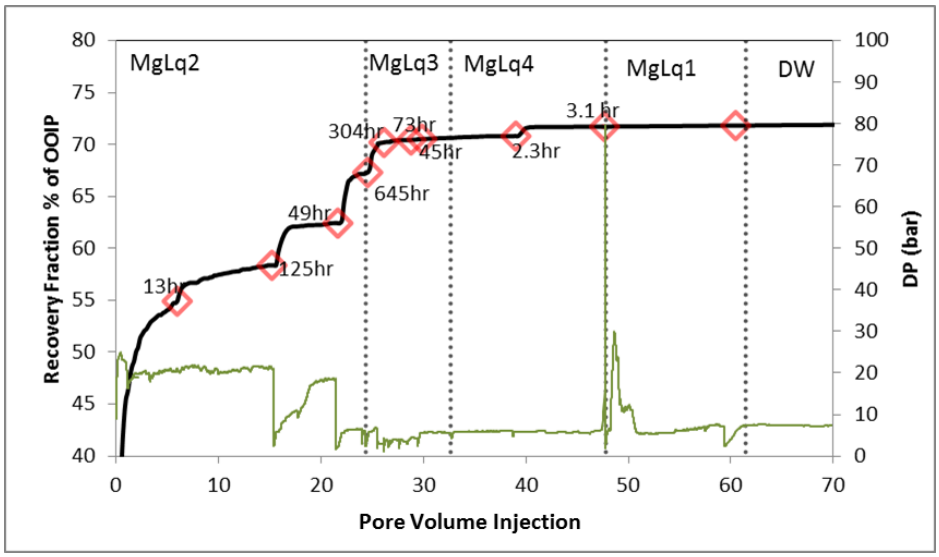


Figure 13: Observed oil recovery and differential pressure across the core plug vs PV magnesium brine injection for the N3X17V core plug.

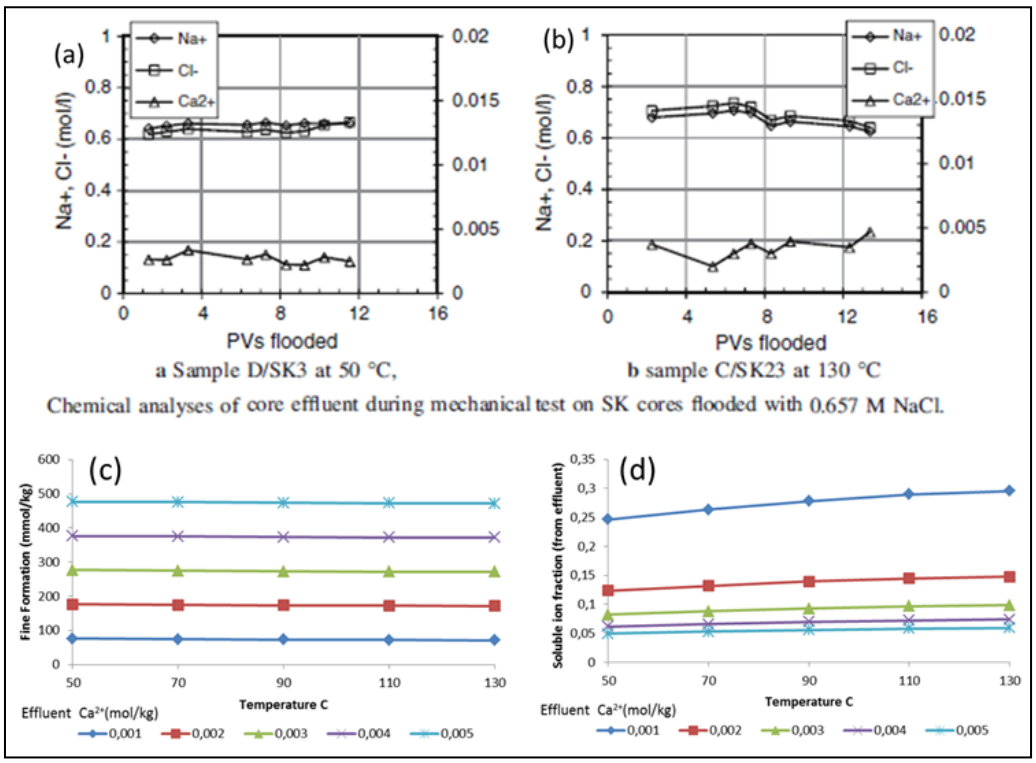


Figure 14: (a-b) Effluent brine composition for flooding 0.657 M NaCl into Stevns Klint outcrop chalk (Megawati et al. 2015).(c-d) effluent brines Ca^{2+} concentration reflects significant supersaturation at flooding conditions from 50 to 130°C, as calculated from Extended UNIQUAC model. Thus calcite attrition can be mistakenly interpreted as dissolution.

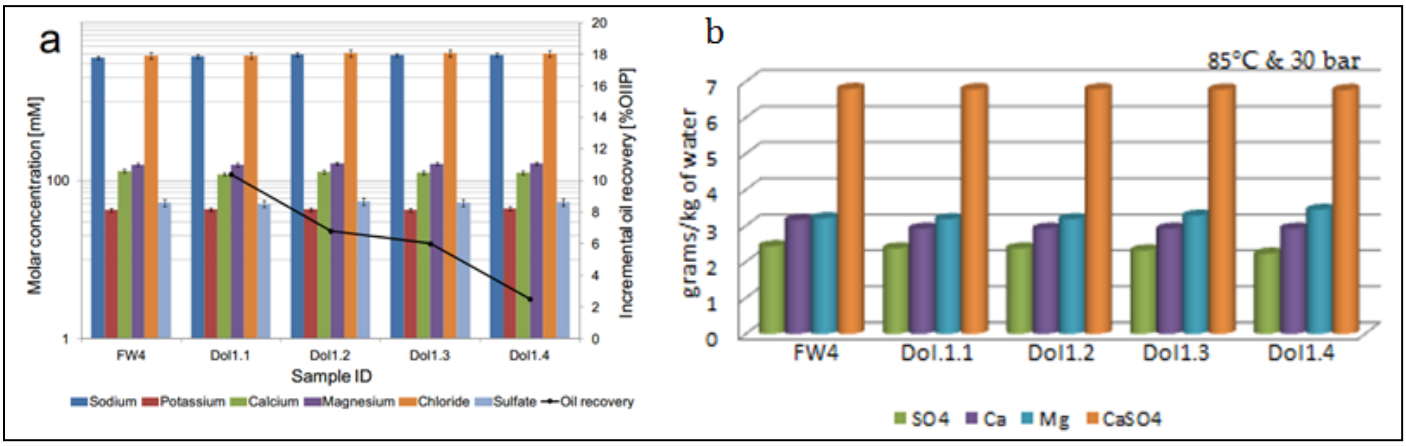
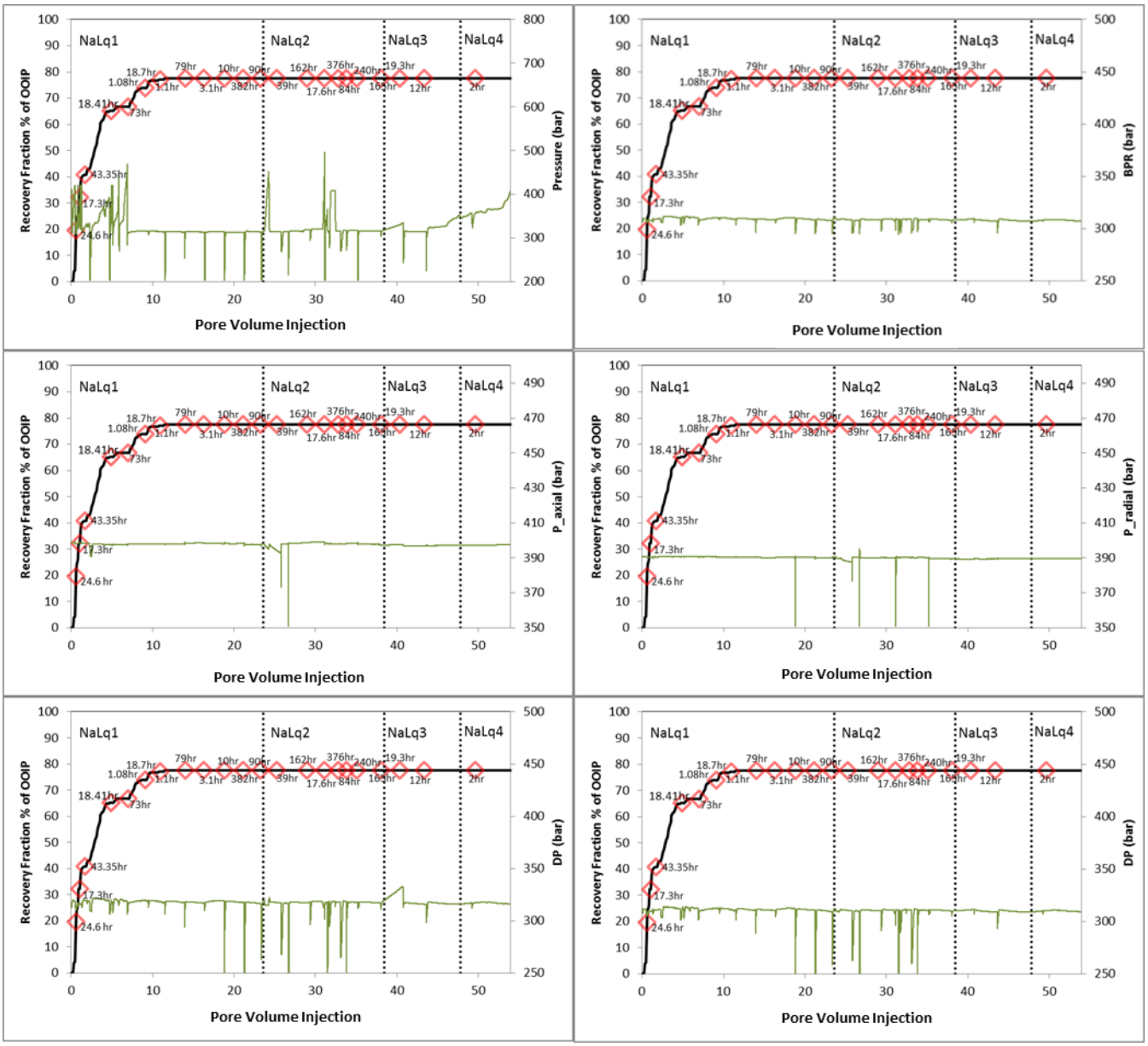
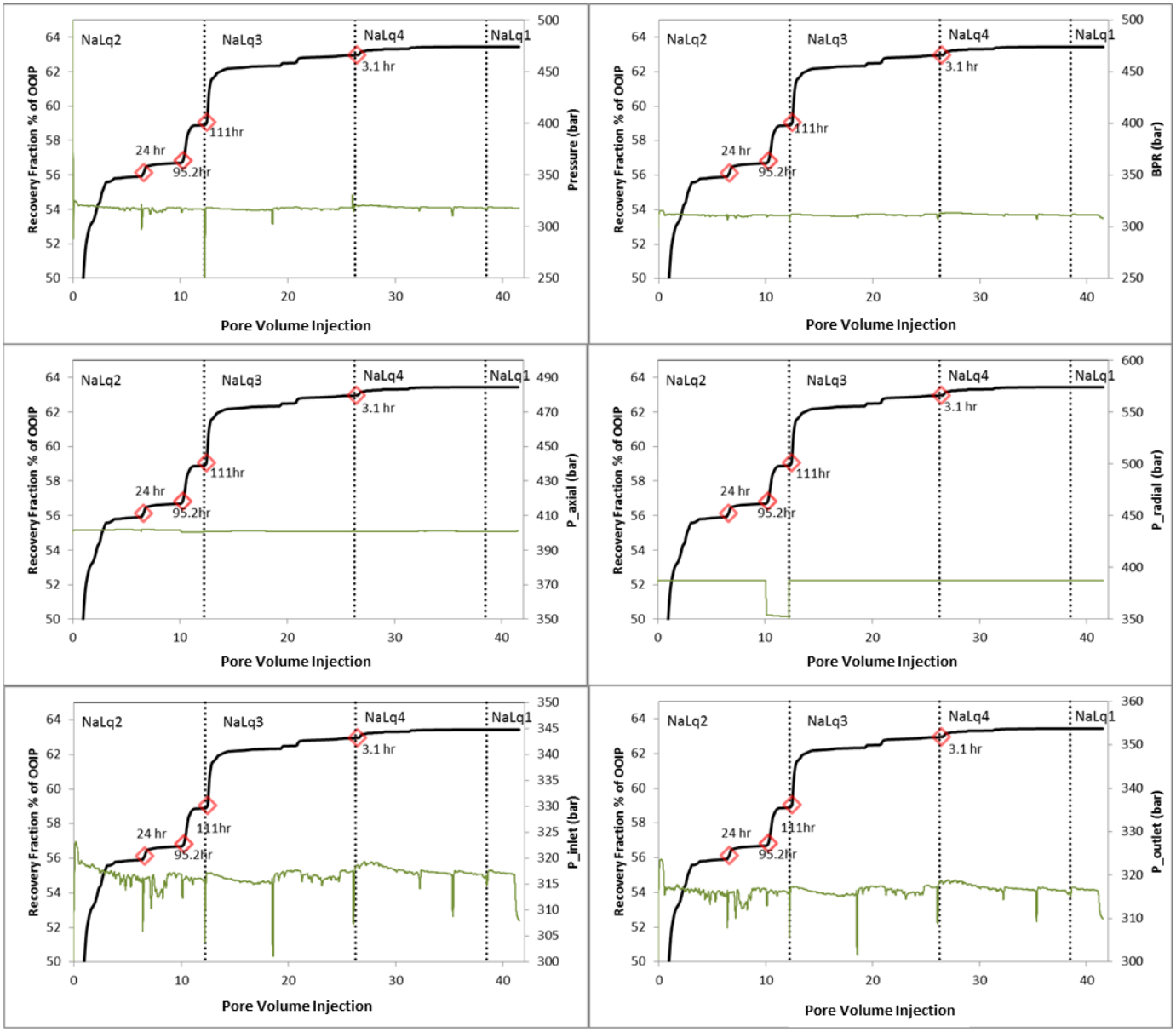


Figure 15: (a) Effluent brine composition for imbibition into dolostone core plugs and corresponding increment in oil recovery for different imbibition experiment (Romanuka et al. 2012).(b) effluent brines Ca^{2+} concentration reflects significant supersaturation at flooding conditions, as calculated from Extended UNIQUAC model. Thus anhydrite attrition can be mistakenly interpreted as dissolution.

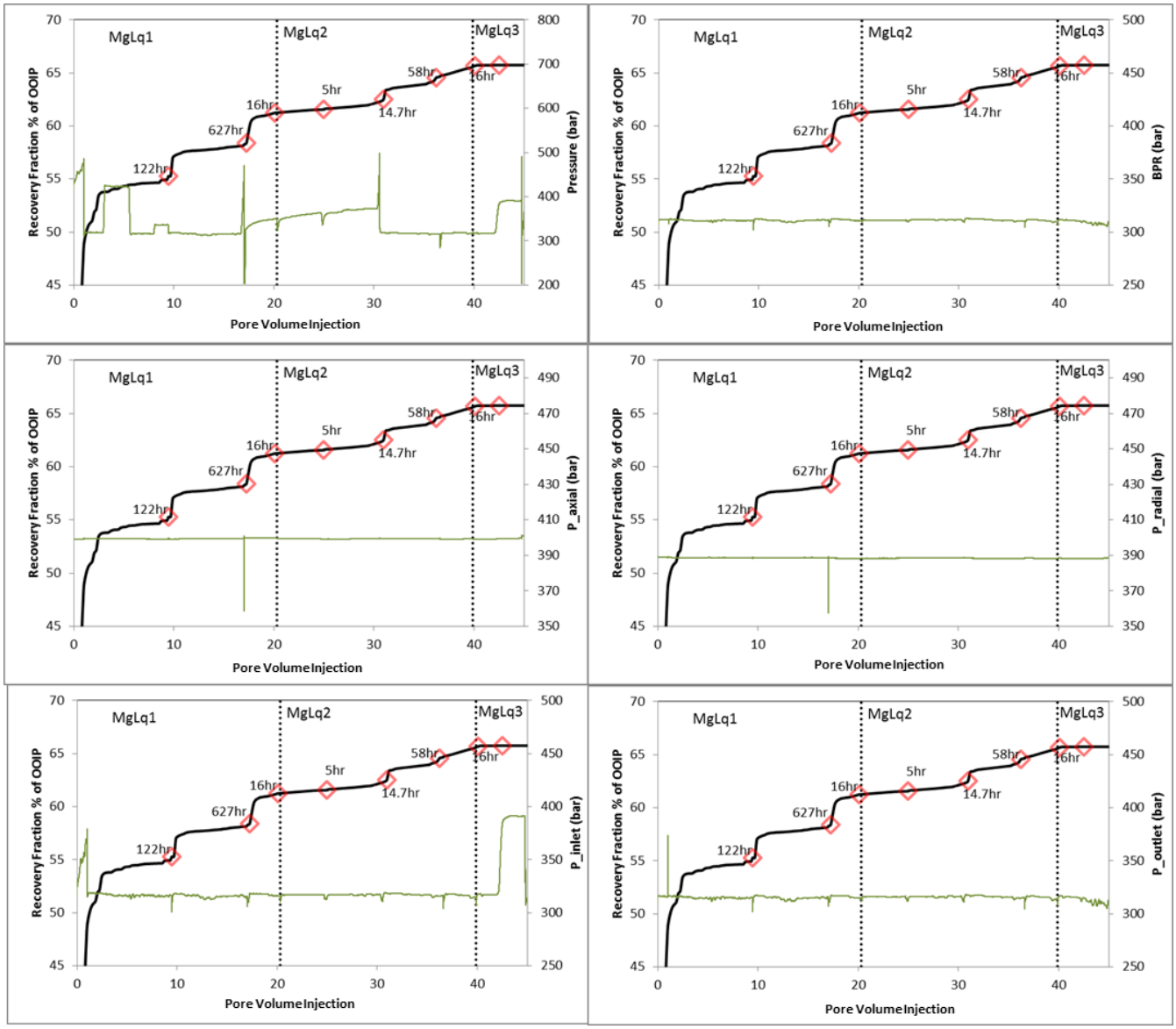
Supplementary Information



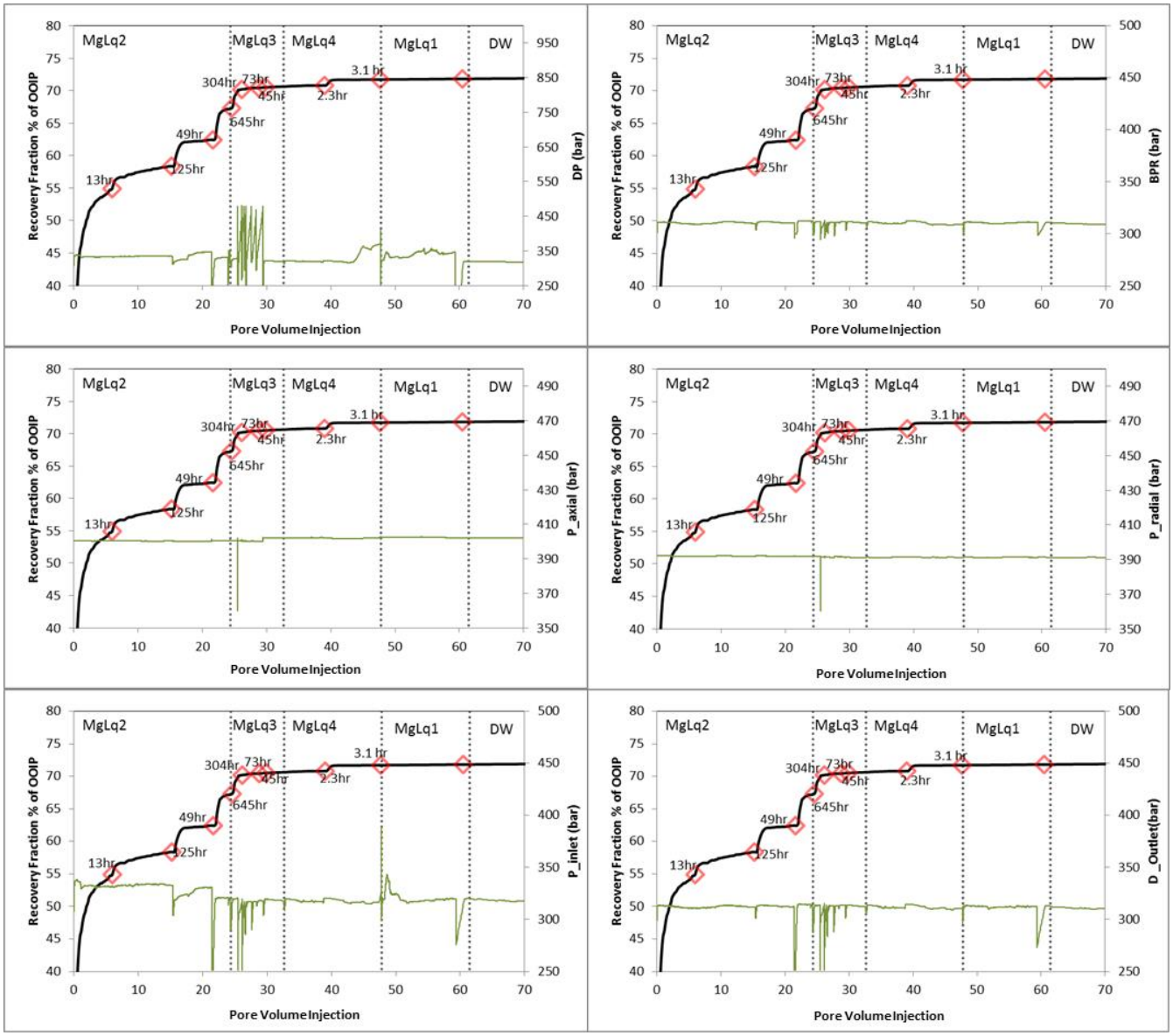
Supplementary Figure 1: Observed oil recovery vs VP sodium brine injection along with continuously monitored pressure profiles (including axial pressure, radial pressure, inlet pressure, outlet pressure, back pressure, pore pressure) for N3X4H core plug.



Supplementary Figure 2: Observed oil recovery vs PV sodium brines injection along with continuously monitored pressure profiles (including axial pressure, radial pressure, inlet pressure, outlet pressure, back pressure, pore pressure) for N3X11H core plug.



Supplementary Figure 3: Observed oil recovery vs PV magnesium brine injection along with continuously monitored pressure profiles (including axial pressure, radial pressure, inlet pressure, outlet pressure, back pressure, pore pressure) for the N3X9H core plug.



Supplementary Figure 4: Observed oil recovery vs PV magnesium brines injected along with continuously monitored pressure profiles (including axial pressure, radial pressure, inlet pressure, outlet pressure, back pressure, pore pressure) for the N3X17V core plug.

Paper XIII

Smart Water-Enhanced Oil Recovery (SmW-EOR) in low temperature Sandstone reservoirs: A case study from the North Sea

Chakravarty, K. H., Ahkami, M., Xiarchos, I., Fosbøl, P. L., & Thomsen, K. (2016) Smart Water-Enhanced Oil Recovery (SmW-EOR) in low temperature Sandstone reservoirs: A case study from the North Sea. ***Journal of Petroleum Science and Engineering*** **(Draft Manuscript: To be submitted)**

Abstract:
Low salinity enhanced oil recovery has been explored for both carbonate and sand stone reservoirs. But high salinity water enhanced oil recovery has only been studied for carbonate reservoirs. In this study, high salinity smart water enhanced oil recovery is investigated for sandstone reservoirs. Core flooding experiments with Green sandstone was conducted at 60 °C. Different compositions of Na and Mg salts were injected into the core plugs. The water flooding experiment showed that high salinity SmW-EOR can be successfully implemented for sandstone reservoirs as well. Beyond the initial oil recovery, variation in composition of injected Na salt brines at constant salinity showed an increment in oil production of 1.5% of OOIP. A similar variation for injected Mg salt brines showed an increase in oil production of 4.22% of OOIP. As suggested for chalks, these experiments show that injection of high concentration of Mg^{2+} and SO_4^{2-} ions can enhance the oil production for sandstone reservoir core plugs as well. This increase in oil production is attributed to two major factors including: (1) Pause and resumption of brine injection; (2) variation in salt composition. Similar water floods with carbonate core plugs show significantly more increase in oil production (increments up to 10.2% of OOIP) following ion substitution on mineral surfaces. These results show that SmW-EOR is possible; and Mg^{2+} and SO_4^{2-} can cause increase in oil production for low temperature sandstone reservoirs. This study suggests that high salinity SmW-EOR can be potentially considered in significantly more oil fields than any previous estimation have shown.

Introduction:
In Pithole City oil reservoir of Pennsylvania, injection of water was first applied in 1865. Subsequently, in all Enhanced Oil Recovery (EOR) methods the injection of water has played a prominent role (Blomberg 1998). Because of its associated cost, traditionally the amount of water injected has been the main consideration for most reservoirs. The composition of the injected water has not been given much attention. Pioneering work by Yildiz and Morrow in 1996 pointed out that tuning the salinity of injection brine could impact the oil recovery performance in sandstones during coreflooding experiments. Extensive laboratory research on oil recovery with salinity variation has been conducted for sandstone core plugs (Tang and Morrow, 1997; Tang and Morrow, 1999; Zhang and Morrow, 2006; Zhang et al. 2007; Lager et al. 2007; Lager et al. 2008a; Shiran and Skauge, 2012; Winoto et al. 2012). These works collectively led to developing low salinity water flooding as a potential EOR method. Changing the injection brine composition to enhance oil recovery in sandstones is a new idea, which was further validated by some field trials or pilot tests (Webb et al. 2004; McGuire et al. 2005; Lager et al. 2008b).

Research has been conducted to explore the possibility of injection brine variation in oil production for carbonate reservoirs (Strand et al. 2006; Zhang et al. 2007; Austad et al. 2008; Zhang et al. 2006; Austad et al. 2005; Puntervold et al. 2009; Gupta et al. 2011; Yildiz et al. 1999; Fernø et al. 2011). It has been shown that high salinity brines with enriched concentrations of SO_4^{2-} ions along with Ca^{2+} and Mg^{2+} ions can significantly enhance oil productions (Zhang et al. 2006).It has been shown that enhancing the concentrations of only divalent ions are beneficial. Reducing the concentrations of Na^+ and Cl^- also benefits oil production as it enhances the effectiveness of divalent ions (Puntervold et al. 2009). Mg^{2+}/Ca^{2+} ion substitution followed by SO_4^{2-} adsorption based wettability alteration (towards water wetness) has been proposed as the primary mechanism (Austad et al. 2008). Further, Advanced Ion management studies have shown that PO_4^{3-} and $B_4O_7^{2-}$ ions can also be used to increase oil production from carbonates (Gupta et al. 2011). This increase in oil production has proved to be dependent on the core plug type and initial mineral wettability (Fernø et al. 2011; Zahid et al. 2010). Nevertheless, high salinity based selective ion variation has proved to be an EOR method for carbonate core plugs which can be used to increase oil production during tertiary oil recovery.

Thereafter, it has been shown that reducing the salinity of the injection brine can lead to enhanced oil recovery for carbonate core plugs as well (Zahid et al. 2012; Yousef et al 2012; Yousef et al. 2011; Romanuka et al . 2012; Austad et al. 2011). Results from tertiary mode core flood tests showed improvements in oil recovery by about 8% with twice reduced-ionic strength seawater (Yousef et al. 2011). Subsequently, further reduction in ionic strength by 10-times led to an additional increment in oil production by 10% of OOIP (Yousef et al. 2011). Anhydrite dissolution during low salinity water flooding and availability of soluble Ca^{2+} and SO_4^{2-} has been proposed to be the primary reason behind the observed increment in oil recovery (Austad et al. 2011). Subsequently, it has been claimed that low salinity brine can cause successful EOR in carbonates if dissolvable anhydrite grains are available as a reservoir mineral. (Austad et al. 2011) Increase in oil production for low salinity water flooding into chalk core plugs containing no anhydrite grains has also been reported in literature (Zahid et al. 2012). This is contradictory to the proposed anhydrite dissolution based wettability alteration mechanism (Austad et al. 2011). Collectively, low salinity brine injection is being studied and discussed in literature to explore its fundamental mechanism and potential applicability in different reservoirs.

Both low salinity (Austad et al. 2011) and high salinity (Austad et al. 2008) water flooding has been studied in literature for carbonate coreplugs. Only low salinity water flooding with sand stone core plugs has been explored preciously in literature (Tang and Morrow, 1999). This study aims to explore the possible influence of high salinity brine composition variation on oil production from green sand cores from the North Sea.

In most previous studies, it has been observed that an increase in oil production for variation in composition and salinity of injection brine is most evident at high temperature conditions (typically above 100°C) (Strand et al. 2006). For optimum oil production, typically 130°C has been recommended to be the most suitable condition for various variations in brine flooding techniques (Puntervold et al. 2009). But not all oil reservoirs have a temperature of 130°C. It is a challenging issue to change the reservoir temperature of low temperature reservoirs being water flooded (Grabowski et al. 2005; Helgeson et al. 1993; Hubert et al. 2012; Nasr-El-Din et al. 2002; Nazina et al. 2013a; Nazina et al. 2013b; Sydansk 1982; Voordouw et al. 1996). A brine variation strate-

gy needs to be developed to particularly address the low temperature reservoirs. This study has been carried out to investigate the possibility of high salinity, ion selective SmW-EOR implementation into low temperature green sand core plugs. Herein; four different sandstone core samples from the Solsort field of the Danish North Sea have been water flooded. In two core plugs, the individual effect of Na^+ salts in the absence of Ca^{2+} and Mg^{2+} have been analyzed. In the other two core plugs, the effect of Mg^{2+} salts in the absence of Na^+ and Ca^{2+} have been analyzed. Pauses in water flooding and reinjection of more of the same brine have been found to increase oil production during low salinity water flooding (Alvarado et al. 2014). Correspondingly, several pauses of different lengths were introduced into the waterflood, to study the effect of individual brines during pauses in waterfloods. The observed oil production along with effluent brine compositions has been used to understand the potential for EOR for low temperature sandstone core plugs.

Experimental

Core Plugs

Four sandstone core plugs with similar lengths and diameters were used in the experiments. The core plugs were from the Solsort field and were provided by DONG Energy. All the samples in this study are from the same oil formation and have similar physical properties such as length, diameter, and porosity (Table 1). Their density is in the range of 2.72 – 2.74 gr/cm^3. Initial porosity of the samples is between 30 - 33%. Permeability of the samples is 156, 130, 94, and 74 mDa for D4, D7H, D3H, and D17, respectively. The specific surface was measured by BET analyses, which is 7.4, 7.4, 8, and 6.3 m2/g for D4, D7H, D3H, and D17, respectively. The specifications of used North Sea crude oil and brine injection saturation are listed in Table 2-5. Water saturation is 0.46, 0.33, 0.34, and 0.48 mD for D3H, D4, D7H, and D17respectively. The CT images (Figure 1-4*Figure 3*) and the CT numbers variation (Table 6), obtained in different stages of experiment, illustrate the homogeneity level of the samples.

Crude oil

In this study, North Sea crude oil was used for the water flooding experiments. Based on the SARA analysis, the viscosity of the crude oil was 8.83 cp and it contained 0.3% of asphaltene. Its acid number and base number were 0.09 and 2.44 (mg KOH/g oil). Acid and base numbers were measured by Metrohm 702 SM Titrino using the method developed by Fan and Buckley (modified version of ASTM D2896 for the base number titration and ASTM D664 for the acid number titration). These values are brought in Table 2. Crude oil was marked by [^{14}C] radio tracer. Radio tracer was provided by Perkin Elmer in the chemical form of stearic acid ($CH_3(CH_2)_{16}{}^{14}COOH$) (Sugiharto et al. 2009). Each one liter of North Sea crude oil was marked by 1.25 ml of solution containing ^{14}C stearic acid in toluene (7.4 MBq/ml). The doped crude oil was used to saturate the core plugs.

Core preparation

All the four core plugs were CT/scanned in their dry form to determine the variation in heterogeneity or fracture by measuring initial density. They were flooded with sequential flooding of toluene and ethanol to ensure thorough cleaning. Cleaned core plugs were dried at 90 ºC and their permeability, and porosity were measured. These data are considered as the initial core properties (Table 1). Thereafter, core plugs were water flooded with formation water (FW: Na^+: 13500; Ca^{2+}: 250; Mg^{2+}: 95; K^+:100; Cl^-: 21000) at 40 ºC and with the injection rate of 0.2 ml/min. Weighing and CT-scanning of the water saturated core plugs was performed. Successively, 5 pore volumes (PV) of crude oil was injected at the rate of 0.2 ml/min to displace the FW in the core plug and reach the irreducible water saturation and the weight and CT-scanning of the core plugs were recorded. The weight of the core plugs and their average CT-number during different stages of the experiment are presented in Table 3 and Table 6. CT-Scans along axial and perpendicular sections of the coreplugs at different stages of the experiment is presented in Figure 1-4*Figure 3*. Core plugs were aged with novel tools, by which the wettability condition of core plugs was monitored by resistivity measurements. Nuclear magnetic resonance (NMR) analyses of the coreplugs at their irreducible water saturation were conducted to investigate the wettability condition of the rock surface. These core plugs were used for water flooding experiments.

Smart waterflood

Two sets of brines were used in the core flooding experiments (Table 4). Petro-physical properties including sound velocity and electric resistivity were continuously recorded during flooding experiments. The produced fluid was collected in the effluent tubes. The amount of produced oil in each tube was measured by image analyses and by using the liquid scintillation method.

The first brine set tagged as the sodium campaign includes: *Na-Lq1*, *Na-Lq2*, *Na-Lq3*, *Na-Lq4*, and *d10NaLq1* (Table 4). *Na-Lq1* contained 0.6 m NaCl, which represents the North Sea water composition, which is currently being injected in the Solsort field. Cl^- was substituted by SO_4^{2-} in *Na-Lq2*, while the Na^+ concentration was kept constant. Keeping the Na^+ concentration constant, *Na-Lq3* contained 0.3 m NaCl and 0.15 m Na_2SO_4. *Na-Lq4* was prepared by using high concentration of Na_2SO_4 (0.75 m) and NaCl (0.6 m) to represent the high saline North Sea brine enriched by SO_4^{2-}. *d10NaLq1* (0.06 m) is made by 10 times diluting *Na-Lq1* to study the influence of injection of low salinity brine into core plugs.

The second brine set is tagged as the magnesium campaign includes: *Mg-Lq1*, *Mg-Lq2*, *Mg-Lq3*, *Mg-Lq4*, and *d10MgLq1* (Table 4). *Mg-Lq1* contained 0.3 m $MgCl_2$ which replicates the impact of Mg^{2+} enriched brine in the absence of SO_4^{2-}. Cl^- was replaced by SO_4^{2-} in *Mg-Lq2*, while the Mg^{2+} concentration was kept constant. *Mg-Lq3* contained $MgCl_2$ (0.3 m) and $MgSO_4$ (0.15 m). Finally, *Mg-Lq4* consisted of $MgCl_2$ (0.3 m) and $MgSO_4$ (0.75 m) which replicates the impact of high concentration of SO_4^{2-} and Mg^{2+}. *d10MgLq1* (0.06 m) represents the diluted sea water. Deionized water (DW) was also injected in both sodium and magnesium campaigns. The densities of the discussed brines were measured at room temperature and are shown in Table 7.

Injection sequence

Four sandstone core plugs were divided into two groups. Each group was water flooded with the same brine set, but with different injection sequences (Table 5). D3H and D7H were water flooded in the sodium campaign. D3H was initially water flooded with *Na-Lq1* for 14.38 (PV) to simulate the reservoir conditions. Water flooding was followed with *Na-Lq2*, *Na-Lq3*, and *Na-Lq4* for 10.86, 8.46, and 14.12 PV, respectively. D7H was initially water flooded with *Na-Lq2* for 10.8 PV until no additional oil was produced. The injection was continued with *Na-Lq3* and *Na-q4*, and *Na-Lq1* for 11.28, 11.32, 11.81 PV, respectively. Subsequently, *d10NaLq1* and DW were injected for 9.92 and 9.82 PV.

D4H and D17H were water flooded in the magnesium campaign. D4H was initially water flooded with *Mg-Lq1* for 16.3 PV to ensure that no additional oil was produced. Thereafter it was water flooded with *Mg-Lq2*, *Mg-Lq3*, and *Mg-Lq4* for 12.04, 10.36, and 10.36 PV, respectively. Diluted magnesium brine *(d10MgLq1*) and DW (deionized water) were injected for 11.63 and 7.97 PV, respectively. D17H was water flooded with a different injection sequence as it was initially water flooded with *Mg-Lq2* for 16.21 PV, thereafter *Mg-Lq3*, and *Mg-Lq4* were injected for 11.04 and 11.07 PV. It was finally injecting with Mg-Lq1 for 9.68 PV. Throughout the experiments, the flooding was paused at regular intervals to provide sufficient time for crude oil – brine – rock interactions. All the experiments were conducted at 60 °C with a radial pressure of 390 bar, an axial pressure of 400 bar, and a back pressure of 300 bar to simulate the reservoir condition. Coreplugs weight and CT-scan images were recorded after flooding to distinguish any possible modification in core properties (Detailed data are presented in Table 3 and 6, Figure 1-4*Figure 3*).

Chemical Analysis

Collected effluents were analyzed with ICP-OES acquired from Agilent 7700s. Nitric acid was used to dilute the samples for 10, 100, and 1000 times to figure out the concentration limit of the equipment. The brines were analyzed for 5 times to ensure the consistency of the experiments. Above 95% consistency was yielded in the obtained brine composition. Composition of various relevant ions including Na^+, Ca^{2+}, Mg^{2+}, SO_4^{2-}, CO_3^{3-} were determined at constant interval in PVI.

Results & Discussion

Core plug D3H was flooded in the sodium campaign. The oil recovery profile is plotted in Figure 9 and a detailed pressure profile is reported in Supplementary Figure 1, while the effluent brine composition is shown in Figure 5. Initially the coreplug was flooded with *Na-Lq1* to mimic the water flooding condition after injection of sea water. The brine was injected for 14.38 pore volume (PV) and the oil recovery was stabilized at 47% after 5 PV of injection. Thereafter, water flooding was paused for 5.6 hours, which resulted in a 0.05% increase in oil recovery. The flooding was continued for another 4 PV but no additional oil recovery was observed. The effluent composition during *Na-Lq1* injection was also monitored (Figure 5). No additional ions were released from the core during continued injection or during pause and reinjection of *Na-Lq1*. The effluent brine composition during brine alteration (substitution of *Na-Lq1* with *Na-Lq2*) was directly correlated to the composition of the injection brine, thus indicating that ion substitution did not lead to any multiple ion exchanges on the mineral surface. The experiment was continued with the injection of *Na-Lq2*. No additional oil was observed after 10.86 PV of injection of *Na-Lq2*. Third injection brine, *Na-Lq3*, was injected after 7.2 hours of pause in the experiment. Oil recovery gradually increased after 4 PV of injection but remained unchanged for the other 4 PV of injection. Finally, *Na-Lq4* was injected for 14.12 PV following a pause of 36.93 hrs. No additional oil was observed in this step even though an additional 12.68 hours pause was introduced into the water flood. Thus variation in Na salt composition for high salinity brines showed a minor increment in oil recovery by 1.5% of OOIP. The first pause in brine injection led to a successful EOR but later introduction of multiple pause in different water floods showed no additional oil recovery.

Core plug D7H was flooded with sodium campaign but in a different injection sequence in comparison with core plug D3H (Figure 10). The oil recovery profile for D7H is plotted in Figure 10 and a detailed pressure profile is reported in Supplementary Figure 2, while the effluent brine composition is shown in Figure 6. It was initially flooded with *Na-Lq2* to investigate the initial oil recovery with sodium sulfate. *Na-Lq2* was injected for 10.8 PV and oil recovery was stabilized after 5 PV at 13.68% of OOIP. Water breakthrough during injection was not observed, since only a small fraction of the existing oil was eventually produced. It is important to scrutinize the efficiency of the water flooding for the observed low oil recovery in this case. The effluent brine composition was analyzed during the initial brine injection. Higher concentrations of Na^+ and Cl^- than in *Na-Lq1* during the first PV of brine injection indicated that the formation water in the core plug was removed from the pore space. Thus the coreplug was well flooded and the injection water did not pass through the core plug along the axial surface. The observed significantly low oil recovery during *Na-Lq2* injection remains unexplained. Injection was continued after 13.3 hours of pause, with injecting of *Na-Lq3*. It was injected for 11.28 PV and no additional oil was recovered. The injection was paused for 104.6 hours and *Na-Lq4* with high concentration of sodium chloride and sodium sulfate was injected. Oil recovery increased for more than 1.06% OOIP in the beginning of injection sequence. This was the first major pause that was introduced in the injection of smart water floods; which also led to a noticeable increment in oil recovery. Injection was continued for 11.32 PV and no additional oil recovery was observed even after 15.58 hours pause during injection sequence. Thereafter *Na-Lq1* was injected for 11.81 PV after a pause of 15.8 hours. Multiple pauses of 18.8 hours and 13.5 hours were also introduced during *Na-Lq1* flooding. But no increment in oil recovery associated with brine alteration or pauses injection was observed. To explore the potential of low salinity water flooding, the

salinity of the injection brine was thereafter reduced. Injection of *d10NaLq1* for 9.92 PV following a pause of 2 hours and introduction of two additional pauses of 16.6 hours and 16.8 hours did not lead to any additional oil recovery. Low salinity brines have consistently been shown to increase oil production from sandstone core plugs and reservoirs (Webb et al. 2004; McGuire et al. 2005; Lager et al. 2008b). It was therefore expected to see a larger increment in oil recovery in this case. The exact reason behind the lack of successful EOR for low salinity *d10NaLq1* injection remains a matter of further research. Finally DW was injected for 9.82 PV. No additional oil was observed during this injection performed with several pauses. For the D7H core plug, the first major pause in flooding led to an additional oil recovery of 1.06% of OOIP, but the ultimate oil recovery remained unexpectedly low at 14.94% of OOIP. The effluent brine composition was identical to the injection brine. No active multiple ion exchange on the mineral surface could be identified. No increment in oil production for low salinity brine injection and low oil yield before initial water breakthrough were unexpected observations and the associated reason remains unexplained.

Core plug D4H was flooded in the magnesium campaign. The oil recovery profile for core plug D4H is plotted in Figure 11 and a detailed pressure profile is reported in Supplementary Figure 3, while the effluent brine composition is shown in Figure 7. First injection step was injection of *Mg-Lq1* (Table 4). It was injected for 16.3 PV and oil recovery was stabilized at 45% of OOIP after 4.5 PV of injection, but remained unchanged until the end of injection of *Mg-Lq1*. Injection was paused for 3.8 hours and 0.25 hours during this step but no additional oil recovery was observed. The effluent brine concentration also did not show noticeable variation throughout the waterflood. Afterwards, *Mg-Lq2* was injected after 20.3 hours of pause. It reflects the effect of substituting magnesium chloride with magnesium sulfate in constant magnesium concentration. Oil recovery was increased for more than 1% of OOIP after injection was started. No release of divalent cations because of desorption of Mg^{2+} from mineral surface (as proposed in the wettability alteration mechanism (Austad et al. 2010)) was observed during the increment in oil recovery. No additional oil recovery was observed after 12.04 PV of injection with a pause of 76.6 hours during injection. Continued increment in oil recovery following multiple pauses was not observed, on this point the green sand core plug behaved different from chalk core plugs,. Neither dissolution/attrition of mineral grain was observed in the effluent. Injection was continued by injecting *Mg-Lq3*, *Mg-Lq4*, *d10MgLq1*, and DW for 10.36, 10.36, 11.63, and 7.97 PV, respectively. Pauses varying from 1.6 hours to 132.6 hours were made during the injection, but no additional oil was recovered. This is similar to the flooding of core plug D7H with sodium brines).

Core plug D17H was water flooded in the magnesium campaign but with a different injection sequence compared to core plug D4H (Table 5). The oil recovery profile for core plug D17H is plotted in Figure 12 and a detailed pressure profile is reported in Supplementary Figure 16. It was initially water flooded by *Mg-Lq2*. It was injected for 16.21 PV and oil recovery was stabilized at 36% after 3.5 PV. There were two pauses for 18.3 and 86.1 hours during this injection step. Each of the pauses was followed by an increase in oil recovery by more than 1%. This observed increment in oil recovery following multiple pauses was only observed during *Mg-Lq2* water flooding in D17H. Injection was continued after 13.8 hours pause, by injecting *Mg-Lq3* for 11.04 PV. The only increase in oil recovery is right after 12.9 hours of pause, while it remained unchanged in other time intervals. Thereafter *Mg-Lq4* was injected after 90.1 hours of pause for 11.07 PV. In contrast to previous core plugs, oil recovery increased gradually for 3% over 9 PV of injection. A pause for 131.4 hours did not have a major effect on the rate of increase in oil recovery. Finally *Mg-Lq1* was injected after 14.9 hours of pause and was continued for 9.68 PV. There was a pause for 69.61 hours but the oil recovery remained unchanged.

Comparative Discussion

Comparing D17H waterflooding with D4H, it is observed that following multiple pauses, the increment in oil recovery during D17H flooding is much higher (with EOR of 4.22% of OOIP) than that observed during flooding of D4H (with EOR of 2.1% of OOIP). Both the core plugs were aged and flooded with the same brines but with different sequences (Table 5). This goes to show that not just the brine sequence but also the injection pattern played a prominent role in the overall increment in oil recovery. After initial stabilization of oil production, only a single increment in oil recovery with D4H was observed following the injection of *Mg-Lq2* after the first major pause in the water flood. During injection of *Mg-Lq2* into core plug D17H, multiple pauses were made and additional oil recovery was observed. Introduction of *Mg-Lq3* and *Mg-Lq4* into the D4H core plug did not produce any additional oil during injection or after pause and reinjection. The same brines showed consistent increment in oil recovery after pause/reinjection in the D17H water flooding. Thus, the injection sequence affected oil recovery considerably. The effluent brine composition during both water floods did not show any increase or decrease in concentration of selective ions (Figure 7 and Figure 8). This indicated that no mineral surface adsorption/desorption of ions took place during the water flood. The observed increment in oil recovery cannot be associated to the wettability alteration mechanism. In chalk core plugs an increment in Ca^{2+} and CO_3^{2-} ion concentrations in the effluent (Paper XI: figure 6-9) indicated calcite attrition. Green sand core plugs contain no carbonate so a similar increment in Ca^{2+} and CO_3^{2-} ion concentrations was neither expected nor observed. The green sand core plugs contained minor amounts of kaolinite clay fines which can also mobilize and release trapped oil from the mineral surface.

CT-scans were conducted to study the movement of clay particles in the core plugs during water flooding (Figures 1-4). CT scans were performed for the dry core plug, to study the overall heterogeneity of the core plug and identify the initial grain and pore volume separately. CT-scan measurement was subsequently conducted after water saturation and oil saturation (irreducible water saturation) of the core plug. This scan was performed to learn about the oil and water spread in the pore volume. A CT-scan was also performed after water flooding to identify the movement of any kaolinite grains in the core plug, by comparing it to the core plug density in the dry form. The obtained CT-scan images during all four stages of water flooding are shown in Figures 1-4. All

core plugs had significantly high CT-numbers at the radial and axial surfaces during all the different stages of flooding. This is unexpected and could have been an end effect during measurements. Therefore the surface end was ignored. Also the CT-scans during the initial dry state and the state after flooding were not axially aligned. Therefore the two average CT-numbers within the back circle (as shown in Figure 1-4) were calculated for comparison. The average CT-numbers along the radial and axial sections are reported in Table 6. When comparing dry and water wet coreplugs, it is observed that the average CT number, which is related to the average density of the core plug, increased by around 300 points as air was replaced by water in the pore space. Thereafter a decrease by 20 points was observed when oil water introduced (as water was partially replaced by oil). After flooding, an increment in average CT-number is expected (since oil is replaced by water). But no selective trend is observed.

In the CT-scan analysis of D3H core plug (Na campaign) an increment by 19 machine units was observed (comparing after flooding CT-scan to Oil saturated core plugs), thus indicating the replacement of oil by water. Also the weight of the sample after water flooding (122.82 g) was more than that during oil saturation (122.82 g) (Table 3). This indicated the expected replacement of oil by injected brine in the coreplug. No major dissolution/ adsorption/precipitation may have taken place as it would have been reflected in the CT-scan numbers and in the weight of the coreplug.

In the D7H core plug (Na campaign) the average CT-number of the core plug showed a decrease by 20 points in both axial and radial measurements. The D7 core plug did not produce much oil. A decrease in average density was therefore not expected. This further shows that release of mineral grains from the coreplug must have taken place during the water flood. The weight of the sample after water flooding (119.21 g) was less than that during oil saturation (119.73. This indicates release of mineral grains during the waterflood.

In the D4H core plug (Mg campaign) the average CT-numbers show no major difference between the S_{irw} conditions and the after flooding condition, even though a significant amount of oil was produced. Along with the release of low density oil and the replacement of oil with injected brine, a fraction of mineral grain must have been produced to keep the average CT numbers constant. CT-scan analysis of both axial and radial sections of the coreplug showed the same trend. The weight of the coreplug after flooding (123.62g) was less than that in the S_{irw} condition (124.4 g) and significantly less than in the S_w condition (125.73 g). This gives further evidence that the Mg brine flooding was associated with the release of mineral grains from the core plug. The exact pore volume of fines production cannot be identified from these measurements.

In the D17H core plug (Mg Campaign) the average CT-number of the core plug showed a decrease by 30 points in both axial and radial measurements. The weight of the sample dropped by 0.75 grams, even though a significant fraction of the oil was produced (40.8 % of OOIP). Although an increment in the weight of the core plug and in the average CT-number is expected with replacement of low density oil with higher density brine, a considerable decrease was observed through the various measurements. This also provides evidence that the smart water floods were associated with release of mineral grains fines form the core plug. The exact pore volume of fines production remains unidentified from these measurements.

These studies collectively show that fines production takes place during smart water flooding in green sand core plugs. The amount of fines production and oil recovery remains dependent on the injection brine composition. Previously, kaolinite movement within sandstone coreplugs has been observed during low salinity water flood using SEM and Micro-CT imaging. In the same line, CT-scan images where attempted to be further processed, so that movement of individual grains can be identified. But the obtained resolution was not good enough to differentiate between the grain volume and pore volume. Thus the exact location in the core plug and the associated mineral which was produced remains unexplored in this study.

There were several pauses during the smart water flooding experiments. Their duration varied from 0.25 hour to more than 100 hours. It was observed that the first major pause in water flooding resulted in an increase in oil production. This increase is independent of injected brine and was not repeated in later pauses. The first major pause in D3H core flooding was during injection of *Na-Lq1* for 5.6 hours, which resulted in an increase in oil production. The increase in oil production can be correlated to the pause in injection because oil production was stabilized prior to the pause. In the core plug D7H, there was a considerable increase in oil production after 104.6 hours of pause. Although this pause was not the first pause, it was the first major pause in the injection sequence. Similarly, in core plug D4H, oil recovery increased after 20.3 hours of pause. It was the first major pause, which occurred after two shorter pauses with the duration of 3.8and 0.25 hours. Core plug D17H, reflects higher potential because oil recovery increased considerably after the first two major pauses. This increase in oil production was replicated in later major pauses.

These low temperature green sand water floodings were similar to the chalk core plug floodings using the same injection brine sequences and temperatures (to be submitted, Chakravarty et al. 2016: Paper XII). In both cases, an increment in oil recovery on variation in composition of individual (Na or Mg) brines was observed. The injection sequence has been shown to influence both ultimate oil recovery and EOR for both chalk and green sand core plugs. Pauses/resumptions of brine injection have been shown to positively influence oil production in both sets of water flooding. An increment in oil recovery for multiple pauses/reinjection was observed for all 4 chalk core plugs. Increment in oil recovery after multiple pauses in green sand core plugs was only observed when *Mg-Lq2* was the first brine injected. The observed increment in oil recovery during multiple pauses was up to 17.8 % of OOIP for Mg brines and11.7% of OOIP for Na brines in chalk reservoirs, while green sand analogs showed an increment in oil recovery of only 4.1% of OOIP and 1.5% of OOIP for Mg and Na brines respectively. The observed increment in oil recovery

after pauses was found to be consistently associated with production of calcite fines from the chalk reservoir core plugs. Evidence of fines production was observed during flooding of green sand core plugs as well but a direct correlation to production data was not possible. During water flooding in chalk reservoir core plugs the decrease in weight between oil saturated and after flooding state (an indication of fines formation) was around 4-7grams, while the same value with green sand core plugs was around 0.2-0.8 grams. Thus the amount of fines production and observed EOR with chalk core plugs was significantly larger than with green sand core plugs. This trend further supports the correlation between fines formation and oil recovery.

Conclusion:

Four green sand core plugs were flooded with different sodium and magnesium brines. It was observed that oil recovery increased after the first major pause of the injection and subsequent resumption of the injection. It can be interpreted as the necessity to provide sufficient time for crude oil- brine- rock interactions. This recovery was not replicated in later pauses, which indicates the limited reaction capability of pore surfaces in green sand reservoir rock. The composition of the injected brine was shown to influence the increment in oil recovery. For Mg brines an increased EOR of 4.1% of OOIP was observed while Na brines only led to an increase of 1.5 % of OOIP. The exact effect of individual ions remains a topic of further investigation. CT-scan analysis and weighing of the core plugs show production of fines from the core plugs during water flooding. From the available data, an exact correlation between oil production and fine mobilization was not observed. The effluent brine composition showed that increments in oil recovery were not associated with adsorption or desorption of any divalent ions. It was observed that injecting low salinity brines and deionized water after high salinity brines did not increase the oil recovery. This study shows that smart variation in brine composition and injection strategy can lead to increments in oil production for low temperature green sand core plugs.

References:

- Alvarado, V., Moradi Bidhendi, M., Garcia-Olvera, G., Morin, B., & Oakey, J. S. (2014, April). Interfacial Visco-Elasticity of Crude Oil-Brine: An Alternative EOR Mechanism in Smart Waterflooding. In SPE Improved Oil Recovery Symposium. Society of Petroleum Engineers.
- Austad, T., RezaeiDoust, A., & Puntervold, T. (2010, January). Chemical mechanism of low salinity water flooding in sandstone reservoirs. In *SPE improved oil recovery symposium*. Society of Petroleum Engineers.
- Austad, T., Shariatpanahi, S. F., Strand, S., Black, C. J. J., & Webb, K. J. (2011). Conditions for a low-salinity enhanced oil recovery (EOR) effect in carbonate oil reservoirs. *Energy & fuels*, *26*(1), 569-575.
- Austad, T., Strand, S., Høgnesen, E. J., & Zhang, P. (2005). Seawater as IOR fluid in fractured chalk. SPE, 93000, 2-4.
- Austad, T., Strand, S., Madland, M. V., Puntervold, T., & Korsnes, R. I. (2008). Seawater in chalk: An EOR and compaction fluid. SPE Reservoir Evaluation & Engineering, 11(04), 648-654.
- Blomberg, J. R. (1998, January). History and potential future of Improved Oil Recovery in the Appalachian Basin. In *SPE Eastern Regional Meeting*. Society of Petroleum Engineers.
- Fan, T., & Buckley, J. S. (2006, January). Acid number measurements revisited. In *SPE/DOE Symposium on Improved Oil Recovery*. Society of Petroleum Engineers.
- Fernø, M. A., Grønsdal, R., Åsheim, J., Nyheim, A., Berge, M., & Graue, A. (2011). Use of Sulfate for Water Based Enhanced Oil Recovery during Spontaneous Imbibition in Chalk. Energy & fuels, 25(4), 1697-1706.
- Grabowski, A., Nercessian, O., Fayolle, F., Blanchet, D., & Jeanthon, C. (2005). Microbial diversity in production waters of a low-temperature biodegraded oil reservoir. *FEMS Microbiology Ecology*, *54*(3), 427-443.
- Gupta R., Smith G. G., Hu L., Willingham T., Cascio M. L. Shyeh J. J., &Harris C. R. (2011, January). Enhanced Waterflood for Carbonate Reservoirs-Impact of Injection Water Composition. In SPE Middle East Oil and Gas Show and Conference. Society of Petroleum Engineers.
- Helgeson, H. C., Knox, A. M., Owens, C. E., & Shock, E. L. (1993). Petroleum, oil field waters, and authigenic mineral assemblages Are they in metastable equilibrium in hydrocarbon reservoirs. *Geochimica et Cosmochimica Acta*, *57*(14), 3295-3339.
- Hubert, C. R., Oldenburg, T. B., Fustic, M., Gray, N. D., Larter, S. R., Penn, K., & Voordouw, G. (2012). Massive dominance of Epsilonproteobacteria in formation waters from a Canadian oil sands reservoir containing severely biodegraded oil. *Environmental microbiology*, *14*(2), 387-404.
- Lager, A., Webb, K. J., & Black, C. J. J. (2007, April). Impact of brine chemistry on oil recovery. In *IOR 2007-14th European Symposium on Improved Oil Recovery*.
- Lager, A., Webb, K. J., Black, C. J. J., Singleton, M., & Sorbie, K. S. (2008a). Low Salinity Oil Recovery-An Experimental Investigation1.*Petrophysics*, *49*(01).
- Lager, A., Webb, K. J., Collins, I. R., & Richmond, D. M. (2008b, January). LoSal enhanced oil recovery: Evidence of enhanced oil recovery at the reservoir scale. In *SPE Symposium on Improved Oil Recovery*. Society of Petroleum Engineers.
- Nasr-El-Din, H. A., Lynn, J. D., Hashem, M. K., & Bitar, G. (2002, January). Field Application of a Novel Emulsified Scale Inhibitor System to Mitigate Calcium Carbonate Scale in a Low Temperature, Low Pressure Sandstone Reservoir in Saudi Arabia. In *SPE Annual Technical Conference and Exhibition*. Society of Petroleum Engineers.

- Nazina, T. N., Pavlova, N. K., Tatarkin, Y. V., Shestakova, N. M., Babich, T. L., Sokolova, D. S., & Belyaev, S. S. (2013a). Microorganisms of the carbonate petroleum reservoir 302 of the Romashkinskoe oilfield and their biotechnological potential. *Microbiology*, *82*(2), 190-200.
- Nazina, T. N., Shestakova, N. M., Pavlova, N. K., Tatarkin, Y. V., Ivoilov, V. S., Khisametdinov, M. R., & Belyaev, S. S. (2013). Functional and phylogenetic microbial diversity in formation waters of a low-temperature carbonate petroleum reservoir. *International Biodeterioration & Biodegradation*, *81*, 71-81.
- Puntervold, T., Strand, S., & Austad, T. (2009). Coinjection of seawater and produced water to improve oil recovery from fractured North Sea chalk oil reservoirs. Energy & fuels, 23(5), 2527-2536.
- Romanuka, J., Hofman, J., Ligthelm, D. J., Suijkerbuijk, B., Marcelis, F., Oedai, S., ... & Austad, T. (2012, January). Low salinity EOR in carbonates. In *SPE Improved Oil Recovery Symposium*. Society of Petroleum Engineers.
- Shaker Shiran, B., & Skauge, A. (2012, January). Wettability and oil recovery by low salinity injection. In *SPE EOR Conference at Oil and Gas West Asia*. Society of Petroleum Engineers.
- Strand, S., Høgnesen, E. J., & Austad, T. (2006). Wettability alteration of carbonates—Effects of potential determining ions (Ca2+ and SO42−) and temperature. Colloids and Surfaces A: Physicochemical and Engineering Aspects, 275(1), 1-10.
- Sugiharto, S., Su'ud, Z., Kurniadi, R., Wibisono, W., & Abidin, Z. (2009). Radiotracer method for residence time distribution study in multiphase flow system. Applied Radiation and isotopes, 67(7), 1445-1448.
- Sydansk, R. D. (1982). Elevated-Temperature Caustic/Sandstone Interaction: Implications for Improving Oil Recovery (includes associated papers 11348 and 11548). *Society of Petroleum Engineers Journal*, *22*(04), 453-462.
- Tang, G. Q., & Morrow, N. R. (1997). Salinity, temperature, oil composition, and oil recovery by waterflooding. *SPE Reservoir Engineering*, *12*(04), 269-276.
- Tang, G. Q., & Morrow, N. R. (1999). Influence of brine composition and fines migration on crude oil/brine/rock interactions and oil recovery. *Journal of Petroleum Science and Engineering*, *24*(2), 99-111.
- Voordouw, G., Armstrong, S. M., Reimer, M. F., Fouts, B., Telang, A. J., Shen, Y., & Gevertz, D. (1996). Characterization of 16S rRNA genes from oil field microbial communities indicates the presence of a variety of sulfate-reducing, fermentative, and sulfide-oxidizing bacteria. *Applied and Environmental Microbiology*, *62*(5), 1623-1629.
- Webb, K. J., Black, C. J. J., & Al-Ajeel, H. (2004). Low Salinity Oil Recovery-Log-Inject-Log. Paper SPE 89379, SPE. In *DOE Symposium on Improved Oil Recovery, Oklahoma*.
- Winoto, W., Loahardjo, N., Xie, S. X., Yin, P., & Morrow, N. R. (2012, January). Secondary and tertiary recovery of crude oil from outcrop and reservoir rocks by low salinity waterflooding. In *SPE Improved Oil Recovery Symposium*. Society of Petroleum Engineers.
- Yildiz, H. O., & Morrow, N. R. (1996). Effect of brine composition on recovery of Moutray crude oil by waterflooding. *Journal of Petroleum science and Engineering*, *14*(3), 159-168.
- Yildiz, H. O., Valat, M., & Morrow, N. R. (1999). Effect of brine composition on wettability and oil recovery of a Prudhoe Bay crude oil. Journal of Canadian Petroleum Technology, 38 (01).
- Yousef, A. A., Al-Saleh, S. H., Al-Kaabi, A., & Al-Jawfi, M. S. (2011). Laboratory investigation of the impact of injection-water salinity and ionic content on oil recovery from carbonate reservoirs. *SPE Reservoir Evaluation & Engineering*, *14*(05), 578-593.
- Yousef, A. A., Al-Saleh, S., & Al-Jawfi, M. S. (2012, January). Improved/enhanced oil recovery from carbonate reservoirs by tuning injection water salinity and ionic content. In *SPE Improved Oil Recovery Symposium*. Society of Petroleum Engineers.
- Zahid, A., Stenby, E. H., & Shapiro, A. A. (2012, January). Smart Waterflooding (High Sal/Low Sal) in Carbonate Reservoirs. In *SPE Europec/EAGE Annual Conference*. Society of Petroleum Engineers.
- Zahid, A., Stenby, E., & Shapiro, A. (2010, June). Improved Oil Recovery in Chalk–Wettability Alteration or Something Else?(SPE-131300). In 72nd EAGE Conference & Exhibition.
- Zhang, P., & Austad, T. (2006). Wettability and oil recovery from carbonates: Effects of temperature and potential determining ions. Colloids and Surfaces A: Physicochemical and Engineering Aspects, 279(1), 179-187.
- Zhang, P., Tweheyo, M. T., & Austad, T. (2007). Wettability alteration and improved oil recovery by spontaneous imbibition of seawater into chalk: Impact of the potential determining ions Ca^{2+}, Mg^{2+}, and SO_4^{2-}. Colloids and Surfaces A: Physicochemical and Engineering Aspects, 301(1), 199-208.
- Zhang, Y., & Morrow, N. R. (2006, January). Comparison of secondary and tertiary recovery with change in injection brine composition for crude-oil/sandstone combinations. In *SPE/DOE Symposium on Improved Oil Recovery*. Society of Petroleum Engineers.
- Zhang, Y., Xie, X., & Morrow, N. R. (2007, January). Waterflood performance by injection of brine with different salinity for reservoir cores. In *SPE Annual Technical Conference and Exhibition*. Society of Petroleum Engineers.

Tables:

Table 1 : Physical and petro-physical properties of core plugs

Coreplug	Length	Diameter	Porosity	Permeability	Gas Density	Pore Volume	S_{wir}	S_o
	mm	mm		mD	g/cm3	cm^3		
D4-Mg	50.61	38.23	0.32	156	2.74	18.59	0.33	0.67
D17-Mg	50.29	38.03	0.32	74	2.73	18.27	0.48	0.52
D3H-Na	49.43	38.21	0.3	94	2.72	17.01	0.46	0.54
D7-Na	49.46	38.15	0.33	130	2.72	18.55	0.34	0.66

Table 2 : North Sea Crude oil properties

Crude Oil	Acid Number	Base Number	Asphaltene	Viscosity
North Sea	(mg KOH/g oil)	(mg KOH/g oil)	(%)	(cp)
	0.09	2.44	0.3	8.83

Table 3: Recorded weight of core plugs at different stages of water flooding

Weight of coreplug (g)	Dry	Water saturated	Oil Saturated	After Flooding
D4-Mg	107.65	125.73	124.40	123.62
D17-Mg	104.83	123.25	122.10	121.35
D3H-Na	107.38	123.48	122.17	122.82
D7-Na	102.01	121.91	119.73	119.21

Table 4: Composition of brines in sodium campaign and magnesium campaign

Na brines mol/kg H_20	NaCl	Na_2SO_4	Total ions	Mg brines mol/kg H_20	$MgCl_2$	$MgSO_4$	Total ions
NaLq1	0.6	0	1.2	MgLq1	0.3	0	1.2
NaLq2	0	0.3	1.2	MgLq2	0	0.3	1.2
NaLq3	0.3	0.15	1.2	MgLq3	0.15	0.15	1.2
NaLq4	0.6	0.75	4.2	MgLq4	0.3	0.75	4.2
d10NaLq1	0.06	0	0.12	d10MgLq1	0.03	0	0.12

Table 5: Sequence of brine injection in four greensand core plugs

Coreplug	Injection sequence						
D3H-Na	FW	Na-Lq1	Na-Lq2	Na-Lq3	Na-Lq4		
D7H-Na	FW	Na-Lq2	Na-Lq3	Na-Lq4	Na-Lq1	d10NaLq1	DW
D4-Mg	FW	Mg-Lq1	Mg-Lq2	Mg-Lq3	Mg-Lq4	d10Lq1Mg	DW
D17-Mg	FW	Mg-Lq2	Mg-Lq3	Mg-Lq4	Mg-Lq1	DW	

Table 6: Recorded average CT-Number of radial and axial sections of core plugs at different stages of water flooding. The measurements are for core plugs at their dry condition, water saturated condition (Sw), irreducible water saturation (Sirw), after water flooding (AF).

Flooded Coreplug	Average CT-Number							
	Radial Section				Axial Section			
	Dry	Sw	Sirw	AF	Dry	Sw	Sirw	AF
D3	1499	1809	1789	1808	1586	1884	1864	1876
D7	1381	1702	1696	1679	1457	1772	1751	1733
D4	1433	1745	1726	1729	1507	1822	1795	1793
D17	1402	1722	1697	1668	1479	1798	1770	1738

Table 7: Density of the injection brines at ambient condition

Na salts	FW	Na-Lq1	Na-Lq2	Na-Lq3	Na-Lq4	d10NaLq1
Density(g/cm3)	1.063	1.035	1.043	1.039	1.142	1.003
Viscosity (cp)						
Mg Salts		Mg-Lq1	Mg-Lq2	Mg-Lq3	MgLq4	d10MgLq1
Density(g/cm3)		1.029	1.036	1.032	1.119	1.003
Viscosity (cp)						

Figures:

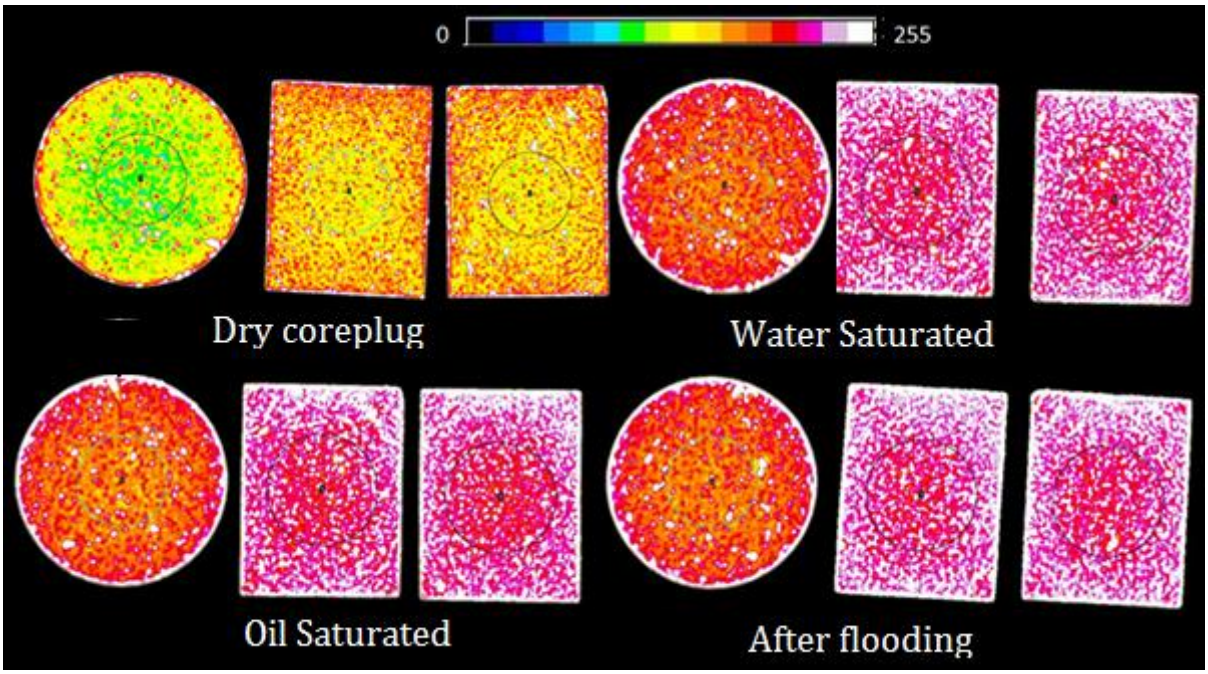


Figure 1: CT-Scan images along axial and perpendicular radial sections of D3H core plug at different stages of experiment.

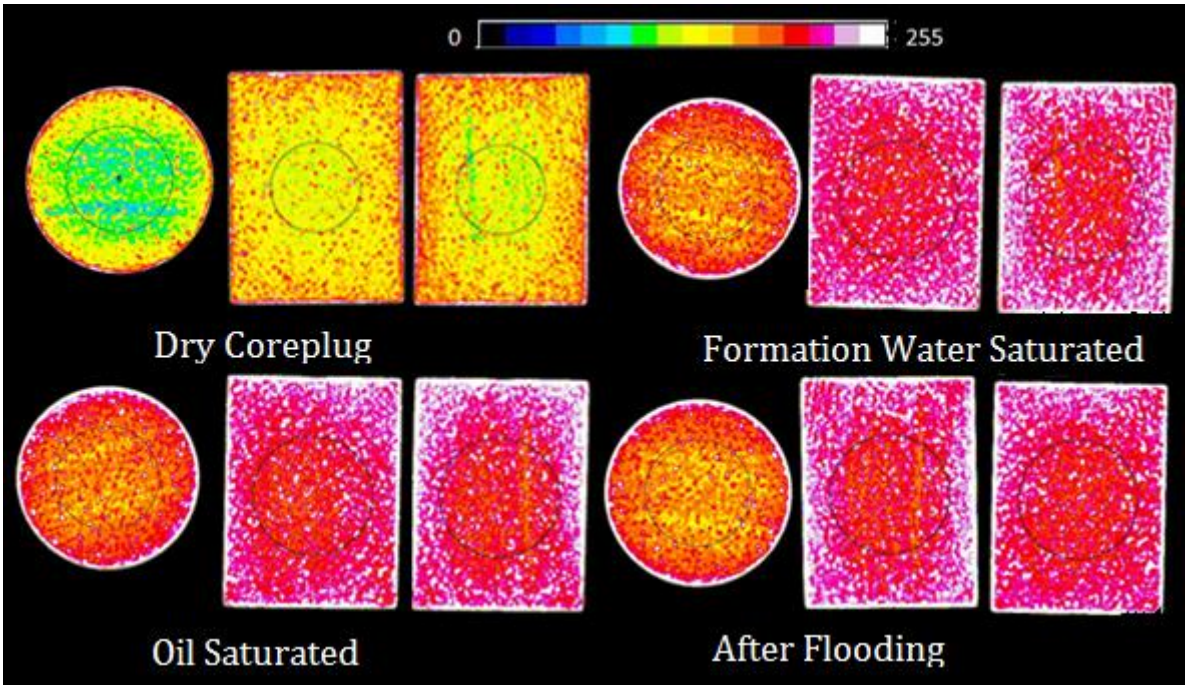


Figure 2: CT-Scan images along axial and perpendicular radial sections of D4H core plug at different stages of experiment.

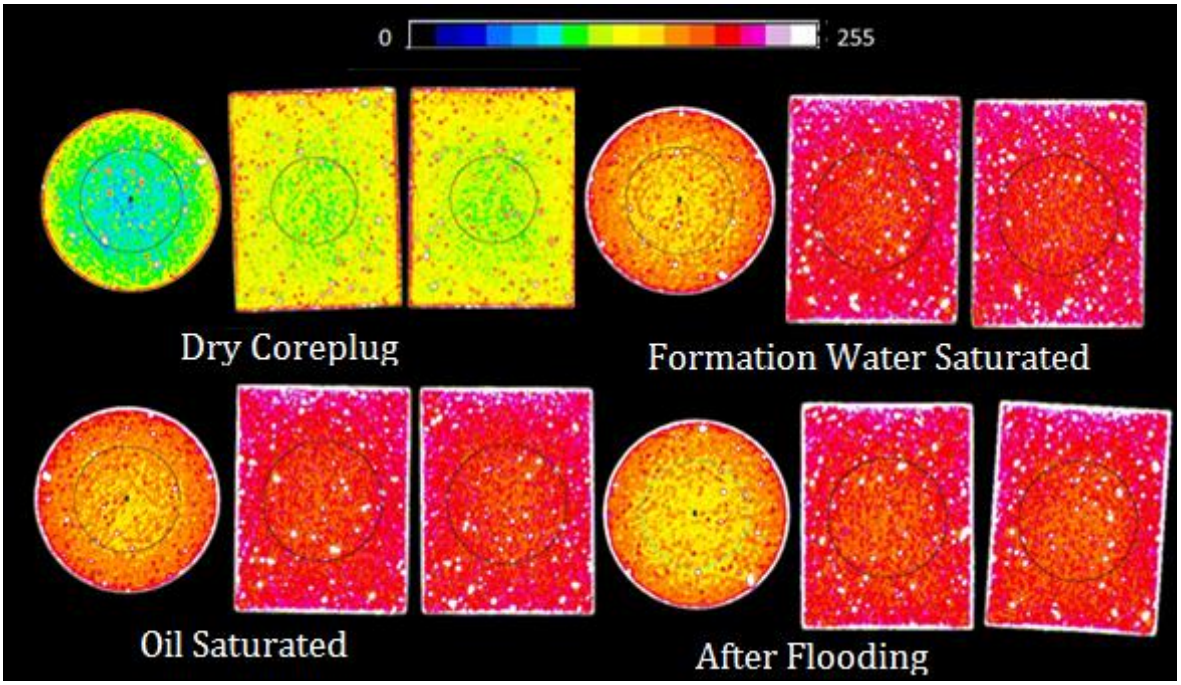


Figure 3: CT-Scan images along axial and perpendicular radial sections of D7H core plug at different stages of experiment.

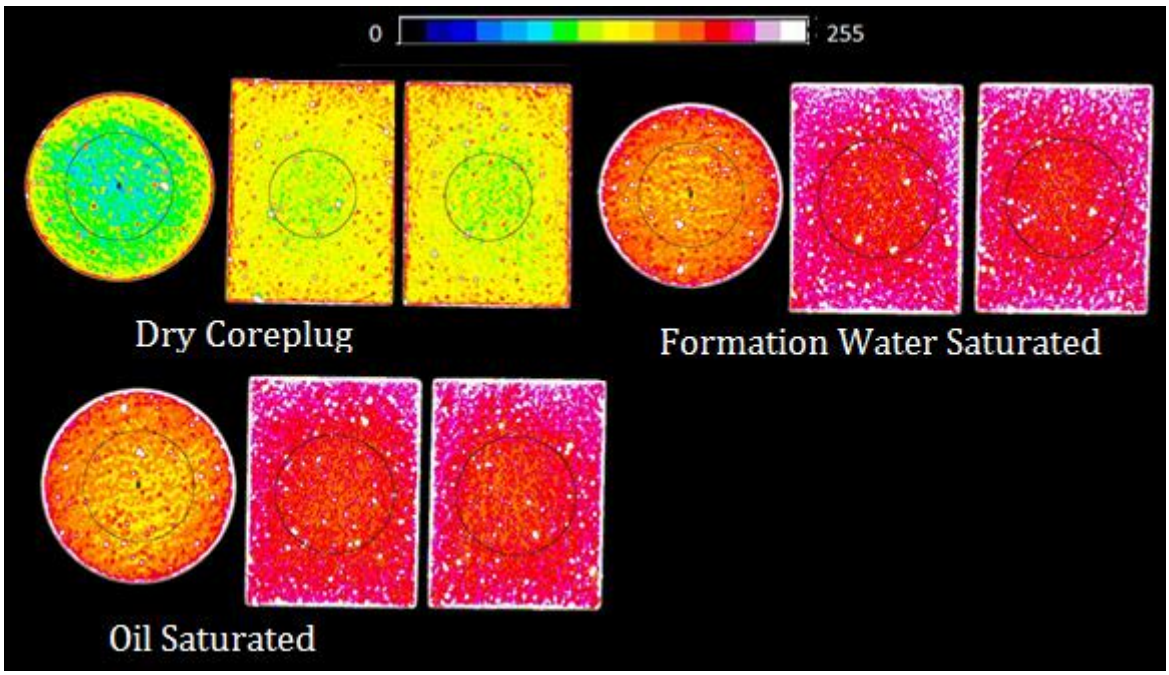


Figure 4: CT-Scan images along axial and perpendicular radial sections of D17H core plug at different stages of experiment.

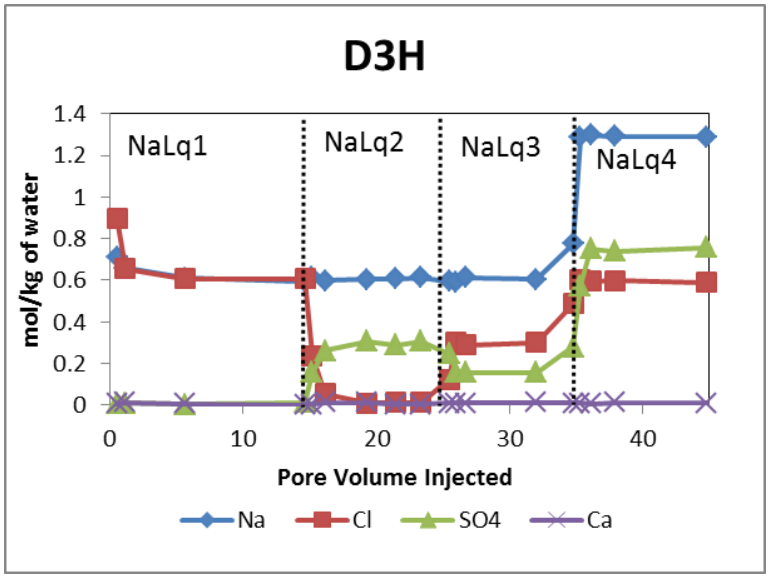


Figure 5: Composition of effluent brines from Core plug D3H vs Pore Volume for injection of sodium campaign.

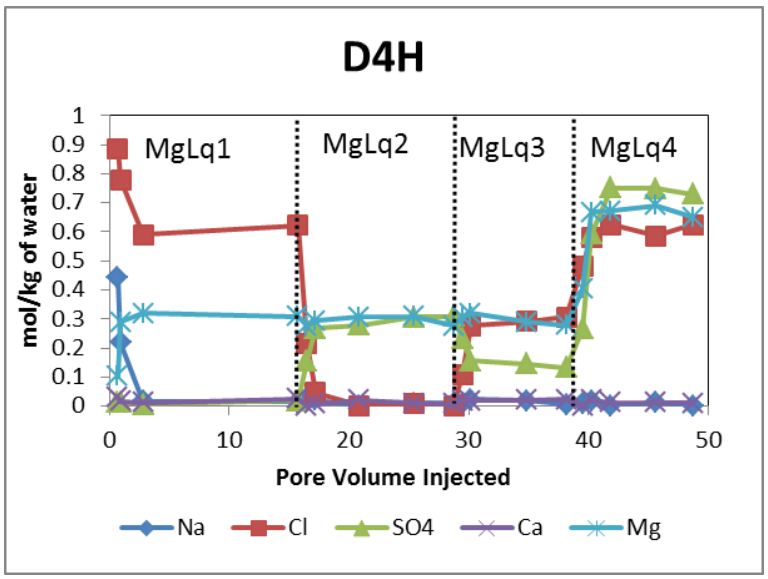


Figure 6: Composition of effluent brines from Core plug D4H vs Pore Volume for injection of magnesium campaign.

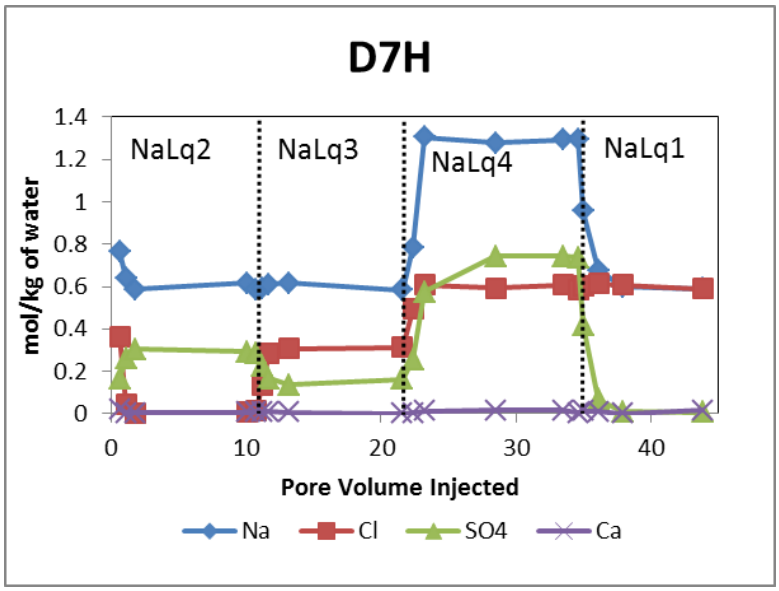


Figure 7: Composition of effluent brines from Core plug D3H vs Pore Volume for injection of sodium campaign.

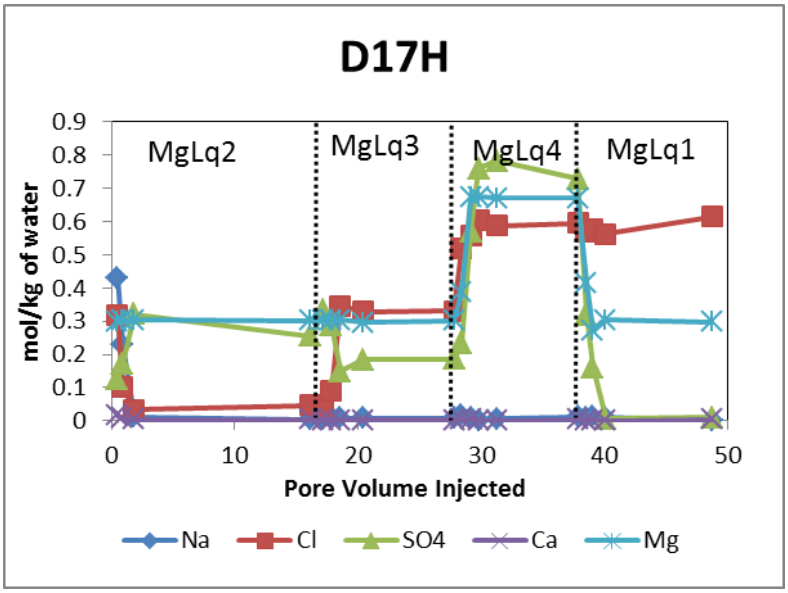


Figure 8: Composition of effluent brines from Core plug D3H vs Pore Volume for injection of magnesium campaign.

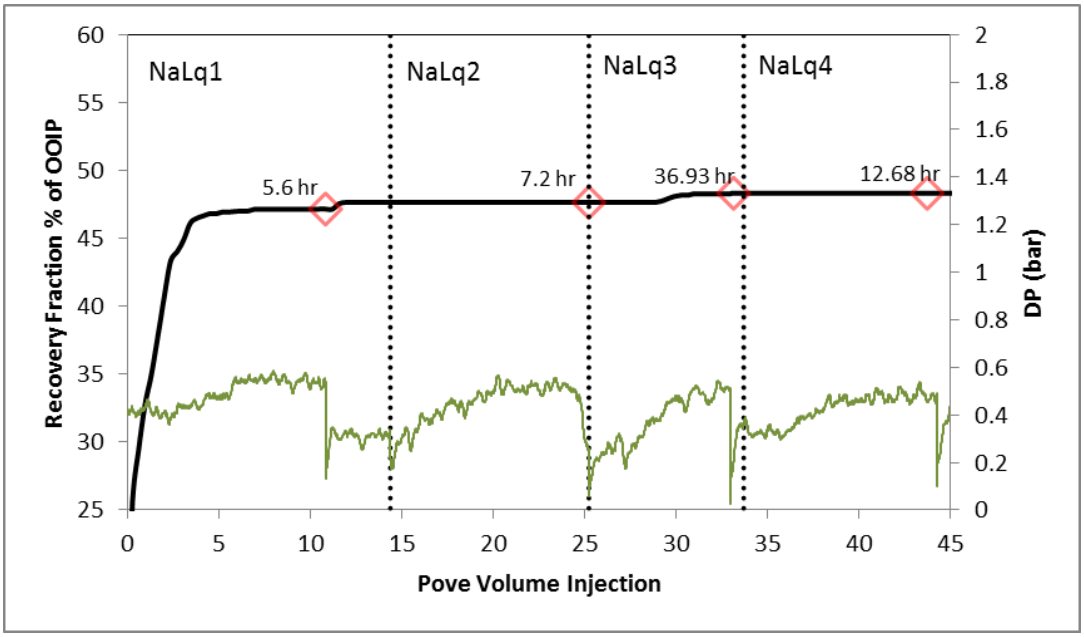


Figure 9: Observed oil recovery and differential pressure across the D3H core plug for injection of sodium campaign.

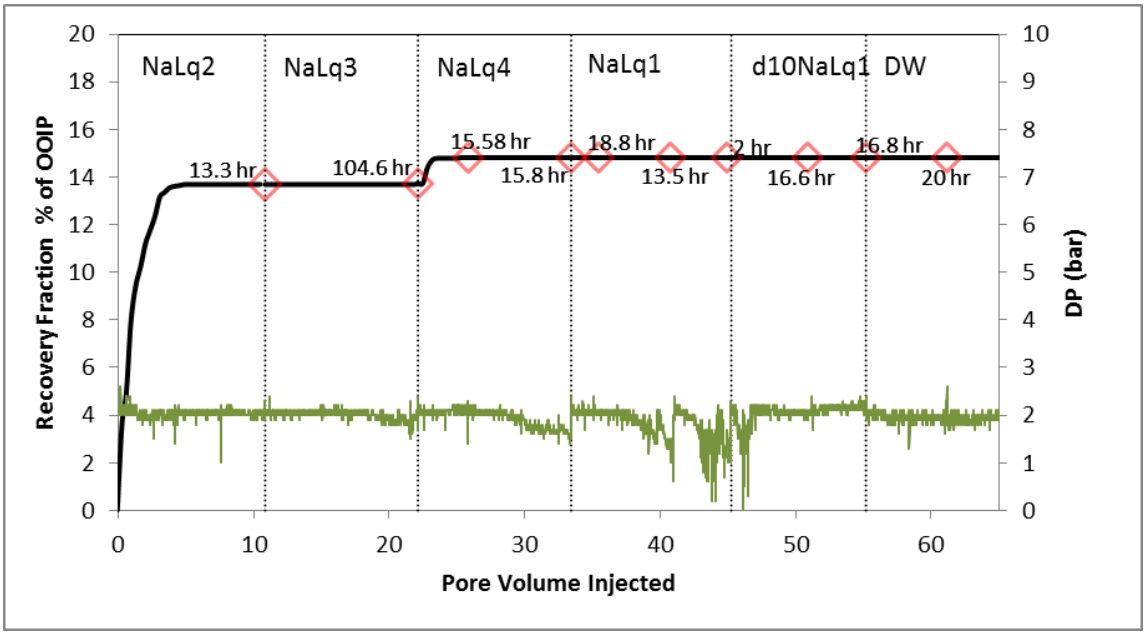


Figure 10: Observed oil recovery and differential pressure across the D7H core plug for injection of sodium campaign.

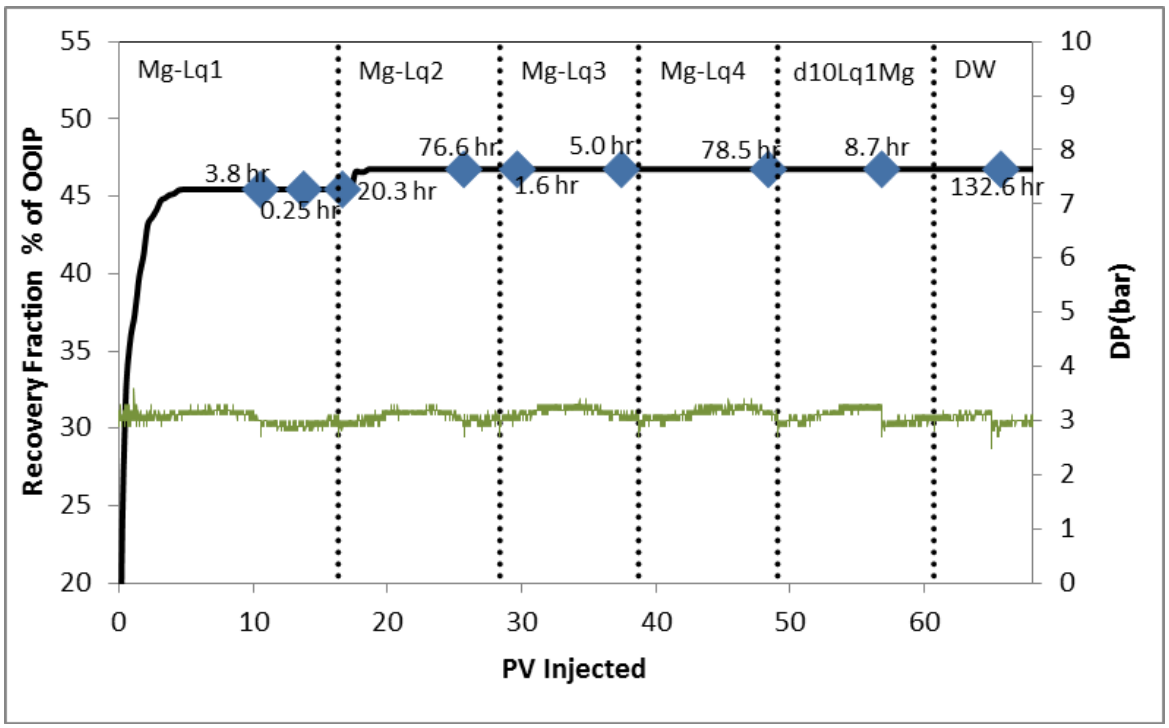


Figure 11: Oil recovery of Core plug D4H vs Pore Volume for injection of magnesium campaign.

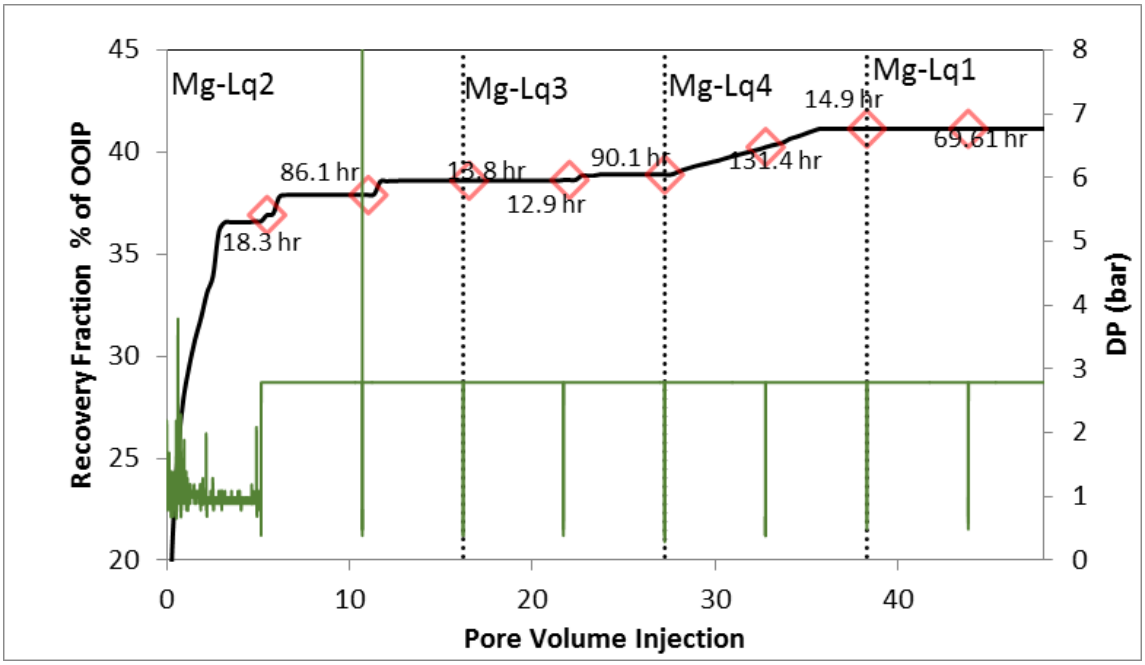
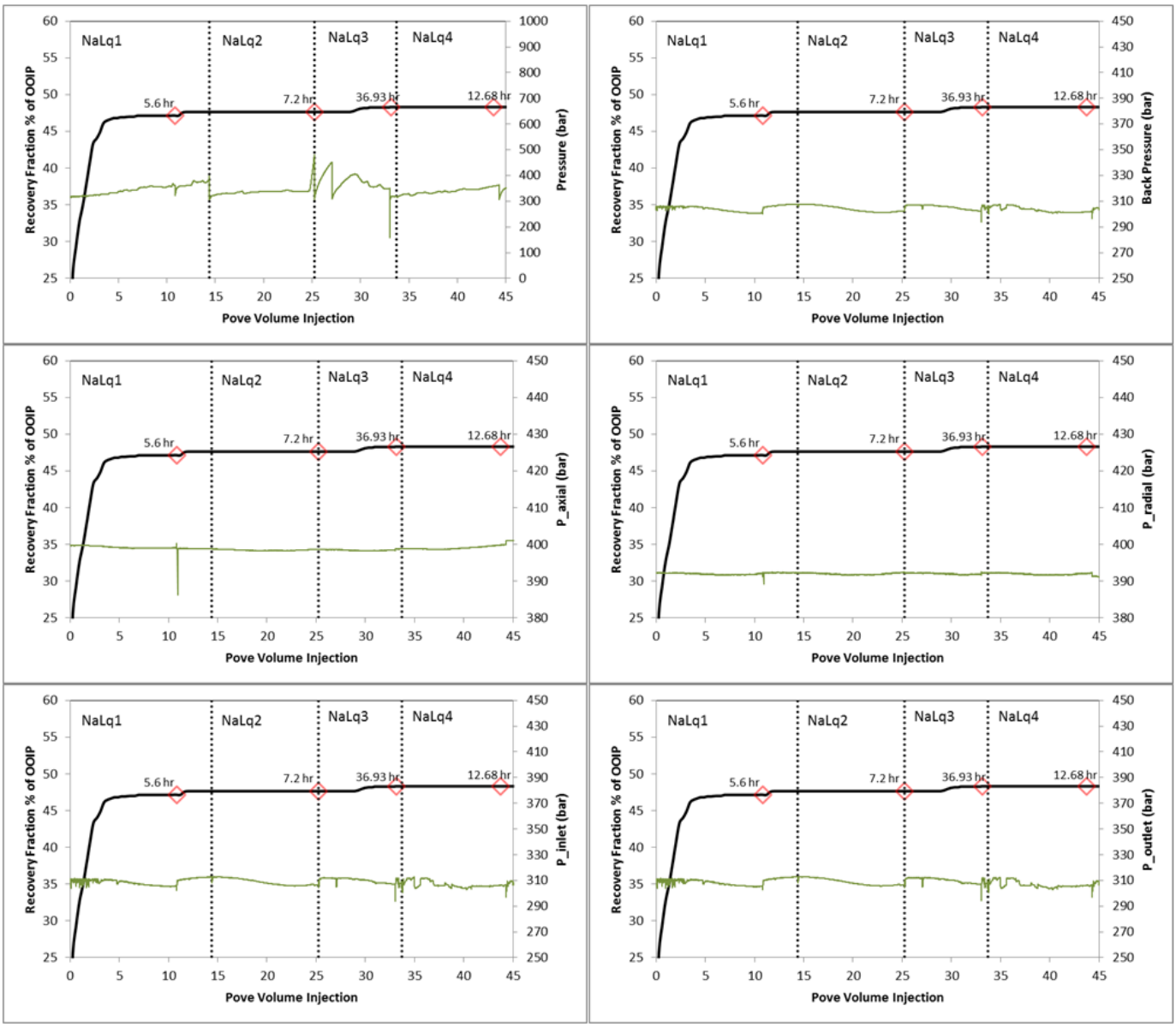
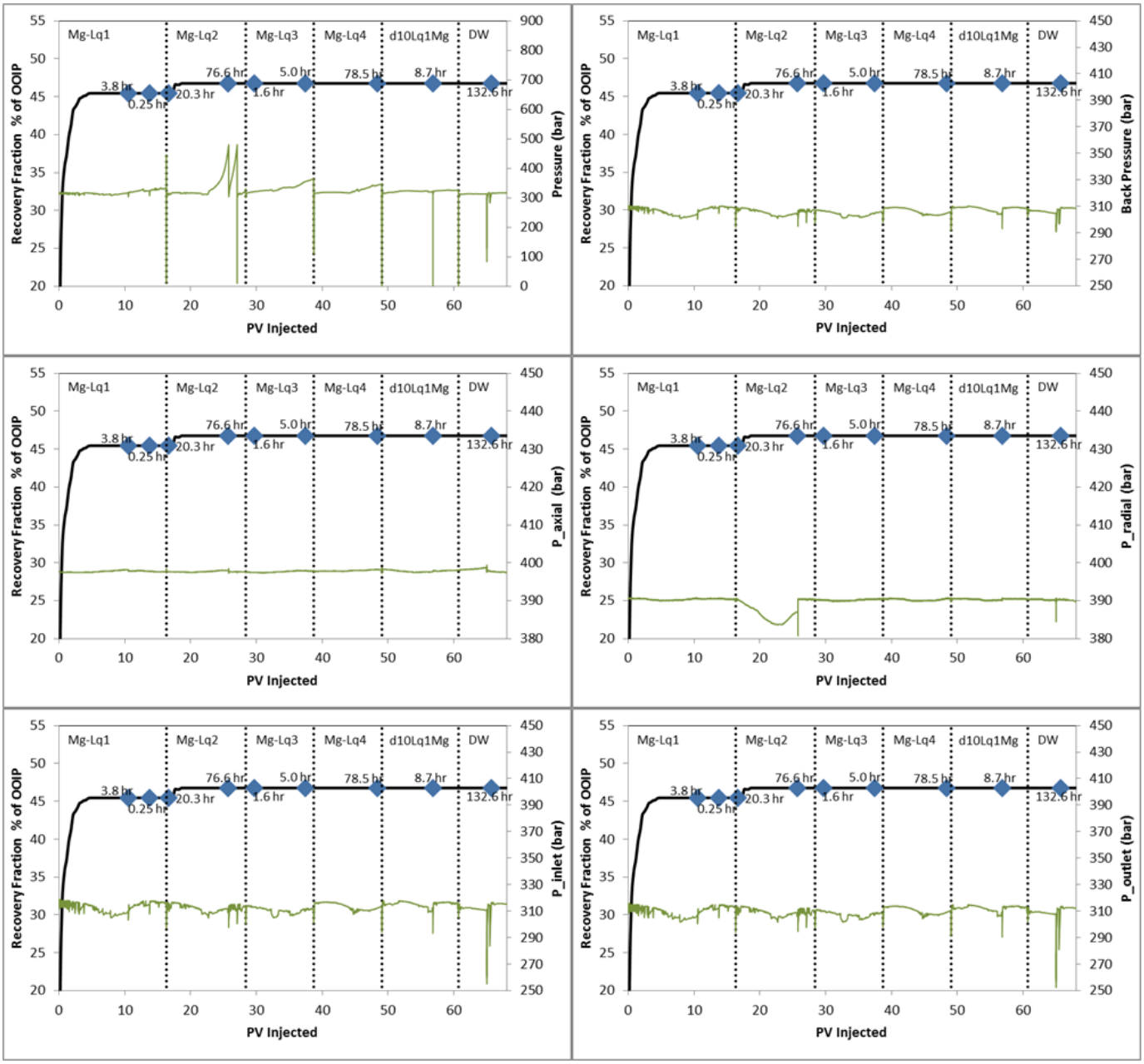


Figure 12 : Oil recovery of Core plug D17H vs Pore Volume for injection of magnesium campaign.

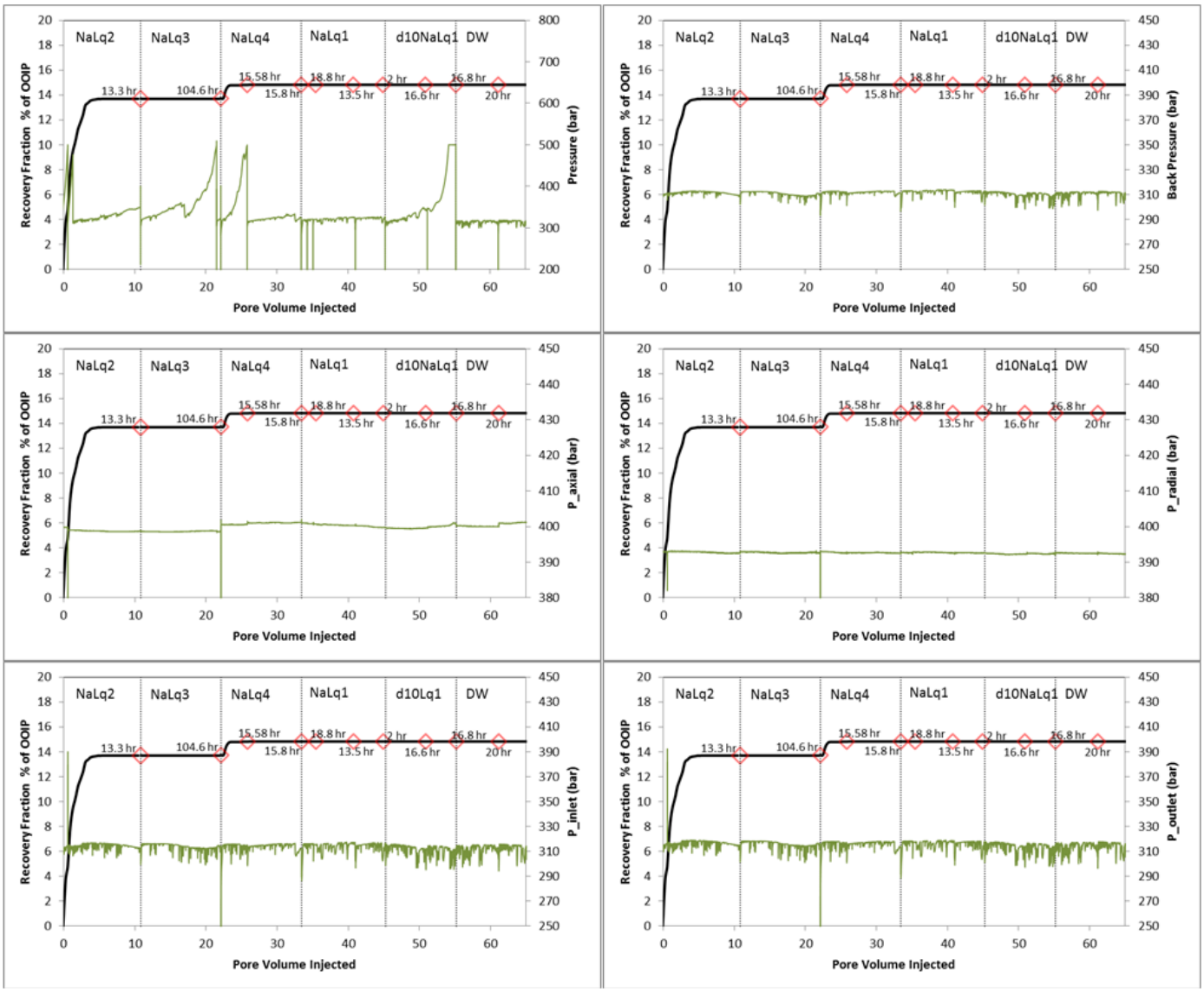
Supplementary Figures



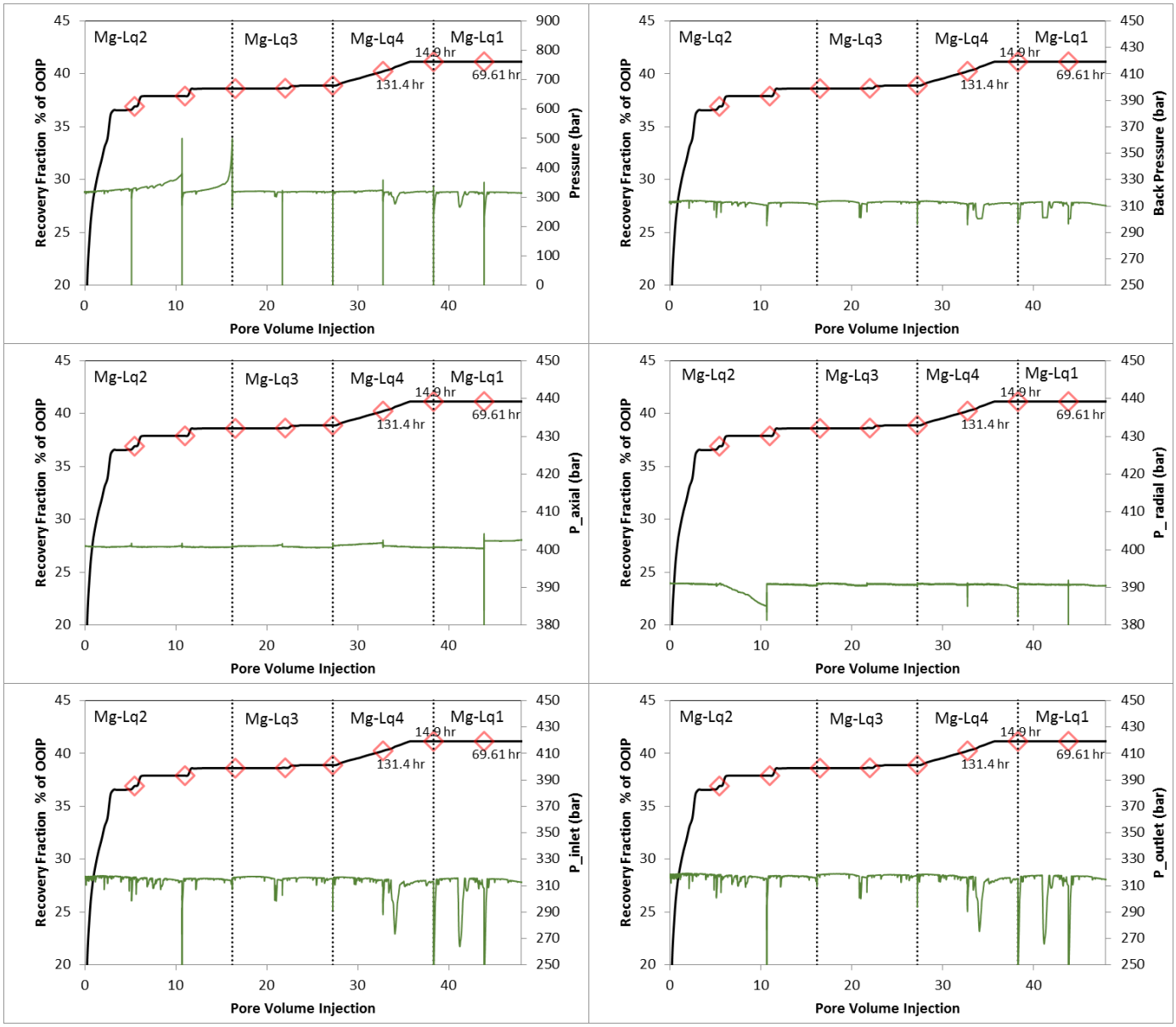
Supplementary Figure 1 : Observed Oil Recovery of core plug D3H Vs Various pressure profiles (including axial pressure, Radial pressure, Inlet Pressure, and Outlet Pressure).



Supplementary Figure 2: Observed Oil Recovery of core plug D4H Vs Various pressure profiles (including axial pressure, Radial pressure, Inlet Pressure, Outlet Pressure, and Back Pressure).



Supplementary Figure 3: Observed Oil Recovery of core plug D7H Vs Various pressure profiles (including axial pressure, Radial pressure, Inlet Pressure, Outlet Pressure, and Back Pressure).



Supplementary Figure 4: Observed Oil Recovery of core plug D17H Vs Various pressure profiles (including axial pressure, Radial pressure, Inlet Pressure, Outlet Pressure, and Back Pressure).

Paper XIV

Parallel injection of multiple brines through various injection wells for optimum fines formation during smart water flooding

Chakravarty, K. H., Fosbøl, P. L., & Thomsen, K. (2016) Parallel injection of multiple brines through various injection wells for optimum fines formation during smart water flooding. ***Journal of Petroleum Science and Engineering*** **(Draft Manuscript: To be submitted)**

Abstract

Understanding the underlying mechanism and identification of the most suitable brine composition that can ensure optimum increase in oil recovery has been the basis of most smart water enhanced oil recovery (EOR) studies. Application of the optimum brine composition remains dependent on field properties, such as production history, sea water sweep efficiency, injection production well network, possible developed preferential flow paths following fractures in the reservoir. This study attempts to explore the possible implementation of smart water EOR in two oil fields (Dan and Halfdan fields) using Extended UNIQUAC modelling. Although these oil fields have similar geological history, they have had significantly different fluid flows throughout their production history. It is observed that ion substitution based optimum fines forming brine injection can be beneficial for Halfdan field and the West flank of the Dan field. Parallel multiple different brine injection, promoting mixing based fines formation has been observed to be more suitable for the A-block and the B-block of the Dan field. Possible core slab equipment and flooding strategy is proposed for further investigation.

What brine composition should be injected: Literature

In past studies, attempts have been made to find the optimum brine composition so that a maximum fraction of the OOIP can be produced from core flooding or imbibition experiments. According to the observed oil productions, use of specific brines such as SW0NaCl (Fathi et al. 2011), SW0NaCl-4SO4 (Fathi et al. 2012) and SW4SO4 (RezaeiDoust et al. 2009) has been recommended. Through Smart water flooding (RezaeiDoust et al. 2009), Low salinity injection (Webb et al. 2003), Advanced Ion Management (Vo et al. 2012), controlled salinity injection (Mahrouqi et al. 2015), and Designed Water injections (Awan et al. 2008) attempts have been made to understand the fundamental mechanism behind increased oil recovery for variation in brine composition. Finding the optimum brine composition that can produce maximum oil recovery has been the common aim of all of these studies. During large scale reservoir implementation the most suitable brine is expected to be ideally injected through all injection wells. For example use of SW0NaCl has been recommended for the entire Ekofisk Field and not any specific injection well (Puntervold et al. 2014).

Based on these recommendations further research has been conducted on large scale preparation of smart waters with high content of potential ions from normal sea water (Ji et al. 2014; Yousef and Ayirala 2014). These salt compositions involve selective compositional variation of individual ions from sea water. Thus they cannot be directly obtained by conducting reverse osmosis of sea water (as used for sandstone fields). Using ultrafiltration, Nano-filtration, and Reverse Osmosis, multiple steps of processing of sea water is required for obtaining the recommended brine solutions (Hassan et al. 1998; Hilal et al. 2005; Yousef and Ayirala 2014; Pontié et al. 2013). Use of multiple process make preparation of smart water both expensive and energy consuming. The alternative method for producing brines with a high content of potential ions is by transporting large amounts of $CaSO_4$, $MgSO_4$ Na_2SO_4 and $MgCl_2$ salts to the offshore rigs from the nearest port. Herein two major benefits of using smart water have to be compromised, including:

- Excessive availability of feed (Kokal and Al-Kaabi 2010): In most other EOR technologies, such as Polymer, Surfactants, Nanoparticles; CO_2 and microbial EOR the feed is not naturally available at oil rigs and has to be manufactured or produced in an industry. In these EOR processes the cost of associated production of primary EOR chemical/feed is inseparable from the overall expenditure during implementation. But in case of smart water flooding, excessive availability of sea water or other aquifer waters is a major benefit, in cost reduction during EOR implementation. If any additional salt has to be produced, the advantage of excessive availability of feed is lost.
- Transportation of salts (Kokal and Al-Kaabi 2010): Smart Water EOR technology is attractive over other EOR processes as it does not require any transportation of chemicals offshore. Several offshore oil fields in the North Sea are being considered for Smart Water EOR implementation. These fields are situated considerable distances from the nearest port city (such as Dan field in Danish North Sea and Esbjerg port city). The transportation of large amounts of additional salts will further increase the overall cost of implementation the technology.

Therefore two major benefits of smart water EOR over other EOR technologies has to be compromised if produced chemicals have to be brought to offshore rigs.

What brine composition should be injected: Extended UNIQUAC calculation

Production of smart water with alteration of the concentration of selected ions from sea water can become an expensive process. Further investigation of the recommended brines has been conducted using the Extended UNIQUAC model (Thomsen and Rasmussen 1999). Use of high content of potential ions (such as SW0NaCl; SW0NaCl-4SO4 and SW4SO4) and avoiding precipitation has been recommended in previous studies (Puntervold et al. 2014). But it has been observed that the recommended brines form precipitate at North Sea reservoir conditions of 130°C (as shown in Paper 9; figure 2-4). Thus an intrinsic contradiction exists with the recommended method for smart water implementation. It has been further observed that precipitation can take place due to two different processes 1. Precipitation can take place on injection of brine because of change in brine speciation with changes in pressure and temperature conditions as the injection brine moves from ambient conditions to reservoir conditions; 2. Precipitation can take place inside the coreplug because of the interaction of the brine with the mineral surface or other brines

present in the pore space. The amount of effective fines formation taking place is calculated by subtracting the precipitation on injection from the total precipitation taking place in the reservoir. For the conducted experiments reported in literature, a consistent correlation between the fines formation and oil recovery has been constantly observed (Chakravarty et al. 2015).

Section I: Fines formation optimization

Using Extended UNIQUAC Model the optimum amount of fines formation should be calculated for various alterations to sea water. Fines formation from brines with high contents of potential ions can be observed in three different ways. 1. Decreasing NaCl concentration; 2. Increasing SO_4^{2-} (divalent anion) concentration; 3. Increasing Ca^{2+} (divalent cation) concentration (Fathi et al. 2011; RezaeiDoust et al. 2009). Using extended UNIQUAC model, the amount of fines formation that shall take place in reservoir conditions has been calculated for all three processes.

- Decreasing Na^+ concentration (Puntervold et al. 2014): Reducing Na^+ by removing NaCl from sea water has been shown to lead to higher amount of fines formation and to increased oil recovery (Puntervold et al. 2014; Chakravarty et al. 2015). The amount of fines formation following a decrease in Na^+ concentration was calculated using Extended UNIQUAC model. For North Sea reservoir conditions (Sunde et al. 1992), variations in pressure (from 50 bars to 400 bars) as well as in temperature 130 ± 10°C have a strong influence on the amount of precipitation taking place on injection and fines formation after ion substitution. Calculated results were plotted in Figure 1. An optimum Na^+ mole fraction (with respect to SW) is observable beyond which effective fines formation taking place inside the core starts decreasing. The optimum amount of fines formation obtained by reducing the NaCl concentration is around 2.5 grams/kg of water. Neither pressure nor temperature variation, show significant alteration to the optimum amount of fine formation; but the Na^+ concentration at which optimum fines formation takes place is significantly dependent on both reservoir pressure and temperature conditions. Injection of SW0NaCl as previously recommended by Puntervold et al. 2014, causes precipitation on injection in all studied cases. Precipitation starts taking place at different fractions of Na^+ depending upon the pressure and temperature conditions.

- Increasing SO_4^{2-} concentration (RezaeiDoust et al. 2009): Increasing the SO_4^{2-} concentration in injection brine has shown to increase oil production in various spontaneous imbibition experiments. Correspondingly, a one to one correlation between fines formation at reservoir condition and oil recovery has also been established. In previous studies the SO_4^{2-} concentration has been enhanced by replacing Cl^- from the solution with SO_4^{2-} (Fathi et al. 2012). Herein the Na^+, Ca^{2+} and Mg^{2+} concentration is kept constant. The amount of fines formation for different SO_4^{2-} concentrations has also been calculated over pressure (from 50 bars to 400 bars) and temperature (70 to 130°C) variations using Extended UNIQUAC model.

  Unlike Na^+ depleted brines, SO_4^{2-} enriched brines exhibit exact optimum concentrations beyond which effective fines formation starts decreasing. But depending upon temperature, the amount of effective fines formation taking place become constant at enriched SO_4^{2-} (mole fraction) beyond which significant additional fine formation is no longer observed. The optimum amount of fines formation obtained by increasing the SO_4^{2-} concentration is around 6.1 grams/kg of water (Figure 2). At reservoir conditions pressure does not show significant alteration to the optimum amount of fine formation. In a previously reported study (Awolayo et al. 2015), the injection of SW8SO4 did not show considerable additional oil recovery while SW4S was observed to be the most optimum concentration. Addition of more SO_4^{2-} ions had no proportional benefits in oil production. The amount of fine formation taking place for SO_4^{2-} brines shows exactly the same behavior. It must be noted that use of SW4SO4 brine has been recommended in various studies; and avoiding precipitation has also been recommended (RezaeiDoust et al. 2009). But SO_4^{2-} enriched brines (SWnSO4 $\forall$ n > 1½) are completely supersaturated at reservoir conditions (Temperature >100°C, Pressure 50 to 400 bars) and on injection precipitation will take place irrespective of the extent of ion substitution. As illustrated by SW4SO4, increased oil recovery can take place in parallel with precipitation on injection provided altering brine composition increases the amount of effective fine formation in the coreplug. The composition at which precipitation begins is not analogues to the composition at which the optimum fines formation or optimum oil recovery is observed.
  Large scale production of SO_4^{2-} brines enriched by replacing Cl^- ions with SO_4^{2-} will require multiple step processing of sea water (Yousef and Ayirala 2014). But instead of replacing Cl^- ions with SO_4^{2-} ions; the SO_4^{2-} concentration can also be selectively enhanced by addition of Na_2SO_4 to sea water. By this method, the Cl^-, Ca^{2+} and Mg^{2+} concentrations are kept constant. Conducting speciation calculation using Extended UNIQUAC model it is observed that the amount of fines formation and the precipitation on injection show similar behavior for two SO_4^{2-} systems. SO_4^{2-} enriched brines have an exact optimum concentration beyond which the effective fines formation starts decreasing. Depending upon temperature, the amount of effective fines formation taking place become constant at high SO_4^{2-} fractions beyond which no significant additional fines formation is longer observed. The optimum amount of fines formation obtained by increasing the SO_4^{2-} concentration is around 5.8 gram/kg water (Figure 3). In this case, the composition at which precipitation begins does also not correspond to the composition at which the optimum fines formation or optimum oil recovery is observed.
  The expense of preparation of SO_4^{2-} enriched brines through both methods should be considered for selecting the most suitable brine.

- Increasing the Ca^{2+} concentration (RezaeiDoust et al. 2009): Enhancing the divalent cation fraction is the third method which can increase the potential ion fraction of the injection brine. Previously, a correlation between fines formation and in-

creased oil recovery has been established for increased Ca^{2+} concentrations. The Ca^{2+} concentration required for optimum fine formation was calculated using extended UNIQUAC model.

In this case it is observed that for Ca^{2+} enriched brines at North Sea reservoir conditions at 130 $\pm$ 10°C both variation in pressure (from 50 bars to 400 bars) and temperature have a strong influence on the amount of precipitation taking place on injection and fines formation after ion substitution.

An optimum Ca^{2+} fraction (with respect to SW) can be identified. Beyond this fraction, the fines formation taking place inside the core starts decreasing. The optimum amount of fines formation obtained by increasing the Ca^{2+} concentration is around 2 grams/kg of water (Figure 4). With increase in pressure the optimum amount of fines formation show steady decrease. The Ca^{2+} concentration at which optimum fine formation takes place is also significantly dependent on both reservoir pressure and temperature conditions.

Section II: Fines formation for no precipitation on injection

Injection of supersaturated brines which can form precipitate near the injection point may not be advisable for reservoirs with very low permeability and small pore throats. For each of the three processes, the maximum amount of potential ions that can be injected without causing precipitation on injection was therefore calculated. The corresponding amount of fines formation taking place in the pore space was also calculated at different pressure and temperature conditions for all three processes.

- Decreasing Na^{+} concentration (Puntervold et al. 2014): The optimum fraction (compared to sea water) up to which the NaCl concentration can be reduced without causing precipitation on injection was calculated at different pressures (1 to 400 bars) and temperatures (110 to 140 °C). The corresponding amount of fines formation taking place after substitution was also calculated using Extended UNIQUAC model. It is observed that the optimum amount of fines formation remains constant for pressure and temperature variation but the fraction up to which sodium can be removed is significantly dependent on the pressure and temperature conditions (Figure 5). Depending upon the reservoir composition the optimum concentration can be obtained.

- Increasing SO_4^{2-} concentration (RezaeiDoust et al. 2009): The optimum fraction (compared to sea water) up to which the SO_4^{2-} concentration can be increased so that no precipitation takes place on injection was calculated at different pressures (1 to 400 bars) and temperatures (100 to 140°C) conditions. The corresponding amount of fines formation taking place after substitution was plotted in Figure 5. It is observed that the fraction of SO_4^{2-} that can be injected without precipitation taking place and the corresponding amount of fines formation both increase with an increase in reservoir pressure. An increase in reservoir temperature (from 100 to 130°C) has the opposite effect. With increase in temperature the amount of SO_4^{2-} that can be injected without causing precipitation on injection decreased and so did the corresponding amount of fines formation. For SO_4^{2-} enriched brines, the optimum fines formation takes place in parallel with precipitation on injection (as observed in Figure 5) and therefore injection of brines with no precipitation on injection does not reflect the optimum fine forming brines. It is observable for all high temperature reservoirs that the injection of SW3SO4 or more sulphate will be associated with precipitation on injection. Therefore recommended brines like SW4SO4 should only be injected with complete awareness that this brine is supersaturated at reservoir condition.

- Increasing the Ca^{2+} concentration (RezaeiDoust et al. 2009): The optimum fraction (compared to sea water) up to which the Ca^{2+} concentration can be increased without precipitation taking place on injection was also calculated using Extended UNIQUAC model. The corresponding amount of fines formation taking place after substitution was also calculated and plotted in Figure 5. The maximum fraction of Ca^{2+} that could be injected in reservoir without precipitation on injection showed significant pressure and temperature dependence. The fraction of Ca^{2+} injection for no associated precipitation showed consistent decrease with increase in temperature. The opposite was observed for pressure variation.

  Unlike SO_4^{2-} enriched brines the corresponding amount of fines formation for Ca^{2+} brines showed increase with increase in temperature. Use of brines such as SW4Ca at 50 bars have been considered supersaturated only at temperatures above 130°C but calculations show that SW4Ca is supersaturated at 100°C. It has been shown that at 100°C and 50 bars for Stevns Klint Chalk that SW4Ca produces significantly higher oil recovery than SW even though precipitation takes place. Therefore for Ca^{2+} enriched brines; increase oil recovery can take place in parallel with precipitation on injection. Therefore injection of brines with no precipitation on injection does not reflect the optimum fine forming or oil producing brines.

Simultaneous variation of the concentrations of more than one ion has also been studied in SW-EOR. Use of brines such as SW0NaCl-4SO4 and SW2Ca4SO4 has been shown to increase oil production significantly (RezaeiDoust et al. 2009). The corresponding Extended UNIQUAC calculation were conducted to identify the extent up to which the concentrations of two ions can be varied so that no precipitation takes place on injection. The calculations were conducted at 400 bars and at temperatures from 120 to 140°C. The maximum fraction of Ca^{2+} that can be added to sea water containing different fractions of Na^{+} was calculated under the constraint that no precipitation took place on injection. The corresponding amount of fines formation was also calculated and plotted in Figure 6a. Similar calculation was conducted for maximum fraction of Na that can be added to sea water containing different fractions of SO4 variation and maximum fraction of Ca that can be added to sea water containing different fractions SO4 variation as shown in Figure 6b and 6c. The obtained results show significant pressure and temperature dependence of the optimum concentration that can be used for injection without precipitation on injection.

The majority of core flooding experiments which were successful in increasing the oil recovery with the use of supersaturated brines (e.g. SW4SO4, or SW0NaCl, RezaeiDoust et al. 2009; Awolayo et al. 2015) have been with outcrop core plugs. In some chalk and limestone reservoirs with low permeability the injection of these supersaturated brines have been shown to cause precipitation and the desired increase in oil recovery has not been observed. In case of reservoir implementation such precipitation on or near the injection point can cause severe production challenges. Therefore the optimum fines formation (with precipitation on injection as discussed in section 1) should be considered for reservoirs through which a smooth flow of supersaturated brine can be assured. As described is section II, smart waters which do not precipitate at reservoir condition can be used. These brine compositions cause fine formation only when ion substitution takes place thus they do not block the preferential water flow along the injection point. Optimum fines formation brines with precipitation on injection are brines that are likely to displace most oil from the pore space because of greater surface adhesion between fines and residue oil. There is an associated risk of major precipitation around the injection point. Fines formation with no precipitation on injection (as described in section II) does not produce maximum fines but has no potentially negative effects on the flow of flooded water. Considering the cost of production of brine and the extent of ion substitution taking place in the coreplug of the particular field the most suitable brine can be identified using the above stated approaches. The composition of sea water and aquifer water can vary with location globally, so cases with specific iteration for maximum fine formation (with or without precipitation on injection) can be conducted using Extended UNIQUAC model for given reservoir pressure temperature conditions. Thus cost effective; composition of brine for optimum oil recovery through single brine injection can be obtained by using this approach.

Discussion

Single optimum brine or multiple brine parallel injection

While recommending smart water compositions for reservoir implementation in all of these studies there is has been a specific objective i.e. to identify suitable brine composition (based on the conducted core plugs experiments). This recommended smart water should be ideally injected through the existing injection well for obtaining optimum oil production. But there are some significant differences between coreplug experiments and reservoir scale smart water floods.

First of all it has been shown that precipitation can take place on injection of recommended brines in the North Sea chalk reservoirs. This precipitation can take place either in the injection pipe or near the injection point depending upon the nucleation kinetics. Alteration in brine speciation because of interactions in the coreplug can further supersaturate the solution. The kinetics of fines nucleation for the two precipitation processes can show a much stronger overall effect for coreplugs (because of limited size of few centimeters) as compared to reservoirs, wherein the injection point and reservoir pores are separated over several 100 meters (Jorgensen 1992). This clear distinction between precipitation on injection and precipitation after brine interaction will be more easily distinguishable at reservoir scale, than at coreplugs (laboratory) scale.

Moreover it must be noted that the flow of injected water in core plugs and in reservoirs can be significantly different. Also different reservoirs can have considerably dissimilar flow patterns because of differences in geological lithology and variation in injection/production well network. In coreplugs a single water front moves across the core plug and pushes the existing fluid (oil and brine) towards the producing end of the cylindrical core plug. By this process, all injected brine pass through the sample pore network and is produced at the specified end.

In the analysis of core flood experiments, it has been observed that alterations in brine speciation (in pore space after injection) and the corresponding fines formation in the reservoir can take place through two major processes (Chakravarty et al. 2015):

1. Injection of smart brine: High concentration of potential ions can cause ion substitution on the mineral surface. And this substitution can thereafter lead to formation of fines. Injection of soluble CO_2 along with brine can also cause dissolution of calcite and formation of anhydrite fine. For a given reservoir, the amount of fines formation and the fines distribution pattern taking place is dependent on the mineral properties, rate of brine injection and the injected brine composition. Herein the alteration of brine speciation is primarily due to interactions on the mineral surface (Chakravarty et al. 2015).
2. Interaction of two different brines: It has also been shown that interaction of two completely soluble salts can cause formation of supersaturated brine when they undergo mixing at reservoir conditions. Alteration of the brine composition in core flooding experiments is commonly implemented. The amount of fines formed due to interaction of the two brines has shown direct correlation to the increase in oil productions (Chakravarty et al. 2015).

Recommending a single smart water composition diminishes the possibility of multiple brine interactions in the reservoir. Unlike core plug experiments, at reservoir scale there are multiple injection points (wells) through which different smart water brines can be injected. Individual smart waters then flow through the preferential flow path towards the associated producing well and can cause fines formation due to their interaction with the mineral surface. This fines formation enhances the mobility of residue oil and causes increased water wetness. But, a fraction of the injection water gets diverted from the preferential flow path (away from the associated producing well) and thus can interact and mix with the brine injected from other injection wells. If different brine compositions are injected through various injection wells, this mixing of brines can further cause fines formation in the reservoir. This additional fines formation due to mixing of brine injected through different injection wells can further enhance the mobility of residue oil in diverted flow regions. Continuous mixing will lead to formation of static fines (or precipitation) which can alter the sweep efficiency of the injected brine. Therefore injection of the most suitable brine through all injection wells may not neces-

sarily produce optimum amounts of oil. Varying the brine composition between different injections well can increase the oil production due to additional fines formation from mixing of the different injected brines.

In other words, the main aim of most studies has been to identify the most suitable brine composition which can produce maximum oil recovery. The actual aim of smart water EOR studies is to develop a method of modified sea water injection which can ensure optimum oil production. And fine formation can not only take place because of individual brines interaction with the mineral surface, but it can also take place because of mixing of two brines injected through different injection wells. This formation of fines (while mixing brines) can further enhance oil production so; injection of same brine composition through all coreplugs may not necessarily lead to optimum oil productions. This concept of fines formation using brine mixing at reservoir can be further explained using the differences between injection/production well network (and geology) of the Dan and the Halfdan fields from the Danish North Sea.

Danish Hydrocarbon oil fields

The Dan field and the Halfdan field are two of the major oil producing chalk reservoir oil fields in the Danish North Sea (Schiøler and Wilson 1993). Both fields are in the Tor formation from Danian and Upper Cretaceous time containing combination of thick, porous and permeable chalk, salt induced structures and an effective early tertiary top seal which makes this region the most producing region in Denmark at the present. The basic geological structure and the injection/production well network for these two fields are significantly different. A brief outline of the geology and production strategy of Dan and Halfdan field is explained below for considering smart water EOR implementation in these.

Halfdan field
The Halfdan Field comprises the Halfdan, Sif and Igor areas and contains a continuous hydrocarbon accumulation. The southwestern part of the field primarily contains oil in Maastrichtian layers, while the area towards the north and east primarily contains gas in Danian layers (Lindgreen et al. 2011). The accumulation is contained in a limited part of the chalk formation, which constitutes a structural trap in earlier geological times. The structure gradually disintegrated, and the oil began migrating away from the area due to later movements in the subsoil. However, the oil and gas deposits have migrated a short distance only due to the low permeability of the reservoir. This porous, unfractured chalk is similar to that found in the western flank of the Dan Field.

Recovery is based on the Fracture Aligned Sweep Technology (FAST) (Rod 2005; Lafond et al. 2010), where long horizontal wells are arranged in a pattern of alternate production and water-injection wells with parallel well trajectories. Varying the injection pressure in the well causes the rock to fracture (Albrechtsen et al. 2001). This generates a continuous water front along the whole length of the well, which drives the oil in the direction of the production wells. The production of gas from Danian layers is based on primary recovery from multilateral horizontal wells, using the reservoir pressure (Albrechtsen et al. 2001). The waterflood efficiency in the field is generally quite good, as a result of a generally regular flood pattern layout. The flow across a coreplug unit in the Halfdan reservoir is very similar to the unidirectional flow in core floods experiments in laboratory scale.

The Halfdan field has produced 64.98 million cubic meters of oil since its production began in 1999. Herein injection of water in 2001 increased the overall production rate to 6.2 million cubic meters in 2005 (Bæk 2013). The production rate has been maintained and its present production is of 4.15 million cubic meters in by 1st January 2014 (Figure 7), while injection has also been maintained around 10-12 million cubic meters per year since 2006 (Bæk 2013). Early application of EOR technologies, (i.e. between secondary oil recovery processes) have shown both increased rate of production and higher ultimate oil recovery. Therefore the already well water flooded Halfdan field can be considered for smart water EOR implementation.

Dan Field
The Dan Field is an anticlinal structure induced through salt tectonics (Jorgensen 1992). A major fault divides the field into two reservoir blocks, which, in turn, are intersected by a number of minor faults (as shown in figure 8). The chalk reservoir has high porosity and low permeability. The Dan Field has a gas cap.

Recovery from the field is based on the simultaneous production of oil and injection of water to maintain reservoir pressure. The Dan field has produced 108.55 million cubic meters of oil since its discovery in 1971 (Bæk 2013). The majority of the production has taken place after sea water injection which was initiated in 1989 and has gradually been extended to the whole field. The recovery of oil is optimized by flooding the reservoir with water to the extent possible. With around 7 million cubic meter of oil production in a year, the rate was maximum during 2000-01 (Figure 7). Presently the recovery takes place from the central part of the Dan Field and from large sections of the flanks of the field (Bæk 2013). Particularly the western flank of the Dan Field, close to the Halfdan Field, has demonstrated good production properties.

As the field attained maturity, the production rate has consistently decreased to 2.04 million cubic meters in 2013. Consistent decrease in production rate and sea water flooding for more than two decades makes it an ideal candidate for consideration of smart water EOR implementation (Bæk 2013).

The Dan field was gradually developed over time and its wells were not designed planned or constructed in the same period. The major fault separates the field in an A-block and a B-block. The Dan West Flank constitutes a third, distinct, part of the Dan field (as shown in figure 8), and continues west into the down flank Halfdan field (Albrechtsen et al. 2001).

- Dan A-block: The Dan A-block is developed with vertical water injectors, most of which are completed with sand-propped fractures. It has been observed that the orientation of these fractures is difficult to control, and some have grown significantly (Hatchell et al. 2007). As a result, the A-block waterflood is characterized by an uneven volumetric sweep and, in some cases, by large injection water short circuits caused by hydraulic fractures (Ovens et al. 1998).
- Dan B-block: The Dan B-block has a number of horizontal injectors. Some zones are fracture stimulated with sand-propped fractures, while others are matrix acid stimulated. In comparison to the A-block, the horizontal injectors offer somewhat better control of the areal sweep, but challenges exist with injection water short circuits (Ovens et al. 1998).
  The flow in both Block A and B of the Dan field in reservoir is therefore not similar to the unidirectional water front movement as observed in laboratory scale core flooding experiments.
- The Dan West Flank (Albrechtsen et al. 2001): The presence of oil in the western flank of the Dan Field was not confirmed until 1998 with the drilling of the MFF-19C well, which also established the existence of the Halfdan Field. The Dan West Flank is largely developed as a parallel line drive, with alternating horizontal injectors and producers using CAJ liner completed wells (Hansen and Nederveen 2002). The waterflood in the Dan West Flank is generally quite effective. Horizontal wells and alternating injector and producing wells ensure unidirectional flow with core plug scale flow behavior being similar to core flooding experiments conducted in laboratory.

Field specific Injection Strategy

Single brine injection

Halfdan field and Dan West Flank have water front based homogenous unidirectional flow; while Dan A-block and Dan B-block inhomogeneous multidirectional flow. Thus compared Dan A-block and Dan B-block, the Halfdan field and Dan West Flank have less mixing opportunity between brine injected through different injection wells. In figure 9 a schematic representation of alternate production/injection horizontal wells is depicted. Through two different injection wells, different brines which are individually soluble at reservoir conditions (for example SW1½Ca and SW1½SO4) can be injected in parallel into the reservoir such that on mixing it leads to fines formation. But in this case each injection well is separated from the next injection well by a production well. Therefore, there is no major possibility of interaction between injected brines from two different injection wells in diverted flow regions. Only near the production wells brine mixing and supersaturation can take place. Formation of small mobile fines near the production well is not beneficial as it can only adhere to the displaced oil which has reached the production well and it cannot interact with the residue oil. Formation of large grain salt precipitation near the production well can only block the flow near production wells and thus can cause hindrance in oil production. Thus, possible alteration (improvement) in sweep efficiency of injected water through precipitation or fine formation due to mixing of two brines cannot be used in these reservoirs.

If flow across any infinitesimally small unit of the reservoir is considered, then a continuous water front's unidirectional movement is observed over time. The standard core flooding experiment exactly mimics this behavior. Herein the flow direction, homogeneity and rate of flow is not altered and has no major local variation. Random selection of any infinitesimally small volume of the reservoir is likely having the same water flow behavior over time (as shown in Figure 9).

Maximum fines formation from individual brine injection following ion substitution should be the primary strategy for SW-EOR implementation in Halfdan field and Dan West Flank. Since the behavior of the reservoir unit volume is exactly like a core water flooding, standard core flooding/imbibition analysis combined with Extended UNIQUAC modelling can be conducted to identify the most suitable brine composition and the extent of ion substitution taking place in the pore space. Use of small cores can be helpful in obtaining SEM high resolution images to identify possible fines formation. In micro CT-scan measurements the use of small cores also can be beneficial. For the Halfdan field and Dan West Flank optimum fines formation through single smart water injection can be considered for possible smart water EOR implementation. Multiple brine parallel injection intended for fines formation in the reservoir may not be advisable for these fields.

Multiple brine parallel injection

In the Dan A-block and Dan B-block of the Dan field, the same SW-EOR strategy may not be most beneficial. As in Dan A-block large fractures have gradually grown, which form the preferential flow path through which the majority of the injected water passes. The associated pore surfaces of the preferential flow path have been heavily flooded and have been significantly exposed to injected Mg from sea water. Thus all possible ion substitution along the mineral surfaces may have already taken place during continued sea water injection. Injection of smart waters will not directly provide any new surfaces for further ion substitution to take place. Note that ion substitution on mineral surface is beneficial for smart water EOR according to observed fine-oil correlation and previously reported wettability alteration mechanism.

If a single smart water is injected through all injection wells into these reservoirs (with large fractures) then the majority of the water will flow through the preferential flow paths. And since the associated pore walls are already exposed to significant fine formation during sea water flooding since 1989, no major ion substitution and thereby fines formation can be expected. Dan A-

block has significant uneven volumetric sweep of injected brine. The fraction of injected smart water that travels through the unswept volumes (with small pore throats) will get access to new surface areas where ion substitution followed by fines formation can take place. These fines can thereby enhance the mobility of the residue oil. But, only a minor fraction of water will continue to flow through these small pore throat regions if a hindrance in flow through the large fractured water short circuits is not engineered.

The injection wells in Dan A-Block do not have a one to one correlation like the one observable in Halfdan field. This indicates that not all injected water moves to the associated production well and a fraction of the injected water from the vertical wells can get diverted towards other existing large fractions. This opens the possibility of interaction of brines injected from two different wells. Therefore parallel injection of (individually soluble but) different brines through different injection wells can cause continued supersaturation in regions of the reservoir where brine mixing can take place. Use of brine combinations such as SW1½Ca and SW1½SO4 can be used to ensure that individual brines remain soluble but on interaction become supersaturated. Using this interaction, precipitation can be engineered in the large fractured preferential flow paths.

During initial interactions the formed supersaturated solution will form small mobile fine particles, which can travel with the flooded water. But the high rate of water flow in the preferential flow path shall also lead to increased fine formation following brine mixing. Compared to small pore throat regions, the growth of grains in the preferential flow path shall be more rapid because of consistent fine formation and grain interaction in the heavily flooded flow paths. The small mobile fines will gradually increase in size and be converted to static fines. Formation of static fines in the preferential flow path will force the water to get diverted towards the unswept volumes. These mixing of brines and precipitation in preferential flow paths can not only increase the overall sweep efficiency of the reservoir but also provide new surfaces for ion substitution followed by further fine formation.

Unlike the Halfdan field, selecting an infinitesimal volume in Dan A-block or B-block will not be analogue to core plug flooding as Multidirectional Flow, Large fractures and uneven symmetric are three major characteristics of Dan A-Block and B-Block; while core floods are unidirectional, wherein mostly large fractures are not present. The Halfdan field is very homogenously flooded, thus selecting a (infinitesimal volume) coreplug and conducting analysis on it gives a reflection of the brine flow in the reservoir. But in case of Dan A-Block there is a lack of homogeneity; thus random selection of an infinitesimal volume (coreplug) does not represent the average reservoir behavior. In Dan A-Block three possibly different flow patterns existent in the reservoirs including (1) Coreplugs near highly flooded large fractures, (2) region in diverted flow with potential of brine mixing and (3) unswept volumes. Therefore, reservoir water flooding in Dan A-Block and B-block containing highly uneven multidirectional flow with possibility of brine mixing (leading to fine formation) cannot be represented in laboratory experiments with unidirectional water front based movement in homogenous core water flood. Herein significant possibility of reservoir flow alteration through fines formation and salt precipitation exist. This can be achieved by injecting different brines which are individually soluble at reservoir condition but on mixing can form supersaturated solutions.

Multiple brine parallel injection (Experimental investigation):

Experimentally the above stated concept cannot be tested using traditional coreplug water flooding equipment as they only provide unidirectional flow opportunity. Therefore to conduct laboratory scale water flooding a few new additions is recommended.

A possible core slab flooding equipment with four injection brines is therefore proposed for mimicking the flow behavior in the Dan A-block. As shown in figure 10 the injection and effluent section of the core flooding equipment can be kept same as to classically used coreplug flooding equipment's. But instead of injecting four brines serially as previously reported, parallel injection can be conducted. Instead of flooding a cylindrical core plug a cubical core slab can be flooded (Figure 11). Use of a core slab ensures that four different brines can be injected in parallel from the different corners. Fluid production at the center of the core slab can be transported to the effluent tubes. The sematic design of the core slab is shown in Figure 12. It can typically contain of two sections, the place and the head. The head can contain the connection to the four injection pipes through which brine can be injected. The head can also contain a hydraulic pump through which the reservoir pressure can be controlled. The fluid in the injection cylinders can be piston controlled through a single ISCO pump thus ensuring same rate of flow through all the channels (Figure 10). With injection of brine from all four corners a pressure difference between the center and the four corners will be developed. Thus it shall ensure flow of fluid towards the effluent connection pipe at the center of the coreplug. Produced fluid from the center can be stored in rotating effluent tubes to conduct radiometric or volumetric oil production and effluent brine analysis.

Herein 3 experiments in similar conditions needs to be conducted to test the hypothesis that: formation of fine through mixing of brines can be used to increase oil production. For example if experiment are to be conducted for brines causing no precipitation on injection for reservoir condition of 130°C and 400 bars (Dan field conditions) the following three brines can be used:

- Case I: From all four injection cylinders SW4Ca0.25SO4 brine can be injected. It represents brine which is individually soluble at reservoir conditions, herein the proportion of Ca^{2+} has been selectively increased by 4 times while the fraction of SO_4^{2-} has been reduced to one fourth. The brine will form fines in reservoir only when ion substitution takes place on mineral surface.

- Case II: From all four injection cylinders SW0.25Ca4SO4 brine can be injected. It represents brine which is individually soluble at reservoir conditions, herein the proportion of SO_4^{2-} has been selectively increased by 4 times while the fraction of SO4 has been reduced to one fourth. This brine shall also form fines in reservoir only when ion substitution takes place on mineral surface.
- Case III: Diagonally in two corners SW4Ca0.25SO4 brine, while SW0.25Ca4SO4 can be injected in from the other two directions. Herein the additional SO_4 produced from brine one can be added to the other brine and vice versa for Ca^{2+}. Thus no new ions need to be injected during smart water EOR implementation. In this case fines formation can not only take place following ion substitution of individual brines, but fines formation can also take place during interactions of two different brines.

Any observed increase in oil production for case III over case I and II will prove that mixing of brines in reservoir can be used for EOR and injection of the same brine through all injection wells may not necessarily lead to optimum oil production. Thereafter Extended UNIQUAC model based core slab flooding can be used to develop a detailed production strategy for further consideration of implementation of smart water EOR in A-Block of Dan field or other similar oil reservoirs.

A reservoir prototype of the Dan field block A is needed where Extended UNIQUAC model can be implemented. Through simulation, possible locations for precipitation in the large fractures can be identified such that brine mixing can be used for alteration of water sweep efficiency. Herein targeted salt precipitation around over grown fractures can be used to even out the volumetric sweep of injected water and reduce flow through water short circuits. Implementation of Extended UNIQUAC model into reservoir simulators can be used for blocking water short circuits by multiple smart water injections through different injection wells in near water short circuits.

Conclusion:

Optimum composition for obtaining maximum fines formation has been calculated for various variations to sea water. It is observed that maximum fines formation and optimum oil recovery can take place, while precipitation occurs on injection. This precipitation on injection may not be acceptable for low permeability tight reservoirs so the composition up to which no precipitation takes place has to be determined. The corresponding amount of fines formation has also to be calculated. Based on these results and injection/production well network smart water EOR implementation strategy has been explored for Dan and Halfdan field. Injection of most cost effective single brine through all injection wells is recommended for Dan field west flank and Halfdan field. While a novel concept of parallel multiple brine injection for mixing based fine formation has been proposed for Dan field A-block and B-block, and core slab flooding equipment has been proposed for further investigation.

References

- Al Mahrouqi, D. A., Vinogradov, J., & Jackson, M. D. (2015, November). Understanding Controlled Salinity Waterflooding in Carbonates Using Streaming Potential Measurements. In *SPE Latin American and Caribbean Petroleum Engineering Conference*. Society of Petroleum Engineers.
- Albrechtsen, T., Andersen, S. J., Dons, T., Engstrøm, F., Jørgensen, O., & Sørensen, F. W. (2001, January). Halfdan: developing non-structurally trapped oil in North Sea Chalk. In *SPE Annual Technical Conference and Exhibition*. Society of Petroleum Engineers.
- Awan, A. R., Teigland, R., & Kleppe, J. (2008). A survey of North Sea enhanced-oil-recovery projects initiated during the years 1975 to 2005. *SPE Reservoir Evaluation & Engineering*, *11*(03), 497-512.
- Awolayo, A., Sarma, H., & AlSumaiti, A. (2015). An Experimental Investigation into the Impact of Sulfate Ions in Smart Water to Improve Oil Recovery in Carbonate Reservoirs. *Transport in Porous Media*, 1-20.
- Bæk M. Oil and Gas Production of Denmark 2013 http://www.ens.dk/sites/ens.dk/files/energistyrelsen/ Nyheder/2014/oil_and_gas_production_in_denmark_2013_uk.pdf
- Chakravarty, K. H., Fosbøl, P. L., & Thomsen, K. (2015, June). Importance of Fines in Smart Water Enhanced Oil Recovery (SmW-EOR) for Chalk Outcrops. In *EUROPEC 2015*. Society of Petroleum Engineers.
- Fathi, S. J., Austad, T., & Strand, S. (2011). Water-based enhanced oil recovery (EOR) by "smart water": Optimal ionic composition for EOR in carbonates. *Energy & fuels*, *25*(11), 5173-5179.
- Fathi, S. J., Austad, T., & Strand, S. (2012, January). Water-Based Enhanced Oil recovery (EOR) by" Smart Water" in Carbonate Reservoirs. In*SPE EOR Conference at Oil and Gas West Asia*. Society of Petroleum Engineers.
- Hansen, J. H., & Nederveen, N. (2002, January). Controlled Acid Jet (CAJ) technique for Effective Single Operation Stimulation of 14,000+ ft long reservoir sections. In *European Petroleum Conference*. Society of Petroleum Engineers.
- Hassan, A. M., Al-Sofi, M. A. K., Al-Amoudi, A. S., Jamaluddin, A. T. M., Farooque, A. M., Rowaili, A., & Al-Tisan, I. A. R. (1998). A new approach to membrane and thermal seawater desalination processes using nanofiltration membranes (Part 1). *Desalination*, *118*(1), 35-51.
- Hatchell, P. J., Jorgensen, O., Gommesen, L., & Stammeijer, J. (2007, January). Monitoring reservoir compaction from subsidence and time-lapse time shifts in the Dan field. In *77th SEG meeting. San Antonio, USA, SEG Technical Program Expanded Abstracts* (pp. 2867-2871).

- Hilal, N., Al-Zoubi, H., Mohammad, A. W., & Darwish, N. A. (2005). Nanofiltration of highly concentrated salt solutions up to seawater salinity.*Desalination*, *184*(1), 315-326.
- Jorgensen, L. N. (1992). Dan Field--Denmark Central Graben, Danish North Sea.
- Kokal, S., & Al-Kaabi, A. (2010). Enhanced oil recovery: challenges & opportunities. *World Petroleum Council: Official Publication*, *2010*, 64-69.
- Lafond, K., Pedersen, L. M., & Christiansen, L. B. (2010, January). FAST Optimization of Line-drive Water Injection. In *SPE EUROPEC/EAGE Annual Conference and Exhibition*. Society of Petroleum Engineers.
- Lindgreen, H., Drits, V. A., Salyn, A. L., Jakobsen, F., & Springer, N. (2011). Formation of flint horizons in North Sea chalk through marine sedimentation of nano-quartz. *Clay Minerals*, *46*(4), 525-537.
- Ovens, J. E. V., Larsen, F. P., & Cowie, D. R. (1998). Making sense of water injection fractures in the Dan field. *SPE Reservoir Evaluation & Engineering*, *1*(06), 556-566.
- Pontié, M., Derauw, J. S., Plantier, S., Edouard, L., & Bailly, L. (2013). Seawater desalination: nanofiltration—a substitute for reverse osmosis?.*Desalination and Water Treatment*, *51*(1-3), 485-494.
- Puntervold, T., Strand, S., Ellouz, R., & Austad, T. (2014, December). Why is it Possible to Produce Oil from the Ekofisk Field for Another 40 Years?. In*International Petroleum Technology Conference*. International Petroleum Technology Conference.
- RezaeiDoust, A., Puntervold, T., Strand, S., & Austad, T. (2009). Smart water as wettability modifier in carbonate and sandstone: A discussion of similarities/differences in the chemical mechanisms. *Energy & fuels*, *23*(9), 4479-4485.
- Rod, M. H. (2005, January). Injection Fracturing in a Densely Spaced Line Drive Waterflood-The Halfdan Example. In *SPE Europec/EAGE Annual Conference*. Society of Petroleum Engineers.
- Schiøler, P., & Wilson, G. J. (1993). Maastrichtian dinoflagellate zonation in the Dan Field, Danish North Sea. *Review of Palaeobotany and Palynology*,*78*(3), 321-351.
- Sunde, E., Beeder, J., Nilsen, R. K., & Torsvik, T. (1992, January). Aerobic microbial enhanced oil recovery for offshore use. In *SPE/DOE Enhanced Oil Recovery Symposium*. Society of Petroleum Engineers.
- Vo, L. T., Gupta, R., & Hehmeyer, O. J. (2012, January). Ion chromatography analysis of advanced ion management carbonate coreflood experiments. In *Abu Dhabi International Petroleum Conference and Exhibition*. Society of Petroleum Engineers.
- Webb, K. J., Black, C. J. J., & Al-Ajeel, H. (2003, January). Low salinity oil recovery-log-inject-log. In *Middle East Oil Show*. Society of Petroleum Engineers.
- Yousef, A. A., & Ayirala, S. C. (2014, April). A novel water ionic composition optimization technology for SmartWater flooding application in carbonate reservoirs. In *SPE Improved Oil Recovery Symposium*. Society of Petroleum Engineers.

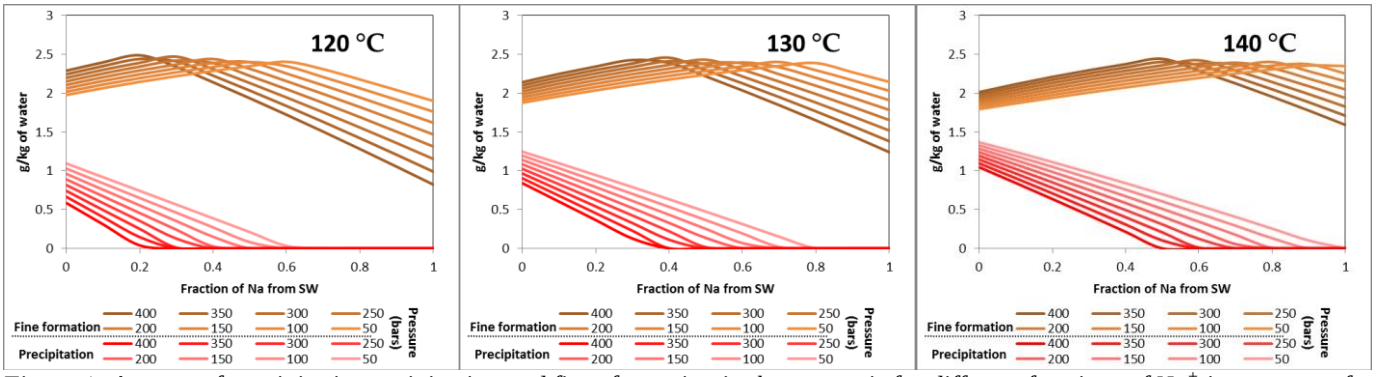


Figure 1: Amount of precipitation on injection and fines formation in the reservoir for different fractions of Na^+ in sea water for different variation in pressure temperature conditions.

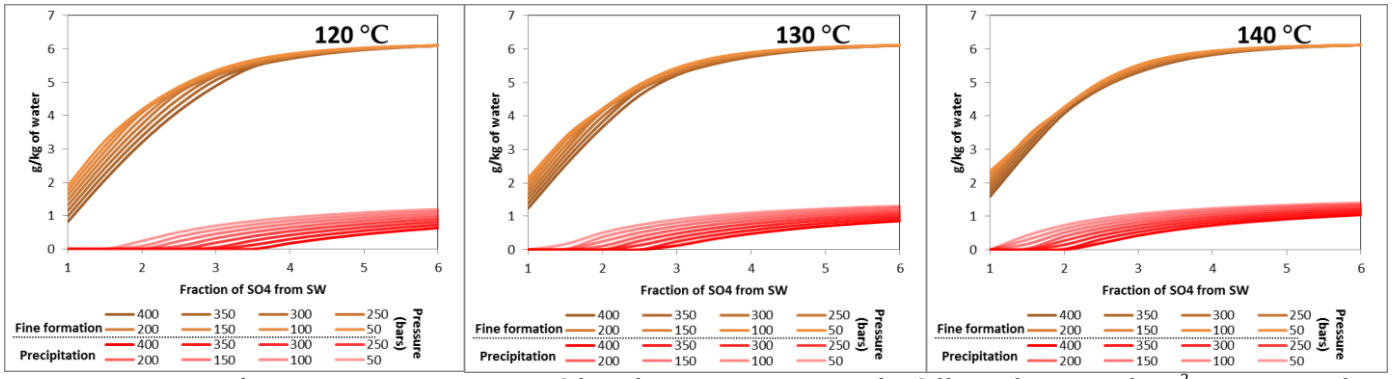


Figure 2: Amount of precipitation on injection and fines formation in reservoir for different fractions of SO_4^{2-} in sea water for different variations in pressure and temperature conditions. The SO_4^{2-} concentration is enriched by replacing of Cl^- (overall salinity remains constant).

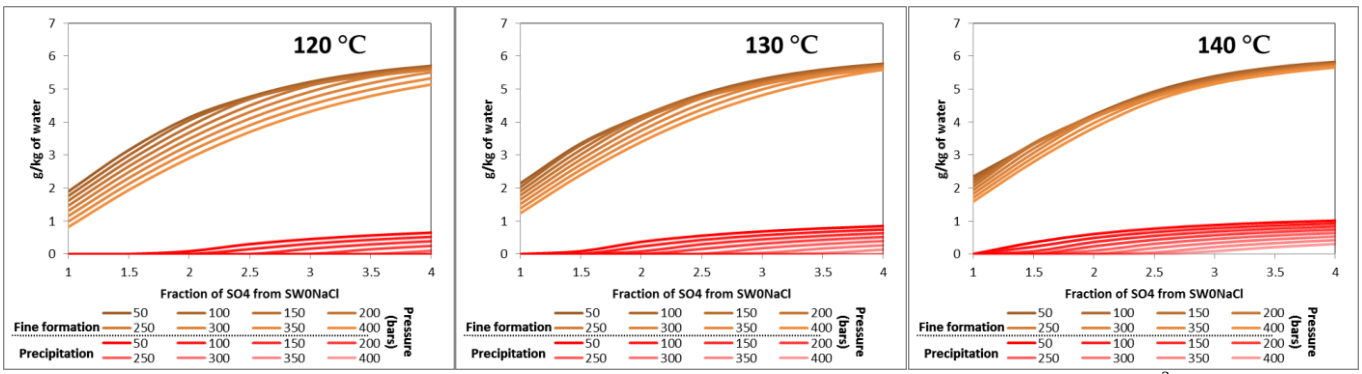


Figure 3: Amount of precipitation on injection and fine formation in reservoir for different fractions of SO_4^{2-} in sea water for different variation in pressure temperature conditions. SO_4^{2-} concentration is enriched by adding Na_2SO_4.

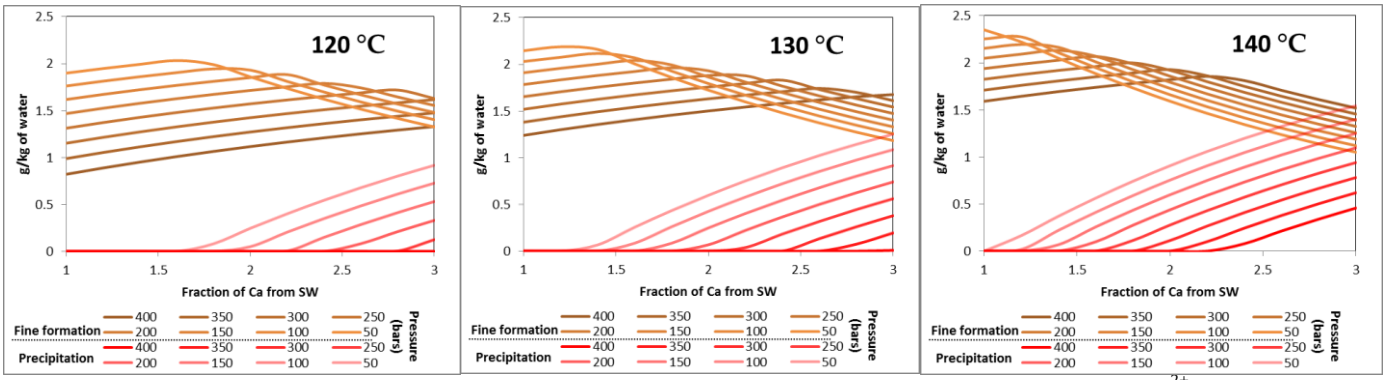


Figure 4: Amount of precipitation on injection and fines formation in reservoir for different fractions of Ca^{2+} in sea water for different variations in pressure and temperature conditions.

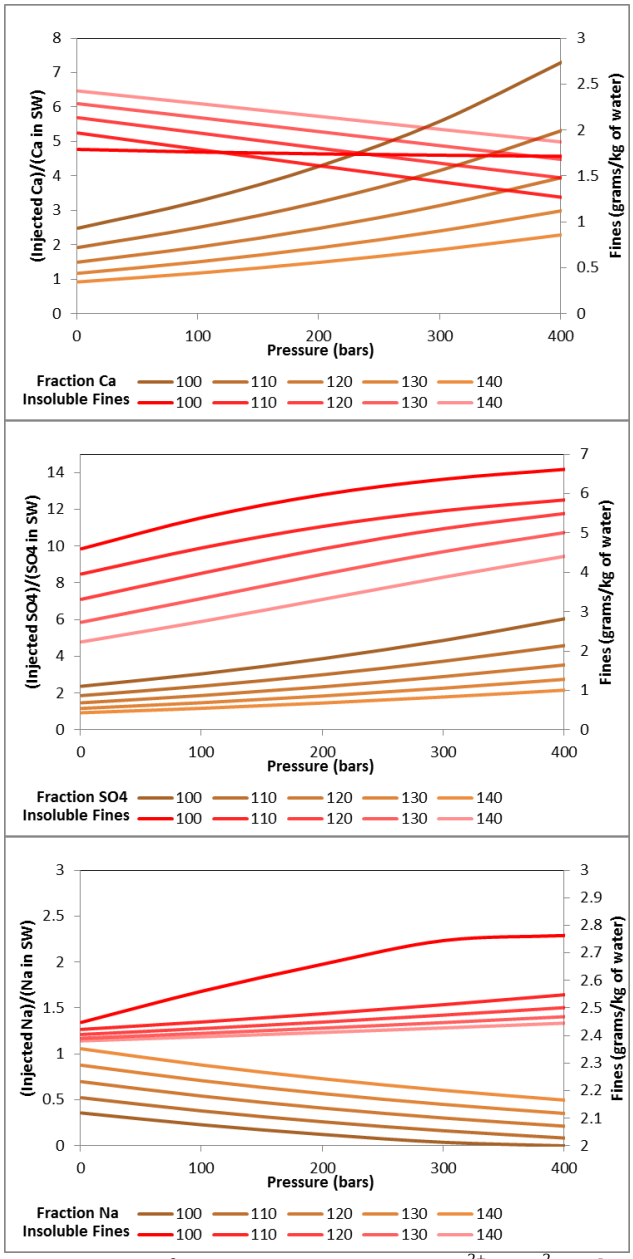


Figure 5: Amount of fines formation in reservoir for optimum variation in Ca^{2+}, SO_4^{2-} and Na^{+} fraction (individually) from sea water so that no precipitation on injection takes place for different variation in pressure and temperature conditions.

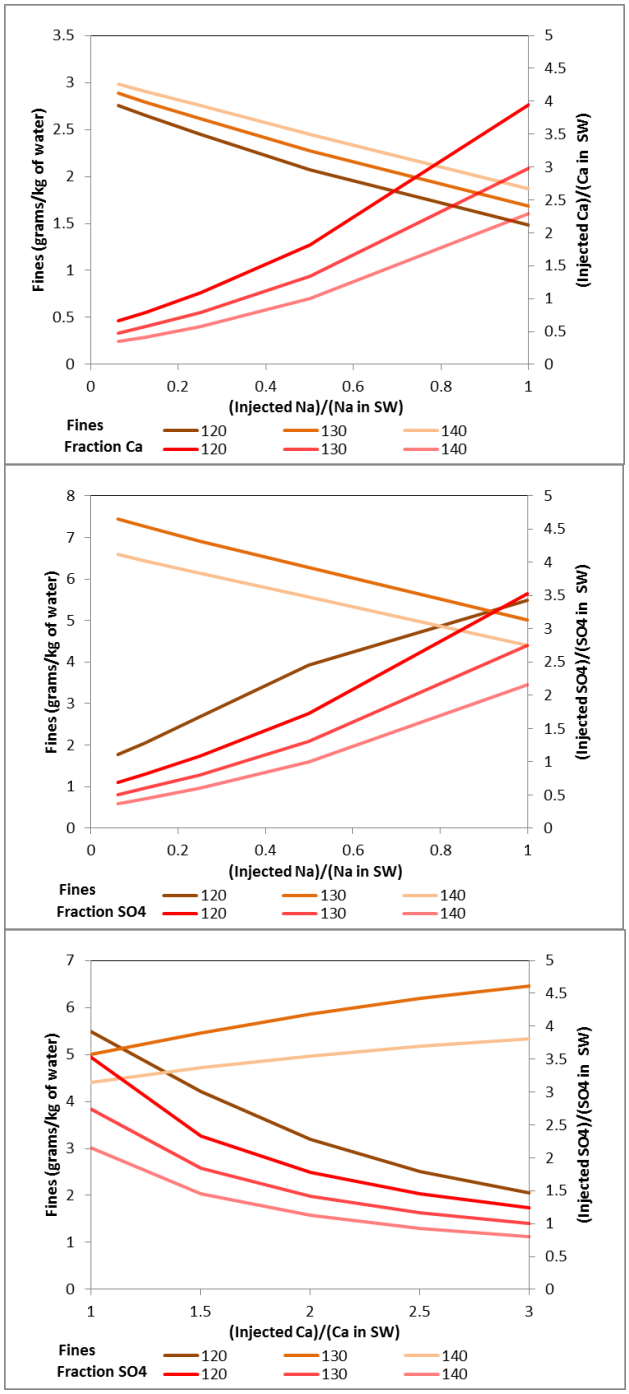


Figure 6: Amount of fine formation in reservoir for multiple ion variation from sea water so that no precipitation on injection for different variation in temperature at 400 bars.

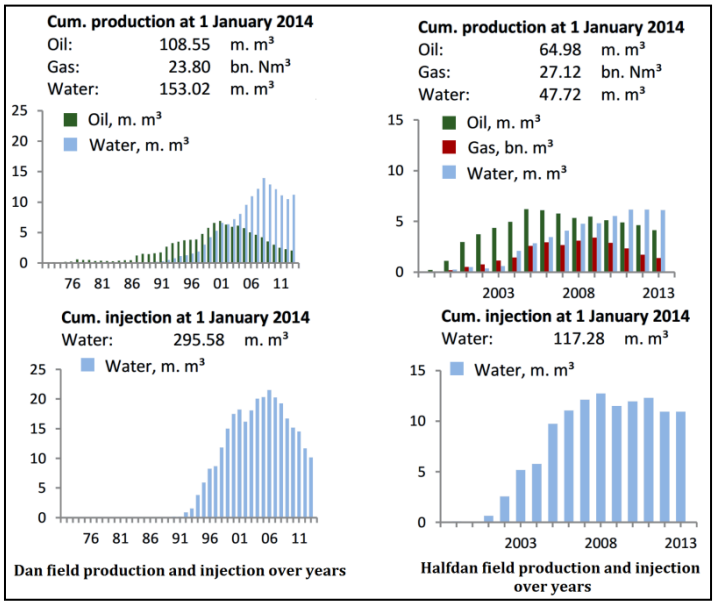


Figure 7: Amount of injected water and produced oil, water and gas from Dan and Halfdan fields during production its production.

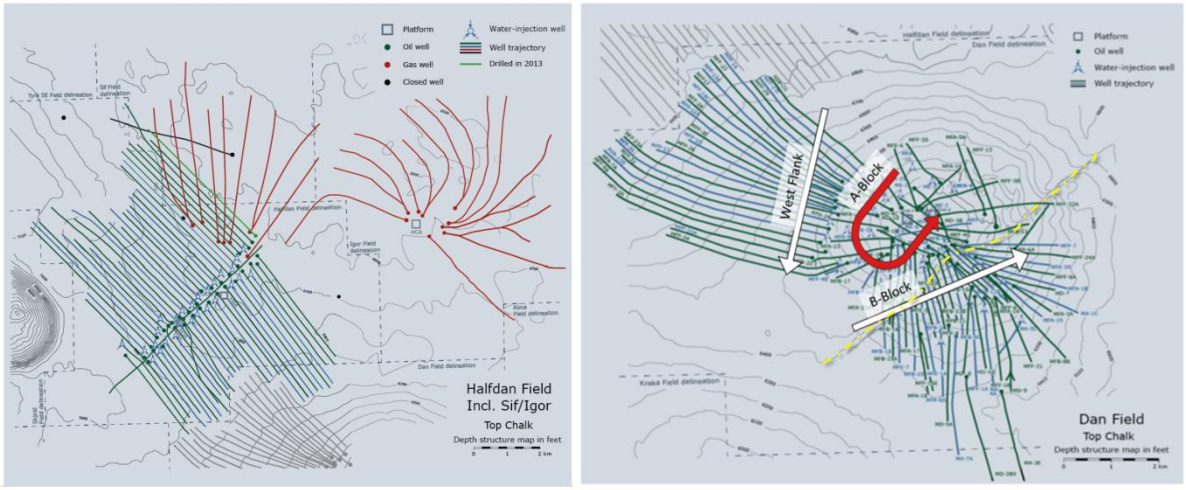


Figure 8: Dan and Halfdan depth structure and exisiting injection production well network. Dan field well network is sub divided in three sections according to its development history.

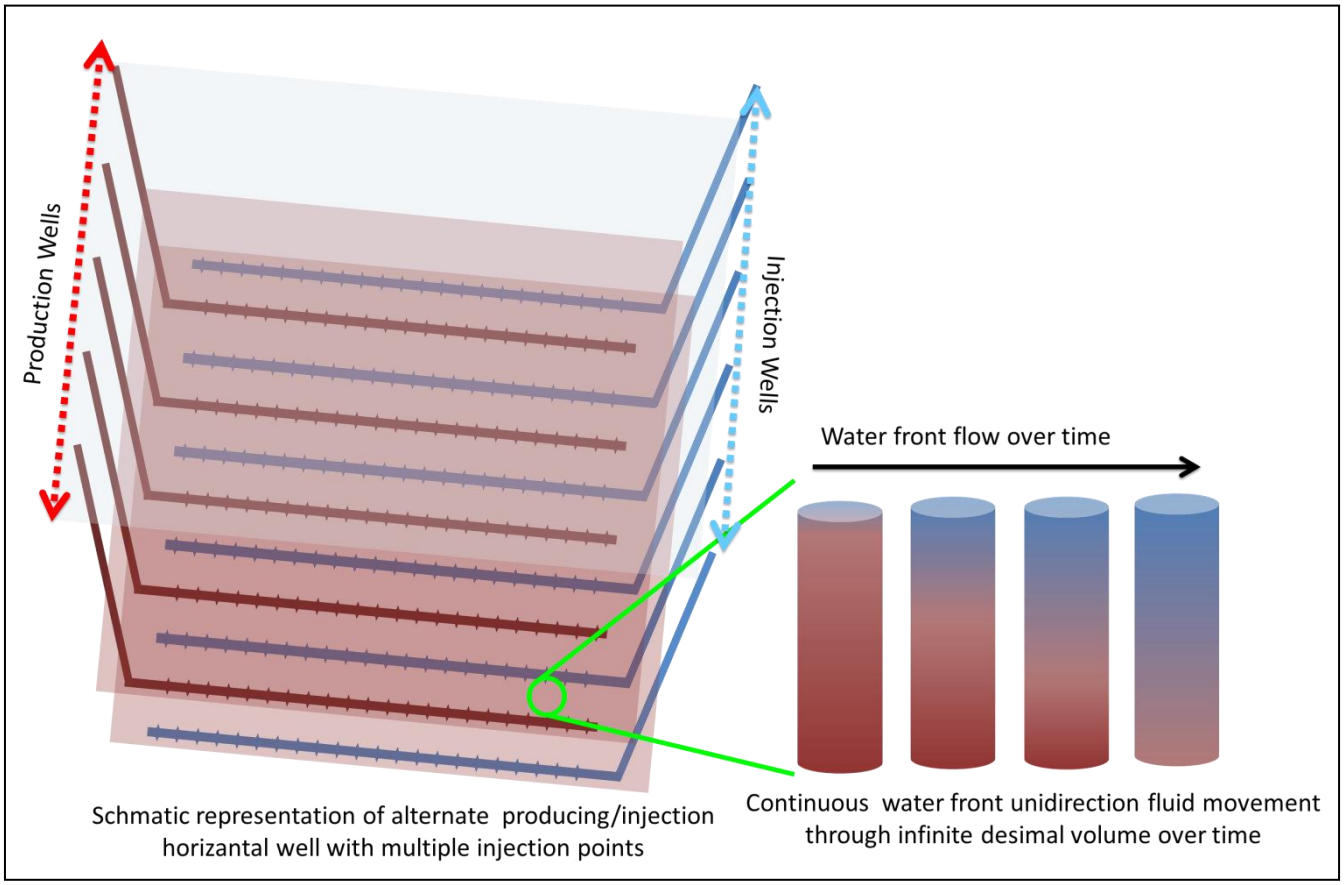


Figure 9: A Scematic representation alternate injection/production horizontal wells in Dan West flank and Halfdan field, show unidirectional water front movement with an infinitetesimal volume being perfectly analogues to laboratory coreflooding expriments.

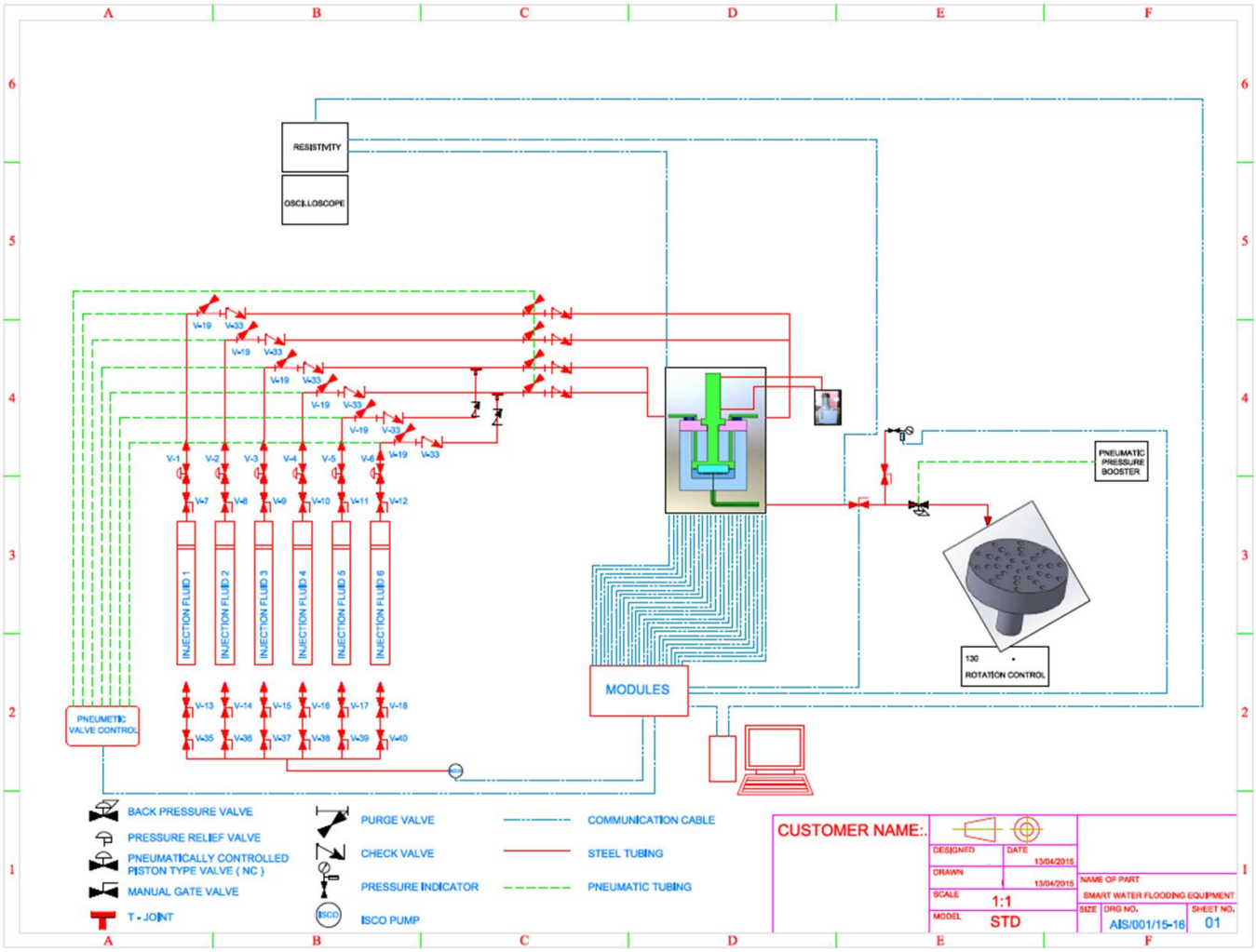


Figure 10: PI diagram of core slab flooding equipment to ensure multiple brine parallel injection.

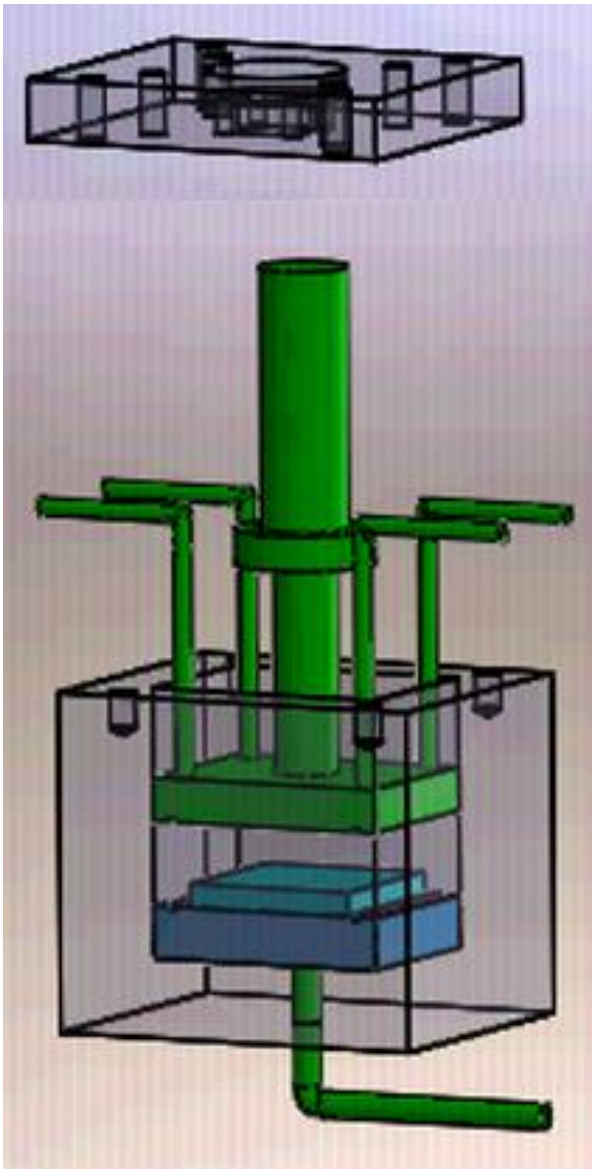


Figure 11: Schematic diagram of core slab flooding equipment (core slab holder section) to ensure four multiple brine parallel injection.

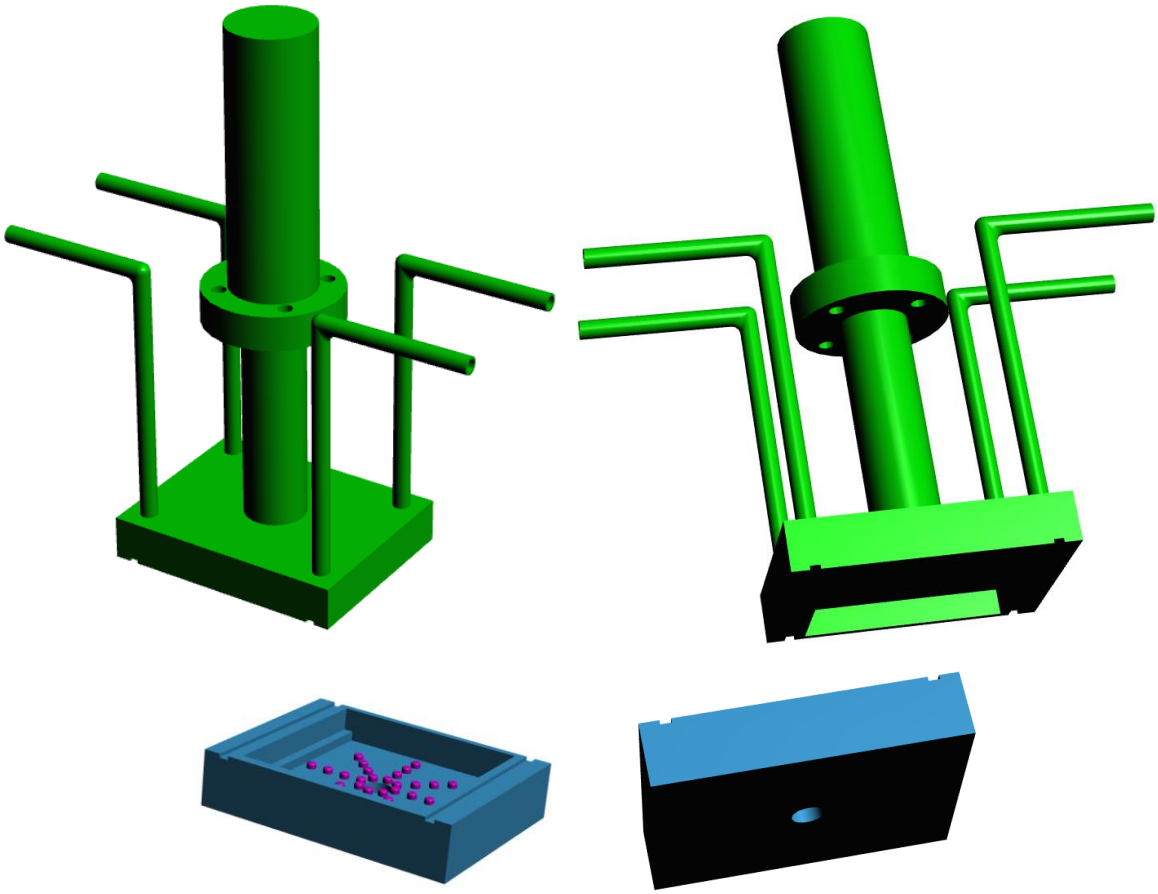


Figure 12: 3 dimensional view presentations of the head and the base of the core slab holder equipment ensuring multiple brine parallel injection.

Paper XV

Extended UNIQUAC Calculation of Solubilities of various smart water floods at reservoir conditions

Chakravarty, K. H., Fosbøl P. L., Thomsen K. Extended UNIQUAC Calculation of Solubilities of various smart water floods at reservoir conditions

Paper XV: Extended UNIQUAC Calculation of Solubilities of various smart water floods at reservoir conditions

Using Extended UNIQUAC model (Thomsen et al. 1996; Thomsen et al. 2004; Iliuta et al. 2000) calculation the brine speciation in reservoir condition of the commonly studied brines in literature has been reported in this study. In reported articles several spontaneous imbibition experiments have been conducted at pressures of 10 bars to 50 bars (Faithi et al. 2010; Faithi et al. 2011; Fernø et al. 2011); while water flooding experiments have been conducted at 70 bars to 400 bars (Paper XI, XII and XIII; Zahid et al. 2010; Zahid et al. 2011). So to include various studies the speciation calculation was conducted from pressure of 1 bar to 400 bars using Extended UNIQUAC model. Consistent reports over the past decade have shown that SmW-EOR can be achieved from temperatures of 70 °C (Austad et al. 2009; Vo et al. 2012; Zahid et al. 2010). SmW-EOR experiments have been conducted at higher temperature as well, ranging from 130 °C to 150°C (Faithi et al. 2011; Fernø et al. 2011; Austad et al. 2009; Vo et al. 2012; Zahid et al. 2010). Therefore for various brines reported in literature the Extended UNIQUAC calculations were conducted over temperature variation from 70 °C to 160°C. From the conducted studies, as shown in Paper VI, VII and IX, the amount of soluble SO_4^{2-}, amount of total soluble potential ions and insoluble potential precipitation salts can be significantly different at reservoir conditions, when compared to the injection brine at room temperature. Furthermore brine speciation on injection at reservoir condition can be significantly different from that in the reservoir after Ca^{2+}/Mg^{2+}ion substitution (as recommended by Austad et al. 2009) have taken place. Therefore speciation calculation was conducted for both cases, including brine properties on injection and brine properties after substitution. In Paper IX it has been shown that, the total precipitation taking place after substitution should remain the dominant factor over the precipitation on injection, for continued increase in oil recovery. Therefore the effective fine formation (i.e. obtained by subtracting the precipitation on injection from the total precipitation taking place after substitution) was also calculated for various brines over the pressure temperature variations. Most of the commonly used brines in literature were used to calculate the brine section taking place at reservoir conditions on injection and after substitution as listed below:

1. SW0NaCl : Sea Water without NaCl (Puntervold et al. 2014; Fathi et al. 2010)
2. SW0NaCl-2SO_4^{2-} : Sea Water without NaCl and twice SO_4^{2-} (Puntervold et al. 2015)
3. SW0NaCl-3SO_4 : Sea Water without NaCl and thrice SO_4^{2-}(Puntervold et al. 2015)
4. SW0NaCl-4SO_4 : Sea Water without NaCl and four times SO_4^{2-}(Puntervold et al. 2014; Fathi et al. 2011)
5. SW-2SO_4: Sea Water with twice SO_4^{2-} (Awolayo et al. 2014)
6. SW-3SO_4: Sea Water with thrice SO_4^{2-} (Strand et al. 2008)
7. SW-4SO_4: Sea Water with four times SO_4^{2-} (Awolayo et al. 2014)
8. SW-8SO_4: Sea Water with eight times SO_4^{2-} (Awolayo et al. 2014)
9. SW-0Ca: Sea Water without Ca^{2+} (Austad et al. 2009, Zang et al. 2006)
10. SW-½Ca: Sea Water with half of the Ca^{2+} ions (Austad et al. 2009, Zang et al. 2006)
11. SW-2Ca: Sea Water with twice Ca^{2+} (Austad et al. 2009, Zang et al. 2006)
12. SW-3Ca: Sea Water with thrice Ca^{2+} (Austad et al. 2009, Zang et al. 2006)
13. SW-4NaCl: Sea Water with 4 times NaCl (Fathi et al. 2010)

1. SW0NaCl : Sea Water without NaCl

SW0NaCl	Precipitation (on injection) :mg / kg of water								
	Pressure (bars)								
Temperature °C	1	50	100	150	200	250	300	350	400
70	28.33	26.58	24.84	23.14	21.49	19.89	18.35	16.86	15.43
80	204.92	62.7	30.25	28.41	26.61	24.85	23.13	21.45	19.83
90	512.77	396.76	272.84	143.62	32.28	30.39	28.53	26.71	24.91
100	769.86	675.91	575.49	470.76	362.02	249.66	134.11	32.45	30.54
110	981.5	905.99	825.19	740.84	653.21	562.63	469.47	374.13	277.09
120	1153.36	1093.18	1028.66	961.21	891.06	818.47	743.75	667.25	589.36
130	1291.08	1243.55	1192.48	1138.97	1083.22	1025.44	965.89	925.09	863.06
140	1400.04	1362.85	1322.78	1304.24	1260.37	1214.82	1167.82	1119.58	1070.38
150	1538.59	1482.84	1451.78	1419.07	1384.83	1349.19	1312.32	1274.41	1235.68
160	1614.15	1591.6	1567.19	1541.43	1514.41	1486.24	1425.91	1396.37	1366.12

SW0NaCl	Soluble SO4 on injection : mg / kg of water								
	Pressure (bars)								
Temperature °C	1	50	100	150	200	250	300	350	400
70	2305.51	2305.51	2305.51	2305.51	2305.51	2305.51	2305.51	2305.51	2305.51
80	2183.87	2283.76	2305.51	2305.51	2305.51	2305.51	2305.51	2305.51	2305.51
90	1968.63	2050.06	2137.02	2227.66	2305.51	2305.51	2305.51	2305.51	2305.51
100	1789.1	1855.01	1925.42	1998.82	2074.99	2153.68	2234.56	2305.51	2305.51
110	1641.49	1694.43	1751.04	1810.1	1871.41	1934.76	1999.88	2066.49	2134.25
120	1521.73	1563.9	1609.07	1656.25	1705.28	1755.97	1808.11	1861.45	1915.73
130	1425.82	1459.12	1494.84	1532.23	1571.14	1611.42	1652.9	1679.64	1723.72
140	1349.93	1375.98	1403.99	1414.89	1446.29	1478.84	1512.39	1546.77	1581.82
150	1249.34	1291.79	1314.22	1337.78	1362.39	1387.96	1414.36	1441.47	1469.14
160	1201.73	1217.6	1234.78	1252.91	1271.93	1291.76	1337.69	1358.9	1380.58

SW0NaCl	Total soluble potential ions, on injection : mg / kg of water								
	Pressure (bars)								
Temperature °C	1	50	100	150	200	250	300	350	400
70	3908.91	3909.61	3910.31	3910.99	3911.65	3912.29	3912.91	3913.51	3914.08
80	3734.84	3876.67	3908.14	3908.88	3909.6	3910.31	3911	3911.67	3912.32
90	3428.68	3544.32	3667.83	3796.6	3907.33	3908.09	3908.83	3909.56	3910.28
100	3173.18	3266.81	3366.84	3471.15	3579.42	3691.27	3806.27	3907.26	3908.03
110	2963	3038.23	3118.68	3202.64	3289.83	3379.93	3472.57	3567.34	3663.78
120	2792.42	2852.36	2916.57	2983.67	3053.42	3125.57	3199.79	3275.75	3353.06
130	2655.78	2703.11	2753.92	2807.11	2862.5	2919.86	2978.95	3019.97	3082.28
140	2547.67	2584.7	2624.54	2643.38	2687.66	2733.58	2780.94	2829.5	2879
150	2411.4	2467.48	2499.01	2532.16	2566.82	2602.84	2640.07	2678.31	2717.36
160	2341.59	2364.1	2388.47	2414.18	2441.16	2469.27	2529.69	2559.57	2590.13

SW0NaCl	Precipitation after substitution : mg / kg of water								
	Pressure (bars)								
Temperature °C	1	50	100	150	200	250	300	350	400
70	2534.47	2438.34	2332.59	2219.09	2097.96	1969.41	1833.79	1691.56	1543.34
80	2734.37	2661.61	2581.56	2495.64	2403.94	2306.61	2203.91	2096.2	1983.93
90	2890.65	2836.14	2776.19	2711.85	2643.18	2570.31	2493.41	2412.76	2328.71
100	3010.68	2970.18	2925.63	2877.84	2826.84	2772.73	2715.64	2655.78	2593.38
110	3101.67	3071.74	3038.83	3003.53	2965.87	2925.93	2883.8	2839.63	2793.6
120	3169.96	3147.92	3123.7	3097.73	3070.03	3040.66	3009.69	2977.23	2943.41
130	3220.85	3204.65	3186.86	3167.8	3147.47	3125.92	3103.21	3079.4	3054.61
140	3258.58	3246.69	3233.63	3219.65	3204.74	3188.95	3172.3	3154.86	3136.69
150	3286.47	3277.73	3268.15	3257.88	3246.95	3235.37	3223.16	3210.38	3197.06
160	3307.03	3300.61	3293.57	3286.03	3278	3269.49	3260.53	3251.14	3241.37

SW0NaCl	Soluble SO4 after substitution : mg / kg of water								
	Pressure (bars)								
Temperature °C	1	50	100	150	200	250	300	350	400
70	555.34	621.93	695.27	774.06	858.23	947.62	1041.99	1141.02	1244.27
80	418.05	468.23	523.49	582.87	646.32	713.71	784.87	859.55	937.44
90	311.41	348.78	389.94	434.17	481.43	531.63	584.64	640.27	698.29
100	230.07	257.67	288.06	320.71	355.58	392.63	431.74	472.79	515.59
110	168.92	189.16	211.44	235.38	260.95	288.09	316.75	346.82	378.16
120	123.44	138.21	154.47	171.94	190.58	210.37	231.26	253.17	276
130	89.89	100.63	112.46	125.15	138.7	153.08	168.25	184.15	200.72
140	65.29	73.09	81.67	90.87	100.69	111.11	122.1	133.62	145.62
150	47.34	52.99	59.2	65.86	72.97	80.51	88.46	96.79	105.46
160	34.28	38.37	42.86	47.68	52.82	58.27	64.01	70.03	76.29

SW0NaCl	Total soluble potential ions ; on injection: mg / kg of water								
	Pressure (bars)								
Temperature °C	1	50	100	150	200	250	300	350	400
70	2128.03	2223.11	2327.78	2440.17	2560.19	2687.62	2822.12	2963.22	3110.31
80	1931.33	2003.1	2082.11	2166.97	2257.6	2353.84	2455.43	2562.02	2673.16
90	1778.13	1831.71	1890.7	1954.05	2021.7	2093.53	2169.37	2248.93	2331.89
100	1660.96	1700.62	1744.28	1791.16	1841.22	1894.37	1950.46	2009.31	2070.66
110	1572.56	1601.74	1633.86	1668.33	1705.13	1744.2	1785.41	1828.65	1873.71
120	1506.57	1527.95	1551.46	1576.7	1603.63	1632.21	1662.36	1693.97	1726.92
130	1457.68	1473.3	1490.47	1508.89	1528.54	1549.39	1571.37	1594.42	1618.43
140	1421.68	1433.06	1445.58	1459	1473.31	1488.49	1504.5	1521.27	1538.74
150	1395.26	1403.55	1412.67	1422.44	1432.86	1443.9	1455.54	1467.74	1480.44
160	1375.92	1381.97	1388.6	1395.72	1403.3	1411.34	1419.81	1428.68	1437.91

SW0NaCl	Effective fine formation : mg / kg of water								
	Pressure (bars)								
Temperature °C	1	50	100	150	200	250	300	350	400
70	2506.14	2411.76	2307.74	2195.95	2076.46	1949.51	1815.43	1674.69	1527.9
80	2529.45	2598.91	2551.3	2467.22	2377.32	2281.75	2180.77	2074.74	1964.1
90	2377.87	2439.38	2503.35	2568.23	2610.9	2539.91	2464.87	2386.05	2303.79
100	2240.82	2294.27	2350.14	2407.08	2464.82	2523.07	2581.53	2623.32	2562.84
110	2120.17	2165.74	2213.63	2262.69	2312.66	2363.3	2414.33	2465.5	2516.51
120	2016.6	2054.74	2095.03	2136.51	2178.97	2222.19	2265.94	2309.97	2354.05
130	1929.76	1961.1	1994.38	2028.82	2064.25	2100.48	2137.31	2154.31	2191.54
140	1858.53	1883.84	1910.84	1915.4	1944.37	1974.12	2004.48	2035.27	2066.3
150	1747.87	1794.89	1816.36	1838.81	1862.12	1886.17	1910.84	1935.96	1961.38
160	1692.88	1709.01	1726.37	1744.59	1763.58	1783.24	1834.62	1854.77	1875.25

2. SW0NaCl-2SO_4^{2-} : Sea Water without NaCl and twice SO_4^{2-}

SW0NaCl-2SO4	Precipitation (on injection) :mg / kg of water								
	Pressure (bars)								
Temperature °C	1	50	100	150	200	250	300	350	400
70	645.16	517.95	379.08	231.22	74.66	18.69	17.19	15.75	14.36
80	902.66	803.97	696.11	581.16	459.34	330.97	196.5	56.48	18.58
90	1108	1032.38	949.65	861.38	767.74	668.99	565.47	457.59	345.89
100	1268.53	1211.18	1148.37	1081.3	1010.09	934.93	856.06	773.82	688.6
110	1392.04	1348.9	1301.62	1251.1	1197.42	1140.72	1081.18	1019.05	954.62
120	1485.89	1453.65	1418.3	1380.51	1340.33	1297.86	1268.86	1222.38	1174.14
130	1556.55	1549.35	1523.3	1495.39	1465.67	1434.21	1401.13	1366.54	1330.62
140	1650.59	1632.78	1613.23	1592.29	1548.28	1525.02	1500.54	1474.92	1448.31
150	1699.1	1685.97	1671.53	1656.08	1639.62	1622.19	1603.85	1584.68	1564.76
160	1736.38	1726.69	1716.06	1704.66	1692.53	1679.67	1666.15	1652	1637.3

SW0NaCl-2SO4	Soluble SO4 on injection : mg / kg of water								
	Pressure (bars)								
Temperature °C	1	50	100	150	200	250	300	350	400
70	4170.79	4260.38	4358.15	4462.22	4572.38	4611.03	4611.03	4611.03	4611.03
80	3990.16	4059.66	4135.58	4216.45	4302.12	4392.36	4486.86	4585.23	4611.03
90	3846.25	3899.5	3957.72	4019.79	4085.6	4154.96	4227.64	4303.35	4381.71
100	3733.85	3774.24	3818.42	3865.56	3915.56	3968.3	4023.6	4081.24	4140.92
110	3647.43	3677.81	3711.05	3746.53	3784.19	3823.92	3865.6	3909.06	3954.08
120	3581.74	3604.46	3629.3	3655.82	3683.97	3713.67	3733.07	3766.31	3800.75
130	3532.2	3536.31	3555.31	3575.59	3597.12	3619.85	3643.7	3668.58	3694.38
140	3468.21	3480.74	3494.5	3509.24	3542.67	3559.64	3577.45	3596.02	3615.27
150	3440.31	3449.56	3459.72	3470.6	3482.18	3494.45	3507.35	3520.85	3534.87
160	3419.72	3426.53	3434.02	3442.04	3450.59	3459.64	3469.16	3479.12	3489.46

SW0NaCl-2SO4	Total soluble potential ions, on injection : mg / kg of water								
	Pressure (bars)								
Temperature °C	1	50	100	150	200	250	300	350	400
70	5593.35	5720.42	5859.11	6006.74	6163.04	6218.29	6218.89	6219.47	6220.02
80	5336.76	5435.33	5543.03	5657.78	5779.36	5907.44	6041.58	6181.24	6218.33
90	5132.25	5207.78	5290.38	5378.47	5471.88	5570.36	5673.57	5781.1	5892.42
100	4972.46	5029.75	5092.44	5159.35	5230.35	5305.27	5383.84	5465.74	5550.58
110	4849.57	4892.66	4939.84	4990.22	5043.71	5100.18	5159.44	5221.24	5285.3
120	4756.18	4788.39	4823.66	4861.32	4901.33	4943.57	4972.93	5019.82	5068.43
130	4685.79	4693.51	4720.13	4748.58	4778.82	4810.77	4844.32	4879.34	4915.68
140	4597.23	4615.01	4634.52	4655.42	4699.74	4723.52	4748.5	4774.57	4801.62
150	4555.11	4568.22	4582.63	4598.06	4614.49	4631.88	4650.19	4669.33	4689.21

160	4523.59	4533.26	4543.88	4555.25	4567.37	4580.2	4593.7	4607.82	4622.5

SW0NaCl-2SO4	Precipitation after substitution : mg / kg of water								
	Pressure (bars)								
Temperature °C	1	50	100	150	200	250	300	350	400
70	2534.47	2438.34	2332.59	2219.09	2097.96	1969.41	1833.79	1691.56	1543.34
80	2734.37	2661.61	2581.56	2495.64	2403.94	2306.61	2203.91	2096.2	1983.93
90	2890.65	2836.14	2776.19	2711.85	2643.18	2570.31	2493.41	2412.76	2328.71
100	3010.68	2970.18	2925.63	2877.84	2826.84	2772.73	2715.64	2655.78	2593.38
110	3101.67	3071.74	3038.83	3003.53	2965.87	2925.93	2883.8	2839.63	2793.6
120	3169.96	3147.92	3123.7	3097.73	3070.03	3040.66	3009.69	2977.23	2943.41
130	3220.85	3204.65	3186.86	3167.8	3147.47	3125.92	3103.21	3079.4	3054.61
140	3258.58	3246.69	3233.63	3219.65	3204.74	3188.95	3172.3	3154.86	3136.69
150	3286.47	3277.73	3268.15	3257.88	3246.95	3235.37	3223.16	3210.38	3197.06
160	3307.03	3300.61	3293.57	3286.03	3278	3269.49	3260.53	3251.14	3241.37

SW0NaCl-2SO4	Soluble SO4 after substitution : mg / kg of water								
	Pressure (bars)								
Temperature °C	1	50	100	150	200	250	300	350	400
70	555.34	621.93	695.27	774.06	858.23	947.62	1041.99	1141.02	1244.27
80	418.05	468.23	523.49	582.87	646.32	713.71	784.87	859.55	937.44
90	311.41	348.78	389.94	434.17	481.43	531.63	584.64	640.27	698.29
100	230.07	257.67	288.06	320.71	355.58	392.63	431.74	472.79	515.59
110	168.92	189.16	211.44	235.38	260.95	288.09	316.75	346.82	378.16
120	123.44	138.21	154.47	171.94	190.58	210.37	231.26	253.17	276
130	89.89	100.63	112.46	125.15	138.7	153.08	168.25	184.15	200.72
140	65.29	73.09	81.67	90.87	100.69	111.11	122.1	133.62	145.62
150	47.34	52.99	59.2	65.86	72.97	80.51	88.46	96.79	105.46
160	34.28	38.37	42.86	47.68	52.82	58.27	64.01	70.03	76.29

SW0NaCl-2SO4	Total soluble potential ions ; on injection: mg / kg of water								
	Pressure (bars)								
Temperature °C	1	50	100	150	200	250	300	350	400
70	2128.03	2223.11	2327.78	2440.17	2560.19	2687.62	2822.12	2963.22	3110.31
80	1931.33	2003.1	2082.11	2166.97	2257.6	2353.84	2455.43	2562.02	2673.16
90	1778.13	1831.71	1890.7	1954.05	2021.7	2093.53	2169.37	2248.93	2331.89
100	1660.96	1700.62	1744.28	1791.16	1841.22	1894.37	1950.46	2009.31	2070.66
110	1572.56	1601.74	1633.86	1668.33	1705.13	1744.2	1785.41	1828.65	1873.71
120	1506.57	1527.95	1551.46	1576.7	1603.63	1632.21	1662.36	1693.97	1726.92
130	1457.68	1473.3	1490.47	1508.89	1528.54	1549.39	1571.37	1594.42	1618.43
140	1421.68	1433.06	1445.58	1459	1473.31	1488.49	1504.5	1521.27	1538.74
150	1395.26	1403.55	1412.67	1422.44	1432.86	1443.9	1455.54	1467.74	1480.44

160	1375.92	1381.97	1388.6	1395.72	1403.3	1411.34	1419.81	1428.68	1437.91

SW0NaCl-2SO4	Effective fine formation : mg / kg of water								
	Pressure (bars)								
Temperature °C	1	50	100	150	200	250	300	350	400
70	1889.3	1920.38	1953.5	1987.87	2023.29	1950.71	1816.59	1675.81	1528.97
80	1831.71	1857.64	1885.44	1914.48	1944.6	1975.63	2007.4	2039.71	1965.35
90	1782.64	1803.76	1826.54	1850.47	1875.43	1901.31	1927.94	1955.17	1982.81
100	1742.15	1759	1777.26	1796.53	1816.75	1837.8	1859.57	1881.95	1904.77
110	1709.63	1722.83	1737.2	1752.42	1768.45	1785.21	1802.62	1820.58	1838.98
120	1684.07	1694.26	1705.39	1717.21	1729.7	1742.8	1740.83	1754.85	1769.26
130	1664.29	1655.3	1663.56	1672.4	1681.8	1691.7	1702.08	1712.86	1723.98
140	1607.99	1613.9	1620.4	1627.35	1656.45	1663.92	1671.76	1679.93	1688.38
150	1587.36	1591.76	1596.61	1601.8	1607.33	1613.17	1619.3	1625.69	1632.29
160	1570.65	1573.91	1577.5	1581.36	1585.47	1589.81	1594.38	1599.14	1604.06

3. **SW0NaCl-3SO_4 : Sea Water without NaCl and thrice SO_4^{2-}**

	Na	Mg	Ca	SO4	HCO3-	Cl-
SW0NaCl-3SO4	0.03	0.045	0.013	0.072	0.002	0

SW0NaCl-3SO4	Precipitation (on injection) :mg / kg of water								
	Pressure (bars)								
Temperature °C	1	50	100	150	200	250	300	350	400
70	856.09	748.13	629.43	502.12	366.35	222.39	70.64	13.52	12.22
80	1068.44	985.67	894.65	797.02	692.89	582.47	466.06	344.09	217.1
90	1235.8	1172.95	1103.83	1029.69	950.62	866.76	778.36	685.74	589.31
100	1365.5	1318.12	1266.02	1210.14	1150.55	1087.36	1020.75	950.96	878.31
110	1464.75	1429.22	1390.16	1348.28	1303.62	1256.27	1206.37	1154.1	1099.69
120	1540.01	1513.46	1484.29	1453.02	1431.32	1396.14	1359.04	1320.16	1279.68
130	1621.73	1589.34	1567.86	1544.8	1520.18	1494.07	1466.52	1437.66	1407.61
140	1673.22	1658.5	1642.32	1624.96	1606.46	1586.84	1547.24	1525.86	1503.59
150	1713.86	1702.93	1690.92	1678.04	1664.3	1649.74	1634.4	1618.34	1601.63
160	1745.68	1737.57	1728.65	1719.09	1708.9	1698.09	1686.71	1674.79	1662.4

SW0NaCl-3SO4	Soluble SO4 on injection : mg / kg of water								
	Pressure (bars)								
Temperature °C	1	50	100	150	200	250	300	350	400
70	6323.8	6399.9	6483.55	6573.22	6668.82	6770.16	6876.96	6916.55	6916.55
80	6174.65	6233	6297.13	6365.87	6439.16	6516.85	6598.72	6684.47	6773.73
90	6057.18	6101.49	6150.18	6202.36	6257.98	6316.93	6379.04	6444.09	6511.79
100	5966.17	5999.58	6036.27	6075.58	6117.47	6161.84	6208.58	6257.52	6308.43
110	5896.51	5921.57	5949.07	5978.51	6009.86	6043.06	6078.01	6114.58	6152.62

120	5843.58	5862.31	5882.84	5904.8	5919.25	5944.58	5971.23	5999.12	6028.11
130	5784.85	5809.4	5825.19	5842.07	5860.02	5879	5898.96	5919.83	5941.51
140	5754.78	5765.14	5776.53	5788.75	5801.78	5815.6	5845.63	5861.25	5877.47
150	5732.38	5740.08	5748.53	5757.6	5767.27	5777.53	5788.33	5799.63	5811.4
160	5715.76	5721.47	5727.75	5734.49	5741.66	5749.27	5757.29	5765.68	5774.41

SW0NaCl-3SO4	Total soluble potential ions, on injection : mg / kg of water								
	Pressure (bars)								
Temperature °C	1	50	100	150	200	250	300	350	400
70	7684.82	7792.72	7911.32	8038.5	8174.1	8317.85	8469.36	8525.88	8526.4
80	7473.05	7555.78	7646.71	7744.22	7848.19	7958.43	8074.6	8196.31	8323
90	7306.22	7369.04	7438.09	7512.11	7591.04	7674.71	7762.88	7855.25	7951.38
100	7176.96	7224.32	7276.36	7332.13	7391.58	7454.59	7520.98	7590.51	7662.86
110	7078.02	7113.54	7152.55	7194.33	7238.86	7286.03	7335.71	7387.71	7441.82
120	7002.91	7029.45	7058.58	7089.76	7111.65	7147.3	7184.84	7224.13	7265.01
130	6922.29	6955.15	6977.22	7000.84	7025.99	7052.61	7080.64	7109.97	7140.46
140	6877.11	6891.8	6907.96	6925.29	6943.77	6963.36	7003.27	7025.14	7047.88
150	6842.81	6853.72	6865.71	6878.57	6892.29	6906.82	6922.14	6938.18	6954.86
160	6816.87	6824.97	6833.87	6843.42	6853.6	6864.39	6875.75	6887.65	6900.03

SW0NaCl-3SO4	Precipitation after substitution : mg / kg of water								
	Pressure (bars)								
Temperature °C	1	50	100	150	200	250	300	350	400
70	2534.47	2438.34	2332.59	2219.09	2097.96	1969.41	1833.79	1691.56	1543.34
80	2734.37	2661.61	2581.56	2495.64	2403.94	2306.61	2203.91	2096.2	1983.93
90	2890.65	2836.14	2776.19	2711.85	2643.18	2570.31	2493.41	2412.76	2328.71
100	3010.68	2970.18	2925.63	2877.84	2826.84	2772.73	2715.64	2655.78	2593.38
110	3101.67	3071.74	3038.83	3003.53	2965.87	2925.93	2883.8	2839.63	2793.6
120	3169.96	3147.92	3123.7	3097.73	3070.03	3040.66	3009.69	2977.23	2943.41
130	3220.85	3204.65	3186.86	3167.8	3147.47	3125.92	3103.21	3079.4	3054.61
140	3258.58	3246.69	3233.63	3219.65	3204.74	3188.95	3172.3	3154.86	3136.69
150	3286.47	3277.73	3268.15	3257.88	3246.95	3235.37	3223.16	3210.38	3197.06
160	3307.03	3300.61	3293.57	3286.03	3278	3269.49	3260.53	3251.14	3241.37

SW0NaCl-3SO4	Soluble SO4 after substitution : mg / kg of water								
	Pressure (bars)								
Temperature °C	1	50	100	150	200	250	300	350	400
70	555.34	621.93	695.27	774.06	858.23	947.62	1041.99	1141.02	1244.27
80	418.05	468.23	523.49	582.87	646.32	713.71	784.87	859.55	937.44
90	311.41	348.78	389.94	434.17	481.43	531.63	584.64	640.27	698.29
100	230.07	257.67	288.06	320.71	355.58	392.63	431.74	472.79	515.59
110	168.92	189.16	211.44	235.38	260.95	288.09	316.75	346.82	378.16
120	123.44	138.21	154.47	171.94	190.58	210.37	231.26	253.17	276

130	89.89	100.63	112.46	125.15	138.7	153.08	168.25	184.15	200.72
140	65.29	73.09	81.67	90.87	100.69	111.11	122.1	133.62	145.62
150	47.34	52.99	59.2	65.86	72.97	80.51	88.46	96.79	105.46
160	34.28	38.37	42.86	47.68	52.82	58.27	64.01	70.03	76.29

SW0NaCl-3SO4	Total soluble potential ions ; on injection: mg / kg of water								
	Pressure (bars)								
Temperature °C	1	50	100	150	200	250	300	350	400
70	2128.03	2223.11	2327.78	2440.17	2560.19	2687.62	2822.12	2963.22	3110.31
80	1931.33	2003.1	2082.11	2166.97	2257.6	2353.84	2455.43	2562.02	2673.16
90	1778.13	1831.71	1890.7	1954.05	2021.7	2093.53	2169.37	2248.93	2331.89
100	1660.96	1700.62	1744.28	1791.16	1841.22	1894.37	1950.46	2009.31	2070.66
110	1572.56	1601.74	1633.86	1668.33	1705.13	1744.2	1785.41	1828.65	1873.71
120	1506.57	1527.95	1551.46	1576.7	1603.63	1632.21	1662.36	1693.97	1726.92
130	1457.68	1473.3	1490.47	1508.89	1528.54	1549.39	1571.37	1594.42	1618.43
140	1421.68	1433.06	1445.58	1459	1473.31	1488.49	1504.5	1521.27	1538.74
150	1395.26	1403.55	1412.67	1422.44	1432.86	1443.9	1455.54	1467.74	1480.44
160	1375.92	1381.97	1388.6	1395.72	1403.3	1411.34	1419.81	1428.68	1437.91

SW0NaCl-3SO4	Effective fine formation : mg / kg of water								
	Pressure (bars)								
Temperature °C	1	50	100	150	200	250	300	350	400
70	1678.38	1690.21	1703.15	1716.97	1731.6	1747.02	1763.14	1678.04	1531.11
80	1665.93	1675.94	1686.9	1698.61	1711.04	1724.14	1737.85	1752.1	1766.83
90	1654.84	1663.19	1672.35	1682.15	1692.56	1703.54	1715.04	1727.02	1739.4
100	1645.18	1652.05	1659.61	1667.69	1676.29	1685.37	1694.89	1704.81	1715.07
110	1636.91	1642.51	1648.66	1655.24	1662.25	1669.66	1677.43	1685.53	1693.91
120	1629.95	1634.45	1639.4	1644.7	1638.7	1644.52	1650.65	1657.06	1663.72
130	1599.12	1615.31	1619	1622.99	1627.28	1631.85	1636.68	1641.74	1646.99
140	1585.36	1588.18	1591.31	1594.68	1598.28	1602.1	1625.05	1628.99	1633.09
150	1572.6	1574.8	1577.22	1579.84	1582.64	1585.62	1588.75	1592.03	1595.42
160	1561.35	1563.04	1564.91	1566.93	1569.1	1571.39	1573.81	1576.34	1578.96

4. **SW0NaCl-4SO_4 : Sea Water without NaCl and four times SO_4^{2-}**

	Na	Mg	Ca	SO4	HCO3-	Cl-
SW0NaCl-4SO4	0.079	0.045	0.013	0.096	0.002	0.0354

SW0NaCl-4SO4	Precipitation on injection :mg / kg of water								
	Pressure (bars)								
Temperature °C	1	50	100	150	200	250	300	350	400
70	894.03	789.62	674.64	551.12	419.17	279.03	131.06	11.09	9.89
80	1093.93	1013.56	925.07	830.04	728.55	620.79	507.02	387.66	263.22

90	1251.96	1190.6	1123.06	1050.55	973.13	890.94	804.21	713.25	618.44
100	1375.01	1328.44	1277.2	1222.2	1163.5	1101.2	1035.49	966.6	894.81
110	1469.76	1434.56	1395.84	1354.3	1309.98	1262.97	1213.4	1161.44	1115.26
120	1542.15	1515.61	1486.43	1455.14	1430.62	1395.38	1358.21	1319.25	1278.66
130	1616	1586.48	1564.78	1541.48	1516.59	1490.19	1462.33	1433.13	1402.71
140	1665.95	1650.93	1634.41	1616.7	1597.8	1577.77	1541.16	1519.3	1496.53
150	1705.91	1694.63	1682.23	1668.92	1654.74	1639.7	1623.85	1607.26	1589.99
160	1737.72	1729.24	1719.92	1709.92	1699.27	1687.97	1676.07	1663.61	1650.65

SW0NaCl-4SO4	Soluble SO4 on injection : mg / kg of water								
	Pressure (bars)								
Temperature °C	1	50	100	150	200	250	300	350	400
70	8600.26	8673.89	8754.95	8841.99	8934.93	9033.63	9137.81	9222.06	9222.06
80	8459.71	8516.39	8578.76	8645.7	8717.17	8793.02	8873.07	8957.03	9044.54
90	8348.62	8391.9	8439.5	8490.56	8545.04	8602.85	8663.82	8727.74	8794.34
100	8262.1	8294.95	8331.06	8369.77	8411.05	8454.82	8500.96	8549.3	8599.64
110	8195.39	8220.23	8247.5	8276.72	8307.85	8340.83	8375.57	8411.95	8443.56
120	8144.24	8162.97	8183.52	8205.5	8222.28	8247.64	8274.34	8302.28	8331.35
130	8091.37	8113.58	8129.53	8146.58	8164.72	8183.9	8204.09	8225.2	8247.14
140	8062.04	8072.62	8084.25	8096.73	8110.04	8124.15	8151.82	8167.79	8184.37
150	8039.99	8047.93	8056.67	8066.04	8076.03	8086.62	8097.78	8109.47	8121.63
160	8023.44	8029.41	8035.98	8043.02	8050.53	8058.48	8066.86	8075.64	8084.77

SW0NaCl-4SO4	Total soluble potential ions, on injection : mg / kg of water								
	Pressure (bars)								
Temperature °C	1	50	100	150	200	250	300	350	400
70	9950.45	10054.83	10169.7	10293.1	10424.9	10564.9	10712.7	10832.3	10832.8
80	9750.98	9831.32	9919.75	10014.6	10116.0	10223.6	10337.2	10456.3	10580.5
90	9593.31	9654.65	9722.14	9794.57	9871.87	9953.89	10040.4	10131.1	10225.7
100	9470.52	9517.08	9568.28	9623.2	9681.78	9743.91	9809.43	9878.1	9949.62
110	9375.89	9411.09	9449.77	9491.23	9535.43	9582.28	9631.65	9683.37	9729.33
120	9303.44	9329.99	9359.13	9390.34	9415.12	9450.81	9488.41	9527.8	9568.78
130	9230.47	9260.44	9282.72	9306.58	9332	9358.92	9387.27	9416.94	9447.79
140	9186.49	9201.48	9217.98	9235.67	9254.54	9274.55	9311.53	9333.89	9357.14
150	9152.72	9163.99	9176.37	9189.66	9203.83	9218.84	9234.67	9251.24	9268.48
160	9126.86	9135.33	9144.64	9154.62	9165.27	9176.55	9188.43	9200.88	9213.82

SW0NaCl-4SO4	Precipitation after substitution : mg / kg of water								
	Pressure (bars)								
Temperature °C	1	50	100	150	200	250	300	350	400
70	2534.47	2438.34	2332.59	2219.09	2097.96	1969.41	1833.79	1691.56	1543.34
80	2734.37	2661.61	2581.56	2495.64	2403.94	2306.61	2203.91	2096.2	1983.93
90	2890.65	2836.14	2776.19	2711.85	2643.18	2570.31	2493.41	2412.76	2328.71

100	3010.68	2970.18	2925.63	2877.84	2826.84	2772.73	2715.64	2655.78	2593.38
110	3101.67	3071.74	3038.83	3003.53	2965.87	2925.93	2883.8	2839.63	2793.6
120	3169.96	3147.92	3123.7	3097.73	3070.03	3040.66	3009.69	2977.23	2943.41
130	3220.85	3204.65	3186.86	3167.8	3147.47	3125.92	3103.21	3079.4	3054.61
140	3258.58	3246.69	3233.63	3219.65	3204.74	3188.95	3172.3	3154.86	3136.69
150	3286.47	3277.73	3268.15	3257.88	3246.95	3235.37	3223.16	3210.38	3197.06
160	3307.03	3300.61	3293.57	3286.03	3278	3269.49	3260.53	3251.14	3241.37

SW0NaCl-4SO4	Soluble SO4 after substitution : mg / kg of water								
	Pressure (bars)								
Temperature °C	1	50	100	150	200	250	300	350	400
70	555.34	621.93	695.27	774.06	858.23	947.62	1041.99	1141.02	1244.27
80	418.05	468.23	523.49	582.87	646.32	713.71	784.87	859.55	937.44
90	311.41	348.78	389.94	434.17	481.43	531.63	584.64	640.27	698.29
100	230.07	257.67	288.06	320.71	355.58	392.63	431.74	472.79	515.59
110	168.92	189.16	211.44	235.38	260.95	288.09	316.75	346.82	378.16
120	123.44	138.21	154.47	171.94	190.58	210.37	231.26	253.17	276
130	89.89	100.63	112.46	125.15	138.7	153.08	168.25	184.15	200.72
140	65.29	73.09	81.67	90.87	100.69	111.11	122.1	133.62	145.62
150	47.34	52.99	59.2	65.86	72.97	80.51	88.46	96.79	105.46
160	34.28	38.37	42.86	47.68	52.82	58.27	64.01	70.03	76.29

SW0NaCl-4SO4	Total soluble potential ions ; on injection: mg / kg of water								
	Pressure (bars)								
Temperature °C	1	50	100	150	200	250	300	350	400
70	2128.03	2223.11	2327.78	2440.17	2560.19	2687.62	2822.12	2963.22	3110.31
80	1931.33	2003.1	2082.11	2166.97	2257.6	2353.84	2455.43	2562.02	2673.16
90	1778.13	1831.71	1890.7	1954.05	2021.7	2093.53	2169.37	2248.93	2331.89
100	1660.96	1700.62	1744.28	1791.16	1841.22	1894.37	1950.46	2009.31	2070.66
110	1572.56	1601.74	1633.86	1668.33	1705.13	1744.2	1785.41	1828.65	1873.71
120	1506.57	1527.95	1551.46	1576.7	1603.63	1632.21	1662.36	1693.97	1726.92
130	1457.68	1473.3	1490.47	1508.89	1528.54	1549.39	1571.37	1594.42	1618.43
140	1421.68	1433.06	1445.58	1459	1473.31	1488.49	1504.5	1521.27	1538.74
150	1395.26	1403.55	1412.67	1422.44	1432.86	1443.9	1455.54	1467.74	1480.44
160	1375.92	1381.97	1388.6	1395.72	1403.3	1411.34	1419.81	1428.68	1437.91

SW0NaCl-4SO4	Effective fine formation : mg / kg of water								
	Pressure (bars)								
Temperature °C	1	50	100	150	200	250	300	350	400
70	1640.43	1648.72	1657.95	1667.97	1678.78	1690.37	1702.72	1680.46	1533.44
80	1640.44	1648.05	1656.48	1665.59	1675.38	1685.82	1696.88	1708.53	1720.71
90	1638.68	1645.54	1653.13	1661.3	1670.05	1679.36	1689.19	1699.51	1710.27

100	1635.66	1641.73	1648.43	1655.64	1663.34	1671.52	1680.14	1689.17	1698.57
110	1631.9	1637.17	1642.98	1649.23	1655.89	1662.96	1670.4	1678.18	1678.34
120	1627.81	1632.31	1637.26	1642.58	1639.41	1645.27	1651.47	1657.98	1664.75
130	1604.84	1618.17	1622.08	1626.31	1630.87	1635.73	1640.87	1646.27	1651.89
140	1592.63	1595.75	1599.21	1602.94	1606.93	1611.17	1631.14	1635.56	1640.16
150	1580.55	1583.1	1585.92	1588.96	1592.21	1595.66	1599.3	1603.11	1607.06
160	1569.31	1571.37	1573.64	1576.1	1578.72	1581.51	1584.45	1587.53	1590.72

5. SW-2SO4: Sea Water with twice SO_4^{2-}

	Na	Mg	Ca	SO4	HCO3-	Cl-
SW-2SO4	0.45	0.045	0.013	0.048	0.002	0.468

SW-2SO4	Precipitation on injection :mg / kg of water								
	Pressure (bars)								
Temperature °C	1	50	100	150	200	250	300	350	400
70	12.46	11.21	9.99	8.82	7.69	6.61	5.56	4.54	3.54
80	15.75	14.33	12.93	11.58	10.28	9.03	7.81	6.63	5.48
90	19.55	17.96	16.38	14.84	13.36	11.91	10.52	9.15	7.83
100	23.8	22.05	20.3	18.58	16.91	15.28	13.69	12.14	10.62
110	91.58	26.49	24.6	22.73	20.89	19.08	17.31	15.56	13.84
120	381.88	241.19	90.21	27.18	25.2	23.24	21.3	19.37	17.47
130	625.24	507.21	380.3	247.24	108.54	27.63	25.55	23.48	21.42
140	827.75	729.1	622.8	511.12	394.49	273.39	148.39	27.76	24.9
150	995.21	913.03	824.27	730.84	633.07	547.69	442.65	334.71	224.46
160	1133.03	1082.82	1009.08	931.28	849.68	764.64	676.55	585.87	493.12

SW-2SO4	Soluble SO4 on injection : mg / kg of water								
	Pressure (bars)								
Temperature °C	1	50	100	150	200	250	300	350	400
70	4611.03	4611.03	4611.03	4611.03	4611.03	4611.03	4611.03	4611.03	4611.03
80	4611.03	4611.03	4611.03	4611.03	4611.03	4611.03	4611.03	4611.03	4611.03
90	4611.03	4611.03	4611.03	4611.03	4611.03	4611.03	4611.03	4611.03	4611.03
100	4611.03	4611.03	4611.03	4611.03	4611.03	4611.03	4611.03	4611.03	4611.03
110	4566.01	4611.03	4611.03	4611.03	4611.03	4611.03	4611.03	4611.03	4611.03
120	4362.3	4461.33	4567.54	4611.03	4611.03	4611.03	4611.03	4611.03	4611.03
130	4191.54	4274.6	4363.86	4457.39	4554.84	4611.03	4611.03	4611.03	4611.03
140	4049.39	4118.8	4193.54	4272	4353.9	4438.89	4526.56	4611.03	4611.03
150	3931.71	3989.53	4051.91	4117.52	4186.12	4244.89	4319.48	4396.08	4474.27
160	3834.65	3868.43	3921.1	3976.61	4034.75	4095.28	4157.93	4222.38	4288.26

SW-2SO4	Total soluble potential ions, on injection : mg / kg of water								
	Pressure (bars)								
Temperature °C	1	50	100	150	200	250	300	350	400
70	6220.79	6221.28	6221.77	6222.24	6222.69	6223.13	6223.55	6223.96	6224.36

80	6219.47	6220.04	6220.6	6221.14	6221.66	6222.16	6222.65	6223.12	6223.58
90	6217.94	6218.58	6219.22	6219.83	6220.43	6221	6221.56	6222.11	6222.64
100	6216.24	6216.95	6217.65	6218.33	6219	6219.66	6220.29	6220.92	6221.52
110	6150.85	6215.17	6215.92	6216.67	6217.41	6218.13	6218.84	6219.54	6220.23
120	5861.51	6001.99	6152.7	6214.89	6215.68	6216.47	6217.25	6218.02	6218.78
130	5618.96	5736.8	5863.47	5996.22	6134.57	6214.71	6215.54	6216.37	6217.2
140	5417.09	5515.57	5621.64	5733.03	5849.32	5970.03	6094.58	6214.66	6217.08
150	5250.03	5332.07	5420.61	5513.78	5611.22	5696.83	5802.3	5910.64	6021.26
160	5112.37	5162.74	5237.07	5315.43	5397.55	5483.08	5571.62	5662.73	5755.88

SW-2SO4	Precipitation after substitution : mg / kg of water								
	Pressure (bars)								
Temperature °C	1	50	100	150	200	250	300	350	400
70	2534.47	2438.34	2332.59	2219.09	2097.96	1969.41	1833.79	1691.56	1543.34
80	2734.37	2661.61	2581.56	2495.64	2403.94	2306.61	2203.91	2096.2	1983.93
90	2890.65	2836.14	2776.19	2711.85	2643.18	2570.31	2493.41	2412.76	2328.71
100	3010.68	2970.18	2925.63	2877.84	2826.84	2772.73	2715.64	2655.78	2593.38
110	3101.67	3071.74	3038.83	3003.53	2965.87	2925.93	2883.8	2839.63	2793.6
120	3169.96	3147.92	3123.7	3097.73	3070.03	3040.66	3009.69	2977.23	2943.41
130	3220.85	3204.65	3186.86	3167.8	3147.47	3125.92	3103.21	3079.4	3054.61
140	3258.58	3246.69	3233.63	3219.65	3204.74	3188.95	3172.3	3154.86	3136.69
150	3286.47	3277.73	3268.15	3257.88	3246.95	3235.37	3223.16	3210.38	3197.06
160	3307.03	3300.61	3293.57	3286.03	3278	3269.49	3260.53	3251.14	3241.37

SW-2SO4	Soluble SO4 after substitution : mg / kg of water								
	Pressure (bars)								
Temperature °C	1	50	100	150	200	250	300	350	400
70	555.34	621.93	695.27	774.06	858.23	947.62	1041.99	1141.02	1244.27
80	418.05	468.23	523.49	582.87	646.32	713.71	784.87	859.55	937.44
90	311.41	348.78	389.94	434.17	481.43	531.63	584.64	640.27	698.29
100	230.07	257.67	288.06	320.71	355.58	392.63	431.74	472.79	515.59
110	168.92	189.16	211.44	235.38	260.95	288.09	316.75	346.82	378.16
120	123.44	138.21	154.47	171.94	190.58	210.37	231.26	253.17	276
130	89.89	100.63	112.46	125.15	138.7	153.08	168.25	184.15	200.72
140	65.29	73.09	81.67	90.87	100.69	111.11	122.1	133.62	145.62
150	47.34	52.99	59.2	65.86	72.97	80.51	88.46	96.79	105.46
160	34.28	38.37	42.86	47.68	52.82	58.27	64.01	70.03	76.29

SW-2SO4	Total soluble potential ions ; on injection: mg / kg of water								
	Pressure (bars)								
Temperature °C	1	50	100	150	200	250	300	350	400
70	2128.03	2223.11	2327.78	2440.17	2560.19	2687.62	2822.12	2963.22	3110.31

80	1931.33	2003.1	2082.11	2166.97	2257.6	2353.84	2455.43	2562.02	2673.16
90	1778.13	1831.71	1890.7	1954.05	2021.7	2093.53	2169.37	2248.93	2331.89
100	1660.96	1700.62	1744.28	1791.16	1841.22	1894.37	1950.46	2009.31	2070.66
110	1572.56	1601.74	1633.86	1668.33	1705.13	1744.2	1785.41	1828.65	1873.71
120	1506.57	1527.95	1551.46	1576.7	1603.63	1632.21	1662.36	1693.97	1726.92
130	1457.68	1473.3	1490.47	1508.89	1528.54	1549.39	1571.37	1594.42	1618.43
140	1421.68	1433.06	1445.58	1459	1473.31	1488.49	1504.5	1521.27	1538.74
150	1395.26	1403.55	1412.67	1422.44	1432.86	1443.9	1455.54	1467.74	1480.44
160	1375.92	1381.97	1388.6	1395.72	1403.3	1411.34	1419.81	1428.68	1437.91

SW-2SO4	Effective fine formation : mg / kg of water								
	Pressure (bars)								
Temperature °C	1	50	100	150	200	250	300	350	400
70	2522	2427.12	2322.59	2210.26	2090.26	1962.8	1828.22	1687.02	1539.79
80	2718.62	2647.27	2568.62	2484.05	2393.65	2297.58	2196.09	2089.56	1978.45
90	2871.09	2818.18	2759.81	2697	2629.82	2558.39	2482.89	2403.61	2320.87
100	2986.88	2948.13	2905.33	2859.25	2809.93	2757.44	2701.95	2643.63	2582.76
110	3010.08	3045.24	3014.22	2980.79	2944.98	2906.84	2866.49	2824.07	2779.75
120	2788.07	2906.73	3033.48	3070.54	3044.83	3017.42	2988.39	2957.85	2925.93
130	2595.6	2697.44	2806.56	2920.55	3038.92	3098.29	3077.65	3055.92	3033.18
140	2430.83	2517.58	2610.83	2708.52	2810.25	2915.55	3023.9	3127.09	3111.78
150	2291.25	2364.7	2443.87	2527.04	2613.88	2687.67	2780.51	2875.67	2972.59
160	2174	2217.79	2284.48	2354.75	2428.31	2504.84	2583.97	2665.26	2748.25

6. SW-3SO4: Sea Water with thrice SO_4^{2-}

	Na	Mg	Ca	SO4	HCO3-	Cl-
SW-3SO4	0.45	0.045	0.013	0.072	0.002	0.42

SW-3SO4	Precipitation on injection :mg / kg of water								
	Pressure (bars)								
Temperature °C	1	50	100	150	200	250	300	350	400
70	11.98	10.75	9.55	8.39	7.28	6.21	5.17	4.15	3.16
80	15.2	13.8	12.42	11.09	9.8	8.56	7.36	6.19	5.05
90	18.93	17.35	15.79	14.27	12.8	11.38	9.99	8.65	7.33
100	305.7	146.78	19.63	17.93	16.28	14.66	13.09	11.55	10.04
110	578.37	447.51	305.54	155.41	20.17	18.38	16.62	14.89	13.18
120	802.68	695.4	578.8	455.29	325.21	189.06	47.41	18.61	16.72
130	985.78	898.11	802.69	701.43	594.63	482.66	366	245.21	120.94
140	1134.37	1062.89	984.97	902.17	814.72	722.9	639.54	540.33	438.11
150	1254.47	1196.26	1146.28	1078.9	1007.6	932.62	854.27	772.92	688.99
160	1381.89	1318.54	1267.05	1212.16	1154	1092.76	1028.69	962.08	893.28

SW-3SO4	Soluble SO4 on injection : mg / kg of water
	Pressure (bars)

Temperature °C	1	50	100	150	200	250	300	350	400
70	6916.55	6916.55	6916.55	6916.55	6916.55	6916.55	6916.55	6916.55	6916.55
80	6916.55	6916.55	6916.55	6916.55	6916.55	6916.55	6916.55	6916.55	6916.55
90	6916.55	6916.55	6916.55	6916.55	6916.55	6916.55	6916.55	6916.55	6916.55
100	6715.3	6827.29	6916.55	6916.55	6916.55	6916.55	6916.55	6916.55	6916.55
110	6523.68	6615.89	6715.87	6821.56	6916.55	6916.55	6916.55	6916.55	6916.55
120	6366.03	6441.62	6523.71	6610.64	6702.13	6797.85	6897.4	6916.55	6916.55
130	6237.26	6299.03	6366.2	6437.43	6512.51	6591.17	6673.08	6757.85	6845.02
140	6132.59	6182.95	6237.79	6296	6357.43	6421.88	6479.79	6550.27	6622.84
150	6047.72	6088.74	6123.16	6171.36	6222.29	6275.77	6331.6	6389.52	6449.21
160	5957.64	6003.99	6041.05	6080.48	6122.16	6165.99	6211.78	6259.32	6308.37

SW-3SO4	Total soluble potential ions, on injection : mg / kg of water								
	Pressure (bars)								
Temperature °C	1	50	100	150	200	250	300	350	400
70	8526.5	8526.99	8527.47	8527.93	8528.38	8528.81	8529.22	8529.63	8530.03
80	8525.2	8525.77	8526.32	8526.85	8527.37	8527.86	8528.34	8528.81	8529.27
90	8523.71	8524.34	8524.97	8525.58	8526.17	8526.74	8527.29	8527.83	8528.35
100	8237.88	8396.67	8523.43	8524.11	8524.77	8525.42	8526.05	8526.67	8527.27
110	7965.87	8096.62	8238.42	8388.35	8523.21	8523.93	8524.64	8525.33	8526.01
120	7742.09	7849.28	7965.73	8089.04	8218.87	8354.73	8496.03	8523.84	8524.6
130	7559.35	7646.94	7742.24	7843.31	7949.87	8061.54	8177.86	8298.26	8422.09
140	7410.92	7482.33	7560.13	7642.74	7729.97	7821.49	7905.14	8004.79	8107.41
150	7290.71	7348.87	7399.26	7467.24	7539.11	7614.62	7693.47	7775.3	7859.66
160	7165.72	7229.19	7281.35	7336.88	7395.64	7457.45	7522.05	7589.16	7658.43

SW-3SO4	Precipitation after substitution : mg / kg of water								
	Pressure (bars)								
Temperature °C	1	50	100	150	200	250	300	350	400
70	2534.47	2438.34	2332.59	2219.09	2097.96	1969.41	1833.79	1691.56	1543.34
80	2734.37	2661.61	2581.56	2495.64	2403.94	2306.61	2203.91	2096.2	1983.93
90	2890.65	2836.14	2776.19	2711.85	2643.18	2570.31	2493.41	2412.76	2328.71
100	3010.68	2970.18	2925.63	2877.84	2826.84	2772.73	2715.64	2655.78	2593.38
110	3101.67	3071.74	3038.83	3003.53	2965.87	2925.93	2883.8	2839.63	2793.6
120	3169.96	3147.92	3123.7	3097.73	3070.03	3040.66	3009.69	2977.23	2943.41
130	3220.85	3204.65	3186.86	3167.8	3147.47	3125.92	3103.21	3079.4	3054.61
140	3258.58	3246.69	3233.63	3219.65	3204.74	3188.95	3172.3	3154.86	3136.69
150	3286.47	3277.73	3268.15	3257.88	3246.95	3235.37	3223.16	3210.38	3197.06
160	3307.03	3300.61	3293.57	3286.03	3278	3269.49	3260.53	3251.14	3241.37

SW-3SO4	Soluble SO4 after substitution : mg / kg of water
	Pressure (bars)

Temperature °C	1	50	100	150	200	250	300	350	400
70	555.34	621.93	695.27	774.06	858.23	947.62	1041.99	1141.02	1244.27
80	418.05	468.23	523.49	582.87	646.32	713.71	784.87	859.55	937.44
90	311.41	348.78	389.94	434.17	481.43	531.63	584.64	640.27	698.29
100	230.07	257.67	288.06	320.71	355.58	392.63	431.74	472.79	515.59
110	168.92	189.16	211.44	235.38	260.95	288.09	316.75	346.82	378.16
120	123.44	138.21	154.47	171.94	190.58	210.37	231.26	253.17	276
130	89.89	100.63	112.46	125.15	138.7	153.08	168.25	184.15	200.72
140	65.29	73.09	81.67	90.87	100.69	111.11	122.1	133.62	145.62
150	47.34	52.99	59.2	65.86	72.97	80.51	88.46	96.79	105.46
160	34.28	38.37	42.86	47.68	52.82	58.27	64.01	70.03	76.29

SW-3SO4	Total soluble potential ions ; on injection: mg / kg of water								
	Pressure (bars)								
Temperature °C	1	50	100	150	200	250	300	350	400
70	2128.03	2223.11	2327.78	2440.17	2560.19	2687.62	2822.12	2963.22	3110.31
80	1931.33	2003.1	2082.11	2166.97	2257.6	2353.84	2455.43	2562.02	2673.16
90	1778.13	1831.71	1890.7	1954.05	2021.7	2093.53	2169.37	2248.93	2331.89
100	1660.96	1700.62	1744.28	1791.16	1841.22	1894.37	1950.46	2009.31	2070.66
110	1572.56	1601.74	1633.86	1668.33	1705.13	1744.2	1785.41	1828.65	1873.71
120	1506.57	1527.95	1551.46	1576.7	1603.63	1632.21	1662.36	1693.97	1726.92
130	1457.68	1473.3	1490.47	1508.89	1528.54	1549.39	1571.37	1594.42	1618.43
140	1421.68	1433.06	1445.58	1459	1473.31	1488.49	1504.5	1521.27	1538.74
150	1395.26	1403.55	1412.67	1422.44	1432.86	1443.9	1455.54	1467.74	1480.44
160	1375.92	1381.97	1388.6	1395.72	1403.3	1411.34	1419.81	1428.68	1437.91

SW-3SO4	Effective fine formation : mg / kg of water								
	Pressure (bars)								
Temperature °C	1	50	100	150	200	250	300	350	400
70	2522.48	2427.59	2323.03	2210.69	2090.67	1963.2	1828.61	1687.4	1540.17
80	2719.17	2647.81	2569.13	2484.55	2394.13	2298.04	2196.54	2090	1978.87
90	2871.71	2818.79	2760.4	2697.57	2630.37	2558.92	2483.41	2404.11	2321.37
100	2704.97	2823.39	2906	2859.91	2810.56	2758.06	2702.55	2644.22	2583.33
110	2523.3	2624.22	2733.28	2848.11	2945.7	2907.55	2867.18	2824.74	2780.41
120	2367.27	2452.52	2544.89	2642.43	2744.81	2851.59	2962.27	2958.61	2926.68
130	2235.06	2306.54	2384.17	2466.36	2552.84	2643.26	2737.2	2834.19	2933.66
140	2124.21	2183.8	2248.66	2317.47	2390.02	2466.04	2532.75	2614.52	2698.57
150	2031.99	2081.47	2121.87	2178.98	2239.35	2302.74	2368.89	2437.46	2508.06
160	1925.14	1982.06	2026.51	2073.87	2123.99	2176.72	2231.84	2289.06	2348.08

7. SW-4SO4: Sea Water with four times SO_4^{2-}

	Na	Mg	Ca	SO4	HCO3-	Cl-
SW-4SO4	0.45	0.045	0.013	0.096	0.002	0.372

SW-4SO4	Precipitation on injection :mg / kg of water								
	Pressure (bars)								
Temperature °C	1	50	100	150	200	250	300	350	400
70	11.51	10.31	9.12	7.98	6.88	5.82	4.79	3.78	2.8
80	26.63	13.28	11.92	10.61	9.34	8.11	6.93	5.77	4.64
90	354.49	194.81	20.85	13.72	12.27	10.86	9.49	8.16	6.86
100	625.63	495.58	353.72	202.84	43.32	14.06	12.5	10.98	9.49
110	847.39	741.94	626.77	504.13	374.3	237.71	94.86	14.23	12.55
120	1027.24	941.99	848.78	749.42	644.13	533.23	417.13	296.35	171.52
130	1172.22	1103.41	1028.12	947.79	862.59	772.77	678.65	580.64	488.16
140	1288.62	1233.12	1172.35	1107.47	1048.53	976.03	899.98	820.71	738.62
150	1391.89	1347.42	1298.65	1246.5	1191.07	1132.51	1071.04	1006.91	940.45
160	1483.86	1447.65	1407.94	1365.49	1305.35	1258.04	1208.34	1156.45	1102.64

SW-4SO4	Soluble SO4 on injection : mg / kg of water								
	Pressure (bars)								
Temperature °C	1	50	100	150	200	250	300	350	400
70	9222.06	9222.06	9222.06	9222.06	9222.06	9222.06	9222.06	9222.06	9222.06
80	9213.57	9222.06	9222.06	9222.06	9222.06	9222.06	9222.06	9222.06	9222.06
90	8982.88	9095.46	9218.06	9222.06	9222.06	9222.06	9222.06	9222.06	9222.06
100	8792.13	8883.81	8983.78	9090.06	9202.39	9222.06	9222.06	9222.06	9222.06
110	8636.1	8710.44	8791.59	8877.95	8969.33	9065.45	9165.92	9222.06	9222.06
120	8509.46	8569.56	8635.23	8705.17	8779.25	8857.23	8938.82	9023.66	9111.32
130	8407.2	8455.72	8508.74	8565.26	8625.16	8688.27	8754.34	8823.1	8887.82
140	8324.82	8363.95	8406.73	8452.36	8493.42	8545.14	8599.34	8655.79	8714.19
150	8251.3	8283.43	8318.57	8356.06	8395.82	8437.76	8481.72	8527.52	8574.94
160	8190.4	8215.92	8243.9	8273.82	8318.16	8352.2	8387.89	8425.09	8463.6

SW-4SO4	Total soluble potential ions, on injection : mg / kg of water								
	Pressure (bars)								
Temperature °C	1	50	100	150	200	250	300	350	400
70	10832.2	10832.6	10833.1	10833.6	10834	10834.4	10834.8	10835.2	10835.6
80	10818.9	10831.4	10832	10832.5	10833	10833.5	10834	10834.5	10834.9
90	10491.6	10651.2	10825	10831.3	10831.9	10832.4	10833	10833.5	10834
100	10220.9	10350.9	10492.6	10643.4	10802.7	10831.1	10831.8	10832.4	10833
110	9999.5	10104.9	10220	10342.5	10472.1	10608.5	10751.1	10831.1	10831.7
120	9819.9	9905.1	9998.2	10097.5	10202.6	10313.2	10429.1	10549.5	10674
130	9675	9743.7	9819	9899.1	9984.2	10073.7	10167.6	10265.2	10358
140	9558.4	9613.8	9674.5	9739.3	9798.6	9871.6	9948.1	10027.9	10110.4
150	9455.4	9500.5	9550	9602.8	9658.8	9717.9	9779.9	9844.6	9911.5
160	9368.4	9404.6	9444.3	9486.7	9547.2	9595.2	9645.4	9697.9	9752.2

SW-4SO4	Precipitation after substitution : mg / kg of water								
	Pressure (bars)								
Temperature °C	1	50	100	150	200	250	300	350	400
70	2534.47	2438.34	2332.59	2219.09	2097.96	1969.41	1833.79	1691.56	1543.34
80	2734.37	2661.61	2581.56	2495.64	2403.94	2306.61	2203.91	2096.2	1983.93
90	2890.65	2836.14	2776.19	2711.85	2643.18	2570.31	2493.41	2412.76	2328.71
100	3010.68	2970.18	2925.63	2877.84	2826.84	2772.73	2715.64	2655.78	2593.38
110	3101.67	3071.74	3038.83	3003.53	2965.87	2925.93	2883.8	2839.63	2793.6
120	3169.96	3147.92	3123.7	3097.73	3070.03	3040.66	3009.69	2977.23	2943.41
130	3220.85	3204.65	3186.86	3167.8	3147.47	3125.92	3103.21	3079.4	3054.61
140	3258.58	3246.69	3233.63	3219.65	3204.74	3188.95	3172.3	3154.86	3136.69
150	3286.47	3277.73	3268.15	3257.88	3246.95	3235.37	3223.16	3210.38	3197.06
160	3307.03	3300.61	3293.57	3286.03	3278	3269.49	3260.53	3251.14	3241.37

SW-4SO4	Soluble SO4 after substitution : mg / kg of water								
	Pressure (bars)								
Temperature °C	1	50	100	150	200	250	300	350	400
70	555.34	621.93	695.27	774.06	858.23	947.62	1041.99	1141.02	1244.27
80	418.05	468.23	523.49	582.87	646.32	713.71	784.87	859.55	937.44
90	311.41	348.78	389.94	434.17	481.43	531.63	584.64	640.27	698.29
100	230.07	257.67	288.06	320.71	355.58	392.63	431.74	472.79	515.59
110	168.92	189.16	211.44	235.38	260.95	288.09	316.75	346.82	378.16
120	123.44	138.21	154.47	171.94	190.58	210.37	231.26	253.17	276
130	89.89	100.63	112.46	125.15	138.7	153.08	168.25	184.15	200.72
140	65.29	73.09	81.67	90.87	100.69	111.11	122.1	133.62	145.62
150	47.34	52.99	59.2	65.86	72.97	80.51	88.46	96.79	105.46
160	34.28	38.37	42.86	47.68	52.82	58.27	64.01	70.03	76.29

SW-4SO4	Total soluble potential ions ; on injection: mg / kg of water								
	Pressure (bars)								
Temperature °C	1	50	100	150	200	250	300	350	400
70	2128.03	2223.11	2327.78	2440.17	2560.19	2687.62	2822.12	2963.22	3110.31
80	1931.33	2003.1	2082.11	2166.97	2257.6	2353.84	2455.43	2562.02	2673.16
90	1778.13	1831.71	1890.7	1954.05	2021.7	2093.53	2169.37	2248.93	2331.89
100	1660.96	1700.62	1744.28	1791.16	1841.22	1894.37	1950.46	2009.31	2070.66
110	1572.56	1601.74	1633.86	1668.33	1705.13	1744.2	1785.41	1828.65	1873.71
120	1506.57	1527.95	1551.46	1576.7	1603.63	1632.21	1662.36	1693.97	1726.92
130	1457.68	1473.3	1490.47	1508.89	1528.54	1549.39	1571.37	1594.42	1618.43
140	1421.68	1433.06	1445.58	1459	1473.31	1488.49	1504.5	1521.27	1538.74
150	1395.26	1403.55	1412.67	1422.44	1432.86	1443.9	1455.54	1467.74	1480.44
160	1375.92	1381.97	1388.6	1395.72	1403.3	1411.34	1419.81	1428.68	1437.91

SW-4SO4	Effective fine formation : mg / kg of water								

	Pressure (bars)								
Temperature °C	1	50	100	150	200	250	300	350	400
70	2522.95	2428.03	2323.46	2211.1	2091.07	1963.58	1828.99	1687.77	1540.53
80	2707.74	2648.32	2569.63	2485.03	2394.59	2298.49	2196.98	2090.42	1979.29
90	2536.15	2641.33	2755.33	2698.13	2630.91	2559.44	2483.92	2404.6	2321.85
100	2385.05	2474.59	2571.91	2674.99	2783.51	2758.66	2703.13	2644.79	2583.89
110	2254.27	2329.79	2412.05	2499.4	2591.57	2688.22	2788.94	2825.39	2781.05
120	2142.71	2205.92	2274.91	2348.3	2425.9	2507.43	2592.56	2680.87	2771.89
130	2048.63	2101.24	2158.74	2220	2284.87	2353.15	2424.56	2498.75	2566.44
140	1969.96	2013.57	2061.28	2112.17	2156.2	2212.91	2272.31	2334.14	2398.07
150	1894.57	1930.31	1969.49	2011.38	2055.88	2102.85	2152.12	2203.46	2256.61
160	1823.17	1852.96	1885.62	1920.53	1972.64	2011.45	2052.19	2094.69	2138.72

8. SW-8SO4: Sea Water with eight times SO_4^{2-}

	Na	Mg	Ca	SO4	HCO3-	Cl-
SW-8SO4	0.45	0.045	0.013	0.192	0.002	0.18

SW-8SO4	Precipitation on injection :mg / kg of water								
	Pressure (bars)								
Temperature °C	1	50	100	150	200	250	300	350	400
70	516.86	367.84	203.94	28.1	5.41	4.38	3.38	2.39	1.41
80	762.76	643.02	511.33	370.06	219.36	59.54	5.32	4.19	3.09
90	964.06	868.32	763.02	650.07	529.6	401.84	267.16	126.07	5.08
100	1127.02	1050.7	966.78	876.76	780.76	678.97	571.68	459.29	342.3
110	1257.87	1197.14	1130.37	1058.76	982.41	901.46	816.15	726.79	633.8
120	1362.4	1314.1	1261	1204.07	1143.38	1079.04	1011.26	940.28	868.66
130	1445.68	1407.24	1364.99	1321.76	1273.68	1222.68	1168.92	1112.6	1053.99
140	1513.28	1482.96	1449.58	1413.77	1375.55	1335.02	1292.29	1247.53	1200.94
150	1574.11	1549.66	1522.78	1493.96	1463.23	1424.07	1390.06	1354.43	1317.35
160	1622.63	1603.09	1581.59	1558.55	1533.99	1507.96	1480.54	1451.84	1421.98

SW-8SO4	Soluble SO4 on injection : mg / kg of water								
	Pressure (bars)								
Temperature °C	1	50	100	150	200	250	300	350	400
70	18084	18189.2	18304.8	18428.7	18444.1	18444.1	18444.1	18444.1	18444.1
80	17910.6	17995.1	18088	18187.6	18293.8	18406.4	18444.1	18444.1	18444.1
90	17768.6	17836.2	17910.4	17990	18074.9	18164.9	18259.8	18359.1	18444.1
100	17653.5	17707.3	17766.5	17829.9	17897.5	17969.2	18044.7	18123.8	18206
110	17560.8	17603.6	17650.7	17701.1	17754.9	17811.8	17871.8	17934.6	17999.9
120	17486.3	17520.4	17557.9	17597.9	17640.6	17685.8	17733.4	17783.2	17833.9
130	17426.5	17453.6	17483.4	17513.7	17548.2	17584.7	17623.2	17663.4	17705.2
140	17378.4	17400.5	17424.8	17450.8	17478.4	17507.6	17538.3	17570.5	17603.9

150	17340.2	17357.4	17376.3	17396.7	17418.3	17447.1	17471.7	17497.4	17524.2
160	17311.2	17324.9	17340.1	17356.3	17373.6	17392	17411.3	17431.5	17452.6

SW-8SO4	Total soluble potential ions, on injection : mg / kg of water								
	Pressure (bars)								
Temperature °C	1	50	100	150	200	250	300	350	400
70	19545.9	19694.9	19858.8	20034.5	20056.7	20057.1	20057.5	20057.9	20058.3
80	19300.1	19419.8	19551.5	19692.7	19843.3	20003	20056.7	20057.2	20057.6
90	19098.8	19194.6	19299.8	19412.7	19533.1	19660.7	19795.2	19936.1	20056.8
100	18935.8	19012.1	19096	19185.9	19281.8	19383.4	19490.6	19602.7	19719.5
110	18804.6	18865.3	18932	19003.6	19079.8	19160.6	19245.7	19334.9	19427.6
120	18699.5	18747.8	18800.8	18857.7	18918.3	18982.4	19050	19120.7	19192.7
130	18615.3	18653.7	18695.9	18739.1	18787.7	18839.3	18893.5	18950.3	19009.3
140	18547.5	18578.5	18612.5	18649	18687.8	18728.9	18772.2	18817.4	18864.5
150	18491.6	18516	18542.9	18571.7	18602.4	18642	18676.6	18712.8	18750.4
160	18448.3	18467.9	18489.3	18512.4	18536.9	18562.9	18590.3	18619	18648.8

SW-8SO4	Precipitation after substitution : mg / kg of water								
	Pressure (bars)								
Temperature °C	1	50	100	150	200	250	300	350	400
70	2534.47	2438.34	2332.59	2219.09	2097.96	1969.41	1833.79	1691.56	1543.34
80	2734.37	2661.61	2581.56	2495.64	2403.94	2306.61	2203.91	2096.2	1983.93
90	2890.65	2836.14	2776.19	2711.85	2643.18	2570.31	2493.41	2412.76	2328.71
100	3010.68	2970.18	2925.63	2877.84	2826.84	2772.73	2715.64	2655.78	2593.38
110	3101.67	3071.74	3038.83	3003.53	2965.87	2925.93	2883.8	2839.63	2793.6
120	3169.96	3147.92	3123.7	3097.73	3070.03	3040.66	3009.69	2977.23	2943.41
130	3220.85	3204.65	3186.86	3167.8	3147.47	3125.92	3103.21	3079.4	3054.61
140	3258.58	3246.69	3233.63	3219.65	3204.74	3188.95	3172.3	3154.86	3136.69
150	3286.47	3277.73	3268.15	3257.88	3246.95	3235.37	3223.16	3210.38	3197.06
160	3307.03	3300.61	3293.57	3286.03	3278	3269.49	3260.53	3251.14	3241.37

SW-8SO4	Soluble SO4 after substitution : mg / kg of water								
	Pressure (bars)								
Temperature °C	1	50	100	150	200	250	300	350	400
70	555.34	621.93	695.27	774.06	858.23	947.62	1041.99	1141.02	1244.27
80	418.05	468.23	523.49	582.87	646.32	713.71	784.87	859.55	937.44
90	311.41	348.78	389.94	434.17	481.43	531.63	584.64	640.27	698.29
100	230.07	257.67	288.06	320.71	355.58	392.63	431.74	472.79	515.59
110	168.92	189.16	211.44	235.38	260.95	288.09	316.75	346.82	378.16
120	123.44	138.21	154.47	171.94	190.58	210.37	231.26	253.17	276
130	89.89	100.63	112.46	125.15	138.7	153.08	168.25	184.15	200.72
140	65.29	73.09	81.67	90.87	100.69	111.11	122.1	133.62	145.62
150	47.34	52.99	59.2	65.86	72.97	80.51	88.46	96.79	105.46

160	34.28	38.37	42.86	47.68	52.82	58.27	64.01	70.03	76.29

SW-8SO4	Total soluble potential ions ; on injection: mg / kg of water								
	Pressure (bars)								
Temperature °C	1	50	100	150	200	250	300	350	400
70	2128.03	2223.11	2327.78	2440.17	2560.19	2687.62	2822.12	2963.22	3110.31
80	1931.33	2003.1	2082.11	2166.97	2257.6	2353.84	2455.43	2562.02	2673.16
90	1778.13	1831.71	1890.7	1954.05	2021.7	2093.53	2169.37	2248.93	2331.89
100	1660.96	1700.62	1744.28	1791.16	1841.22	1894.37	1950.46	2009.31	2070.66
110	1572.56	1601.74	1633.86	1668.33	1705.13	1744.2	1785.41	1828.65	1873.71
120	1506.57	1527.95	1551.46	1576.7	1603.63	1632.21	1662.36	1693.97	1726.92
130	1457.68	1473.3	1490.47	1508.89	1528.54	1549.39	1571.37	1594.42	1618.43
140	1421.68	1433.06	1445.58	1459	1473.31	1488.49	1504.5	1521.27	1538.74
150	1395.26	1403.55	1412.67	1422.44	1432.86	1443.9	1455.54	1467.74	1480.44
160	1375.92	1381.97	1388.6	1395.72	1403.3	1411.34	1419.81	1428.68	1437.91

SW-8SO4	Effective fine formation : mg / kg of water								
	Pressure (bars)								
Temperature °C	1	50	100	150	200	250	300	350	400
70	2017.6	2070.49	2128.64	2190.98	2092.55	1965.02	1830.4	1689.16	1541.92
80	1971.61	2018.58	2070.22	2125.58	2184.57	2247.06	2198.59	2092	1980.84
90	1926.58	1967.82	2013.16	2061.77	2113.58	2168.46	2226.24	2286.69	2323.62
100	1883.66	1919.47	1958.85	2001.07	2046.07	2093.75	2143.96	2196.48	2251.07
110	1843.79	1874.59	1908.45	1944.76	1983.46	2024.47	2067.65	2112.83	2159.79
120	1807.56	1833.82	1862.69	1893.65	1926.65	1961.61	1998.43	2036.94	2074.75
130	1775.17	1797.41	1821.86	1846.03	1873.79	1903.24	1934.28	1966.79	2000.61
140	1745.3	1763.73	1784.04	1805.87	1829.19	1853.92	1880	1907.32	1935.74
150	1712.35	1728.07	1745.36	1763.92	1783.72	1811.29	1833.1	1855.94	1879.71
160	1684.4	1697.52	1711.97	1727.47	1744	1761.52	1779.98	1799.3	1819.38

9. SW-0Ca: Sea Water without Ca^{2+}

	Na	Mg	Ca	SO4	HCO3-	Cl-
SW-2Ca	0.45	0.045	0	0.192	0.002	0.49

SW-0Ca	Precipitation on injection :mg / kg of water								
	Pressure (bars)								
Temperature °C	1	50	100	150	200	250	300	350	400
70	0	0	0	0	0	0	0	0	0
80	0	0	0	0	0	0	0	0	0
90	0	0	0	0	0	0	0	0	0
100	0	0	0	0	0	0	0	0	0
110	0	0	0	0	0	0	0	0	0
120	0	0	0	0	0	0	0	0	0
130	2.3	2.3	2.3	2.3	2.3	2.3	2.3	2.3	2.3

140	9.39	9.39	9.39	9.39	9.39	9.39	9.39	9.39	9.39
150	17.21	17.21	17.21	17.21	17.21	17.21	17.21	17.21	17.21
160	25.34	25.34	25.34	25.34	25.34	25.34	25.34	25.34	25.34

SW-0Ca	Soluble SO4 on injection : mg / kg of water								
	Pressure (bars)								
Temperature °C	1	50	100	150	200	250	300	350	400
70	2305.5	2305.5	2305.5	2305.5	2305.5	2305.5	2305.5	2305.5	2305.5
80	2305.5	2305.5	2305.5	2305.5	2305.5	2305.5	2305.5	2305.5	2305.5
90	2305.5	2305.5	2305.5	2305.5	2305.5	2305.5	2305.5	2305.5	2305.5
100	2305.5	2305.5	2305.5	2305.5	2305.5	2305.5	2305.5	2305.5	2305.5
110	2305.5	2305.5	2305.5	2305.5	2305.5	2305.5	2305.5	2305.5	2305.5
120	2305.5	2305.5	2305.5	2305.5	2305.5	2305.5	2305.5	2305.5	2305.5
130	2305.5	2305.5	2305.5	2305.5	2305.5	2305.5	2305.5	2305.5	2305.5
140	2305.5	2305.5	2305.5	2305.5	2305.5	2305.5	2305.5	2305.5	2305.5
150	2305.5	2305.5	2305.5	2305.5	2305.5	2305.5	2305.5	2305.5	2305.5
160	2305.5	2305.5	2305.5	2305.5	2305.5	2305.5	2305.5	2305.5	2305.5

SW-0Ca	Total soluble potential ions, on injection : mg / kg of water								
	Pressure (bars)								
Temperature °C	1	50	100	150	200	250	300	350	400
70	3399.2	3399.2	3399.2	3399.2	3399.2	3399.2	3399.2	3399.2	3399.2
80	3399.2	3399.2	3399.2	3399.2	3399.2	3399.2	3399.2	3399.2	3399.2
90	3399.2	3399.2	3399.2	3399.2	3399.2	3399.2	3399.2	3399.2	3399.2
100	3399.2	3399.2	3399.2	3399.2	3399.2	3399.2	3399.2	3399.2	3399.2
110	3399.2	3399.2	3399.2	3399.2	3399.2	3399.2	3399.2	3399.2	3399.2
120	3399.2	3399.2	3399.2	3399.2	3399.2	3399.2	3399.2	3399.2	3399.2
130	3398.5	3398.5	3398.5	3398.5	3398.5	3398.5	3398.5	3398.5	3398.5
140	3396.5	3396.5	3396.5	3396.5	3396.5	3396.5	3396.5	3396.5	3396.5
150	3394.2	3394.2	3394.2	3394.2	3394.2	3394.2	3394.2	3394.2	3394.2
160	3391.9	3391.9	3391.9	3391.9	3391.9	3391.9	3391.9	3391.9	3391.9

SW-0Ca	Precipitation after substitution : mg / kg of water								
	Pressure (bars)								
Temperature °C	1	50	100	150	200	250	300	350	400
70	2456.36	2353.51	2240.78	2120.27	1992.13	1856.66	1714.24	1565.42	1410.84
80	2676.78	2598.75	2513.16	2421.61	2324.2	2221.15	2112.77	1999.47	1881.73
90	2849.63	2791.2	2727.08	2658.44	2585.38	2508.05	2426.68	2341.56	2253.08
100	2982.45	2939.15	2891.62	2840.73	2786.53	2729.14	2668.72	2605.5	2539.75
110	3082.89	3051.06	3016.12	2978.7	2938.83	2896.61	2852.15	2805.61	2757.19
120	3157.92	3134.66	3109.12	3081.77	3052.64	3021.77	2989.27	2955.23	2919.82
130	3213.45	3196.52	3177.93	3158.02	3136.82	3114.35	3090.69	3065.91	3040.13
140	3254.28	3241.98	3228.48	3214.02	3198.62	3182.31	3165.13	3147.14	3128.41

150	3284.17	3275.23	3265.43	3254.94	3243.76	3231.93	3219.47	3206.41	3192.82
160	3305.98	3299.49	3292.37	3284.75	3276.63	3268.04	3258.99	3249.52	3239.65

SW-0Ca	Soluble SO4 after substitution : mg / kg of water								
	Pressure (bars)								
Temperature °C	1	50	100	150	200	250	300	350	400
70	608.72	680.08	758.38	842.16	931.3	1025.62	1124.84	1228.57	1336.37
80	457.02	510.91	570.09	633.47	700.95	772.4	847.6	926.27	1008.05
90	338.79	378.92	423.02	470.27	520.63	573.97	630.15	688.95	750.1
100	248.59	278.13	310.6	345.42	382.54	421.89	463.34	506.75	551.91
110	180.94	202.48	226.17	251.58	278.68	307.41	337.69	369.4	402.42
120	130.88	146.48	163.63	182.04	201.67	222.48	244.42	267.41	291.34
130	94.23	105.46	117.81	131.07	145.2	160.2	176	192.56	209.8
140	67.6	75.65	84.52	94.02	104.16	114.91	126.25	138.12	150.48
150	48.37	54.13	60.47	67.27	74.52	82.21	90.31	98.8	107.63
160	34.55	38.66	43.19	48.04	53.21	58.7	64.48	70.53	76.83

SW-0Ca	Total soluble potential ions ; on injection: mg / kg of water								
	Pressure (bars)								
Temperature °C	1	50	100	150	200	250	300	350	400
70	1683.65	1785.47	1897.14	2016.58	2143.64	2278.04	2419.37	2567.1	2720.6
80	1466.48	1543.52	1628.08	1718.59	1814.94	1916.91	2024.21	2136.42	2253.06
90	1296.8	1354.3	1417.45	1485.09	1557.13	1633.42	1713.74	1797.79	1885.18
100	1166.98	1209.41	1256.04	1306	1359.25	1415.66	1475.08	1537.28	1601.98
110	1069.28	1100.32	1134.44	1171.02	1210.01	1251.33	1294.86	1340.45	1387.89
120	996.7	1019.26	1044.06	1070.65	1099	1129.04	1160.71	1193.87	1228.38
130	943.31	959.64	977.58	996.81	1017.31	1039.05	1061.95	1085.94	1110.92
140	904.34	916.11	929.04	942.91	957.69	973.36	989.87	1007.16	1025.16
150	876.03	884.5	893.81	903.79	914.43	925.7	937.57	950.01	962.96
160	855.55	861.65	868.34	875.52	883.16	891.26	899.8	908.74	918.04

SW-0Ca	Effective fine formation : mg / kg of water								
	Pressure (bars)								
Temperature °C	1	50	100	150	200	250	300	350	400
70	2456.36	2353.51	2240.78	2120.27	1992.13	1856.66	1714.24	1565.42	1410.84
80	2676.78	2598.75	2513.16	2421.61	2324.2	2221.15	2112.77	1999.47	1881.73
90	2849.63	2791.2	2727.08	2658.44	2585.38	2508.05	2426.68	2341.56	2253.08
100	2982.45	2939.15	2891.62	2840.73	2786.53	2729.14	2668.72	2605.5	2539.75
110	3082.89	3051.06	3016.12	2978.7	2938.83	2896.61	2852.15	2805.61	2757.19
120	3157.92	3134.66	3109.12	3081.77	3052.64	3021.77	2989.27	2955.23	2919.82
130	3211.15	3194.22	3175.63	3155.72	3134.51	3112.05	3088.39	3063.61	3037.83
140	3244.88	3232.58	3219.08	3204.62	3189.22	3172.91	3155.73	3137.74	3119.01
150	3266.95	3258.02	3248.21	3237.72	3226.55	3214.71	3202.25	3189.2	3175.61

160	3280.64	3274.14	3267.02	3259.4	3251.29	3242.7	3233.65	3224.17	3214.31

10. SW-½Ca: Sea Water with half of the Ca^{2+} ions

	Na	Mg	Ca	SO4	HCO3-	Cl-
SW-2Ca	0.45	0.045	0.0065	0.192	0.002	0.49

SW-½Ca	Precipitation on injection :mg / kg of water								
	Pressure (bars)								
Temperature °C	1	50	100	150	200	250	300	350	400
70	5.96	4.96	3.96	2.98	2.01	1.04	0.08	0	0
80	8.27	7.11	5.96	4.83	3.73	2.64	1.55	0.46	0
90	11.04	9.7	8.38	7.08	5.81	4.56	3.32	2.08	0.84
100	14.27	12.75	11.24	9.75	8.29	6.86	5.44	4.03	2.62
110	17.94	16.24	14.53	12.85	11.2	9.56	7.95	6.34	4.74
120	21.97	20.11	18.22	16.36	14.51	12.67	10.85	8.46	8.46
130	26.26	24.25	22.21	20.18	18.15	16.13	14	14	14
140	30.66	28.55	26.39	24.22	22.05	20.16	20.16	20.16	20.16
150	35.05	32.87	30.63	26.66	26.66	26.66	26.66	26.66	26.66
160	39.31	37.1	33.18	33.18	33.18	33.18	33.18	33.18	33.18

SW-½Ca	Soluble SO4 on injection : mg / kg of water								
	Pressure (bars)								
Temperature °C	1	50	100	150	200	250	300	350	400
70	2305.5	2305.5	2305.5	2305.5	2305.5	2305.5	2305.5	2305.5	2305.5
80	2305.5	2305.5	2305.5	2305.5	2305.5	2305.5	2305.5	2305.5	2305.5
90	2305.5	2305.5	2305.5	2305.5	2305.5	2305.5	2305.5	2305.5	2305.5
100	2305.5	2305.5	2305.5	2305.5	2305.5	2305.5	2305.5	2305.5	2305.5
110	2305.5	2305.5	2305.5	2305.5	2305.5	2305.5	2305.5	2305.5	2305.5
120	2305.5	2305.5	2305.5	2305.5	2305.5	2305.5	2305.5	2305.5	2305.5
130	2305.5	2305.5	2305.5	2305.5	2305.5	2305.5	2305.5	2305.5	2305.5
140	2305.5	2305.5	2305.5	2305.5	2305.5	2305.5	2305.5	2305.5	2305.5
150	2305.5	2305.5	2305.5	2305.5	2305.5	2305.5	2305.5	2305.5	2305.5
160	2305.5	2305.5	2305.5	2305.5	2305.5	2305.5	2305.5	2305.5	2305.5

SW-½Ca	Total soluble potential ions, on injection : mg / kg of water								
	Pressure (bars)								
Temperature °C	1	50	100	150	200	250	300	350	400
70	3657.3	3657.7	3658.1	3658.5	3658.9	3659.3	3659.7	3659.7	3659.7
80	3656.4	3656.9	3657.3	3657.8	3658.2	3658.6	3659.1	3659.5	3659.7
90	3655.3	3655.8	3656.3	3656.9	3657.4	3657.9	3658.4	3658.9	3659.4
100	3654	3654.6	3655.2	3655.8	3656.4	3657	3657.5	3658.1	3658.7
110	3652.5	3653.2	3653.9	3654.6	3655.2	3655.9	3656.5	3657.2	3657.8
120	3650.9	3651.7	3652.4	3653.2	3653.9	3654.6	3655.4	3656.7	3656.7
130	3649.2	3650	3650.8	3651.6	3652.4	3653.2	3654.8	3654.8	3654.8

140	3647.4	3648.3	3649.1	3650	3650.9	3652.7	3652.7	3652.7	3652.7
150	3645.7	3646.5	3647.4	3650.4	3650.4	3650.4	3650.4	3650.4	3650.4
160	3644	3644.8	3648.1	3648.1	3648.1	3648.1	3648.1	3648.1	3648.1

SW-½Ca	Precipitation after substitution : mg / kg of water								
	Pressure (bars)								
Temperature °C	1	50	100	150	200	250	300	350	400
70	2503.29	2404.3	2295.55	2179.01	2054.81	1923.18	1784.51	1639.29	1488.16
80	2711.95	2637.03	2554.7	2466.43	2372.33	2272.57	2167.43	2057.3	1942.64
90	2875.11	2819.06	2757.46	2691.41	2620.97	2546.29	2467.56	2385.07	2299.17
100	3000.32	2958.77	2913.09	2864.12	2811.9	2756.52	2698.14	2636.96	2573.24
110	3095.05	3064.44	3030.8	2994.73	2956.28	2915.51	2872.52	2827.48	2780.56
120	3165.94	3143.49	3118.83	3092.39	3064.21	3034.33	3002.84	2969.85	2935.48
130	3218.57	3202.15	3184.12	3164.8	3144.21	3122.38	3099.38	3075.28	3050.18
140	3257.43	3245.43	3232.27	3218.16	3203.14	3187.21	3170.44	3152.86	3134.56
150	3286.01	3277.25	3267.63	3257.34	3246.37	3234.76	3222.52	3209.7	3196.35
160	3306.99	3300.58	3293.55	3286.03	3278.02	3269.53	3260.6	3251.24	3241.49

SW-½Ca	Soluble SO4 after substitution : mg / kg of water								
	Pressure (bars)								
Temperature °C	1	50	100	150	200	250	300	350	400
70	576.6	645.21	720.68	801.63	887.98	979.55	1076.09	1177.25	1282.59
80	433.17	484.86	541.74	602.78	667.92	737.03	809.92	886.33	965.92
90	321.72	360.17	402.5	447.93	496.43	547.91	602.21	659.15	718.47
100	236.81	265.13	296.31	329.78	365.51	403.44	443.47	485.43	529.16
110	173.1	193.8	216.58	241.05	267.17	294.89	324.14	354.81	386.77
120	125.86	140.9	157.46	175.24	194.21	214.35	235.59	257.86	281.07
130	91.15	102.04	114.02	126.88	140.6	155.16	170.52	186.62	203.39
140	65.83	73.68	82.32	91.6	101.49	111.99	123.06	134.66	146.74
150	47.44	53.09	59.31	65.99	73.11	80.66	88.62	96.96	105.65
160	34.13	38.2	42.67	47.47	52.59	58.01	63.73	69.72	75.95

SW-½Ca	Total soluble potential ions ; on injection: mg / kg of water								
	Pressure (bars)								
Temperature °C	1	50	100	150	200	250	300	350	400
70	1898.07	1996.01	2103.68	2219.14	2342.24	2472.76	2610.32	2754.42	2904.45
80	1692.64	1766.57	1847.87	1935.08	2028.11	2126.78	2230.82	2339.84	2453.38
90	1532.61	1587.73	1648.36	1713.41	1782.83	1856.47	1934.14	2015.55	2100.35
100	1410.32	1451.02	1495.8	1543.86	1595.13	1649.54	1706.92	1767.08	1829.75
110	1318.25	1348.1	1380.93	1416.16	1453.75	1493.63	1535.7	1579.8	1625.74
120	1249.73	1271.5	1295.44	1321.13	1348.54	1377.61	1408.27	1440.41	1473.89
130	1199.16	1214.99	1232.39	1251.05	1270.96	1292.07	1314.33	1337.66	1361.96
140	1162.08	1173.56	1186.17	1199.7	1214.13	1229.42	1245.55	1262.44	1280.03

150	1135.01	1143.32	1152.46	1162.25	1172.69	1183.76	1195.43	1207.65	1220.37
160	1115.3	1121.33	1127.94	1135.03	1142.59	1150.59	1159.03	1167.87	1177.07

SW-½Ca	Effective fine formation : mg / kg of water								
	Pressure (bars)								
Temperature °C	1	50	100	150	200	250	300	350	400
70	2497.32	2399.34	2291.59	2176.03	2052.79	1922.13	1784.43	1639.29	1488.16
80	2703.68	2629.92	2548.73	2461.59	2368.59	2269.93	2165.88	2056.83	1942.64
90	2864.07	2809.36	2749.08	2684.32	2615.16	2541.73	2464.24	2382.98	2298.33
100	2986.05	2946.01	2901.85	2854.37	2803.6	2749.66	2692.69	2632.92	2570.62
110	3077.1	3048.19	3016.26	2981.88	2945.08	2905.94	2864.57	2821.13	2775.82
120	3143.96	3123.38	3100.6	3076.03	3049.7	3021.66	2991.99	2961.38	2927.01
130	3192.31	3177.89	3161.9	3144.61	3126.05	3106.24	3085.38	3061.28	3036.18
140	3226.76	3216.88	3205.87	3193.94	3181.09	3167.05	3150.27	3132.69	3114.39
150	3250.96	3244.37	3237	3230.67	3219.71	3208.09	3195.85	3183.03	3169.68
160	3267.68	3263.48	3260.37	3252.85	3244.84	3236.35	3227.41	3218.05	3208.3

11. SW-2Ca: Sea Water with twice Ca^{2+}

	Na	Mg	Ca	SO4	HCO3-	Cl-
SW-2Ca	0.45	0.045	0.026	0.192	0.002	0.542

SW-2Ca	Precipitation on injection :mg / kg of water								
	Pressure (bars)								
Temperature °C	1	50	100	150	200	250	300	350	400
70	21.47	19.89	18.32	16.82	15.37	13.97	12.64	11.35	10.12
80	25.78	24.05	22.33	20.66	19.04	17.47	15.95	14.49	13.07
90	30.48	28.64	26.79	24.98	23.2	21.47	19.78	18.14	16.54
100	35.44	33.53	31.59	29.67	27.77	25.89	24.05	22.25	20.48
110	75.11	38.56	36.57	34.58	32.6	30.62	28.67	26.73	24.81
120	450.62	263.72	67.49	39.57	37.54	35.51	33.48	31.44	29.42
130	781.45	616.52	443.49	266.14	85.01	40.4	38.33	36.25	34.16
140	1072.43	926.63	773.77	617.23	457.46	295.02	130.5	41	38.88
150	1328.14	1198.98	1063.68	925.2	783.99	640.51	495.3	348.94	202.06
160	1552.8	1438.14	1318.11	1195.35	1070.23	943.2	814.73	685.32	569.55

SW-2Ca	Soluble SO4 on injection : mg / kg of water								
	Pressure (bars)								
Temperature °C	1	50	100	150	200	250	300	350	400
70	2305.5	2305.5	2305.5	2305.5	2305.5	2305.5	2305.5	2305.5	2305.5
80	2305.5	2305.5	2305.5	2305.5	2305.5	2305.5	2305.5	2305.5	2305.5
90	2305.5	2305.5	2305.5	2305.5	2305.5	2305.5	2305.5	2305.5	2305.5
100	2305.5	2305.5	2305.5	2305.5	2305.5	2305.5	2305.5	2305.5	2305.5
110	2281	2305.5	2305.5	2305.5	2305.5	2305.5	2305.5	2305.5	2305.5
120	2018.3	2149.5	2287.1	2305.5	2305.5	2305.5	2305.5	2305.5	2305.5

130	1787.2	1902.8	2024.1	2148.4	2275.3	2305.5	2305.5	2305.5	2305.5
140	1584	1686.1	1793.1	1902.8	2014.6	2128.4	2243.5	2305.5	2305.5
150	1405.5	1495.9	1590.6	1687.5	1786.2	1886.6	1988.1	2090.4	2193
160	1248.7	1328.9	1412.8	1498.6	1586.1	1674.8	1764.5	1854.9	1934.1

SW-2Ca	Total soluble potential ions, on injection : mg / kg of water								
	Pressure (bars)								
Temperature °C	1	50	100	150	200	250	300	350	400
70	4432.6	4433.3	4433.9	4434.5	4435.1	4435.6	4436.2	4436.7	4437.2
80	4430.9	4431.6	4432.3	4433	4433.6	4434.2	4434.8	4435.4	4436
90	4429	4429.8	4430.5	4431.2	4431.9	4432.6	4433.3	4434	4434.6
100	4427	4427.8	4428.6	4429.4	4430.1	4430.9	4431.6	4432.3	4433
110	4390.3	4425.8	4426.6	4427.4	4428.2	4429	4429.8	4430.5	4431.3
120	4016.8	4203.1	4398.6	4425.4	4426.2	4427	4427.8	4428.6	4429.5
130	3687.9	3852.2	4024.5	4201.2	4381.6	4425.1	4425.9	4426.7	4427.6
140	3398.7	3543.9	3696.1	3851.9	4010.9	4172.6	4336.3	4424.8	4425.7
150	3144.7	3273.2	3407.8	3545.6	3686.1	3828.8	3973.2	4118.8	4264.8
160	2921.5	3035.6	3154.9	3277	3401.4	3527.7	3655.4	3783.9	3899.8

SW-2Ca	Precipitation after substitution : mg / kg of water								
	Pressure (bars)								
Temperature °C	1	50	100	150	200	250	300	350	400
70	2571.26	2478.8	2376.94	2267.49	2150.51	2026.19	1894.83	1756.88	1612.9
80	2759.33	2689.11	2611.8	2528.73	2439.99	2345.7	2246.1	2141.52	2032.39
90	2906.71	2853.87	2795.71	2733.25	2666.55	2595.7	2520.9	2442.37	2360.46
100	3020.37	2980.87	2937.4	2890.75	2840.95	2788.08	2732.27	2673.72	2612.66
110	3106.98	3077.58	3045.24	3010.56	2973.54	2934.26	2892.82	2849.36	2804.06
120	3172.39	3150.57	3126.59	3100.87	3073.44	3044.34	3013.66	2981.48	2947.96
130	3221.48	3205.31	3187.55	3168.51	3148.21	3126.69	3104	3080.22	3055.44
140	3258.16	3246.19	3233.04	3218.95	3203.93	3188.02	3171.24	3153.67	3135.36
150	3285.5	3276.62	3266.88	3256.45	3245.34	3233.56	3221.15	3208.16	3194.62
160	3305.83	3299.25	3292.02	3284.29	3276.05	3267.33	3258.14	3248.51	3238.49

SW-2Ca	Soluble SO4 after substitution : mg / kg of water								
	Pressure (bars)								
Temperature °C	1	50	100	150	200	250	300	350	400
70	530.4	594.41	664.99	740.92	822.15	908.53	999.87	1095.86	1196.1
80	401.39	449.77	503.11	560.48	621.84	687.08	756.05	828.52	904.17
90	300.91	337.13	377.04	419.95	465.83	514.61	566.15	620.29	676.79
100	223.97	250.87	280.52	312.38	346.43	382.61	420.83	460.96	502.83
110	165.79	185.67	207.57	231.09	256.23	282.92	311.11	340.69	371.53
120	122.23	136.87	152.98	170.28	188.76	208.37	229.08	250.79	273.43
130	89.85	100.59	112.42	125.11	138.65	153.03	168.2	184.1	200.67

140	65.91	73.78	82.44	91.73	101.65	112.16	123.26	134.88	146.99
150	48.28	54.04	60.37	67.16	74.41	82.1	90.2	98.69	107.53
160	35.32	39.53	44.16	49.13	54.42	60.03	65.95	72.15	78.6

SW-2Ca	Total soluble potential ions ; on injection: mg / kg of water								
	Pressure (bars)								
Temperature °C	1	50	100	150	200	250	300	350	400
70	2613.13	2704.54	2805.3	2913.65	3029.51	3152.7	3282.91	3419.71	3562.53
80	2428.2	2497.42	2573.71	2655.72	2743.39	2836.58	2935.07	3038.52	3146.51
90	2283.8	2335.73	2392.94	2454.41	2520.11	2589.92	2663.67	2741.11	2821.92
100	2172.91	2211.59	2254.18	2299.93	2348.81	2400.73	2455.55	2513.1	2573.12
110	2088.79	2117.46	2149.01	2182.89	2219.07	2257.48	2298.02	2340.56	2384.91
120	2025.59	2046.76	2070.05	2095.06	2121.74	2150.06	2179.94	2211.27	2243.93
130	1978.42	1994.02	2011.18	2029.59	2049.23	2070.06	2092.03	2115.07	2139.07
140	1943.39	1954.87	1967.49	1981.03	1995.47	2010.78	2026.92	2043.84	2061.45
150	1917.46	1925.9	1935.19	1945.14	1955.74	1966.99	1978.85	1991.27	2004.2
160	1898.31	1904.52	1911.35	1918.66	1926.46	1934.72	1943.43	1952.55	1962.05

SW-2Ca	Effective fine formation : mg / kg of water								
	Pressure (bars)								
Temperature °C	1	50	100	150	200	250	300	350	400
70	2549.78	2458.9	2358.61	2250.67	2135.13	2012.21	1882.19	1745.52	1602.78
80	2733.55	2665.06	2589.46	2508.07	2420.94	2328.22	2230.14	2127.03	2019.31
90	2876.23	2825.23	2768.91	2708.27	2643.34	2574.23	2501.11	2424.23	2343.92
100	2984.92	2947.33	2905.81	2861.08	2813.18	2762.18	2708.21	2651.46	2592.17
110	3031.87	3039.01	3008.67	2975.97	2940.94	2903.64	2864.15	2822.63	2779.24
120	2721.77	2886.84	3059.09	3061.29	3035.89	3008.83	2980.18	2950.04	2918.54
130	2440.03	2588.79	2744.05	2902.36	3063.2	3086.28	3065.66	3043.96	3021.28
140	2185.73	2319.56	2459.26	2601.71	2746.46	2892.99	3040.73	3112.66	3096.48
150	1957.35	2077.63	2203.19	2331.24	2461.34	2593.05	2725.85	2859.21	2992.56
160	1753.03	1861.1	1973.91	2088.94	2205.82	2324.12	2443.41	2563.18	2668.93

12. SW-3Ca: Sea Water with thrice Ca^{2+}

	Na	Mg	Ca	SO4	HCO3-	Cl-
SW-2Ca	0.45	0.045	0.052	0.192	0.002	0.594

SW-4Ca	Precipitation on injection :mg / kg of water								
	Pressure (bars)								
Temperature °C	1	50	100	150	200	250	300	350	400
70	30.81	29	27.18	25.4	23.67	21.98	20.34	18.76	17.23
80	35.63	33.74	31.84	29.95	28.1	26.29	24.51	22.77	21.08
90	420.56	161.71	36.77	34.82	32.89	30.98	29.09	27.22	25.39
100	861.09	636.92	398.83	152.05	37.88	35.91	33.95	32	30.06
110	1244.58	1051.01	845.23	631.77	411.39	184.96	38.95	36.95	34.95

120	1575.81	1409.18	1231.79	1047.57	857.22	661.49	461.25	257.44	51.06
130	1859.99	1716.94	1564.43	1405.84	1241.76	1072.88	899.97	723.85	545.43
140	2102.32	1979.88	1849.11	1712.9	1571.78	1426.35	1277.29	1125.33	971.25
150	2307.86	2203.37	2091.54	1974.85	1853.75	1728.77	1600.5	1469.59	1336.73
160	2481.4	2392.46	2297.08	2197.36	2093.69	1986.52	1876.36	1763.78	1649.39

SW-4Ca	Soluble SO4 on injection : mg / kg of water								
	Pressure (bars)								
Temperature °C	1	50	100	150	200	250	300	350	400
70	2305.5	2305.5	2305.5	2305.5	2305.5	2305.5	2305.5	2305.5	2305.5
80	2305.5	2305.5	2305.5	2305.5	2305.5	2305.5	2305.5	2305.5	2305.5
90	2036.9	2218.5	2305.5	2305.5	2305.5	2305.5	2305.5	2305.5	2305.5
100	1729	1886.2	2053.1	2226.2	2305.5	2305.5	2305.5	2305.5	2305.5
110	1461.4	1597	1741.1	1890.6	2045	2203.7	2305.5	2305.5	2305.5
120	1230.6	1347.2	1471.3	1600.1	1733.3	1870.3	2010.5	2153.1	2297.6
130	1032.9	1132.8	1239.4	1350.2	1464.9	1582.9	1703.7	1826.8	1951.6
140	864.6	950	1041.2	1136.2	1234.7	1336.2	1440.2	1546.3	1653.8
150	722	794.7	872.6	953.9	1038.3	1125.4	1214.8	1306	1398.6
160	601.8	663.6	729.9	799.3	871.4	945.9	1022.5	1100.8	1180.4

SW-4Ca	Total soluble potential ions, on injection : mg / kg of water								
	Pressure (bars)								
Temperature °C	1	50	100	150	200	250	300	350	400
70	5470.9	5471.7	5472.4	5473.1	5473.8	5474.5	5475.1	5475.8	5476.4
80	5469	5469.8	5470.5	5471.3	5472	5472.7	5473.5	5474.2	5474.8
90	5086.7	5344.6	5468.5	5469.3	5470.1	5470.9	5471.6	5472.4	5473.1
100	4648.7	4872	5109.1	5355	5468.1	5468.9	5469.7	5470.5	5471.2
110	4267.7	4460.4	4665.3	4877.8	5097.2	5322.7	5467.7	5468.5	5469.3
120	3939	4104.7	4281.2	4464.5	4653.9	4848.6	5047.9	5250.7	5456.1
130	3657.2	3799.3	3950.9	4108.6	4271.7	4439.7	4611.6	4786.7	4964.1
140	3417.1	3538.7	3668.5	3803.8	3944	4088.5	4236.6	4387.6	4540.6
150	3213.6	3317.3	3428.2	3544.1	3664.2	3788.3	3915.6	4045.5	4177.4
160	3042	3130.1	3224.7	3323.5	3426.3	3532.6	3641.8	3753.4	3866.8

SW-4Ca	Precipitation after substitution : mg / kg of water								
	Pressure (bars)								
Temperature °C	1	50	100	150	200	250	300	350	400
70	2599.9	2510.54	2412.04	2306.13	2192.87	2072.43	1945.08	1811.23	1671.42
80	2775.51	2707.04	2631.61	2550.57	2463.94	2371.87	2274.58	2172.38	2065.68
90	2914.17	2862.1	2804.78	2743.22	2677.47	2607.62	2533.85	2456.4	2375.6
100	3022.07	2982.69	2939.36	2892.86	2843.2	2790.49	2734.86	2676.47	2615.59
110	3105.14	3075.46	3042.83	3007.81	2970.46	2930.82	2888.99	2845.13	2799.42
120	3168.58	3146.27	3121.74	3095.44	3067.39	3037.64	3006.27	2973.38	2939.11

130	3216.77	3200.01	3181.6	3161.87	3140.83	3118.52	3095.01	3070.37	3044.7
140	3253.24	3240.66	3226.84	3212.03	3196.26	3179.54	3161.91	3143.45	3124.23
150	3280.77	3271.32	3260.95	3249.83	3238	3225.46	3212.24	3198.4	3183.99
160	3301.53	3294.43	3286.63	3278.29	3269.4	3259.98	3250.06	3239.67	3228.85

SW-4Ca	Soluble SO4 after substitution : mg / kg of water								
	Pressure (bars)								
Temperature °C	1	50	100	150	200	250	300	350	400
70	511.3	573.13	641.35	714.78	793.37	877.02	965.52	1058.6	1155.87
80	390.96	438.12	490.14	546.1	605.96	669.64	736.99	807.77	881.71
90	296.49	332.18	371.51	413.81	459.03	507.11	557.93	611.32	667.05
100	223.46	250.29	279.86	311.64	345.6	381.68	419.8	459.82	501.58
110	167.64	187.73	209.86	233.63	259.03	285.99	314.46	344.34	375.49
120	125.35	140.34	156.85	174.58	193.51	213.6	234.81	257.05	280.23
130	93.5	104.66	116.96	130.15	144.23	159.18	174.94	191.46	208.68
140	69.62	77.92	87.06	96.87	107.33	118.43	130.13	142.39	155.16
150	51.77	57.94	64.73	72.01	79.77	88.01	96.69	105.79	115.25
160	38.46	43.04	48.08	53.48	59.24	65.35	71.78	78.52	85.54

SW-4Ca	Total soluble potential ions ; on injection: mg / kg of water								
	Pressure (bars)								
Temperature °C	1	50	100	150	200	250	300	350	400
70	3627.46	3715.79	3813.2	3918	4030.13	4149.44	4275.64	4408.32	4546.96
80	3454.89	3522.39	3596.79	3676.79	3762.34	3853.32	3949.5	4050.58	4156.13
90	3319.1	3370.27	3426.64	3487.23	3551.99	3620.82	3693.54	3769.91	3849.62
100	3213.83	3252.4	3294.88	3340.5	3389.24	3441.01	3495.68	3553.06	3612.92
110	3133.14	3162.1	3193.97	3228.19	3264.72	3303.51	3344.45	3387.4	3432.18
120	3071.8	3093.48	3117.33	3142.92	3170.24	3199.22	3229.8	3261.87	3295.29
130	3025.44	3041.64	3059.46	3078.57	3098.96	3120.59	3143.4	3167.31	3192.21
140	2990.54	3002.64	3015.94	3030.2	3045.41	3061.53	3078.53	3096.35	3114.9
150	2964.36	2973.38	2983.3	2993.94	3005.28	3017.3	3029.97	3043.24	3057.05
160	2944.73	2951.47	2958.87	2966.8	2975.26	2984.22	2993.66	3003.54	3013.84

SW-4Ca	Effective fine formation : mg / kg of water								
	Pressure (bars)								
Temperature °C	1	50	100	150	200	250	300	350	400
70	2569.09	2481.54	2384.86	2280.73	2169.2	2050.44	1924.73	1792.46	1654.18
80	2739.88	2673.29	2599.77	2520.61	2435.83	2345.58	2250.07	2149.6	2044.59
90	2493.6	2700.38	2768.01	2708.4	2644.57	2576.64	2504.76	2429.18	2350.2
100	2160.97	2345.77	2540.53	2740.8	2805.32	2754.58	2700.9	2644.47	2585.53
110	1860.56	2024.44	2197.59	2376.04	2559.06	2745.85	2850.04	2808.18	2764.46
120	1592.76	1737.09	1889.95	2047.86	2210.17	2376.15	2545.01	2715.94	2888.05
130	1356.78	1483.07	1617.16	1756.02	1899.06	2045.63	2195.03	2346.51	2499.27

140	1150.92	1260.77	1377.72	1499.13	1624.47	1753.18	1884.62	2018.12	2152.97
150	972.9	1067.94	1169.4	1274.98	1384.24	1496.68	1611.74	1728.81	1847.26
160	820.13	901.96	989.54	1080.92	1175.7	1273.46	1373.7	1475.89	1579.46

13. SW-4NaCl: Sea Water with 4 times NaCl

	Na	Mg	Ca	SO4	HCO3-	Cl-
SW-2Ca	0.45	0.045	0.052	0.192	0.002	0.594

SW-4NaCl	Precipitation on injection :mg / kg of water								
	Pressure (bars)								
Temperature °C	1	50	100	150	200	250	300	350	400
70	2.66	1.68	0.69	0	0	0	0	0	0
80	3.49	2.39	1.28	0.16	0	0	0	0	0
90	4.32	3.08	1.82	0.55	0	0	0	0	0
100	5.12	3.71	2.26	0.81	0	0	0	0	0
110	5.84	4.22	2.56	0.88	0	0	0	0	0
120	6.4	4.54	2.62	0.67	0	0	0	0	0
130	6.69	4.55	2.32	0.04	0	0	0	0	0
140	6.53	4.06	1.47	0	0	0	0	0	0
150	5.68	2.81	0	0	0	0	0	0	0
160	3.7	0.32	0	0	0	0	0	0	0

SW-4NaCl	Soluble SO4 on injection : mg / kg of water								
	Pressure (bars)								
Temperature °C	1	50	100	150	200	250	300	350	400
70	2305.5	2305.5	2305.5	2305.5	2305.5	2305.5	2305.5	2305.5	2305.5
80	2305.5	2305.5	2305.5	2305.5	2305.5	2305.5	2305.5	2305.5	2305.5
90	2305.5	2305.5	2305.5	2305.5	2305.5	2305.5	2305.5	2305.5	2305.5
100	2305.5	2305.5	2305.5	2305.5	2305.5	2305.5	2305.5	2305.5	2305.5
110	2305.5	2305.5	2305.5	2305.5	2305.5	2305.5	2305.5	2305.5	2305.5
120	2305.5	2305.5	2305.5	2305.5	2305.5	2305.5	2305.5	2305.5	2305.5
130	2305.5	2305.5	2305.5	2305.5	2305.5	2305.5	2305.5	2305.5	2305.5
140	2305.5	2305.5	2305.5	2305.5	2305.5	2305.5	2305.5	2305.5	2305.5
150	2305.5	2305.5	2305.5	2305.5	2305.5	2305.5	2305.5	2305.5	2305.5
160	2305.5	2305.5	2305.5	2305.5	2305.5	2305.5	2305.5	2305.5	2305.5

SW-4NaCl	Total soluble potential ions, on injection : mg / kg of water								
	Pressure (bars)								
Temperature °C	1	50	100	150	200	250	300	350	400
70	3919.1	3919.5	3919.9	3920.2	3920.2	3920.2	3920.2	3920.2	3920.2
80	3918.8	3919.3	3919.7	3920.1	3920.2	3920.2	3920.2	3920.2	3920.2
90	3918.5	3919	3919.5	3920	3920.2	3920.2	3920.2	3920.2	3920.2
100	3918.2	3918.7	3919.3	3919.9	3920.2	3920.2	3920.2	3920.2	3920.2
110	3917.9	3918.5	3919.2	3919.9	3920.2	3920.2	3920.2	3920.2	3920.2

120	3917.6	3918.4	3919.2	3919.9	3920.2	3920.2	3920.2	3920.2	3920.2
130	3917.5	3918.4	3919.3	3920.2	3920.2	3920.2	3920.2	3920.2	3920.2
140	3917.6	3918.6	3919.6	3920.2	3920.2	3920.2	3920.2	3920.2	3920.2
150	3917.9	3919.1	3920.2	3920.2	3920.2	3920.2	3920.2	3920.2	3920.2
160	3918.7	3920.1	3920.2	3920.2	3920.2	3920.2	3920.2	3920.2	3920.2

SW-4NaCl	Precipitation after substitution : mg / kg of water								
	Pressure (bars)								
Temperature °C	1	50	100	150	200	250	300	350	400
70	2534.47	2438.34	2332.59	2219.09	2097.96	1969.41	1833.79	1691.56	1543.34
80	2734.37	2661.61	2581.56	2495.64	2403.94	2306.61	2203.91	2096.2	1983.93
90	2890.65	2836.14	2776.19	2711.85	2643.18	2570.31	2493.41	2412.76	2328.71
100	3010.68	2970.18	2925.63	2877.84	2826.84	2772.73	2715.64	2655.78	2593.38
110	3101.67	3071.74	3038.83	3003.53	2965.87	2925.93	2883.8	2839.63	2793.6
120	3169.96	3147.92	3123.7	3097.73	3070.03	3040.66	3009.69	2977.23	2943.41
130	3220.85	3204.65	3186.86	3167.8	3147.47	3125.92	3103.21	3079.4	3054.61
140	3258.58	3246.69	3233.63	3219.65	3204.74	3188.95	3172.3	3154.86	3136.69
150	3286.47	3277.73	3268.15	3257.88	3246.95	3235.37	3223.16	3210.38	3197.06
160	3307.03	3300.61	3293.57	3286.03	3278	3269.49	3260.53	3251.14	3241.37

SW-4NaCl	Soluble SO4 after substitution : mg / kg of water								
	Pressure (bars)								
Temperature °C	1	50	100	150	200	250	300	350	400
70	555.34	621.93	695.27	774.06	858.23	947.62	1041.99	1141.02	1244.27
80	418.05	468.23	523.49	582.87	646.32	713.71	784.87	859.55	937.44
90	311.41	348.78	389.94	434.17	481.43	531.63	584.64	640.27	698.29
100	230.07	257.67	288.06	320.71	355.58	392.63	431.74	472.79	515.59
110	168.92	189.16	211.44	235.38	260.95	288.09	316.75	346.82	378.16
120	123.44	138.21	154.47	171.94	190.58	210.37	231.26	253.17	276
130	89.89	100.63	112.46	125.15	138.7	153.08	168.25	184.15	200.72
140	65.29	73.09	81.67	90.87	100.69	111.11	122.1	133.62	145.62
150	47.34	52.99	59.2	65.86	72.97	80.51	88.46	96.79	105.46
160	34.28	38.37	42.86	47.68	52.82	58.27	64.01	70.03	76.29

SW-4NaCl	Total soluble potential ions ; on injection: mg / kg of water								
	Pressure (bars)								
Temperature °C	1	50	100	150	200	250	300	350	400
70	2128.03	2223.11	2327.78	2440.17	2560.19	2687.62	2822.12	2963.22	3110.31
80	1931.33	2003.1	2082.11	2166.97	2257.6	2353.84	2455.43	2562.02	2673.16
90	1778.13	1831.71	1890.7	1954.05	2021.7	2093.53	2169.37	2248.93	2331.89
100	1660.96	1700.62	1744.28	1791.16	1841.22	1894.37	1950.46	2009.31	2070.66
110	1572.56	1601.74	1633.86	1668.33	1705.13	1744.2	1785.41	1828.65	1873.71
120	1506.57	1527.95	1551.46	1576.7	1603.63	1632.21	1662.36	1693.97	1726.92

130	1457.68	1473.3	1490.47	1508.89	1528.54	1549.39	1571.37	1594.42	1618.43
140	1421.68	1433.06	1445.58	1459	1473.31	1488.49	1504.5	1521.27	1538.74
150	1395.26	1403.55	1412.67	1422.44	1432.86	1443.9	1455.54	1467.74	1480.44
160	1375.92	1381.97	1388.6	1395.72	1403.3	1411.34	1419.81	1428.68	1437.91

References:

- Austad, T., Strand, S., & Puntervold, T. (2009, September). Is wettability alteration of carbonates by seawater caused by rock dissolution. In *Paper SCA2009-43 presented at the International Symposium of the Society of Core Analysts held in Noordwijk, The Netherlands, September* (pp. 27-30).
- Awolayo, A., Sarma, H., & AlSumaiti, A. M. (2014, March). A Laboratory Study of Ionic Effect of Smart Water for Enhancing Oil Recovery in Carbonate Reservoirs. In *SPE EOR Conference at Oil and Gas West Asia*. Society of Petroleum Engineers.
- Fathi, S. J., Austad, T., & Strand, S. (2010). "Smart Water" as a Wettability Modifier in Chalk: The Effect of Salinity and Ionic Composition. *Energy & fuels*, *24*(4), 2514-2519.
- Fathi, S. J., Austad, T., & Strand, S. (2011). Water-based enhanced oil recovery (EOR) by "smart water": Optimal ionic composition for EOR in carbonates. *Energy & fuels*, *25*(11), 5173-5179.
- Fathi, S. J., Austad, T., & Strand, S. (2012, January). Water-Based Enhanced Oil recovery (EOR) by" Smart Water" in Carbonate Reservoirs. In*SPE EOR Conference at Oil and Gas West Asia*. Society of Petroleum Engineers.
- Iliuta, M. C., Thomsen, K., & Rasmussen, P. (2000). Extended UNIQUAC model for correlation and prediction of vapour–liquid–solid equilibria in aqueous salt systems containing non-electrolytes. Part A. Methanol–water–salt systems. *Chemical Engineering Science*, *55*(14), 2673-2686.
- Puntervold, T., Strand, S., Ellouz, R., & Austad, T. (2014, December). Why is it Possible to Produce Oil from the Ekofisk Field for Another 40 Years?. In*International Petroleum Technology Conference*. International Petroleum Technology Conference.
- Puntervold, T., Strand, S., Ellouz, R., & Austad, T. (2015). Modified seawater as a smart EOR fluid in chalk. *Journal of Petroleum Science and Engineering*, *133*, 440-443.
- Strand, S., Austad, T., Puntervold, T., Høgnesen, E. J., Olsen, M., & Barstad, S. M. F. (2008). "Smart water" for oil recovery from fractured limestone: a preliminary study. *Energy & fuels*, *22*(5), 3126-3133.
- Thomsen, K., Iliuta, M. C., & Rasmussen, P. (2004). Extended UNIQUAC model for correlation and prediction of vapor–liquid–liquid–solid equilibria in aqueous salt systems containing non-electrolytes. Part B. Alcohol (ethanol, propanols, butanols)–water–salt systems. *Chemical engineering science*,*59*(17), 3631-3647.
- Thomsen, K., Rasmussen, P., & Gani, R. (1996). Correlation and prediction of thermal properties and phase behaviour for a class of aqueous electrolyte systems. *Chemical Engineering Science*, *51*(14), 3675-3683.
- Vo, L. T., Gupta, R., & Hehmeyer, O. J. (2012, January). Ion chromatography analysis of advanced ion management carbonate coreflood experiments. In *Abu Dhabi International Petroleum Conference and Exhibition*. Society of Petroleum Engineers.
- Zahid, A., Shapiro, A., Stenby, E. H., & Yan, W. (2012). Managing injected water composition to improve oil recovery: A case study of North Sea chalk reservoirs. *Energy & Fuels*, *26*(6), 3407-3415.
- Zahid, A., Stenby, E. H., & Shapiro, A. A. (2010, January). Improved Oil Recovery in Chalk: Wettability Alteration or Something Else?. In *SPE EUROPEC/EAGE Annual Conference and Exhibition*. Society of Petroleum Engineers.
- Zhang, P., Tweheyo, M. T., & Austad, T. (2006). Wettability alteration and improved oil recovery in chalk: The effect of calcium in the presence of sulfate. *Energy & fuels*, *20*(5), 2056-2062.